

Quantitative Thin-Layer Chromatography

A Practical Survey



Quantitative Thin-Layer Chromatography

Bernd Spangenberg • Colin F. Poole • Christel Weins

Quantitative Thin-Layer Chromatography

A Practical Survey



Prof. Dr. Bernd Spangenberg Hochschule Offenburg FB Maschinenbau und Verfahrenstechnik Badstr. 24 77652 Offenburg Germany spangenberg@fh-offenburg.de

Christel Weins Hasenfeld 7 66132 Bischmisheim Saarland Germany c.weins@mail.intersaar.de Colin F. Poole Wayne State University Dept. Chemistry Cass Avenue 5101 48202 Detroit Michigan USA cfp@chem.wayne.edu

ISBN 978-3-642-10727-6 e-ISBN 978-3-642-10729-0 DOI 10.1007/978-3-642-10729-0 Springer Heidelberg Dordrecht London New York

Library of Congress Control Number: 2010938374

© Springer-Verlag Berlin Heidelberg 2011

This work is subject to copyright. All rights are reserved, whether the whole or part of the material is concerned, specifically the rights of translation, reprinting, reuse of illustrations, recitation, broadcasting, reproduction on microfilm or in any other way, and storage in data banks. Duplication of this publication or parts thereof is permitted only under the provisions of the German Copyright Law of September 9, 1965, in its current version, and permission for use must always be obtained from Springer. Violations are liable to prosecution under the German Copyright Law.

The use of general descriptive names, registered names, trademarks, etc. in this publication does not imply, even in the absence of a specific statement, that such names are exempt from the relevant protective laws and regulations and therefore free for general use.

Cover design: WMXDesign GmbH, Heidelberg, Germany

Printed on acid-free paper

Springer is part of Springer Science+Business Media (www.springer.com)

Preface

Thin-layer chromatography (TLC) is a rather ignored quantification technique. The method is widely used for education purposes and qualitative analysis. The analysis of herbs, in particular, is often performed by TLC due to the simultaneous separation of different samples facilitating their differentiation at first glance. The aesthetic results of individual coloured TLC zones are certainly appreciated by many people who enjoy looking at such results. Another critical aspect of TLC is the humidity dependence of adsorption chromatography. This is certainly the major reason why adsorption TLC was labelled "irreproducible" and "unreliable" and why industry prefers closed systems such as HPLC. Another reason for avoiding TLC is that analyses using highly automated HPLC were generally superior to TLC, which relies more on the skill of the analyst. Last, but not least, the odour of vanillin reagent reminded laboratory staff on a daily basis that chemical analysis is a part of chemistry and not computer science.

All these aspects that spoke against TLC are now just history. Modern equipment and working practices have overcome all these problems. TLC calibration curves are now linear over more than three orders of magnitude. Modern sample application, development chambers, and reagent spray or dipping devices provide the required degree of automation, reliability, and independence of the local environment (temperature, humidity, etc.) associated with robust analytical methods. Nevertheless, quantitative TLC, unlike HPLC, is still mostly done in resource-limited laboratories with incomplete instrument support.

This book is written as a self-study guide for professional scientists to refresh their understanding of modern TLC. It presents the complete theory of quantitative TLC analysis. It is also written for newcomers who want to use quantitative TLC but have limited access to older books which are often unavailable or difficult to obtain. The main concept was to collect in one place all the knowledge necessary to perform quantitative TLC. The chapters follow a modular style facilitating access to information relevant to the individual operations of a successful TLC analysis. The book starts with a chapter on history followed by a chapter on theory (including practical hints for fast and reliable method development). Chapter 3 introduces the different stationary phases and Chap. 4 the various mobile phases. Chapter 5

vi Preface

describes sample pre-treatment techniques and methods for sample application. Chapter 6 deals with the different development techniques. Chapter 7 adopts a dictionary-like style to introduce the many methods of general and specific staining reactions for visualization. Chapter 8 concentrates on analysis linked to bio-effective methods bridging the gap with biology. Chapter 9 describes all known measurement methods for evaluating TLC separations. Chapters 10 and 11 contain the theory for spectrometric methods linked to Chap. 12 that deals with chemometric methods of data analysis to maximize the information contained in the measured data. The book ends with two chapters (Chaps. 13 and 14) on basic statistics and planning and validation of TLC analyses.

Our hope is that this book will demonstrate that quantitative planar chromatography is a practical alternative in liquid/solid and liquid /liquid separations. We hope that the liquid/solid separation method, which is TLC's strength, will thus find new friends. In 1987 Friedrich Geiss wrote in the preface of his book *Fundamentals of Thin Layer Chromatography* "TLC is here to stay". We believe indeed that TLC will consolidate its position in analytical chemistry. Taking the biological measurement techniques of Chap. 8 into account, we hope that TLC will even extend its range and position among separation methods.

Offenburg Detroit, MI Saarbrücken October 2010 Bernd Spangenberg Colin F. Poole Christel Weins

Acknowledgements

From my time in the industry, I personally remember the delighted expressions of laboratory staff looking at a nicely stained TLC plate. I remember in the mid-1980s that TLC was widely used for quantification purposes. I also remember that my technicians were always suspicious of TLC due to its non-linear calibration curves. It was difficult for them to accept that a doubling of the amount of substance did not result in a doubling of the measurement signal. All this was the reason for me to write a TLC book that helps to overcome this problem. I am indebted to the ladies of the Offenburg library who nearly instantly provided the desired papers for this book. I wish to thank Trisha Cornforth for her help in interpreting my German text into English, and I wish to thank my wife Marion and my daughter Johanna for their understanding and patience.

Offenburg October 2010 Bernd Spangenberg

Contents

1	Histo	ory of Planar Chromatography	1
	1.1	History of Paper Chromatography (PC)	1
	1.2	History of Thin-Layer Chromatography	7
	1.3	The History of Quantitative Planar Chromatography	8
	Refe	rences	10
2	The	oretical Basis of Thin Layer Chromatography (TLC)	13
	2.1	Planar and Column Chromatography	13
	2.2	TLC Capillary Flow	15
	2.3	TLC Distribution Equilibrium	18
		2.3.1 Adsorption Chromatography	18
		2.3.2 Partition Chromatography	20
	2.4	The Retardation Factor (R_f)	22
		2.4.1 The Empirical R_f Factor	22
		2.4.2 The Thermodynamic $R'_{\rm f}$ Factor	24
	2.5	Mobile Phase Composition	25
	2.6	Transfer of TLC Separations to Columns	27
	2.7	The $R_{\rm m}$ Value	28
	2.8	Temperature Dependence of TLC Separations	29
	2.9	Advanced Theoretical Considerations	30
	2.10	Indices Characterizing Separation and Resolution	37
	2.11	Zone Broadening in Planar Chromatography	40
		2.11.1 The <i>A</i> term	40
		2.11.2 The <i>B</i> term	41
		2.11.3 The <i>C</i> term	42
		2.11.4 Local Plate Height <i>H</i>	42
		2.11.5 The van Deemter Equation	43
	2.12	Optimum Separation Conditions in TLC	45
		Separation Number	47
	2.14	Real Plate Height	50
		rences	

x Contents

3	The Stationary Phase in Thin-Layer Chromatography	53
	3.1 Activating and Deactivating Stationary Phases	
	3.2 Snyder's Adsorption Model	55
	3.3 Layer Characteristics	
	3.3.1 Layer Thickness (d_f)	59
	3.3.2 Average Particle Size (d _p)	60
	3.3.3 Particle Size Distribution	60
	3.3.4 Specific Surface Area (O _s)	60
	3.3.5 Pore Volume (V_p)	61
	3.3.6 Average Pore diameter (P _d)	61
	3.4 The Most Important Stationary Phases in TLC	62
	3.4.1 Aluminium Oxide	62
	3.4.2 Magnesium Silicate	62
	3.4.3 Silica Gel	63
	3.4.4 Chemically Bonded Silica Gel Layers	66
	3.4.5 Kieselguhr	67
	3.4.6 Cellulose	68
	3.4.7 Polyamides	70
	3.4.8 Ion Exchange Resins	71
	3.4.9 Chiral Phases	72
	3.4.10 Layers with Fluorescent Indicators	73
	3.4.11 Making Your Own Plates	73
	3.5 Light Absorption on Plate Surfaces	74
	References	77
4	The Mobile Phase in Adsorption and Partition Chromatography	
	4.1 Solvent Characteristics	81
	4.2 Solvent Theory for Adsorption Chromatography	
	(According to Snyder)	
	4.2.1 Solvent Strength (ε^0)	
	4.2.2 Solvent Strength of Binary Mixtures	
	4.3 Solvent Theory in Partition Chromatography	
	4.3.1 Solvent Theory (According to Snyder)	
	4.3.2 Other Methods for Characterizing Solvents	
	4.4 Optimizing Solvent Composition	
	4.5 The PRISMA Model (According to Nyiredy)	
	4.6 Solvent Additives	
	4.7 Appendix: Solvent Properties	
	References	103
5	Preparing and Applying Samples	105
3	5.1 Sample Preparation	105
	5.1.1 The QuEChERS Approach	105
	5.1.2 Solid-Phase Extraction	105
	5.1.3 Stir Bar Sorptive Extraction	108
	2.1.2 3H Dai 901phyc Danacholl	100

Contents xi

	5.2	The Dosage Quality	108
		Choice of Application Position	112
		Practical Application Methods	113
		5.4.1 Sample Application via Plate Contact	113
		5.4.2 Sample Application Without Plate Contact	114
		5.4.3 Sample Application via Contact Spotting	114
		5.4.4 Plate Overloading and Incomplete Drying	116
		erences	117
6	Basi	is for TLC Development Techniques	119
	6.1	Influence of the Vapour Phase	119
	6.2	Chamber Types for Linear Development	123
		6.2.1 N-Chambers ("Trough Chambers")	123
		6.2.2 S-Chamber ("Small Chamber")	124
		6.2.3 Vario-KS-Chamber	125
		6.2.4 The H-Chamber ("Horizontal Chamber")	125
	6.3	Controlling Separations via the Vapour Phase	126
		6.3.1 Solvent Composition During Separation	126
		6.3.2 Plate Pre-loading via the Vapour Phase	130
	6.4	Circular Separations	133
	6.5	Solvent Gradients	134
		6.5.1 Theory of Solvent Gradients	134
		6.5.2 Evaporation-Controlled Gradient Elution	140
		6.5.3 Multiple Development in TLC	142
		6.5.4 Automated Multiple Development (AMD)	143
	6.6	Normal Phase Separations with Water-Containing Solvents	145
	6.7	Plate Development with Forced Flow	147
		6.7.1 Rotation Planar Chromatography (RPC)	147
		6.7.2 Over-pressure Layer Chromatography (OPLC)	147
	6.8	Two Dimensional TLC (2D TLC)	148
		6.8.1 Development in Orthogonal Directions	148
		6.8.2 Grafted TLC	149
		6.8.3 Stability Test and SRS Technique	151
	6.9	Drying the Plate	153
		erences	153
7		cific Staining Reactions	155
	7.1	Chemical Reactions Prior to Separation (Pre-chromatographic	
		Derivatization)	157
		7.1.1 Sample Enrichment by Pre-chromatographic	
		Derivatization	157
		7.1.2 Pre-chromatographic In Situ Derivatization	159
		7.1.3 Pre-chromatographic Staining	163
		7.1.4 Reagents in the Mobile Phase	167

xii Contents

	7.2	Post-chromatographic Reactions (Derivatization After	
		Development)	168
		7.2.1 Fluorescence Enhancer	170
		7.2.2 pH and Redox Indicators	171
		7.2.3 Universal Reagents (Charring Reagents)	172
		7.2.4 Aldehyde Reagents	173
		7.2.5 CH- and NH-Reacting Reagents	176
		7.2.6 Boron-Containing Reagents	180
		7.2.7 Alkaline Reagents	182
		7.2.8 Chloramine-T Reagent	183
		7.2.9 Diazotization Reactions	184
		7.2.10 Iodine-Starch and Wursters Reagents	185
		7.2.11 Reactions with Metal Reagents	187
		7.2.12 Reagents for Metal Cations	190
	7.3	Reactions via the Gas Phase	191
		7.3.1 Ammonium Bicarbonate Reagent	192
		7.3.2 Tin(IV) Chloride Reagent	192
		7.3.3 Formic Acid Reagent	193
		7.3.4 Hydrogen Chloride Reagent	193
		7.3.5 Trichloroacetic Acid Reagent	193
		7.3.6 Nitric Acid Reagent	194
	7.4	Thermal Treatment of TLC Plates	194
		Activity Analysis Using Chemical Reagents	194
		7.5.1 Folin–Ciocalteu Reagent	195
		7.5.2 Checking for Free Radical Scavenger Activity	
		Using DPPH Reagent	195
		7.5.3 Nucleophilic Reaction Ability	196
	Ref	erences	197
8	Bio	effective-Linked Analysis in Modern HPTLC	201
	8.1	Principle of the Method	202
		8.1.1 Contaminant Analysis in the Environment and Food	
		and the Principle of Bioactivity-Based Analysis	202
		8.1.2 Aims and Fundamental Aspects of Bioeffective-Linked	
		Analysis by Thin-Layer Chromatography	203
		8.1.3 HPTLC as a Method for Bioeffective-Linked Analysis	203
	8.2	General Rules for the Analysis of Bioeffective Compounds	205
	8.3	Enzyme Tests	206
		8.3.1 Urease-Inhibition Test for Heavy Metals	206
		8.3.2 Analysis Using Redox Enzymes	207
		8.3.3 The Detection of Cholinesterase Inhibitors	208
	8.4	Inhibition of Photosynthesis by Herbicides	216
		8.4.1 Reagent Preparation	216
		8.4.2 Hill Reaction	217
		8.4.3 Detection Using Algae	217

Contents xiii

	8.5 Detecting Bioeffective Compounds with Photobacteria	218
	8.5.1 Practical Use of Photobacteria	218
	8.5.2 Reaction Time Optimization	220
	8.5.3 Applications of Photobacteria	221
	8.6 Detection of Fungicidal- and Antibiotical-Active Substances	
	in Environmental Samples	222
	8.6.1 Determining Fungicides	222
	8.6.2 Screening of Pesticides in Food and Surface Water	
	8.6.3 Detection of Compounds by Antibiotic Activity	223
	8.7 Yeast Estrogen Screen	225
	References	227
9	Planar Chromatography Detectors	231
	9.1 Transmittance Measurements in Thin-Layer Chromatography	231
	9.1.1 The Lambert-Beer Law	232
	9.2 Reflectance Measurements in TLC and HPTLC	
	9.2.1 The Kubelka–Munk Equation	234
	9.2.2 Reflectance Measurements with a Diode-Array Scanner	237
	9.2.3 Spatial Resolution on the Plate	239
	9.2.4 Spectral Distribution on HPTLC Plates	240
	9.2.5 Spectral Evaluation Algorithm	
	9.2.6 Video-Densitometric Measurements	
	9.3 Infrared and Raman Detection in Thin-Layer Chromatography	247
	9.3.1 Analysis of Thin-Layer Chromatograms by Diffuse	
	Reflectance Infrared Fourier Transformation	247
	9.3.2 Analysis of Thin-Layer Chromatograms by Near-Infrared	
	FT-Raman Spectroscopy	248
	9.3.3 Analysis of Thin-Layer Chromatograms by Surface-Enhanced	
	Raman Scattering Spectrometry	249
	9.4 Mass Spectrometric Detection in TLC	
	9.4.1 Direct Plate Extraction (SSSP)	
	9.4.2 MALDI Techniques (MALDI-MS)	
	9.4.3 Atmospheric Pressure Mass Spectrometry	
	9.5 Thin-Layer Radiochromatography (TL-RC)	
	9.5.1 Direct Radioactivity Measurements on TLC Plates	
	9.5.2 Phosphor Imaging	
	References	257
10	· · · · · · · · · · · · · · · · · · ·	261
	10.1 The Lambert Cosine Law	261
	10.2 Theory of Diffuse Reflectance	263
	10.2.1 Special Case a: The Reversal Reflectance Formula	267
	10.2.2 Special Case b: The Fluorescence Formula	267
	10.2.3 Special Case c: The Kubelka–Munk Expression	268

xiv Contents

	10.3	Mass-Dependent Reflection	270
		Simplifying the Expression	274
		rences	274
	***	L MY O.Y	255
11		rescence in TLC Layers	277
		Theory of Fluorescence and Phosphorescence	277
		Fluorescence Enhancement	280
	11.3	Quantification in TLC by Fluorescence	282
		11.3.1 Low Sample Concentration Fluorescence in Light	
		Scattering Media	283
		11.3.2 High Sample Concentration Fluorescence in Light	
		Scattering Media	284
	11.4	Contour Plots for Fluorescence Evaluation	285
	11.5	TLC Plates Containing a Fluorescent Dye	285
	Refer	rences	288
10	CI	A HDWLC	200
12		nometrics in HPTLC	289
	12.1	Calculation of R _F Values	289
	12.2	Compound Identification Using UV–Visible and	
		Fluorescence Spectra	291
	12.3	Correlation Spectroscopy	293
		12.3.1 Theory of Correlation Spectroscopy	293
		12.3.2 Combination of R_F and UV–Visible Spectral	
		Library Search	296
		12.3.3 Zone Purity Check	296
	12.4	Selection of the Measurement Wavelength	298
	12.5	Statistical Photometric Error (Detector Variance)	301
		12.5.1 Reciprocal Model	301
		12.5.2 Absorbance Model	302
		12.5.3 Kubelka–Munk Model	303
		12.5.4 Fluorescence model	304
		12.5.5 Minimizing the Statistical Photometric Error	305
	12.6	Diode Bundling and Data Smoothing	305
	12.7	Signal Integration: Area or Height Evaluation?	307
	12.8	Deconvolution of Overlapping Peaks	308
	12.9	New Visualization Methods for Plots	310
	Refer	rences	313
13	Ctat!	otics for Quantitative TLC	315
13		stics for Quantitative TLC	315
	13.1		
	13.2	Variance and Precision	316
		13.2.1 Definition of Variance	316
		13.2.2 Relative Variance	318
		13.2.3 Quantification of Relative Variance	319

Contents xv

	13.3	Trueness, Precision, and Accuracy	320
	13.4	The Gauss Distribution	321
		13.4.1 Area of the Gauss Distribution	322
		13.4.2 Quantiles of the Gauss Distribution	322
		13.4.3 Test for a Normal Distribution	324
	13.5	Student's Distribution (<i>t</i> Distribution)	325
	13.6	Error Propagation	326
	13.7	Calibration Methods	328
		13.7.1 The Linear Calibration Function	329
		13.7.2 Estimating $\overline{X_C}$	330
		13.7.3 Estimating a and $\overline{Y_{\rm C}}$	331
		13.7.4 Estimating the variances of a and $\overline{Y_C}$	333
	13.8	The F-Test	334
	13.9	The Linear Regression Variance	334
		The Analytical Function of Linear Regression	335
		Quantitative Analysis Using External Standards	338
		Second-Order Calibration Function	339
		Analytical Function of the Second-Order Calibration	343
		Risk of Systematic Error	345
	13.14	13.14.1 Constant Systematic Error	345
		13.14.2 Proportional Systematic Error	345
	12 15	•	
		Use of Internal Standards	346
		Standard Addition Method	347
		Mean t Test	350 351
	Refer	ences	331
14	Dlann	sing on Analysis and Validation in TLC	353
14		ning an Analysis and Validation in TLC	
		Terms Used in Validation	353
		Method Validation	354
		14.2.1 Testing Specificity	354
		14.2.2 Quantifying Analytes	357
		14.2.3 General Aspects of Calibration	358
		14.2.4 Linearity and Working Range	359
		14.2.5 Choosing a Calibration Function	360
		14.2.6 External Standard Calculation	362
		14.2.7 Optimized Calibration Methods	362
		14.2.8 Precision	363
		14.2.9 Accuracy	364
		14.2.10 Confidence Interval	367
		14.2.11 Limit of Detection and Limit of Quantification	367
		14.2.12 Robustness	370
	14.3	Control Charts as Quality Indicators in Routine Analysis	372
	Refer	ences	373
Ind	ev		375

Chapter 1 History of Planar Chromatography

Generally speaking, spectroscopy and spectrometric methods such as infra-red (IR) spectroscopy and ultra-violet (UV) spectrophotometry are incapable of carrying out complete analysis of complicated mixtures. As a consequence, the individual substances must be separated from one another before spectrophotometric determination can take place.

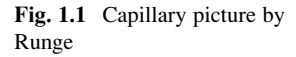
Chromatography is the term used to describe all separation methods, based on the distribution of compounds between two separate phases. In thin-layer chromatography (TLC), one phase is fixed on a plate (stationary phase) and the other phase is mobile and migrates through the stationary phase (mobile phase). During the chromatographic development process, the mixture to be separated is distributed between the stationary and mobile phases.

Paul Karrer had been involved in developing new identification methods for two decades before he spoke about them at the 1947 IUPAC Congress. During his main lecture he declared "... no other discovery has exerted as great an influence and widened the field of organic chemistry investigation as much as Michail Semenovich Tswett's chromatographic adsorption analysis" [1].

Indeed, modern analysis would be unthinkable without column and planar chromatography. In the long run, modern developments such as the reversed-phase (RP) technique or high-performance thin-layer chromatography (HPTLC) ensure that TLC is frequently used as a separation process [2].

1.1 History of Paper Chromatography (PC)

Writing his book *Libri naturalis historiae* in ancient Rome, Caius Plinius (Pliny the Elder) mentioned using papyrus impregnated with gall-apple extract to identify the addition of iron sulphate in verdigris (copper acetate) [1]. Plinius used papyrus to hold chemical substances where various reagents were mixed and brought to a reaction due to capillary flow in the papyrus. Thus papyrus was used to carry out

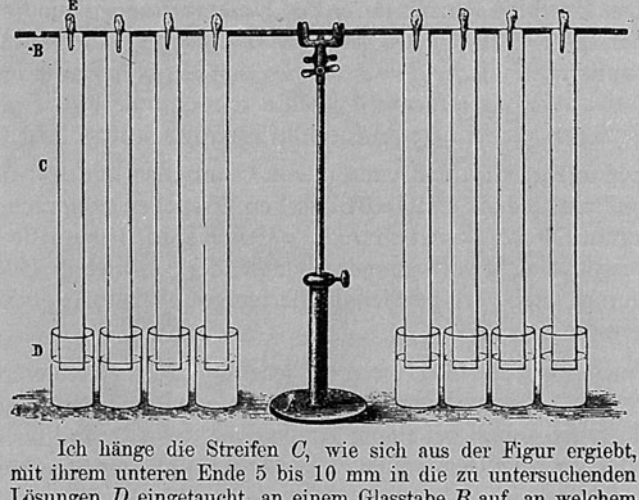




analysis but no substances were separated. The true origins of modern chromatography are of a more recent date. In 1850, Runge (1794–1867) first used paper to differentiate between colour dyes. Runge was the first to use "the power of the hairs in paper" to separate individual substances out of a mixture (Fig. 1.1). He wrote: "Due to the power of its hollow hairs, it (the paper) was capable of separating drops of liquid into component parts according to their individual fluidity, to form a picture with a dark centre and paler outer circles or completely non-coloured rings" [3].

Runge's book (German title *Bildungstrieb der Stoffe*) became famous for its colourful pictures and descriptions as active examples of the "living power in plants and animals". At the World Exhibition held in Paris in 1855, he was awarded a special medal for his book [4]. Like Plinius' paper analysis, Runge used various mixtures to see how they would react on paper [5]. Runge was the first person to deliberately use the characteristics of paper to separate substances, although similar work had been carried out during the same decade by Schönbein (1799–1868). The latter published his experiments in 1861, describing how he had cut unglued paper into strips and dipped them in dissolved dyes [5].

He noticed that the water from the dissolved dyes always moved through the fabric quicker than the dyes themselves and that various dyes moved at different speeds. Goppelsröder (1837–1919) later extended these experiments to kieselguhr and wood fibres. In 1906, a summary of his work concluded that paper manufactured by the company "Schleicher und Schüll", in Düren, Germany, showed the best results [6]. However, as he himself wrote in 1910 "Naturally such dyes cannot be



nit ihrem unteren Ende 5 bis 10 mm in die zu untersuchenden Lösungen D eingetaucht, an einem Glasstabe B auf, an welchem sie mit Hilfe jener hölzernen Klammern E festgehalten werden, wie sie zum Aufhängen der Wäsche in den Haushaltungen dienen. Ich lasse die Streifen je nach den Lösungsmitteln 15 Minuten bis ein oder mehrere Stunden, selbst bis 12 Stunden hängen. Nachher hebe ich sie aus den Flüssigkeiten heraus

Fig. 1.2 Separation on paper strips according to Goppelsröder [7]

completely separated from one another during the first capillary attempt" because "the lower layers still contain small residual amounts of those dyes which have mostly moved upward" [7, 8].

The deficiency of all the so-called frontal analysis separation publications up until then was that the solvent used for the sample and the mobile phase were identical. As Goppelsröder correctly observed, that meant each new separation needed a new sample solution, thus continually contaminating separated substance zones (Fig. 1.2).

Quite independently of Goppelsröder, Reed tried separating many dissolved salts by "selective absorption in bibulous paper". It is historically interesting to note that his article published in 1893 finishes with the statement: "I have obtained satisfactory results ... by using tubes containing powdered kaolin that had been slightly pressed down, on which the solution was placed and allowed to soak downwards" [9, 10].

It was the brilliant Russian botanist Tswett (1872–1919), born in Italy and educated in Switzerland, who actually discovered chromatography in 1903. He made the distinction between sample, mobile, and stationary phase, as well as the single application of a sample and the permanent effect of the mobile phase. He was the first to make a successful separation of leaf dyes by means of chromatography

columns [11–16]. Tswett used icing sugar, insulin, CaCO₃, aluminium oxide, and many other adsorbents as stationary phases. In 1906, he wrote:

"There is a definite adsorption sequence according to which the substances can displace each other. The following important application is based on this law. When a chlorophyll solution in petrol ether is filtered through the column of an adsorbent (I mainly use calcium carbonate which is tightly packed into a narrow glass tube), then the dyes will be separated according to their adsorption sequence from the top down in various coloured zones, as the more strongly adsorbed dyes displace the more weakly retained. This separation is practically complete if, after passing the dye solution through the adsorbent column, the latter is washed with pure solvent [13]".

This is the first description of placing a sample on the stationary phase, the effect of the (clean!) mobile phase on the sample, as well as the creation of substance zones and their broadening in the course of the elution. The genius of Tswett's discovery can be recognized by the fact that Goppelsröder had hung paper strips in hundreds of solutions for more than 40 years without making the obvious conclusion (as seen from today's point of view) that the paper strips should be further developed after immersion in clean solutions.

In the first of his three articles, published in 1906 in *Berichte der Deutschen Botanischen Gesellschaft* (Reports of the German Botanical Society) [13, 14], Tswett first mentioned the words "chromatogram" and "chromatography", both concepts he had devised himself (Fig. 1.3). He wrote:

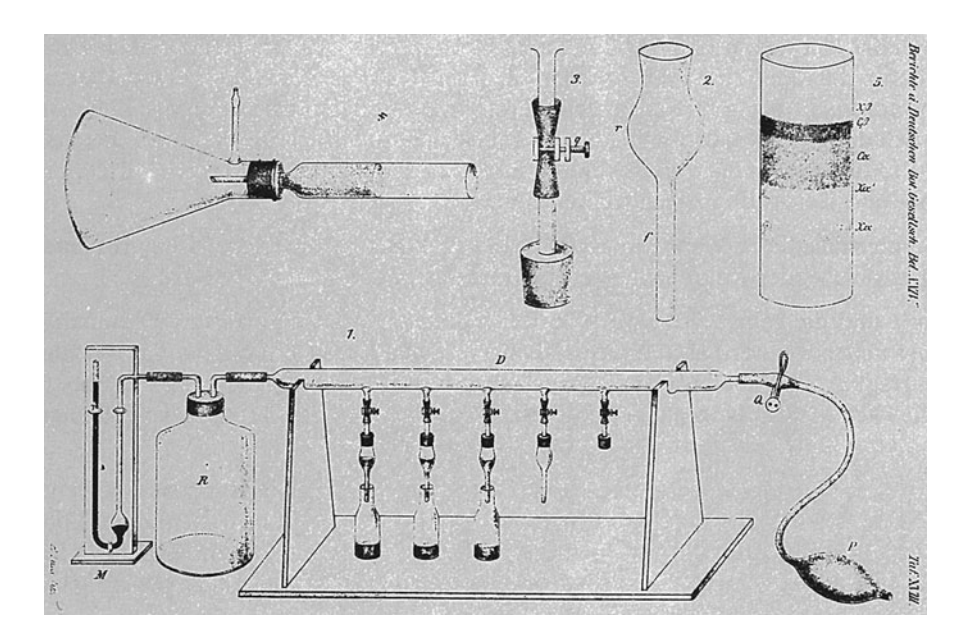


Fig. 1.3 Tswett's apparatus for column chromatography [14]. The small columns were activated by slight over-pressure. Shows chromatography carried out under pressure

"Like light rays in the spectrum, the different components of a dye mixture, obeying a law, are separated on the calcium carbonate column and can thus be qualitatively and quantitatively determined. I call such a preparation a chromatogram and the corresponding method the chromatographic method [13]".

Tswett associated the concept of "chromatography" with the literal translation of "colour description" and was convinced he had discovered a universally applicable method. He wrote [13]:

"Of course, the described adsorption phenomena are not only confined to chlorophyll dyes. It is to be assumed that all kinds of coloured or colourless chemical compounds are subject to the same laws. So far I have successfully examined lecithin, alkannin, prodigiosin, sudan, cyanin, solanorubin as well as acid derivates of chlorophylline".

Tswett listed over 100 substances he had tested for their adsorption capacities [13]. He definitely carried out his first experiments with filter paper although nowadays we cannot be sure whether Tswett really invented paper chromatography. However, the invention of chromatography as a separation method using filled columns can definitely be attributed to him, and he even recognized the method's full potential. In 1906, he wrote:

"Now the question can be proposed whether the chromatographic method can be raised to a chromatometric power. It would be desirable to express the quantities of dyes simply in volumes of adsorbent saturated by them. The experiments which I have performed to this end have thus far led to no satisfactory results [14]".

A further step on the way to modern TLC was the discovery of circular paper chromatography by Grüss in about 1908. Following on work by Goppelsröder, and in a similar way to Runge, Grüss dropped samples (mainly enzymes) onto the centre of a round filter paper. After the formation of rings, he added water to the centre of the paper, and a second water application caused complete separation of the substances. Grüss used colour-creating reagents to make colourless zones visible, using the name "chromogram" for the "rows of coloured sections lined up beside one another" [17].

Schönbein and Göppelsröder's work on "capillary analysis" was continued by Liesegang who went way ahead of his predecessors with a remarkable piece of work on 15 May 1943. He described his work under the title *Cross-Capillary Analysis*:

"A drop of a dye mix was left to dry on the corner of a sheet of filter paper about 20×20 cm in size. When water was allowed to soak through by a capillary process, the result was a narrow strip of colour. In contrast to normal capillary analysis, separating into individual colour strips is not usually as sharp as can be achieved by chromatographic analysis by subsequent development. Further separation can be achieved by drying the paper and again hanging it in the water so it rises perpendicularly to the first capillary direction. Moreover, the kind of polymerisation of individual dyes can thus be spatially separated by observing their mobility rate. The capillary rise of water can be replaced by organic fluids and the filter paper replaced by a gypsum plate, etc." [18]".

Because the Second World War was raging at the time, this extremely important advance in paper chromatography remained unrecognized and did not influence later researchers [19].

In 1930, Willstädter gave the only German translation of a Tswett dissertation (dated 1910) to Richard Kuhn (1900–1967). This led to a renaissance of Tswett's chromatographic methods in the 1930s. In 1938, Kuhn was awarded the Nobel Prize for his work on column chromatographic separations of carotenoids. His assistant Winterstein played an important role in disseminating information about "column adsorption chromatography" through numerous lectures and experimental demonstrations. This insured that the breakthrough in column adsorption chromatography was not lost this time around. It was also a 1933 Winterstein lecture at Cambridge that inspired Martin to carry out his first basic experiments in chromatography [1].

In the 1930s, Martin constructed large apparatuses to achieve "against the current extraction" to thus separate substances with similar chemical characteristics. Together with Synge, he explored this method of alternately shaking an extraction medium to separate amino acids. Much effort went into designing apparatuses to facilitate rapid equilibrium of both fluids. In retrospect, Martin wrote in 1975 [1]:

"I suddenly realized it was not necessary to move both liquids because the required conditions were fulfilled if I just moved one of them ... Synge and I took silica gel intended as a drying agent from a balance case, ground it up, sifted it and added water ... We put this mixture of silica gel and water into a column ... One foot of in this apparatus' tubing could do substantially better separations than all the machinery we had constructed until then".

Martin and Synge received the 1952 Nobel Prize for chemistry for their discovery of distribution chromatography.

Two years after his fundamental recognition of distribution chromatography, 1944, together with Consden and Gordon, Martin published a further variation of the chromatographic separation process. He named this method "a Partition Chromatographic Method Using Paper" [20]. The authors published an exact description of their simple apparatus:

"a strip of filter paper with the substances applied, with the upper end dipped in a trough filled with water-saturated medium. The filter paper was folded over the upper edge so that the solution could not be soaked up by capillarity. The whole experiment took place in the vapour-saturated atmosphere of a closed chamber".

This type of chromatography revolutionized chemical analysis, significantly facilitating the identification of amino acids derived from proteins. Previously, it required several years to analyse a protein, but this simple separation method shortened the work to a few days! By 1954 more than 4,000 publications had already been published on the subject of paper chromatography. As a contemporary scientist laconically remarked: "Paper chromatography is so widely used that it is impossible to make more than a rough estimate of its applications" [21].

1.2 History of Thin-Layer Chromatography

In 1889, Beyerinck published a separation of substances by diffusion in gelatine smeared on a glass plate [22]. However, this was a first attempt without further consequences to carry out planar chromatography with a stationary phase other than paper.

In 1938, encouraged by Tswett's work, Izmailov (1907–1961) and Shraiber (1904–1992) transferred the results of column chromatography to the so-called open columns. These researchers spread thin layers (about 2 mm) of various sorbents such as lime, magnesium oxide, or aluminium oxide on glass plates [23–26] and performed separations similar to those of Grüss.

In 1992, Shraiber described the discovery of TLC as follows:

"The use of column chromatography for the analysis of pharmaceutical samples took a lot of time. This limited the application of the method throughout pharmaceutical analysis. For this reason our thoughts and efforts were directed to studying opportunities for accelerating the separation process for complex samples [24, 25]".

Furthermore, *Shraiber* stated that the original idea for planar chromatography derived from Tswett. She wrote:

"Thin layer chromatographic adsorption analysis was elaborated as a result of a number of experiments based on the separation of a mixture of compounds into zones on a thin layer of adsorbent using one drop of sample. Developing M. S. Tswett's idea, it was demonstrated that the planar adsorbent layer is an analog of the chromatographic column [24–27]".

In 1949, Meinhardt and Hall introduced a significant technical improvement to "surface chromatography". They fixed the aluminium oxide sorbent onto a glass plate with starch as a binding agent [28]. This resulted in stable plates without splits. Kirchner Miller and Keller modified the method according to Meinhardt and Hall. They added the sorbent's zinc silicate and zinc cadmium sulphide as indicators to visualize UV absorbing compounds. Thus substances could be observed on the plate without dyeing or destroying them, under short-wavelength UV light (254 nm) as zones of reduced fluorescence. They named their coated glass strips "chromato strips" and used them for the separation of terpenes. They wrote: "Very unreactive compounds can be located by spraying with concentrated sulfuric—nitric acid mixture and heating to cause charring of the compounds". They came to the following conclusion: "Of the numerous adsorbents tested, silicic acid proved to be the best for terpenes" [29].

In 1954, Reitsema used glass plates (size $12.5 \text{ cm} \times 17.5 \text{ cm}$) coated with silica gel, naming them "chromato-plates". He achieved a high sample throughput by simultaneously applying and developing several samples [30].

TLC's essential breakthrough, both as an analytical separation method and in establishing its name, was the achievement of Stahl (1924–1986). From 1955 onwards he definitively standardized the separation technique and introduced it into routine analysis [31]. Stahl used 20×20 cm glass plates covered with various sorbents. He published his manual in 1962 and Randerath's book was dated the

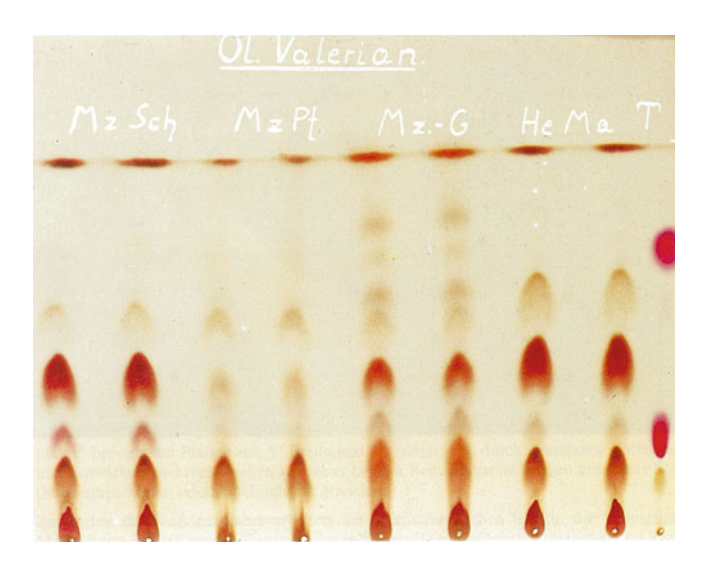


Fig. 1.4 One of the first TLC plates developed by Stahl in 1956 [1], showing a valerian oil separation. The plate was sprayed with SbCl₃ solution in CHCl₃ and subsequently heated

same year; both made the method world famous under the abbreviation "TLC" (Fig. 1.4) [32, 33].

The next improvements were made at the beginning of the 1970s by Kaiser at the Institute of Chromatography in Bad Dürkheim (Germany) [34]. He prepared silica gel plates without a binder using silica particles of a small size (5 µm) with a narrow size distribution. The separation time was decisively reduced from hours to minutes, while simultaneously improving resolution [34]. This led to the 1977 publication of Kaiser's book *HPTLC – High Performance Thin Layer Chromatography*, which facilitated the adoption of this improved technique [35].

In the middle of the 1970s, Halpaap at Merck (Darmstadt, Germany) invented the so-called high performance thin-layer chromatography (HPTLC) silica gel plates in 10×10 cm format and launched them on the market [36]. The RP-18-HPTLC plate arrived in 1980, followed by Jost and Hauck's amino plate in 1982, the Cyano HPTLC plate in 1985 and the Diol HPTLC plate in 1987 [37].

1.3 The History of Quantitative Planar Chromatography

In 1953, Cramer indicated various possibilities for obtaining quantitative results by means of paper chromatograms [38]. In 1954, a Merck company brochure noted:

"There is a proportional relationship between the size of the spot and the logarithm of the substance concentration. Therefore, if equal spot sizes of two solutions of the same substance are "chromatographed" and also result in spots of equal size, both solutions must contain equal concentrations (within an accuracy span of about 10%). The spot size

can also be determined in this way, so that solutions of various (known) concentrations can be chromatographed and compared with spots of an unknown solution concentration. The spot sizes can either be determined by measuring the surface area or by cutting out the spots and weighing them. Sports can also be evaluated by photometric means. The paper is made transparent by soaking it for five minutes in a mixture with equal parts of α -bromonaphthalene and liquid paraffin (DAB 6). After drying, the spots can be measured with the aid of a photo-electric detector" [39]".

It was also common practice to cut out zones from the layer and determine the amount of substance present by extraction with a micro-soxhlet apparatus as well as by a subsequent colorimetric concentration determination. In the early days of TLC, it was only possible to determine the contents by scratching off the spot and extracting the sample. Despite this primitive quantification method, Kirchner obtained an amazing average error of only 2.8% in 1954 [40].

In 1960, Hefendehl published a method for measuring thin-layer chromatograms without destroying them based on the transmission of light by the layer. He sprayed the thin-layer plate with a paraffin–ether solution (1+1, V/V) to make the plate transparent and then evaluated it by photographic means [41].

In 1963, Barrett and Dallas used TLC plates treated with sulphuric acid for charring. They used a chromo-scan densitometer and also recorded densitograms in the reflectance mode [42, 43].

In 1964, Jork (1933–1993) published the first densitogram measured in the reflectance mode from a stained TLC plate. He used a chromo-scan densitometer produced by the company *Joyce & Loeble* (Newcastle, England). By automatic integration of the peak areas, he obtained good reproducibility with errors less than 1% [43, 44].

After about 1964, quantitative TLC by spectrophotometry in the reflectance mode based on Jork's work became the accepted measurement method. Jork illuminated untreated TLC plates with monochromatic light and recorded the intensity of the light reflected by the plate, depending on its position and wavelength [43].

If a ray of light illuminates the TLC layer, each individual layer particle absorbs light. However, most of the light is scattered and reflected by the plate. This reflected light permits rapid and, most importantly, non-destructive quantification of the substance zones on the plate. The Zeiss KM2 spectrophotometer (that was adapted by Jork as KM3) was later capable of routinely measuring densitograms as well as spectra in the reflectance, transmittance, and fluorescence modes (Fig. 1.5) [45, 46].

The first successful quantitative measurements were carried out with a digital camera by Prosek and Kaiser in 1984 [36, 47]. At the beginning of the 1970s, Ebel had combined a TLC scanner capable of measuring light in the reflectance and transmittance modes with a desktop computer to control the plate photography, which was thus capable of evaluating the received reflectance data [48].

The first spectra of a light fibre TLC scanner in the range of 300–700 nm were published by Hamman and Martin [49]. The first combination of a TLC scanner with a diode-array detector (DAD detector) was published by Bayerbach and



Fig. 1.5 The first TLC scanner (ZR3), constructed by Jork for Zeiss, Germany [45]

Gauglitz in 1989 [50]. In 1998, J&M Company (Aalen, Germany) brought out the first diode-array light scanner for HPTLC plates [51]. For a complete overview of more than 50 years of TLC publications and instrumentation development, see [51].

References

- 1. Wintermeyer U (1989) Die Wurzeln der Chromatography. GIT, Darmstadt
- 2. Issaq HJ (ed) (2002) A century of separation science. Dekker, New York
- 3. Runge FF (1950) Farbenchemie III, Berlin, p 15
- 4. Bussemas HH, Harsch G, Ettre LS (1994) Friedlieb Ferdinand Runge (1794–1867): self-grown pictures as precursors of paper chromatography. Chromatographia 38:243–254
- Schönbein CF (1861) Ueber einige durch die Haarröhrchenanziehung des Papiers hervorgebrachten Separationswirkungen, Pogg Ann 24:275–280
- Goppelsröder F (1906) Anregung zum Studium der auf Capillaritäts- and Adsorptionserscheinungen beruhenden Capillaranalyse. Helbing & Lichtenhalm, Basel
- Goppelsröder F (1910) Capillaranalyse beruhend auf Capillaritäts- und Adsorptionserscheinungen. Steinkopff, Dresden
- 8. Ettre LS (2001) The pre-dawn of paper chromatography. Chromatographia 54:409-414
- 9. Reed L (1893) Notes on capillary separation of substances in solution. Chem News 67:261–264
- 10. Heines SV (1969) Three who pioneered in chromatography. J Chem Educ 46:315-316
- 11. Tswett MS (1905) Trudy Varshavskogo Obshchestva Estestvoispytatelei Otdelenie Biologii 14:20–39 English translation by Berezkin VG, [15]
- 12. Tswett M (1906) Zur Ultramikroskopie. Ber dtsch botan Ges 24:234-244
- Tswett M (1906) Physikalisch-chemische Studien über das Chlorophyll. Die Absorption. Ber dtsch botan Ges 24:316–323
- 14. Tswett M (1906) Adsorptionsanalyse and chromatographische Methode. Anwendung auf die Chemie des Chlorophylls. Ber dtsch botan Ges 24:384–393 English translation by Strain HH, Sherma J, Tswett M (1967) Adsorption analysis and chromatographic methods. Application to the chemistry of the chlorophylls. J Chem Edu 44:238–242
- 15. Berezkin VG (ed) (1990) Chromatographic adsorption analysis. Selected works of M.S. Tswett. Ellis Harwood, New York, pp 70–74

References 11

 Ettre LS, Sakodynskii KI (1993) M.S. Tswett and the discovery of chromatography I: early work (1899-1903). Chromatographia 35:223–231

- 17. Grüss J (1912) Biologie und Kapillaranalyse der Enzyme, Berlin
- 18. Liesegang RED (1943) Kreuz-Kapillaranalyse. Naturwissenschaften 31:348
- Ettre LS, Sakodynskii KI (1993) M.S. Tswett and the discovery of chromatography II: completion of the development of chromatography (1903-1910). Chromatographia 35:329–338
- Consden R, Gordon AH, Martin AJP (1944) Qualitative analysis of proteins: a partition chromatographic method using paper. J Biochem 38:224–232
- 21. Wilson ID (2000) The Chromatographic Society Communicator 3:12-17
- 22. Beyerinck MW (1889) Ein einfacher Diffusionsversuch. Z. Physik. Chem. 3:110-112
- 23. Izmailov NA, Shraiber MS (1936) Farmatsiya 3:1-7
- 24. Berezkin V (1995) The discovery of thin layer chromatography (foreword). J Planar Chromatogr 8:401–405, English translation of [23] and [25] by Izmailov NA, Shraiber MS. Spot chromatographic adsorption analysis and its application in pharmacy communication I:401–405
- 25. Shraiber MS (1972) In: Chmutov KV, Sakodynsky KI (eds) Uspekhi Khromatografii (Advances in chromatography), Nauka, Moscow, pp 31–32
- Shostenko YuV, Georgievskii VP, Levin MG (2000) History of the discovery of thin-layer chromatography. J Anal Chem 55:904–905
- 27. Berezkin VG, Dzido TH (2008) Discovery of thin layer chromatography by N.A. Izmailov and M.S. Shraiber. J Planar Chromatogr 21:399–403
- 28. Meinhard JE, Hall NF (1949) Surface chromatography. Anal Chem 21:185-188
- 29. Kirchner JG, Miller JM, Keller GJ (1951) Separation and identification of some terpenes by a new chromatographic technique. Anal Chem 23:420–425
- 30. Reitsema RH (1954) Characterisation of essential oils by chromatography. Anal Chem 26:960–963
- 31. Stahl E, Schröter G, Renz R (1956) Dünnschicht-Chromatographie, Pharmazie 11:633-637
- 32. Stahl E (1962) Dünnschicht-Chromatographie. Springer, Berlin
- 33. Randerath K (1962) Dünnschicht-Chromatographie, Chemie, Weinheim
- 34. Kreuzig F (1998) The history of planar chromatography. J Planar Chromatogr 11:322-324
- 35. Zlatkis A, Kaiser RE (1977) HPTLC high performance thin-layer chromatography. Elsevier, Amsterdam
- 36. Ripphahn R, Halpaap H (1975) Quantitation in high-performance micro-thin-layer chromatography. J Chromatogr 112:81–96
- Wall PE (2005) Thin-layer chromatography. A modern practical approach. RSC chromatography monographs. RSC, Cambridge
- 38. Cramer F (1953) Papierchromatographie 2. Aufl. Chemie, Weinheim, pp 36–37, 63–68
- 39. Säulen Chromatographie, Papierchromatographie, Merck Darmstadt 1954
- 40. Kirchner JG, Miller JM, Rice RG (1951) Quantitative determination of bi-phenyl in citrus fruits and fruit products by means of chromatostrips. J Agric Food Chem 2:1031–1033
- 41. Hefendehl FW (1960) Dokumentation and quantitative Auswertung von Dünnschicht-Chromatogrammen. Planta Med 8:65–70
- 42. Barrett CB, Dallas MSJ, Pudley FB (1963) The quantitative analysis of triglyceride mixtures by thin layer chromatography on silica impregnated with silver nitrate. Am Oil Chem Soc 40:580–584
- 43. Touchstone JC, Sherma J (1979) Densitometry in thin layer chromatography. Wiley, New York
- Jork H (1963) Dünnschicht-Chromatographie zur Kennzeichnung natürlich vorkommender Harze and Balsame, Deutsch. Apotheker-Zeitung 102:1263–1267
- 45. Jork A (1966) Direkte spektralphotometrische Auswertung von Dünnschicht-Chromatogrammen im UV-Bereich. Z Anal Chem 221:17–33
- 46. Jork H (1968) Die direkte quantitative dünnschicht-chromatographische Analyse. Fresenius Anal Chem 234:311–326

- 47. Prosek M, Medija A, Katic M, Kaiser RE (1984) Quantitative evaluation of TLC. Part 7: scanning with micro D-cam. CAL 4:249–251
- 48. Ebel S, Herold G, Kocke J (1975) Quantitative evaluation of thin-layer chromatograms: multicomponent analysis from calibration curves and by internal standard. Chromatographia 8:569–572
- 49. Hamman BL, Martin MM (1966) A versatile spectrophotometric scanner for large TLC plates. Anal Biochem 15:305–312
- 50. Bayerbach S, Gauglitz G (1989) Spectral detection in thin-layer chromatography by linear photodiode array spectrometry. Fresenius Z Anal Chem 335:370–374
- 51. Sherma J, Morlock G (2008) Chronology of thin layer chromatography with focus on the instrumental progress. J Planar Chromatogr 21:471–477

Chapter 2 Theoretical Basis of Thin Layer Chromatography (TLC)

2.1 Planar and Column Chromatography

In column chromatography a defined sample amount is injected into a flowing mobile phase. The mix of sample and mobile phase then migrates through the column. If the separation conditions are arranged such that the migration rate of the sample components is different then a separation is obtained. Often a target compound (analyte) has to be separated from all other compounds present in the sample, in which case it is merely sufficient to choose conditions where the analyte migration rate is different from all other compounds. In a properly selected system, all the compounds will leave the column one after the other and then move through the detector. Their signals, therefore, are registered in sequential order as a chromatogram. Column chromatographic methods always work in sequence. When the sample is injected, chromatographic separation occurs and is measured. This type of chromatography is known as "Online Chromatography".

The different column chromatographic methods can be distinguished by their phase systems. Gas chromatography uses an inert gas such as nitrogen or helium as the mobile phase. In liquid chromatography the mobile phase is a liquid with a constant or varied composition altered during the separation process. A separation employing a constant mobile phase composition is known as an isocratic separation. If the mobile phase composition is varied during the separation this is called a *gradient* separation. A pump is used to move the mobile phase through the column at a suitable velocity. Separations are optimized by first selecting a suitable column and then varying the mobile phase composition to achieve the desired resolution in an acceptable time.

For planar separations like TLC, different samples are usually applied to the stationary phase before it is contacted by the mobile phase which begins to migrate through it in a definite direction. The movement of the mobile phase through the stationary phase is referred to as the development step. After development the mobile phase is removed by evaporation and detection is performed in the

stationary phase. The record of the detector response plotted against the separation distance is called a densitogram.

Separations by planar chromatography occur in parallel in contrast to the sequential approach of column chromatography. This situation has advantages and disadvantages: a sequential process like column chromatography facilitates automation in which a fixed protocol is commonly employed for a batch of samples.

Planar chromatographic separations are more flexible but not easily automated, and the sequence of manual steps commonly used makes validation of the method more difficult and has led, for instance, to the fact that the pharmaceutical industry hardly ever uses planar chromatography to check medicinal products (Fig. 2.1).

Another important difference between planar chromatography and column chromatography lies in a more flexible use of the stationary phase. A new stationary phase is needed for each separation in planar chromatography, thus preventing any cross-contamination from one sample to another. Thus even heavily contaminated samples can be applied to the stationary phase without sample cleanup. Sample components are not usually overlooked during detection because the whole separation can be scanned. Column chromatography only measures those substances that leave the

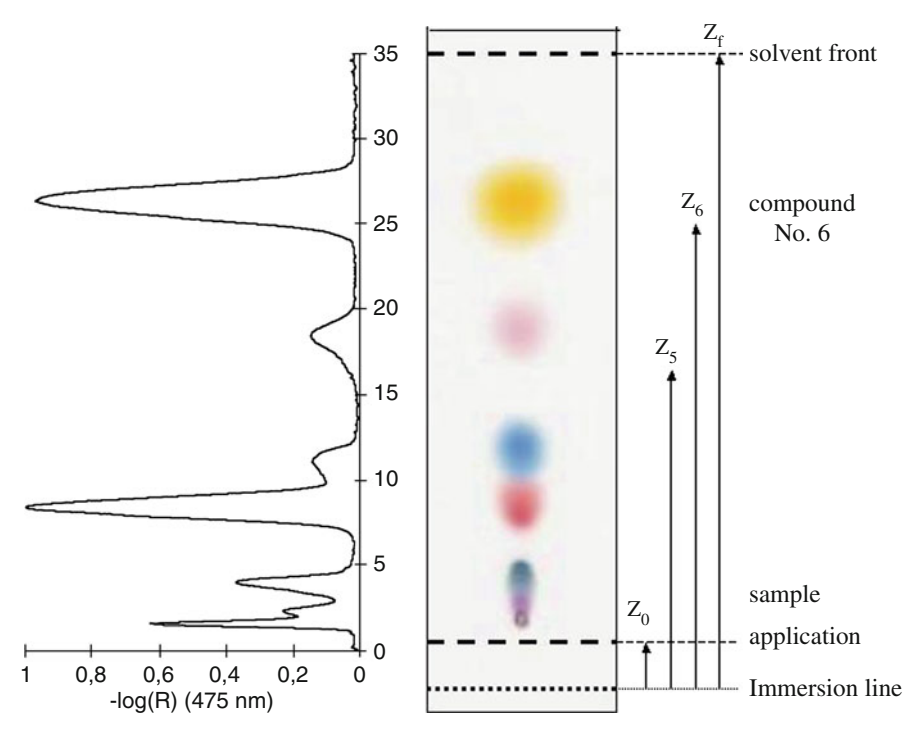


Fig. 2.1 Separation of six dyes (CAMAG III mix, no. 032.8003), with the relevant densitogram, on a SiO_2 plate, developed with toluene. With increasing R_f values: Ciba F-II (*violet*), indophenol (*indigo blue*), ariabel red (*red*), sudan blue II (*blue*), sudan IV (*scarlet red*) and (6) N,N-dimethylaminobenzene (*yellow*)

column. Those that remain on the column may be easily overlooked. It is also difficult to observe decomposition on the column during the separation process.

A significant difference between the two separation methods lies in the method of detection. In column chromatography, the sample is determined in the mobile phase and this restricts the number of useable liquids. Liquid chromatography is dominated by reversed-phase separations in which 90% or so of the separations employ a mobile phase consisting of acetonitrile or methanol in water or an aqueous buffer. In TLC, the mobile phase is removed before detection, so it cannot interfere with the measurements. On the other hand, detection is now performed in the stationary phase, which is an opaque medium, leading to its own compromises with the manner in which detection is facilitated or hindered.

In principle, column and planar chromatographic processes represent different separation methods, each with its own strengths and weaknesses. Many people see non-existent rivalry between TLC and HPLC, but both methods can be applied as appropriate because they complement each other.

2.2 TLC Capillary Flow

The significant difference between HPLC and TLC lies in the way the mobile phase permeates the stationary phase. In HPLC, a pressure gradient imposed along the column is responsible for the flow of mobile phase, but in classical TLC the mobile phase moves through the layer by capillary forces. In TLC textbooks many variations of the classical TLC approach are described [1–11]. These include a whole series of processes in which the flow is forced through the layer and referred to collectively as forced-flow methods. If the mobile phase flow is maintained through the layer by placing an electric field across the layer the method is referred to as electro-planar chromatography (EPC). Analogous to HPLC the layer can be sealed at the normally open surface and pressure used to drive the mobile phase through the layer by a series of methods collectively referred to as overpressure layer chromatography or optimum performance laminar chromatography (OPLC). There are also additional methods like rotation planar chromatography (RPC), where the mobile phase flow is induced by centrifugal force. All the abovementioned methods will not be further discussed here, as we will concentrate on classical TLC methods, where capillary forces control the flow of mobile phase.

In TLC, the porous stationary phase can be modelled as a bundle of extremely fine capillaries, whereby the mobile phase cohesion is distinctively superior to the capillary wall adhesion. The surface tension of the mobile phase is thus noticeably reduced, creating a pressure difference that propels the liquid through the capillaries. This type of mobile phase flow in TLC is known as *capillary TLC*, to distinguish it from *forced-flow TLC*.

The upward flow of the mobile phase comes to a standstill in a vertical chamber when the static counter-pressure caused by the rising fluid equals the surface tension forces. During development in a horizontal chamber, it is only the increasing friction force that brings the capillary flow to a stop after a while. In the case of a dipped TLC plate, the position of the solvent front moves rapidly at first and then gradually slows down. The total distance (Z_f) that the front moves is a square root function of time:

$$Z_f = \sqrt{\chi t}. (2.1)$$

The proportionality factor χ is known as the flow constant. This relationship expresses the fact that the capillary flow is not constant. This relationship is not valid when the mobile phase evaporates from the layer surface or condenses from the vapour phase. In developing chambers with a large gas volume, this is invariably the case. The adsorption and desorption of the mobile phase components by the layer then vary in a complicated way. To obtain reproducible mobile phase migration, it is important to use developing chambers with as little gas space as possible. In larger chambers, the evaporation of the mobile phase can be effectively suppressed by saturating the gas space with the mobile phase before developing the TLC plate.

The following expression for the flow constant takes into consideration both the internal friction caused by the capillary flow and the static counter-pressure from the rising mobile phase, but not vapour exchange [6,11,12]:

$$\chi = 2k_0 d_p \frac{\gamma}{\eta} \cos \vartheta \tag{2.2}$$

with

 k_0 permeability constant $k_0 = 6-8 \times 10^{-3}$

 $d_{\rm p}$ the average particle size of the stationary phase

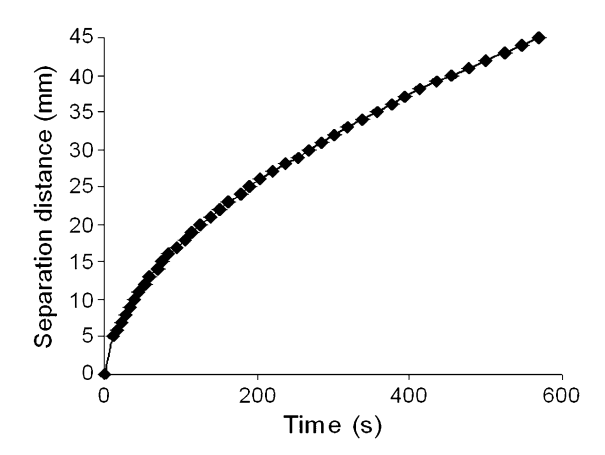
 η viscosity of the mobile phase surface tension (permeability)

 $\cos \vartheta$ cosine of the wetting angle ϑ

The higher the viscosity η and the lower the surface tension γ of the mobile phase, the slower the front will move (Fig. 2.2). The viscosity and surface tension quotient is referred to as the permeation factor. The permeation factor provides a standard measure of the mobile phase front velocity. The greater the permeation factor, the faster the mobile phase will flow through the layer. The permeation factor for di-isopropyl ether is 9.1, while for 1-propanol it is 1.05. Di-isopropyl ether migrates three times faster than 1-propanol:

$$(Z_{\rm f})^2 = \left(2k_0 d_{\rm p} \frac{\gamma}{\eta} \cos \vartheta\right) t. \tag{2.3}$$

Fig. 2.2 Solvent front velocity for methanol in a horizontal developing chamber (NH₂ plate)



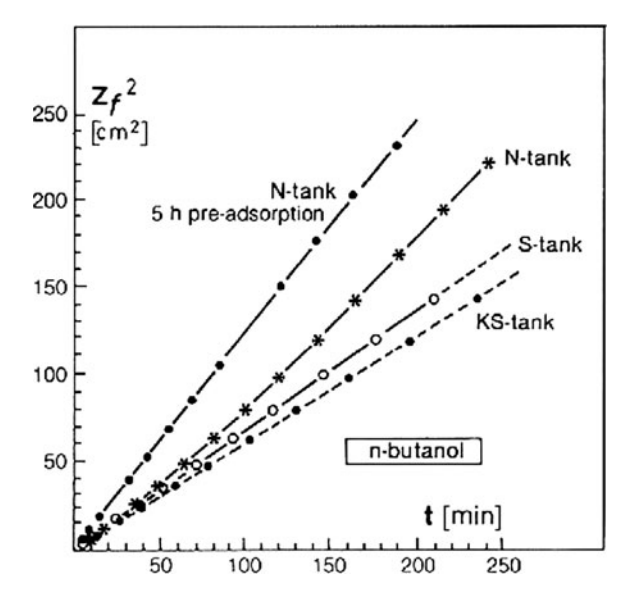


Fig. 2.3 Plot of the separation distance squared $Z_{\rm f}^2$ for various mobile phases against the time for development (From [6] with permission. © Hüthig.)

There is little difference in the time required for development between a horizontal and a vertical plate. If the development distance Z_f is measured at various intervals and plotted as (Z_f^2) against time, the results form a series of straight lines (Fig. 2.3).

For a low polarity mobile phase, the cosine of the contact angle is usually about one and can therefore be neglected in the above relationship. This is not the case for chemically bonded layers like RP-18 where the cosine of the contact angle can be reduced to zero in extreme cases. When the layer is no longer wet by the mobile

phase, capillary forces are inadequate for flow, but this may be reversed if a surfactant is added to an aqueous mobile phase [6]. Equation (2.3) indicates a lower flow rate for layers prepared from smaller particles. The front moves a shorter distance per time unit. Development on HPTLC plates with an average particle size $d_{\rm p} < 10~\mu{\rm m}$ takes longer than for TLC plates with mean particle diameters of about 40 $\mu{\rm m}$.

2.3 TLC Distribution Equilibrium

After the samples are applied to a TLC plate, the plate is placed in contact with the mobile phase and its development begins. During development, the substances applied to the plate are distributed between two distinct phases, the stationary and the mobile phases. The sample components interact with both the stationary and mobile phases according to whether the mechanism is dominated by adsorption or absorption process. In the first case the mechanism is called adsorption chromatography and in the second case partition chromatography.

2.3.1 Adsorption Chromatography

Adsorption is a characteristic property of surfaces, particularly solid surfaces. Adsorption in TLC occurs at the surface of the particles of the stationary phase, which are in contact with the mobile phase. The forces involved in adsorption processes are van der Waal's forces, dipole-type interactions, and complexation interactions like hydrogen bonding.

For chromatographic separations, the adsorption process must be reversible and only involves physical interactions. On inorganic oxide layers the more polar groups a compound has the stronger it is adsorbed. A compound's structure and the system temperature also play a role in adsorption. Steric factors affect the extent of interactions with active sites on the surface of the layer and higher temperatures tend to weaken polar interactions in general due to the greater motion of the adsorbed species.

The balance of adsorption interactions at a constant temperature depends only on the solute concentration at the adsorbent surface and its concentration in the mobile phase. The ratio of the equilibrium concentration of a substance in the stationary and the mobile phases is the distribution coefficient K for adsorption chromatography, also known as the repartition coefficient [6]:

$$K = \frac{c_{\rm S}[g/g]}{c_{\rm m}[g/{\rm cm}^3]},$$

where

K repartition coefficient (dimension g/cm³)

 $c_{\rm S}$ substance concentration in the stationary phase

 $c_{\rm m}$ substance concentration in the mobile phase

The repartition coefficient has the dimension of cm³/g [6].

When the solute concentration in the sorbing phase logarithmically decreases with its concentration in the mobile phase, the situation is described as an isotherm according to Feundlich. If there is a linear relationship between the amount of adsorbed substance and the concentration in the liquid phase, and if it shows a saturation effect as all adsorption centres are covered, this is described as a Langmuir isotherm. Both processes result in concave adsorption isotherms.

It really does not matter what the relationship looks like, the important aspect is to work in the linear region of the isotherm, which will produce Gaussian-shaped peaks. Asymmetric zones will result at higher concentrations, in the range of the curved relationship. The stationary phase is overloaded here, so the mobile phase cannot bind more solute in spite of an increasing concentration. Non-adsorbed solute will migrate through the stationary phase faster than expected, a phenomenon known as "tailing" because the substance trails a line behind it like a tail (Fig. 2.4).

In the concave region of the adsorption isotherm, more of the substance is adsorbed by the stationary phase than in the linear region of the isotherm. This case is described as "fronting". In adsorption chromatography, the stationary phase generally consists of silica gel, aluminium oxide, kieselguhr, or magnesium silicate.

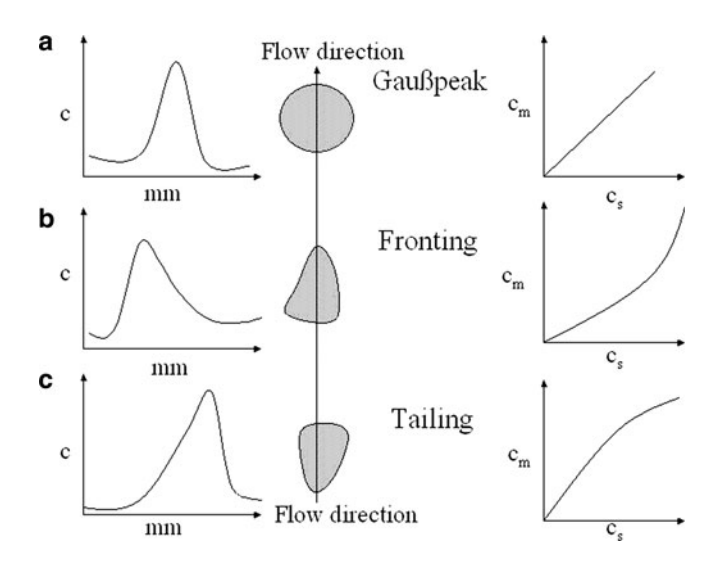


Fig. 2.4 Representation of the relationship between spot shape and the sorption isotherm. (a) Gaussian profile, (b) fronting, and (c) tailing [9]

These substances are all polar and can easily store water in an activated condition. Such phases can be desiccated by heating, thus releasing and reactivating the active sites of the stationary phase. In return, water effectively de-activates the stationary phase. In adsorption chromatography, adsorption of water quickly leads to phase over load, explaining why a small amount of water can lead to a significant alteration in retention behaviour during adsorption chromatography.

2.3.2 Partition Chromatography

In the middle of the 1930s, Martin developed an apparatus for counter-current extraction, to separate substance with similar properties by distributing them between two immiscible solvents. Working with Synge in 1940, he noticed that the separation of mixtures could be carried out when merely one liquid was immobilized and the other flowed over it. Martin and Synge saturated silica gel with water and allowed chloroform to flow through this stationary phase. In this way, they were able to separate very similar substances from one another. Similar to silica gel, cellulose, kieselguhr, and aluminium oxide can adsorb water and thus act as the stationary phase in partition chromatography. The sample is distributed between water and the organic mobile phase according to Nernst's distribution law. From this observation it is only a small step to paper chromatography, where the stationary phase consists of water immobilized by cellulose. The concept of paper chromatography was published by both researchers in 1943.

In partition chromatography, separation depends on the relative solubility of the sample components in two immiscible solvents brought into contact with each other according to the Nernst's distribution law:

$$K = \frac{c_{\rm S}}{c_{\rm m}} = \frac{V_{\rm m} m_{\rm S}}{V_{\rm S} m_{\rm m}}.$$

Here,

K partition coefficient (dimensionless) $c_{\rm S}$ substance concentration in the stationary phase $c_{\rm m}$ substance concentration in the mobile phase $V_{\rm S,m}$ volume of the stationary or mobile phase substance mass in the stationary or mobile phase

Nernst's law indicates that the quotient between the concentration of each substance in the mobile phase $(c_{\rm m})$ and the stationary phase $(c_{\rm s})$ at a given temperature is a constant, the so-called partition coefficient. The above-mentioned mass dependence of the partition coefficients is a result of the concentration definition:

$$c = \frac{n}{V} = \frac{m/M}{V},$$

where

n substance amountM molar mass

Because a substance is distributed between the mobile and stationary phases, the substance amount n can also stand for mass m. In reality, the partition coefficient K is independent of the total substance concentration resulting in a linear isotherm. This type of distribution is called a Nernst function. However, if dissociation or association occurs in either phase, such as acid/base proton transfer or complex formation resulting in a convex or concave deviation from a Nernst distribution, then tailing or fronting zones are observed in planar partition chromatography. Thus the range from K = 1 to K = 10 is ideal for partition chromatography.

The dominant features in adsorption chromatography are the surface phenomena, and in partition chromatography the decisive role is played by the distribution between the two liquid phases. Therefore, in adsorption chromatography, the type, position, and number of the solute's functional groups control the separation, while the solute's overall polarity plays the same role in partition chromatography. However, there are no absolutely distinct differences between the two methods. For example, liquid-coated silica gel phases can have unoccupied adsorption sites, which can act as adsorption centres. In the so-called "end-capped" phases, adsorption-active centres are partially blocked by chemical reactions. For example, cellulose phases work by using surface-bound water as the stationary phase. If a dry cellulose layer is used for a separation, the cellulose primarily serves as an adsorption phase and thereby desiccates the mobile phase. Thus amino acids on a dry cellulose layer may be well separated in the first separation section but then "smeared" in the second. This is because the water required for the formation of the stationary phase is no longer available from the mobile phase. Chemically bonded aminopropyl phases behave like hydrophilic distribution phases. An acid mobile phase protonates the NH₂ groups, forming cationic centres. This modified stationary phase then acts as a surface-active ion exchanger.

Chemically bonded cyanopropyl layers show particularly ambivalent properties with respect to the retention mechanism. Separations by adsorption chromatography are observed with low polarity mobile phases. With mobile phases containing water the retention mechanism changes to reversed-phase partition chromatography. Due to this ambivalent behaviour, cyanopropyl layers are particularly appropriate for 2D separations (Fig. 2.5).

Whether partition or adsorption chromatography is involved in the final separation is of less importance. The vital question is whether the separation can be reliably reproduced. Densitograms with symmetrical peaks verify that the separation occurs in the linear region of the isotherm where acceptable reproducibility can be expected.

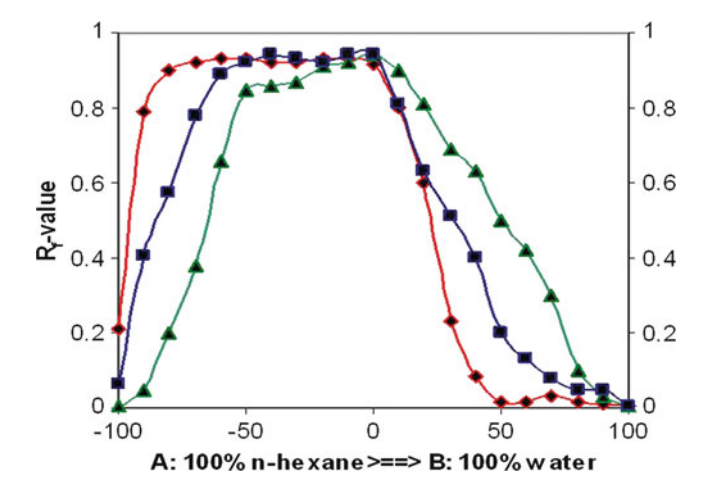


Fig. 2.5 Separation behaviour of steroids on a chemically bonded cyanopropyl layer, under adsorption conditions (**a**) and reversed-phase partition conditions (**b**). The labelling of the *x*-axis refers to percent composition with acetone [Source: Merck, with permission.]

Thus, a distribution value can always be calculated in the case of symmetrical peaks; it is irrelevant whether this is attributed to partition or adsorption chromatography. The best way of defining this distribution value is via the mass of a substance found in the stationary phase (m_s) and the mobile phase (m_m) :

$$k = \frac{n_{\rm S}}{n_{\rm m}} = \frac{m_{\rm S}}{m_{\rm m}} = K \frac{V_{\rm S}}{V_{\rm m}}.$$
 (2.4)

The distribution expression *k* is called the retention factor and is connected to the distribution coefficient via the phase ratio for the system.

2.4 The Retardation Factor (R_f)

2.4.1 The Empirical R_f Factor

The $R_{\rm f}$ factor is used for the qualitative evaluation of a TLC separation. It is the quotient of the distance of the substance zone from the sample origin to the front of the mobile phase $(z_{\rm f})$. Historically, Goppelsröder was the first person to use this $R_{\rm f}$ value (relation to front expression) to characterize planar separations:

$$R_{\rm f} \equiv \frac{z_{\rm s}}{z_{\rm f} - z_{\rm 0}},\tag{2.5}$$

where

- $z_{\rm s}$ distance of the substance zone from the sample origin (mm)
- $z_{\rm f}$ solvent front migration distance (mm)
- z_0 distance between immersion line and sample origin (mm)

By definition, the $R_{\rm f}$ value cannot exceed 1. To avoid the decimal point, the $R_{\rm f}$ value is sometimes multiplied by 100 and then described as the $hR_{\rm f}$ value. The value of the retardation factor in a given separation system at constant temperature depends entirely on the characteristic properties of the separated substances. It is important for identification purposes that $R_{\rm f}$ values are accurate and reproducible, but this is difficult to achieve, since it is almost impossible to adequately control all the experimental conditions that influence the separation process (Fig. 2.6).

This problem is avoided by defining a retardation factor for a standard substance (R_{st}) that has been already separated in the system:

$$R_{\rm st} = \frac{z_{\rm s}}{z_{\rm st}}.$$

Here,

- $z_{\rm s}$ distance of the substance zone from the sample origin (mm)
- $z_{\rm st}$ distance of the standard substance zone from the sample origin (mm)

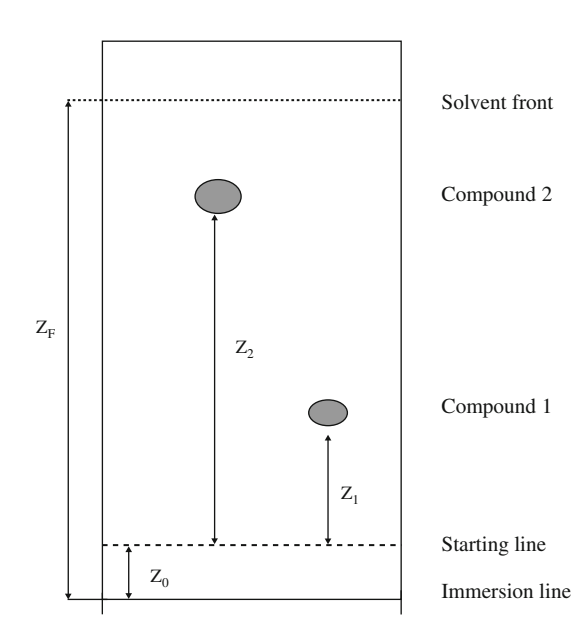


Fig. 2.6 Calculation of $R_{\rm f}$ values

2.4.2 The Thermodynamic R'_{f} Factor

While only an empirical $R_{\rm f}$ value can be provided from a densitogram, the thermodynamic $R_{\rm f}'$ value (also known as the true $R_{\rm f}$ value) correctly represents the behaviour of the substance in the separation system. The thermodynamic $R_{\rm f}'$ value is defined as the fraction of time the analyte is dissolved in the mobile phase $(t_{\rm m})$ in relation to the total development time $(t_{\rm ms})$:

$$R_{\rm f}' = \frac{t_{\rm m}}{t_{\rm m} + t_{\rm S}}.$$

Here,

 $t_{\rm m}$ time analyte is dissolved in the mobile phase $t_{\rm s}$ time analyte is associated with the stationary phase

The relationship between the mass of the substance in the mobile and stationary phases is independent of time. Assuming a constant distribution between phases, the mass distribution for an analyte is described by

$$R_{\rm f}' = \frac{m_{\rm m}}{m_{\rm m} + m_{\rm S}},$$

where

 $m_{\rm m}$ sample mass in the mobile phase $m_{\rm s}$ sample mass in the stationary phase

Reverting to a concentration definition (c=n/V=m/MV), it follows that

$$R_{\mathrm{f}'} = \frac{c_{\mathrm{m}}V_{\mathrm{m}}}{c_{\mathrm{m}}V_{\mathrm{m}} + c_{\mathrm{S}}V_{\mathrm{S}}} = \frac{V_{\mathrm{m}}}{V_{\mathrm{m}} + \frac{c_{\mathrm{S}}}{c_{\mathrm{m}}}V_{\mathrm{S}}},$$

where

 $c_{S,m}$ sample concentrations in the stationary or mobile phase (mol/L) $V_{S,m}$ mobile or stationary phase volumes (L)

If the partition coefficient relationship is applied to this equation, the result is called the *Martin–Synge* equation:

$$R_{\rm f}' = \frac{1}{1 + K \frac{V_{\rm S}}{V_{\rm m}}} = \frac{1}{1 + k}.$$
 (2.6)

Here,

K partition coefficient*k* retention factor

The empirically measured R_f values are only identical with the thermodynamic R_f' values if one of the following conditions can be applied:

- If the phase ratio remains constant for the whole layer
- If the mobile phase composition does not change during development
- If the stationary phase is free of solvent prior to development
- If the solvent front velocity is the same as the mobile phase velocity at the spot position

But these conditions are never fulfilled in the real world. Therefore the observed $R_{\rm f}$ value will always be smaller than the "true" or thermodynamic $R_{\rm f}'$ value. $R_{\rm f}$ values ranging from 62 to 100% of the thermodynamic $R_{\rm f}'$ values are quoted in the relevant literature. A reasonable approximation for the thermodynamic $R_{\rm f}'$ value is obtained by multiplying the observed $R_{\rm f}$ value by 1.1. Moreover, here the $R_{\rm f}$ value is used without differentiating between the "measured" or "thermodynamic" values. If not mentioned further, the abbreviation $R_{\rm f}$ is taken to mean a correctly measured $R_{\rm f}$ value identical with the thermodynamic value.

2.5 Mobile Phase Composition

The mobile phase composition is rarely constant over the whole separation distance. Some deviations are nearly always observed near the sample origin and the solvent front. Therefore only use measured $R_{\rm f}$ values in the range 0.05–0.9 when selective solvation of the stationary phase leading to demixing is not a problem.

The observed distribution of the components of a ternary mobile phase mixture on a silica gel layer is shown in Fig. 2.7. The mobile phase consists of low polarity mesitylene and polar benzyl alcohol (mixed with ethyl acetate). At a 40 mm separation distance the mesitylene front gradient can be observed with a decrease in the concentration of benzyl alcohol. The explanation is simple. The relative concentration of mesitylene in the mobile phase is increased at the expense of the benzyl alcohol; the more polar benzyl alcohol is selectively adsorbed by active sites on the silica gel layer. Mesitylene, less strongly adsorbed by silica gel, is enriched in the mobile phase and forms a gradient at the solvent front. This illustrates an important feature of separations employing the development mode:

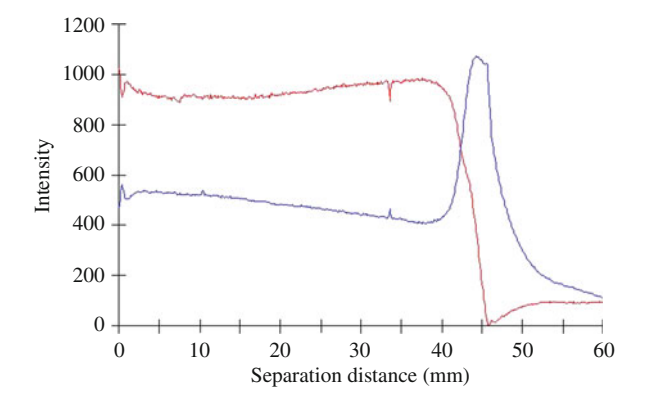


Fig. 2.7 Mobile phase composition of an ethyl acetate, benzyl alcohol, and mesitylene mixture (18+1+1, V/V) on a silica gel HPTLC plate. At the start of the development, the mesitylene concentration lies below that of benzyl alcohol

A solvent front composition gradient is formed in all types of development chromatography. The mobile phase composition is not identical with the solvent mixture chosen for separation. The composition gradient is formed during development, due to the mutual interactions between the mobile and stationary phases.

Figure 2.7 shows typical adsorption chromatography with normal phase development, that is, with a mobile phase composition that is less polar than the stationary phase. Substances of low polarity migrate within the low polarity solvent front gradient. Thus some separations can produce strong front signals caused by the low polarity sample components that migrate within the solvent front gradients. Figure 2.7 demonstrates that the benzyl alcohol concentration in the mobile phase drops off rapidly at a separation distance of 40 mm. The rather volatile mesitylene gathers at the front. In this system a constant mobile phase composition occurs only up to a separation distance of 40 mm. In this mobile phase $R_{\rm f}$ values higher than 0.85 are meaningless since unseparated substances in this region move with the solvent front gradient.

It can also be deduced from Fig. 2.7 that all substances with $R_{\rm f}$ values < 0.85 have been overrun by the low polarity gradient at the solvent front. Therefore all substance with a separation distance less than 40 mm have spent some time migrating in the solvent front gradients. This explains why the measured $R_{\rm f}$ values differ from the "correct" thermodynamic $R_{\rm f}'$ values.

Figure 2.8 illustrates a typical plot of the composition for a ternary mobile phase containing methanol in a normal-phase separation employing an octadecylsiloxane-bonded silica gel layer. The mobile phase consists of equal volumes of mesitylene and benzyl alcohol in methanol. In this case it is mesitylene, which has a higher affinity for the low polarity stationary phase RP-18 than benzyl alcohol and is selectively absorbed from the mobile phase by the layer. The main component of the mobile phase is the relatively polar methanol, which washes out the benzyl

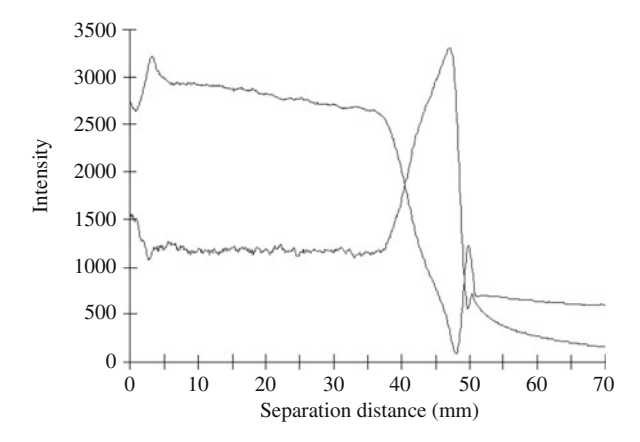


Fig. 2.8 Change in solvent composition of a mixture of methanol, benzyl alcohol and mesitylene (18+1+1, V/V) on an RP-18 HPTLC plate. At first the concentration of mesitylene lies above that of benzyl alcohol

alcohol resulting in a broad solvent front gradient. Under these conditions, polar substances remain unseparated within the front gradients. The small mesitylene signal in front of the benzyl alcohol peak indicates the evaporated mesitylene, which was adsorbed by the layer and is now absorbed by the moving solvent front. A change in the mobile phase composition can be seen below a separation distance of 5 mm. Here, the proportion of mesitylene in the mobile phase is less than in the original solvent mixture. Mesitylene is enriched in the first 5 mm of the stationary phase while the benzyl alcohol concentration is reduced. After a separation distance of about 5 mm the new equilibrium between phases forms a constant mobile phase composition. This explains why the $R_{\rm f}$ values below 0.1 and above 0.85 should not be used for substance characterization.

2.6 Transfer of TLC Separations to Columns

The $R_{\rm f}$ value characterizes the migration distance of the analyte for conditions pertaining to TLC. However, a substance can only move over the plate while dissolved in the mobile phase; otherwise it remains in place. If a substance has an $R_{\rm f}$ value of 0.2, then it must have spent 1/5 of the development time in the mobile phase and 4/5 of the development time in the stationary phase. The value for the retention factor k is thus calculated with k=4. The above-mentioned relationship between the $R_{\rm f}'$ value and the retention factor must be valid in order to arrive at the $R_{\rm f}'$ value of 0.2:

$$R_{\rm f}' = \frac{1}{k+1} = \frac{t_{\rm m}}{t_{\rm m} + t_{\rm S}}.$$

The $R_{\rm f}'$ value is an analyte-specific constant for a given stationary and mobile phase combination. Thus, layer and column techniques have a common retention factor, as shown by the equation

$$k = \frac{t_{\rm S}}{t_{\rm m}} = \frac{1 - R_{\rm f}'}{R_{\rm f}'}.$$
 (2.7)

Transferring separation conditions from planar separations to HPLC has practical advantages since TLC separations are faster, in general, and less expensive than non-optimized separations by HPLC. The precondition for transferring retention data from TLC to column chromatography is that the distribution coefficient must be identical in both systems. This is the case, when using the same stationary and mobile phases. The Martin–Synge equation (2.6), set out according to the partition coefficient, yields

$$K = \frac{1 - R_{\rm f}'}{R_{\rm f}'} \frac{V_{\rm m}}{V_{\rm S}} \tag{2.8}$$

If TLC and HPLC distribution coefficients are set as equal and if $V_{\rm m}$ represents the mobile phase volume and W the sorbent weight, the following relationship results between TLC and HPLC separations:

$$\left\{\frac{V_{\rm m}}{W}k\right\}_{\rm HPLC} = \left\{\frac{V_{\rm m}}{W}\frac{1 - R_{\rm f}'}{R_{\rm f}'}\right\}_{\rm TLC}.$$

From the transformed Martin–Synge equation, it follows that the quotient of the $R_{\rm f}'$ values in the TLC equation is the same as the retention factor in HPLC. If divided by $V_{\rm m}/W$, it results in the following expression

$$k_{\text{HPLC}} = \frac{\{V_{\text{m}}/W\}_{\text{TLC}}}{\{V_{\text{m}}/W\}_{\text{HPLC}}} \frac{1 - R_{\text{f}}'}{R_{\text{f}}'}$$

If the weight of the stationary phases and volumes of the mobile phases are known, the R_f' values determined by TLC can be used to calculate the retention factors expected for an HPLC separation. To avoid weight and volume determinations, the separation systems can be calibrated by experimentally establishing the relationship between the TLC and HPLC separations for a series of standards and using this information to predict HPLC separations for other substances once TLC data have been obtained [13].

2.7 The $R_{\rm m}$ Value

The thermodynamic R_f' value is not linearly related to the structural properties of a molecule. However, a linear correlation with structure exists if a logarithmic form of the R_f' value is used. This so-called R_m value was introduced in 1950 by Bate-Smith and Westall [14]:

$$R_{\rm m} = \lg\left(\frac{1}{R_{\rm f}'} - 1\right) = \lg(k).$$
 (2.9)

The expression for the $R_{\rm m}$ value when inserted in the Martin–Synge equation (2.8) yields

$$R_{\rm m} = \lg \frac{V_{\rm S}}{V_{\rm m}} + \lg K. \tag{2.10}$$

By applying equation $\Delta \mu^0 = RT \ln K = 2.3RT \lg K$ for the chemical potential, it affords the important *Martin* relationship:

$$R_{\rm m} = \lg \frac{V_{\rm S}}{V_{\rm m}} + \frac{\Delta \mu^0}{2.3RT}.$$
 (2.11)

The chemical potential $\Delta\mu^0$ describes the free energy change resulting from the transfer of a mole of analyte under standard conditions between phases. The Martin relationship is based on thermodynamic considerations and is valid for adsorption as well as partition chromatography. Martin explained the remarkable separating powers of chromatography by using this equation. If two molecules are only slightly different, for example, differ only in a single structural element, their difference in chemical potential is proportional to the structural element. This explains why large molecules with small structural differences can be separated. For separation, the individual structural differences are important, not the relative differences [7].

The Martin equation serves as a basis for quantitative structure–retention relationships. In the ideal case, the chemical potential of a substance is the sum of the partial contributions of its structural elements (atoms, functional groups, and bonds). Substance $R_{\rm m}$ values can be calculated from homologous substances as a multiple of the basic structure, as illustrated in Fig. 2.9 for different aliphatic carboxylic acids. If a member's $R_{\rm m}$ values are known, then further $R_{\rm m}$ values for additional members can be deduced.

2.8 Temperature Dependence of TLC Separations

The effect of temperature on thin layer separations is relatively weak in comparison with other influences. A change in temperature has a noticeable effect on the equilibrium composition of the mobile phase in contact with the stationary phase. Distribution constants are temperature dependent as are sorption isotherms. Higher temperatures favour evaporation of the more volatile components of the mobile phase into the gas phase as well as reducing the viscosity of the mobile phase. Furthermore, the temperature-dependent water content of the vapour phase plays an important role in adsorption chromatography. It is a well-known fact that TLC separations based on adsorption are generally stable and run well in temperate

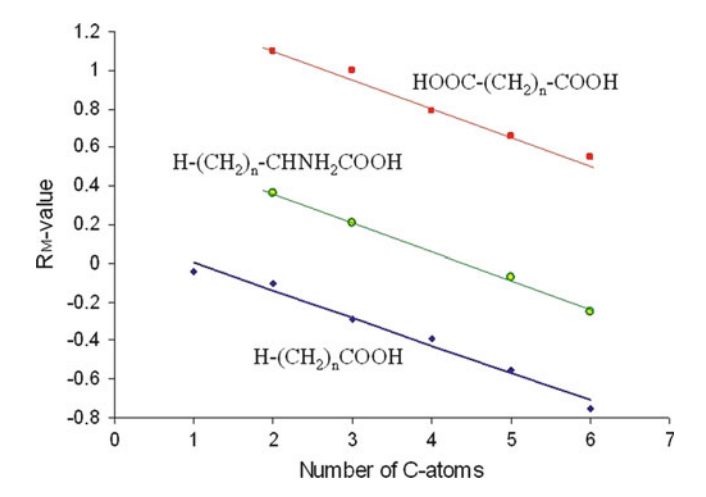


Fig. 2.9 $R_{\rm m}$ values of aliphatic acids (From [15].)

climate zones but are a total disaster on hot summer days in the tropics. High air humidity obviously makes a difference and there is a temperature effect as well. The above temperature-dependent factors partially compete with each other, thus making it almost impossible to exactly predict the effect that changes in temperature have on a TLC separation. The Martin relationship combines temperature and $R_{\rm m}$ values in a single equation where the $R_{\rm m}$ value increases as the temperature decreases. Thus R_f values should increase as the temperature declines at a constant absolute humidity for the gas phase [6]. At a constant relative humidity, the observed $R_{\rm f}$ values rise with decreasing temperature. Thus, it can be concluded that the higher the temperature, the lower the stationary phase activity. Moreover, mobile phase viscosity declines at higher temperatures, thus increasing the velocity constant. This results in a higher separation of the zone centres but with increased spot diameters. Therefore, there is no substantive argument in favour of performing TLC separations at higher temperatures. On the other hand, some separations are only successful at low temperatures. For example, the separation of polycyclic aromatic hydrocarbon on caffeine-impregnated silica gel layers at -20° C [16, 17].

In summary, it can be stated that temperature changes in the region of $\pm 10^{\circ} C$ cause little to no alteration in the separation process, provided that the humidity of the system is kept constant. In practice, this means that a laboratory does need to maintain temperate temperatures to carry out TLC separations.

2.9 Advanced Theoretical Considerations

Chromatographic separations are determined by a combination of kinetic and thermodynamic properties. Thermodynamic properties are responsible for the retention behaviour and selectivity. Kinetic properties determine zone broadening during a separation [18].

The process of chromatographic separation can be compared to a liquid–liquid distribution in a separating funnel, except that the equilibrium between phases occurs several thousand times in a chromatographic separation. In addition, in a chromatographic separation the mobile phase passes through the stationary phase while the two phases are merely brought into contact and separated in a typical liquid–liquid distribution experiment. In column chromatography a substance is permanently distributed between both phases but only moves when in the mobile phase. A simulation of these processes, transferred to TLC, leads to the sample moving through the TLC layer in the form of a binominal distribution. Assuming that a certain amount of analyte n was applied to a TLC layer before contacting the mobile phase, the total substance amount is concentrated in a small zone and the mobile phase has not yet had any contact with the sample, this situation is represented by the equation

$$\left\{\frac{0}{n}\right\} = \frac{n_{\text{mobile phase}}}{n_{\text{stationary phase}}} = n(\gamma + \beta)^{0}.$$

The nominator in this equation represents the mobile phase and the denominator the stationary phase. The meaning of γ and β will be explained below. Equilibrium has yet to be established between the two phases, as all the sample n still lie in the starting zone of the stationary phase. After adding the mobile phase, some sample is distributed between the stationary and mobile phases, according to their individual retention factors. The factor $n_{\rm S}$ refers to the amount of substance that remains in the stationary phase and $n_{\rm m}$ to the amount dissolved in the mobile phase. At this moment the following expression is valid for the substance in the stationary phase:

$$n_{\rm S}=kn_{\rm m}$$
.

As the amount of sample is conserved, it must be distributed between both phases, and the following expression is also valid:

$$n = n_{\rm S} + n_{\rm m}$$

If the upper equation is substituted into the lower one, this leads to the expression

$$n = n_{\rm m}(k+1)$$

and after rearrangement, it becomes

$$n_{\rm m} = \frac{1}{(k+1)} n \equiv \beta n.$$

From the sample applied n, the fraction βn will move into the mobile phase. The equation below represents the fraction of the amount of sample n, which remains in the stationary phase:

$$n_{\rm S} = k n_{\rm m} = \frac{k}{(k+1)} n \equiv \gamma n.$$

The fraction of immobilized sample that remains in the stationary phase is given by γn . The expressions for β and γ allow a shorter description of the separation processes. By definition, the fraction β changes phase while the fraction γ remains behind, thus leading to $\beta + \gamma = 1$.

In the next step, fresh mobile phase contacts the sample zone pushing the fraction $n\beta$ of sample molecules onto a clean area of the plate. The fraction $n\gamma$ of the sample is immobilized by the stationary phase and does not move. After the first equilibrium, the situation is represented as follows:

$$\left\{\frac{0}{n\gamma} + \frac{n\beta}{0}\right\} = \frac{n_{\text{mobile phase}}}{n_{\text{stationary phase}}} = n(\gamma + \beta)^{1}.$$

The next equilibrium can be described as follows. The fraction of n in the mobile and stationary phases will be distributed according to their retention factors. From the substance amount remaining in the stationary phase, the fraction β of the amount $n\gamma$ will move into the mobile phase (i.e. $\beta n\gamma$), while the fraction γ of $n\gamma$ (i.e. $\gamma n\gamma$) remains at the sample origin in the stationary phase. From the substance amount $n\beta$ in the mobile phase, the fraction γ will move into the stationary phase (i.e. $\gamma n\beta$), while the fraction β of $n\beta$ remains in the mobile phase. If further clean mobile phase is introduced, then we have

$$\left\{ \frac{0}{\gamma n \gamma} + \frac{\beta n \gamma}{\gamma n \beta} + \frac{\beta n \beta}{0} \right\} = \frac{n_{\text{mobile phase}}}{n_{\text{stationary phase}}} = n(\gamma + \beta)^2.$$

If the individual fractions of n from the stationary and mobile phases are summed at the end of the three equilibrium stages described above, the results can be represented by a binominal expression. The exact form depends on the number of equilibrium stages. For x number of equilibria the result is represented by $n(\beta + \gamma)^x$

After many equilibria a useful picture of the distribution of a sample on the TLC layer results. For low retention factors $(k \cong 1)$ and for an infinite number of equilibria, the binominal distribution merges into a Guassian distribution of the type

$$f(x) = n \frac{1}{\sqrt{2\pi x \gamma \beta}} e^{-(z - x \gamma)^2 / 2x \gamma \beta}.$$

It has often been said that substances move along the TLC plate as a sequence of Gaussian-shaped zones. This statement can only be regarded as approximate, since even the longest TLC plate lacks the capacity to allow for an infinite number of equilibrium stages. Therefore, TLC peaks recorded in a densitogram are correctly described as binominal functions. Nevertheless, the Gauss function still remains a

satisfactory approximation for many TLC separations using high performance layers. The distribution of the substance amount n as a Gaussian distribution, characterized by a mean value z_S and variance σ , is defined as follows:

$$f(x) = n \frac{1}{\sigma \sqrt{2\pi}} e^{-(x-z_S)^2/2\sigma^2}.$$
 (2.12)

For $x=z_S$ the e-function is 1 and the Gaussian function approaches a maximum height of $f(z_S)$ = $(1/\sigma\sqrt{2\pi})\times 1$. The value z_S of a peak in a densitogram must be taken where the signal reaches its highest value. The width of a Gaussian distribution is defined as the distance between the median of the recorded peak and the inflection points. This width measurement is described as the standard deviation of the peaks. The square of the standard deviation is called the variance (σ^2) .

Figure 2.10 illustrates the distribution of a constant amount of caffeine at different migration distances. The caffeine was applied to the plate, recorded (narrow peak at the start), developed a short distance, and then recorded again. This process was repeated nine times. Note that the caffeine signal widens with each development. If the square of the separation distance (z_s) is divided by the variance, this will at first result in a more or less constant value:

$$\frac{z_{\rm S}^2}{\sigma_{\rm S}^2} = \frac{(x\gamma)^2}{x\gamma\beta} = x\frac{\gamma}{\beta} = xk \equiv N'. \tag{2.13}$$

The product of the retention factor k and the number of distribution steps provides a constant value x representing the efficiency as well as the migration

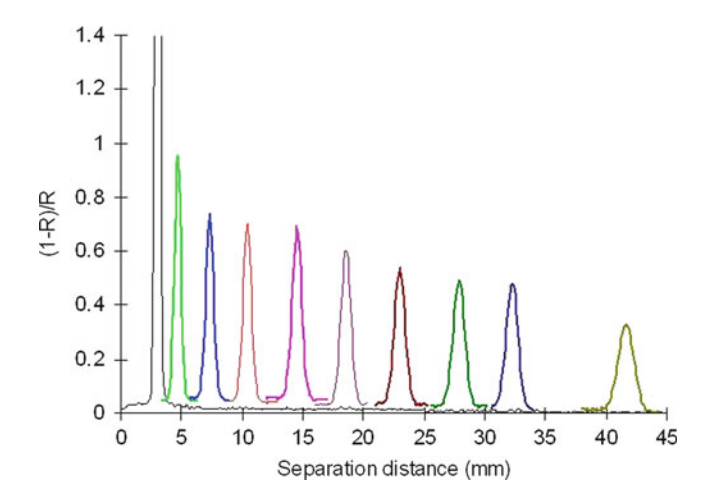


Fig. 2.10 The distribution of a constant amount of caffeine on a TLC plate at different migration distances

distance in a TLC separation. This product of efficiency and migration distance is called the "real number of theoretical plates" and is represented by the symbol N'. If the relationship is formulated according to the standard deviation σ of the peaks recorded in a densitogram, this results in the following equation:

$$\sigma_{\rm S} = \frac{1}{\sqrt{N}} z_{\rm S}.\tag{2.14}$$

Here,

 $\sigma_{\rm S}$ standard deviation

 $z_{\rm S}$ substance migration distance

N' real number of theoretical plates

This expression is generally valid and means that the peak width $(2\sigma_S)$ increases with longer migration distances z_S , as is clearly shown in Fig. 2.10. Thus it follows that a chromatographic system can only separate a finite number of samples because an infinitely long separation distance would lead to infinitely broad peaks.

The expression "number of theoretical plates" or "plate number" in column chromatography refers to the column length corresponding to a single equilibration stage. The plate number in column chromatography can be calculated directly from a chromatogram because each substance, independent of its retention time, must migrate the same distance defined by the column length. In contrast, each separated substance in TLC has associated with it a different migration distance defined as a fraction of the solvent front migration distance. Therefore, in thin-layer chromatography, the maximum plate number N determined at the solvent front position should be corrected for each substance in the chromatogram by the fraction of the solvent front migration distance they migrated using their R_f values [6,11]:

$$N' = NR_{\rm f}. \tag{2.15}$$

If the value of the peak width at base for a Gaussian peak is used, with $w = 4\sigma$ (or more accurately, $w = 2 \times 1.96\sigma$), the following relationship is valid:

$$N' = \left(\frac{z_{\rm S}}{\sigma_{\rm S}}\right)^2 = 16\left(\frac{z_{\rm S}}{w_{\rm B}}\right)^2,\tag{2.16}$$

where

N' real plate number

 $z_{\rm S}$ substance migration distance

 $w_{\rm B}$ peak width at base = 4σ

N' describes the theoretical plate number for each substance corresponding to the fraction of the plate number for the solvent front migration distance that each substance migrates over.

The plate number at the solvent front migration distance N represents the maximum value possible for that separation. It is an inflated value because separations cannot be achieved at the solvent front at which N is calculated:

$$N = \frac{1}{R_{\rm f}} \left(\frac{z_{\rm S}}{\sigma_{\rm S}}\right)^2 = 16z_{\rm S} \frac{(z_{\rm f} - z_0)}{w_{\rm B}^2}.$$
 (2.17)

Here,

N plate number at the solvent front migration distance

 $\sigma_{\rm S}$ standard deviation of the substance

 $w_{\rm B}$ peak width at base for the substance = $4\sigma_{\rm S}$

For those substances that reside at the sample application position there is no interaction with the mobile phase, and the migration distance is zero. For those substances that migrate at the solvent front there is no interaction with the stationary phase, and the number of equilibrium steps is therefore zero. In either case, this will make N or N' zero as well. The value for N is larger than zero only for substances with an $R_{\rm f}$ value in the range $0 < R_{\rm f} < 1$. A chromatographic separation can only take place when the separation performance of the system is other than zero.

Figure 2.11 shows a separation of six dyes, demonstrating the increase in peak width with increasing migration distance z_s . A densitogram allows peak widths at base and migration distances to be extracted for calculation of plate numbers

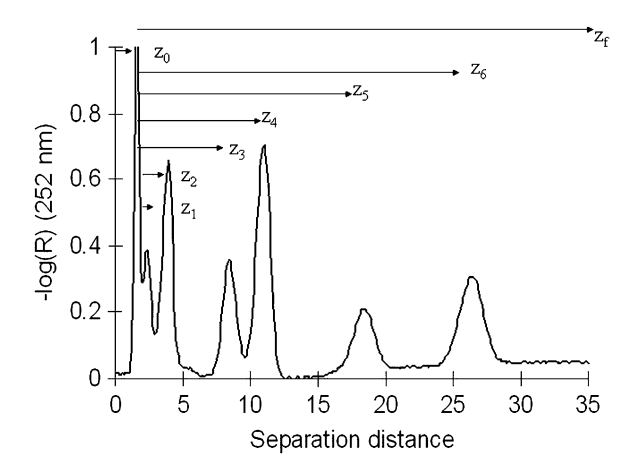


Fig. 2.11 Densitogram illustrating the separation of six dye substances measured at 252 nm (CAMAG dye mix no. III)

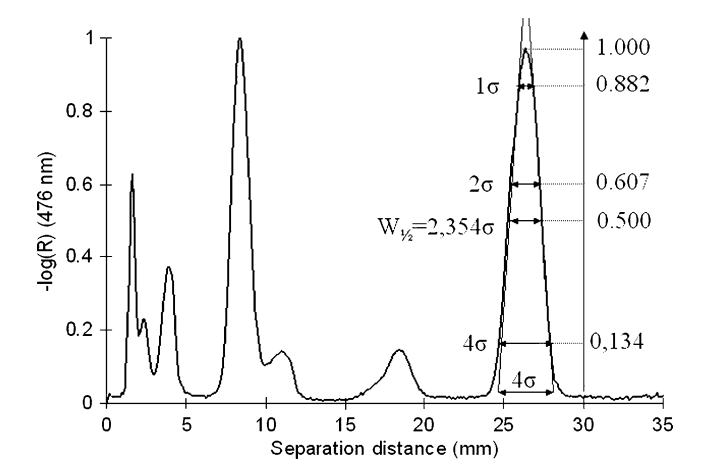


Fig. 2.12 Gaussian-like peaks in the densitogram recorded at 476 nm for the separation of a dye mixture (CAMAG dye mix III)

using (2.16) (see Fig. 2.12). Plate numbers up to 5,000 are achieved in TLC. Plate numbers up to 300,000 have been described for HPLC [6], although plate numbers < 25,000 are more typical for columns in general use.

The standard deviation of a peak is often determined by the peak width at half height rather than by the peak width at base. The height of a Gaussian peak is described by the fore factor of the e-function $(1/\sigma\sqrt{2\pi})$. The Gaussian function value at median peak height $H_{\rm P}/2$ is given by

$$\frac{H_{\rm P}}{2} = \frac{1}{2\sigma\sqrt{2\pi}} = \frac{1}{\sigma\sqrt{2\pi}} e^{-(x)^2/2\sigma^2}.$$

From which it can be concluded that

$$2 = e^{(x)^2/2\sigma^2}$$
 and $\ln 2 = \frac{(x)^2}{2\sigma^2}$.

The peak width at half height w_H runs from -x to +x. Thus

$$w_{\rm H}^2 = 8\sigma^2 \ln 2 = 5.545\sigma^2. \tag{2.18}$$

The relationship for the plate number can also be written in the following form when the peak width at half height is used as a surrogate determination of the standard deviation for a Gaussian peak recorded in a densitogram:

$$N = 5.545z_{\rm S} \frac{(z_{\rm f} - z_0)}{w_{\rm H}^2}.$$
 (2.19)

2.10 Indices Characterizing Separation and Resolution

How can a separation be improved? Of course you would like to separate a substance from all the other sample components so that it can be correctly quantified. For this purpose a chromatographic system must be selected that provides sufficient differentiation of the $R_{\rm f}$ values of the individual substances. At the completion of the development step the substance zones occupy the space defined by the solvent front migration distance characterized by a location ($R_{\rm f}$ value) and a distribution that can be approximately represented by a Gaussian function. Because of dispersion, individual zones occupy space on the layer that depends on their $R_{\rm f}$ value and system properties.

The peak area of the Gaussian distribution is proportional to the amount of substance contained in the spot. The peak width at base (w_B) of a Gaussian peak is a measure of the space occupied by the scanned zone on the TLC plate. This can be calculated for an individual substance by using the distance z_S according to

$$w_{\rm B} = \frac{4}{\sqrt{NR_{\rm f}}} z_{\rm S}.\tag{2.20}$$

The resolution, R_S , of two neighbouring Gaussian curves (two peaks) is defined by the quotients from the difference between the two maximum signals (z_{S1} and z_{S2}) and the arithmetic mean of their peak widths at base (w_{B1} and w_{B2}):

$$R_{\rm S} \equiv \frac{z_{\rm S2} - z_{\rm S1}}{\frac{w_{\rm B1} + w_{\rm B2}}{2}} = 2 \frac{z_{\rm S2} - z_{\rm S1}}{w_{\rm B1} + w_{\rm B2}} = \frac{z_{\rm S2} - z_{\rm S1}}{2(\sigma_1 + \sigma_2)}.$$

For $R_{\rm S}=0.5$ the distance between peaks is $\sigma_1+\sigma_2\approx 2\sigma$,-called a " 2σ separation". The two peaks still overlap each other by about 20%. However, the two components can still be recognized. At a resolution of 1, the peaks are almost completely separated. The peak profiles only overlap by 3%, corresponding to a 4σ separation (Fig. 2.13).

A resolution of 1.25 is sufficient for quantitative measurements by scanning densitometry. A resolution greater than 1.5 is unnecessary for quantifying overlapping peaks since the overlap of the peaks is less than 0.3%. Of course, this is only true for symmetrical peaks adhering to a Guassian profile. In the case of fronting or tailing peaks, a 10σ separation is required for reliable quantification, which corresponds to a resolution of $R_{\rm S}=2.5$.

From the definition of the $R_{\rm f}$ value, $z_{\rm S}=R_{\rm f}(z_{\rm f}-z_0)$, and with the simplification $\sigma_1 \approx \sigma_2 \approx \sigma$ the expression for the resolution can be transformed into

$$R_{\rm S} = \frac{(R_{\rm f2} - R_{\rm f1})(z_{\rm f} - z_{\rm 0})}{4\sigma}.$$

With $(z_f - z_0) = z_{S1}/R_{f1}$ and application of (2.14), it follows that

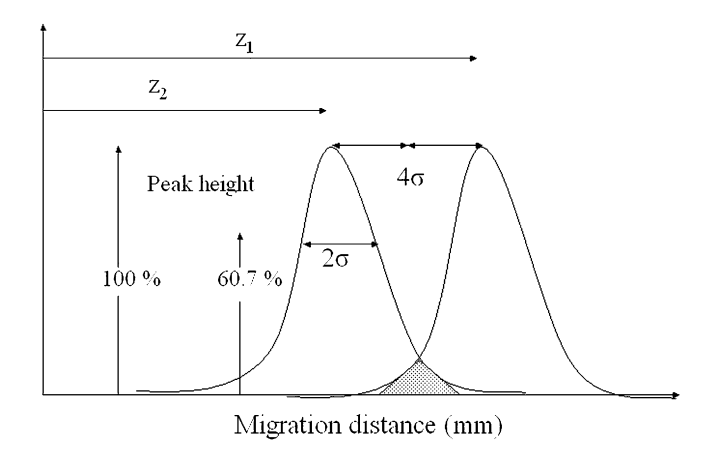


Fig. 2.13 Separation of neighbouring peaks according to the 4σ peak separation definition

$$R_{\rm S} = \frac{(R_{\rm f2} - R_{\rm f1})}{R_{\rm f1}} \frac{z_{\rm S1}}{4\sigma} = \left(\frac{R_{\rm f2}}{R_{\rm f1}} - 1\right) \frac{1}{4} \sqrt{NR_{\rm f}}.$$

The value of R_f is calculated from the mean value of R_{f1} and R_{f2} . Given that $R_f = 1/(1+k)$ it follows that

$$R_{\rm S} = \frac{1}{4} \sqrt{NR_{\rm f}} (k_1 - k_2) R_{\rm f2} = \frac{1}{4} \sqrt{NR_{\rm f}} \frac{(k_1 - k_2)}{k_2} k_2 R_{\rm f2}.$$

Using the expression for the retention factor of the second substance $k_2 = (1 - R_{f2})/R_{f2}$, Snyder's equation for resolution in TLC is obtained [6, 19, 20]:

$$R_{\rm S} = \frac{1}{4} \sqrt{NR_{\rm f}} (1 - R_{\rm f2}) \left(\frac{k_1}{k_2} - 1 \right).$$

$$\mathbf{a} \quad \mathbf{b} \quad \mathbf{c}$$
(2.21)

According to Snyder's equation, the resolution of two substances is influenced by three factors:

- (a) The first term in the Snyder equation describes the layer quality. This is characterized by the plate number NR_f and is dominated by the contribution of diffusion to zone broadening for well-prepared layers. Resolution can be improved by an increase in the plate number but only in proportion to the square root of NR_f . Increasing the R_f value is predicted to increase the resolution of two closely migrating peaks but this is not the case since resolution goes through a maximum at around an R_f value of 0.3. This is because of the opposing contributions of the first two terms in (2.21).
- (b) The second term in (2.21) contradicts the sense of the first. The greater the $R_{\rm f}$ value, the lower the resolution of two closely migrating zones. All substances

migrating with the solvent front have an R_f value of one and a resolution of $R_S = 0$. All substances that migrate in the region close to the solvent front have a limited number of interactions with the stationary phase and the probability of their separation is low.

(c) The selectivity term depends on the ratio of the retention factors. The greater the difference for the retention factors, the higher the chromatographic selectivity and the higher will be the resolution. The selectivity term is a measure of the ability of the separation system to distinguish between the two substances by their capability for different intermolecular interactions in the mobile and stationary phases.

Equation (2.21) can also be interpreted differently. The first two terms (**a** and **b**) describe the "potential resolution" of the TLC system. It is also a general measure of the locally variable separation performance of a chromatographic system at a particular migration distance. It can be used to calculate the actual resolution (R_S) of a pair of substances, by multiplying the terms **a** and **b** by the term **c** [6]. By adopting the abbreviation $Q^2 = R_f(1-R_f)^2$ both the terms **a** and **b** of (2.21) can be described as follows (with $R_f \sim R_{f2}$):

$$NQ^2 = NR_{\rm f}(1 - R_{\rm f})^2 = \left[\sqrt{NR_{\rm f}}(1 - R_{\rm f2})\right]^2.$$

The product NQ^2 is proportional to the resolution squared and known as the "effective plate number".

If R_{12} is replaced by the retention factor, the above equation can be written as

$$NQ^2 = NR_f \left(1 - \frac{1}{1 + k_2}\right)^2 = N' \left(\frac{k_2}{1 + k_2}\right)^2.$$
 (2.22)

The variation of the effective plate number with $R_{\rm f}$ values is evaluated graphically in Fig. 2.14.

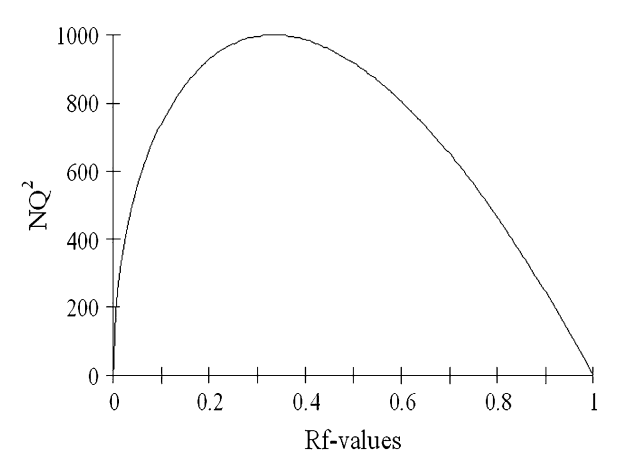


Fig. 2.14 Effective plate number, as a function of R_f values with N = 6,751, according to [21]

According to Fig. 2.14, the highest effective plate number is obtained with $R_{\rm f}$ values of about 0.33. Satisfactory separations are only achieved in the $R_{\rm f}$ region from 0.05 to about 0.9. For critical separations, the system should be adjusted so that critical pairs have an average $R_{\rm f}$ value around 0.33. In TLC it is extremely difficult to improve the plate quality (represented by \sqrt{N}) by a factor of more than 2–3. However, the selectivity can be improved by a factor 10–50 through an intelligent choice of the mobile and stationary phases. In practice, it is usually more productive to optimize the mobile phase composition for a chosen stationary phase [6].

2.11 Zone Broadening in Planar Chromatography

We can distinguish between three different processes that contribute to zone broadening in TLC, commonly referred to as the A, B, or C terms [6, 20, 22-30].

2.11.1 The A term

The A term is determined by the heterogeneity of the layer, which results from variations in the local packing density, the distribution of particle sizes and shapes, and the presence of additives in the layer such as binders and visualization indicators. Layer heterogeneity is responsible for flow heterogeneity. Flow is slower through the internal porosity system than through the interparticle spaces [6]. This effect is called Eddy diffusion and is directly proportional to the particle diameter. Guiochon and Siouffi were the first researchers to substitute the term Eddy diffusion (from the Giddings approach) for the considerably slower processes of liquid chromatography. They also used the dimensionless Knox constant to describe the packing quality of the layer [6]:

$$\sigma_{\rm xA}^2 = A \frac{\sqrt[3]{d_{\rm p}^4}}{\sqrt[3]{D_{\rm m}R_{\rm f}t}}$$

 $d_{\rm p}$ particle size

 $D_{\rm m}$ diffusion coefficient in the mobile phase (cm²/s)

t time spent in the mobile phase (s)

A Knox constant

2.11.2 The B term.

Sample molecules in the mobile phase diffuse in all directions. According to Einstein's law of diffusion, a substance zone broadens with time, as determined by its diffusion coefficient. Zone broadening in the mobile phase, expressed as variance σ^2 , can be written as

$$\sigma^2 = 2D_{\rm m}t$$

where

 $D_{\rm m}$ diffusion coefficient in the mobile phase (cm²/s) t time spent in the mobile phase (s)

The longitudinal zone broadening (σ_x), i.e. the zone spreading in the flow direction, is calculated from the zone broadening due to diffusion, corrected to account for the space occupied by the impenetrable sorbent particles, the labyrinth factor, and introducing the retardation factor to account for the fraction of the separation time the sample spends in the mobile phase:

$$\sigma_{\rm vB}^2 = 2D_{\rm m}\lambda_{\rm m}R_{\rm f}t = BD_{\rm m}R_{\rm f}t.$$

Here,

 $\sigma_{\rm x}$ longitudinal spot spreading

 $\lambda_{\rm m}$ labyrinth factor (mobile phase)

t time spent in the mobile phase (s)

B Knox constant

A similar situation is true for the transversal standard deviation σ_v across the flow direction.

Partition chromatography requires a further contribution to account for longitudinal zone broadening [20, 22–27]. The fraction of sample in the solvated stationary phase with a diffusion coefficient (D_s) and labyrinth factor for of the stationary phase (λ_s) will slowly exchange with sample in the mobile phase resulting in additional longitudinal zone broadening expressed by [28]

$$\sigma_{\rm xB}^2 = 2\bigg(\lambda_{\rm m}D_{\rm m} + \frac{1 - R_{\rm f}}{R_{\rm f}}\lambda_{\rm S}D_{\rm S}\bigg)R_{\rm f}t$$

 $\sigma_{\rm x}$ longitudinal spot spreading

 $\lambda_{\rm m}$ labyrinth factor (mobile phase)

 $D_{\rm m}$ molecule diffusion coefficient (mobile phase)

 $\lambda_{\rm S}$ labyrinth factor (stationary phase)

 $D_{\rm S}$ molecule diffusion coefficient (stationary phase)

t time (s)

This relationship demonstrates that in partition TLC, zone broadening from diffusion results from contributions that occur in both the mobile and stationary phases. In the direction of development, zones broaden with an increase in $R_{\rm f}$ values influenced by diffusion in the solvated stationary phase [6]. This results in the formation of elliptical zones. For smaller $R_{\rm f}$ values there are few interchanges between the stationary and mobile phases and the zones remain round or compact. At higher $R_{\rm f}$ values, the substance has few interchanges with the stationary phase and spends most of its time in the mobile phase, and thus hardly diffuses into the pores of the stationary phase. Zone broadening depends almost exclusively on diffusion in the mobile phase, with a sample zone forming a diffuse circle.

2.11.3 The C term

The C term accounts for delays caused by mass transfer processes during sorption and desorption of solute molecules. It is inversely proportional to the separation time and the diffusion coefficient and proportional to the square of the particle diameter [26]:

$$\sigma_{\rm xC}^2 = C \frac{d_{\rm p}^2}{D_{\rm m} R_{\rm f} t}.$$

Here,

 σ_{xC} non-equilibrium process zone broadening

 $d_{\rm p}$ particle size

 $D_{\rm m}$ diffusion coefficient in mobile phase (cm²/s)

t time (s)

C Knox constant

The sum of all the variations then describes the total variance of the zone broadening process:

$$\sigma_{\mathrm{S}}^2 = \sigma_{\mathrm{xA}}^2 + \sigma_{\mathrm{xB}}^2 + \sigma_{\mathrm{xC}}^2.$$

2.11.4 Local Plate Height H

As already mentioned, N (the plate number for the complete separation length) describes the separation capacity of a chromatographic system, i.e. the larger the N is, the more substances can be separated. Instead of giving the plate number, the

local plate height H is frequently given as a chromatographic separation characteristic. This is obtained by dividing the total separation distance by N [6]:

$$H \equiv \frac{z_{\rm f} - z_0}{N} = R_{\rm f} \sigma_{\rm S}^2 \frac{z_{\rm f} - z_0}{z_{\rm S}^2} = \frac{\sigma_{\rm S}^2}{z_{\rm S}}.$$
 (2.23)

The expression *H* represents an (imaginary) fraction of the plate length over which, in theory, one equilibration step in the separation is achieved [6]. The "H value" is encapsulated in the acronym HETP (height equivalent to a theoretical plate).

2.11.5 The van Deemter Equation

The van Deemter equation describes the relationship between the local plate height H and the individual factors that lead to zone broadening. This equation was originally developed for gas chromatography and later used in liquid chromatography. Guiochon and Siouffi published an adaptation for TLC [6, 28]. This equation illustrates the relationship between molecular diffusion, mass transport, and the local plate height H. It enables the optimum velocity to be forecast in column chromatography and the optimum separation distance in TLC. The equation also allows us to predict which particle and pore diameters afford optimum separation performance for the stationary phase. Therefore the modified van Deemter equation made a decisive contribution to the successful development of HPTLC layers.

The solvent front velocity, which corresponds to the local mobile phase velocity for the sample zone, is calculated according to the general definition of velocity:

$$u = \frac{z_{\rm f} - z_0}{t}.$$

Given that $(z_f-z_0)=z_S/R_f$ the following is valid:

$$R_{\rm f}t = R_{\rm f} \frac{(z_{\rm f} - z_0)}{u} = \frac{z_{\rm S}}{u}$$

Divided by z_S , the sum of all variations can be described as a local plate height:

$$H = \frac{\sigma_{\mathrm{S}}^2}{z_{\mathrm{S}}} = \frac{\sigma_{\mathrm{xA}}^2 + \sigma_{\mathrm{xB}}^2 + \sigma_{\mathrm{xC}}^2}{z_{\mathrm{S}}}.$$

A modified van Deemter equation designed for adsorption chromatography can be written as follows [28]:

$$H = Ad_{\rm p} \left(\frac{d_{\rm p}}{D_{\rm m}}u\right)^{1/3} + \frac{BD_{\rm m}}{u} + C\frac{d_{\rm p}^2}{D_{\rm m}}u. \tag{2.24}$$

Here.

```
D_{\rm m} solute diffusion coefficient (mobile phase)
d_{\rm p} average particle size
u mobile phase velocity, u=(z_{\rm f}-z_0)/t
A-C Knox equation coefficients [29]
```

Constant A characterizes the quality of the stationary phase, B the axial diffusion, and C the resistance to mass transport in the layer.

The value of H is mainly dependent on u (the mobile phase velocity). If the mobile phase moves slowly through the layer, diffusion dominates; broadening the separating zones resulting in a poor separation. If the mobile phase moves too quickly through the layer, equilibrium is not fully established and again a poor separation results. For any separation there is an optimum mobile phase velocity corresponding to a minimum value for H. This optimum situation depends decisively on the particle size (d_p) of the layer.

According to Giddings [30], the first term (the A term) in the van Deemter equation describes the Eddy diffusion and mass transport in the mobile phase. This diffusion in all directions is due to various different local flow velocities in the stationary phase. The usual cause is varying particle geometry of the packing. The more uniform the packing of the stationary phase, the lower the value of constant A. A further contribution to eddy diffusion arises from the difference in local velocity within the layer. Velocity gradients exist within the interparticle channels, with a greater difference between flow velocity in the middle and at the sides of the larger channels than in narrower channels. Smaller particles promote smoother flow, so there is less diffusion. Of course, one cannot keep on reducing particle size, since the channels would get too narrow and be easily blocked.

The second term of the van Deemter equation (the B term) describes the effects of the mobile phase on molecular diffusion. This term has already been discussed in the section on "zone broadening in TLC". The mobile phase velocity is inversely proportional to zone broadening. Consequently, the contribution of the B term to zone broadening decreases with increasing mobile phase velocity. In TLC, zone broadening is most noticeable for longer separation distances and at higher $R_{\rm f}$ values. This is a consequence of the use of capillary forces to promote and maintain the flow of mobile phase and is a considerable disadvantage for TLC compared with pneumatically regulated column systems.

The third expression in the modified van Deemter equation (*C* term) takes into consideration that adsorption and desorption of the sample from the stationary phase needs time. Some molecules are adsorbed and therefore fixed in position while others move forwards with the mobile phase, resulting in zone dispersion in the flow direction. As this effect is also connected with the packing surface, it directly depends on the squared particle diameter. Furthermore, it also takes into consideration that molecules in thin layers can move to the surface of the layer faster than those in thicker layers. A faster re-dissolution process also reduces dispersion [18].

2.12 Optimum Separation Conditions in TLC

In GC or HPLC an optimum mobile phase velocity is calculated as the minimum H value from the van Deemter relationship. Unfortunately, as Geiss rightly points out [6], the mobile phase velocity for TLC is not constant and, as a consequence, the value of H depends on the position of each zone in the chromatogram. Therefore stating an optimum mobile phase velocity is not relevant for TLC. However, the location dependence of the local plate height can be eliminated by creating a new value (H/z_f) for the local plate height. If this quotient for the local plate height is integrated for the space between the sample application point and the solvent front migration distance (from z_0 to z_f) an average plate height H_M is obtained which is independent of the mobile phase velocity but not the flow velocity constant χ . Geiss called this expression "the observed average plate height", which is the sum of all local plate heights passed through during the development [6]. The TLC expression for the local van Deemter equation must be integrated over the whole separation distance [6, 28]:

$$\overline{H_{\rm M}} = \frac{1}{\int_{z_0}^{z_{\rm f}} {\rm d}z_{\rm f}} \int_{z_0}^{z_{\rm f}} H {\rm d}z_{\rm f} = \frac{1}{z_{\rm f} - z_0} \int_{z_0}^{z_{\rm f}} (A d_{\rm p} \left(\frac{d_{\rm p}}{D_{\rm m}} u\right)^{1/3} + \frac{B D_{\rm m}}{u} + C \frac{d_{\rm p^2}}{D_{\rm m}} u) {\rm d}z_{\rm f}.$$

By introducing the local flow velocity $u = dz_f/dt = \chi/2z_f$ (derived from the flow relationship $z_f^2 = \chi t$), this equation can be solved:

$$\overline{H_{\rm M}} = \frac{3}{2} A \left(\frac{d_{\rm p}^4 \chi}{2 D_{\rm m}} \right)^{1/3} \frac{z_{\rm f}^{2/3} - z_0^{2/3}}{z_{\rm f} - z_0} + \frac{B D_{\rm m}}{\chi} (z_{\rm f} + z_0) + \frac{C \chi d_{\rm p}^2}{2 D_{\rm m} (z_{\rm f} - z_0)} \ln \frac{z_{\rm f}}{z_0}. \quad (2.25)$$

The A term and the C term can be minimized by small d_p . The diffusion coefficient of the sample in the mobile phase (D_m) is difficult to optimize since it appears in the nominator of the second term as well as in the denominator of the first and third terms. The major contribution from diffusion appears in the B term.

According to Einstein's diffusion law, a zone boundary will expand in all direction in time t by $2D_{\rm m}t$. Consequently, separations should be reasonably fast to minimize band broadening. Unfortunately, the flow of the mobile phase is hindered by small particles in the stationary phase, which reduces the A and D terms and enlarges the B term. Using a mobile phase with small diffusion constants will limit zone broadening as much as possible [6]. Small velocity constants also reduce the influence of the B and C terms. In addition, it should be noted that for z_0 values close to zero the logarithmic expression tends towards very large values. The distance between immersion line and sample application zone should not be too short. According to Saunders and Snyder [6, 31], the optimum relationship for $z_{\rm f}$ to z_0 should lie between 7 and 33.

As demonstrated in (2.25) and Fig. 2.15, $H_{\rm M}$ achieves a minimum value for a fixed development length. For a value of $z_0=1$ cm, the optimum development

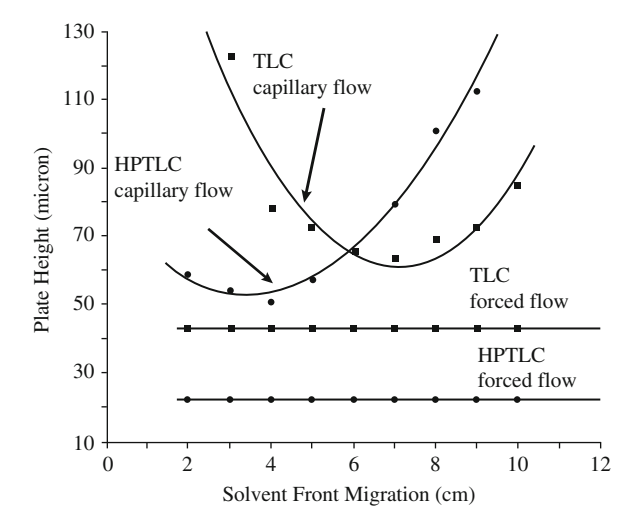


Fig. 2.15 The variation of observed plate height as a function of solvent front migration distance for conventional (TLC) and high-performance (HPTLC) silica gel layers, under capillary flow and forced flow conditions (Taken from [33] with permission. © Elsevier.)

Table 2.1	Typical TLC and HPTLC data, taken from [181

J1		
Parameter	TLC	HPTLC
$\overline{D_{\mathrm{m}}}$	$2.8 \times 10^{-5} \text{ cm}^2/\text{s}$	
$d_{\rm p}$	8.8 µm	6.0 μm
Knox constants		
A	2.83	0.75
B	1.18	1.56
C	0.84	1.42
Flow constant		
χ	$0.044 \text{ cm}^2/\text{s}$	$0.019 \text{ cm}^2/\text{s}$

length for a TLC separation is between 7 and 15 cm [18]. Thus Stahl's standard values for classic TLC: $z_0 = 1$ cm and $z_f = 10$ cm [6] were extremely well chosen. As shown in Fig. 2.15, the optimum development length for HPTLC is about 4 cm [18]. The minimum plate height for capillary flow separations is always higher than for forced flow. HPTLC plates with smaller particles than TLC plates provide better separations, but a development distance of 5 cm should not be exceeded (Table 2.1) [33].

What conclusions can be drawn from (2.25)? The ideal situation is to maintain a constant flow for the whole separation distance, a condition which is only fulfilled in Optimum Performance Laminar Chromatography (OPLC). However, further details about this special method will not be discussed here.

An essential practical point is the importance of working with TLC plates with a small particle size distribution. This can be achieved by using high-performance thin layer plates. Moreover, the stationary phase should be homogenously packed,

which argues against preparing plates yourself and for purchasing industrially manufactured products.

If possible one should also use a solvent with low diffusivity in order to minimize zone broadening. In any case, development should always take place over the optimum separation distance [6]. Belenkii recommends using plates with $d_{\rm p}=10~\mu{\rm m}$ and a development length of $z_{\rm f}=10~\rm cm$ for substances of low molecular weight and layers with $d_{\rm p}=5~\mu{\rm m}$ and a development length of $z_{\rm f}=5~\rm cm$ for substances of higher molecular weight [12].

The D term is minimized if the sample to be separated has a large stationary phase diffusion coefficient (D_s). This is more often the case in partition chromatography than in adsorption chromatography.

Van Deemter plots for layers prepared with particles smaller than 10 μ m show constantly rising lines instead of the typical hyperbolic curves. Obviously, only the *B* term (due to molecule diffusion in the mobile phase) contributes to peak broadening for these layers. All other contributions to band broadening can be neglected. Thus $H_{\rm M}$ for small particle sizes ($d_{\rm p} < 10~\mu{\rm m}$) is reduced to the following [28]:

$$H_{\rm M} = \frac{B}{\chi}(z_{\rm f} + z_0).$$

This equation demonstrates that a low plate height is achievable only for separations over a short distance. Therefore plates with larger particles must be used for separations over longer distances. In general, after choosing the plate material and optimum mobile phase, the analyst can only improve a separation by choosing an optimum development length.

2.13 Separation Number

A separation method that satisfactorily separates many substances must be rated higher than a separation system that can separate only a few substances. The separation number introduced by Kaiser provided the basis for an evaluation of the separation capacity of chromatographic systems [32]. The separation number describes the number of zones that can be separated with a resolution of 4σ . In TLC this corresponds to the situation where the distance between two adjacent peaks in a densitogram is equal to the sum of their peak widths at half height. The peak width at half height $w_{\rm H}$ can be expressed as a linear function of the development length. To calculate the separation number for TLC, Kaiser used an average peak width at half height value obtained by summing the peak width at half height for a sample zone at the origin and a sample zone at the solvent front obtained by extrapolation from a series of real peak widths recorded in a densitogram:

$$\overline{w_{\rm H}} = \frac{1}{2} (w_{\rm H(start)} + w_{\rm H(front)}).$$

The average effective separation distance is calculated correspondingly as

$$\overline{z_{\mathbf{M}}} = \frac{1}{2}(z_{\mathbf{f}} - z_{\mathbf{0}}),$$

with the definition for the separation number (SN)

$$SN \equiv \frac{\overline{z_M}}{\overline{w_H}} - 1$$

or

$$SN = \frac{(z_f - z_0)}{w_{H(start)} + w_{H(front)}} - 1.$$
 (2.26)

The separation number describes the number of separated zones over the separation distance $(z_f - z_0)$. To calculate separation numbers, the peak widths at half height can be determined according to the relation

$$N' = \left(\frac{z_{\rm S}}{\sigma_{\rm S}}\right)^2 = 5.545 \frac{z_{\rm S}^2}{w_{\rm HS}^2},$$

which proposes a linear relationship between the separation distance and the peak width at half height:

$$w_{\rm H} = w_{\rm H(start)} + w_{\rm HS} = w_{\rm H(start)} + \sqrt{\frac{5.545}{N'_{\rm real}}} z_{\rm S}.$$

Dye	Separation distance (mm)	W _H (mm)
Ciba F-II	0.92	0.73
Indophenol	2.57	0.83
Ariabel red	6.96	1.01
Sudan blue	9.53	1.10
Sudan IV	16.9	1.83
Dimethyl-aminobenzene	24.9	2.11
Front	34.8	

As an example of the calculation, the separation of a dye mixture on silica gel (Fig. 2.11) provides the following values:

The slope of the plot of the peak width at half height against the separation distance yields a slope a=0.0611 (Fig. 2.16). The intercept, calculated as peak

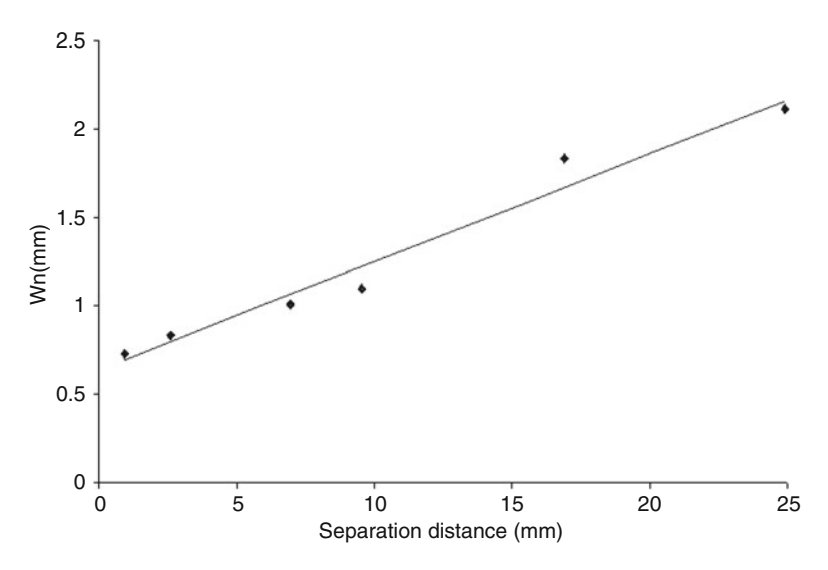


Fig. 2.16 Plot of the peak width at half height against separation distance for six dyes (CAMAG dye mixture, see Fig. 2.11). From the slope, the real plate number was calculated as N' = 1486. The sample application zone width was calculated from the intercept: $W_{\text{H(Start)}} = 0.64$ mm

width at half height $w_{\rm H(start)}$, is 0.64 mm. The real plate number is calculated from the slope as

$$N'_{\text{real}} = \frac{5.545}{a^2} = 5.545 \left(\frac{z_{\text{f}} - z_0}{w_{\text{H(Front)}} - w_{\text{H(Start)}}} \right)^2, \tag{2.27}$$

which takes into account zone broadening during the separation process.

$$N'_{\text{real}} = \frac{5.545}{a^2} = \frac{5.545}{0.06109^2} = 1,486$$

The peak width at half height for a compound migrating with the solvent front is calculated as

$$w_{\rm H(front)} \sqrt{\frac{5.545}{N'}} (z_{\rm f} - z_0).$$

With the experimental total separation distance of $(z_f-z_0)=38$ mm it follows that

$$w_{\rm H(front)} = w_{\rm H(start)} + \sqrt{\frac{5.545}{1486}} 34.8 \,\mathrm{mm} = 2.77 \,\mathrm{mm}.$$

Combining (2.26) and (2.27) with $5.545 = 4\ln(4)$ provides an expression for the separation number [32]:

$$SN = \frac{1}{2} \sqrt{\frac{N'_{\text{real}}}{\ln(4)}} \frac{w_{\text{H(Front)}} - w_{\text{H(Start)}}}{w_{\text{H(Front)}} + w_{\text{H(Start)}}} - 1. \tag{2.28}$$

For the dye mixture a separation number SN = 9 is obtained, a value that is fairly typical for TLC. Maximum separation numbers are achieved by making application zones as small as possible. With the chosen separation system, it is no longer possible to influence sample diffusion. However, spot geometry can be optimized by using appropriate equipment.

2.14 Real Plate Height

The theory of zone broadening is based on the unrealistic assumption that zone broadening only depends on processes that occur development. To account for the unavoidable zone broadening during sample application, the plate height must be corrected for zone broadening during sample application. This is described as a real plate height $H_{\rm real}$. Kaiser suggested a simple and practical method for determining real plate heights [29–32]. The analyte peak width at half height ($w_{\rm HS}$) is calculated as the sum of the application width at half height ($w_{\rm H(start)0}$) and the signal width ($w_{\rm Hreal}$) caused by chromatographic development:

$$w_{\text{Hreal}} = w_{\text{H(start)}} + w_{\text{HS}}.$$

For the real plate height

$$H_{\text{real}} = \frac{z_{\text{f}} - z_{0}}{N'_{\text{real}}} \tag{2.29}$$

and substituting for N'_{real}

$$H_{\text{real}} = \frac{\left(w_{\text{H(front)}} - w_{\text{H(start)}}\right)^2}{5.545(z_f - z_0)}.$$
 (2.30)

In the case of the CAMAG dye mixture, the real plate height is calculated as $H_{\rm real}=23.5~\mu m$.

In order to compare TLC methods, the experimentally determined real plate heights should be quoted according to (2.30).

References 51

References

 Fried B, Sherma J (1999) Thin layer chromatography – techniques & applications. Dekker, New York

- 2. Fried B, Sherma J (eds) (1996) Practical thin layer chromatography: a multidisci-plinary approach. CRC, Boca Raton
- 3. Poole CF (2001) In: Nyiredy Sz (ed) Planar chromatography. A retrospective view for the third millennium. Springer, Budapest
- Sherma J, Fried B (eds) (1995) Handbook of thin-layer chromatography, 2nd edn. Dekker, New York
- 5. Grinberg N (1990) Modern thin layer chromatography. Dekker, New York
- 6. Geiss F (1987) Fundamentals of thin layer chromatography. Huethig, New York
- 7. Poole CF (2003) The essence of chromatography. Elsevier, Amsterdam
- 8. Hahn-Deinstrop E (2007) Applied thin layer chromatography: best practice & avoidance of mistakes, 2nd edn. Wiley, New York
- Wagner H, Bladt S (1996) Plant drug analysis thin layer chromatography atlas. Springer, New York
- 10. Frey HP, Zieloff K (1993) Quantitative and qualitative thin layer chromatography (Grundlagen and Praxis). Chemie, Weinheim
- 11. Kraus Lj, Koch A, Hoffstetter-Kuhn S (1995) Thin layer chromatography. Springer, Berlin
- 12. Belenkii B, Kurenbin O, Litvinova L, Gankina E (1990) A new approach to optimization in TLC. J Planar Chromatogr 3:340–347
- 13. Reuke S, Hauck HE (1995) Thin-layer chromatography as a pilot technique for HPLC demonstrated with pesticide samples. Fresenius J Anal Chem 351:739–744
- 14. Bate-Smith EC, Westall RG (1950) Chromatographic behavior and chemical structure in some naturally occurring phenolic substances. Biochim Biophys Acta 4:427-440, 2. The tea catechins 441–444
- Canić VD, Perišić-Janjić NU (1974) Separation of aliphatic and aromatic organic acids on starch thin-layers. Chromatographic behaviour and chemical structure. Z Anal Chem 270:16–19
- Funk W, Glück V, Schuch B, Donnevert G (1989) Polynuclear aromatic hydrocarbons (PAHs): charge transfer chromatography and fluorimetric determination. J Planar Chromatogr 2:28–32
- Funk W, Donnevert G, Schuch B, Glück V, Becker J (1989) Quantitative HPTLC determination of six polynuclear aromatic hydrocarbons (PAH) in water. J Planar Chromatogr 2:317–319
- Poole CF, Fernando WPN (1992) Some musings on the measurement and interpretation of theoretical plate height in thin layer chromatography. J Planar Chromatogr 5:323–333
- 19. Snyder LR (1968) Principles of adsorption chromatography. Dekker, New York
- Guiochon G, Bressolle F, Siouffi A (1979) Study of the performance of thin-layer chromatography IV. Optimization of experimental conditions. J Chromatogr Sci 17:368–386
- 21. Jänchen D (1977) In Zlatkis A, Kaiser RE (eds) HPTLC high performance thin-layer chromatography. Elsevier, Amsterdam, pp 129–145
- 22. Guiochon G, Siouffi A, Engelhardt H, Haláz I (1978) Study of the performance of thin-layer chromatography I. A phenomenological approach. J Chromatogr Sci 16:152–157
- Guiochon G, Siouffi A (1978) Study of the performance of thin-layer chromatography II.
 Band broadening and the plate height equation. J Chromatogr Sci 16:470

 –481
- Guiochon G, Siouffi A (1978) Study of the performance of thin-layer chromatography III.
 Flow velocity of the mobile phase. J Chromatogr Sci 16:598–609
- Guiochon G, Körösi G, Siouffi A (1980) Study of the performance of thin-layer chromatography V. Flow rate in reversed phase plates. J Chromatogr Sci 18:324–329
- Belenkii BG, Nesterov VV, Gaukina ES, Semirnov MM (1967) A dynamic theory of thin layer chromatography. J Chromatogr 31:360–368

- Belenkii BG, Kolevov UI, Nesterov VV (1975) Theory of thin-layer chromatography. Effect
 of the structure of the adsorption layer on spreading of spots. J Chromatogr 107:265–283
- 28. Siouffi AM, Bressolle F, Guiochon G (1981) Optimization in thin-layer chromatography. Some practical considerations. J Chromatogr 209:129–147
- 29. Knox JH (1976) In Simpson CF (ed) Practical high performance liquid chromatography. Heyden, London
- 30. Giddings JC (1965) Dynamics of chromatography, Part I. Dekker, New York
- 31. Saunders DL, Snyder LR (1970) In: Zlatkis A (ed) Advances in chromatography. Chromatography symposium, Houston, pp 307–321
- 32. Zlatkis A, Kaiser RE (1977) HPTLC High performance thin-layer chromatography. Elsevier, Amsterdam, pp 15–38
- 33. C. F. Poole, S. K. Poole, Multidimensionality in planar chromatography, J. Chromatogr. A 703 (1995) 573 612

Chapter 3 The Stationary Phase in Thin-Layer Chromatography

Uncoated Silica gel is the dominant stationary phase used in thin-layer chromatography (TLC). This constitutes an important difference to HPLC where most separations are carried out on chemically bonded phases by partition chromatography in the reversed-phase mode. Normal-phase separations by HPLC on inorganic oxide sorbents are uncommon due in part to poor retention reproducibility resulting from the difficult to avoid adsorption of trace amounts of water from the mobile phase. In contrast to HPLC, therefore, there are no significant problems in using normal phase systems for TLC.

On the contrary, adsorption chromatography is far more important in TLC than partition chromatography. This is clearly demonstrated by statistically evaluating 1,752 relevant publications from 1979 to 1985 (see Table 3.1). Silica gel layers are preferred over all other stationary phases [1]. Besides silica gel, aluminium oxide, kieselguhr, magnesium oxide, and magnesium silicate (Florisil®) are also among the most frequently used adsorption stationary phases. Furthermore, under certain circumstances, kieselguhr and silica gels can also act as chromatographic distributors if the mobile phase obviously contains a certain amount of water. Chemically bonded, silica-based phases and even silica coated with a thick film of solvent are suitable for partition chromatography. Retention on cellulose layers and papers is largely dominated by partition into an adsorbed water matrix. Modified cellulose phases or synthetic organic ion-exchange resins containing ionic groups are used for ion-exchange chromatography. Polyamide phases can act as ion exchangers as well as partition systems. Polysaccharide and polyamide gels, most commonly dextrans, are used for separations by size-exclusion chromatography. Exclusion chromatography constitutes a particular form of TLC tailor-made for the separation of polymers, most often using dextran or polyamide gels.

Phase type	TLC (%)	HPTLC (%)
Silica gel G and H	73.3	73.5
Cellulose	5.2	3.1
Polyamide	1.8	1.4
Bonded phases	5.5	22.0
Aluminium oxide	2.6	_
Kieselguhr	0.3	_
Gels	0.4	_

Table 3.1 The stationary phases (TLC and HPTLC) used in the years 1979–1985 [1]

3.1 Activating and Deactivating Stationary Phases

The activity of the stationary phase is the controlling factor for normal-phase separations on inorganic oxide layers. The sorbent activity of the stationary phase is made up of two contributions: an energy term and the specific surface area. The adsorption energy is determined by interactions with specific sites of different energy, the distribution of these sites on the surface of the adsorbent, and the accessible surface area of the adsorbent. The active sites may bind reversibly with water or other polar contaminants or components of the mobile phase modifying their interactions with sample components. This process is sometimes referred to as deactivation, and the deactivating agents are called modifiers. Water is the most commonly used modifier in normal-phase chromatography, but other strongly polar substances such as glycerine, glycol, or substances with strongly polar (particularly hydrogen bonding) functional groups can also act as modifiers. On inorganic oxide stationary phases, solvents of low polarity such as hexane are unable to absorb sufficient water to obtain a stable deactivated layer. In this case acetonitrile is a better choice of modifier. For non-selective adsorbents such as activated carbon, suitable modifiers are non-polar solvents such as toluene or stearic acid. Incompatibility with spectroscopic detection is one of the several reasons why carbon adsorbents are little used in TLC.

A stationary phase is completely deactivated, when a modifier occupies all surface-active sites. The chromatographic process is then (usually) dominated by a partition mechanism. In TLC the concentration of modifier in the stationary phase is mostly established before separation via the gas phase. For this purpose, the layer is first activated at temperatures above 100°C and then stored at ambient humidity so that the layer can absorb the appropriate amount of water from the gas phase. Alternatively, the layer can be deactivated from the liquid phase. However, to produce a defined activity the plate can also be preactivated by a flow medium. For this purpose, the plate is developed with a solvent that contains the desired deactivator concentration. An additional benefit of this method is the simultaneous decontamination of the stationary phase, as low polarity residues acquired from the laboratory air or from the plastic packaging of the plate are carried along with the solvent front gradients. Label adhesives are also often a source of contamination of the stationary phase.

In principle a large number of active centres will not necessarily result in better separations. In practice the opposite is often the case. Alterations in activity can even cause reversal of the migration sequence. The surface energy of the layer should be constant at all positions in the stationary phase. In addition, the plate must be evenly coated and be undamaged by cracks.

It is difficult to measure the surface energy, which is mostly determined by the chromatographic result, and consequently it is hard to compare the adsorption strength of the various stationary phases with one another. In general, it is impossible to answer the question whether silica gel is more active than aluminium oxide.

3.2 Snyder's Adsorption Model

Snyder [2] devised an adsorption model for TLC that accounts for the contribution of intermolecular interactions to the adsorption process and the complementary contributions of the adsorbent and mobile phase to the retention mechanism. In adsorption chromatography, the dimensionless partition coefficient (thermodynamic adsorption coefficient) is expressed by the following relationship:

$$K = \frac{c_{\rm S}}{c_{\rm m}},$$

where

 $c_{\rm S}$ sample concentration in the stationary phase

 $c_{\rm m}$ sample concentration in the mobile phase

The real adsorption coefficient K_a is often not dimensionless and is expressed in the units of cm³/g:

$$K_{\rm a} = \frac{c_{\rm S}}{c_{\rm m}} V_{\rm a},$$

where

K_a adsorption coefficient

 $c_{\rm S}$ concentration of sample in the adsorbed solvent layer

 $c_{\rm m}$ concentration of sample in the mobile phase

 $V_{\rm a}$ volume of the adsorbed monolayer per gram of adsorbent

The parameter V_a is the volume of a monolayer at which the active sites of the adsorbent are occupied by solvent molecules. The volume of the solvent monolayer is proportional to the active surface of the stationary phase. The greater the value of V_a , the higher the activity of the stationary phase. After complete deactivation

(when the whole active surface is occupied, e.g. by water), $V_{\rm a}$ will be equal to zero, resulting in $K_{\rm a}=0$ and $R_{\rm f}=l$ (which makes $R_{\rm m}=\infty$) [3]. The "thermodynamic adsorption coefficient" describes the difference between the adsorption energy of the sample molecules $(E_{\rm p})$ and the solvent molecules $(E_{\rm m})$, which displaced the sample molecules from the surface:

$$\lg K - \lg V_a = \lg \frac{c_S}{c_m} = \frac{{\mu_S}^0}{2.3RT} - \frac{{\mu_m}^0}{2.3RT} = E_p - E_m.$$

The adsorption energy of a sample molecule is a function of the sample molecule f(p) itself. This function includes the polarity of the compound and its structure. Its surface energy $f(A_i)$ must also be taken into consideration as a function of the stationary phase surface:

$$E_{\rm p} = f(A_{\rm i})f(p) = \alpha_{\rm a}S^0.$$

The total adsorption energy for all solvent molecules $E_{\rm m}$ depends on the surface energy of the stationary phase $f(A_{\rm i})$ as well as on the properties of the mobile phase $f({\rm m})$. In this equation $\alpha_{\rm a}$ expresses the adsorbent activity and is given as the value $\alpha_{\rm a}=1$ for an aluminium oxide adsorbent with the highest activity; the highest activated aluminium oxide adsorbent; S^{O} represents the sample's adsorption energy:

$$E_{\rm m} = f(A_{\rm i})f(m) = \alpha_{\rm a}\varepsilon^0 A_{\rm P}.$$

The surface size (i.e. the space needed by a sample molecule on the adsorbent surface) is abbreviated to A_P . The solvent parameter ε^0 describes the characteristics of the mobile phase. For the logarithmic adsorption coefficient, it follows

$$\lg K_{\mathbf{a}} = f(A_{\mathbf{i}})[f(p) - f(m)] + \lg V_{\mathbf{a}}$$

with

$$f(A_i)[f(p) - f(m)] = \alpha_a(S^0 - \varepsilon^0 A_P)$$

and by introducing the expression for the $R_{\rm m}$ value gives

$$R_{\rm m} = \lg \frac{V_{\rm S}}{V_{\rm m}} + \lg K_{\rm a}$$

from which the fundamental relationship for adsorption chromatography is obtained [2, 3]:

$$R_{\rm m} = \lg \frac{V_{\rm S}}{V_{\rm m}} V_{\rm a} + \alpha_{\rm a} (S^0 - \varepsilon^0 A_P). \tag{3.1}$$

The weight of the stationary phase is easier to determine than its volume. The quotient $V_{\rm S}/V_{\rm m}$ in Snyder's relationship stands for the volumes of the stationary and mobile phases and can be replaced by their weights $W_{\rm a}/V_{\rm P}$, where $W_{\rm a}$ indicates the weight of the TLC layer (g) and $V_{\rm P}$ the solvent-accessible pore volume. One gram of the TLC layer can be covered by a monolayer of solvent having a volume $V_{\rm a}$. Thus, $V_{\rm a}$ is an appropriate parameter to describe the layer activity. It is zero if the sorbent is completely deactivated (and the $R_{\rm f}$ value then equals 1). Therefore, Snyder's relationship for adsorption chromatography can also be written as [2, 3]

$$R_{\mathrm{m}} = \lg rac{W_{\mathrm{a}}}{V_{\mathrm{P}}} V_{\mathrm{a}} + lpha_{\mathrm{a}} (S^0 - arepsilon^0 A_{\mathrm{P}}),$$

where

 $V_{\rm a}$ volume of the adsorbed solvent monolayer per gram of adsorbent

 $W_{\rm a}$ weight of the TLC layer (g)

 $V_{\rm P}$ pore volume (cm³) freely accessible to the solvent

 α_a energy components of the activity parameters ($\alpha_a=1$ for most active aluminium oxide)

 S^0 adsorption energy of the sample

 ε^0 solvent parameter

 $A_{\rm P}$ space needed by a sample molecule at an adsorption centre

The greater the value of V_a , the greater the stationary phase activity. If V_a is zero after complete deactivation, it follows that $R_m = -\infty$, and the R_f value is 1. In this case, all the sample molecules will be transported through the layer without delay, and no more adsorption will take place by the stationary phase.

The practical significance of Snyder's relationship (3.1) is relatively low because "trial and error" is generally much quicker for solving problems than calculating activity parameters. Moreover, experimental activity and separation have nothing to do with one another. It is a mistake to believe that highly active adsorbents can separate better than deactivated materials. The value of the equation lies more in the possibility of standardizing adsorbents, because $R_{\rm m}$ values for similar substances on an identical adsorbent are linearly related.

According to Geiss, to characterize new stationary phases, relative values of α and $\lg(V_aV_s/V_m)$, indicated here as α' and $\lg(V_aV_s/V_m)'$, should be determined by the separation of polyphenylenes with hexane at various relative humidity levels [3]. The measured R_m values when plotted against a relative measure, e.g. the number of rings, allows values for α' to be calculated from the slope and $\lg(V_aV_s/V_m)'$ from the intercept (Fig. 3.1). Such values can be quickly determined and are satisfactory for comparing the adsorption strength of new stationary phases for TLC.

3.3 Layer Characteristics

The first commercially available TLC plates were prepared with adsorbent particles approximately $20 \mu m$ in diameter with a relatively broad particle size distribution.

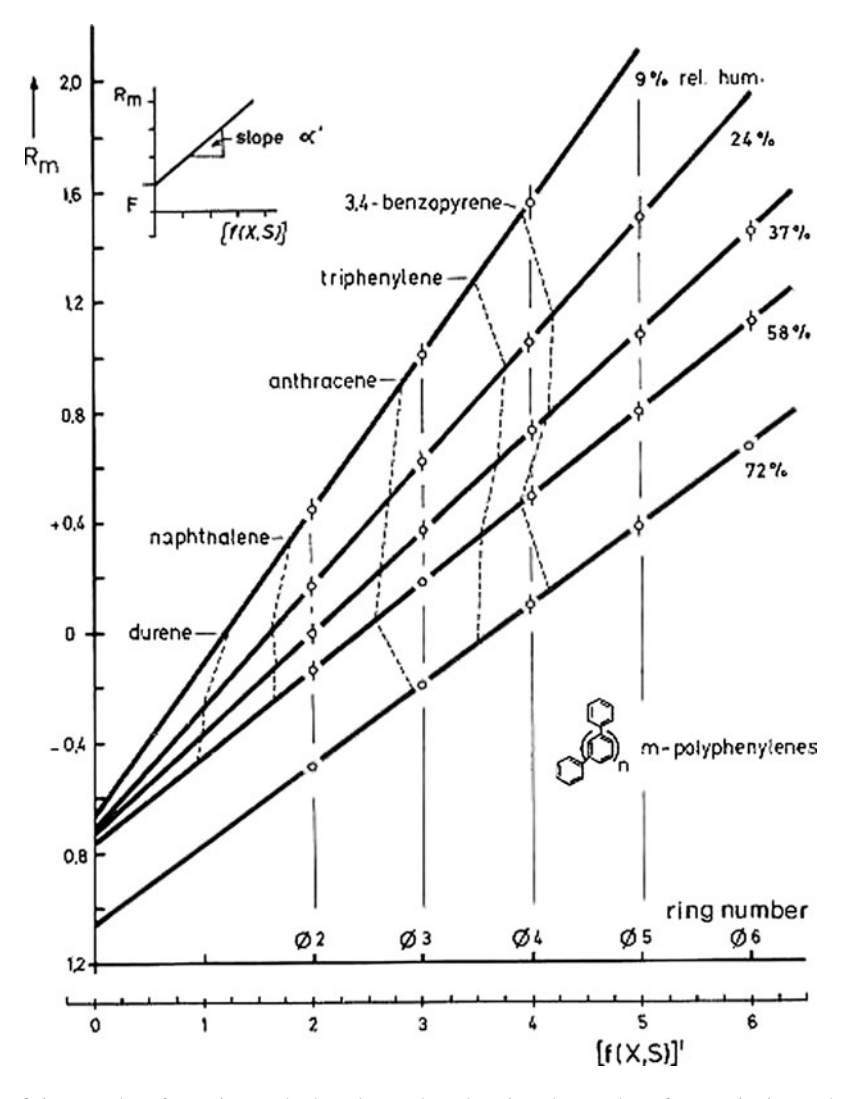


Fig. 3.1 $R_{\rm m}$ values for various polyphenylenes plotted against the number of aromatic rings. Their slopes correspond to their Geiss α' value. The intercept equals $\lg(V_{\rm a}V_{\rm S}/V_{\rm m})'$ (From [3] with permission. © Hüthig.)

Stahl, one of the founders of modern TLC, used layers of this type [4]. Plates for preparative layer chromatography (PLC) had even larger particle sizes than indicated above.

Over the period 1968–1973, intensive efforts were made to improve the separation characteristics of the layers described above [1]. The concept of "high-performance thin-layer chromatography" (HPTLC) first appeared in 1973. In this technique,

Plate size 20×20 10×10 6×3.6 (c Plate thickness $100-250$ $100-200$ 10 (μm) Particle size (μm) $8-10$ $6-8$ None Application volume(μL) $1-5$ $0.1-5$ $0.01-0.1$ Separating distance (cm) $6-15$ $3-7$ $1-3$ Max. spot diameter of application (mm) $3-6$ $1-1.5$ $0.5-1$ Separating time (min) $30-200$ $3-20$ $1-5$ Separating distance (cm) $10-15$ $3-8$ $1-3$ Plate height (μm) $35-75$ $23-25$ $-$ Tracks per plate 10 $9-18$ 6 Detection limits in reflectance (ng) $1-5$ $0.5-1$ 0.5 Detection limits in fluorescence (pg) $50-100$ $5-10$ 5	Parameter	TLC	HPTLC	UTLC
Particle size (μm) 8–10 6–8 None Application volume(μL) 1–5 0.1–5 0.01–0.1 Separating distance (cm) 6–15 3–7 1–3 Max. spot diameter of application (mm) 3–6 1–1.5 0.5–1 Separating time (min) 30–200 3–20 1–5 Separating distance (cm) 10–15 3–8 1–3 Plate height (μm) 35–75 23–25 – Tracks per plate 10 9–18 6 Detection limits in reflectance (ng) 1–5 0.5–1 0.5	Plate size	20×20	10 × 10	6 × 3.6 (cm)
Application volume(μL) 1–5 0.1–5 0.01–0.1 Separating distance (cm) 6–15 3–7 1–3 Max. spot diameter of application (mm) 3–6 1–1.5 0.5–1 Separating time (min) 30–200 3–20 1–5 Separating distance (cm) 10–15 3–8 1–3 Plate height (μm) 35–75 23–25 – Tracks per plate 10 9–18 6 Detection limits in reflectance (ng) 1–5 0.5–1 0.5	Plate thickness	100-250	100-200	10 (μm)
Separating distance (cm) 6–15 3–7 1–3 Max. spot diameter of application (mm) 3–6 1–1.5 0.5–1 Separating time (min) 30–200 3–20 1–5 Separating distance (cm) 10–15 3–8 1–3 Plate height (μm) 35–75 23–25 – Tracks per plate 10 9–18 6 Detection limits in reflectance (ng) 1–5 0.5–1 0.5	Particle size (µm)	8-10	6–8	None
Max. spot diameter of application (mm) 3–6 1–1.5 0.5–1 Separating time (min) 30–200 3–20 1–5 Separating distance (cm) 10–15 3–8 1–3 Plate height (μm) 35–75 23–25 – Tracks per plate 10 9–18 6 Detection limits in reflectance (ng) 1–5 0.5–1 0.5	Application volume(µL)	1–5	0.1-5	0.01 - 0.1
Separating time (min) $30-200$ $3-20$ $1-5$ Separating distance (cm) $10-15$ $3-8$ $1-3$ Plate height (μ m) $35-75$ $23-25$ $-$ Tracks per plate 10 $9-18$ 6 Detection limits in reflectance (ng) $1-5$ $0.5-1$ 0.5	Separating distance (cm)	6–15	3–7	1–3
Separating distance (cm) $10-15$ $3-8$ $1-3$ Plate height (μ m) $35-75$ $23-25$ $-$ Tracks per plate 10 $9-18$ 6 Detection limits in reflectance (ng) $1-5$ $0.5-1$ 0.5	Max. spot diameter of application (mm)	3–6	1-1.5	0.5-1
Plate height (μm) 35–75 23–25 – Tracks per plate 10 9–18 6 Detection limits in reflectance (ng) 1–5 0.5–1 0.5	Separating time (min)	30-200	3-20	1–5
Tracks per plate 10 9–18 6 Detection limits in reflectance (ng) 1–5 0.5–1 0.5	Separating distance (cm)	10-15	3–8	1–3
Detection limits in reflectance (ng) 1–5 0.5–1 0.5	Plate height (µm)	35–75	23-25	_
· 6/	Tracks per plate	10	9–18	6
Detection limits in fluorescence (pg) 50–100 5–10 5	Detection limits in reflectance (ng)	1–5	0.5-1	0.5
	Detection limits in fluorescence (pg)	50–100	5–10	5

Table 3.2 Characteristic properties of layers used for TLC [5, 6]

layers with particle sizes between 5 and 15 µm and a relatively narrow particle-size distribution were used. Results obtained by using this new kind of plate were published by Zlatkis and Kaiser in 1977 [5].

Comparisons between TLC and HPTLC plates have definitely been decided in favour of HPTLC (Table 3.2). On HPTLC layers the detection limits for both absorption and fluorescence are lower than for TLC layers [6, 7]. Development times are also shorter than for TLC layers and resolution is about 20% better. Selectivity, though, is independent of particle size.

At the beginning of 1980, Andreev published an article with data from his "optimum" TLC separating layer [8]. Andreev suggested reducing the layer thickness to less than 15 μ m, well below the 100 μ m typical of conventional HPTLC plates. Almost 20 years later, Merck introduced ultra-thin layers with a layer thickness of 10 μ m, a specific surface of 350 m²/g, and a specific pore volume of 0.3 mL/g as UTLC (ultra-thin-layer chromatography) [9]. All three plate types (TLC, HPTLC, and UTLC) are commercially available today. The sale of HPTLC plates are increasing but traditional TLC plates still dominate the market for precoated plates: 80% of all plates sold worldwide are TLC plates. Only the future will tell whether the market will accept HPTLC and UTLC plates.

All stationary phases in TLC, UTLC, or HPTLC can be sorted in ascending order based on their polarity: RP-18, other chemically bonded silica gel phases, paper, cellulose, starch, gypsum (CaSO₄), silica gel (SiO₂), fluorisil (magnesium silicate), magnesium oxide (MgO), and aluminium oxide (Al₂O₃). In order to characterize the properties of these layers, a set of parameters discussed below are important.

3.3.1 Layer Thickness (d_f)

The layer thickness for modern TLC and HPTLC plates lies between 0.1 and 0.25 mm. For preparative TLC, layers of 1.0–2.0 mm are available. The layer

thickness for UTLC is $10 \mu m$. Employing thinner layers decreases the development time. The mobile phase velocity is $1.5{\text -}2.5$ times faster for HPTLC layers of $0.1 \mu m$ thickness compared with those of $0.2 \mu m$. The separated zones are narrower resulting in lower detection limits both in absorption and fluorescence by a factor of about $1.1{\text -}1.5$ [10]. The layer thickness does not influence the plate number or the selectivity of the stationary phase.

3.3.2 Average Particle Size (d_p)

Historically, classical TLC plates started with an average particle size of about 30 μ m, which was gradually reduced over time to values around 9 μ m for modern TLC plates. HPTLC plates have an average particle size between 6 and 8 μ m. As explained above, a reduction in average particle size does not necessarily lead to an increase in the separation capacity. On the contrary, plates with particle sizes around 3 μ m exhibit a lower separation performance than plates prepared with 5 μ m particles when capillary forces are responsible for maintaining the mobile phase velocity. This is due to the reduction in the velocity of the mobile phase associated with the decrease in particle size accompanied by an increase in analyte diffusion [11].

3.3.3 Particle Size Distribution

The particle size distribution is just as important, if not more so, than the average particle size in determining the layer quality (Fig. 3.2). As a general rule, the narrower the particle size distribution is, the more homogeneous is the packing density of the layer, and the higher the layer performance is. The principal difference in the properties of precoated HPTLC layers compared with precoated TLC layers is the narrower particle size distribution of the former. The particle size distribution affects the mobile phase velocity, since an increase in the particle size distribution results in an increase in the fraction of small particles in the layer [11].

3.3.4 Specific Surface Area (O_s)

The specific surface areas of TLC sorbents can be measured and fall into the range from 100 to $500 \text{ m}^2/\text{g}$. According to Snyder's relationship [1, 3], the substance retention increases linearly with an increase in the value of the specific surface area. The precondition for this is that the sample has free access to the active adsorption centres, which depends on the pore size of the adsorbent.

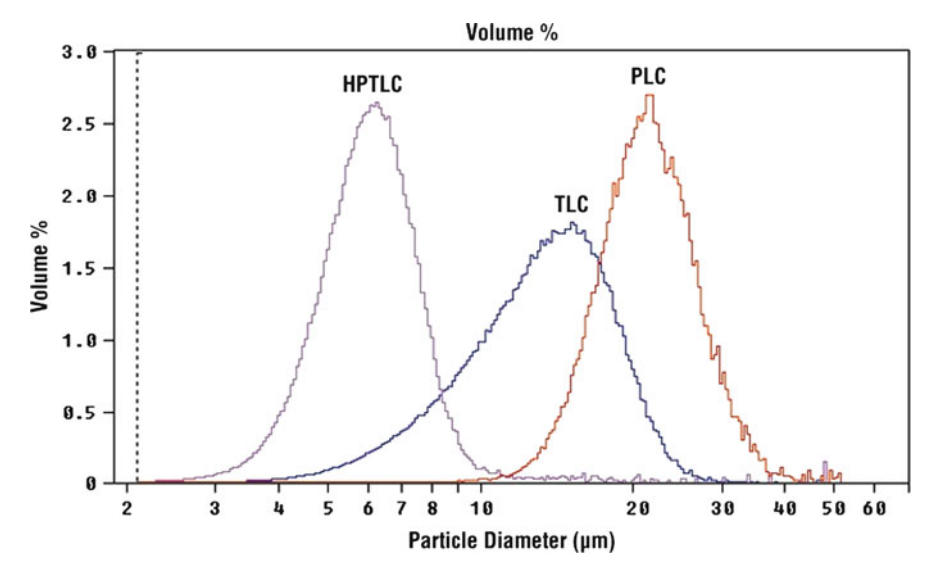


Fig. 3.2 Typical particle size distribution for TLC, HPTLC, and PLC layers (With permission from Merck, Darmstadt, Germany.)

3.3.5 Pore Volume (V_p)

For porous materials the pore volume is the volume of liquid (mobile phase) required to fill the internal pores for 1 g of stationary phase. It is closely linked with the specific surface area and pore diameter and lies between 0.8 and 1.2 mL/g for TLC sorbents (except for monolithic UTLC plates which have a pore volume of 0.3 mL/g). The mobile phase velocity decreases with increasing pore volume [11].

3.3.6 Average Pore diameter (P_d)

The average pore diameter for TLC sorbents is between 5 and 10 nm. The pore size distribution is more important, however, than the average pore diameter itself. Ideally, the variance for the distribution of pore sizes should be small. The average pore diameter is calculated by [12]

$$P_{\rm d} = 4 \frac{V_{\rm p}[\rm mL/g]}{O_{\rm s}[\rm m^2/g]} [\rm nm],$$

where

 $V_{\rm p}$ pore volume

 $O_{\rm s}$ specific surface area

All commercial TLC plates are standardized according to this parameter. Various characteristics of the most important layer materials will be presented later in detail. A good overview is to be found in Grinberg [1].

3.4 The Most Important Stationary Phases in TLC

3.4.1 Aluminium Oxide

Aluminium oxide for TLC is derived from clay by dehydration at 500° C. Like silica gel, it belongs to the group of ionic-polar adsorbents but has a slightly lower activity level than silica gel. The average particle size for commercially available Al_2O_3 sorbents for TLC lies between 5 and 40 μ m with a specific surface area of 150-200 m²/g. The pore volume lies between 0.1 and 0.4 mL/g, while the average pore size varies from 2 to 35 nm. The average surface concentration of OH groups is about $13 \ \mu$ mol/m². The pore volume and the surface activity can be influenced by the dehydration temperature.

Various surface functional groups are responsible for retention on aluminium oxide layers. Coordinative unsaturated Al³⁺-centres act as Lewis acids for compounds with π -electron systems and other nucleophilic or basic groups. O^{2-} groups in the crystal grid can act as basic centres for acidic functional groups. Furthermore, the polar AlOH group functions as a weak proton donor. Aluminium oxide phases are especially suited to separating aromatic compounds. Aluminium oxide is slightly alkaline (apparent pH 9-10), but during the manufacturing process the apparent pH can be adjusted to neutral (pH 7 - 8) or acid (pH 4-4.5). Acidic aluminium oxide contains remnants of aluminium chloride while basic aluminium oxide contains some sodium aluminates. Only neutral aluminium oxide consists of pure aluminium oxide. The water content is an important parameter for aluminium oxide adsorbents and is adjusted by some manufacturers in order to achieve a defined activity. Gypsum (CaSO₄) or organic polymers, mostly polyacrylamides (homo- or co-polymerisates), are used as binders for the manufacture of TLC plates. Aluminium oxide is an active catalyst and can react with samples containing ketone and ester groups, among others.

3.4.2 Magnesium Silicate

This rarely used adsorbent is commercially available as Florisil[®]. Its polarity lies between that of aluminium oxide and silica gel. It has no known catalytic activity. Florisil[®] is often used in preparative TLC as well as in column chromatography [1].

3.4.3 Silica Gel

Silica gel is by far the most important TLC adsorbent. It is prepared by acid precipitation from sodium silicate (Na₂SiO₃) solution. Control of the surface area is achieved by varying the precipitation conditions and by special after-treatments to attain specific surface areas of 400–800 m²/g. The pore volume is 0.5–1.2 mL/g, and the average pore size lies between 4 and 12 nm. The average surface concentration of OH groups is about 8 µmol/m², corresponding to about 5 OH groups per square millimetre. Gypsum, starch, or organic binders are used to fix the silica gel to a support surface. The sorption characteristics of silica gel are due to surface silanol (SiOH) groups. These are weakly dipolar and strongly hydrogen bonding. Silanol groups activated by impurities in the silica gel matrix behave as weak acids. Silica gel can bind up to three molecular layers of water. The top two layers can be reversibly removed by dry solvents or by heating at 120°C. Above 200°C, silanol groups can irreversibly eliminate water. When heated above 1,000°C silica gel almost completely loses its activity with the disappearance of silanol groups from the surface. Consequently, silica gels should not be heated to above 180°C in the laboratory, if the structural characteristics responsible for retention in TLC are to be retained. The most common silica gel for TLC is "Silica Gel 60" which has a pore size of 6 nm (60 Å). Irregular silica gels are commonly used for layer preparation in a nominal particle size range from 20 to 5 µm for different types of plates (as discussed in the previous section). Layers prepared with spherical particles are manufactured by Merck (Darmstadt, Germany) under the trade name LiChrospher® (Fig. 3.3).

The development times for layers prepared from LiChrospher silica gel particles are about 20% shorter than those for irregularly shaped silica gel particles. Diffusion is partially suppressed giving more compact spots and better resolution (Fig. 3.4). Selectivity is not influenced by the particle shape. DurasilR[®] and Nano-DurasilR[®] are precoated plates manufactured by Macherey-Nagel (Düren, Germany). They have hard, water resistant, and wettable layers on which a pencil can be used to write on their surface without damaging the layer. Similar plates are also available from Whatman (Poole, UK). This company also produces a silica gel 60 material called Partisil[®] K6, an extremely pure silica gel for TLC.

Silica gel layers are often impregnated with various chemicals by dipping, spraying, or as additives included in the mobile phase. Exposing the plate to ammonia, acetic acid, or formic acid vapours in a developing chamber can alter the apparent pH value of the layer. Of the many modifications achievable by using additives [1], the formation of layers impregnated with silver cations or boric acid is particularly noteworthy. Silver-impregnated silica gels can separate lipids that are only differentiated by a single double bond [13]. This process can even separate cis/trans-isomers [14] as well as organic sulphonic acids [13], cholesteryl derivates [15], steroids [16], and chinones [17]. The separation of unsaturated fatty acids using silver-impregnated layers is the most common example of this modification [1]. The separation mechanism is based on the reversible formation of π -complexes

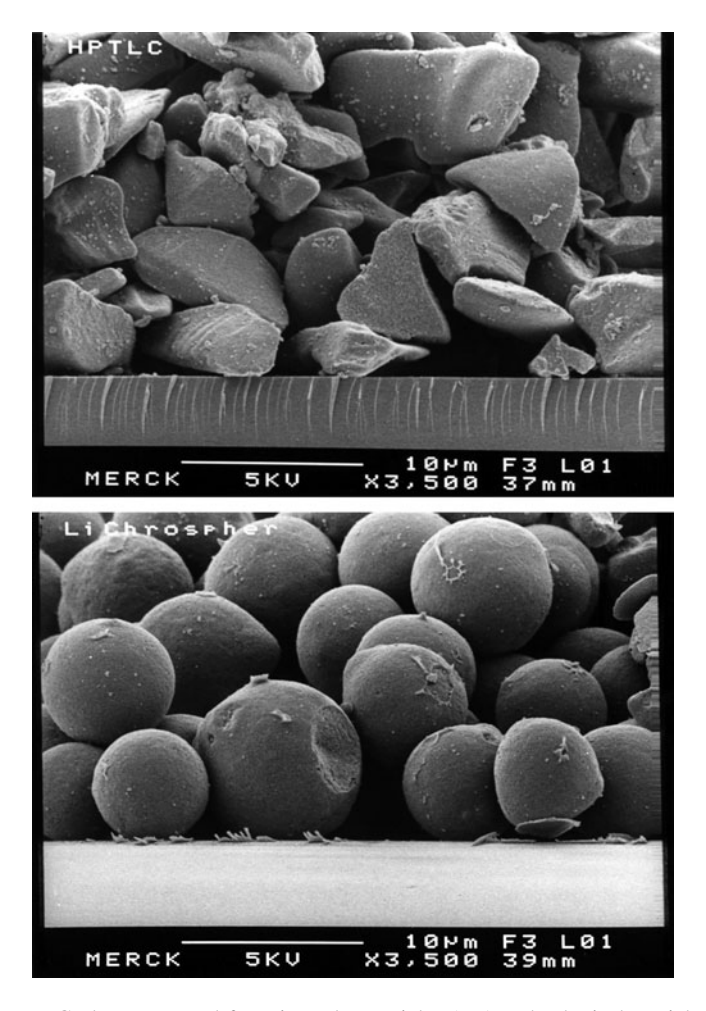


Fig. 3.3 HPTLC plates prepared from irregular particles (*top*) and spherical particles (*bottom*) (Photographs taken by scanning electron microscopy and reprinted with permission from Merck, Darmstadt, Germany.)

between silver ions and isolated double bonds. A silica gel plate can be impregnated with silver nitrate by immersing it in a 3% AgNO₃ solution (methanol-water 93+7, V/V) for about 3 min, followed by drying the plate at 100°C in a drying oven. Silver-impregnated plates must be stored in the dark. They are also stable for a long time when stored in hexane. Analytes containing vicinal hydroxyl groups can be effectively retained on silica gel layers impregnated with boric acid. Triglycerides [18, 19], phospholipids [20, 21], and urethane derivates [22] can also be separated by this technique, which is commonly used in sugar analysis [1, 23]. Silica gel can be impregnated with EDTA for the improved separation of phospholipids [24], cephalosporines [25], tetracyclines [26], as well as heavy metals [27].

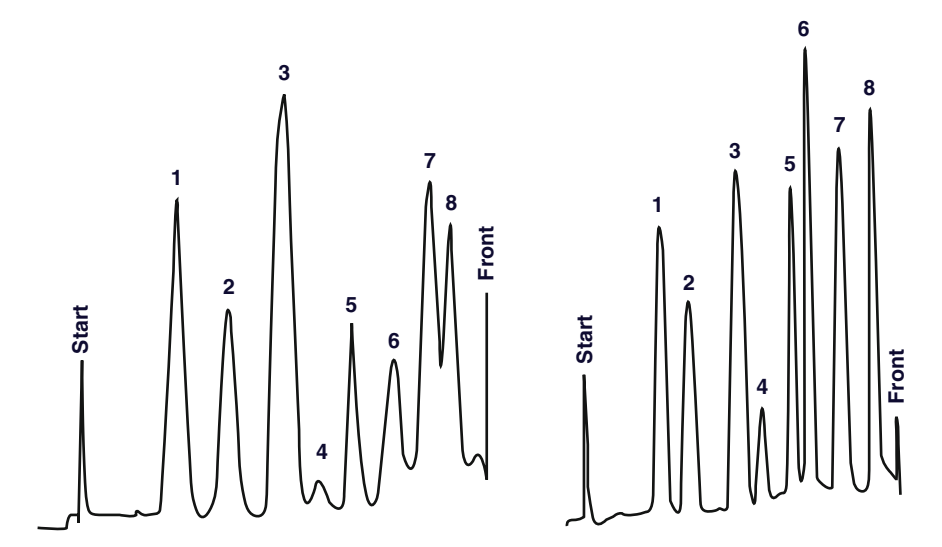


Fig. 3.4 Separation of hexazinone, metoxuron, monuron, aldicarb, azinphos-methyl, prometryn, pyridat, and trifluralin with petroleum ether/acetone (70+30, V/V) as the mobile phase on silica gel KG 60 (*left*) and on LiChrospher[®] KG 60 (*right*) with migration distances of 6 and 5 cm, respectively (Printed with permission from Merck, Darmstadt, Germany.)

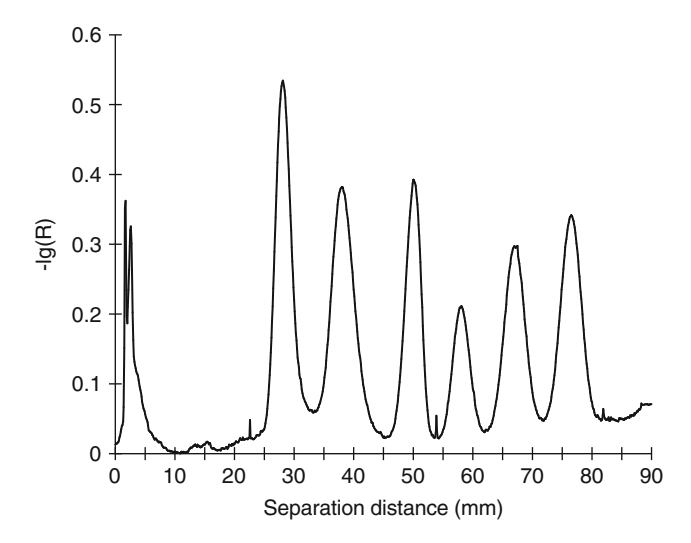


Fig. 3.5 The separation of uric acid (1), cytosine (27), guanine (38), caffeine (51), adenine (59), uracil (68), and thymine (82) on silica gel with isopropanol–toluene–aq. NH₃ (25%) (6+3+1, V/V) as the mobile phase. The hR_f values are given in parentheses

A general overview of separations employing EDTA and boric acid impregnated layers is given in [28]. The separation of polycyclic aromatic hydrocarbons on caffeine-impregnated silica gel layers is also well known [29]. The formation of

charge-transfer complexes is responsible for improving the separations (Fig. 3.5). For enhanced fluorescence detection of lipophilic compounds silica gel layers impregnated with berberine (2 mg/100 mL, dissolved in methanol) have been used [30].

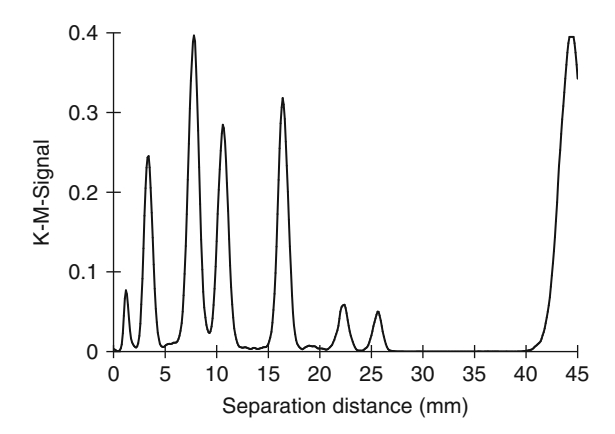
3.4.4 Chemically Bonded Silica Gel Layers

The reactive silanol groups on the silica surface facilitate chemical modification by reaction with organosilane reagents containing different substituent groups [1, 31]. These materials are called chemically bonded phases and are suitable for a wide range of applications. Organic polymers are typically used as binders to stabilize the layers. Silica gel layers reacted with silanes containing hydrocarbon groups are suitable for reversed-phase chromatography with aqueous mobile phases. Commercially available reversed-phase plates are labelled RP-1, RP-2, RP-8, or RP-18 according to the chain length of the major alkane substituent attached to silicon. Amino-, cyano-, and diol-modified layers are also interesting because of their different characteristics to the alkylsiloxane-bonded silica layers. To improve stability, diol, NH₂ and CN groups are bonded to the silica gel matrix via an *n*-propyl group (-CH₂-CH₂-CH₂-). These layers can be eluted with both water (reversed-phase) and non-aqueous (normal-phase) mobile phases. For chemically bonded silica gel layers, this provides the following polarity order (from polar to non-polar):

$$\begin{split} \text{SiO}_2 > -\text{CH}_2 - \text{CH}_2 - \text{CH}_2 - \text{CH}_2 - \text{CH}_2 - \text{CH}_2 - \text{CN}, \\ -\text{CH}_2 - \text{CHOH} - \text{CH}_2 - \text{OH} > -\text{CH}_2 - \text{CH}_3 (\text{RP} - 2) > -(\text{CH}_2)_7 \\ -\text{CH}_3 (\text{RP-8}) > -(\text{CH}_2)_{17} - \text{CH}_3 (\text{RP-18}) \end{split}$$

The various chemically bonded silica gel phases all have different microstructures that have been well characterized [1, 32]. For phases with short chains the bonded substituents are orientated vertically to the silica gel surface while those with longer chain substituents are linked and more disordered. The chain length also affects the accessible pore volume and pore diameter because these groups are of significant size with respect to the space they are located in [32]. The slightly basic amino phase is favoured for separating acids of all kinds, vitamins, phenols, purines, steroids, nucleotides, and sugars (Fig. 3.8). Depending on the pH of the mobile phase the amino group can be neutral or protonated forming a cationic NH₃⁺ group. In the protonated form it behaves as a weak anion exchanger. The amino phase is chemically active and can react with carbonyl groups. Mobile phases containing ketones and aldehydes should not be used for separations with this phase. If, after separation, the aminopropyl phase is heated to about 120°C (or a higher temperature), carbonyl groups react with the NH₂ group, losing water and forming strongly fluorescent zones, whereby a N=C function is probably created. This reaction affords an elegant way of detecting sugars [33].

Fig. 3.6 Separation of α - and β -carotene, chlorophyll a and b, luteine, violaxanthine, and neoxanthine on a reversed-phase RP-18 layer with methanol–acetone–water (30+30+5, V/V) as mobile phase



The RP-18 layer has prevailed among the non-polar bonded phases because it provides for classic partition separations analogous to reversed-phase chromatography in HPLC. Compared with HPLC, a limitation, however, is that the stationary phase is not adequately wet by highly aqueous mobile phases resulting in an inadequate or no flow of mobile phase through the layer. Reversed-phase layers with a low bonding density (6% compared to 32% typical of fully bonded reversed-phase layers) are available from several manufacturers to overcome this problem, but their retention properties are different to high-bonding density layers, in part due to the presence of accessible silanol groups in relatively high concentration. Alkylsiloxane-bonded layers are well suited for the separation of non-polar to moderately polar substances (Fig. 3.6). Reversed-phase layers have particle sizes between 5 and 25 μ m, a nominal pore size of 6 nm, and a layer thickness of 0.2–0.25 mm. Gypsum and organic binders are used to immobilize reversed-phase layers to their support.

Chemically bonded phases can be prepared in the laboratory to extend the range of stationary phases and degree of modification available beyond those of commercial precoated layers [34, 35]. There are many simple procedures that allow the modification of standard silica gel plates as required. A straightforward method is as follows: dry the silica gel plate at 110°C for about 2 h; excluding all water, make a 1–2% solution of a di- or trichloroalkylsilane in dry toluene and then, with their glass backs facing one another, dip two plates at a time in this solution; for optimum reagent distribution in the stationary phase remove air bubbles by sonnicating the plates and solution for 15 min; allow the plates to stand in the solution protected from the atmosphere for 12 h; finally, dry the plates at 110°C for 2 h. The resulting reaction is shown in Fig. 3.7.

3.4.5 Kieselguhr

The name "kieselguhr" (of German origin) describes the fossil skeletons of silica algae. More than 90% of kieselguhr consists of silicic acid with the residue Al₂O₃,

Fig 3.7 Reaction scheme to produce chemically bonded phases [34, 35]

Fe₂O₃, MgO, TiO₂, CaO, and carbonates. Kieselguhr is found in geological deposits and is only suitable for use as a TLC adsorbent after a complete and lengthy purification procedure. Compared with silica gel, it has a larger pore volume of 1-3 mL/g. The average pore size lies between 10³ and 10⁴ nm, and so, the specific surface area is relatively small at 1–5 m²/g. Particle sizes for materials used for TLC are typically between 5 and 40 μm, and gypsum is generally used as a binder to fix the material to the support plate. Due to its low activity, kieselguhr is used to dilute silica gel and also as a material for concentration zones. In addition, its large pore volume makes it suitable for use as a "supporting phases" for partition chromatography. In this case, the plates are soaked with paraffin or silicone oil and used in reversed-phase chromatography or coated with polar solvents for use in normal-phase chromatography, Besides water, dimethyl sulphoxide, ethylene glycol, and ethylenediamine (or other polar solvents) are commonly used as coatings. This type of chromatography is really a form of liquid-liquid partition chromatography because there is no covalently bonded phase involved. An advantage is the ease with which partitioning systems can be formed but on the other hand the physically supported liquid films are unstable and during the development step may migrate with the solvent front often observed by an irregular baseline in the densitogram.

Silica gel 50,000 is available as a kieselguhr substitute. Silica gel 50,000 is highly porous and absolutely inert. It has chromatographic characteristics similar to those of kieselguhr but can be produced without contamination. It has an average pore diameter of 5,000 nm, a specific pore volume of about 0.6 mL/g and a specific surface area of 0.5 m 2 /g. Silica gel 50,000 is equally well suited for use in partition chromatography as a substitute for kieselguhr. Organic binders are generally used for immobilizing the layer to its support.

3.4.6 Cellulose

Cellulose is a glucose polymer with useful properties as a sorbent for TLC. Natural cellulose retains its fibre structure (its average cellulose polymerization grade

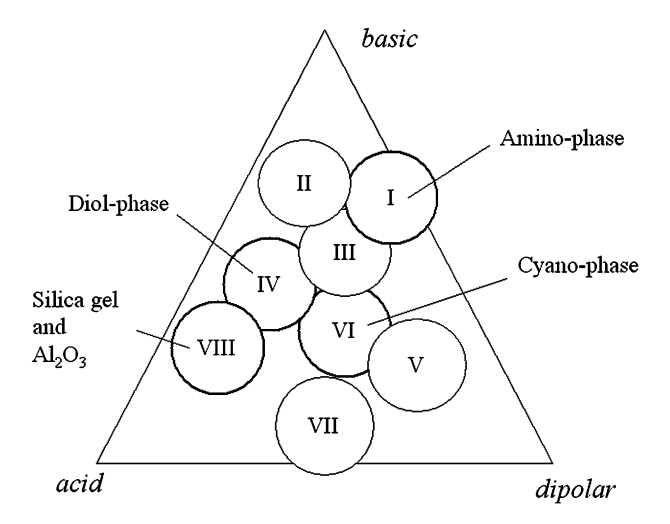


Fig. 3.8 Selectivity diagram of TLC stationary phases [3]

lies between 300 and 600 glucose units). The hydrolysed form "micro-crystalline cellulose" contains from 40 to 200 glucose units and possesses a large swelling capacity. Cellulose used for TLC has a fibre length of 2–20 µm, which is just about the same as its particle size. Short fibres prevent the mobile phase moving too quickly along the long fibres, a phenomenon that is not observed on untreated cellulose. Consequently, separated zones are therefore more compact than in paper chromatography. The specific surface area for treated celluloses is about 2 m²/g. Binders are not necessary since cellulose is a good self-adhesive, owing to its large number of OH groups. Cellulose mainly absorbs water when it swells, but can also absorb other polar solvents such as ethanol, through hydrogen bonding to the OH groups of the glucose units. Consequently, cellulose can be used as a polar stationary phase in partition chromatography. On the other hand, cellulose is easily chemically modified by introducing an acetyl group for use in reversed-phase chromatography (acetylated cellulose is used to manufacture cigarette filters to adsorb polycyclic aromatic hydrocarbons). Cellulose also contains small amounts of carboxylic acid groups (from lignin) and has some cation-exchange capacity. Cellulose can also be modified by chemical reactions to introduce ion-exchange groups. The following are some useful ion-exchange types:

Cation exchangers

- Cellulose phosphate (–OPO(OH)₂)
- Carboxymethylcellulose (CM–) (–OCH₂COOH)
- Cellulose citrate (–OOC(CH₂COOH)₂OH)
- Oxycellulose (–COOH)
- Sulphomethylcellulose (–OCH₂SO₃H)
- Sulfoethylcellulose (–OCH₂CH₂SO₃H)

Anion exchangers

- Diethylaminoethylcellulose (DEAE-) (-OCH₂CH₂NH⁺(CH₂CH₃)₂)
- Triethylaminoethylcellulose (TEAE–)(–OCH₂CH₂N⁺(CH₂CH₃)₃)
- Aminoethylcellulose (AE–)(–OCH₂CH₂NH₃⁺)
- p-Aminobenzylcellulose (PAB-)(-OCH₂C₆H₄NH₃⁺)

Cellulose layers are mainly used in biochemistry for the separation or isolation of proteins, amino acids (Fig. 3.9), phosphates, and nucleotides. Weak retention of small organic compounds limits their application to compounds typically separated on silica gel and chemically bonded phases. Phosphates and anionic amino acids can be separated on modified cellulose layers. An important application in biochemistry is the separation and clean-up of sensitive compounds such as egg albumin, proteins, enzymes, hormones, and nucleotides.

3.4.7 Polyamides

Two types of polyamides, polyamide-6 and polyamide-11, are used as sorbents for TLC. Polyamide phases possess the functional group –NH–COO–, whereby the figure given in the name indicates the number of CH₂ groups next to the NH group. There are also polyamide phases where the –NH group has been acetylated.

The amide group affords selectivity for hydrogen-bonding functional groups. Polyamide-6 is rather hydrophilic in contrast to polyamide-11 and is used mainly

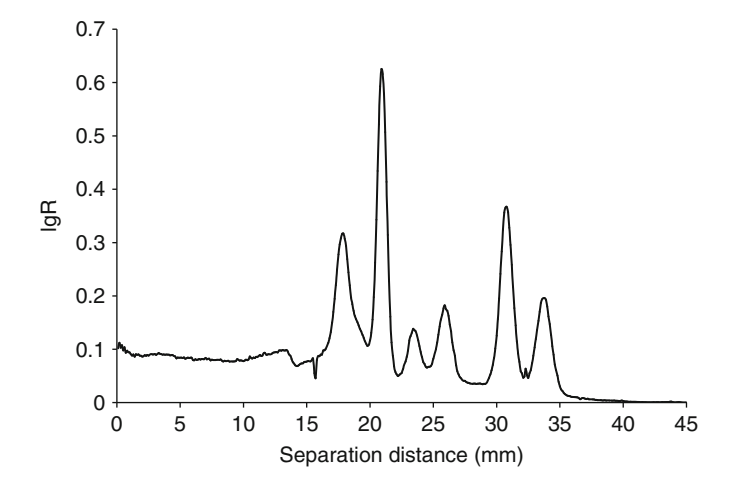
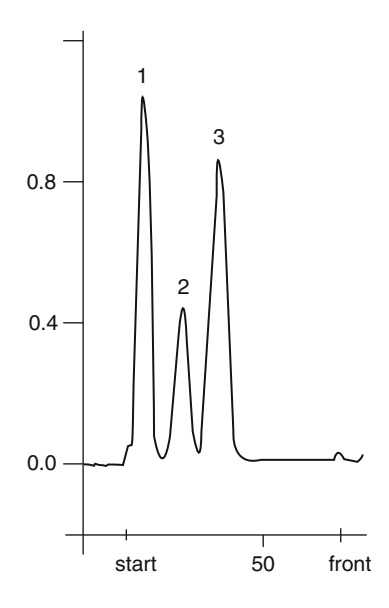


Fig. 3.9 Separation of amino acids (aspartic acid, glutamic acid, histidine, tyrosine, valine, and isoleucine) on cellulose with 1-butanol–acetic acid–water (4+1+1, V/V) as mobile phase (double development including ninhydrin in the second development for visualization of the amino acids after heating at 80°C for 10 min to form red zones)

Fig. 3.10 Separation of *p*-nitroaniline (1), *m*-nitroaniline (2), and *o*-nitroaniline (3) on polyamide-6 as the stationary phase with carbon tetrachloride–acetic acid (9+1, V/V) as mobile phase (detection at 400 nm) (Published with permission from Macherey-Nagel, Düren, Germany.)



for reversed-phase separations (Fig 3.10). The outstanding feature of polyamide phases is their high loading capacity, which is attributable to their large swelling capacity. Polyamide plates can also be used for preparative separations and are generally sold without binders.

Polyamide phases are particularly good at separating polar, water-soluble compounds such as phenols and carboxylic acids, or natural products that contain such groups. They are equally good at separating isomeric compounds. Polyamide is unstable in the presence of strong acids or bases [31].

3.4.8 Ion Exchange Resins

Commercially available cation or anion exchangers mixed with silica gel and organic binders are used for special purposes. Such phases are useful for separating polar compounds such as amino acids, proteins, amino sugars, amino carboxylic acids, and antibiotics as well as anions and cations. Cation exchangers generally consist of polystyrene–divinylbenzene resins modified to introduce acidic functional groups in from 4 to 12% of the number of aromatic rings. Sulphonic acid (–SO₃H), phosphoric acid (–PO(OH)₂), or carboxylic acids (–COOH) are used. The phenol group (–OH) can also be used as a weak acid. Anion exchangers are formed by introducing polystyrene resins with quaternary amine groups such as a –N(CH₃)₃ $^+$ Cl $^-$.

3.4.9 Chiral Phases

The resolution of enantiomers in chromatography is achieved by the formation of reversible diastereomeric complexes with a stationary phase or after conversion to diastereoisomers by reaction with a chiral reagent and separation in an achiral system [36]:

$$\lg K = \frac{1}{2.3RT} (\mu_{R}^{0} - \mu_{S}^{0}),$$

where

K partition coefficient μ_R^0, μ_S^0 chemical potential of two diastereomers

Diastereomers should be separated at low temperature because, according to Martin's relationship the partition coefficient decreases as the temperature increases, i.e. the separation would also decrease in quality [36].

Cellulose is a chiral polymer capable of separating enantiomers. Modified forms of microcrystalline cellulose, such as cellulose triacetate, similarly permit the separation of enantiomers [36]. Chiral stationary phases can also be prepared by impregnating achiral layers with an appropriate chiral reagent capable of forming diastereomeric complexes with the compounds to be separated. For this purpose silica gel is often used in conjunction with L-proline or hydroxy-L-proline. Other chiral amino acids can be used too. Cu(II) ions are also required since the complexes formed involve coordination to copper.

In principle, all substances that form Cu(II) complexes can be resolved into their enantiomeric forms [34, 36–38]. This special type of copper-impregnated plate is available as CHIRALPLATE® from Macherey-Nagel (Düren, Germany).

A further chiral separation method uses enantiomeric additives dissolved in the mobile phase, for example, camphor derivatives, D-galactaric acid, or erythromycin. Diol-plates are often used for this kind of separation [36]. Modified and unmodified β -cyclodextrin, bovine serum albumin, or macrolide antibiotics are used as mobile-phase resolving agents usually with RP-18 layers [36]. Also the possibility of prechromatographic chiral derivatization of enantiomers (e.g. using Marfey's reagent [39]) forming diastereomers, which can be separated by a non-chiral stationary phase, should be mentioned.

The so-called imprinted phases add a relatively new development to chiral separations. A polymer is synthesized in the presence of an enantiomeric template molecule such as quinine. The template molecule leaves its imprint in the polymer and after washing out, these "chiral holes" retain their ability to recognize different chiral structures [40].

Table 3.3 List of various TLC plate codes [41]

Code/symbol	Meaning
G	Gypsum (13%) is used as binder
H	Plate without binder
R	Material is especially cleaned
P	Preparative plates
W	Water wettable plates
F	Layer contains a fluorescence indicator
F ₂₅₄ , 366	Excitation wavelengths of fluorescence indicators
F _{254S}	Acid-resistant fluorescence indicator
40, 60, etc.	Average pore size of the layer (Å)
C	Layer divided into separating parts
RP	Reversed phase
RP-8, -18	Reversed phase with C-8 or C-18 hydrocarbon chain
AMD	Automated Multi-development
NH_2	Hydrophilic chemically bonded layer with 3-aminopropyl groups
CHIR	Chiral plate for separation of enantiomers by ligand exchange
CN	Hydrophilic chemically bonded layer with 3-cyanopropyl groups
DIOL	Hydrophilic chemically bonded layer with spacer bonded propanediol groups

3.4.10 Layers with Fluorescent Indicators

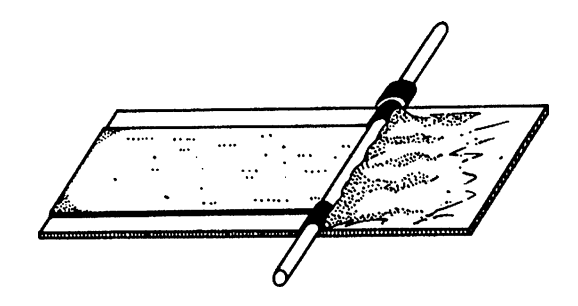
Commercially available plates with fluorescent indicators facilitate the visualization of substances that absorb UV light. Green fluorescence is produced by manganese-activated zinc silicate and blue fluorescence by magnesium tungstate contained in the layer. However, only the magnesium tungstate indicator is "acid stable". Such plates are coded with an "F" for fluorescence and the indication of the excitation wavelength. More useful plate characterizations are listed in Table 3.3

3.4.11 Making Your Own Plates

TLC plates are usually purchased ready-made. Repeatable production of standardized silica gel or aluminium oxide is not easy and generally exceeds the capacities of even a well-equipped laboratory. Of course you can buy readymade phases and coat them yourself, but such plates will never attain the high quality of those purchased. Moreover, if the production time is taken into consideration, the price advantage is absolutely minimal. Nevertheless, there are circumstances where it may be desirable to prepare plates in the laboratory. For example, plates containing silver ions are unstable and cannot be stored for long and, therefore, must be made shortly before use.

Furthermore, commercially available plates are relatively expensive, so laboratories in underprivileged countries cannot always afford them. In some areas, there

Fig. 3.11 A simple apparatus for spreading an even layer of sorbent on a planar support with the aid of a glass rod and two strips of rubber tubing (From [42] with permission. © Wiley-VCH.)



are no sources for industrially produced plates or sorbents, etc., and natural substances must be used instead.

For example, a TLC plate with a cellulose stationary phase can be made from a slurry of 27 g starch and 3 g gypsum (CaSO₄) suspended in 20 mL of water and 10 mL of ethanol [19, 43]. For silica gel plates, silica gel is mixed with 5–13% gypsum and suspended in 85% ethanol–water (8.6+1.4, V/V). The slurry is applied to the glass support by a glass rod with a strip of rubber tube attached either side (as a means of controlling thickness and width). The glass rod acts as a roller and evenly distributes the suspension on the support (see Fig. 3.11). After spreading, the layer is dried at room temperature and activated at 120° C. Easily fabricated plates containing readily available farina starch can separate organic acids, amino acids, vitamins E and D₂, and anthocyanins as well as fructose, glucose, and sucrose [19]. It fully demonstrates that good analyses can be carried out by simple means.

3.5 Light Absorption on Plate Surfaces

The manner of the interaction of light with the plate surface is an important criterion for plate selection because quantitative measurements depend on the layer's absorption characteristics. The spectral distribution of light reflected from the layer surface is generally not identical to that of the source. Depending on the wavelength, part of the light is absorbed by the plate surface. Diode array detection provides a reliable and simple means for determining the extent of the wavelength-dependent plate absorption. Evaluation is carried out according to the following expression:

$$A(\lambda) = -\lg\left(\frac{I(\lambda)}{I_{\text{MgO}}(\lambda)}\right)$$
(3.2)

 $I(\lambda)$ distribution of spectral light reflected by the TLC plate $I_{\rm MgO}(\lambda)$ reflected spectral light distribution of (MgO) white standard

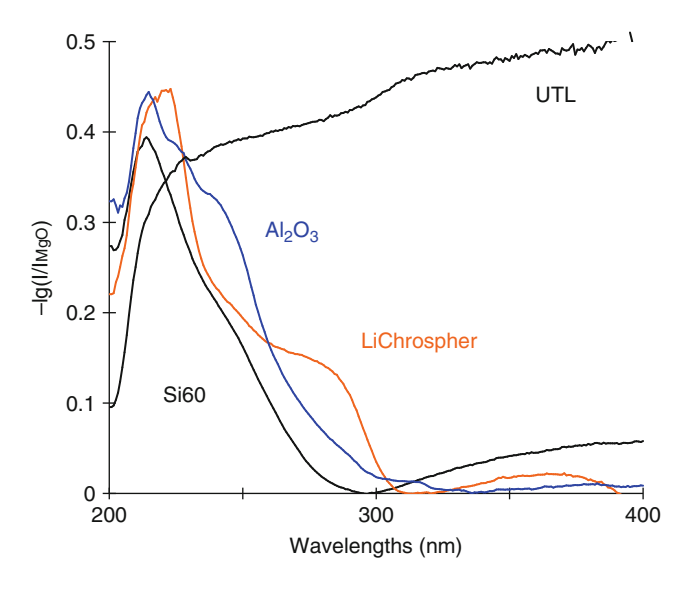


Fig. 3.12 The loss of light from spherical and irregular particle silica gel layers (Si_{60}), an UTLC plate, and an aluminium oxide phase compared with magnesium oxide

As a white standard for comparison purposes, magnesium oxide (MgO) powder is placed in slightly compressed layers beside the plate to be measured at an equal distance from the measuring interface. The intensity for the white standard ($I_{\rm MgO}$) and the reflected light from the stationary phases (I) are recorded at various wavelengths. The calculated value for $A(\lambda)$ describes the fraction of light loss from the plate surface in comparison to the white standard. At an absorption value of A=1, only 1/10 of the MgO surface light intensity is reflected. At a value of A=0.5, it is only about one third the intensity of the white standard.

Figure 3.12 compares various silica gel phases (Si_{60} , irregular particles and LiChrospher[®] spherical particles) with the reflection spectrum of aluminium oxide. Above 300 nm, all inorganic phases (with the exception of the UTLC layer) reflect light with intensity comparable to the magnesium oxide coating.

This demonstrates that the absorption of light by a layer plate strongly depends on the stationary phase used because in the range below 300 nm, the chemically modified plate surfaces absorb more light than silica gel. For all the plates shown in Fig. 3.12, below 300 nm, only about one third of the light intensity is reflected (A = 0.48), compared with the magnesium oxide surface. LiChrospher[®] and Si₆₀ plates differ slightly in their light-scattering ability, which can be attributed to their different binders. There is almost no noticeable difference between aluminium oxide and silica gel.

One interesting aspect of the UTLC plate is that it reflects only about one third of the light intensity over the whole spectral range compared with the other plate surfaces. This is a consequence of the layer's extreme thinness (only $10~\mu m$) and its corresponding transmission loss. All other layers are $100~\mu m$ thick. Another

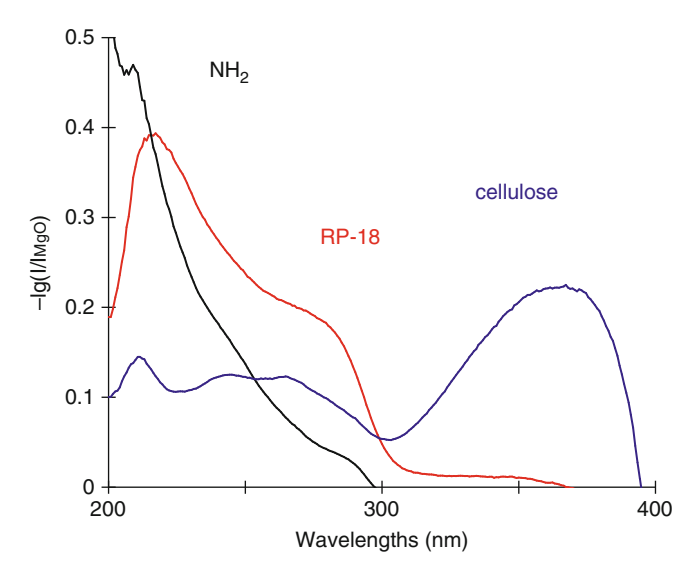


Fig. 3.13. The light loss from -NH₂, RP-18, and cellulose layers compared with MgO

interesting aspect of the UTLC plate is its low light absorption at 200 nm because this layer does not contain a separate binder. It seems that the absorption of the other plates at 220 nm is not due to the silica gel and aluminium oxide, but due to the contamination of the stationary phase, probably with Fe³⁺ ions, derived from iron vessels used in the production process.

Chemically bonded stationary phases in the region below 250 nm show an increasing loss of light, as shown in Fig. 3.13. The amino group absorbs more light than the RP-18 layer. The absorption spectra of RP-2, RP-8, and RP-18 phases are absolutely identical.

Figure 3.13 also illustrates the percent light loss from a cellulose layer. Cellulose has the most functional groups, and its strong absorption in the UV between 300 and 400 nm is not surprising. The relatively strong absorption of cellulose above 300 nm compared with silica gel, aluminium oxide, and chemically bonded phases is equally unsurprising. Nevertheless, all stationary phases provide unlimited use for measurements in the range below 400 nm. The only restriction is that the amino phase is less effective for measurements in the range below 230 nm, where this layer absorbs light very strongly.

Kieselguhr and ion-exchange phases merely reflect one tenth of the light reflected from a magnesium oxide surface at wavelengths below 250 nm (see Fig. 3.14). We must assume that contamination is inevitable with such a natural product as kieselguhr.

The ion-exchange layers based on organic polymers show strong absorptions below 300 nm, severely limiting their use in this range. In particular, signals can be seen at 220 and 280 nm, caused by the phenyl groups of the polymers. In the range below 250 nm, Nylon-6 and Nylon-11 show intense absorption bands, considerably

References 77

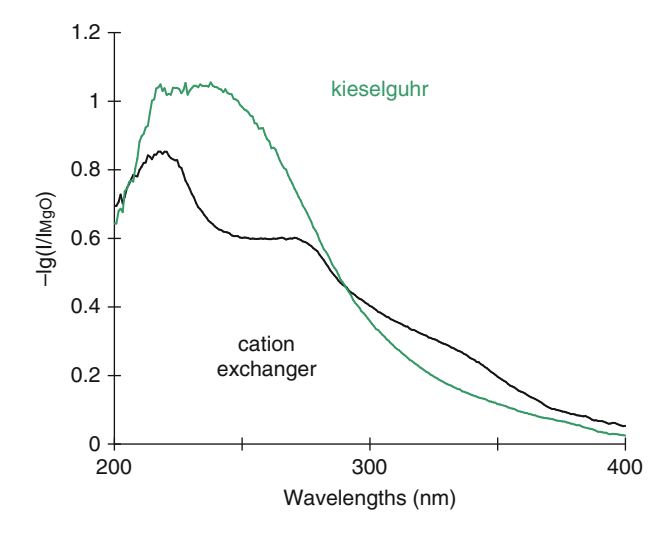


Fig. 3.14 Light loss from a kieselguhr and a cation exchanger phase compared with MgO

more intense than even the amino phases. Kieselguhr, ion-exchange resins, and polyamide phases, therefore, should only be used for reflectance measurements in the range above 300 nm.

References

- 1. Grinberg N (ed) (1990) Modern thin-layer chromatography. Dekker, New York
- 2. Snyder LR (1968) Principles of adsorption chromatography. Dekker, New York
- 3. Geiss F (1987) Fundamentals of thin layer chromatography. Huethig, Heidelberg
- 4. Stahl E (1969) Thin-layer chromatography. A laboratory handbook. Springer, Berlin
- Zlatkis A, Kaiser RE (eds) (1977) High performance thin layer chromatography. Elsevier, Amsterdam
- 6. Poole CF (1988) Progress in planar chromatography. Anal Chem 4:209–213
- 7. Poole CF, Poole SK (1994) Instrumental thin-layer chromatography. Anal Chem 66:27A–37A
- Andreev LV (1982) High performance thin-film chromatography in biological studies. J Liq Chromatogr 5:1573–1582
- 9. Hauck HE, Bund O, Fischer W, Schulz M (2001) Ultra-thin layer chromatography (UTLC) a new dimension in thin layer chromatography. J Planar Chromatogr 14:234–236
- Poole SK, Ahmed HD, Belay MT, Fernando WP, Poole CF (1990) The influence of layer thickness on the chromatographic and optical properties of high performance silica gel thin layer chromatography plates. J Planar Chromatogr 3:133–140
- 11. Litvinova LS, Kurenbin OI (1991) An equation expressing the effect of sorbent characteristics on eluent flow velocity in thin layer chromatography. J Planar Chromatogr 4:402–405
- 12. Wheeler A (1955) In: Emmett PH (ed) Catalysis, vol II. Reinhold, New York
- Nikolova-Damyanova B, Momchilova Sv (2005) Silver ion thin-layer chromatography of fatty acids. A survey. J Liq Chromatogr Rel Technol 24:1447–1466
- 14. Wall PE (1997) Argentation HPTLC as an effective separation technique for the cis/trans isomers of capsaicin. J Planar Chromatogr 10:4–9

- Wardas W, Pyka A (1998) Visualizing agents for cholesterol derivatives. J Planar Chromatogr 11:70–73
- Li T, Li J, Li H (1995) Modified and convenient preparation of silica impregnated with silver nitrate and its application to the separation of steroids and triperpenes. J Chromatogr A 715:372–375
- 17. Lightenthaler H, Börner K (1982) Separation of prenylquinones, prenylvitamins and phenols on thin-layer plates impregnated with silver nitrate. J Chromatogr 242:196–201
- 18. Brühl L, Schulte E, Thier H-P (1994) Composition and structures of triglycerides of human milk and some base components for infant milk formulas. Fat Sci Technol 96:147–154
- Aubourg SP, Sotelo CG, Gallordo JM (1990) Zonal distribution of fatty acids in Albacore (Thunnus alalunga) triglycerides and their changes during cooking. J Agric Food Chem 38:255–257
- Colarow L (1989) Quantification of phospholipid classes on thin-layer plates with a fluorescence reagent in the mobile phase. J Planar Chromatogr 2:19–23
- 21. Hegewald H (1996) One-dimensional thin-layer chromatography of all known D-3 and D-4 isomers of phosphoinositides. Anal Biochem 242:152–155
- Sempore BG, Bezard JA (1994) Separation of monoacylglycerol enantiomers as urethane derivatives by chiral-phase high performance liquid chromatography. J Liq Chromatogr 17:1679–1694
- 23. Lato M, Brunelli B, Ciuffini G, Mezzetti T (1968) Bidimensional thin-layer chromatography of carbohydrates on silica gel impregnated with boric acid. J Chromatogr 34:26–34
- Ruiz JI, Ochoa B (1997) Quantification in the subnanomolar range of phospholipids and neutral lipids by monodimensional thin-layer chromatography and image analysis. J Lipid Res 38:1482–1489
- 25. Bhushan R, Parshad U (1996) Separation and identification of some cephalosporins on impregnated TLC plates. Biomed Chromatogr 10:256–260
- Naidong W, Hua S, Roets E, Hoogmartens J (1994) Purity control of six tetracyclines by semiquantitative TLC with fluorescence detection. J Planar Chromatogr 7:297–300
- 27. Sharma SD, Misra S, Gupta R (1993) Normal phase, reversed phase and chelation thin layer chromatographic studies of some toxic metal ions in two component solvent systems containing DMSO: quantitative separation of Pb²⁺ from Hg₂²⁺, Hg²⁺, Tl⁺, Bi³⁺, Sn⁴⁺, and Sb³⁺. J Liq Chromatogr 16:1833–1843
- 28. Kovács-Haday K, Balázs E (1993) Thermoanalytical study of the impregnation of silica gel layers. J Planar Chromatogr 6:463–466
- 29. Funk W (1989) Polynuclear aromatic hydrocarbons (PAHs): charge transfer chromatography and fluorimetric determination. J Planar Chromatogr 2:28–32
- 30. Membrado L, Cebolla VL, Matt M, Gàlvez EM, Domingo MP, Vela J, Beregovtsova N (2002) Hydrocarbon group-type analysis by thin layer chromatography and scanning densitometry. J Planar Chromatogr 15:268–273
- 31. Wan KT, Weinstein B (1972) In: Niederwieser A, Pataki G (eds) Progress in thin layer chromatography, vol 3. Ann Arbor Science Publishers, Ann Arbor
- 32. Berendsen GE, Pikart KA, de Galan L (1980) Preparation of various bonded phases for HPLC using monochlorosilanes. J Liq Chromatogr 3:1437–1464
- 33. Spangenberg B, Arranz I, Stroka J, Anklam E (2003) A simple and reliable HPTLC method for the quantification of the intense sweetner Sucralose[®]. J Liq Chromatogr Rel Technol 26:2729–2739
- Gilpin RK, Sisco WR (1976) Preparation and characterization of chemically bonded thinlayer chromatographic plates. J Chromatogr 124:257–264
- 35. Ericson M, Blomberg LG (1980) Modification of HPTLC plates by in situ chemical bonding with non-polar and polar organosilanes. J High Resolut Chromatogr Chromatogr Commun 3:345–350
- 36. Lepri L (1997) Enantiomer separation by TLC. J Planar Chromatogr 10:320–331

References 79

37. Nyiredi Sz (ed) (2000) Planar chromatography, a retrospective view of the third millennium. Springer, Budapest

- 38. Perišić-Janjić N, Vujičić B (1997) Analysis of some food components by thin-layer chromatography on unconventional layers. J Planar Chromatogr 10:447–452
- 39. Bushan R, Brückner H (2004) Marfey's reagent for chiral amino acid analysis: a review. Amino acids 27:231–247
- Suedee R, Songkram Ch, Petmoreekul A, Sangkunakup S, Sankasa S, Kongyarit N (1998)
 Thin-layer chromatography using synthetic polymers imprinted with quinine as chiral stationary phase. J Planar Chromatogr 11:272–276
- 41. Hahn-Deinstrop E (1992) Stationary phase sorbents. J Planar Chromatogr 5:57-61
- 42. Randerath K (1965) Dünnschicht-Chromatographie. Chemie, Weinheim
- 43. Frey H-P, Zieloff K (1993) Qualitative und quantitative Dünnschichtchromatographie, Grundlagen und Praxis. Chemie, Weinheim

Chapter 4 The Mobile Phase in Adsorption and Partition Chromatography

In thin-layer chromatography (TLC), there are only three degrees of freedom in which the chromatographic results can be seriously influenced. They are (1) the polarity of the stationary phase in partition chromatography or its activity in adsorption chromatography; (2) the selection of the mobile phase; and (3) the composition of the vapour phase in contact with the layer. Although all three factors can change a separation, the most important for method development is the mobile phase composition.

The separation process in TLC begins with the equilibrium between the mobile and stationary phases. This is quite different from HPLC, where a reproducible separation can only be achieved after equilibrium is established. In TLC, the *mobile phase* (the solvent) only comes into contact with the dry stationary phase after the start of the separation. Its composition depends on the original solvent composition, which is modified by interactions with the stationary phase and the vapour phase, and may change further during the development process. Moreover, the dry layer is not the real stationary phase, since this is modified by the sorption of components from the mobile phase.

If the sorbent surface is directly involved in the separation, this is known as *adsorption chromatography*. If the stationary phase merely affords a mechanism to immobilize a liquid phase, this is described as *partition chromatography*. The solvent decisively determines the type of separation. During this process a *front gradient* is formed, which is enriched in the solvent components.

In summary, the term "mobile phase" should not be used as a synonym for "solvent" as this is incorrect for over 90% of TLC systems [1, 2].

4.1 Solvent Characteristics

Solvents have a double function in chromatography: they are responsible for transporting the sample and for creating the separation system. The solvent's strength determines its ability to transport the sample through the system, and its

selectivity determines whether a separation is obtained. For transport the sample must be dissolved by the mobile phase, and for separation it must be retained by the stationary phase.

Dissolving a substance requires integrating it into the structure of the solvent. The necessary energy (solvation energy) is supplied by placing solvent molecules closely around the analyte, thus forming a shell-like analyte solvent complex. In fact the increasing solvent entropy provides the energy necessary to integrate the analyte into the solvent structure. The mixing of two solutions takes a similar course. Both lose their individual structure in favour of a statistically determined partition of one solvent in the other. A new mixture will not be formed if the dissipation energy is insufficient for an integration process. Water and *n*-hexane for example are immiscible because the forces between hexane molecules are much greater than the forces between hexane and water molecules. Mixing in this case will result in two immiscible phases. The general rule is that "like dissolves like". We distinguish between "hydrophilic" and "hydrophobic" solvents, depending on their ability to mix with water, with hydrophilic solvents selectively forming solutions with hydrophilic compounds and vice versa.

When a dissolved substance migrates through the layer, its solvent shell interacts directly with the stationary phase. Inorganic ions (like metal cations or NO_3^- , PO_4^{3-} , etc.) mostly form stable water complexes, which cannot be disrupted by non-polar organic solvent molecules. This is the reason why ions can hardly be dissolved in organic solvents. However, if these ions are combined with a large and hydrophobic counterion, the result will be a soluble ion pair that can be used in partition chromatography.

In principle, any liquid can be used as a solvent in TLC as long as the liquid is of the required purity. Unfortunately, this is not always the case with chloroform because it is generally stabilized with ethanol. In the past, chloroform was incorrectly positioned in the eluotropic series because its ethanol content was overlooked. Other restrictions to consider are that solvents should be of low toxicity, should possess neither a too high nor a too low vapour pressure, and should be chemically inert. All chlorinated hydrocarbons such as methylene chloride or chloroform are hazardous to human health. They should not be used as solvents, as far as this is practical. If they must be used, because of the non-availability of suitable alternative, the solvents should be disposed of in separate waste containers reserved for chlorinated solvents.

Cancer-causing substances such as benzene or carbon tetrachloride should also be avoided. Diethyl ether is also a problem because of its high vapour pressure. All ethers (e.g. dialkyl ether, dioxane, tetrahydrofuran, etc.) eventually form explosive peroxides. These solvents should be stored in brown bottles, as peroxides are formed by light in the presence of oxygen. The only exception is *tert*-butyl methyl ether (MTBE), which is incapable of forming peroxides. This ether, however, is resistant to microbiological degradation and should not be allowed to contaminate the natural environment.

A general problem concerns the widely varying water content of solvents, especially if their containers are left open to the atmosphere for a significant

time. Therefore, it is advisable to keep only small portions of solvents at the workplace and regularly replace them with fresh solvent from a closed container.

Solvent selection is made initially to obtain sufficient selectivity to solve a separation problem. For this, solvent viscosity or, more exactly, solvent permeation factor should not be too high, in order to keep the development time as short as possible and to minimize zone diffusion. Furthermore, wherever possible, single solvents should be used as mobile phases. Only when the desired selectivity cannot be obtained with single solvents, binary, ternary, or quaternary mixtures are used in their place. Higher order solvent mixtures are usually unnecessary. Beware of publications that suggest a mixture of immiscible solvents to obtain an upper or lower phase for development purposes. Adjusting such biphasic system is extremely temperature dependent and thus the system is not very stable. Avoid using "old" solvent systems that have been stored for a while because their compositions are unstable. Mixtures of acids and alcohols react relatively quickly, forming esters. The basic rule should be make a fresh solvent mixture for each use. It is perhaps obvious without saying that a used solvent mixture cannot be re-used as it nearly always changes its composition during the development, because the composition of the solvent mixture is different from the composition of the mobile phase. To avoid unnecessary waste, stock solvent volumes should be kept to a minimum (a few millilitre) each time. For preparing solvent mixtures, pipettes are more accurate than graduated cylinders.

The selection of a solvent composition may be largely empirical, but more systematic approaches will generally be more successful. A modifier (mostly a polar solvent) is used in adsorption chromatography to adjust (meaning to reduce) the number of active adsorption sites on the stationary phase. This depends not only on the amount of modifier in the mobile phase but also on the strength of the mobile phase. For a low polarity solvent mixture a larger amount of modifier will be adsorbed by the stationary phase than if the solvent mixture has a higher polarity. In the latter case, more solvent molecules will also be adsorbed by the stationary phase.

The polarity of a solvent mixture can be adjusted by dilution with a weaker solvent. In adsorption chromatography, pentane, hexane, cyclohexane, or heptane is mostly used for this purpose, but any low polarity solvent will suffice. On the other hand, For reversed-phase chromatography, water is usually used as a weak solvent. A modifier is not necessary for reversed-phase separations because there are a few active sites on the stationary phase. A mediator may be used to obtain a single phase for solvents immiscible with water. The mediator is often the main component of the mixed solvent. Recommendation for suitable solvent mixtures – at least for adsorption chromatography – is provided by *Snyder's* theory.

4.2 Solvent Theory for Adsorption Chromatography (According to Snyder)

In the competition between sample and solvent molecules to occupy active centres on the sorbent surface in adsorption chromatography, the following characteristics should be noted:

- Even small quantities of hydrophilic molecules (e.g. water) de-activate, i.e. quickly block all active centres, and therefore have an enormous influence on separations. At higher concentrations, an adsorbed film of water covering the surface is formed, and the adsorption separation changes into a partition separation.
- Humidity of air exerts a great influence on the $R_{\rm f}$ value.
- Sample over loading leads to tailing.
- Inorganic oxide adsorbents afford separations according to polarity or to the number and type of functional groups rather than according to size. Hydrogenbonding interactions play an important role.
- The mobile phase contains low to moderate amounts of polar solvents mostly of low volatility. The type of developing chamber, in particular, the size of the evaporation space, has a greater influence on the separation than is observed for partition chromatography.

Snyder's fundamental relationship for adsorption chromatography can be expressed as [1-3]

$$R_{\rm m} = \lg \frac{W_{\rm a}}{V_{\rm P}} V_{\rm a} + \alpha_{\rm a} (S^0 - \varepsilon^0 A_{\rm P}),$$
 (4.1)

where

V_a volume of adsorbed solvent monolayer per gram of adsorbent

 $W_{\rm a}$ weight of adsorbent layer (g)

 $V_{\rm P}$ pore volume freely accessible to the solvent (cm³)

 α_a energy components of activity parameters, with $\alpha_a=1$ for the most highly active aluminium oxide

 S^0 adsorption energy of the sample

 ε^0 solvent parameter

 $A_{\rm P}$ area occupied by a sample molecule (at adsorption centre)

Snyder's equation describes the influence of the most important parameters of a chromatographic system on the $R_{\rm m}$ value. The layer parameters are contained in the logarithmic portion of the expression for the phase ratio. The strength of the mobile phase is described by the activity parameter. The sample properties are contained in the parameter S^0 (sample adsorption energy) and $A_{\rm P}$ (area occupied by a sample molecule on the adsorbent surface). The solvent parameter (ε^0) represents the characteristic properties of the mobile phase. One sample molecule occupies an area $A_{\rm P}$ and can displace a corresponding number of solvent molecules that were adsorbed at the active centres on this surface area. This process releases adsorption energy S^0 . For aliphatic compounds the adsorption energy is defined as zero.

Ideally, all the above parameters are independent of each other. In practice, however, the adsorption energy of different samples depends on the properties of the adsorbent. The same is true for A_P and the solvent parameter ε^0 . From a qualitative point of view, Snyder's equation indicates that the greater the adsorption energy S^0 of a sample molecule, the greater the R_m value of this substance and the

smaller its $R_{\rm f}$ value; the greater the solvent parameter (ε^0) the greater the $R_{\rm f}$ value; and for compounds of low polarity, which cannot saturate the sorption centres because $\varepsilon^0=0$ and $S^0=0$, only the first part of (4.1) is relevant. For $S^0\ll A_{\rm P}\varepsilon^0$ (the mobile phase minimizes interactions with the adsorbent), the $R_{\rm m}$ value becomes negative, and the $R_{\rm f}$ value shifts towards one. For $S^0\gg A_{\rm P}\varepsilon^0$ (the mobile phase cannot displace the sample from the adsorbent), the $R_{\rm m}$ value becomes positive, and the $R_{\rm f}$ value shifts towards zero [1–3].

4.2.1 Solvent Strength (ε^0)

The solvent strength in adsorption chromatography (according to Snyder [1, 2]) describes the influence of the solvent molecules on the adsorption of sample molecules. Snyder defines solvent strength as a quotient of the adsorption energy (E_P) of the solvent molecules that are desorbed by the sample and the space (A_P) originally occupied by the solvent molecules on the surface of the stationary phase. The solvent strength parameter then describes the adsorption energy of a solvent molecule per unit surface area of the adsorbent [1]:

$$\varepsilon^0 = \frac{E_{\rm P}}{A_{\rm P}} = \frac{\Delta G^\circ}{2.3RTA_{\rm P}}.\tag{4.2}$$

Here

 $E_{\rm P}$ adsorption energy of the solvent molecule

 $A_{\rm P}$ adsorption area required by a solvent molecule

 ΔG° standard free energy change

This definition of solvent strength shows that ε^0 is not only a function of the solvent but also a function of the properties of the stationary phase.

To determine the solvent strength, a mobile phase of strength $\varepsilon^0 = 0$ (e.g. pentane) is allowed to migrate through an adsorbent with activity $\alpha_a = 1$ (highly active aluminium oxide) from which the parameters A_P and S^0 (or C) are determined from measurement of the resulting R_m values according to (4.1):

$$R_{\rm m} = \lg rac{W_{
m a}}{V_{
m P}} V_{
m a} + lpha_{
m a} S^0 - lpha_{
m a} A_{
m P} arepsilon^0 = C - lpha_{
m a} A_{
m P} arepsilon^0.$$

For solvents of different strength on a given layer, a plot of the $R_{\rm m}$ values against the solvent strength results in a straight line with a slope $\alpha_{\rm a}A_{\rm P}$ and intercept C. Setting $\varepsilon^0=0$ for pentane and calculating $\alpha_{\rm a}A_{\rm P}$ and C, the ε^0 value can be determined by $R_{\rm m}$ measurements for any solvent. Tabulation of the ε^0 values in descending order is referred to as an *eluotropic series* [2]. They are valid for different $\alpha_{\rm a}$ $A_{\rm P}$ values, and a large number of values are available for aluminium oxide and silica gel.

4.2.2 Solvent Strength of Binary Mixtures

For binary mixtures, Snyder deduced a logarithmic relationship between the solvent strength of the mixture and its composition [2]. From (4.1), it follows with $R_{\rm m} = \lg k$ (k = being retention factor) for the difference of the two $R_{\rm m}$ values:

$$R_{\mathrm{m_B}} - R_{\mathrm{m_A}} = \lg\left(\frac{k_{\mathrm{B}}}{k_{\mathrm{A}}}\right) = \alpha_{\mathrm{a}} A_{\mathrm{P}} (\varepsilon_{\mathrm{A}}^0 - \varepsilon_{\mathrm{B}}^0).$$

For a mixture of two solvents A and B, the analogous equation $(R_{\rm mB}-R_{\rm mAB})$ is valid. With the simplification

$$\frac{k_{\rm B}}{k_{\rm AB}} \approx \frac{n_{\rm B}}{n_{\rm A} + n_{\rm B}} = N_{\rm B},$$

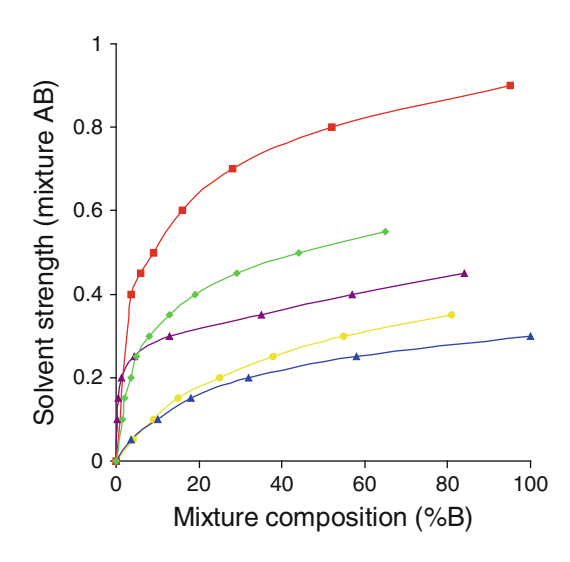
which holds for $N_{\rm B} > 0.2$ and for $\alpha_a(\varepsilon_A^0 - \varepsilon_B^0) > 0.2$, the equation can be reduced to

$$\varepsilon_{AB}^{0} = \varepsilon_{B}^{0} + \frac{\lg(N_{B})}{\alpha_{a}A_{PB}}.$$
(4.3)

 $N_{\rm B}$ mole fraction of the more polar component B $\alpha_{\rm a}$ activity parameter (for Al₂O₃), lying between 0 and 1, for SiO₂ it is 0.7) $A_{\rm PB}$ area required by a molecule B on the adsorbent surface

Equation (4.3) can be verified experimentally, as shown in Fig. 4.1. A low percentage of a polar solvent in n-pentane, n-octane, or dichloromethane strongly

Fig. 4.1 Solvent strength ε_{AB}^0 of binary mixtures AB at increasing volume fraction of the polar solvent B. From *top* to *bottom*: dichloromethane in octane, diethyl ether in pentane, methyl *tert*-butyl ether in octane, methyl acetate in pentane, and methanol in dichloromethane [2]



	(MG/d_{20})	SiO_2	Al_2O_3	$A_{ m P}$
<i>n</i> -Pentane	114.9	0.0	0.0	5.9
<i>n</i> -Octane	163.0	0.0	0.0	7.6
Isopropyl ether	142.0	0.28	0.28	5.1
Toluene	106.5	0.22	0.29	6.8
Benzene	89.2	0.25	0.32	6.0
Ethyl ether	104.4	0.43	0.38	4.5
Methylene				
chloride	64.4	0.3	0.4	4.1
1,2-Dichloroethane	63.7	0.32	0.47	4.8
MTBE	119.1	0.35	0.48	_
Acetone	73.8	0.5	0.58	4.2
Methyl ethyl				
ketone	89.3		0.51	4.6
THF	81.2	0.53	0.45	5.0
Acetonitrile	52.7	0.6	0.55	3.1
Ethyl acetate	98.1	0.48	0.6	4.5
Dioxane	85.5	0.6	0.61	6.0
Methanol	40.6	0.7	0.95	8.0
2-Propanol	76.8	0.6	0.82	8.0

Table 4.1 Properties of solvents for use in TLC. Listed are the molar masses in g/mol and solvent strength ε^0 and A_P [2, 4, 5]

increases the solvent strength. At higher concentrations of the polar solvent, the mixtures gradually reach an asymptotic value. The figure clearly shows that there is a logarithmic connection between the solvent strength and the mixture composition.

Theoretical discussion also shows that the solvent's strength is dependant on the activity parameter α_a . Binary mixtures, therefore, cannot be placed exactly in the eluotropic series [2]. Therefore, the eluotropic series is not a sufficient tool for mobile phase optimization, as solvent proton acceptor, proton donor, and dipole characteristics are not taken into consideration. However, the eluotropic series provides sufficient information for a first, careful prediction concerning the influence of solvents on analyte R_f values.

As an example let us calculate the solvent strength of the mixture 75% benzene (A) and 25% acetonitrile (B) (Table 4.1). The mole fraction for the more polar solvent is

$$N_{\rm B} = \frac{0.25 \times 0.55}{0.25 \times 0.55 + 0.75 \times 0.32} = 0.364.$$

Geiss [2] gives for $\varepsilon_{\rm B}^0 \geq 0.38, A_{\rm P} \approx 10$. The solvent strength according to (4.3) can be calculated as

$$\varepsilon_{AB}^0 = 0.6 + \frac{lg(0.364)}{0.7 \times 10} = 0.54.$$

The experimental value is 0.58 [2].

ε^0	DCE/OCT	MTBE/OCT	ACN/PEN	MTBE/DCE	ACN/DCE	MeOH/DCE
0.00	0	0	0	0	0	0
0.05	3.5					
0.10	10	0.2	0.3			
0.15	18	0.6	0.6			
0.20	32	1.4	1.1			
0.25	58	4.3	2			
0.30	100	13	3.5	0	0	0
0.35		35	8	30	12	
0.40		57	24	60	30	3.5
0.45		84	52	88	55	6
0.50			88		88	9
0.60			100		100	16
0.70						28
0.80						52
0.00						05

Table 4.2 Solvent mixtures with equal solvent strengths ε^0

DCE 1,2-dichloroethane; OCT n-octane; MTBE methyl tert-butyl ether; ACN acetonitrile; PEN n-pentane; MeOH methanol [2]

Geiss [2] published a proposal to accelerate method development, based on the concept of solvent strength. To determine the necessary solvent strength for a separation, he suggested 13 solvent mixtures listed in bold in Table 4.2. An optimum separation is achieved at an $R_{\rm f}$ value of 0.33. If you know the necessary solvent strength for this $R_{\rm f}$ value, you can optimize the selectivity of the separation by combining the individual mixtures with one another (at the same solvent strength). The solvent strength of the new mixture can be calculated via (4.3). Good results are achievable relatively quickly with this empirical process.

For reversed-phase systems, an eluotropic series can also be used to roughly estimate retention, taking two restrictions into consideration. In reversed-phase separations, the solvent strength increases with decreasing polarity. Water is the strength adjusting solvent with a solvent strength of zero. The selection of modifiers and mediators is restricted to just a few water miscible solvents.

4.3 Solvent Theory in Partition Chromatography

In partition chromatography, the sample is distributed between the stationary and the mobile phase. A separation is observed if the sample components have different partition coefficients:

$$K = \frac{c_{\rm s}}{c_{\rm m}}.$$

Here

K partition coefficient (repartition coefficient)

 $c_{\rm s}$ substance concentration in the stationary phase

 $c_{\rm m}$ substance concentration in the mobile phase

Partition chromatography in TLC can be recognized by the following characteristics:

- The stationary phase is formed by the solvent during development. Water, methanol, ethanol, acetonitrile, and tetrahydrofuran are the preferred solvents to create a stationary phase. Cellulose, 3-aminopropylsiloxane-bonded silica, or silica gel serves as a support for immobilizing the stationary liquid phase.
- The solvent has high water content, and all active centres are deactivated.
- Humidity has nearly no influence on the $R_{\rm f}$ value as in adsorption chromatography.
- The "thickness" of the liquid phase must be large enough that the sample can be dissolved in it like in a "real" liquid.
- Systems with water as the stationary phase have an advantage for separating very polar substances, such as sugars, acids, or amino acids, with a standard solvent mixture (butanol, acetic acids, water (4+1+1, V/V)).
- Separations using RP-18 layers can be described as partition process, carried out with a lipophilic stationary phase and hydrophilic mobile phases. RP-2 layers do not exhibit pure partition chromatography because the "thickness" of the coating is too thin.
- Zone broadening is greater than for adsorption chromatography, because the broadening process is no longer negligible in the stationary phase.

Partition chromatography can be impressively demonstrated by separating amino acids with butanol/water mixtures. For example, if you use a dry cellulose layer and reduce the water content in the mobile phase, the sample zones can "smear" at high $R_{\rm f}$ values if there is insufficient water in the upper part of the plate to provide for the stationary phase.

4.3.1 Solvent Theory (According to Snyder)

In reversed-phase HPLC and in TLC, the solvent selectivity model according to Snyder is most often used for partition systems [4, 5]. Snyder classified solvents based on their interactions with three solutes determined by their gas-liquid partition coefficients corrected for differences in solvent size, polarizability, and dispersion interactions. Each value was then corrected empirically to give a value of zero for the polar distribution constants for saturated hydrocarbon solvents. For these calculations, he took advantage of a database of gas-liquid partition coefficients assembled by Rohrschneider in 1973 for 81 solvents dissolved in n-octane, toluene, ethanol, methyl ethyl ketone, dioxane, and nitromethane [5]. Snyder chose the solutes nitromethane, ethanol, and dioxane as probes for a solute's capacity for dipole-type, hydrogen-bond donor, and hydrogen-bond acceptor interactions, respectively [6]. As an example, for ethanol the $R'_{\rm m}$ value was calculated from

$$R_{\textit{m}}'(\mathbf{x})_{\mathrm{Ethanol}} \equiv \lg \left(\frac{K(\mathbf{x})_{\mathrm{Ethanol}} V_{\mathbf{m}}(\mathbf{x})}{\left(K(\mathbf{x})_{\mathrm{Octane}} V_{\mathbf{m}}(\mathbf{x})\right)^{\frac{V_{m}}{V_{\mathrm{mOctane}}}}} \right),$$

where

K(x) partition coefficient of solvent x (e.g. acetone), here dissolved in ethanol

 $V_{\rm m}$ molar volume (mL/mol) $V_{\rm m}(x)$ mol volume of solvent x

 $K(x)_{\text{Octane}}$ partition coefficient of the solvent dissolved in n-octane (as reference

value)

 $V_{\rm m}$ Ethanol $V_{\rm m_{Ethanol}}$ mol volume of ethanol

 $V_{\rm m}$ Octane $V_{\rm m_{Octane}}^{\rm m}$ MG_{Octane}/d_{20_{Octane}} = 114.23/0.703 = 163 mL/mol

The value of $R_{\rm m}'(x)$ is thus proportional to the free energy difference of the solvent (x), related to the energy value of n-octane with the same molar volume. Snyder calculated the $R_{\rm m}'$ value of all 81 solvents for the liquids n-octane, toluene, ethanol, methyl ethyl ketone, dioxane, and nitromethane according to the above relationship. A more detailed description of his calculation can be found in [7]. The calculated $R_{\rm m}'(x)$ values for n-hexane, isooctane, and cyclohexane in the various liquids are all similar and exhibit the smallest $R_{\rm m}'(x)$ values. Thus, Snyder determined the average values of these three $R_{\rm m}'(x)$ values (n-hexane, isooctane, and cyclohexane) for each solvent and subtracted them from all 81 $R_{\rm m}'(x)$ results. The corrected $R_{\rm m}''(x)$ values for n-hexane, isooctane, and cyclohexane were of course zero. The corrected $R_{\rm m}''(x)$ value for ethanol in the solvent x was calculated as

$$R_{\rm m}''({\rm x})_{\rm Ethanol} \equiv \log(K'')_{\rm Ehanol}$$

= $R_{\rm m}'({\rm x})_{\rm E} - 1/3\{R_{\rm m}'(n{
m -Hexane}) \times R_{m}'(Isooctane) \times R_{m}'(Cyclohexane)\}.$

Next Snyder defined a polarity index (P') as the standard measure for the capacity of a solvent to interact with various liquids such as n-octane, ethanol, dioxane, methyl ethyl ketone, or nitromethane. To take proton acceptor, proton donor, and dipole properties into account, Snyder used the partition coefficients of the liquid dissolved in ethanol (proton donor), dioxane (proton acceptor), and nitromethane (dipole character). The n-octane data served as the reference value. He rejected the partition coefficients of the liquids with methyl ethyl ketone because they correlated with the ethanol data [6].

From these data Snyder then calculated $\log (K'')$ values which he summed to give the P' value:

$$P' \equiv \log(K'')_{\text{Ethanol}} + \log(K'')_{\text{Dioxane}} + \log(K'')_{\text{CH}_3 \text{NO}_3}.$$

Using this relationship, the strength of the interactions of the solvents with the liquids ethanol, dioxane, and nitromethane can be calculated, e.g. $x_e = \log(K'')_{\text{Ethanol}}/P'$. Thus the following is valid:

$$P' = x_{e}P' + x_{d}P' + x_{n}P' \quad (x_{e} + x_{d} + x_{n} = 1). \tag{4.4}$$

Here.

P' polarity scale (solvent strength parameter)

 $x_{\rm e}$ proportion of solvent interacting capacity with ethanol (proton donor character)

 $x_{
m d}$ proportion of solvent interacting capacity with dioxane (proton acceptor character)

 x_n proportion of solvent interaction capacity with nitromethane (dipole character)

The solvent strength parameter (ε^0) is only conditionally comparable with the polarity scale P' as it was obtained by a completely different approach. A workable simplification can be used

$$\varepsilon^0 \approx 0.1 P'. \tag{4.5}$$

The three experimentally determined selectivity parameters (x_d, x_e, x_n) characterize the important features of a solvent mixture. They always sum up to one. The values for the individual solvents are listed in Appendix 4.7. Various corrections have been carried out, based on new measurements of partition coefficients for triethylamine, chloroform, and methylene chloride. Methylene chloride has now been re-classified from polarity group V to group VII [8].

Taking into account the various polar distribution constants (selectivity parameters) for all solvents resulted in a classification that revealed eight clusters (or groups) (Fig. 4.2). Each group includes solvents with similar characteristics. Solvent strength adjusting solvents (e.g. *n*-pentane, isooctane, cyclohexane, and hexane) are not classified in any group because their solvent strength is zero and

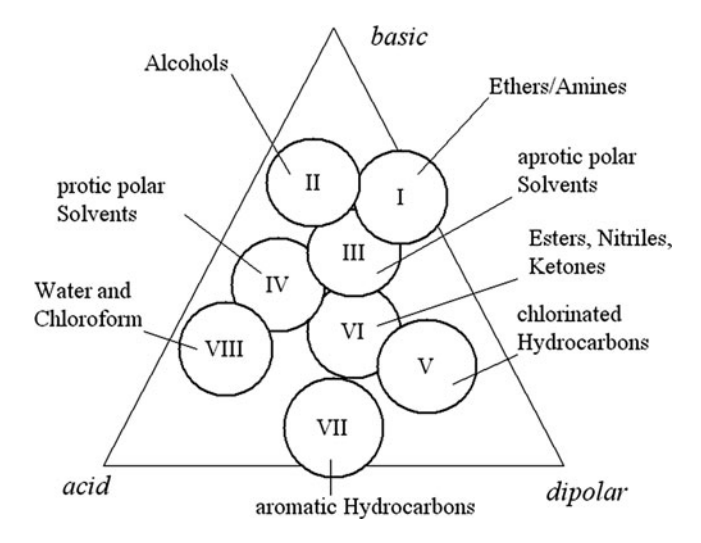


Fig. 4.2 Classification of solvents in various selectivity groups (according to Snyder [6])

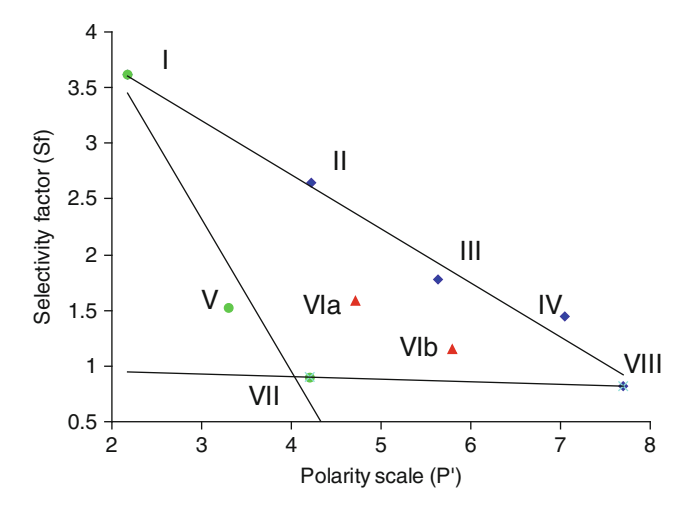


Fig. 4.3 The selectivity factors (S_f) , plotted against the solvent strength (P') [9, 10]

they have no selectivity. As the sum of the selectivity factors is always one by definition, the quotient of two factors is sufficient to determine all three values. The definition of this selectivity factor (S_f) is attributed to Nyiredy [9, 10]:

$$S_{\rm f} = \frac{x_{\rm e}}{x_{\rm d}}$$
.

Here.

 $S_{\rm f}$ selectivity factor

x_e proton acceptor character

 $x_{\rm d}$ proton donator character

If the averaged selectivity factors of a group are plotted against their solvent strengths, the result is two straight lines (Fig. 4.3).

The solvent clusters I–IV and VIII form one line and the solvent clusters I, V, and VII the other. Solvent cluster I (ethers and amines) show the highest selectivity factors, i.e. the greatest proton acceptor effects. Solvent clusters VIII and VII show the lowest proton acceptor characteristics. Clusters VIa and VIb lie between the two straight lines. Solvents from both of these clusters are suitable as solvent mediators. They include ethyl acetate, methyl ethyl ketone, cyclohexanone, dioxane, acetone, and acetonitrile.

4.3.2 Other Methods for Characterizing Solvents

There are other methods for characterizing solvents besides the two approaches presented above (see [11] for further information). However, we will only describe

the "solvatochromic approach," according to Reichardt [4, 12]. Reichardt based his approach on work by Dimroth. He used the spectroscopic behaviour of the substance known as "Reichardt's dye" to characterize various solvents. A polarity parameter can be determined from the solvent-dependant spectral shift. This widespread method used for characterizing solvents in organic chemistry did not succeed in chromatography against competition from Snyder's polarity index. By the way, Reichard's dye method can be used to measure the water content of a TLC sorbent [13].

4.4 Optimizing Solvent Composition

The aim of optimizing the mobile phase composition is to achieve a more satisfactory separation. Following the theoretical considerations in Chap. 2, an optimum separation of two components occurs at $R_{\rm f}$ values of around 0.33. The purpose of optimizing solvent compositions is therefore to migrate a critical substance pair such that their $R_{\rm f}$ values lie at approximately 0.33. The choice of solvent composition is decisive for several reasons.

- The solvent composition must move the analyte to an advantageous $R_{\rm f}$ value determined by its solvent strength.
- The selectivity of the solvent composition determines the resolution of the two substances and thus the quality of the separation. The selectivity parameters are responsible for the resolution.
- Diffusion should be as low as possible during the separation. Consequently, the development time should be as short as possible.

While the first two points have been dealt with already, we must take another look at the separation time. For complete wettability (a wetting angle of $\vartheta = 0$ which results in $\cos \vartheta = 1$), (2.1) can be written as

$$Z_{\mathrm{f}} = \sqrt{2k_0d_{\mathrm{p}}\frac{\gamma}{\eta}t},$$

Where

 $Z_{\rm f}$ solvent front migration distance (mm)

t development time

 k_0 permeability constant, $k_0 = 6-8 \times 10^{-3}$

 $d_{\rm p}$ average particle size of the stationary phase

 γ/η quotient of the surface tension and the viscosity of the mobile phase

The greater the value of $d_{\rm p}$, the faster the front moves. Therefore, many separations are carried out on TLC plates with large particle sizes. The γ/η ratio should be large so that the development takes place as quickly as possible. Unfortunately, this statement is not quite as straightforward as it may seem, because even solvents with

a small γ/η ratio (e.g. *n*-butanol) achieve good separations because, although the separation takes longer, zone broadening is suppressed by its relatively high viscosity. In spite of this, the substitution of *n*-butanol by 1-propanol often provides improved separations.

It is difficult to estimate the separation quality of a solvent when so many parameters can influence the separation. The relevant literature contains many practical articles about help from $R_{\rm m}$ values and diverse chemometric processes and theoretical separation techniques [11, 14]. Other publications concentrate on theoretical assessments of separation behaviour or computer-simulated chromatographic systems. Yet the number and variety of these attempts is itself evidence for a present lack of reliability of simulation methods. Occasionally, a computer can provide help with a search for a solvent, but no computer program is yet available to successfully design a solvent system without a laboratory. Therefore, the analyst is still very much in demand for solving separation problems and the famous adage of "trial and error" is still the most successful [4, 11, 15].

In adsorption chromatography, the best separating conditions can be ascertained with the aid of a triangle diagram as shown in Fig. 4.4 [16–19]. If you imagine that the inner triangle can be rotated, then moving the lower point to the polarity region of your sample moves the other points to the correct system conditions for the separation. To separate polar analytes (e.g. hydrophilic compounds, ions), the stationary phase should be inactive and the mobile phase should be polar (i.e. hydrophilic). For separating lipophilic (non-polar) analytes, the stationary phase should be active and the mobile phase non-polar (lipophilic).

"Like dissolves like" is the principle for partition chromatography (Fig. 4.5). If you know the chemical structure of your analyte, you can determine the necessary solvent polarity, as the polarity of a compound is determined by its functional groups. As far as functional groups are concerned, the following ranking of increasing polarity is valid: RH, RN(CH₃)₂, RCOOCH₃, RNH₂, ROH, RCONH₂, RCOOH.

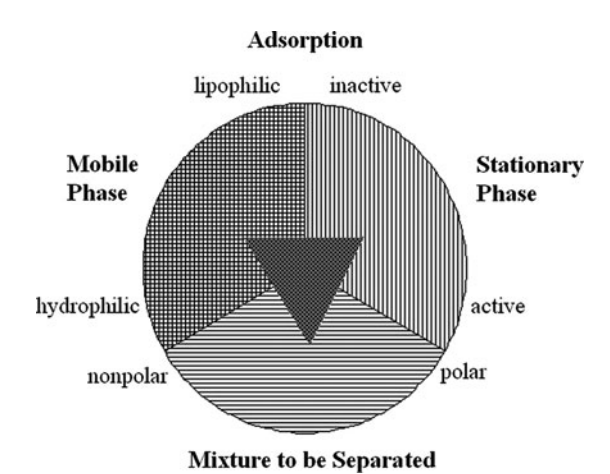
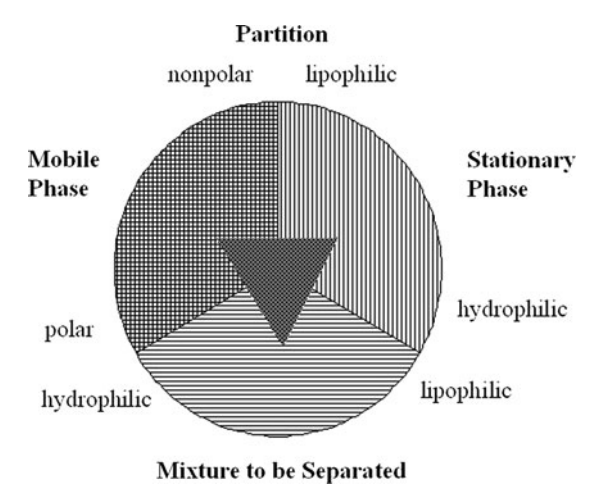


Fig. 4.4 Selectivity triangle for choosing solvents in adsorption chromatography.

Fig. 4.5 Selectivity triangle for choosing solvents in partition chromatography



For separating lipophilic substances, the stationary phase should be lipophilic and the mobile phase more polar. For separating hydrophilic substances, the stationary phase should be hydrophilic and the mobile phase non-polar.

The statement "like dissolves like" is also true for acids and bases. Acids should be separated with acidic solvents such as acetic acid, formic acid, or solvents containing dilute hydrochloric acid. Bases are best separated by adding modifiers containing a basic functional group or diluted ammonia to the mobile phase. Often the relevant literature contains important hints on how to identify the best solvent system for a particular sample [19, 20].

If you cannot find any literature for the stationary phase, begin your investigation with a silica gel 60 HPTLC plate. To achieve a rough overview of elution behaviour, try out at least one solvent from each selectivity group of Snyder's classification. The various selectivity groups or clusters are shown in Fig. 4.2. All available individual data concerning the various pure substances used as solvents in TLC are listed in Table 4.6 in Appendix.

There are a number of azeotropic solvent mixtures that neither enrich nor deplete either of their partners during development. These azeotropic mixtures can be treated like pure substances (see Table 4.3).

Taking toxicity and polarity ranges into account, the following mobile phases, Table 4.4, are often suggested for screening purposes.

The separation should be assessed with each solvent or solvent mixture listed in Table 4.4. The quickest and easiest way is to use aluminium-backed silica gel cards. Use scissors (or better a twin cutter) to cut them into handy strips. Merely a few microlitres of solvent in a small container is sufficient to judge separation behaviour over a roughly 4 cm development. For colourless compounds, zone positions can be determined by using layers containing an indicator activated by UV light. Optimum migration distances for a critical pair correspond to $R_{\rm f}$ values of 0.3–0.4. If the $R_{\rm f}$ value is too high, the solvent strength must be reduced. If it is necessary to raise the

Solvent	(mL)	P' Value	b.p. (°C)	
Propanol	(20.3)	2.6	66.2	
+ 2-propyl ether	(115.6)			
Methyl acetate	(52.3)	2.9	50.8	
+ methanol	(22.5)			
+ cyclohexane	(43.25)			
CH ₂ Cl ₂	(70.0)	3.3	37.8	
+ methanol	(9.2)			
CHCl ₃	(62.6)	3.5	59.4	
+ ethanol	(9.9)			
Acetone	(85.3)	3.7	53.0	
+ cyclohexane	(41.8)			
CHCl ₃	(59.5)	3.8	53.4	
+ methanol	(15.9)			
Methanol	(22.4)	4.4	54.0	
+ methyl acetate	(88.5)			
Ethanol	(118.5)	4.5	78.2	
+ water	(4.0)			
CHCl ₃	(11.6)	4.6	79.9	
+ 2-butanon	(103.2)			
Methanol	(15.2)	5.4	55.5	
+ acetone	(111.3)			

Table 4.3 Azeotropic solvent mixtures with their P' values and boiling points

Table 4.4 Mobile phases used to start an optimization process

Group	Name	P Value
0	<i>n</i> -Pentane	0.0
I	Methyl tert-butyl ether	2.7
II	2-Propanol + methanol	3.9 + 5.1
III	2-Methoxyethanol	5.5
IV	Acetic acids	6.0
V	Methylene chloride	3.1
VI	Ethyl acetate + acetone	4.4 + 5.1
VII	Toluene	2.4

 $R_{\rm f}$ value, the solvent's strength should be increased. If substances move into the desirable $R_{\rm f}$ region, but do not separate from one another, vary the solvent composition but keep the same solvent strength.

Figure 4.1 shows that the solvent strength of a binary solvent mixture is a function of mobile phase composition. Higher selectivity can be attained by adding not more than 5% of the stronger solvent to the weaker solvent. In this region, small changes in composition show large alterations in solvent strength. Mixtures with over 50% volume fraction of the stronger solvent are often recommended because such mixtures show relatively constant solvent strength, even with small alterations in their composition [2].

The so-called spot test is sometimes recommended for solvent optimization (Fig. 4.6). It involves applying about $1-2 \mu L$ of the sample to a plate [15] as a



Fig. 4.6 Using spot tests to optimize the separation of a CAMAG dye mixture (on silica gel) with $35 \,\mu\text{L}$ each of cyclohexane, diethyl ether, *tert*-butyl methyl ether, methylene chloride, toluene, and ethyl acetate (from *top left* to *bottom right*). Methylene chloride and toluene show the best separation

spot. Then place the point of a micropipette containing about 35 μ L of solvent on the centre of the spot, and then allow the solvent to run out. This creates a series of rings of about 1–1.5 cm diameter. This circular process is to be used when no aluminium-backed plates are available because glass plates are difficult to divide into sections.

However one must be careful in assessing the spots because transforming circular R_f values to linear chromatography is governed by the following relationship:

$$(R_{\rm f})_{\rm linear} = (R_{\rm f})_{\rm circular}^2.$$
 (4.6)

This equation shows that a circular chromatogram results in larger $R_{\rm f}$ values than for linear development. To transfer circular chromatographic results to a linear development, the rings for the critical pair should be moved to about half of the ring diameter.

If you have developed individual spots on a TLC plate, mark the circumference of the solvent front with a pencil. After drying, mark all sample rings with a diameter of more than half of the solvent front. These spot tests provide usable solvents. When transferring separations to linear chambers, however, you must take into consideration that these preliminary tests were performed without chamber saturation [2].

4.5 The PRISMA Model (According to Nyiredy)

The PRISMA model proposed by Nyiredy et al. [21, 22] has a great advantage for method development in that it does not need any computer algorithms or prior knowledge of the analytes. To determine the optimum quaternary solvent mixture,

you, at first, establish the solvent strength for the separation providing the desired range of $R_{\rm f}$ values and then dilute any number of additional solvents with a strength adjusting solvent to bring them into the required solvent strength range.

By visual comparison the three solvents that demonstrate the best initial separations are selected for optimization. The three solvents are diluted to the required solvent strength. These three mixtures with solvent strengths $P_{\rm A}', P_{\rm B}', P_{\rm C}'$ represent the three corners of an equilateral triangle of composition 1/0/0, 0/1/0, and 0/0/1. The edges of this triangle describe single solvents; the side's binary mixtures while the composition of all the ternary mixtures lay on the surface. The shape of the prism in the third dimension arises when the solvent strength is added to the triangle. A regular prism occurs if these three components are reduced to an equal solvent strength with a solvent strength adjusting solvent.

For example, Fig. 4.7 illustrates the solvent system of chloroform, methylene chloride, and methyl *tert*-butyl ether. The aim is to make a mixture of these three solvents with a solvent strength of 2.7.

The polarity scale for the mixture is calculated according to

$$P' = x_{\text{A}} P_{\text{MTBE}}' + x_{\text{B}} P'_{\text{CHCl}_3} + x_{\text{C}} P_{\text{CH}_2\text{Cl}_2}'.$$

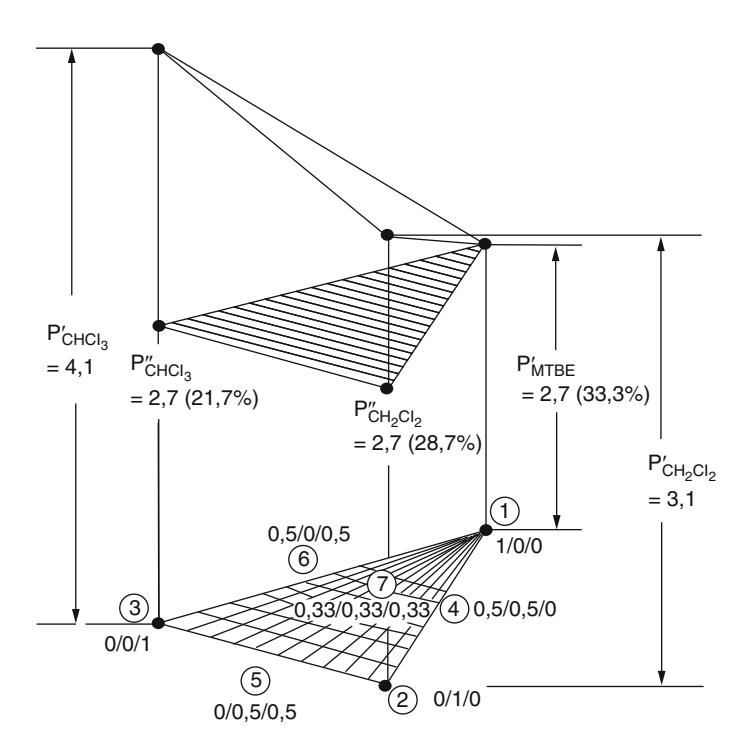


Fig. 4.7 PRISMA model for solvent system CHCl₃, CH₂Cl₂, and methyl *tert*-butyl ether (From [3] with permission. © Wiley-VCH.)

4.6 Solvent Additives 99

The P' value of the methyl *tert*-butyl ether is exactly 2.7, so it can be used without diluting. The divisor x_A receives the value 0.33.

Chloroform has a polarity of $P_{\text{CHCl}_3}' = 4.1$ and methylene chloride a value of $P_{\text{CH}_2\text{Cl}_2}' = 3.1$, so both solvents must be diluted with heptane to a value of P' = 2.7. Thus, the chloroform proportion is $x_B = 0.33 \times 2.7/4.1 = 0.217$.

The calculation for methylene chloride is $x_B = 0.33 \times 2.7/3.1 = 0.287$.

$$P_{ABC}' = 33\% MTBE + 21.7\% CHCl_3 + 28.7\% CH_2 Cl_2 + (11.3 + 4.3)\%$$
 heptane.

Then choose new selectivity points on the surface $(P_{\rm A}'/P_{\rm B}'/P_{\rm C}')$ so that they always sum up to 10. Use these various mixtures of the three original solvents (e.g. 1/1/8 or 1/8/1 or 8/1/1 on the outer edges or 3/3/3 in the middle) to optimize the separation (between $R_{\rm f}=0.2$ and 0.8 with the best resolution at $R_{\rm f}=0.33$). This kind of trial will usually lead to the optimum quaternary solvent system for the separation. The PRISMA model combines solvent strength and solvent selectivity in a graphical manner, visualizing the process, and thus aiding the identification of an optimum solvent mixture.

4.6 Solvent Additives

Besides modifiers, strength adjusting solvents, and mediators, additives are also used for some separations. They are mostly buffers that keep the pH of the solvents in a pre-determined region. To determine the pH of a buffer, the buffer equation derived from the logarithmic dissociation equation of an acid (HA) to protons (H^+) and their corresponding anion (A^-) can be used:

$$pH \equiv -\lg(c^{H^{+}}) = pK_{S} + \lg\frac{c_{A^{-}}}{c_{HA}}.$$
 (4.7)

If the concentration of the acids and the corresponding anions are equal, the logarithmic expression is zero, and thus the following is valid:

$$pH = pK_S$$

Therefore, it is simple to make buffers with a pH equal to the pK_S of the buffer system. You only have to weigh out the same molar amounts of acid and salt or base and salt. In everyday laboratory practice, you start with the salt and add a solution of the acid or base until the desired pH is attained. It should be noted that a buffer functions in a pH window of about \pm 30% around its pK_S value (Table 4.5). When an aqueous buffer is mixed with a miscible organic solvent, the pH of the solution changes because of changes in the solvation of the anion and is not easily calculated

resulting in a burier with $pri = pk_S$	
Buffer system	pK_S value
H ₃ PO ₄ /H ₂ PO ₃ ⁻	1.96
HCOOH/COOH ⁻	3.7
CH ₃ COOH/CH ₃ COO ⁻	4.75
$H_2PO_3^-/HPO_4^{2-}$	6.16
$H_3BO_3/H_2BO_3^-$	9.24
NH ₄ ⁺ /NH ₃	9.25
HCO_3^-/CO_3^{2-}	10.4
HPO_4^{2-}/PO_4^{3-}	12.3

Table 4.5 p K_S values for various buffer systems suitable for TLC. Both substances are mixed in a molar relationship 1:1 resulting in a buffer with pH = p K_S

from the volume fraction of organic solvent present in the mixture. It is not unusual for the composition of the mobile phase to be indicated with the pH given for the aqueous buffer used in its preparation. However, this will not be the pH of the mobile phase used for the separation.

How does a buffer alter the migration behaviour of an analyte? Acid HA is partitioned between the mobile and stationary phases:

$$[HA]_m \to [HA]_s + [A^-]_s + [H^+]_s$$

For the acid HA, an apparent partition coefficient K^* can be written as

$$K^* = \frac{[c_{\text{HA}}]_{\text{s}} + [c_{\text{A}^-}]_{\text{s}}}{[c_{\text{HA}}]_{\text{m}}}$$

With the definition of the acid constant in the stationary phase $K_s = [c_{H^+}c_{A^-}/c_{HA}]_s$ and the definition of the partition coefficient $K=[c_{HA}]_s/[c_{HA}]_m$, an apparent partition coefficient K^* can also be written as

$$K^* = \frac{[c_{\text{HA}}]_{\text{s}}}{[c_{\text{HA}}]_{\text{m}}} + \frac{[c_{\text{A}^-}]_{\text{s}}[c_{\text{H}^+}]_{\text{s}}[c_{\text{HA}}]_{\text{s}}}{[c_{\text{HA}}]_{\text{m}}[c_{\text{H}^+}]_{\text{s}}[c_{\text{HA}}]_{\text{s}}} = K \left[1 + \frac{K_{\text{s}}}{c_{\text{H}^+}} \right]_{\text{s}}$$

By entering the apparent partition coefficient into the definition of the $R_{\rm m}$ value (2.10), it follows

$$R_{\rm m} = \lg \frac{V_{\rm s}}{V_{\rm m}} + \lg K^* = \lg \frac{V_{\rm s}}{V_{\rm m}} + \lg K + \lg \left[1 + \frac{Ks}{C_{\rm H^+}}\right]_{\rm s}.$$

With the definition of the pH (4.7) and the p K_s for the stationary phase (p K_s = -lg K_s), it follows for a strong acid (pH \gg p K_s) or $K_s/c_H^+ \gg 1$ [2]:

4.6 Solvent Additives 101

Fig. 4.8 The separation of paraquat, diquat, mepiquat, chloromequat, and difenzoquat (from bottom to top) with a solvent mix of 1-propanol—methanol and 0.5, 1, 1.5, 2, 2.5 M aqueous NaCl solution (4+4+12, V/V). The compounds were stained with tetraphenyl borate/HCl in water and show fluorescence when illuminated with UV light at 366 nm



$$R_{\rm m} = \lg K \frac{V_{\rm s}}{V_{\rm m}} + pH - pK_{\rm s}. \tag{4.8}$$

The following is true for ionized analytes: their $R_{\rm m}$ values rise linearly with an increase of the pH of the stationary phase. Thus the $R_{\rm f}$ value correspondingly decreases as the pH of the stationary phase rises. An important point in this connection is that the pH and $R_{\rm f}$ values of ionized analytes (acids, bases, and salts) change, but not the $R_{\rm f}$ values of neutral analytes.

For the separation of ionic compounds, the mobile phase should provide a sufficient number of counterions. For this purpose, potassium bromide, lithium chloride, ammonium chloride, or sodium acetate is often used, since these salts are reasonably soluble in organic solvents. The retention behaviour can also be influenced via the concentration of counterions. Figure 4.8 shows the separation of some cationic compounds in the presence of different concentrations of sodium chloride. The influence of the salt concentration on the separation can clearly be recognized. Without added salt, the cationic compounds remain unseparated at the point of application. All cationic compounds migrate from the origin only if the sodium chloride concentration is greater than about 1 M.

Ion-pair interactions are introduced to dissolve ionic compounds in low polarity mobile phases. A lipophilic anion is added to cationic compounds or vice versa. Salts of pentane- or hexanesulphonic acids are often used to dissolve cations. Anions can be dissolved by cetylpyridinium chloride. In the ion pair, the two opposing charges neutralize each other, and the lipophilic shell provides compatibility with low polarity solvents.

Adding boric acid has proved useful for separating sugars or polyalcohols, since boric acid forms complexes selectively with *cis*-1,2-diol groups. The same is true for crown ethers, which form lipophilic complexes with Li⁺, Na⁺, and K⁺. Chiral reagents, such as cyclodextrins, form diastereomeric insertion complexes with chiral samples that can be separated by chromatography [23].

4.7 Appendix: Solvent Properties

Table 4.6 Polarity scale, weighting factors, and group membership (with interpolated values for reversed-phase chromatography in brackets)

Solvent	P' Value	x _e	$x_{\rm d}$	$\chi_{\rm n}$	Group	$\gamma/\eta (25^\circ)^+$
n-Hexane	0.1	_	_	_	0	56
<i>n</i> -Pentane	0.1	_	_	_	0	67
Cyclohexane	0.2	_	_	_	0	28
Di- <i>n</i> -butyl ether	2.1	0.44	0.18	0.38	I	91
Di-isopropyl ether	2.4	0.48	0.14	0.38	I	91
Toluene	2.4	0.25	0.28	0.47	VII	48
Triethylamine	1.9 (2.2)	0.56 (0.66)	0.12 (0.08)	0.32 (0.26)	I	52
Methyl- <i>t</i> -butyl ether	2.7	0.49	0.14	0.37	I	72
Diethyl ether	2.8	0.53	0.13	0.34	I	71
Methylene chloride	3.1 (4.3)	0.29 (0.27)	0.18 (0.33)	0.53	V (VII)	62
n-Octanol	3.4	0.56	0.18	0.25	II	3.7
1,1-Dichlorethane	3.5	0.30	0.21	0.49	V	41
2-Propanol	3.9	0.55	0.19	0.27	II	8.7
n-Butanol	3.9	0.56	0.19	0.25	II	8.3
THF	4.0 (4.4)	0.38	0.20	0.42	III	56
1-Propanol	4.0	0.54	0.19	0.27	II	11
t-Butanol	4.1	0.56	0.20	0.24	II	7.3
Chloroform	4.1 (4.3)	0.25 (0.31)	0.41 (0.35)	0.34 (0.34)	VIII	47
Ethanol	4.3 (3.6)	0.52	0.19	0.29	II	19
Ethyl acetate	4.4	0.34	0.23	0.43	VIa	52
Bis-(2-ethoxyethyl)-Ether	4.6	0.37	0.21	0.42	VIa	_
Cyclohexanone	4.7	0.36	0.22	0.42	VIa	40*
Methyl ethyl ketone	4.7	0.35	0.22	0.43	VIa	57
Dioxane	4.8	0.36	0.24	0.40	VIa	26
Chinolin	5.0	0.41	0.23	0.36	III	26
Acetone	5.1 (3.4)	0.35	0.23	0.42	VIa	74
Methanol	5.1 (3.0)	0.48	0.22	0.31	II	38
Pyridine	5.3	0.41	0.22	0.36	III	39
Methoxy ethanol	5.5	0.38	0.24	0.38	III	18
Benzyl alcohol	5.7	0.40	0.30	0.30	IV	_
Acetonitrile	5.8 (3.1)	0.31	0.27	0.42	VIb	75
Acetic acid	6.0	0.39	0.31	0.30	IV	21
Formic acid	6.0	_	_	_	IV	_
Nitromethane	6.0	0.28	0.31	0.41	VII	_
Methyl formamide	6.0	0.41	0.23	0.36	III	_
DMF	6.4	0.39	0.21	0.40	III	40
Ethylene glycol	6.9	0.43	0.29	0.28	IV	2.3
DMSO	7.2	0.39	0.23	0.39	III	2.4
m-Cresol	7.4	0.38	0.37	0.25	VIII	2.8
Dodecafluoroheptanol	8.8	0.33	0.40	0.27	VIII	_
Formamide	9.6	0.37	0.33	0.30	IV	17
Water	10.2 (0.0)	0.37	0.37	0.25	VIII	73

 γ/η [m/s], *value of methyl butyl ketone, *italics*: values according to [8]

References 103

References

- 1. Snyder LR (1968) Principles of adsorption chromatography. Dekker, New York
- 2. Geiss F (1987) Fundamentals of thin-layer chromatography. Hüthig, Heidelberg, pp 278–286
- 3. Frey H-P, Zieloff K (1993) Qualitative und quantitative Dünnschichtchromatographie, Grundlagen and Praxis. Chemie, Weinheim
- Barwick VJ (1997) Strategies for solvent selection a literature review. Trends Anal Chem 16:293–309
- Rohrschneider L (1973) Solvent characterization by gas-liquid partition coefficients of selected solutes. Anal Chem 45:1241–1247
- Snyder LR (1978) Classification of solvent properties of common liquids. J Chromatogr Sci 16:223–234
- Snyder LR (1974) Classification of solvent properties of common liquids. J Chromatogr A 92:223–234
- 8. Rutan SC, Carr PW, Cheong WJ, Park JH, Snyder LR (1978) Re-evaluation of the solvent triangle and comparison to solvachromic based scales of solvent strength and selectivity. J Chromatogr 463:21–37
- Nyiredy Sz (1997) Solvent classification for liquid chromatography. In: Chromatography, celebrating Michael Tswett's 125th birthday. InCom Sonderband, Düsseldorf, pp 231–239
- Nyiredy Sz, Fatér Z, Szabady B (1994) Identification in planar chromatography by use of retention data measured using characterized mobile phases. J Planar Chromatogr 7:406–409
- Poole CF, Dias NC (2000) Practioner's guide to method development in thin-layer chromatography. J Chromatogr A 892:123–142
- 12. de Juan A, Fonrodona G, Casassas E (1997) Solvent classification based on solvatochromic parameters: a comparison with the Snyder approach. Trends Anal Chem 16:52–62
- Spangenberg B, Kaiser RE (2007) The water content of stationary phases. J Planar Chromatogr 20:307–308
- 14. Cavalli E, Truong TT, Thomassin M, Guichard C (1993) Comparison of optimization methods in planar chromatography. Chromatographia 35:102–108
- 15. Reich E, George T (1997) Method development in HPTLC. J Planar Chromatogr 10:273-280
- 16. Kraus Lj, Koch A, Hoffstetter-Kuhn S (1996) Dünnschichtchromatographie. Springer, Berlin
- 17. Randerath K (1967) Thin layer chromatographie, 2. Auflage. Springer, Berlin
- 18. Hahn-Deinstrop E (1992) Stationary phases, sorbents. J Planar Chromatogr 5:57-61
- Stahl E (ed) (1969) Thin-layer chromatography. A laboratory handbook, 2 edn. Springer, Berlin, Heidelberg
- 20. Gasparič J, Králové H (1992) Chromatography on thin layers impregnated with organic stationary phases. Adv Chromatogr 31:153–252
- Nyiredy Sz, Meier B, Erdelmeier CAJ, Sticher O (1985) PRISMA: a geometrical design for solvent optimisation in HPLC. J High Resolut Chromatogr 8:186–188
- 22. Nyiredy Sz, Dallenbach-Tölke K, Sticher O (1988) The PRISMA optimization system in planar chromatography. J Planar Chromatogr 1:336–342
- 23. Han SM, Armstrong DW (1990) Chiral separation via charge transfer. Chem Anal 108:81-100

Chapter 5 Preparing and Applying Samples

Sample application decisively influences the separation quality and fidelity of quantitative information. The important fact is that they both can be affected by the choice of experimental conditions [1–4]. Sample application, however, only indirectly influences the selectivity of a separation system. A poor application merely hinders the achievement of the maximum possible selectivity, thus preventing the highest separation quality from being achieved. Furthermore, sample application should always be done automatically if quantification is required, since the variance of the application volume is one of the main contributors to the overall experimental error.

5.1 Sample Preparation

Except in rare cases, samples must be simplified prior to analysis with two objectives in mind: to enrich the analytes and to deplete any disturbing matrix. In the simplest case, solid samples are dissolved in a suitable solvent prior to sample application. In an ideal case, for example, the sample is mixed with water and methylene chloride forming two phases. The analyte is distributed to the organic phase while the matrix remains in the aqueous phase. This classical liquid—liquid extraction can be carried out with various solvents. The important point is that two phases are formed.

5.1.1 The QuEChERS Approach

Acetonitrile, tetrahydrofuran, or acetone can be used for extraction purposes even though these solvents are totally miscible with water. In the presence of a high salt concentration (e.g. NaCl, MgSO₄), the organic phase will separate from the aqueous phase. Experience has shown that centrifugation can accelerate phase

	1	1	<i>C</i> 1
Solvent (10 mL)	P' value	Salt amount	Volume of upper phase
2-Propanol	3.9	4 g MgSO ₄ ·6 H ₂ O + 1 g NaCl	12.4 mL
Tetrahydrofuran	4.0	4 g MgSO ₄ ·6 H ₂ O + 1 g NaCl	10.4 mL
Ethanol	4.3	8 g K ₂ CO	11.4 mL
Dioxane	4.8	$4 \text{ g MgSO}_4 \cdot 6 \text{ H}_2\text{O} + 1 \text{ g NaCl}$	3.4 mL
Acetone	5.1	$4 \text{ g MgSO}_4 \cdot 6 \text{ H}_2\text{O} + 1 \text{ g NaCl}$	9.0 mL
Acetonitrile	5.8	$4 \text{ g MgSO}_4 \cdot 6 \text{ H}_2\text{O} + 1 \text{ g NaCl}$	9.8 mL

Table 5.1 List of solvents for the QuEChERS approach (calculated for 10 mL of aqueous sample) with the amount of salt required to form two phases and the volume of the organic phase

separation. This new sample preparation method is known as the QuEChERS approach (the abbreviation of quick, easy, cheap, effective, rugged, and safe) and was developed for use in pesticide residue analysis [5] and the analysis of pharmaceuticals in blood [6] (Table 5.1).

For the standard procedure, 10 g samples are homogenized for 1 min with 10 mL of acetonitrile or another solvent. After adding 4 g MgSO₄ and 1 g NaCl, the sample vial is shaken to dissolve the salts and then centrifuged. The organic phase can be applied directly to the layer. Acetonitrile is the standard solvent for the extraction of pesticides from water-rich fruits and vegetables. Ethyl acetate, acetone, and tetrahydrofuran are more suitable for water-poor matrices.

An advantage of acetonitrile is that water can be easily removed by drying with MgSO₄. The addition of NaCl influences the polarity of the aqueous phase allowing a degree of control over the amount of matrix extracted.

5.1.2 Solid-Phase Extraction

The most frequently applied sample preparation method involves no more than dissolving the sample in a liquid, followed by filtering and evaporating the solution to dryness. The dry sample is taken up in a small volume of another volatile solvent and then applied to the layer. The treated sample usually contains matrix remains, but these do not cause a problem in TLC since each plate is used only once. On the other hand, for HPLC column re-use is essential and further clean-up using solid-phase extraction (SPE) is required. This approach is also beneficial for TLC separations [7–9].

SPE involves fife steps. First, the cartridge is equilibrated with a non-polar or slightly polar solvent, which wets and cleans the surface. Second, the sample solvent (water, buffer, or organic solvent) is passed through the column to condition the cartridge. Third, the sample is applied to the cartridge and sucked through the sorbent packing, where, ideally, the analytes are retained and matrix components run to waste. After the sample is loaded (fourth step), the cartridge is washed with water, buffer, or solvents to remove further impurities. In the ideal case the matrix will be completely removed from the cartridge. As last step the analyte is eluted with a small amount of a strong solvent. Non-polar samples can be eluted with hexane, dichloromethane, acetonitrile, ethanol, or 2-propanol. Medium-polar and

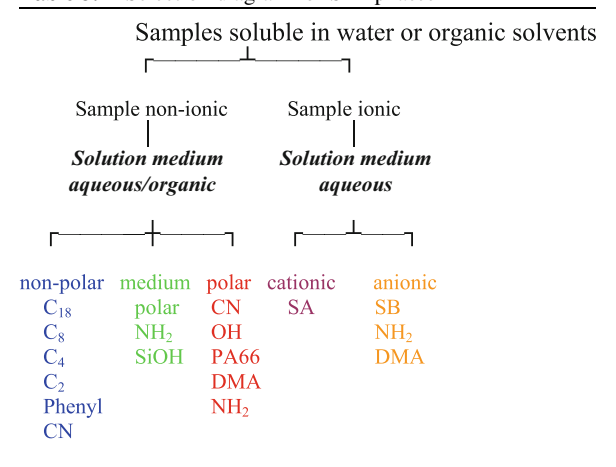
polar samples can be eluated with chloroform, dichloromethane, ethyl acetate, methanol, ethanol, or water. Mostly non-polar solvents are used because TLC analytes are typically semi-polar or non-polar compounds. Vacuum suction is a suitable method for elution with small volumes of a strong solvent. Special equipment is commercially available for the above purpose and allows samples to be processed in parallel. A typical apparatus for SPE using vacuum suction is shown in Fig. 5.1.

For SPE, typically about 1 g of sorbent in a short polyethylene or glass column is used. Sorbent selection is dictated by the need to provide a suitable breakthrough volume for the analytes of interest and to maintain compatibility with the sample solvent. Table 5.2 lists the sorbent types commonly used for different analytes.

Fig. 5.1 Solid-phase extraction by hydrostatic pressure (*left*) and SPE by vacuum suction (*right*)



Table 5.2 Selection diagram for SPE phases



Phenyl phenyl substituted, PA66 nylon 66, DMA dimethylamino substituted, SA benzenesulphonic acid, SB quaternary amines

Anion exchange sorbents are derivatized with positively charged functional groups, mostly quaternary ammonium or aminopropyl groups that retain negatively charged anions. The analytes are eluted with a solvent of appropriate pH and/or ionic strength to displace the analytes from the sorbent in a small volume of solvent.

Cation exchange sorbents are derivatized with functional groups that retain positively charged cations. Weak cation exchange sorbents contain aliphatic carboxylic acids, and strong cation exchangers contain aliphatic sulphonic acid groups. Weak cation exchangers are negatively charged at pH values above 5. Strong cation exchangers are negatively charged at lower pH values. Cationic analytes can be eluted by acids and/or salt solutions [7–9].

The SPE procedure delivers clean sample solutions, but is time consuming and relatively expensive. One advantage of this method is that it avoids using large quantities of organic solvents, and analytes from water samples can also be easily enriched [10].

5.1.3 Stir Bar Sorptive Extraction

An interesting development for extraction with a small amount of sorbent is the so-called stir bar sorptive extraction [11, 12]. A stir bar is a magnetic bar used to stir a mixture. For extraction purposes, special polysiloxane coated stir bars are used. The polysiloxane outer coating serves as the extraction phase. The sample solution is simply stirred with this stir bar for some hours, whereby the analytes are enriched in the lipophilic polysiloxane phase. The stir bar is removed from the solution and the analytes recovered by immersing the stir bar in a small amount of organic solvent.

No matter which sample preparation method is chosen, the simplest method is likely to produce the lowest analytical error. In addition, the sample preparation error is generally much greater than the instrumental measurement uncertainty error. One should not underestimate the advantages of using a disposable layer in TLC. Even strongly contaminated sample solutions can be directly placed on the layer without any preparation, which considerably reduces the error in sample preparation to mere sample application. In any case, such simple methods are to be recommended in preference to complicated sample preparation procedures because they help avoid mistakes.

5.2 The Dosage Quality

The application width of a sample is the deciding factor in optimizing the separation. The expression for the separation number according to Kaiser's equation (2.28) is

$$\mathrm{SN} = \sqrt{\frac{N_{\mathrm{real}}'}{5.545}} \frac{w_{\mathrm{H(Front)}} - w_{\mathrm{H(Start)}}}{w_{\mathrm{H(Front)}} + w_{\mathrm{H(Start)}}} - 1.$$

Resolved for the real plate number (measured for peaks at half height)

$$\sqrt{\frac{N'_{\text{real}}}{5.545}} = (\text{SN} + 1) \frac{w_{\text{H(Front)}} + w_{\text{H(Start)}}}{w_{\text{H(Front)}} - w_{\text{H(Start)}}}$$

and for resolution taking $N' = NR_f$ into account

$$R_S = \left(\frac{k_1}{k_2} - 1\right) (1 - R_{f2}) \sqrt{\frac{N'_{real}}{16}}$$

which if the peak width at half height and not at base is used, results in

$$R_{S} = \left(\frac{k_{1}}{k_{2}} - 1\right) (1 - R_{f2}) (SN + 1) \frac{w_{\text{H(Front)}} + w_{\text{H(Start)}}}{w_{\text{H(Front)}} - w_{\text{H(Start)}}}.$$
 (5.1)

According to Kaiser, the dosage quality $Q_{\rm D}$ can be determined by the following expression:

$$Q_{\rm D} \equiv \frac{w_{\rm H(Front)} - w_{\rm H(Start)}}{w_{\rm H(Front)} + w_{\rm H(Start)}}.$$
 (5.2)

It has a maximum value of $Q_D = 1$ if $w_{H(Start)} = 0$. For $w_{H(Start)} > 0$, (5.2) takes values smaller than 1. With (5.2), the expression for the selectivity can be written as

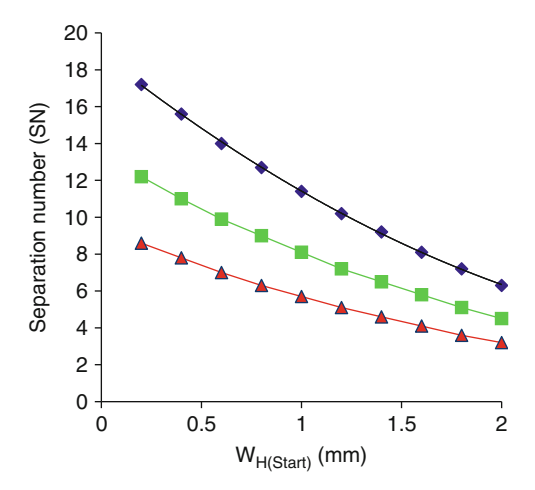
$$\left(\frac{k_1}{k_2} - 1\right) = \left(\frac{1}{(1 - R_{f2})(SN + 1)}\right) R_S Q_D. \tag{5.3}$$

The best quantification results are found for a separation system with high selectivity. Equation (5.3) states that for achieving a high selectivity it is necessary to have a good resolution (R_S) and an optimum in dosage quality (Q_D). An optimum in dosage quality means achieving application widths ($w_{H(Start)}$) that are as narrow as possible. Effective focusing is achievable only by using strong solvents, which provide large R_f values, thus creating narrow bands. The effect is multiplied if focusing is repeated.

From equation (2.28), it is clear that the separation number increases with narrower application bands. In other words, the selectivity increases with smaller application bandwidths or spot diameters.

Figure 5.2 shows the separation numbers depending on application bandwidth according to Kaiser's formula for various real plate numbers (N' = 500, 1,000, and 2,000). The separation numbers decline relatively rapidly with increasing application bandwidth. For large application bandwidths of 1.5 mm and above, separation numbers greater than 10 are unachievable. It can be estimated that, even for an optimum separating systems (N' = 2,000) and application bandwidth of 0.2 mm, maximum separation numbers of about 20 can be achieved. Commonly, separation numbers are less than 10.

Fig. 5.2 Variation of the separation number with application bandwidth $w_{\text{H(Start)}}$ (with $w_{\text{H(Front)}} = 3 \text{ mm}$) for various plate numbers (with N' = 2,000, 1,000, and 500, from the *top downwards*)



Spot application always includes a conflict. A large spot containing as much sample as possible should be applied to achieve the best possible sensitivity, but a smaller diameter spot is needed to increase resolution. Applying the highest possible concentration of the sample solution in several millimetre-long bands can solve this problem. Thus even $10\,\mu L$ of sample with an application bandwidth of not more than 1~mm can be applied to the plate.

The elution strength of the sample solvent is of decisive importance for the application bandwidth. The general rule is that a solvent of the lowest possible strength should be used so that the sample zone does not expand appreciably during sample application. In adsorption chromatography, whenever possible, the sample should be dissolved in a solvent like hexane or any other non-polar solvent. For reversed-phase chromatography water or methanol—water mixture is more appropriate.

If the sample solvent has already been established (because there is no other sample preparation possible or because large amounts of the sample must be applied to the plate), the application band or spot should be focussed with a strong mobile phase during an initial short development. This focusing step can be repeated as many times as needed by interspersing a drying step after each short development.

The effect is based on the fact that the zone is compressed with each development step even before it starts moving. With n short developments, the zone width is given by [7]

$$\sigma_n = \sigma_0 (1 - R_{\rm f})^n, \tag{5.4}$$

where

 σ_n zone width after n focussing steps

 $\sigma_{\rm o}$ zone width before focussing

 $R_{\rm f}$ R_f value in focussing solvent

Another possibility is to use plates with concentration zones. Such plates have an application area and a separate separation area. The application area consists of weakly active or non-retaining adsorbents. This technique goes back to Abbott and Thomas and was used for the first time in 1965 [13]. Kieselguhr or Si_{50000} is often used as material for the application area; the application size is not important on plates with concentration zones, as shown in Fig. 5.3a. At the start of development, the whole sample moves into the separation area and becomes focussed into a tight band independent of its application position. The separation begins with a narrow application bandwidth, and thus correspondingly high separation numbers and good resolutions can be achieved. Spot-shaped applications, however, are a disadvantage, as can be scene for tracks 1, 2, and 6 in Fig. 5.3b. Round application zones lead to an irregular mass distribution for the band-shaped starting zones leading to half-moon shaped separation zones as well as incomplete separations.

If the sample is applied in the zigzag mode, large volumes can be applied to the sample application area without a great loss of resolution at the separation stage. Such an application is shown in track 4 of Fig. 5.3.

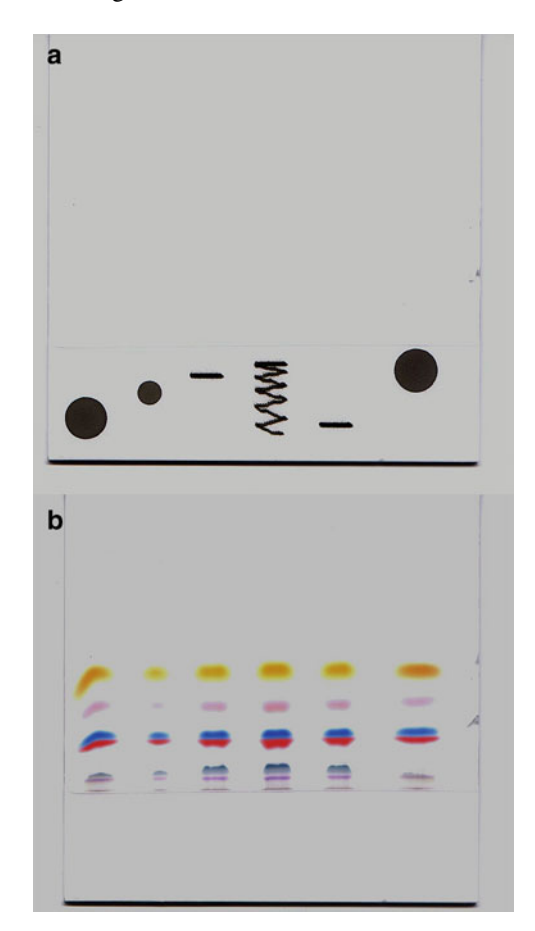


Fig. 5.3 Using an HPTLC plate with application zone: (a) after application, (b) after development

Using plates with concentration zones has a further advantage. Strongly polar substances, salts, and polymers that might interfere in the separation are immobilized on the application area. Application onto a concentration zone does not contaminate neighbouring tracks, even if large volumes are applied as spots. Thus the application zone serves as a kind of "guard column" that can be used for sample clean-up.

5.3 Choice of Application Position

The application position z_0 at the immersion line has an important influence on the separation efficiency and development time. According to Poole, the choice of application position with respect to the mobile phase entry position (z_0) has a significant influence on the plate height of a separation system [14]. The distance between the solvent introduction and application position should, according to Poole, lie between 4 and 6 mm in HPTLC and between 5 and 10 mm in TLC. At greater

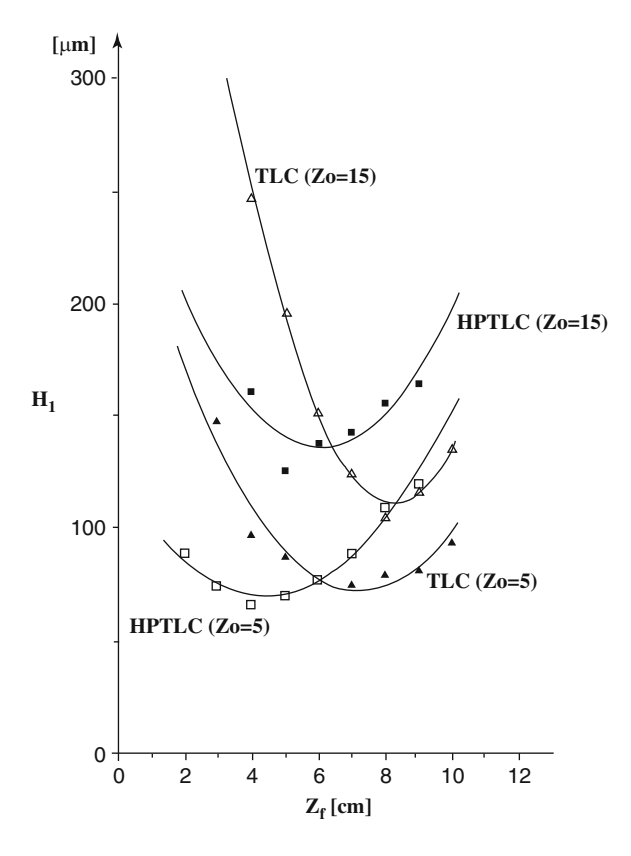


Fig. 5.4 Plot of the plate height against the solvent front migration distance for various TLC and HPTLC separations, each measured at two different sample application positions ($z_0 = 5$ and 15 mm (From [14] with permission. © Akadémiai Kiadó.)

distances, the plate height increases for the separation. This is shown in Fig. 5.4. The solvent flow velocity is the reason why the application position should not be too near the immersion line. At high mobile phase velocities, there may be insufficient time to instantaneously dissolve the sample resulting is an extended application zone, and the sample appearing to be smeared over the layer after separation. This can also be concluded from the expression for the observed median plate height $\overline{H_{\rm M}}$ in (2.25). For $z_0=0$, this expression indicates a high value and low separation performance:

$$\overline{H_{
m M}} pprox \ln rac{z_{
m f}}{z_0}$$
 .

Industrially manufactured TLC plates are of high quality, but their coating can still vary from one area of a plate to another, which can have a direct influence on quantitative results.

In order to compensate for such quality differences, samples and standards should be applied alternately, referred to as the data-pair technique [15]. Thus, incorrect results can be avoided, since both analytes and standards are separated on the same section of poor-quality plate. A critical aspect of all layers is the coating area at the sides where the layer thickness varies the most. Therefore the outermost edge (about 1 cm) of the plate should not be used for separations.

5.4 Practical Application Methods

5.4.1 Sample Application via Plate Contact

The easiest way to apply a sample solution to a TLC plate is to use capillaries (Fig. 5.5). Disposable glass capillary tubes are commercially available in sizes of 0.5, 1.0, 2.0, and 5.0 μ L. The capillary tubes act as very small bulb pipettes. They completely fill with the designated volume when simply dipped into the



Fig. 5.5 Various disposable capillary tubes with holder and suction cap

sample solution. A standard deviation of not more than 1% is achievable when using the same capillary tube for a series of sample applications.

Do not use graduated capillary tubes for measuring different sample volumes because it is too difficult to exactly reproduce the applied volume. With glass capillary tubes you should also take care not to apply samples that are too aqueous. Aqueous samples should be diluted with methanol to about 30% (V/V) methanol so that the glass is adequately wetted to fill the capillary. Glass capillaries are only suitable for applying samples as spots and should be used for a single sample only and then discarded because of the high probability of cross-contamination between samples. A complete application system is commercially available with calibrated, re-usable glass or metal capillary tubes, from CAMAG under the trade name Nanomat[®] [2]. An automatic application system (TLS 100), in which a wide range of different volumes can be applied by use of 1-, 10-, and 100- μ L syringes, is available from the Lothar Baron laboratory company in Reichenau, Germany. Application as spots and bands is possible [16].

5.4.2 Sample Application Without Plate Contact

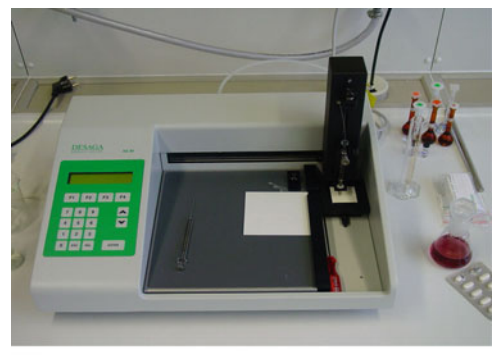
If the sample is applied with a capillary tube, there is always a danger that this contact will damage the plate surface. The spray-on method is more elegant and, with suitable nozzles, the sample solution can be applied to the layer without touching the surface. Attainable spot diameters of less than $100~\mu m$ are possible. There are also various semi-automatic or completely automatic sample applicators available for the precise application of sample solutions using the spray-on method. Omori has listed all such application systems available [16] (Fig. 5.6).

The great advantage of automatic application lies in the higher precision of the spray-on methods and the greater speed of sample application compared with manual techniques. However, once you start using even a semi-automatic application system, TLC starts to lose its status as a relatively inexpensive separating technique. For quantitative TLC, automated sample application is virtually essential to ensure an even distribution of sample within the separated zones interrogated using scanning densitometry (Fig. 5.7).

5.4.3 Sample Application via Contact Spotting

The "contact-spotting process" facilitates the application of large sample volumes with small spot diameters onto a TLC plate [2]. The TRANSPOTTM 1010, from Clarke Analytical Systems, Sierra Madre, California, is no longer commercially available. Vacuum suction applied to the underside of a Teflon® tape is used to form a series of sample wells capable of holding up to $100~\mu L$ of solution (Fig. 5.8a, b). Each sample is added to a well along with a small volume of transfer fluid (such as

Fig. 5.6 AS 30, a semiautomatic sample application system from DESAGA (*above*) and Linomat V (*below*) from CAMAG (Photographs published by permission from DESAGA, Heidelberg, Germany and CAMAG, Muttenz, Switzerland.)





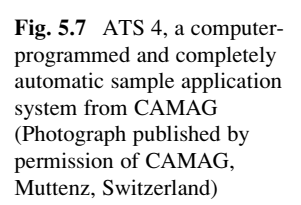




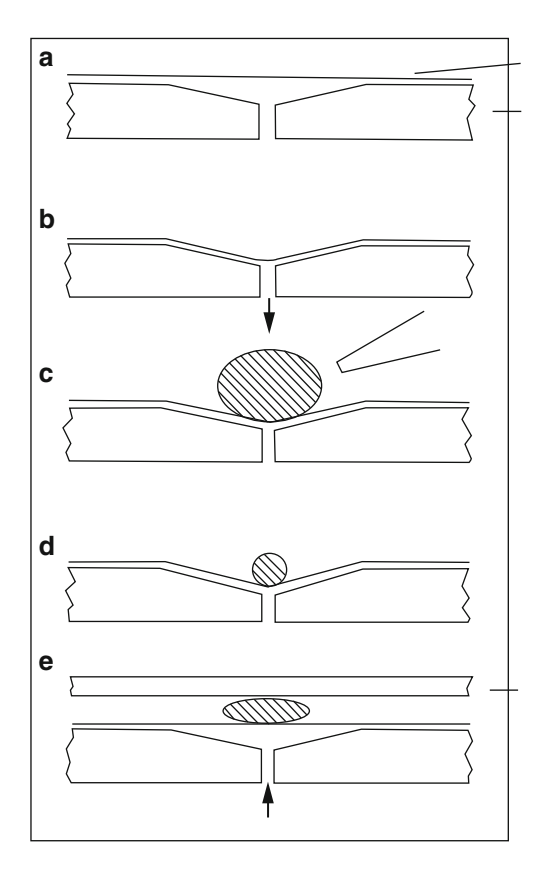
Fig. 5.8 Sample application by contact spotting.

(a) Polymer film covering an application well;

(b) application of vacuum to the polymer film;

(c) application of sample solution to a sample well created in b; (d) sample solvent evaporated; and

(e) sample transfer onto the TLC layer (From [17] with permission. © Hüthig).



glycerine or dimethyl sulphoxide to avoid formation of crystalline solids incapable of quantitative transfer to the layer in the application step) (Fig. 5.8c). The sample solution is evaporated by a warm nitrogen stream leaving a residue dissolved in the transfer fluid of a much smaller volume than the original sample solution (Fig. 5.8d). A TLC plate is placed over the Teflon[®] tape with the stationary phase side facing the sample wells. Switching the vacuum to positive pressure causes the tape to press against the layer simultaneously transferring the samples as small spots to the layer (Fig. 5.8e).

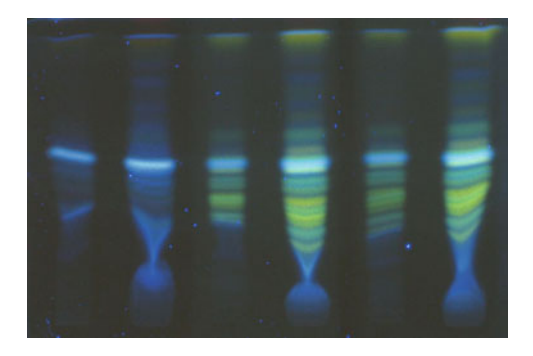
The method is especially suitable for trace analysis and for applying large sample volumes [18].

5.4.4 Plate Overloading and Incomplete Drying

Sample volume or mass overload is a possibility in TLC as in any other chromatographic system. Depending on the matrix, an HPTLC plate with a 200- μ m-thick layer can tolerate a maximum sample volume of 5–20 μ L applied as a spot

References 117

Fig. 5.9 Separation of a Gingko extract on silica gel using ethyl acetate, formic acid, and acetic acid in water (100+11+11+22, V/V) as mobile phase. The application volume was 1 μ L for tracks 1, 3, and 5, and 5 μ L for tracks 2, 4, and 6



without disturbing the separation process. Too much matrix can block the pores of the sorbent preventing solvent flow through the application zone at the start of development. In this case, the applied sample volume must be reduced.

Figure 5.9 shows the separation of a Gingko extract applied in 1 and 5 μL volumes and stained with three different reagents.

The $5-\mu L$ sample volume remained wet even when the separation started. The mobile phase became mixed with the sample solvent resulting in the distorted band shapes. Needless to say,improvement in the drying of the sample application zone before development is recommended.

References

- Kaiser RE (1988) Scope and limitations of modern planar chromatography. Part 1. Sampling. J Planar Chromatogr 1:182–187
- 2. Fenimore DC (1980) In: Bertsch W, Hara S, Kaiser RE, Zlatkis A (eds) Instrumental HPTLC. Huethig, Heidelberg, pp 81–95
- Jänchen DE (1977) In:Zlatkis A, Kaiser RE (eds) HPTLC: high performance thin-layer chromatography. Elsevier, New York, pp 129–146
- 4. Nyiredy Sz (ed) (2001) Planar chromatography, a retrospective view for the third millennium. Springer, Budapest, pp 120–136
- Anastassiades M, Lehotay SJ, Stajhbaher D, Schenk FJ (2003) Fast and easy multiresidue method employing acetonitrile extraction/partitioning and "dispersive solid-phase extraction" for the determination of pesticide residues in produce. J AOAC Int 86:412-431
- Plössl F, Giera M, Bracher F (2006) Multiresidue analytical method using dispersive solidphase extraction and gas chromatography/ion trap mass spectrometry to determine pharmaceuticals in whole blood. J Chromatogr A 1135:19–26
- 7. Thurman EM, Mills MS (1998) Solid-phase extraction: principles and practice. Wiley-VCH, Weinheim
- 8. Simpson NJK (2000) Solid-phase extraction: principles, techniques, and applications. CRC, London
- 9. Fritz JS (1999) Analytical solid-phase extraction. Wiley-VCH, Weinheim
- 10. Sherma S, Fried B (eds) (1996) Handbook of thin-layer chromatography. Dekker, New York
- 11. Baltussen E, Sandra P, David F, Cramers C (1999) Stir bar sorptive extraction (SBSE), a novel extraction technique for aqueous samples: theory and principles. J Microcol 11:737–747

- 12. Sánchez-Rojas F, Bosch-Ojeda C, Cano-Pavón JM (2009) A review of stir bar sorptive extraction. Chromatographia 69:S79–S94
- 13. Abbott DC, Thomson J (1965) The preparation and uses of multi-band chromatoplates. J Chem Ind 310:310
- 14. Poole CF, Fernando WPN (1992) Some musings on the measurement and interpretation of theoretical plate height in thin-layer chromatography. J Planar Chromatogr 5:323–333
- 15. Ebel S (1996) Quantitative analysis in TLC and HPTLC. J Planar Chromatogr 9:4–15
- Omori T (2001) In: Nyiredy Sz (ed) Planar chromatography, a retrospective view for the third millennium. Springer, Budapest, pp 120–136
- Bauer K, Gros L, Sauer W (1989) Dünnschichtchromatographie. Alfred Hüthig, Heidelberg 1989
- 18. Fenimore DC, Meyer CJ (1979) Contact spotting: a new approach to sample application in thin-layer chromatography. J Chromatogr 186:555–561

Chapter 6 Basis for TLC Development Techniques

Selecting the sorbent and solvent and minimizing the application zone widths are important factors on the way to obtaining optimum separating conditions. In this respect, TLC is very flexible with many possible methods. Thus, it provides additional opportunities not available to other chromatic processes, for example, using the vapour phase to influence separations. TLC uses an open system in which the mobile and stationary phases are formed during separation. This occurs between sorbent and solvent, under the influence of the vapour phase, and depends on the choice of the developing chamber [1, 2].

From (2.21) and (2.29), we can derive (6.1):

$$R_{\rm S} = \left(\frac{R_{\rm f2}}{R_{\rm f1}} - 1\right) \frac{1}{2} \sqrt{\frac{z_{\rm f} - z_{\rm 0}}{\ln(4)H_{\rm real}}}.$$
 (6.1)

Equation (6.1) demonstrates that resolution does not increase linearly with the separation distance but with the square root of the separation distance. We can conclude that a satisfactory resolution requires a minimum migration distance $z_{\rm f}$, which means a minimum separation time. It also requires a good coating material, which is expressed in (6.1) by a low $H_{\rm real}$.

6.1 Influence of the Vapour Phase

The mobile phase is formed during separation due to equilibration between solvent and sorbent. However, for many years, analysts overlooked the effects of the vapour phase on the flow conditions. It was not until 1968 that de Zeeuw drew attention to the decisive influence exerted by the vapour phase in a developing chamber. He demonstrated that considerable amounts of solvent are adsorbed by a dry layer via the vapour phase and could be involved in the separation (Fig. 6.1 demonstrates these processes). Thus, de Zeeuw was the first person to recommend using the vapour phase as a further degree of freedom in optimising chromatographic separations by TLC.

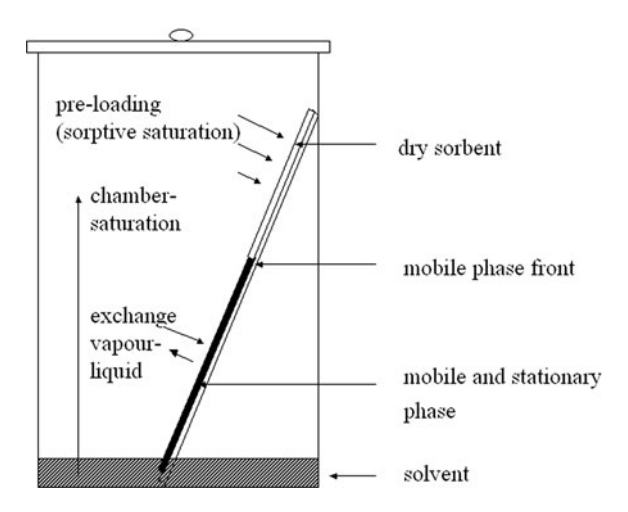


Fig. 6.1 Terms related to TLC development and saturation [2, 3])

The uptake of vapour from the vapour phase is termed sorption [2, 3]. The sorption volume depends on the history of the TLC plate and can be controlled by the type of chamber used. Geiss described this in detail [2, 3]. According to Raoult's law, the concentration relationship of solvent components in the vapour phase corresponds to the concentration ratio in the solvent. After a certain time, a dynamic equilibrium is formed in such a way that many solvent molecules enter the vapour phase, as molecules are precipitated into the liquid phase or onto the stationary phase. The relationship between the concentrations in the solvent, the vapour phase, and the stationary phase thus remains stable.

Chamber saturation is the description of this situation, with the vapour phase remaining unsaturated until chamber saturation is achieved. If a TLC plate is placed in a developing chamber, solvent molecules from the evaporation phase precipitate onto the plate: sorptive saturation takes place on the plate surface. The plate is described as pre-loaded. *Pre-loading* results in the masking of active centres by solvent vapour-phase molecules. *Sorptive saturation* means the separation layer is in a state of equilibrium with the saturated vapour phase. Sorptive saturation, therefore, represents extreme pre-loading of the layer. If the pore volume of the sorbent layer is completely filled with solvent, this is called *capillary saturation* [2, 3].

If a solvent is poured into a chamber and the TLC plate is immediately introduced, the vapour phase will not have had time to reach saturation. A dry TLC plate needs more than 30 min to reach saturation with solvent molecules from the vapour phase (see Fig. 6.2). Yet if the dry TLC plate had been placed in a saturated chamber previously, the layer will be saturated within about 5 min (see Fig. 6.3). The capillary saturation of the sorbent layer enlarges the surface area of the solvent, which increases vapour exchange during the separation. As the lighter and more volatile solvent components are more easily evaporated, an enrichment of these components will take place on the plate surface. For an unsaturated chamber, more solvent will be needed than for a saturated chamber when the plate is developed over a particular distance.

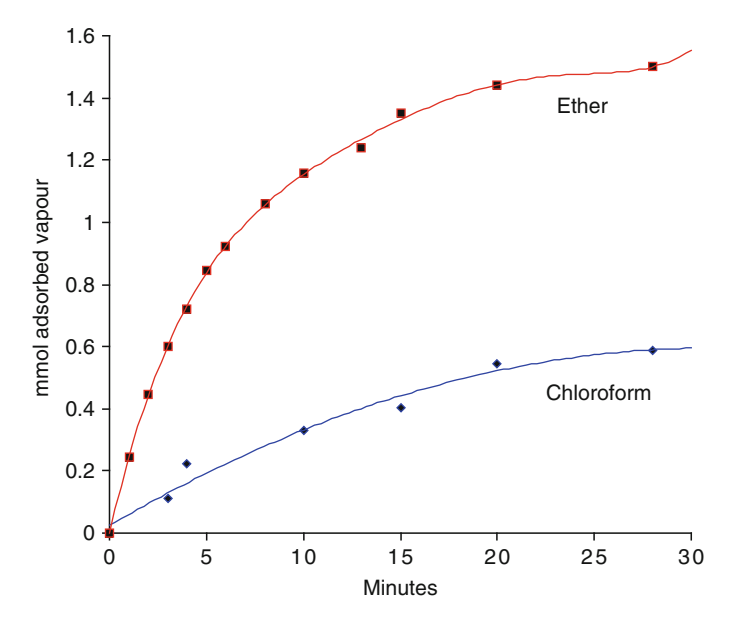


Fig. 6.2 Vapour-phase adsorption of diethyl ether (red) and chloroform (blue) by a silica gel plate (without chamber saturation [1])

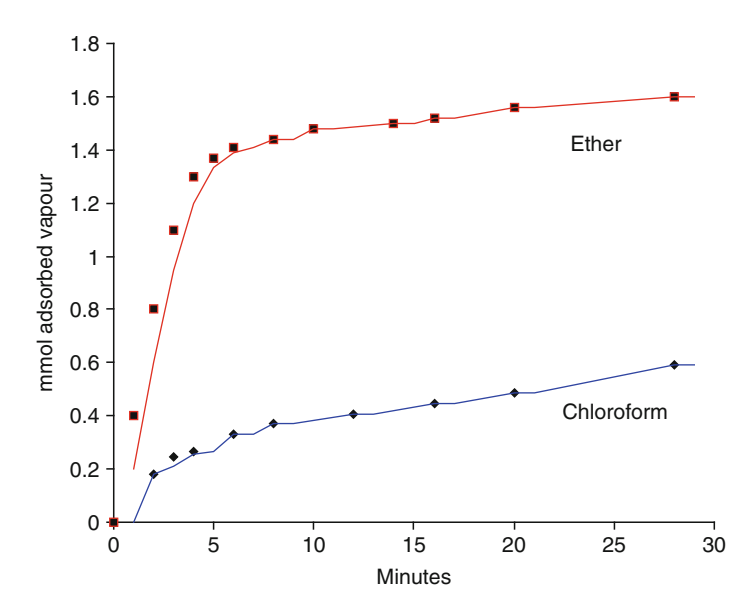


Fig. 6.3 Vapour-phase adsorption of ether (red) and chloroform (blue) on a silica gel plate (with chamber saturation [1])

A dry plate takes up volume $V_{\rm m}$ of solvent to fill the empty pore volume, so a pre-evaporated plate will reduce its effective vacant volume by $V_{\rm v}$, because the plate has already taken up that amount of solvent during pre-evaporation. During development of such a pre-evaporated plate, a substance moves over the distance z_x . This distance is proportional to the solvent volume taken up by the plate during development, hence $z_x \approx (V_{\rm m} - V_{\rm v})$.

From the definition of the R_f value, it follows that the distance moved by the substance is also proportional to the R_f value, hence

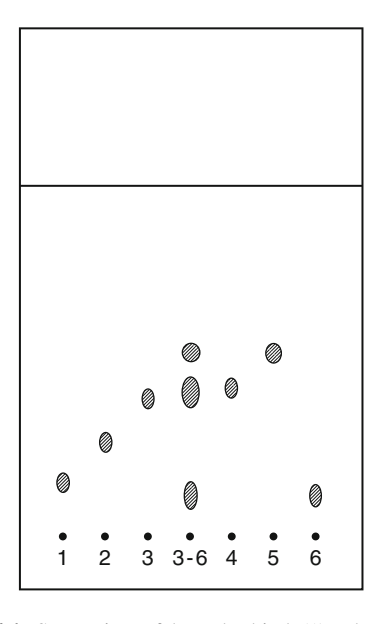
$$z_r = R_f(z_f - z_0).$$

Combining both equations shows that the $R_{\rm f}$ value is proportional to the solvent volume, which was uptaken during development:

$$z_{\rm f} \approx R_{\rm f} \approx (V_{\rm m} - V_{\rm v}).$$

If the reduced solvent flow due to pre-loading is taken into account, it is easy to demonstrate that for the same solvent, developed over the same distance (equal z_f values), test substances do not move as far as in unsaturated chambers.

Better resolution is often obtained in unsaturated chambers than in a saturated chamber. A greater separation distance leads to better resolution, which is the consequence of (6.1) [1]. This can be clearly seen in the separation shown in Fig. 6.4. While compounds 3 and 4 are not completely separated in the saturated



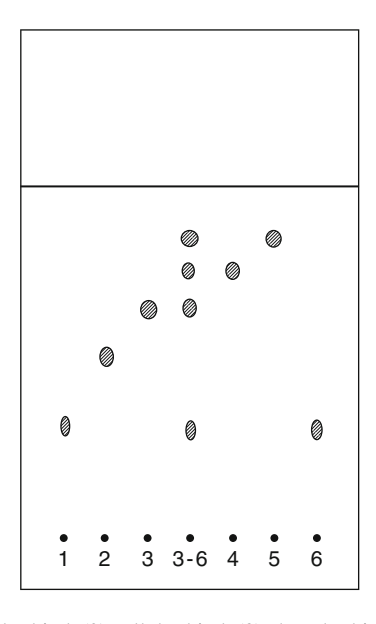


Fig. 6.4 Separation of heptobarbital (1), phenobarbital (2), allobarbital (3), hexobarbital (4), methyl-phenobarbital (5), and bromisoval (6) on silica gel with chloroform/diethyl ether 75+25 (V/V): saturated chamber (*left*) and unsaturated chamber (*right*) (From [1] with permission. © Elsevier.)

chamber, satisfactory separation is achieved in the unsaturated chamber. If a trough chamber is lined with filter paper and wetted so that the solvent can evaporate over a large surface area, sorbent-layer saturation is attained in about 5 min. It is easier to reproduce separations with chamber saturation than for unsaturated conditions.

In order to create reproducible working conditions, Brenner and Niederwieser introduced the BN-chamber for horizontal development, which prevents solvent vapour uptake [4, 5]. Thus the BN-chamber was a predecessor to the *Vario-KS-chamber*.

6.2 Chamber Types for Linear Development

Most TLC separations are carried out in linear chambers, so we will not discuss the interesting subject of circular development in detail here. The usual linear chamber types can be divided into two categories: N-chambers and S-chambers.

6.2.1 N-Chambers ("Trough Chambers")

"N" stands for "Normal". Chambers of this type have a gas space of 5–10 cm. In chambers without a solvent-saturated filter paper lining, it can take several hours to attain chamber saturation. The relatively large vapour space can thus serve as a buffer to perform development without chamber saturation. However, the chamber must be cleaned and dried when there is a change of solvent, because that is the only way to prevent cross-contamination. In any case, working with chamber saturation needs filter paper-lined and wetted chamber sides. The filter paper distributes the solvent in the vapour space via its large surface area. That is the only way to ensure that chamber saturation will be obtained within a few minutes after closing the chamber with its lid.

A double-trough chamber can be used to pre-load a TLC plate (Fig. 6.5). The plate should stand in a dry trough while the solvent is pored into the second trough.



Fig. 6.5 Several doubletrough chambers in various sizes (Published with permission from CAMAG, Muttenz, Switzerland.)

As a function of storage time the layer is gradually loaded with solvent via the vapour phase. The double-trough chamber is tilted to start development, thus filling the dry trough where the TLC plate is located with solvent.

6.2.2 S-Chamber ("Small Chamber")

"S" in the chamber name stands for "small" referring to a vapour space of less than 3 mm. In an S-chamber, the TLC plate is sealed on three sides. The solvent is introduced at the fourth (open) side. At the start of development, the small (less than 5-cm^3 -size vapour space) is completely unsaturated as there are no solvent molecules in the vapour space. Thus the TLC layer is also unsaturated. Because of the small volume available, chamber saturation occurs very quickly in an S-chamber but only over the already developed plate surface. Convection can be practically excluded because of the small gas space. Development is possible without any pre-loading(Fig. 6.6). This type of development is easy to reproduce and the R_f values remain constant.

Trough chambers permit TLC plates to develop vertically. Such "standing chambers" were the very first chambers used for TLC and described by Stahl in 1959 [3]. The horizontal S-chamber represents an elegant variation of the vertical S-chamber. In this kind of chamber (and in the Vario-KS-chamber), the solvent is transferred onto the sorbent via a glass plate. Its advantage lies in a slightly shorter development time, as the vertical gravitational component is no longer present. Furthermore, this type of chamber allows both sides of a plate to be simultaneously developed. If you use a 10×10 cm HPTLC plate with an optimum development distance of 4–5 cm, you can double the number of samples separated. As the plate lies in a horizontal chamber with the layer downwards, it is also possible to carry out separations with chamber saturation. Pre-loading the layer is also possible. For this container (6) is filled with solvent, and plate (2) is removed. Of course, this container can be filled with different solutions. If plate (2) is replaced, separation is possible without a significant vapour phase. It is essential when using the S-chamber that the sides of the plate are sealed so that no vapour phase can leave the vapour space. If the vapour space is unsealed, spots will migrate in the direction of the vapour flow. This effect is shown in Fig. 5.3, left track.

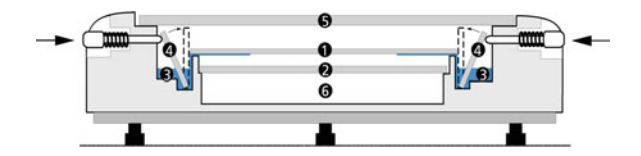


Fig. 6.6 Cross-section of a horizontal S-chamber with HPTLC plate (1), gas space boundaries (1+2), solvent (3), connection to the sorbent (4), and covering plate (5), pre-loading container (6) when (2) is removed (Printed with permission from CAMAG, Muttenz, Switzerland.)

6.2.3 Vario-KS-Chamber

The Vario-KS-chamber (KS stands for "chamber saturation"; in German, "KammerSättigung") is a further development of the horizontal chamber mainly devised by Geiss, Schlitt, and Klose [2, 6–8]. Like a horizontal chamber, this type of chamber can be used for one-side plate development and has various solution tanks that permit up to six different solvents for pre-conditioning or development (Fig. 6.7).

By marking out a 10×10 cm HPTLC plate, six separated tracks are formed and six different vapour spaces created using six solvents. This type of chamber is ideally suited for rapid solvent optimization.

6.2.4 The H-Chamber ("Horizontal Chamber")

The *H-chamber*, (horizontal chamber) developed by Kraus, is distinguished by its extremely simple construction. The chamber also has a reservoir for pre-conditioning. A glass frit conducts the solvent from the storage reservoir onto one side of the plate that is placed with the layer downwards [6]. Pouring the solvent into the solvent container starts the development. DESAGA markets the H-chamber in sizes 5×5 cm and 10×10 cm. The small H-chamber is ideal for rapid separations using a few tracks, for example, qualitative determination of pharmaceuticals for identity checking. The 5×5 cm HPTLC plates are commercially available or can be cut to size from standard plates with a special glass plate cutter(Fig. 6.8).

A good overview of the various chamber types can be found in [9].



Fig. 6.7 A Vario-KS-Chamber (*top*, *right*) with scoring unit. For pre-conditioning, the layer is placed over the main chamber body on the *left side* where six trays are scratched out. For development, the plate is slid to the *right side* with no vapour below (With permission from CAMAG, Muttenz, Switzerland.)



Fig. 6.8 H-chambers (according to Kraus) with a 10×10 cm and a 5×5 cm HPTLC plate (With permission of DESAGA, Heidelberg, Germany.)

6.3 Controlling Separations via the Vapour Phase

6.3.1 Solvent Composition During Separation

The development of a thin-layer chromatogram is a complicated process because the solvent phase meets a dry stationary phase, thus being subjected to a frontal chromatographic separation. If the mobile phase is a mixed solvent, the individual components can interact with the stationary phase and are extracted depending on their relative affinity for the stationary phase. The mobile phase component most strongly bound by the layer is removed first, leaving behind those components of the mobile phase that are weakly bound, forming a front gradient. In an extreme case, each of the solvent components will form its own adsorption area indicated by a sharp change in the mobile phase composition. Such behaviour is extremely difficult to describe theoretically.

For example, if the solvent combination of benzyl alcohol (modifier), mesitylene (strength adjusting solvent), and ethyl acetate (mediator) (1+1+10, V/V) encounters a dry silica gel phase (which is a typical situation in normal-phase chromatography), it creates a mobile phase that produces the expected front gradient. Otherwise, the partition relationships between the modifier and strength adjusting solvent remain stable over the whole development distance (see Fig. 2.7).

If the mediator is not ethyl acetate but methanol, the partition relationships between mesitylene and benzyl alcohol is shown in Fig. 6.9. Methanol is more polar than benzyl alcohol. Therefore methanol functions as a modifier in a mixture with mesitylene and benzyl alcohol. It occupies the active centres of the sorbent and forms part of the stationary phase. Benzyl alcohol is allotted the role of a mediator in this separation system.

As shown in Fig. 6.9, the solvent strength adjusting solvent (mesitylene) and the mediator (benzyl alcohol) form the front gradients one after the other, although the benzyl alcohol front gradient lies in the middle of the mesitylene gradient, resembling a double signal. Otherwise, the concentration of benzyl alcohol remains constant over the first 40 mm separation distance. Mesitylene shows a gradient over the whole separation distance, i.e. a constantly changing concentration. In an extreme case there will be as many fronts formed, as there are solvent components with different polarity [2]. As these fronts need space, the effective separation distance is reduced, which is an overwhelming argument for using pure solvents and no mixtures.

The solution mediator has an important influence on the characteristics of the mobile phase. For example, in the above case methanol is replaced by the less polar

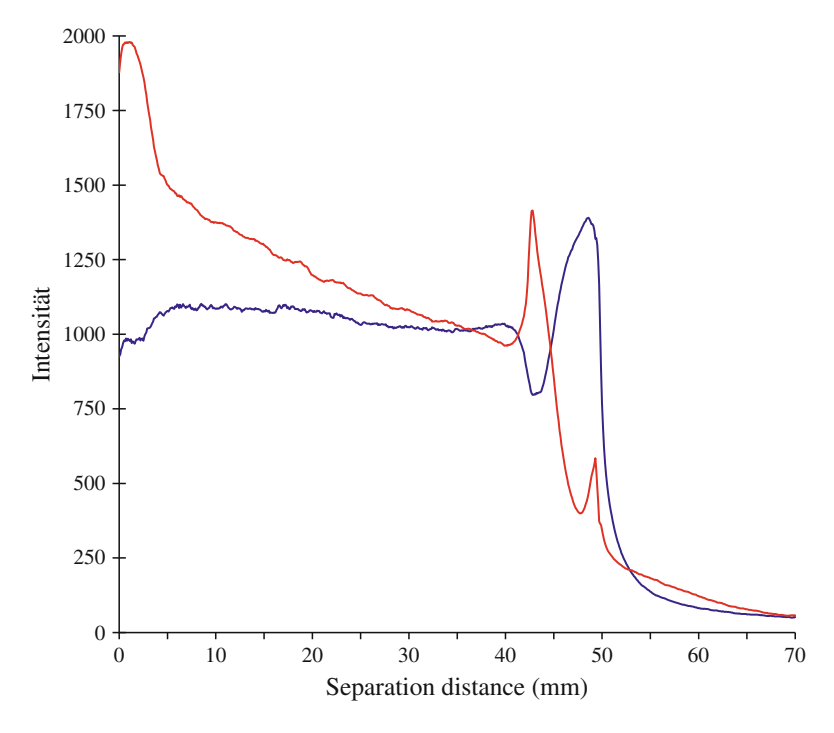


Fig. 6.9 Composition of the mobile phase: mesitylene (*red*) and benzyl alcohol (*blue*) with methanol on a 0.1-mm silica gel Si 60 layer in a saturated chamber (prewashed plate). Mobile phase: methanol (modifier), mesitylene (strength adjusting solvent), benzyl alcohol (mediator) (18+1+1, V/V)

methylene chloride as a mediator. Figure 6.10 shows the mesitylene and benzyl alcohol composition of the mobile and stationary phases over the total separation distance. Apart from the initial disturbance at the start, the benzyl alcohol demonstrates a constant composition over a separation distance of about 30 mm.

It is worth noting the de-mixing zone at the separation distance of 30 mm. Such a sharp change in the solvent composition is known as a β -front and works like a second front gradient. The β -front is formed as follows: Due to the relatively non-polar mediator methylene chloride, relatively large amounts of polar benzyl alcohol saturates the active centres and thus forms the stationary phase in conjunction with silica gel. This task is carried out by methanol in Fig. 6.9. In this way, the modifier benzyl alcohol is depleted in the mobile phase and retained by the layer. The plate shows this enrichment of benzyl alcohol and the depleted mesitylene at separation distances below 30 mm. Mesitylene is hardly adsorbed by the sorbent in comparison to benzyl alcohol. Thus mesitylene migrates over the plate without much delay and forms the front gradients. The mobile phase loses its modifier in the front section of the separation (above 30 mm separation distance) and the front signal

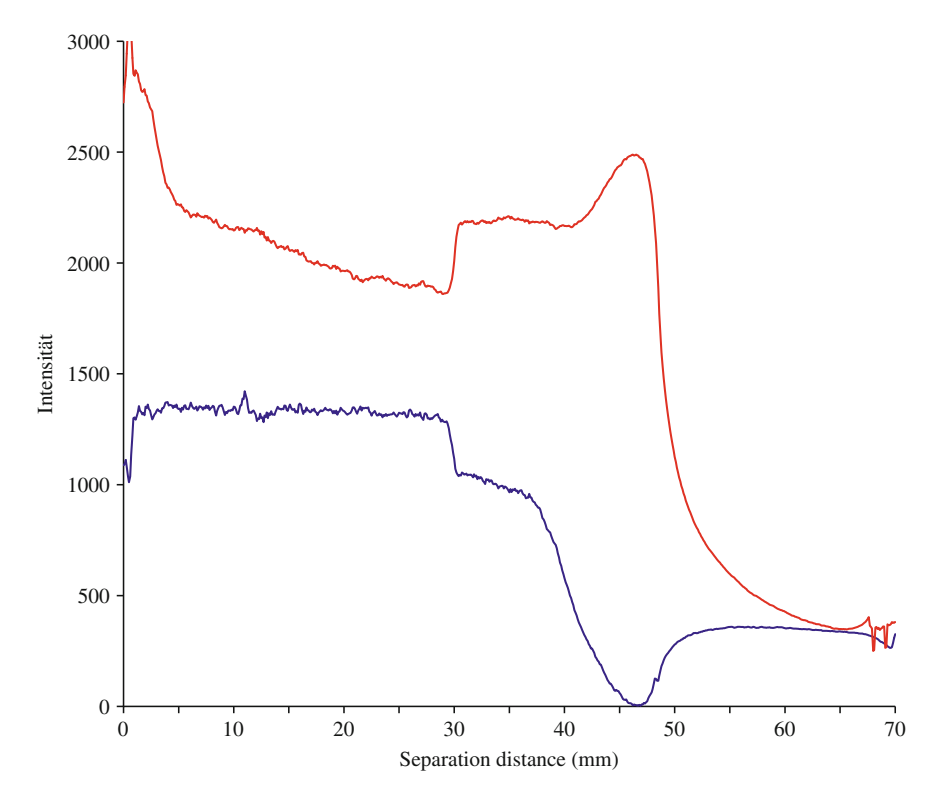


Fig. 6.10 The mobile phase composition of mesitylene (top, in red) and benzyl alcohol (below, in blue) with methylene chloride as mediator on a 0.1-mm silica gel Si 60 layer (saturated chamber, washed plate). Mobile phase: CH₂Cl₂ (mediator), mesitylene (solvent strength adjusting solvent), and benzyl alcohol (modifier) (18+1+1, V/V)

contains absolutely no benzyl alcohol, so the modifier forms a kind of "negative" front gradient. The benzyl alcohol concentration even lies below the amount coming from the vapour phase, because the concentration of benzyl alcohol increases again beyond the front at 47 mm.

The dryer the layer, the more active centres remain un-occupied, and the more modifier that will be absorbed. A dry layer therefore adsorbs more polar modifier to form the stationary phase than is the case for a water-saturated stationary phase. The β -front thus moves correspondingly slower on a dry layer than on a water-deactivated layer.

A β-front is not popular in TLC because it hinders the development of a constant, stable composition for the mobile and stationary phases over the whole separation distance. Moreover, in the region of a β-front, neither the expression for the R_f values nor the expression for the chromatographic resolution is valid. Nevertheless, β-fronts are occasionally used to separate substances where a sharp change of solvent works as a gradient that can produce very sharp zones. Niederwieser and Honegger first used a β-front as a TLC mobile phase gradient [4, 5]. Figure 6.11 shows the practical use of a β-front to determine Sucralose in soft drinks. Sucralose is an artificial sweetener, which contains polar groups (5 OH groups) as well as 3 non-polar Cl groups. Due to its ambivalent structure, sucralose exhibits a strong R_f value shift even with the smallest of mobile phase alterations.

Thus the separation is not very robust. To obtain constant R_f values, the mobile phase composition must be measured exactly. A β -front formed on an unconditioned amino phase with the mobile phase acetonitrile–water (8+2, V/V) in an

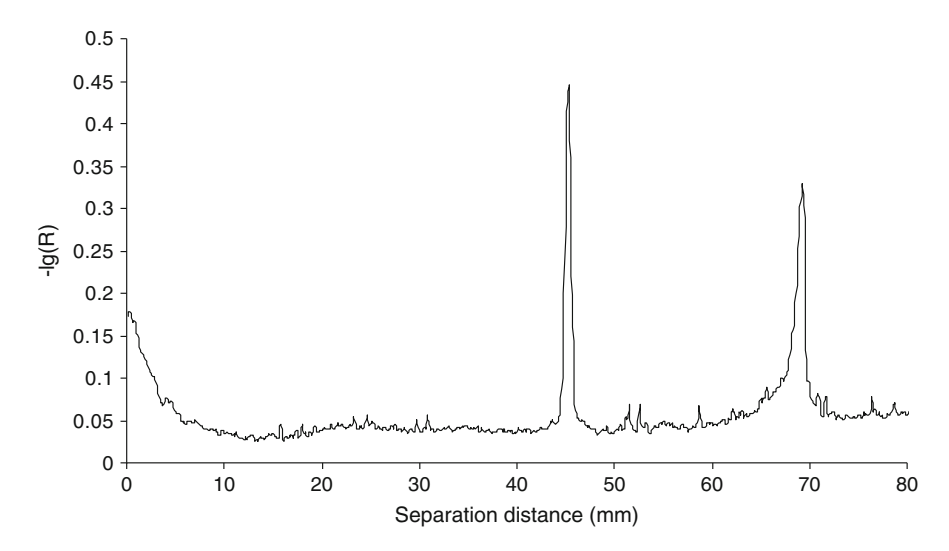


Fig. 6.11 Separation of 150 ng sucralose $^{\circledR}$ (at 45 mm separation distance) on an amino plate in an S-chamber without pre-loading and acetonitrile—water (8+2, V/V) as mobile phase. The sucralose signal appears sharp because the substance is running in a β -front. Pre-loading with acetonitrile could make the β -front disappear

S-chamber "catches" the sucralose and causes a very narrow substance zone with good detection limits and a robust $R_{\rm f}$ value. Thus sucralose can be easily identified by its $R_{\rm f}$ value. The β -front can be avoided if the separation is carried out under the same conditions in a saturated trough chamber. Due to the saturation of the active centres of the stationary phase by adsorption of the polar component of the mobile phase via the gas phase, the mobile phase is not depleted in the polar component, and a β -front is no longer formed.

If the stationary phase has been pre-conditioned with a solvent, all the necessary mobile phase components are already present, so no β -front will be formed. In particular, pre-conditioning hinders the formation of β -fronts in separations employing S- or H-chambers.

6.3.2 Plate Pre-loading via the Vapour Phase

Pre-loading the adsorbent layer with solvent increases the (virtual) velocity of the solvent front. In this case, part of the stationary phase already has been filled with solvent via the vapour phase. The pre-loading results in smaller R_f values in comparison to a non-preconditioned layer. The advantage is that β -fronts are mostly avoided. The relationship of the R_f values for pre-loaded and non-loaded layers corresponds to the relationship between the pore volume and capillary-filled pore volume. In practice, the value of the fraction varies between 1.0 and 1.6 [2]:

$$R_{\rm f}' = \frac{V_{\rm m}}{V_{\rm m} - V_{\rm v}} (R_{\rm f})_{\rm pre-loaded}. \tag{6.2}$$

Here

 $R_{\rm f}'$ R_f value without plate pre-loading (true $R_{\rm f}$ value)

 $V_{\rm m}$ pore volume of the plate

 $V_{\rm v}$ pre-loading volume

The sorbed solvent amount (V_v) can be determined by measuring the true R_f' value and the R_f' value under pre-loaded conditions. The pre-loading volumes can be calculated directly if the expression is resolved to V_v :

$$V_{
m v} = V_{
m m} - rac{V_{
m m}}{{R_{
m f}}'} (R_{
m f})_{
m pre-loaded}$$

Figure 6.12 shows a plate pre-loaded with mesitylene developed over a separation distance of 45 mm. During development, the true front had already pushed together the pre-loaded mesitylene, forming a broad, easily visible front gradient. The true front can be recognized at separation distance of about 30 mm. That is the maximum distance sample molecules can move. Pre-loading the plate with mesitylene has reduced the maximum separation distance of 45 mm down to about 30 mm, i.e. decreased by about 1/3. Thus no $R_{\rm f}$ values greater than $R_{\rm f}=0.7$ can be observed

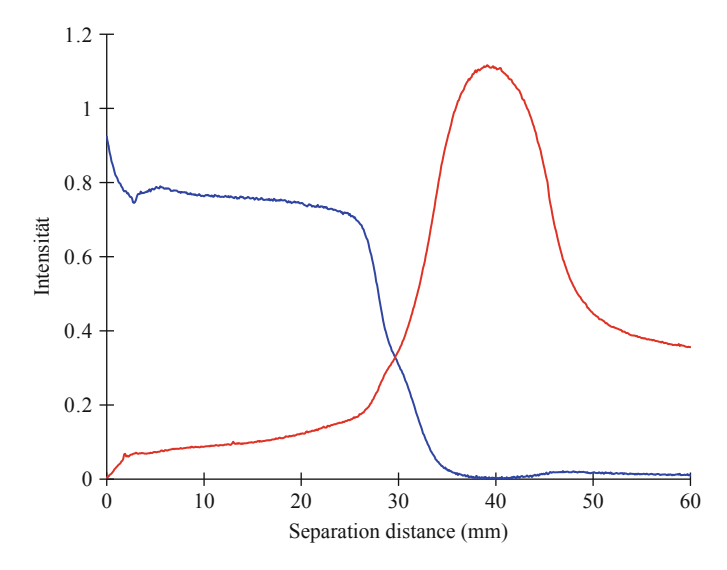


Fig. 6.12 Mobile phase composition of mesitylene–benzyl alcohol–ethyl acetate (1+1+18, V/V) for a silica gel layer sorptively saturated over mesitylene–ethyl acetate (1+5, V/V) for 10 min. The mesitylene front gradient can be seen between 30 and 45 mm separation distances

when the visible front is used as a reference for calculating $R_{\rm f}$ values. This problem of pre-loaded plates was expressly referred to by Geiss [3]. An $R_{\rm f}$ value of 0.7 in the system shown in Fig. 6.12 indicates that the substance is running with the front gradient, that is, it cannot spend time in the stationary phase. If the "true" front cannot be recognized, this could mean that the analyst might try to optimize a separation that is not a separation at all.

An interesting point in adsorption chromatography is the adjustment of activity due to defined relative humidity in order to deliberately adjust the layer activity. Geiss lists a number of mixtures suitable for adjusting relative humidities [2]. A change in the water content of the separation layer, and thus a change in its activity, can be achieved by heating the plate to about 110°C and storing this activated plate at different relative humidities (Table 6.1).

A simple way of adjusting the water content of a separation layer is storing the plate over different concentrations of sulphuric acid. Using sulphuric acid avoids working with different salt solutions (Table 6.2).

Figure 6.13 shows the separation of a dye mixture in a Vario-KS-chamber at different relative humidity levels. The activity of the stationary phase is reduced from left to right. Low humidity provides low $R_{\rm f}$ values. The dyes migrate only minimal distances and are not completely separated. Increasing pre-loading with water deactivates more of the active centres and increases the separation distances. The optimum separation potential of this system is obtained at 72% relative humidity.

If the track is pre-loaded over pure water, all the active centres are saturated, the various dyes will no longer be retained and all will run, unseparated, with the front

Table 6.1 Relative humidity over saturated salt solutions (from [2])

Solid phase	%Relative humidity
$H_3PO_4 + 1/2 H_2O$	9
LiCl · H ₂ O	15
K(CH ₃ COO)	22.7
CaCl₂ · 6 H₂O	32.3
NaI	38.4
$K_2CO_3 \cdot 2 H_2O$	44
$NaHSO_4 \cdot H_2O$	52
NaBr ⋅ 2 H ₂ O	58
CuCl ₂ · 2 H ₂ O	67
NaCl	75.7
KCl	85
$Na_2SO_4 \cdot 10 H_2O$	93
CaSO ₄ · 5 H ₂ O	98

Table 6.2 List of relative humidity over sulphuric acid (from [2])

Weight% H ₂ SO ₄	%Relative humidity
10	96
25	83
35	66
45	46
55	26
60	16
65	10
70	4

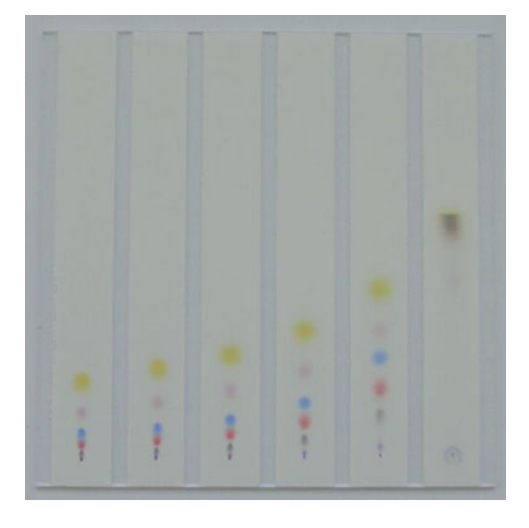


Fig. 6.13 Dye separations with toluene on Si 60 layer at various relative humidity levels. From *left to right*: 4%, 16%, 26%, 46%, 66%, and 96% relative humidity

gradient. The result can be seen on track 6. This example shows that for developing a TLC method, at least as far as adsorption chromatography is concerned, the vapour phase must be taken into consideration. The Vario-KS-chamber is eminently suited for optimizing such separations [2].

In summary, the largest $R_{\rm f}$ values can be observed in an ideal unsaturated S-chamber. This type of chamber shows separations with the "correct" $R_{\rm f}$ values. By using trough chambers, the layer is more or less pre-loaded. Therefore a separation process is only reproducible in an ideally saturated chamber. This is the only way to avoid β -fronts.

6.4 Circular Separations

Up until now, layer development has been described as a linear process. The solvents move from one side of the plate to the opposite side. In addition to linear development there are two circular development modes that should be mentioned briefly: centrifugal and centripetal development [2].

Centrifugal development or elution means "fleeing from the centre". The solvent is introduced by a wick, which is placed in the middle of the layer. Samples are applied in a circle of small diameter near the centre. Development occurs radially from the plate centre to the sides.

In linear elution the throughput of solvent S from the reservoir is constant and $S \approx z$. In centrifugal development the solvent throughput is related to the separation distance z by $S \approx \pi z^2$. Geiss [2] gives the relationship between the centrifugal and linear R_f values as

$$(R_{\rm f})_{\rm linear} = (R_{\rm f})_{\rm centrifugal}^2.$$
 (6.3)

The circular centrifugal $R_{\rm f}$ values are higher than their linear counterparts, with the exception of $R_{\rm f}=0$ and $R_{\rm f}=1$, where they must, of course, be equal. The increase in the $R_{\rm f}$ values is greater in the lower range [2]. This favours the separation of components with small $R_{\rm f}$ values without disadvantaging the separation of components with higher $R_{\rm f}$ values.

If a plate is developed from the outside towards the centre, this is called centripetal development. This technique was first described by Van Dijck and is sometimes also called "anti-circular development" [10]. In a *centripetal development*, the solvent is introduced in a circle from the plate sides and flows towards the centre. Centripetal means "seeking the centre". The sample is applied on an outer circle of large diameter near the plate sides. This allows the separation of a large number of samples. Forty-eight samples applied as spots on a 10×10 cm HPTLC plate can be separated simultaneously within about 4 min [10]. In linear and centrifugal development, the mobile phase flow decreases quadratically with time. The wetted area decreases quadratically with the time, and, consequently, the solvent front velocity is constant.

Centripetal development can be performed by placing the mobile phase inside a petri dish with the sides wrapped with filter paper. The HPTLC plate is placed with the layer side downwards on the paper-wrapped petri dish rim [11]. In the centripetal mode, $R_{\rm f}$ values are smaller than in the linear mode. At high $R_{\rm f}$ values the centripetal technique shows better results than the linear technique. Multiple developments in the centripetal mode are often preferable because of the fast elution time.

To transfer centripetal R_f values into linear R_f values, use (6.4) according to Geiss [2]:

$$(R_{\rm f})_{\rm linear} = 1 - \left[1 - (R_{\rm f})_{\rm centripetal}\right]^2. \tag{6.4}$$

Equation (6.4) is only valid for a single component solvent in the absence of pre-loading.

The development sequence of circular separations is not basically different from that of linear development but mostly provides sharper separations. This is shown in Fig. 6.14 in comparison to Fig. 6.13. The layer can also be loaded with 10–100 times more samples than in linear development [10]. The disadvantages of circular separations lie in the central solvent introduction, which often causes a strongly disturbed solvent profile.

6.5 Solvent Gradients

6.5.1 Theory of Solvent Gradients

In HPLC, the composition of the mobile phase is often continuously altered during elution. Such gradient chromatography is mainly responsible for the very high separation numbers in HPLC. Also in TLC, suggestions were made for the continuous alteration of the mobile phase composition. However, theoretical considerations indicate that solvent gradients would result in a higher zone capacity but with lower resolution [12]. For separations with a constant mobile phase composition the resolution maximum occurs at an $R_{\rm f}$ value of 0.33. This corresponds to a separation system k value of about k=2, as can be easily deduced from the relationship $k=(1-R_{\rm f})/R_{\rm f}$. A TLC separation always takes place in an $R_{\rm f}$ range of about 0.05–0.95, which corresponds to k values of 0.05–19. Substances can only be separated from one another; therefore, if their k values lie in a range of $10^{2.6}$. Substances with k values outside this range will either move only a short distance from the sample origin or migrate with the solvent front, that is they will move outside the $R_{\rm f}$ range of 0.05–0.95. Thus these substances do not have the potential to be separated from one another.

If a sample contains many components of different polarity, a TLC system can be adjusted to optimum separation conditions for only a few of these substances. 6.5 Solvent Gradients 135

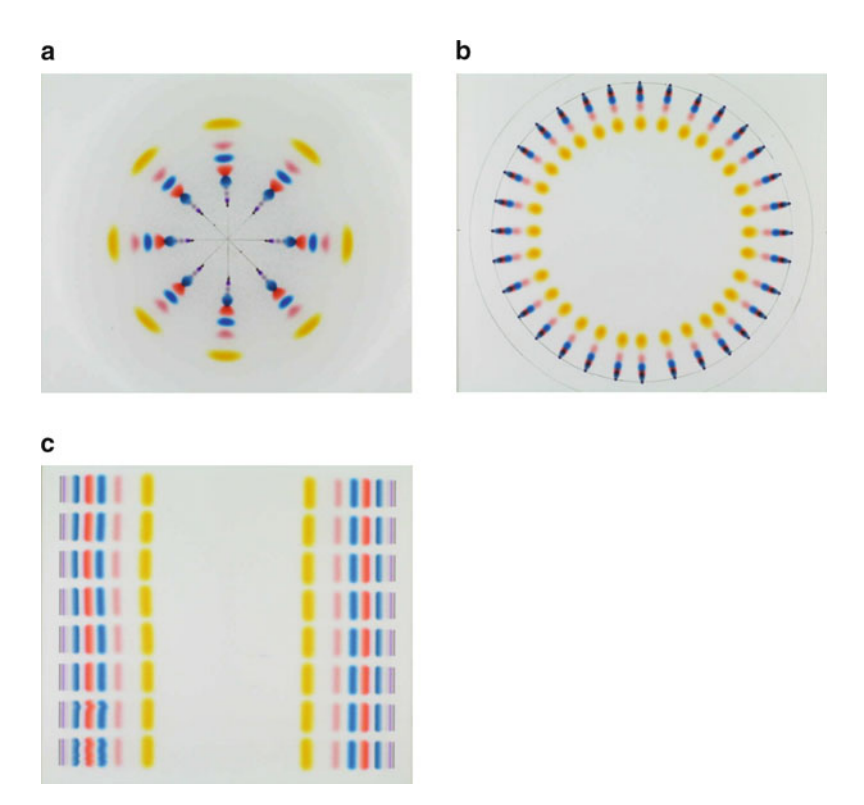


Fig. 6.14 Separation of a dye mixture with toluene in (a) centrifugal, (b) centripetal, and (c) linear development (simultaneously from both sides) modes. At low $R_{\rm f}$ values the centrifugal technique shows better results than the centripetal and linear development modes. The centripetal technique favours the resolution of zones with high $R_{\rm f}$ values. In addition, observe the transversal zone broadening of the centrifugal separation in contrast to centripetal development. The linear development allows bandwise application, which results in bar-shaped zones

The other compounds will either remain at the start line or move with the solvent front. Thin-layer chromatography only has a relatively small polarity window for separating compounds.

Figure 6.15 shows the separation of a dye mixture with various solvents with an approximately fixed solvent front migration distance. The development at far left was carried out with cyclohexane. The mixture remained almost motionless, although one can just make out a slightly red "shimmer" beyond the application zone.

The solvents for tracks 2–4 (toluene, cyclohexane-methyl *tert*-butyl ether, and methylene chloride) move the components of the dye mixtures apart, while nearly all the dyes on tracks 5 and 6 (tetrahydrofuran and ethyl acetate) migrate with the solvent front. Thus only the solvents on tracks 3 and 4 are suitable for the separation of all the dye components.

Fig. 6.15 Separation of a CAMAG dye mixture with (from *left to right*) cyclohexane, cyclohexane and methyl *tert*-butyl ether (9+1, V/V), toluene, CH₂Cl₂, tetrahydrofuran, and ethyl acetate with same front distance. Also notice the increased transversal zone broadening from *left to right*



Tracks 3 and 4 beautifully illustrate that all the dyes in the mixture can be separated by a fixed mobile phase composition. You merely have to choose the solvent (like toluene or methylene chloride) that produces the best resolution, that is the solvent that spreads all dye components over the whole separating distance. However, let us recall that TLC can only separate a few substances with k values in the range of about $10^{2.6} = 400$. If there is a mixture whose k values are different by more than 400, these cannot be separated using a fixed mobile phase composition.

In 1969, Snyder and Saunders published an article that dealt with the basics of the TLC-gradient technique [12]. Their theoretical results are sufficiently important that they should be briefly explained here.

Snyder and Saunders imagined two substances applied at a position on a TLC plate with a series of solvent zones moving over them. The separation takes place over the total distance L using the solvent amount V_0 . On an HPTLC plate, L lies within the range of 4–8 cm, and V_0 has a maximum value of about 1.4 mL for a 10×10 cm plate.

In the first separation step, the solvent amount V_1 flows through the centre of the two substance zones. Both substances migrate a distance L_1 towards the solvent front. The partition of the substances in the stationary phase volume V_s , or the mobile solvent volume V_m , is described by the retention factor k (according to (2.7)):

$$k = \frac{t_{\rm s}}{t_{\rm m}} = \frac{L_{\rm s}}{L_{\rm m}} = \frac{1 - R_{\rm f}'}{R_{\rm f}'}$$

The retention factor provides the link between planar and column chromatography. It describes the time a substance spends in the mobile or stationary phases ($t_{\rm m}$ and $t_{\rm s}$) equivalent to the relationship between migration time and retention in the stationary phase for TLC.

In Snyder and Saunders model, equal volumes migrate equal distances, so the pore size of the stationary phase is assumed to be a constant. When the solvent

6.5 Solvent Gradients 137

fraction V_1/V_0 passes over both substances, they will move the relative distance L_1/L . The retention factor k_1 is given by

$$k_1 = \frac{V_1/V_0}{L_1/L}$$
.

The relative migration distances R_{f1} of both substances can be deduced from this relationship, if the solvent volume V_1 has passed this pair of substances, hence (6.5):

$$\frac{L_1}{L} \equiv R_{\rm f1} = \frac{V_1/V_0}{k_1}.\tag{6.5}$$

By analogy, the centre of both zones migrates the relative distance $R_{\rm f2}$, if volume V_2 passes through both zones. When i solvent volumes have passed through the zones, they have migrated the relative distance $\sum R_{\rm f_i}$. The distance migrated by the solvent front $L_{\rm F}$ while volume element i passes through the zones can be expressed as

$$L_{\mathrm{F}} = L \left[\sum_{0}^{i} \left(V_i / V_0 \right) + \sum_{0}^{i} R_{\mathrm{f}_i} \right].$$

Separation ends when the solvent front reaches the end of the migration distance, thus $L_{\rm F}=L$.

Therefore, a separation can be simulated as long as the following relationship is valid:

$$\sum_{0}^{i} (V_i/V_0) + \sum_{0}^{i} R_{f_i} \le 1.$$
 (6.6)

Figure 6.16 graphically describes the whole process. According to (2.22), the effective plate number NQ² is defined as

$$NQ^{2} = NR_{f} \left(\frac{k_{2}}{1+k_{2}}\right)^{2} = \frac{N}{R_{f}} \left(R_{f} \frac{k_{2}}{1+k_{2}}\right)^{2}$$

$$= \frac{N}{\sum_{i=1}^{j} \left(\prod G_{m}\right)^{2} R_{f_{i}}} \left[\sum_{i=1}^{j} \left(\prod G_{m}\right) R_{f_{i}} \frac{k_{i}}{(1+k_{i})}\right]^{2}, \tag{6.7}$$

where

NQ² effective plate number

 $R_{\rm f_i}$ relative migration distance in volume i

 $G_{\rm m}$ zone compression factor

 k_i retention factor for the ith solvent

N plate number at the solvent front migration distance

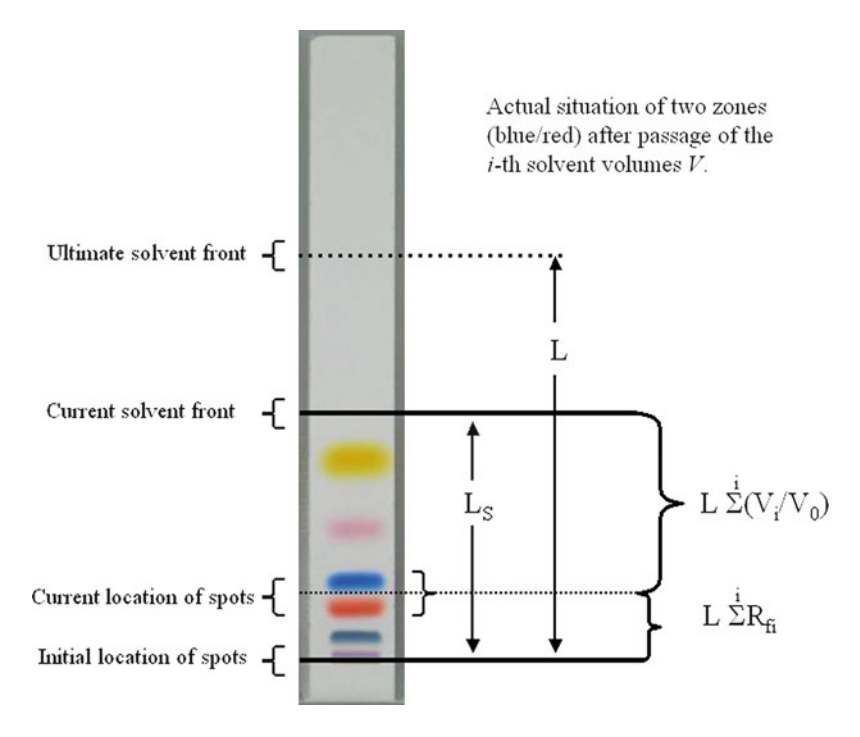


Fig. 6.16 Gradient elution TLC after passage of the ith solvent through the two bands of interest

Snyder and Saunders calculated the effective plate number of a gradient separation for various k values according to (6.7). For this they first simulated a substance pair migration according to (6.5), for solvent fractions passing through the substance zones until condition (6.6) is fulfilled. The effective plate numbers NQ^2 calculated in this way (for $G_m = 1$) are plotted in black in Fig. 6.17 against the logarithm of the retention factor k. The function shows the shape of the effective plate number with respect to the retention factor as shown in Fig. 2.14. As already mentioned, noticeable separation steps can be achieved only in a retention factor range about $-0.6 < \lg(k) < +2$.

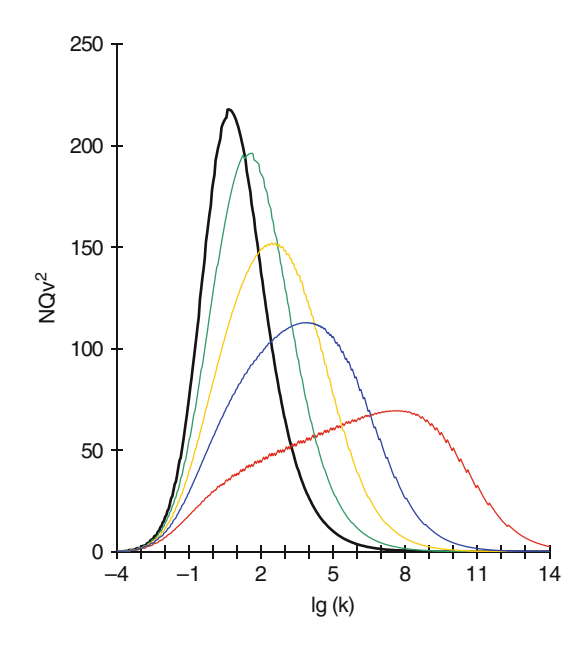
The advantage of Snyder and Saunders' rather complicated formula for the effective plate number is that the effective plate number of a gradient development can now be simulated. However, to do so one must also take into consideration that an alteration in the solvent strength will compress the zones.

The compression factor can be calculated from (5.4) or (6.11) with $R_f = k/(1+k)$:

$$G_{\rm m} = \frac{\sigma_{i+1}}{\sigma_i} = \frac{(1 - R_{\rm f(i+1)})}{(1 - R_{\rm f(i)})} = \frac{k_{i+1}(1 + k_i)}{k_i(1 + k_{i+1})},\tag{6.8}$$

6.5 Solvent Gradients 139

Fig. 6.17 Effective plate numbers dependent on retention factors (for N = 1486) without gradient (*black*) and with gradient steepness of b = 2 (*green*), 4 (*yellow*), 6 (*blue*), and 10 (*red*)



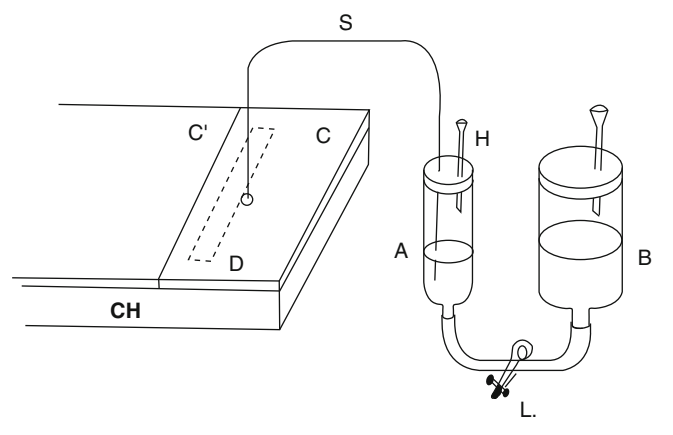


Fig. 6.18 Simple gradient development device for use with a horizontal developing chamber. The solvent in A is successively mixed with a stronger solvent from B (from [13)

Where

G_m zone compression factor

 σ_i compression in zone i

 σ_{i+1} compression in zone i+1

The compression factor has a multiplying effect and is taken into consideration in (6.7) in the form of a geometric expansion.

Figure 6.18 shows how the solvent strength can be altered during a development by mixing two solvents (A and B). The R_m values ($\lg k$ values) change linearly with

the solvent composition. The retention factors change during the simulated passage of the solvent flow through the zone pair. This can be modelled using the following formula:

$$\lg(k)^* = \lg(k) - b\frac{V_i}{V_0}. (6.9)$$

Here,

 $lg(k)^*$ simulated retention factor

lg(k) retention factor at the start of the gradient

b steepness (slope) of the gradients

 $V_{\rm i}$ volume of the mixing chamber

 $V_{\rm i}$ added volume dose in the *i*th gradient step

 V_0 total volume for the development

The results of the simulation for various slopes b, plotted against the retention factor at the start, are also plotted in Fig. 6.17. It can be seen that the zones broaden with increasing gradient steepness. With a value of b=10, substances in the k range higher than 10^{10} can be potentially separated. However, the effective plate number is reduced to about a quarter of that for a separation with a constant mobile phase composition.

In general, gradients reduce resolution (indicated as the effective plate number) while simultaneously extending the separation range to include mixtures of a wider polarity. The loss of resolution compared with an isocratic development is the price paid for an increase in the zone capacity for mixtures of a wider polarity [2, 12]. Therefore, a critical substance pair should be separated with a constant mobile phase composition, because this will achieve the highest resolution. If substances with different polarity are to be separated in a single run, for example, for screening purposes, gradient conditions are preferred. From further simulations, Snyder and Saunders also deduced that for TLC, a gradient in the stationary phase is more advantageous than altering the mobile phase during development [12].

A good TLC gradient is always an anti-parallel gradient. A gradient is defined as anti-parallel when it works against the solvent direction, that is, when compounds with higher R_f values are more retained than those at lower R_f values. On the contrary, a gradient working in parallel reduces resolution, because it extends the migration of substances in the direction of the solvent front and increases zone widths [12].

6.5.2 Evaporation-Controlled Gradient Elution

An anti-parallel gradient in the stationary phase is obtained by increasing the layer thickness or by increasing the layer activity in the solvent direction. Altering the solvent composition towards a weaker solvent strength during a separation also produces an anti-parallel gradient. Geiss also suggested variations in temperature,

6.5 Solvent Gradients 141

altering pH values, or locally impregnating the TLC plate as other possible methods for creating gradients [2]. All these approaches are complicated to perform and not in widespread use.

The simplest method for generating a layer gradient is to exploit activity gradients using different humidity levels in a Vario-KS-chamber. A silica gel plate is preconditioned over troughs with different relative humidities to activate or deactivate the layer. For example, an anti-parallel gradient could start with 98% relative humidity and attain 9% relative humidity at the end of the development distance.

The composition of the mobile phase can also be changed via the vapour phase to carry out a simple gradient development. Figure 6.19 shows a separation obtained with a mobile phase of ethyl acetate—mesitylene—benzyl alcohol (18+1+1, V/V) developed over a vapour phase of pure mesitylene. The main component of the mobile phase consists of ethyl acetate. This evaporates from the plate surface during development while mesitylene simultaneously condenses from the vapour phase onto the layer. Thus, the fraction of mesitylene in the mobile phase continually increases during development while that of the ethyl acetate decreases. This process is not linear because the velocity of the solvent front is continuously reduced whereas the mesitylene condensation remains stable.

In addition, mesitylene is also condensed on dry plate areas. From about 25 mm separation distance, this surplus of mesitylene present on the not-yet developed plate area forms a large front gradient and reduces the fraction of benzyl alcohol in the solvent. Thus the mobile phase shown in Fig. 6.19 is almost entirely based on non-linear processes. The result is the non-linear shape of the mesitylene gradient formed during development.

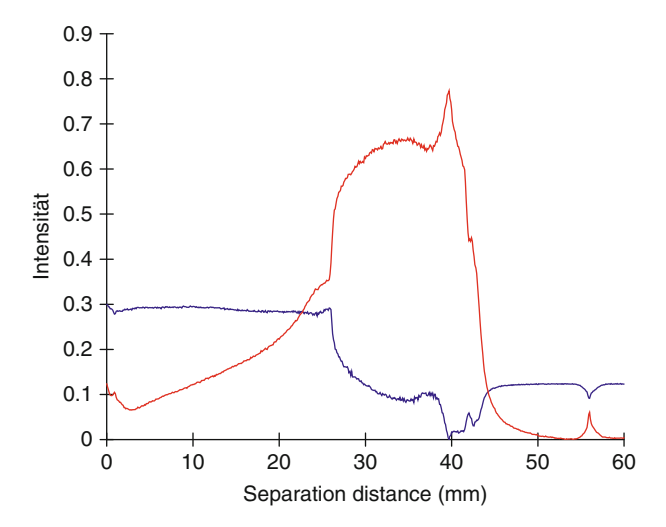


Fig. 6.19 The solvent composition of a mobile phase consisting of mesitylene (red) and benzyl alcohol (blue), mixed with ethyl acetate (1+1+18, V/V). The plate was developed in the presence of mesitylene vapour to a separation distance of 45 mm

6.5.3 Multiple Development in TLC

Multiple development can improve resolution and/or extend the polarity range in a separation. If the same solvent and same solvent front migration distance is used for each development, the resulting $R_{\rm fn}$ values depend on the $R_{\rm f}$ value observed in the first development. In the first development step the analyte moves according to its $R_{\rm f}$ value over the distance $z_{n0}=(z_{\rm f}-z_0)\,R_{\rm f}$. The plate is dried and the solvent moves the distance $(z_{\rm f}-z_0)$, and the analyte will move the fraction $z_{n1}=(z_{\rm f}-z_0)\,R_{\rm f}\,(1-R_{\rm f})$, because in the second development the analyte starts from position z_{n0} . The plate is dried and developed once again over the distance $(z_{\rm f}-z_0)\,R_{\rm f}\,(1-R_{\rm f})^2$ and so on. In the nth repetition, the analyte moves the distance $z_n=(z_{\rm f}-z_0)\,R_{\rm f}\,(1-R_{\rm f})^n$. The sum of all distances the analyte moves after n developments is

$$z_{sn} = \sum_{i=0}^{n} (z_{f} - z_{0}) R_{f} (1 - R_{f})^{i} = (z_{f} - z_{0}) [1 - (1 - R_{f})^{n}].$$

Taking the definition of the R_f value (2.5) into account $[R_{fn}=z_{sn}/(z_f-z_0)]$, we obtain (6.10) [14]:

$$R_{\rm fn} = 1 - (1 - R_{\rm f})^n. ag{6.10}$$

Here.

 $R_{\rm fn}$ $R_{\rm f}$ value after n developments

 $R_{\rm f}$ R_f value after a single development

n number of developments

The separation distance between two zones ($\Delta R_{\rm f} = R_{\rm f2} - R_{\rm fl}$) in multiple development reaches a maximum after a certain number of developments and then decreases as the slower moving zone catches up with the faster moving zone as they approach the solvent front. The optimum number of developments can be empirically estimated [14] as

$$n_{\rm opt} \approx \frac{1}{R_{\rm f1,2}} - 1,$$

where $R_{\rm f1,2}$ is the mean $R_{\rm f}$ value of the two substances. This equation reaches a value of 1 for $R_{\rm f1,2}=0.5$ and provides optimum repetition values $n_{\rm opt}>1$ only for $R_{\rm f}$ values < 0.4. Separations by multiple development should not be carried out for substances with values of $R_{\rm f}>0.4$ because such separations deteriorate the separation quality in comparison with a single development [2].

6.5 Solvent Gradients 143

6.5.4 Automated Multiple Development (AMD)

Multiple development is the simplest method of performing a TLC-gradient separation. The separation is carried out using either short or maximum development distances. After each development, the layer is dried and the whole process is repeated once again using another solvent. However, during later elution steps, the solvent front first meets the spot, which has moved the shortest distance. Within this spot, the part with a smaller $R_{\rm f}$ value is contacted first by the solvent front and gradually moves towards zones with higher $R_{\rm f}$ values, thus compressing the zone width.

A combination of multiple development with an incremental mobile phase composition gradient is known as "AMD", the acronym for "automated multiple development". The method was first proposed by Perry and introduced in an automated form by Burger in 1984 [15, 16]. The AMD system is commercially available, working as a fully automated system under computer control. The plate is exposed to the solvent vapours for a fixed time, then developed for a fixed distance, and finally dried. Automated layer conditioning via the vapour phase is also possible for any or all development steps. In general, anti-parallel gradients are used in AMD. Strong solvents are employed for the first 5–10 development steps. The sample zones are thus focussed, which has a positive effect on resolution.

The relationship between the zone width and $R_{\rm f}$ value is as follows. The distance from the bottom of the lowest sample zone (or sample application position) to the solvent entry position (immersion line) is z_0 , see Fig. 6.20, and is the same distance

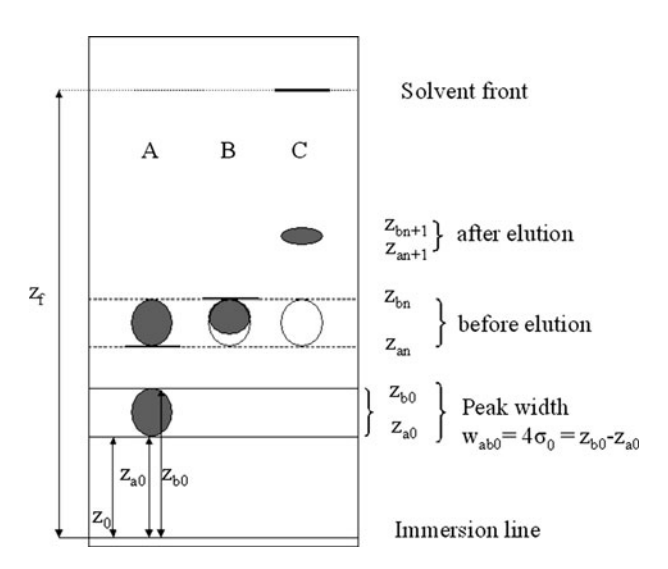


Fig. 6.20 Zone width abbreviations and illustration of the zone refocusing mechanism (a) before development, (b) during development, (c) after development

for the lower zone z_{a1} after the first development over the distance z_f , then from the definition of the R_f value [17]:

$$z_{a1} - z_{a0} = R_f(z_f - z_0),$$

$$z_{a1} = (R_f z_f - R_f z_{a0}) + z_{a0} = z_f R_f + z_{a0} (1 - R_f).$$

The same holds for the upper zone z_{b1} after a single development from z_{b0} to z_f . Let us call the difference of $z_{b0} - z_{a0} = w_{ab0} = 4\sigma_0$ and $z_{b1} - z_{a1} = w_{ab1} = 4\sigma_1$

$$z_{b1} - z_{a1} = w_{ab1} = w_{ab0}(1 - R_f).$$

Hence

$$\sigma_1 = \sigma_0(1 - R_f), \tag{6.11}$$

Where

 σ_1 peak width after the first development

 σ_0 original peak width

The spot compression is proportional to the R_f value, as shown by the following equation after n developments:

$$\sigma_n = \sigma_0 (1 - R_f)^n, \tag{6.12}$$

Where

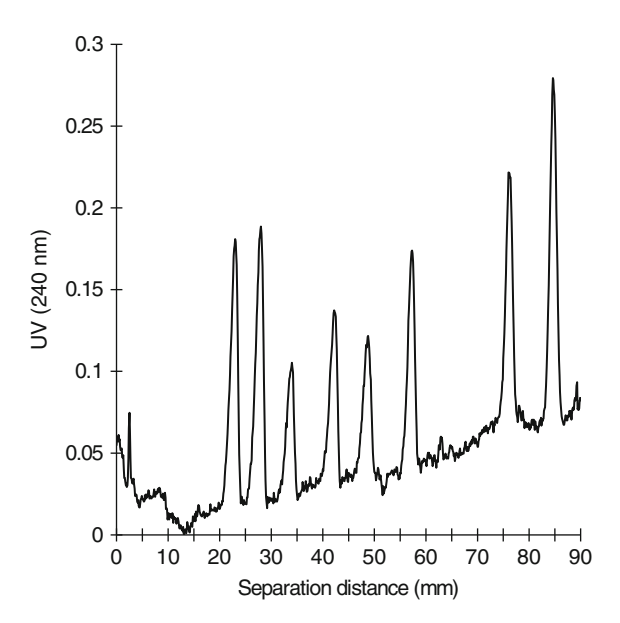
 σ_n peak width after *n* developments

 σ_0 original peak width

A spot compression will result, if the spot is developed with strong mobile phases because according to (6.11), a high $R_{\rm f}$ value ($R_{\rm f}\approx 1$) immediately render $\sigma_n\approx 0$. Therefore focussing with strong solvents at the beginning of the development achieves very small zone widths. Thus AMD allows the direct application of up to 50 μ L sample volumes without loss of resolution, because the application band is compressed (focussed) during the first few development steps, using strong solvents.

Immediately after sample application and focussing, the plate is developed with an anti-parallel gradient of 20–30 individual steps in which the solvent front migration distance is extended a few millimetres at each development step. After drying, in each new development the solvent front encounters the dried substance zone and compresses it. The substances are further focussed by the anti-parallel gradient when they move, that is when they dissolve in the mobile phase. The solvent strength of the anti-parallel gradient diminishes as the number of development step increases. For gradient k values beyond 20, a substance stops moving and remains immobilized on the layer. As the substances literally "fall out" of the mobile phase, the weakening gradient in subsequent steps cannot bring these zones

Fig. 6.21 AMD separation of monuron, chlorotoluron, desethylatrazine, cyanazine, methobromuron, propazine, vinclozoline, and pendimethaline (500 ng, each, and vinclozoline 1 μ g), developed with the gradients given in Fig. 6.22



back into solution. This prevents substance zones broadening by diffusion, because these compounds no longer enter the mobile phase [16–21]. The result is a separation with narrow zone widths as shown in Fig. 6.21.

Figure 6.22 shows a typical AMD composition gradient over 25 development steps. With each new development, the solvent front is incremented almost 4 mm. The anti-parallel gradient starts with the polar solvent (methyl *tert*-butyl etheracetonitrile) and ends with n-hexane.

AMD can achieve relatively large separation numbers (greater than 10). The large application volumes possibly facilitate the determination of sample concentrations below 1 mg/L without enriching the sample. Thus, AMD is well suited to environmental screening [22, 23] as well as separating complex samples, for example, in food analysis [24].

6.6 Normal Phase Separations with Water-Containing Solvents

Very polar substances can be successfully separated on silica gel layers using solvents that contain water. In such separations, adsorbed water forms the stationary phase and the method is known as Hydrophilic Interaction Chromatography (HILIC).

This provides an obvious advantage compared with normal-phase separations employing organic solvents and extends the application range to highly polar compounds, including ions. Figure 6.23 illustrates the separation of positively

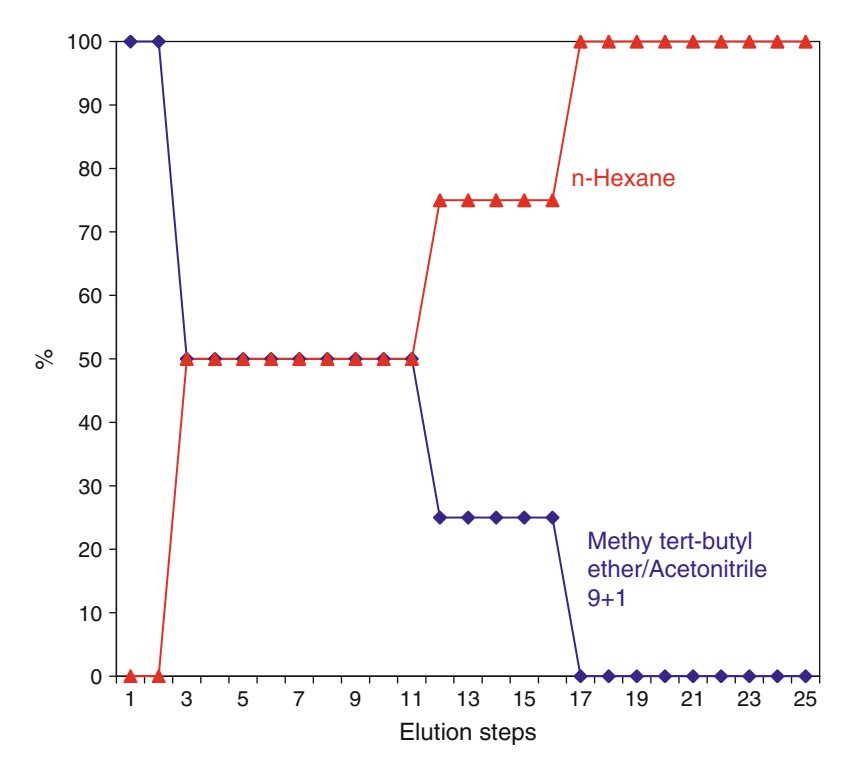
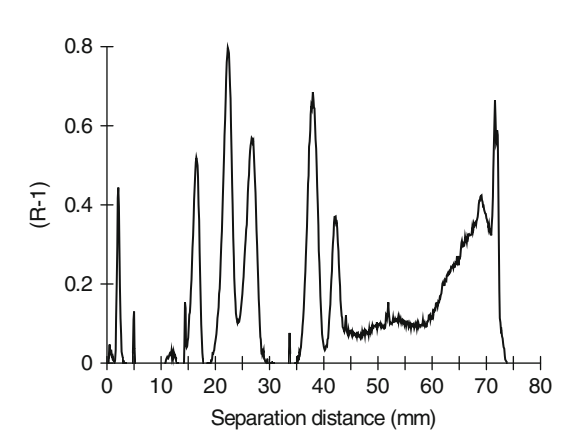


Fig. 6.22 Typical AMD composition gradient

Fig. 6.23 Separation of paraquat, diquat, mepiquat, chloromequat, and difenzoquat (from *left to right*) with the solvent mixture 1-propanol—methanol–2.5 M aqueous NaCl (1+1+3, V/V). The compounds were stained with tetraphenyl borate/HCl and measured by fluorescence from 560 to 590 nm



charged compounds on silica gel with a mobile phase containing up to 60% (V/V) water. The separation takes about 50 min because the mobile phase is very viscose, yet good separations with sharp zones are achieved.

6.7 Plate Development with Forced Flow

A major disadvantage of TLC compared with HPLC is the decrease in the mobile phase velocity with increasing development distances. Like HPLC there are a number of methods that can be used to elute or develop a TLC plate with a mobile phase under forced flow conditions [25].

The simplest method is to place the TLC plate in a horizontal chamber with the layer facing upward. The layer is covered with a counter plate leaving a narrow strip at the end of the layer uncovered from where the solvent is evaporated resulting in a continuous flow of mobile phase. In this experiment Nyiredy observed constant solvent velocity [25].

6.7.1 Rotation Planar Chromatography (RPC)

Rotation planar chromatography is carried out when the plate rotates around its central point while the mobile phase is simultaneously applied to its centre. Centrifugal forces propel the mobile phase outwards with a spin velocity that can reach up to 1,500 rpm (rotations per minute). To determine the separated analytes the process is interrupted before the mobile phase reaches the outside edge of the plate. For preparative separations, the mobile phase is usually allowed to elute the sample components off the layer and into a trough for collection or online detection. Apparatus for preparative rotation planar chromatography is available under the trade names Rotachrom[®] [26] or ExtraChrom[®] [25].

6.7.2 Over-pressure Layer Chromatography (OPLC)

If a TLC plate is sealed from above and the solvent is forced by pressure through the stationary phase, we have the planar equivalent to HPLC. The simplest way of carrying this out is to seal the TLC plate from below with a strong glass plate under pressure with the mobile phase supplied at the centre [27]. Kaiser managed to achieve sharp separation zones using such a simple apparatus. He carried out circular separations within a few minutes, as well as performing anti-circular separations (in which the solvent flows from the outside inwards). Circular separations produce optimum separation conditions for substances with low $R_{\rm f}$ values. The opposite is true for anti-circular separations. Kaiser stated that two anti-circular separations carried out sequentially are the equivalent of a linear separation [27].

Tyihák and co-workers introduced the linear high pressure horizontal development technique in 1979 [28]. Separation conditions similar to HPLC are attained at pressures up to 100 bars. A difference to HPLC lies in the possibility of separating samples in parallel. Detection can be carried out off-line on the plate after development or online when the separated zones are eluted from the layer into the detector.

Fig. 6.24 Correlation between the observed average plate height \overline{H} and the separation distance for TLC and HPTLC layers with different particle sizes. Conventional development was performed in saturated and unsaturated normal chambers (N_s and N_{us}) and a separation without a vapour phase (U_M) where the layer is covered by a glass plate (from [28])

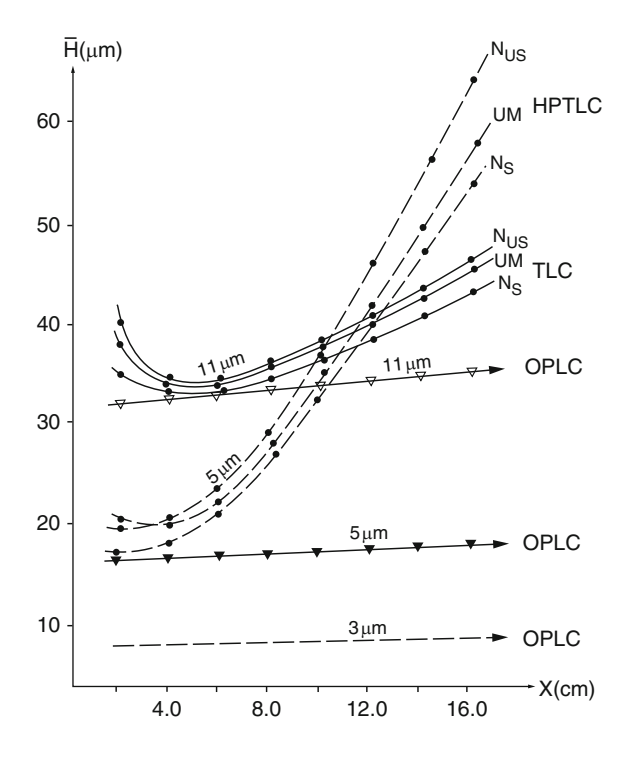


Figure 6.24 illustrates the change in plate heights \overline{H} with the separation distance for layers of different particle size using conventional and OPLC developments. The advantage of HPTLC over TLC is clearly illustrated as well as the advantages of the OPLC mode.

The decisive point in favour of OPLC is that the separation quality represented by the average plate height is independent of the separation distance. OPLC requires complicated equipment and specially sealed plates. Such requirements have so far prevented this interesting method from finding widespread use.

6.8 Two Dimensional TLC (2D TLC)

6.8.1 Development in Orthogonal Directions

2D chromatography dates back to Consden who designed a method using separate developments in different directions [29]. With the same mobile phase and two orthogonal developments the zone number and component resolution is expected to increase by $\sqrt{2}$. By choosing mobile phases of different selectivity for the orthogonal developments, very high zone capacities are theoretically possible

although the correct experimental conditions to achieve these separations are difficult to obtain. In its normal implementation a single sample is spotted at one corner of the TLC plate and developed in solvent A to the opposite edge of the layer, the plate is then dried and rotated through 90° and developed a second time with solvent B in the direction orthogonal to the first development. In another variant the sample is spotted at the four corners of the layer with samples spotted at the middle between the four samples which are then developed simultaneously towards the centre of the layer in a horizontal developing chamber. After drying, the TLC plate is turned through 90° and again developed with solvent B. The identification of individual spots is carried out in relation to the position of the standards. If two standards are applied on a 10×10 cm HPTLC plate, four 2D separations can be obtained, each with two standard tracks (Fig. 6.25).

If a 2D plate is simultaneously developed in this way, with two different solvents starting on either side, four different solvent combinations can be simultaneously tested on a single plate. There is a quantification problem with 2D separation because slit scanners cannot readily quantify such separations. In this case videodensitometry provides an elegant solution.

To perform a 2D separation on two different stationary phases, a narrow strip of the TLC plate can be chemically modified to create a different type of sorbent. The first separation is then performed on this chemically modified strip. Such two-phase layers for TLC are commercially available from Whatman as "Multi-K dual phase" plates. The company sells a 20×20 cm silica gel TLC plate with a 3-cm-wide edge-strip coated with RP-18 material. Unfortunately, similar HPTLC plates are not available.

6.8.2 Grafted TLC

A 2D separation using different stationary phases can be performed by cutting an HPTLC plate (glass plates are best) into small strips. One strip is used to separate a sample using the full length of the layer. After drying, the strip is clamped on a second plate with a different stationary phase, so that both layers come into contact. Small magnets provide a practical method for holding the two plates together. This procedure is called "grafting". It can avoid the problem that the different stationary phases required for a separation are not commercially available. You can simply construct your own combination [30].

Some hints should be noted to observe good result. If the first dimension of the separation is carried out on an RP-18 plate, separate the sample and then cut the plate into narrow strips about 1 cm wide. Graft these strips onto the second plate, e.g. one with a silica gel phase. To do the grafting, scratch away the stationary phase of the second plate to create a space for the strip from the first layer. Place the strip from the first separation layer-side down onto the cleared area of the second plate and, with a gentle dragging movement, make contact with the stationary phase on the second plate. It is essential for a good separation that both layers have contact over the whole distance. Position a spacer (a glass strip) on the other side of the

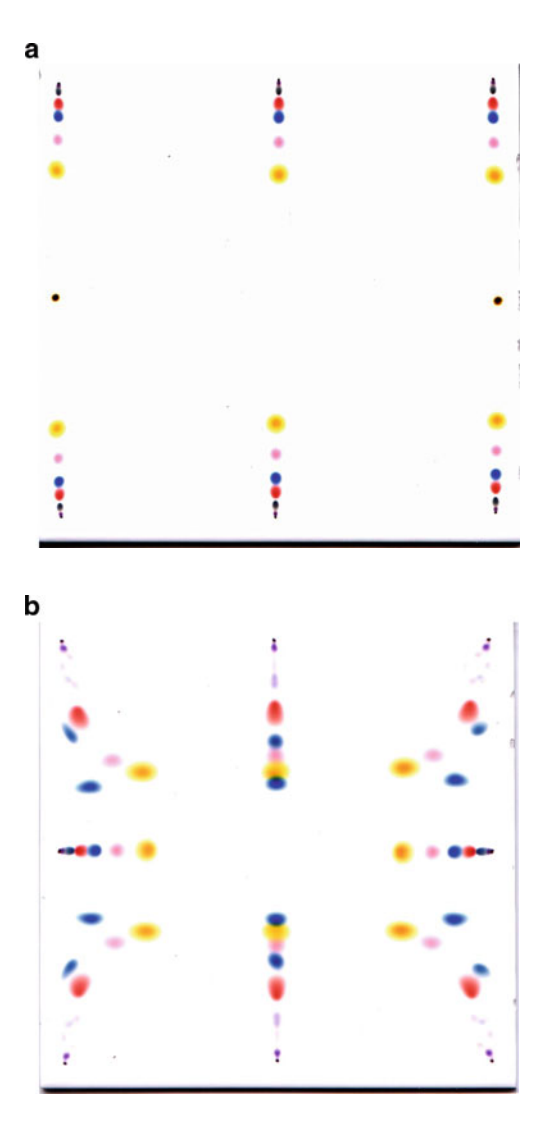


Fig. 6.25 (a) 2D separation (dye mixture on silica gel) after the first elution with solvent A (toluene). (b) 2D separation after the second development with solvent B (methyl *tert*-butyl ether). Visible are four 2D separations and four standard tracks

second plate. Cover the whole construction with an opposing plate and fix it (held in position) with two magnets (Fig. 6.26).

Now bring the narrow strip with the first separation phase in contact with the solvent. The solvent transfers the substances onto the second stationary phase. The contact between the two stationary phases must be good so that the substance spots remain compact.

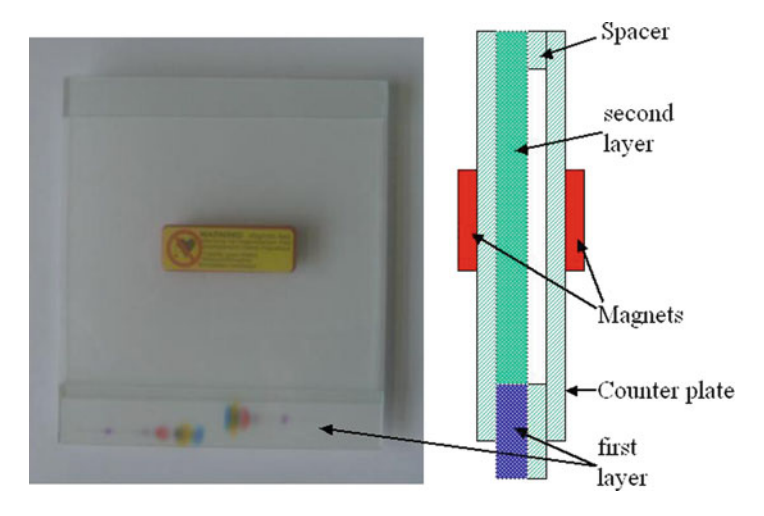


Fig. 6.26 A grafted separation track at a 10×10 cm HPTLC plate (left). The diagram at right schematically describes the procedure

6.8.3 Stability Test and SRS Technique

2D development methods facilitate the identification of compounds that decompose under the conditions used for the separation. The test is easy to carry out: The sample is applied to one corner (or all four corners) of the layer and developed with the chosen solvent. After drying, the TLC plate is rotated through 90° and again developed with the same solvent. If the separated substances do not decompose during development, they lie on a diagonal after the second development. Substances that can be seen beside the diagonal have an altered chemical structure, which occurred during the separation and indicates that the corresponding substance is unstable.

Figure 6.27 shows the 2D separation of a dye mixture. After a 2D separation with toluene, all the substances lie on a diagonal line, which shows that none of the substances decomposed during the development step. When the stability of a sample to TLC conditions is in doubt this method should be used for general screening before more detailed studies begin.

The large surface of a TLC plate can catalyse decomposition reactions, which can be revealed using the SRS method [31]. In this way the robustness of a separation can be tested concerning oxygen, light, heat, moisture, and reactions with the mobile phase. In the SRS method (separation, reaction, separation) the sample is separated in the first direction with solvent (S), then subjected to a stressing reaction (R), followed by separation in the second dimension using the same solvent (S).

Figure 6.28 shows the SRS separation of a dye mixture. After the first separation with toluene, the dried plate was exposed to an HCl atmosphere. After the second

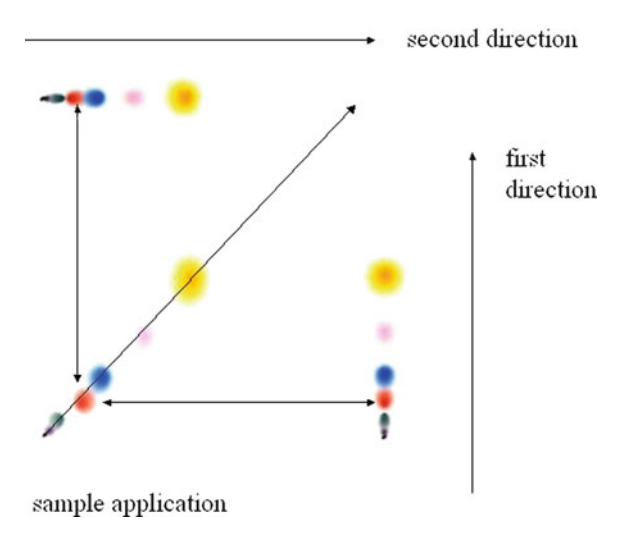


Fig. 6.27 Distribution of a 2D separation of a dye mixture with toluene on silica gel. The separated substances all lie on the diagonal, thus demonstrating that they did not decompose during separation

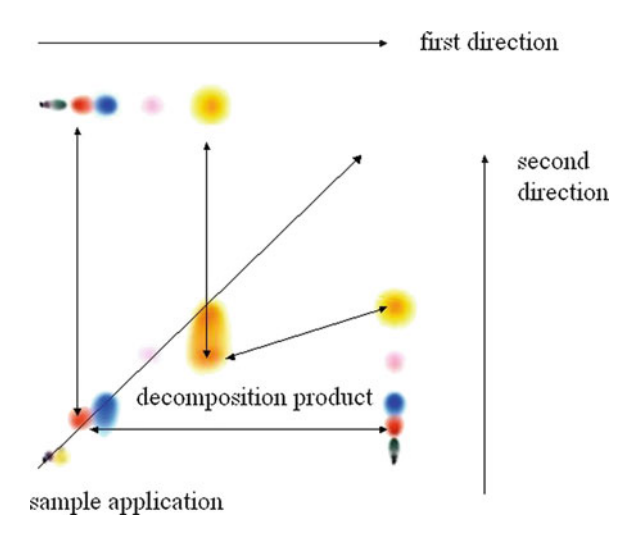


Fig. 6.28 An SRS separation of a dye mixture with toluene on silica gel. The substance with the highest $R_{\rm f}$ value decomposed during the reaction step. Substances that react during deliberate "stressing" of the sample can be recognized by their divergence from the diagonal. This process can be used to test whether a separation is robust

separation with toluene, one substance is partially protonated. This "decomposition" can easily be identified by the different behaviour of the "decomposing product" indicating that separating this compound in an HCl atmosphere should be avoided.

References 153

6.9 Drying the Plate

After development, the TLC plate must be dried to facilitate densitometric measurements. Unfortunately, the drying step is often not given sufficient attention. Indeed, most textbooks do not even mention it at all.

However, drying the plate is one of the deciding factors in quantitative TLC analysis [32]. During the drying process the mobile phase evaporates from the plate surface. The mobile phase is distributed throughout the stationary phase but is exhausted from the layer only at its surface. The mobile phase carries the analytes to the plate surface as it evaporates where they become enriched. This is very important because the closer a substance is located to the sorbent surface, the higher its response in scanning densitometry. For quantitative evaluation, therefore, it is essential that the analyte distribution remains constant [33] during the drying process. The consequences are obvious. Never dry the plate with a hairdryer because that would unevenly warm the plate. Even drying can be achieved with a heating plate roughly the same size as the TLC plate. A convection oven is also a suitable choice. Passing a laminar stream of air or nitrogen over the plate surface can also be effective. The simplest method to dry a plate is to place it somewhere without air movement. Avoid waving the plate around in your hand and drafty storage places where the plate cannot dry evenly.

References

- de Zeeuw RA (1968) The role of solvent vapour in thin-layer chromatography. J Chromatogr 32:43–52
- 2. Geiss F (1987) Fundamentals of thin-layer chromatography. Huethig, Heidelberg, pp 278–286
- Geiss F (1988) The role of the vapour in planar chromatography. J Planar Chromatogr 1:102–115
- Niederwieser A, Brenner M (1965) Polyzonale Dünnschichtchromatographie. Chromatographische Fliessmittelentmischung und ihre Anwendung zur Trennung von Substanzgemischen, Teil 1 und 2. Experimentia 21:50–54, 105–109
- Niederwieser A, Honegger CC (1966) Gradient techniques in thin-layer chromatography. Adv Chromatogr 2:123–167
- 6. Kraus L (1993) Concise practical book of thin-layer chromatogaphy. Desaga, Heidelberg
- Geiss F, Schlitt H, Klose A (1965) Zur Reproduzierbarkeit in der Dünnschichtchromatographie. Einfluß von Luftfeuchtigkeit, Kammerform und Atmosphäre auf das chromatographische Resultat. Z Anal Chem 213:331–346
- 8. Geiss F, Schlitt H (1968) Ein Neues, Vielseitiges Entwicklungssystem zur Dünnschicht-Chromatographie (KS-Variokammer). Chromatographia 1:392–402
- 9. Dzido TH (2001) In: Nyiredy Sz (ed) Planar chromatography, a retrospective view for the third millennium. Springer, Budapest, pp 68–87
- Kaiser RE (1978) Anticircular high performance thin-layer chromatography. HRC CC 1: 164–168
- 11. Kariko K, Tomasz J (1979) A simple device for anticircular thin-layer-chromatography. HRC&CC 2:247

- Snyder LR, Saunders DL (1969) Resolution in thin-layer chromatography with solvent or absorbent programming. Comparisons with column chromatography and normal thin-layer chromatography. J Chromatogr 44:1–13
- Soczewinski E, Matsik G (1985) A simple device for gradient elution in equilibrium sandwich chambers for continuous thin-layer chromatography. J Liq Chromatogr Rel Technol 8:1125–1238
- Jeanes A, Wise CS, Dimler RJ (1951) Improved techniques in paper chromatography of carbohydrates. Anal Chem 23:415–420
- Perry JA (1973) Programmed multiple development in thin layer chromatography. J Chromatogr Sci 11:447–453
- Burger K (1984) DC-PMD, Dünnschicht-Chromatographie mit Gradienten-Elution im Vergleich zur Säulenflüssigkeits-Chromatographie. Fresenius Z Anal Chem 318:228–233
- 17. Jupille TH, Perry JA (1974) Programmed multiple development. Spot behavior during solvent advance; a mathematical treatment. J Chromatogr 99:231–242
- 18. Zietz E, Ricker I (1989) Methods to monitor pesticides in ground and drinking water by HPTLC/AMD according to drinking water regulations. J Planar Chromatogr 2:262–267
- 19. De La Vigne U, Jänchen D (1990) Determination of pesticides in water by HPTLC using automated multiple development (AMD). J Planar Chromatogr 3:6–9
- Burger K, Köhler J, Jork H (1990) Application of AMD to the determination of crop protection agents in drinking water. J Planar Chromatogr 3:504–510
- Poole CF, Belay MT (1991) Progress in automated multiple development. J Planar Chromatogr 4:345–359
- Lodi G, Betti A, Menziani E, Brandolini V, Tosi B (1991) Some aspects and examples of automated multiple development (AMD) gradient optimization. J Planar Chromatogr 4:106–110
- 23. Butz S, Stan H-J (1995) Screening of 256 pesticides in water by thin-layer chromatography with automated multiple development. Anal Chem 67:620–630
- Morlock GE (1996) Analysis of pesticide residues in drinking water by planar chromatography. J Chromtogr A 754:423–430
- Nyiredy Sz (2003) Progress in forced-flow planar chromatography. J Chromatogr A 1000:985–999
- 26. Nyiredy Sz, Both L, Sticher O (1989) Rotachrom $^{\$}$: a new instrument for rotation planar chromatography (RPC). J Planar Chromatogr 2:53–61
- 27. Kaiser RE (1987) Einführung in die Hochdruck-Planar-Flüssig-Chromatographie (High pressure planar liquid chromatography). Huethig, Heidelberg
- 28. Mincsovics E, Ferenczi-Fodor K, Tyihák E (1996) In: Sherma J, Fried B (eds) Handbook of thin-layer chromatography, 2nd edn. Dekker, New York, pp 171–203
- 29. Consden R, Gordon AH, Martin AJP (1944) Qualitative analysis of proteins: a partition chromatographic method using paper. Biochem J 38:224–232
- 30. Nyiredy Sz (ed) (2001) Planar chromatography, a retrospective view for the third millennium. Springer, Budapest, pp 112-113
- 31. Stahl E (ed) (1969) Thin-layer chromatography. A laboratory handbook, 2nd edn. Springer, Berlin
- 32. Prosek M, Golc-Wondra A, Vovk I, Zmitek J (2005) The importance of controlled drying in quantitative TLC. J Planar Chromatogr 18:408–414
- 33. Rimmer JG (1968) Sample distribution in the TLC layer. Chromatographia 1:219–220

Chapter 7 Specific Staining Reactions

An undoubted advantage of TLC is the simplicity of qualifying a separation. Coloured compounds can be seen by eye. Compounds absorbing only below 400 nm can be visualized by incorporating a fluorescent dye in the layer. Illuminating the plate with light of 256 nm will induce fluorescence. A sample zone covers the dye and inhibits fluorescence, so the zone is visible as a dark band. Illuminating the plate with light of 366 nm can identify substances with native fluorescence. Under these conditions you can observe most of the fluorescent substances by eye.

If all the above-mentioned methods fail, TLC separations can be visualized without destruction by exposing the layer to iodine vapour. Some iodine crystals stored in a closed jar instantly form a violet vapour phase. Placing a plate in this jar will enrich the stationary phase with iodine. Lipophilic sample zones will enrich iodine more efficiently than clean areas of the plate. Substance zones are visualized as brown bands on a nearly white background. Removing the plate from the iodine vapour causes the iodine to evaporate. The visualization procedure also works in reverse. Iodine is removable without any reactions from the separated zones. The duration of staining is sufficient for taking a photograph. It is insufficient for densitometric measurements, but staining can be irreversibly fixed when the plate is dipped for 2 s in a 0.5% (w/v) aqueous starch solution.

Figure 7.1 shows an HPTLC plate stained with iodine vapour. The sensitivity of this staining can be seen at the lower middle of the plate. A brown spot indicates fat from a thumb print because the plate was held without gloves.

Water is another universal detection reagent for lipophilic compounds. The plate is dipped in water for 1 s and then wiped with a window wiper. The plate is placed on a black background. The wetted plate is translucent except where the lipophilic zones are located. Here the plate is not wetted enough to let the black colour of the background pass. As a result the plate shows white zones on a black background.

Figure 7.2 shows a fungicide separation on silica gel. The lipophilic fungicides are visible as white zones on a black background. After drying, the zones can be made visible once again. The method is suitable for taking a photograph. Densitometric measurements are not possible.

Fig. 7.1 An iodine-stained silica gel HPTLC plate. The compounds doxylamine (*left*, *below*), metoclopramide (*right*, *below*), zopiclone (*right*, *above*), and tramadole (*left*, *above*) were separated in amounts of 250–1,000 ng using ethyl acetate–methanol–aqueous NH₃ (25%) (85+10+5, V/V) as mobile phase. There is a standard mixture in the middle (*above* and *below*)

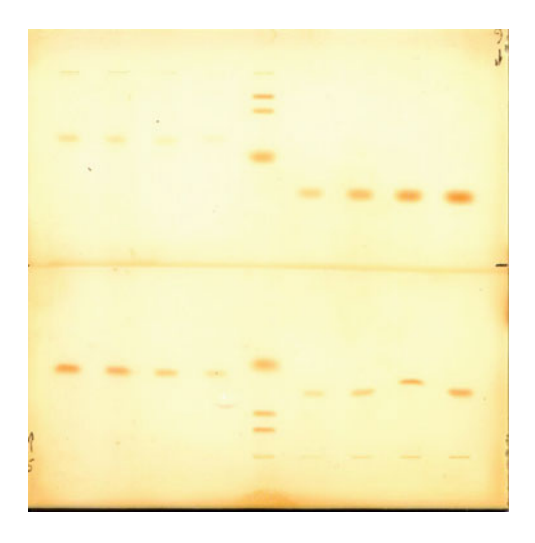


Fig. 7.2 Separation of fungicides (*white zones*) on a silica gel plate visualized by dipping in water



TLC is an open separation method. Open means that the layer is accessible, facilitating the application of chemical reagents. The advantage of having a large number of reagents forming dyes or fluorescent compounds in more or less specific reactions should not be underestimated. These reagents can be used as a "chemical" detector. Commonly used reagents are listed in [1–9]. A more-or-less specific staining reaction in combination with an absorption or fluorescence detector can make TLC separations extremely specific. A general drawback is that staining increases measurement error due to the extra steps required. Staining for quantitative purposes, therefore, should be used only when selectivity is not sufficient without staining.

Two different methods can be distinguished in principle. Staining can be carried out before separation (referred to as pre-chromatographic derivatization) or after separation (referred to as post-chromatographic derivatization). Both methods have their advantages and disadvantages. In most cases a post-chromatographic staining step is used because pre-chromatographic staining brings an additional substance (the reagent) onto the layer, which may interfere with the separation. Nevertheless, pre-chromatographic derivatization has its uses.

7.1 Chemical Reactions Prior to Separation (Pre-chromatographic Derivatization)

Pre-chromatographic reactions can distinguish compounds with similar or identical chromophors but different chemical properties. This reaction can enhance the stability of compounds to avoid chemical reactions during the separation. A pre-chromatographic derivatization can be used to turn volatile compounds into stable derivatives. It can change their extraction properties, improve light absorption, or induce fluorescence. The drawback is that the reagent can contaminate the sample. In addition, this contamination must be separated from the analyte.

7.1.1 Sample Enrichment by Pre-chromatographic Derivatization

Heavy metals can react with dithizone forming coloured complexes at pH values < 4.5. This pre-treatment procedure has two advantages. Only the most problematic heavy metal cations Cd^{2+} , Pb^{2+} , Ni^{2+} , Hg^{2+} , Cu^{2+} , Zn^{2+} , Mn^{2+} , Sn^{2+} , Bi^{3+} , and Co^{2+} will react under these conditions. Other cations do not interfere. The reaction products are extractable with ethyl acetate or dichloromethane, improving detection limits by a factor of more than 100. Separation by reversed-phase chromatography makes quantification possible because the dithiozonates are stable for more than 1 h, which is not the case on silica gel (Fig. 7.3) [10–13].

The ligand 4-(2-pyridylazo)resorcinol (PAR) also forms coloured and extractable complexes with heavy metal cations, which can be separated on cellulose layers using toluene–chloroform (50+5, V/V) [13].

The V, Mo, Mn, Fe, Co, Ni, Rh, Pd, Os, Ir, Pt, Cu, Zn, Hg, Tl, Pb, and Te cations form green, yellow, orange-yellow, brown, or white extractable complexes with 1-hydroxy-2-pyridinthione in the pH range from 3 to 8. The complexes can be separated on silica gel using dichloromethane—tetrahydrofuran (9+1, V/V) as mobile phase [15-17].

Diethyldithiocarbamate forms stable and extractable complexes at pH 8.5 with the metal ions Mn^{2+} , Fe^{3+} , Co^{2+} , Ni^{2+} , Cu^{2+} , Zn^{2+} , Pd^{2+} , Ag^+ , Cd^{2+} , In^{3+} , Sn^{4+} , Sb^{3+} , Pt^{4+} , Au^{3+} , Hg^+ , Tl^+ , Tl^{2+} , Pb^{2+} , and Bi^{3+} [18].

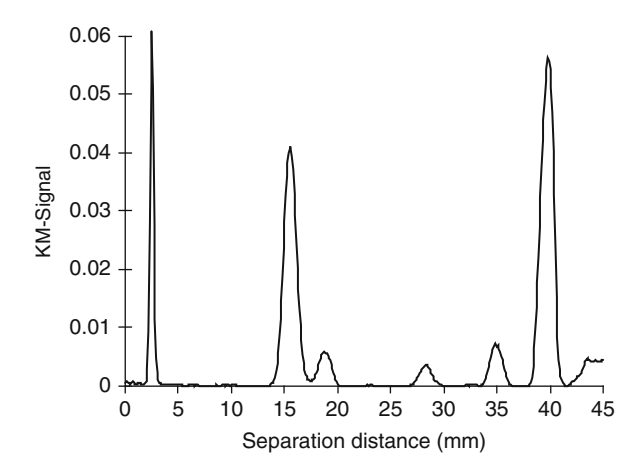


Fig. 7.3 Separation of heavy metal dithizone complexes, separated on an RP-18 plate with water–acetonitrile–ethanol (3+15+5, V/V) as mobile phase scanned in the wavelength range 313–324 nm. The densitogram shows the separation of Hg²⁺ (*orange*, 16 mm), Ni²⁺ (*violet*, 19 mm), Cu²⁺ (*green-brown*, 28 mm), Cd²⁺ (*red-orange*, 35 mm), and Pb²⁺ (*blue-green*, 40 mm) [14]

Structures of dithizone (1), 4-(2-pyridylazo)resorcinol (PAR) (2), 1-hydroxy-2-pyridinthione (3), and diethyldithiocarbamate (4)

Similar to heavy metals, formaldehyde in teeth can be quantified at very low levels using a pre-chromatographic derivatization reaction. The procedure is based on the reaction of dimedone with formaldehyde forming a stable dye. For quantification, cleaned teeth (0.25 g) were pulverized and formaldehyde extracted with a methanol solution containing 0.05–3 mg/ml dimedone. The suspension was centrifuged, and an extract (20 $\mu L)$ was applied to the layer and developed using chloroform–dichloromethane (1:3) as the mobile phase. The extracts were quantified by scanning densitometry at 275 nm [19].

A very sensitive pre-chromatographic reaction was published by Funk for selenium. Selenium reacts with 2,3-diaminonaphthalene forming a red-orange fluorescing extractable compound (Reaction 7.1) [20].

Volatile aldehydes and ketones react with 2,4-dinitrophenylhydrazine forming coloured hydrazones. It is possible to determine traces of acetone and formaldehyde in air by gas/solid reactions followed by photometric determination [21]. Lipophilic aldehydes and related carbonyl compounds in rat and human urine react with

Reaction 7.1 Reaction of selenium dioxide with 2,3-diaminonaphthalene

2,4-dinitrophenylhydrazine forming hydrazones extractable with dichloromethane [22]. The hydrazones are not air stable. 4-Hydrazino-7-nitrobenzofurazane (NBD-hydrazine) or *N*-methyl-4-hydrazino-7-nitrobenzofurazane (Methyl-NBD-hydrazine) reacts with aldehydes and ketones and forms extractable and air stable red to reddish-yellow products, which can be separated on silica gel [23].

$$NH_2$$
 NH_2
 NH_2

Structures of 2,4-dinitrophenylhydrazine (1), 4-hydrazino-7-nitrobenzofurazane (NBD-hydrazine) (2), and *N*-methyl-4-hydrazino-7-nitrobenzofurazane (Methyl-NBD-hydrazine) (3)

The compound NBD-hydrazine was first used as a pre-chromatographic reagent to form fluorescent derivatives by Frei [25]. The main disadvantage of hydrazines is that they form products in two isomeric forms (*cis*- and *trans*-forms) that may be separated by TLC. That is why in Fig. 7.4 the signal for acetaldehyde–methyl-NBD-hydrazone is such a broad peak at 24 mm separation distance.

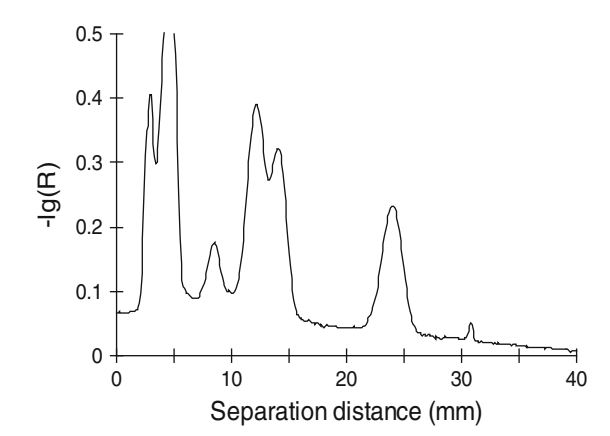
7.1.2 Pre-chromatographic In Situ Derivatization

Group-specific pre-chromatographic reactions can be used to modify the analyte, improve separation selectivity, improve analyte stability, reduce analyte reactivity, and increase the sensitivity of the detection method.

The requirements of such a reaction are [26]:

- Single, stable, reaction products
- High yields in all concentration ranges
- Simple and fast reaction

Fig. 7.4 Separation of acetaldehyde–methyl-NBD-hydrazone (24 mm) from methyl-NBD-hydrazine (4 mm) and degradation products on silica gel layers. Solvent: Cyclohexane–*n*-butanol–toluene (9+1+1, V/V) [24]



- No interference from excess reagent with the separation
- No "convergence" of the chromatographic properties (e.g. by the introduction of large molecular groups that dominate the separation characteristics of the compounds)

In 1953, Miller and Kirchner [27] published an elegant derivatization method for TLC separations, called the sample overspotting method. The sample is applied to the layer band-wise. A reagent solution is then sprayed over the sample zone. For favourable reaction conditions, the overspotted band should not be totally dry. Dimethyl sulphoxide at high temperatures is a beneficial solvent for this reaction. A reaction time of not more than 10 min and reaction temperatures of 60–100°C are mostly sufficient for a complete reaction, due to the small reaction zone. A glass plate can be used to cover the zone to avoid evaporation of the reaction solvent. Covering the reaction zone with a glass plate and a reaction temperature of less than 100°C will reduce the yield if water is a reaction product. Reviews can be found in [1, 26].

7.1.2.1 Oxidation

Oxidation reactions are among the most frequently applied in situ pre-chromatographic reactions. They are used to enhance analyte stability. Phenothiazine, for example, can be oxidized by spraying with 10–20% H₂O₂ and subsequent drying at 60°C [28]. Hydroxyl groups react with a 10% aqueous solution of NaIO₄ at 50°C to form carbonyl compounds. An example is the oxidation of 17-hydroxicorticosteroids, which form 17-ketosteroides [1, 26]. The oxidation of polycyclic aromatic hydrocarbons by atmospheric oxygen at 100°C is catalysed by trifluoroacetic acid [29]. Bis-3,4-benzpyrenyl forms 3,4-benzpyrenyl in the presence of iodine vapour at room temperature (a rare reaction of iodine vapours in TLC) [30].

7.1.2.2 Reductions

In situ reductions are mostly performed using sodium borohydride (NaBH $_4$) as a 1–10% (W/V) solution in ethanol or methanol. This solution must be diluted 1:1 with 0.1 M aqueous sodium hydroxide solution. The zone is neutralized with acid after 30 min reaction [1, 26]. Compounds reduced include carbonyl groups and disulphides.

7.1.2.3 Hydrolyses

Hydrolytic reactions on a TLC plate can be performed in acid or alkaline conditions. For example, sulphonamides can be shown hydrolysed by HCl vapour at 100°C [31]. The HCl vapour at 100°C can be produced from a few drops of hydrochloric acid in a twin-trough chamber. Flavone, cumarin, and triterpene glycosides can be hydrolysed by spraying the application zone with 10% hydrochloric acid in ethanol. The plate is then exposed to the vapours of concentrated hydrochloric acid—ethanol (1+1, V/V) in a twin-trough chamber at 50–55°C for 4–5 h. After drying at 90°C the application zone is overspotted with 25% NH₃ solution dissolved in ethanol (1+1, V/V) [26, 32].

For alkaline hydrolysis, a 7% (W/V) potassium or sodium hydroxide solution in ethanol is used. Esters can be hydrolysed simply by overspotting the application zone [26, 33]. For carbamates, a glass plate covering the overspotted application zone is required to accommodate a reaction temperature of 170°C for 20 min [26, 34]. Glycosides can be hydrolysed when the plate is stored for 24–48 h in an ammonia atmosphere [35].

7.1.2.4 Halogenations

Bromine and chlorine vapour can react with unsaturated substances in the presence of light [26].

Chlorination

Cholesterol reacts with thionyl chloride (SOCl₂) in the vapour phase within 4 h at ambient temperature [32]. Compounds such as caffeine, codeine, acetanilides, urea, melamine, cyanuric acid, and triazine herbicides react with chlorine at ambient temperature in seconds [36–38]. Chlorine can be conveniently produced from potassium permanganate and a few drops of concentrated hydrochloric acid.

Bromination

Phenylbutazone and cholestanol undergo bromination when sprayed with 0.1% (V/V) Br₂ solution in dichloromethane [39, 40]. Much simpler is bromination using bromine vapours. Bromine vapours are conveniently formed by the addition of a few drops of concentrated sulphuric acid to an aqueous solution containing equal amounts of sodium bromide and sodium bromate. At ambient temperature, capsaicinoids are completely brominated [1, 26]. Bromination can be used to distinguish between reacting and non-reacting barbiturates and thiobarbiturates [1, 26, 36].

Iodination

Iodination of pyridine, pyrrole, quinoline, isoquinoline, and indole alkaloids at room temperature over 10 or more hours has been reported [26]. Iodinations are not suitable for analytical purposes due to the long reaction time. Polycyclic aromatic hydrocarbons, naphthylamines, and phenolic steroids form dimeric reaction products with iodine vapours [30]. Iodine vapours can be generated by placing a few crystals of iodine in a closed chamber.

7.1.2.5 Nitrations

Aromatic nitro compounds are often strongly coloured. They frequently form coloured derivatives with quinoids in alkaline conditions [26]. Polycyclic aromatic hydrocarbons react with concentrated nitric acid in dry conditions (e.g. in the presence of P_2O_5) within 20 min [26, 29]. Naphthol reacts completely with concentrated nitric acid at 105° C for 30 min when overspotted [37]. The wide range of available reactions makes nitrations so valuable, especially in forming diazocations from aromatic amines.

7.1.2.6 Diazotizations

Diazotizations are used for identification of aromatic amines or benzodiazepines. Sample bands are sprayed with sodium nitrite in 1 M hydrochloric acid and heated at 105° C for 5 min. After cooling, 5% α -naphthol solution is overspotted forming an azo dye [26]. Diazotizations can be easily performed by overspotting the application zone with a saturated solution of fast blue salt B in ethanol at ambient temperature [1].

7.1.2.7 Esterification

Esterification can be used to derivatize hydroxyl and carboxylic acid groups. It can be used to distinguish primary, secondary, and tertiary alcohols. Tertiary alcohols

react much slower than the other alcohols [1, 26]. Esterification of alcohols is mostly done by reaction with trifluoroacetic anhydride. Aflatoxins, ochratoxin A, sterigmatocystin, and patulin can be esterified at ambient temperature by overspotting with trifluoroacetic anhydride [41]. A mixture of pyridine and acetic anhydride (1+1, V/V) can transform mycotoxins in 5 min at room temperature into acetic esters [42]. This mixture can also be used for gas phase reactions [43]. Carboxylic acids such as sorbic acid or benzoic acid react with a 0.5% (W/V) solution of 4-bromophenacyl bromide in N,N-dimethylformamide. The reagent is overspotted and the reaction takes place at 80° C within 40 min [1, 26]

7.1.3 Pre-chromatographic Staining

A number of reagents react specifically with defined functional groups, transforming the analyte into a dye or fluorescent substance. High cost or absorbing/fluorescence properties may render some of these reagents unsuitable for use as dipping solutions. Overspotting with a small amount (not more than 2 μ L) is possible, especially when strong fluorescent dyes are formed. Funk, Frei, and Wintersteiger reported conditions for use with different reagents to transform analytes into fluorescent compounds [20, 36, 41, 44–46].

7.1.3.1 Reactions with Carbonyl Compounds

Compounds containing a carbonyl group can react in situ with 2,4-dinitrophenyl-hydrazine, isonicotinic acid hydrazide, or phenylhydrazine [1].

Structures of phenylhydrazine (1), isonicotinic acid hydrazide (2), and 2-diphenylacetyl-1,3-indandion-1-hydrazone (3)

Kirchner was the first to describe reactions of nitrophenylhydrazine directly on a TLC plate [27]. 2,4-Dinitrophenylhydrazine (10 mg) in 10 mL methanol/acetic acid (10+1, V/V) was overspotted on the sample zones [1]. Some reactions require additional heating up to 100° C. Progesterone reacts with 2,4-dinitrophenylhydrazine (10 mg) dissolved in 10 mL ethanol containing 30 μ L of concentrated hydrochloric acid. After overspotting, the reaction needs 5–10 min at 100° C for complete

reaction [47]. In a similar manner aldehydes and ketones such as carvone, menthone, acetophenone, 4-benzochinon derivatives, and steroid ketones react with isonicotinic acid hydrazide [1]. The reagent solution is prepared from 10 mg isonicotinic acid hydrazide dissolved in 1 mL ethanol to which 5 μ L trifluoroacetic acid or 10 μ L concentrated acetic acid is added [1].

Phenylhydrazine in the presence of dilute sulphuric acid also reacts with carbonyl groups. The mycotoxin patulin can be transformed into a fluorescent compound by overspotting with 2 μ L of a solution of 50 mg phenylhydrazine in 9 mL methanol and 1 mL dimethyl sulphoxide to which 100 μ L concentrated sulphuric acid is added. The reaction requires about 10 min at 100°C. The product can be separated on silica gel with methyl *tert*-butyl ether–heptane (8+2, V/V) [46, 48].

Dansyl hydrazine reacts with carbonyl groups and forms fluorescent reaction products.

$$O = S - NH_2$$
 $O = S - NH_2$
 $O =$

Structures of dansyl hydrazine (1), dansyl chloride (2), and dansyl azirine (3)

The sample application zone is overspotted with an aliquot of a solution prepared from 30 mg dansyl hydrazine in 4.5 mL methanol and 50 μ L DMSO. After heating to 195°C for 2 min the separation is performed. Molock quantified acrylamide after reaction with dansyl hydrazine and separation of the product on silica gel with ethyl acetate as the mobile phase. [49].

Ketones react with the DIH reagent (2-diphenylacetyl-1,3-indandion-1-hydrazone). A solution of the reagent is prepared by mixing 7 mg 2-diphenylacetyl-1,3-indandion-1-hydrazone with 1 mL methanol—toluene (1+1, V/V) and adding a single drop of concentrated hydrochloric acid. After overspotting, the plate is heated at 100°C for 10 min [50].

7.1.3.2 Reactions with SH-, NH- and OH Groups

Pre-chromatographic dansylation with dansyl chloride has the advantage that excess of reagent can be separated from the zone of interest as well as from fluorescent by-products (e.g. dansyl hydroxide) [26]. Dansyl chloride is not suitable for post-chromatographic derivatization because the whole plate background will fluoresce blue. Dansyl chloride reacts specifically with NH- and OH-groups. For β -blockers, oestriol, morphine, and derivatives of morphine, a solution of 5–20 mg dansyl chloride in 1 mL of acetone is overspotted on the sample zones and then neutralized by spraying with a 8% aqueous Na₂CO₃ solution. For neutralization the

plate can be stored as well for 10 min in NH_3 vapour. In either case, the plate is heated to 120° C for 15 min to complete the reaction [1, 51].

The neutralizing step is not necessary for reactions with primary or secondary amines, or phenols [41, 51]. Carbamates and urea herbicides like metoxurone, diurone, and linurone must be hydrolysed prior to derivatization. For this the application zone is overspotted with a few microlitres of a 1 M aqueous NaOH solution (2 g in 50 mL of water). Sometimes additional heating (up to 180°C, for 20–30 min) is necessary [1].

Dansyl azirine reacts only with SH-groups forming fluorescent derivatives [52, 53]. The reagent is prepared from 10 mg of dansyl aziridine dissolved in 1 mL methanol to which a few drops of phosphate buffer are added to give a pH of 8.2. The application zone is overspotted with the reagent, covered with a glass plate, and heated at 60°C for 60 min to complete the reaction [52, 53].

Fluorescamine reacts with amino acids and primary and secondary amines forming strongly fluorescent derivatives. The reagent is prepared by dissolving 0.3–1.0 mg fluorescamine in 1 mL of acetone. After overspotting, the reaction starts at a pH of 8–10, which can be achieved by overspotting with a buffer solution. After 30 min the plate is developed in the dark. Fluorescamine solution (which is expensive) remains stable for a month at 4°C [51, 54].

Structures of fluorescamine (1), 2,4-dinitrofluorobenzene (2), NBD-chloride (3), and 3,5-dinitrobenzoyl chloride (4)

2,4-Dinitrofluorobenzene (DNFB reagent) is suitable for derivatizing amino acids and peptides [55]. The reagent also reacts with alcohols forming 2,4-dinitrobenzene ethers and hydrogen fluoride. The application zone is overspotted with a 4% (W/V) solution of DNFB in acetone. The plate must be heated at 190°C for 10–40 min to complete the reaction [1, 55]. The reagent should not be used with amino plates. Besides 2,4-dinitrofluorobenzene, numerous reagents are described for the derivatization of alcohols. The most important is NBD-chloride. 7-Chlor-4-nitrobenzo-2-oxa-1,3-diazole (NBD-chloride reagent) reacts with phenols, mercaptans, primary and secondary amines, amino acids, peptides, sulphonamides, and alkaloids under alkaline conditions. [1, 26]. The reagent solution is prepared from 10–20 mg NBD-Cl dissolved in 10 mL ethanol, methanol, or acetonitrile. The sample application zone must first be overspotted with 1 μ L of an alkaline solution (for example, 2 g NaHCO3 or 5 g NaOH dissolved in 100 mL of water). The reagent solution is sprayed onto the application zone after drying [1, 51]. This results in the formation of coloured zones with yellow-green fluorescence when illuminated with

UV light at 365 nm. The reagent can be used on silica gel and RP-18 layers but not on amino plates [1].

NBD-Cl is used to synthesize 4-hydrazino-7-nitrobenzofurazane (NBD-hydrazine) and *N*-methyl-4-hydrazino-7-nitrobenzofurazane (Methyl-NBD-hydrazine), used to prepare fluorescent derivatives of aldehydes and ketones. The reagent solution for overspotting is prepared from 10 mg NBD-hydrazine or 10 mg methyl-NBD-hydrazine in 1 mL methanol containing a drop of concentrated phosphoric acid. Two microlitres of the reagent solution is applied to each sample zone and the reaction is completed within a few minutes at room temperature [23, 24].

3,5-Dinitrobenzoyl chloride is used for the pre-chromatographic derivatization of alcohols [1]. The reagent solution is prepared by dissolving 1.0 g of 3,5-dinitrobenzoyl chloride in 7.5 mL of p-xylene and 1 mL of tetrahydrofuran. Alcohols react at 185°C directly on the plate. After reaction, excess reagent is hydrolysed with 10% (W/V) aqueous sodium hydroxide solution [56].

7.1.3.3 Derivatization of Carboxylic Acids

Carboxylic acids, such as sorbinic acid, benzoic acid, or C_6 – C_{24} lipid acids, react rapidly with dansyl semipiperizide and dansyl semicadaverine forming strongly fluorescent derivatives [1, 26, 57].

$$O = S - NH$$

$$O = S - N$$

$$O =$$

Structures of dansyl semicadaverine (1) and dansyl piperizide (2)

The reagent solution is prepared by dissolving 10 mg of dansyl piperazide or dansyl semicadaverine in 1 mL of methanol. After overspotting the sample, the water formed by reaction must be removed. This can be done by overspotting with a 1% (W/V) solution of N,N'-dicyclohexylcarbodiimide in diethyl ether. This should be done with care since this compound is a known carcinogen. The plate is then air dried before development [57].

7.1.3.4 Reactions with Alcohols and Amines

Isocyanates and phenylisocyanates, such as *o*-nitrophenylisocyanate [1, 56], react with alcohols, amines, and amino acids forming well-defined products.

Naphthylisocyanate and fluoresceine isothiocyanate both act as selective reagents for alcohols and amines forming coloured or strongly fluorescent urethane, urea, or thiourea derivatives. Naphthylisocyanate reacts with alcohols and amino acids to form yellow non-fluorescent dyes. The reagent solution is prepared by dissolving 10 mg naphthylisocyanate in 1 mL xylene to which 100 µL triethylamine is added. Primary and secondary amines react at 95°C within 30 min. Tertiary alcohols react within 2 h at 140°C [58].

Fluoresceine isothiocyanate forms strongly fluorescent derivatives with amino acids (Reaction 7.2). The reagent solution is prepared from 10 mg fluoresceine isothiocyanate dissolved in 1 mL of xylene to which 100 μL of triethylamine is added. The sample is overspotted with this solution and a solution of 1%~N,N'-dicyclohexylcarbodiimide dissolved in diethyl ether, to remove water. After applying the reagent solutions, the plate is heated to $100^{\circ} C$ for several minutes. In some cases it is necessary to cover the application zone with a glass plate. Both reagents must be freshly prepared.

7.1.4 Reagents in the Mobile Phase

Primary amino acids react with ninhydrin at 80°C forming a red dye. Secondary amines, such as praline, form a yellow derivative. Ninhydrin can be dissolved in the mobile phase prior to development. In this way it is uniformly distributed over the layer. After development the plate is heated at 80°C for 10 min, and ninhydrin reacts forming dyes.

Reaction 7.2 Reaction of fluoresceine isothiocyanate with amino acids forming a fluoresceine thiourea derivative

Structure of ninhydrin

This approach is also successful for fluorescamine and 8-anilino-naphthalen-1-sulphonic acid reagents [1] and is especially suited for quantitative evaluations because the error-dependent step of spraying or dipping in the reagent is avoided. A drawback of this method is that water in the mobile phase can inhibit the reaction. In this case higher temperatures above 100°C are necessary.

Amino acids can be separated on cellulose using n-butanol—acetic acid—water (4+1+1, V/V) as mobile phase (see Fig. 3.9). For a complete reaction, less than 20 mg of ninhydrin dissolved in 10 mL of mobile phase is all that is required.

7.2 Post-chromatographic Reactions (Derivatization After Development)

Post-chromatographic reactions are a powerful tool for qualification and quantification of TLC separations. More than 300 different staining reagents are known for this application [1, 2, 9, 59]. The purpose of this section is not to discuss all known reactions but to highlight those chosen for quantitative determinations. Reagents requiring complicated handling with multiple application steps or forming unstable derivatives are not discussed.

A general problem is that some chemicals are toxic and should be handled with appropriate care. For example, the toxicity of sodium nitroprusside (Na₂[Fe (CN)₅NO]) is often underestimated, and the numerous reagent mixture containing this compound for selective detection of aldehydes, amines, alkaloids, urea and thiourea compounds, sulphonamides, and sugars, as well as for –S–S- and –SH-groups, will not be discussed here. Known carcinogenic compounds such as benzidine and *o*-phenylenediamine are not discussed, nor picric acid, which is an explosion hazard.

Staining reactions are mostly done by hand spraying but this method is not suitable for quantification. Hand spraying results in an irregular distribution of reagent over the layer. Spraying for quantification should be done by using computer-controlled spraying equipment, as shown in Fig. 7.5. The reagent is uniformly distributed over the layer using a minimum of reagent, which makes the use of expensive compounds possible. A few millilitres is sufficient for spraying a whole plate. The amount of reagent is reproducibly sprayed which assists in maintaining constant evaluation conditions. Sequence spraying, or spraying different solutions at different plate locations, is no problem.

Fig. 7.5 A computercontrolled reagent sprayer (With permission by DESAGA, Heidelberg, Germany.)

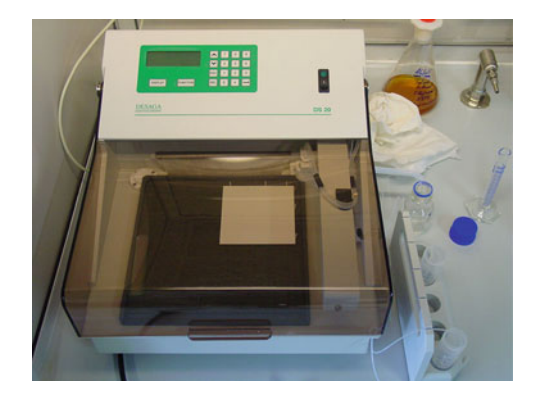
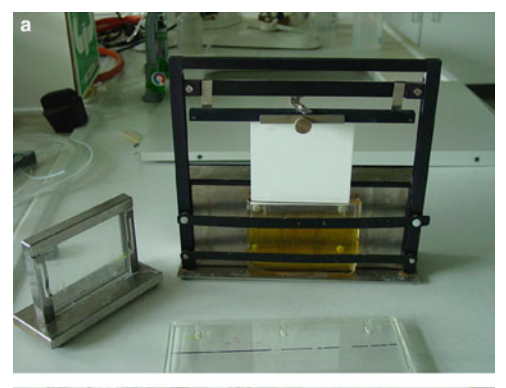
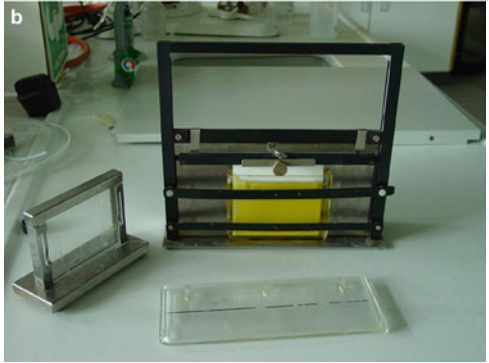


Fig. 7.6 Dipping equipment (from Baron company, Reichenau, Germany). (*Above*) before dipping, (*below*) during dipping





If a computer controlled reagent sprayer is unavailable then plate dipping is the method of choice. This requires a fully automated dipping apparatus. Dipping by hand results in zones of higher reagent concentration perpendicular to the direction of development, which makes quantitative evaluations impossible (Fig. 7.6).

Dipping systems are available from various distributors and are not expensive. The drawback of the method is that a volume of 45–90 mL of reagent solution is

necessary, depending on the size of the plate (10×10 cm or 10×20 cm). After dipping, uniformly heating of the whole plate is often recommended. A drying oven is sufficient, but this oven must be able to control the temperature precisely. More convenient and requiring less space are heating plates, which are also available from different distributors.

Sponge pads are an alternative to dipping or spraying. The sponge pad is pressed onto the plate to transfer the reagent solution to the layer. Sponge pads and a mechanical press for controlling the application pressure are commercially available and suitable for quantitative evaluations [60].

Staining reagent solutions are mostly formulated for spraying [2, 9, 60]. Spraying a 10×10 cm plate results in the transfer of approximately $200~\mu\text{L}$ of solution to the layer. Dipping the same plate may transfer up to 2 mL of solution to the layer. This explains the difference in reagent concentrations required. The concentration of dipping solutions is commonly a factor of 10–20 less than for a spray reagent [1]. All pre-chromatographic reagents presented in this chapter are calculated (if not stated otherwise) for a dipping process.

Post-chromatographic derivatization reagents for TLC are often used in environmental analysis, in forensic science, and in pharmaceutical analysis. For the detection of plant materials, the use of staining reactions is well known and widely used [61]. The classic book of plant analysis by Wagner and Bladt [9] lists over 50 reagents for the identification of more than 250 species of plants. With just five reagents, 70% of all applications using post-chromatographic reactions can be accomplished. The most useful reagents are the vanillin reagent (19%), Dragendorff reagent (16%), the reagent after Neu (15%), the anisaldehyde reagent (11%), and the potassium hydroxide reagent (9%). This observation suggests that no laboratory needs to maintain an inventory of all known reagents when a few well-chosen reagents are sufficient to accomplish most tasks.

7.2.1 Fluorescence Enhancer

Many reagents have been used to enhance fluorescence. The most popular is liquid paraffin dissolved in dichloromethane (3+7, V/V), but other lipophilic compounds are used as well [1]. For some polar analytes dipping in methanolic or aqueous solutions of surfactants is recommended, for example, 2 g of sodium *n*-hexenesulphonate or *n*-octanesulphonate dissolved in 40 mL of water or methanol [62]. Also effective is dipping in a 10% (W/V) solution of polyethylene glycol 600 (PEG 600) or polyethylene glycol 4000 (PEG 4000) in methanol or acetone, or ethylene glycol in methanol (1+1, V/V), or a solution of 20% triethanolamine in 2-propanol, or triton-X-100 in chloroform (1+4, V/V). Enhancement factors of 10–300 have been observed on silica gel layers [1]. The effect on RP-18 plates is observable but enhancement factors less than 2 are more common [62].

Plate dipping enhances fluorescence by blocking the analyte-layer contact. Fluorescent signals are enhanced because radiationless pathways are no longer

available. This is the main enhancement effect, restricted to low concentrations of analyte on silica gel. The enhancement effect on RP-18 plates by dipping is mainly caused by blocking of analyte to analyte contact and minor blocking of analyte-layer contact [62].

In the reverse process, lipophilic analytes without fluorescence, such as fatty acids, cholesterol, and phospholipids, are often visualized by dipping the plate in solutions of fluorescent compounds. Recommended are rhodamine B, rhodamine 6G, nile red (all 0.5-2 mg dissolved in 100 mL of methanol-water 8+2, V/V), pinacryptol yellow, 2,7-dichlorfluoresceine, primuline (direct yellow 7) or acridine orange (0.1-1 mg, dissolved in 100 mL of methanol), berberine (0.2-1 mg dissolved in 100 mL of methanol), and 8-anilino-naphthalen-1-sulphonic acid (ANS reagent: 100 mg, dissolved in 40 mL 0.1 M aqueous sodium hydroxide mixed with 57 mL of citric acid, containing 21 g citric acid and 8 g sodium hydroxide per litre of water) [1]. As a standard reagent berberine is often used, because the yellowgreen fluorescence of this reagent is nearly enhanced by all lipophilic compounds. Here dipping enhances the light emission of the fluorescing zones, because the analytes block the reagent-layer contact. For example the ANS reagent shows nearly no fluorescence in water or on silica gel plates. In the presence of lipophilic analytes in solution or on plate, the contact to the solvent or the layer is reduced causing a brilliant blue-green fluorescence.

7.2.2 pH and Redox Indicators

To stain acids or bases, pH indicator substances are commonly used. These dyes change their colour with changes in pH. Bromocresol green is the standard reagent for the detection of acids or bases. The reagent solution is prepared from 20 mg of bromocresol green dissolved in 10 mL of ethanol with the addition of 1 mL of 0.1 M aqueous sodium hydroxide for the detection of acids or 1 mL of 0.2% (W/V) aqueous citric acid solution for the detection of bases.

Acids change the colour of 2,6-dichlorophenolindophenol (*Tillmans*' reagent, 40 mg dissolved in 100 mL of ethanol) from blue to red. Acridine orange (20 mg dissolved in 100 mL ethanol) changes its fluorescence emission in the pH range pH 8–10 from green-yellow to yellow, 1-naphthol (100 mg dissolved in 100 mL ethanol) from colourless to blue-green (pH 7–9), umbelliferone (10 mg dissolved in 100 mL ethanol) from orange to blue (pH 6.5–8), thioflavine (100 mg dissolved in 100 mL ethanol) from colourless to green, acridine (10 mg dissolved in 100 mL ethanol) from green to blue (pH 4.5–6), and resorufine (10 mg dissolved in 100 mL ethanol) from colourless to orange (pH 4–6).

Strong reducing agents such as ascorbic acid can be detected with 2,6-dichlor-ophenolindophenol or tetrazole blue (each 40 mg dissolved in 100 mL methanol). 2,6-Dichlorophenolindophenol changes colour from blue (oxidized form) to colourless (reduced form, which shows a green fluorescence at 365 nm) [1]. Tetrazole blue

changes colour by reduction from colourless to blue-violet in the presence of ammonia vapour.

Compounds having weak reducing properties, such as aromatic amines, phenols, phenolic steroids, enamine ketones, enol ketones, thiosulphates, isothiosulphates, and thiourea derivatives, can be detected using FeCl₃ and potassium hexacyanoferrate(III) (*Barton's* reagent). During this reaction a blue dye is formed (Turnbull's blue) according to the equation

$$[Fe(CN)_6]^{3-} + Fe^{2+} \rightarrow [Fe^{3+}Fe^{2+}(CN)_6]^+$$

The reagent solution is prepared from 18 mL of recrystallized potassium hexacyanoferrate(III) solution (80 mg $K_3[Fe(CN)_6]$ dissolved in 18 mL water) and 2 mL FeCl₃ solution (40 mg dissolved in 2 mL water). To this 1 mL of concentrated hydrochloric acid (36%) is added and the volume brought to 100 mL with methanol. Reducing compounds form iron(II) ions, which form the dye in conjunction with iron(III) ions. The reagent is stable for 2 weeks and can be used with all types of layers [1].

The vanadate (V)–sulphuric acid reagent (*Mandelin's* reagent) oxidizes sugars, glycol, carboxylic acids, steroids, vitamins, aromatic amines, and phenols. During the reaction the yellow vanadate(V) ion (VO $_2$ ⁺) is reduced forming the blue vanadate(IV) ion (VO $_2$ ⁺). The reagent solution is prepared from 600 mg of ammonium vanadate (NH $_4$ ⁺) $_3$ VO $_4$ dissolved in 47.5 mL water to which 2.5 mL of concentrated sulphuric acid is carefully added [1]. The dried plate is dipped for 2 s in the reagent solution and heated to 100–120°C for 5 min, resulting in blue zones on a light yellow background for reducing compounds. Silica gel and cellulose plates can be used.

Hydrogen peroxide (H_2O_2) reacts with many aromatic carboxylic acids and thiabendazole forming blue fluorescing zones when illuminated with UV light at 365 nm. Hydrogen peroxide is a strong oxidizing reagent. It is assumed that the aromatic acids are oxidized at first, but the details of the full reaction mechanism are not known. The reagent solution contains 1–3 mL 30% H_2O_2 made up to 100 mL with water. The reaction with thiabendazole requires addition of 10 mL acetic acid. The plate is dipped for 2 s in the reagent solution and must be illuminated for some minutes at 365 nm.

7.2.3 Universal Reagents (Charring Reagents)

All charring reagents, in one form or another, assist in the conversion of carbon-containing compounds into brown-black zones when heated to 80–120°C without destroying the stationary phase. The method is applicable to compounds on inorganic oxide layers but not chemically bonded, polymeric, or cellulose layers. Cellulose, RP-phases, and all stationary phases containing an organic binder turn dark when treated as described above. The most common charring reagent is sulphuric acid containing manganese or copper salts as catalysts.

The manganese reagent is prepared from 100 mg $MnCl_2$ ·2 H_2O dissolved in 30 mL of water and 30 mL methanol. After mixing, 2 mL of concentrated H_2SO_4 is carefully added with cooling. The copper reagent is prepared from 3 g Cu-II acetate (dissolved in 100 mL 8% aqueous H_3PO_4) and 100 mL of acetic anhydride and concentrated H_2SO_4 (9+1, V/V).

Molybdatophosphoric acid $(H_3Mo_{12}O_{40}P)$ oxidizes nearly all organic analytes forming a blue-grey dye. The reagent is prepared from 250 mg of molybdatophosphoric acid dissolved in 50 mL of methanol. The dipped plate is heated to $120^{\circ}C$ until blue-grey zones are visible.

7.2.4 Aldehyde Reagents

Aldehydes can react with -NH₂ and -CH₂-groups under acid conditions with elimination of water forming C=C or N=C bonds (schiff base or azomethine according to Schiff). Schiff bases very often show strong fluorescence.

The reactivity of these reagents is determined by the reactivity of the aldehyde group and by the acid used. Formaldehyde and furfural are by far the most reactive aldehydes followed by aromatic aldehydes. Less reactive are aliphatic aldehydes such as glucose and thymol. Reagent solutions prepared with sulphuric acid are more reactive than those prepared with phosphoric or hydrochloric acid. When using concentrated sulphuric acid in the preparation of reagent solutions the acid should be added with cooling. The combination of methanol and sulphuric acid might form methyl sulphate, which is a known carcinogen. Therefore, none of these reagents should be used for hand spraying. All aldehyde reagents have limited stability and are no longer usable when the colour has turned to red-violet.

The most reactive aldehyde reagent is the mixture of formaldehyde in sulphuric acid (Marquis' reagent). The reagent solution is prepared from 0.2 mL formaldehyde solution in water (37%), 9 mL of methanol, and 1 mL of concentrated H_2SO_4 . The plate is dipped for 2 s in the reagent solution and kept at $120^{\circ}C$ for 20 min. Aromatic hydrocarbons, alkaloids, morphine, codeine, thebaine, amphetamines, and tannins react under these conditions.

The most important aldehyde reagent is without doubt the vanillin reagent. 3-Hydroxy-4-methoxybenzaldehyde (vanillin) is used in conjunction with different acids (H₂SO₄, HCl, H₃PO₄). The vanillin–sulphuric acid reagent is prepared from 100 mg vanillin, 1 mL of concentrated sulphuric acid, and 9 mL ethanol or diethyl ether. For the vanillin–hydrochloric acid reagent, 100 mg vanillin in 9 mL ethanol is sprayed first on the layer which is subsequently sprayed with concentrated hydrochloric acid. The vanillin–phosphoric acid reagent is prepared from 100 mg vanillin in 4 mL ethanol and 5 mL concentrated H₃PO₄. The reagent containing HCl reacts with phenols, catechins, and alkaloids. The mixture containing sulphuric acid can be used to detect steroids, essential oils, terpenes, carotenoids, phenols, catechins, flavonoids, ginsenosides, fatty acids, and antibiotics.



Fig. 7.7 Separation of ethyl acetate extracted Iceland moss (CETRARIA ISLANDICA) on HPTLC Si 60 F₂₅₄ with acetone, methanol, formic acid, toluene (5+5+10+80, v/v), chamber saturation, stained with anisaldehyde reagent

Tracks: 1-6 show Iceland moss extract, 7 caffeic acid, 8 anethole, 9 usnic acid, 10, 11 Iceland moss extract, 12 oak moss, 13 usnea moss, 14 usnea tincture, (with permission by CAMAG, Muttenz, Switzerland)

The anisaldehyde reagent is widely used in photochemical analysis (Fig. 7.7). The reagent solution is prepared from 50 μ L of 4-methoxybenzaldehyde (anisaldehyde) and 1.0 mL acetic acid diluted with 10 mL methanol or diethyl ether. To this mixture 0.5 mL concentrated H₂SO₄ (Ekkerts' reagent) is carefully added. The analytes form coloured zones after heating to 100–110°C for 10 min. Antioxidants, steroids, prostaglandins, sugars, phenols, glycosides, sapogenins, essential oils, antibiotics, and mycotoxins are detected as red or blue zones. Several reagents using 4-dimethylaminobenzaldehyde are known. After dipping, the plate must be stored at 120°C for 20 min.

The reagent solution is prepared from 50 mg 4-dimethylaminobenzal dehyde in 10 mL of acetic acid and 0.5 mL concentrated $\rm H_3PO_4$ and is known as EP reagent. Terpenes and sequite rpenes are stained. Ehrlich's reagent is prepared from 100 mg 4-dimethylaminobenzal dehyde dissolved in 10 mL methanol, and 0.5 mL HCl (35%) is added. This reagent reacts with sulphonamides, mycotoxins, pesticides, alkaloids, and pyridine-containing compounds.

The mixture of 100 mg 4-dimethylaminobenzaldehyde in 9.5 mL water and 0.5 mL concentrated H₂SO₄ is known as *van Urk's* reagent. Stained are primary amines, alkaloids, indole alkaloids, and carbamate pesticides.

2-Methoxybenzaldehyde or pyridoxal (200 mg each dissolved in 35 mL methanol + 5 mL H₃PO₄) is a useful general reagent. In general, it is necessary to keep the plate at 120°C for some minutes.

Structures of vanillin (1), anisaldehyde (2), 4-dimethylaminobenzaldehyde (3), cinnamaldehyde (4), and furfural (5)

Very interesting are reactions using cinnamaldehyde because this compound can react with less reactive NH_2 groups. For the preparation of cinnamaldehyde reagent, $80~\mu L$ of cinnamaldehyde is dissolved in 40~mL acetone. Then 2.4~mL of $85\%~H_3PO_4$ is added. The plate is dipped for 2~s in the reagent solution and heated to $130^{\circ}C$ for 10~min. Methyl carbamate, ethyl carbamate, and acrylamide can be separated on silica gel with methyl *tert*-butyl ether–cyclohexane (7+3,~V/V) as mobile phase. All compounds react with cinnamaldehyde forming fluorescent zones [63]. The detection limit is in the lower nanogram range. The reagent is stable for 2 days and cannot be used with amino plates.

Glucose in combination with sulphuric acid reacts with less reactive amides and can be used to stain carbamate esters. For the preparation of glucose reagent, 300 mg glucose is dissolved in 40 mL water and 1 mL concentrated $\rm H_2SO_4$. The reagent is stable for about a week. The plate is dipped for 2 s in the reagent solution and heated to 80–120°C for 10 min. Carbamate esters react to form brown zones, which show fluorescence when illuminated with light of 366 nm. Glucose in combination with phosphoric acid (2 g glucose dissolved in 40 mL water and 10 mL 85% $\rm H_3PO_4$ and topped up with methanol to 80 mL) stains aromatic amines even at 45°C.

Furfural is a very reactive substance and can even react with carbamate ester. The dried plate must first be dipped into a 1% solution of furfural in acetone and then in a 10% sulphuric acid solution in acetone, and slightly heated if necessary. Both solutions can be mixed (1+1, V/V) but this furfural reagent is stable for only 1 day. This reagent can also be used to detect sugars or acids.

The aniline–phthalic acid reagent is used to detect mono- and oligosaccharides as coloured and mostly fluorescing zones with a white background [1]. The reagent solution is prepared from 0.9 mL aniline and 1.66 g phthalic acid dissolved in 100 mL acetone. The dried plate is dipped for 1 s in the reagent solution and then heated at $80{\text -}130^{\circ}\text{C}$ for $20{\text -}30$ min.

Structure of orcinole (1), 1,3-naphthalenediol (2), and 1-naphthol (3)

With the orcinole reagent (250 mg 1,3-dihydroxy-5-methylbenzene and 100 mg FeCl $_3$ dissolved in 95 mL ethanol and 5 mL concentrated H $_2$ SO $_4$) nearly all sugar aldehydes react within 15 min at 100°C forming blue-violet zones. 1,3-Naphthalenediol reacts in a similar way with sugars forming coloured zones. The reagent solution is prepared from 200 mg of 1,3-naphthalenediol dissolved in 90 mL ethanol and 10 mL 85% phosphoric acid. The plate is dipped for 2 s in the reagent solution and then heated at 100–105°C for 5–10 min. The 1-naphthol reagent (150

mg 1-naphthol in 10 mL ethanol, mixed with 1.6 mL concentrated sulphuric acid, and topped up with 40 mL ethanol and 0.4 mL water) reacts in a similar manner.

The aniline-aldose reagent uses the same reaction principle for the detection of organic acids. The reagent solution is prepared from 2 mL freshly distilled aniline dissolved in 18 mL ethanol. In a second solution, 2 g glucose is dissolved in 20 mL of water. Both solutions are mixed (20 mL each) and made up to 100 mL with 1-butanol directly before use [1]. In the presence of organic acids coloured zones are formed after heating at 90–140°C for 10 min. The reagent is not particularly sensitive but acids in the upper nanogram range can be detected.

Reagents containing a ketone group are rare. Anthrone (9,10-dihydro-9-oxoan-thracene) reacts with keto-sugars forming yellow zones. The reagent solution is prepared from 300 mg anthrone dissolved in 10 mL acetic acid and 20 mL ethanol to which 3 mL 85% phosphoric acid and 1 mL water are added. The anthrone reagent is stable for several weeks at 4°C.

7.2.5 CH- and NH-Reacting Reagents

Aldehyde reagents can react with CH-active and NH-active groups, and it is possible to use reagents containing these groups for the detection of aldehydes and ketones.

The dimedone-phosphoric acid reagent reacts with keto-sugars. The reagent solution is prepared from 300 mg dimedone (5,5-dimethylcyclohexane-1,3-dione) dissolved in 90 mL ethanol and 10 mL 85% phosphoric acid. After dipping in the reagent solution the plate is heated to 110°C for 15–20 min. Ketoses appear as yellow spots on a white background. The spots show a blue fluorescence when illuminated with UV light at 366 nm [59]. The dimedone reagent reacts readily with formaldehyde.

The indanedione reagent is prepared from 0.5 mg 1,3-dioxoindane dissolved in 20 mL water and 0.3 mL 36% hydrochloric acid. Carotenoid aldehydes react at room temperature [59].

4-Aminohippuric acid, 2-aminophenol, 4-anisidine and *o*-phenylenediamine all have an –NH₂-group, which can react with carbonyl compounds forming Schiff bases.

Structures of 4-aminohippuric acid (1), o-aminophenol (2), 4-anisidine (3), and o-phenylenediamine (4)

A 0.3% (W/V) solution of 4-aminohippuric acid in ethanol (4-aminohippuric acid reagent) can be used without addition of acid. Sugar aldehydes form characteristic fluorescent products after heating at 140° C for 10 min. The o-aminophenol reagent (300 mg o-aminophenol dissolved in 95 mL ethanol and 5 mL 85% phosphoric acid) reacts in a similar manner with reducing sugars producing brown zones [59]. The 4-anisidine reagent is prepared from 100 mg 4-anisidine and 100 mg phthalic acid dissolved in 50 mL ethanol. After dipping in the reagent solution the plate is heated to 100° C for 10 min. Keto-acids react in the same manner with o-phenylenediamine reagent (1 g o-phenylenediamine·HCl dissolved in 8 mL water added to 50 mL ethanol and 1.5 mL concentrated H_2SO_4). All aromatic amines should be handled with care because they are suspected to cause cancer.

Phenylhydrazine, isonicotinic acid hydrazide, and 2,4-dinitrophenylhydrazine react with carbonyl groups forming coloured or fluorescent derivatives. The phenylhydrazine and 2,4-dinitrophenylhydrazine reagent solutions are prepared by dissolving 50 mg of the hydrazine in 15 mL ethanol and adding 15 mL H₃PO₄ (85%). The dried plate is dipped for 2 s in the reagent solution and then heated to 110°C for 10–20 min. Aldehydes and ketones form yellow of orange-yellow zones on a white background with the 2,4-dinitrophenylhydrazine reagent. The phenylhydrazine reagent forms colourless but strongly fluorescent zones when illuminated with UV light at 365 nm. The reagent solutions are stable for several days. The isonicotinic acid hydrazide reagent solution is prepared from 100 mg pyridine-4-carbonic acid hydrazide dissolved in 9 mL ethanol and 1 mL acetic acid. The dried plate is dipped for 10 s in the reagent solution. Keto-steroids, such as testosterone, form coloured hydrazones, which show fluorescence when excited at 365 nm. The reagent can be used with silica gel and cellulose layers and is stable for days when stored at 4°C.

Urea–HCl reagent reacts with the carbonyl group of ketoses forming blue derivatives. The reagent solution is prepared from 2.5 g urea dissolved in 10 mL of 2 M HCl and made up to 50 mL by adding ethanol. The plate is dipped for 2 s in the reagent solution and heated to $100-120^{\circ}$ C for 10 min [1].

7.2.5.1 4-Aminoantipyrine Reagent (Emerson reagent)

A 2% solution of 4-aminoantipyrine (4-amino-2,3-dimethyl-1-phenyl-3-pyrazoline–5-one) in ethanol is sprayed over the layer followed by 8% aqueous potassium hexacyanoferrate(III) solution. The plate is placed in chamber saturated with ammonia vapour. Phenols give red spots on a light yellow background (Reaction 7.3).

7.2.5.2 MBTH Reagent (Besthorn Reagent)

3-Methyl-2-benzothiazolin-3-one hydrazone hydrochloride salt (MBTH·HCl) is a sensitive reagent for aldehydes and ketones. The reagent solution is prepared from

Reaction 7.3 Reaction of 4-aminoantipyrine with phenol

$$H_3C$$
 NH_2
 H_3C
 NH_2
 NH_2

Reaction 7.4 Reaction of MBTH with aldehydes and oxidation to the blue MBTH cation

0.5-1.0~g MBTH·HCl dissolved in 100~mL methanol or a mixture of methanol and water (1+1,~V/V). This solution may need to be filtered before use. The dipping solution is stable for a few days. The dried plates are dipped for 1~s in the reagent solution and heated at $110-120^{\circ}C$ for up to 2~h. MBTH reacts with carbonyl compounds forming blue-violet zones on a light yellow background. The zones fluoresce yellow or orange when illuminated at 365~nm (Reaction 7.4).

The dipped plates turn blue within days due to reaction with oxygen. The reagent can be used on silica gel, cellulose, and amide plates [1]. MBTH reacts with phenols when oxidized by cerium(IV) sulphate forming red zones on a blue background. These conditions are not favourable for quantification by scanning densitometry.

7.2.5.3 2,6-Dibromochinone-4-chlorimide (Gibbs' Reagent)

Gibbs'reagent is used for staining aromatic compounds (phenols, amines, aromatic hydrocarbons, indoles, and compounds like barbiturates and phenoxyacetic acid herbicides), which have no substituent in the *para* position (see Reaction 7.5).

Reaction 7.6 Reaction of 1,2-naphthoquinone-4-sulphonate with aniline

The reagent solution is prepared from 100 mg of 2,6,-dibromochinone-4-chlorimide dissolved in 10 mL of dimethyl sulphoxide, saturated with sodium bicarbonate and made up to 100 mL with dichloromethane or ethanol. The plate is dipped for 5 s in the reagent solution and then heated at 110°C for some minutes. The reagent must be freshly prepared for each application. 2,6-Dibromochinone-4-chlorimide (the two bromine atoms in Gibbs' reagent are replaced by chlorines) is less reactive than Gibbs' reagent and reacts mainly with aromatic amines and phenols, which are not substituted in the *para* position. Well known is the reaction with capsaicin forming a blue dye [64]. The reaction product with phenol is the blue dye 2,6-dichlorophenolindophenol (*Tillmans*' reagent). The reagent is produced and used in the same way as described for Gibbs' reagent [1].

7.2.5.4 1,2-Naphthoquinone-4-sulphonic Acid Reagent (Folins' Reagent)

Folin's reagent reacts with amino acids, peptides, aromatic and aliphatic amines, piperidine derivatives, alkaloids, and phenolic aromatic sulphides, sulphones, and sulphoxides. The reagent solution is prepared from 500 mg 1,2-naphthoquinone-4-sulphonate dissolved in 30 mL water, 65 mL ethanol, and 5 mL acetic acid. For reaction with amino acids and aliphatic amines, dissolve 200 mg 1,2-naphthoquinone-4-sulphonate in 100 mL of 5–10% (W/V) aqueous sodium bicarbonate solution [1]. This solution must be freshly prepared while the acetic acid reagent is stable for a week (Reaction 7.6).

Primary amines and substances with reactive methylene groups form intensely coloured derivatives with a quinoid structure. Proline and hydroxyproline react as well. The detection limits are in the lower nanogram range. This reagent is not suitable for use with amino phases.

7.2.5.5 7-Chloro-4-nitrobenzo-2-oxa-1,3-diazol Reagent (NBD-Chloride Reagent)

NBD-chloride (NBD-Cl) reacts with phenols, thiols, primary and secondary amines, amino acids, peptides, sulphonamides, and alkaloids [1]. During the reaction, hydrogen chloride is formed. The reagent itself shows no fluorescence and can be used in dipping solutions.

Structure of 7-chloro-4-nitrobenzo-2-oxa-1,3-diazolreagent (NBD-chloride)

The reagent solution is prepared from 40–80 mg NBD-Cl dissolved in 40 mL ethanol, methanol, or acetonitrile. The formation of hydrogen chloride makes alkaline conditions necessary. After separation, the dried plate is dipped in sodium acetate solution (10 g sodium acetate dissolved in 20 mL water and diluted with 40 mL methanol). The plate is dried and dipped for 1 s in the NBD-Cl solution. Coloured zones result, which show a yellow-green fluorescence when illuminated with UV light (365 nm). The reagent can be used with silica gel and RP-18 phases but should not be used with amino phases [1].

7.2.6 Boron-Containing Reagents

7.2.6.1 Natural Product Reagent (Neu Reagent)

Diphenylboric acid- β -ethylamino ester (which is named Neu reagent after Neu) reacts with nearly all flavonoids forming coloured zones. The plate is dipped for 1 s in a 1% (W/V) solution of diphenylboric acid- β -ethylamino ester in methanol (100 mg dissolved in 20 mL methanol or ethyl acetate) and then in a 5% (W/V) solution of polyethylene glycol 4000 (PEG-4000) dissolved in ethanol. Diphenylboric acid anhydride can be used instead of diphenylboric acid- β -ethylamino ester.

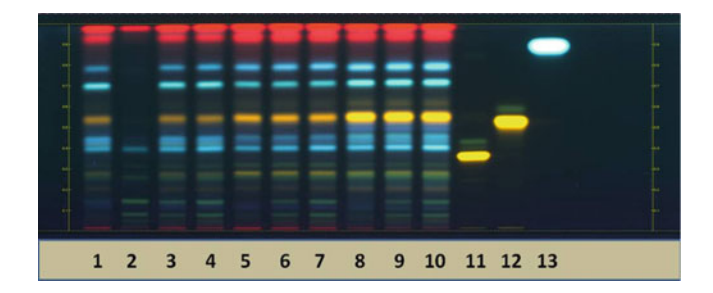


Fig. 7.8 Common horsetail herb ($E_{QUISETUM\ ARVENSE}$) extracted with methanol on HPTLC Si 60 F_{2.54} with ethyl acetate, water, acetic acid, formic acid (134+36+15+15 v/v), chamber saturation, stained with NEU-reagent and illuminated with UV-light at 366 nm [9]

Tracks: 1, 5, 8 Common horsetail herb, 2 Marsh horsetail herb (*Equisetum Palustre*), 3, 4, 6, 7, 9, 10, combinations, 11 rutin, 12 hyperoside, 13 caffeic acid, (with permission by CAMAG, Muttenz, Switzerland)

Brilliant colours appear when the plate is illuminated with UV light (256 nm and 356 nm), see Fig. 7.8. The reagent is stable for days when stored at 4°C.

Structure of diphenylboric acid-β-ethylamino ester (Neu-Reagent).

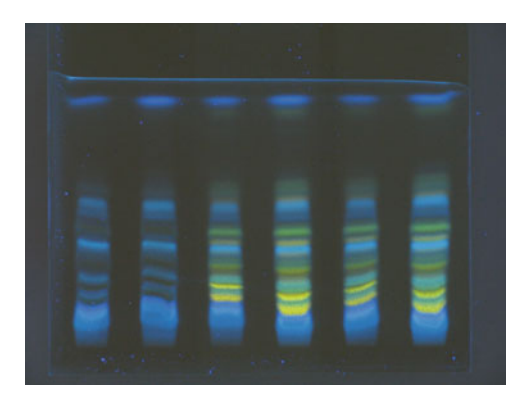
7.2.6.2 Diphenylboric Acid Anhydride-Salicylic Aldehyde Reagent (DOOB Reagent)

The DOOB reagent reacts with primary amines, amino acids, antibiotics, hydrazines, and substituted anilines forming blue fluorescent zones when illuminated with UV light at 365 nm. The reagent provides lower detection limits for amino acid than fluorescamine [1]. The reagent solution is prepared from 35 mg diphenylboric acid anhydride and 25 mg salicylic aldehyde dissolved in 100 mL dichloromethane. The compound 2,2-diphenyl-1-oxa-3-oxonia-2-borata-naphthalene (DOOB) is formed. The dried plate is dipped for 2 s in the reagent solution and heated at 110°C for 10–20 min (Reaction 7.7).

The reaction is very sensitive and the coloured zones are stable for weeks when stored in the dark. The reagent can be used for silica gel, RP-18, and aluminium oxide plates. Amino and polyamide plates are not suitable. The reagent mixture is stable for several hours when stored at 4° C [65].

Reaction 7.7 Formation of 2,2-diphenyl-1-oxa-3-oxonia-2-borata-naphthalene (DOOB) from diphenylboric acid and salicylic aldehydes

Fig. 7.9 Separation of a primulae flos extract on silica gel using ethyl acetate–acetic acid–formic acid–water (100+11+11+26, V/V) as mobile phase. Tracks 1 and 2 are stained with tetraphenylborate reagent, tracks 3 and 4 with Neu reagent and tracks 5 and 6 with 1% diphenylboric acid anhydride in methanol



7.2.6.3 Tetraphenylborate Reagent

Tetraphenylborate reacts specifically with quaternary ammonium compounds such as paraquat and diquat. The plate was immersed for 2 s in the reagent solution consisting of 50 mg sodium tetraphenylborate (Na[B(C₆H₅)₄] dissolved in 50 mL of water containing 50 μ L 10 M hydrochloric acid. The staining solution is stable for 8 h at ambient temperature. The wet plate is illuminated for 5 min by intense light of 254 nm and then 10 min at 365 nm. This reagent can be used to transform paraquat, diquat, mepiquat, chloromequat, difenzoquat, codeine, pilocarpine, and papaverine into blue fluorescing zones. Dipping for 2 s in a solution of ethylene glycol and methanol (1+1, V/V) enhances the fluorescence by a factor of 2. The fluorescence remains stable for a month when the plate is stored in the dark (Fig. 7.9) [66, 67].

7.2.7 Alkaline Reagents

Strong alkaline reagents such as potassium and sodium hydroxide react with cumarin glycosides, anthraquinones glycosides (Bornträger reaction), thiophosphoric acid pesticides, nitrophenyl esters, acethylcholine, sennosides, steroids, and dinitrophenylhydrazone forming coloured zones that fluoresce strongly when

illuminated at 365 nm. The reagent solution is prepared from 1 g KOH (or NaOH) dissolved in 3–10 mL of water made up to 25 mL with ethanol. The dried plate is dipped for 2 s in the reagent solution and heated to 100–200°C for 5–30 min. Often it is necessary to cover the layer with a glass plate to keep the water in the stationary phase. The reagents can be used with silica gel, cellulose, and polyamide layers.

7.2.8 Chloramine-T Reagent

Chloramine-T contains 25% active chlorine and is used for chlorination and oxidation reactions. A reaction takes place under either acid or alkaline conditions. The dried plate is dipped first in the chloramine-T reagent solution and subsequently in acid (or alkaline) solution.

Structure of chloramine-T

For chloramine-T acid reagent solution, 2.5 g chloramine-T is dissolved in 20 mL water and diluted with methanol to 50 mL. After dipping the plate in the chloramine-T reagent solution, it is dipped in a solution of 2.5 mL concentrated H₂SO₄ or HCl carefully mixed with 47.5 mL ethanol. In some cases it is sufficient to store the wet plate for 10 min in HCl vapour. Purines (e.g. caffeine, theophylline, or the obromine) form red-violet zones. The plate is dipped for 2 s in the chloramine-T reagent solution, stored for 10 min in HCl vapour, and then heated at 110°C for some minutes to remove excess chlorine. The plate is then stored in ammonia vapour for 10 min and heated to 110°C [1]. Purines react forming red zones with blue or yellow fluorescence when illuminated with UV light at 365 nm. Steroids and sterins, such as cholesterol, estrogens, and testosterone, react forming yellowbrown zones with yellow fluorescence (UV light at 365 nm). Digitalis glycosides react with chloramine-T trichloroacetic acid reagent (Jensen's reagent) forming yellow or blue fluorescent zones. The reagent solution is prepared from 5 g trichloroacetic acid and 0.2 g chloramine-T dissolved in 1 mL water and then mixed with 9 mL methanol. This solution is made up to 50 mL with dichloromethane. The dried plate is dipped for 2 s in the reagent solution and then heated to 100–150°C for 5–30 min [1].

Phenols and flavonoids react with chloramine-T NaOH reagent forming yellow or purple derivatives, which fluoresce when illuminated with UV light at 365 nm. The reagent solution is prepared from 2.5 g chloramine-T dissolved in 25 mL water to which 250 mg of solid sodium hydroxide is added and then diluted with 25 mL methanol. The dried plate is dipped for 2 s in the reagent solution, kept for 5 min at

ambient temperature, and then heated to 120°C for 5 min [1]. Chloramine-T reagents can be used for all plate types. The Jensen's reagent is stable for a week at 4°C. Other chloramine-T reagents are stable at 4°C for days.

7.2.9 Diazotization Reactions

Primary aromatic amines form diazo cations with nitrite ions. The diazo cation reacts with phenols forming intensely coloured dyes. This reaction can be used for the analysis of aniline derivatives and phenols.

Diazotization reactions can be used in different ways. Diazo cations can be formed by the reaction of NH_2 -groups with NO^+ produced from NO_2^- . The diazo cation subsequently reacts with a phenolic group. This is the reaction pathway of the Bratton–Marshall reagent and Paulys' reagent.

A second more convenient method is to dip the dried plate in a solution of a stable diazonium compound. This avoids complicated reaction pathways. Commonly fast black salt K, 4-nitrobenzodiazonium tetrafluoroborate, or fast blue salt B is used. By far the most important reagent is the fast blue salt B.

The fast blue salt B reagent solution is prepared from 75 mg fast blue salt B dissolved in 5 mL water and 15 mL methanol. This solution is diluted by stirring with a mixture of 55 mL methanol and 25 mL dichloromethane. The reagent preparation should be done carefully because all diazonium compounds are reactive and suspect carcinogens. Diazonium reagents should not be used for hand spraying.

$$\begin{array}{c} H_3C - O \\ N = N^{\downarrow} \\ CI^{-} \\ \end{array} \qquad \begin{array}{c} CI^{-} \\ O - CH_3 \\ \end{array}$$

Structure of fast blue salt B

The dried plate is placed for 10 min in an ammonia atmosphere and then instantly dipped for 5 s in the fast blue B salt reagent solution. Sometimes better results are achieved when fast blue salt B is dissolved in 0.1% (W/V) methanolic sodium or potassium hydroxide. Phenols, amines, tanning agents, cumarins, cannabinols, and flavonols form coloured zones on a colourless background. The solution is stable for one day and can be used with silica gel, alumina, cellulose, polyamide, and reversed-phase layers.

The Pauly reagent contains sulphanilamide and sodium nitrite. The reagent solution is prepared from 500 mg sulphanilamide dissolved in 50 mL water to which 1 mL concentrated HCl and 3 mL 1-butanol are added. Immediately before use 500 mg sodium nitrite is added. The dry plate is dipped into the reagent solution for 2 s and after 5–10 min the plate is dipped in 10% (W/V) aqueous sodium carbonate solution. Phenols, aromatic amines, and heterocyclic compounds react to form coloured zones.

The Bratton–Marshall reagent is mostly used for the determination of benzodiazepines. The dried plate is placed in a double through chamber together with 5 mL of a 20% (W/V) aqueous sodium nitrite solution. To the sodium nitrite solution 10 drops of concentrated hydrochloric acid is added. In the closed chamber, NO and NO_2 are produced, which react with amino groups forming diazo cations. After 10 min, the plate is placed in a fume hood for 1 min to remove all NO_2 . The plate is then dipped for 1 s in a solution of 0.5 g N-(1-naphthyl)ethylenediamine dihydrochloride dissolved in 5 mL water and diluted to 50 mL with ethanol [1]. At room temperature, coloured zones appear on a colourless background. Some benzodiazepines without a free amino group can be hydrolysed first by exposing the plate to HCl fumes at 110° C for 30 min [1, 68, 69].

7.2.10 Iodine-Starch and Wursters Reagents

To determine nitrogen-containing compounds, such as aromatic amines, nitroaromatic compounds, triazines, melamine, acrylamide, nucleotides, urethane, and amino acids, as well as aniline, carbamate, and urea pesticides, the plate is placed in a chlorine atmosphere for some minutes. Chlorine reacts with nitrogen groups to form chlorine derivatives. Chlorine can be prepared by mixing 10 mL KMnO₄ solution (300 mg dissolved in 10 mL water) and 10 mL 36% hydrochloric acid in a double-trough chamber [1]. The plate is placed for 5 min in the chlorine atmosphere. Excess chlorine is removed by placing the plate for 1 min in a fume hood. The plate is then dipped for 2 s in Wursters blue reagent. Chlorine reacts with nitrogen groups to form chlorine derivatives, which oxidizes the Wursters blue reagent forming a quinoid structure. These compounds are detectable at 608 nm. The detection limit for pesticides is between 5 and 100 ng per zone. Wursters blue reagent is more stable than Wursters red reagent or the *o*-toluidine reagent. Nevertheless, all dipped plates should be scanned immediately because the blue colour fades within 1 h.

7.2.10.1 Wursters Red Reagent

N,*N*-dimethyl-1,4-phenylenediammonium dichloride (DPDD reagent) is oxidized by peroxides to Wursters red, a quinoid-imine compound (Reaction 7.8).

Reaction 7.8 Formation of Wursters red

A similar reagent is produced from o-toluidine and potassium iodide. In this case, 50 mg o-toluidine dissolved in 1 mL acetic acid and 200 mg potassium iodide dissolved in 1 mL water are mixed and made up to 50 mL with water. This reagent reacts like Wursters blue reagent and is stable at 4°C for 2 weeks.

7.2.10.2 Wursters Blue Reagent

N,N,N',N'-Tetramethyl-1,4-phenylenediammonium dichloride reacts when oxidized like *Wursters* red reagent forming a quinone compound. The reagent solution is prepared from 100 mg N,N,N',N'-tetramethyl-1,4-phenylenediammonium dichloride (TPDD) dissolved in 4 mL water and 5 mL methanol to which 1 mL acetic acid is added. Sometimes it is sufficient to dissolve 500 mg TPDD in acetone. The dried plate is dipped for 2 s in the reagent solution. The reagent is suitable for silica gel and aluminium oxide layers.

$$\begin{array}{c} H_3C \\ H - N^{\dagger} \\ H_3C \\ CI^- \end{array} \begin{array}{c} CI^- \\ CH_3 \\ CH_3 \end{array}$$

Structure of Wursters blue

The two Wurster reagents show different reaction behaviour. There are many more reactions described using Wursters blue reagent [1].

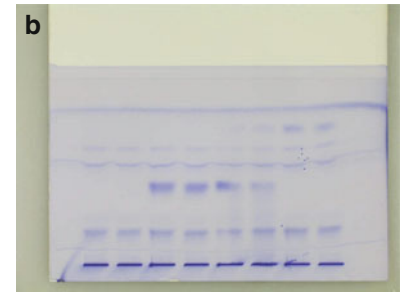
7.2.10.3 Iodine-Starch Reagent

The iodine-starch reagent reacts similar to Wursters blue reagent and produces comparable detection limits. The stained plates are stable and do not change colours like *Wursters* blue stained plates. The reagent solution is prepared from 250 mg potassium iodide dissolved in 25 mL water and 750 mg starch (according to Zulkowsky), dissolved in 25 mL water and diluted with 30 mL ethanol. The reagent is stable for 1 day and can be used with all plate types as a spray reagent. For the dipping solution, a mixture of 600 mg potassium iodide dissolved in 15 mL water and 600 mg starch dissolved in 15 mL water are added and the mixture is diluted with 18 mL ethanol. After chlorine treatment the plate is dipped for 1 s in the iodine-starch reagent solution. The blue-violet colour appears instantly due to the release of iodine, which reacts with starch forming a deeply coloured insertion product. Zones can be detected between 400 and 500 nm (Fig. 7.10).

Fig. 7.10 Separation of milk (tracks 1 and 2) and milk to which 80 ng melamine (1,3,5triazine-2.4.6-triamine) was added (tracks 3 and 4). On tracks 5 and 6 milk was spiked with 80 ng melamine and cyanuric acid (2,4,6trihydroxy-1,3,5 triazine, 200 ng) and on tracks 7 and 8 milk was spiked only with cyanuric acid. The plates were stained with iodine-starch reagent and Wursters blue reagent. The mobile phase was 2propanol-dichloromethanewater (3+1+1, V/V) [70]



Iodine-starch reagent



Wursters blue reagent

7.2.11 Reactions with Metal Reagents

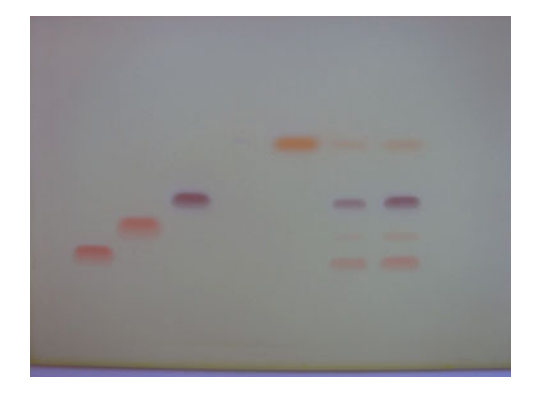
7.2.11.1 Phosphate Detection Using Ammonium Molybdate

Ammonium molybdate $(NH_4)_6[Mo_6O_{21}]$ reacts specifically with phosphate ions forming a blue dye. The reagent solution is prepared from 100 mg ammonium molybdate and 100 mg ascorbic acid dissolved in 12 mL water (by use of an ultrasonic bath) and diluted with 12 mL methanol. The reagent is suitable for use with cellulose layers and is stable for a day. The dried plate is dipped for 2 s in the reagent solution and heated to 55°C for 10 min. Zones containing phosphates appear blue on a colourless background.

7.2.11.2 Dragendorff Reagent

Dragendorff reagent (according to Munier and Macheboeuf) stains all nitrogencontaining compounds forming red or red-blue zones on a light yellow background. Alkaloids appear as red-orange zones. Atropine, nicotine, narceine, and phenothiazine produce violet zones (Fig. 7.11).

Fig. 7.11 Separation of paraquat, diquat, mepiquat, chloromequat, and difenzoquat on silica gel (from *bottom to top*) with the solvent 1-propanol–methanol–2N aqueous sodium chloride solution (4+4+12, V/V). The plate was stained with Dragendorff reagent [65]



Solution A: 100 mg Bi(NO₃)₂·5 H₂O dissolved in 1 mL acetic acid diluted with 4 mL water.

Solution B: 300 mg potassium iodide dissolved in 2 mL water.

The reagent solution is prepared by mixing $500 \,\mu\text{L}$ of solution A and $500 \,\mu\text{L}$ of solution B with 2 mL acetic acid diluted to $10 \,\text{mL}$ with water. The plate is dipped for 5 s in the reagent solution and then heated to 80°C if necessary. Polyethylene glycol and other polyethers are stained red-orange when $200 \,\text{mg}$ BaCl₂ is added to $10 \,\text{mL}$ of the reagent solution [2]. Heating is unnecessary for staining glycols. Both solutions (A and B) are stable in the dark for 1 month. The final reagent is stable for weeks at ambient temperature. All plate types can be used.

7.2.11.3 Antimony(III) Chloride Reagent (Carr-Price Reagent)

The Carr-Price reagent stains analytes containing double bonds. The active agent is the antimony(V) cation, which is present in antimony(II) solutions. The assumption is that SbCl₅ reacts with alcohol groups forming [SbCl₃OH]⁻ and a coloured analyte cation. The cation is stabilized by the double bonds. Compounds reacting include vitamin A, corticoids, terpenes, sterins, steroids, gallic acid, sapogenins, glycosides, flavonoids, and phospholipids. The zones often show fluorescence when illuminated with UV light at 356 nm. The reagent solution is prepared from 500 mg SbCl₃ dissolved in 12 mL chloroform. Some publications describe the addition of 3 mL acetic acid or 1 mL sulphuric acid [1]. The dried plate is dipped for 1 s in the reagent solution and heated to 110–120°C for 5–10 min. The reagent can be used with silica gel and aluminium oxide layers. It must be freshly prepared for each use.

7.2.11.4 Silver Nitrate Reagent

The silver nitrate reagent is suitable for the detection of compounds containing chlorine and bromine. Detection limits are between 20 and 100 ng per zone [69].

For preparation of the dipping solution, 10 mg of silver nitrate is dissolved in 6 mL water and then 10 mL acetone is added. Alternatively, 500 mg of silver nitrate in 1 mL water is diluted to 100 mL with ethanol. Both solutions are stable in the dark for several weeks [69]. In addition a dipping solution can be prepared by combining 100 mg silver nitrate dissolved in 1 mL water with 20 mL of 2-phenoxyethanol and diluted to 200 mL with acetone. Then one drop of 30% H_2O_2 solution is added. This solution is stable at 4°C for 4 days [69]. The dried plates are dipped for 5 s in the silver nitrate reagent solution. The wet plate is illuminated by sunlight or a bright lamp for approximately 30 min. Silver nitrate forms AgCl or AgBr with chlorine- or bromine-containing compounds. During the illumination process small silver particles are produced from these silver compounds, which cause the black to brown colour of the zones. The reagent can be used with silica gel and cellulose layers. It is possible to dip the plate in a 1% (W/V) aqueous solution of silver nitrate prior to the separation and then illuminate the plate with UV light at 256 nm.

7.2.11.5 Aluminium Chloride Reagent

Aluminium(III) and iron(III) cations form complexes with aromatic hydroxyl ketones. Flavonoids, mycotoxins (e.g. zearalenone, ochratoxin A, citrinin, or sterigmatocystin), cholesterol, triglycerides, and phospholipids react with a dipping solution prepared from 0.2 to 1.0 g AlCl $_3$ ·6 H $_2$ O dissolved in 100 mL ethanol in 1 s at room temperature forming yellow fluorescent zones under UV light at 365 nm. In some cases, the plate must be heated to 80–100°C for 10 min. The reagent can be used with all layers. Sometimes a saturated solution of zirconium oxychloride (ZrOCl $_2$) in methanol results in higher fluorescence. With this treatment the mycotoxin sterigmatocystin could be detected at 1 ng per zone [42]. The reagent is stable for 1 month.

7.2.11.6 Iron(III) Chloride Reagent

The reagent solution is prepared from 1 g FeCl₃·6H₂O dissolved in 5 mL water and diluted to 100 mL with ethanol. The plate is dipped for 1 s in the reagent solution and then heated to 110°C for 10 min. Flavonoids react to form red- or blue-violet zones, flavonoids and glycosides form green or red-green, or red-brown zones, catechin forms a green zone, tannins form blue, and phenothiazine light red zones. Alkaloids and indoles form coloured zones even at room temperature when 2 mL 70% perchloric acid is added to the reagent solution (reagent according to Salkowsky) [1]. The reagent solution is stable for a month and can be used with all layer types.

7.2.11.7 Iodoplatinate Reagent

Organic nitrogen compounds, such as alkaloids, quaternary ammonium compounds, thiols, thio ethers, and sulphoxides, can be stained using the iodoplatinate

reagent. Detection limits for urethanes and some alkaloids are 10 ng per zone. For penicillin derivatives, they are 50 ng per zone [1].

The reagent solution is prepared from 100 mg hexachloroplatinic acid dissolved in 10 mL water (or 1 M HCl for detecting benzodiazepines). This solution is mixed with 90 mL 1.5% (W/V) aqueous potassium iodide solution. The mixture is stable for a week at 4°C [71].

The dried plate is dipped for 1–4 s in the reagent solution. At room temperature, different coloured zones appear on a slightly pink background. Silica gel and aluminium oxide plates can be used.

7.2.11.8 Palladium Dichloride Reagent

The palladium dichloride reagent reacts with sulphur-containing compounds (e.g. mercaptans, disulphides, phenothiazine, and thiophosphoric esters) forming yellow-brown to black zones. It can be used to detect allium species [9]. The reagent solution is prepared from 100 mg palladium dichloride dissolved in 1 ml concentrated HCl and diluted to 20 mL with ethanol. The dried plate is dipped for 1 s and heated to 110°C for 10 min forming yellow or brown spots on a pale brown background [71]. The reagent can be used for all plate types and has good storage properties.

7.2.12 Reagents for Metal Cations

7.2.12.1 Alizarin Reagent

A large number of compounds form coloured complexes with metal cations, which can be used to determine metals [72–74]. The most versatile reagent for this purpose is alizarin [1]. The reagent solution is prepared from 50 mg alizarin dissolved in 50 mL ethanol. The dried plate is dipped for 1 s in the reagent solution and then stored for 1 min in an ammonia vapour atmosphere. Metal cations react forming red-violet zones on a weak red-violet background. Dipping the plate in 1% (W/V) boric acid solution prepared with methanol—water (9+1, V/V) and heating at 100° C for 2–5 min forms red zones on a light yellow background. The plates must be scanned immediately because the colours are not very stable.

Structures of alizarin (1), 8-hydroxychinoline (2), and rubeanic acid (3)

Metals reacting include Li, Cu, Ag, Au, Be, Mg, Ca, Sr, Ba, Zn, Cd, Hg, Al, Ga, Sc, In, La, Sn, Pb, Ti, Zr, As, V, Sb, Bi, Se, Cr, Mn, Fe, Co, Ni, Pd, and Pt. The reagent can be used with silica gel and cellulose plates. The reagent solution is stable for a month.

7.2.12.2 8-Hydroxyquinoline Reagent

The reagent solution is prepared from 50 mg 8-hydroxyquinoline dissolved in 50 mL ethyl acetate or ethanol–water (8+2, V/V). The dried plate is dipped for 5 s in the reagent solution and then exposed to ammonia vapour for 5 min forming yellow zones with yellow to yellow-red fluorescence when illuminated with UV light at 254 nm. Metals reacting include Be, Mg, Ca, Sr, Ba, Sn, Cr, Fe, Al, Ni, Co, Cu, Bi, Zn, Cd, and Hg in their +2 or +3 oxidation states. The reagent solution is stable for several days and is suitable for use with silica gel and cellulose layers.

7.2.12.3 Selenium Determination Using 2,3-Diaminonaphthalene

The reagent solution is prepared from 10 mg 2,3-diaminonaphthalene [11] dissolved in 1 mL cyclohexane to which a single drop of H_3PO_4 is added. Selenium (IV) reacts with the reagent solution forming red fluorescent zones when illuminated with UV light of 366 nm.

Selenomethionine can be hydrolysed to SeO_2 when the plate is placed at 110° C in a nitric acid atmosphere for 30 min [75]. Silica gel and cellulose layers can be used. The reagent is stable at 4° C for 1 day.

7.2.12.4 Rubeanic Acid Reagent

A 0.5% (W/V) solution of thiooxamide (ethanedithioamide) dissolved in methanol reacts with Pb^{2+} , Co^{2+} , Cu^{2+} , Mg^{2+} , Ni^{2+} , Hg^+ , and Bi^{3+} at room temperature. After dipping, the plate is placed in an ammonia vapour atmosphere. The reagent is stable for several weeks and can be used with all types of layers.

7.3 Reactions via the Gas Phase

Reactions via the gas phase result in a uniform distribution of reagent over the layer and are particularly well suited for quantitative evaluations.

7.3.1 Ammonium Bicarbonate Reagent

Segura and Gotto published in 1974 the first so-called vapour phase fluorescence (VPF) reaction using ammonium bicarbonate [76]. This salt decomposes when heated releasing ammonia which reacts with nearly all analytes containing C=O groups forming fluorescent derivatives. Independent of their structure all carbonyl compounds can be determined when excited at 380 nm with emission at 450 nm. The method is suitable for inorganic oxide layers with inorganic binders, but layers containing organic binders or bonded phases, polymeric, and cellulose layers form weak fluorescent backgrounds that interfere in the detection of analytes (Fig. 7.12).

In some cases, even compounds without carbonyl groups react forming fluorescent zones [76]. The completely dry plate is heated for 30 min in a closed chamber at 100–180°C in the presence of ca. 50 mg ammonium bicarbonate. The resulting light brown coloured zones show strong fluorescence, which can be enhanced using liquid paraffin–dichloromethane (3+7, V/V) as a dipping solution. Using amino plates, the same reaction can be performed in the absence of ammonium bicarbonate.

7.3.2 Tin(IV) Chloride Reagent

Tin(IV) chloride stains sterins, steroids, sapogenins, terpenes, fatty acids, amino acids, purines, pyrimidines, sugars, flavonoids, and phenols forming yellow fluorescent

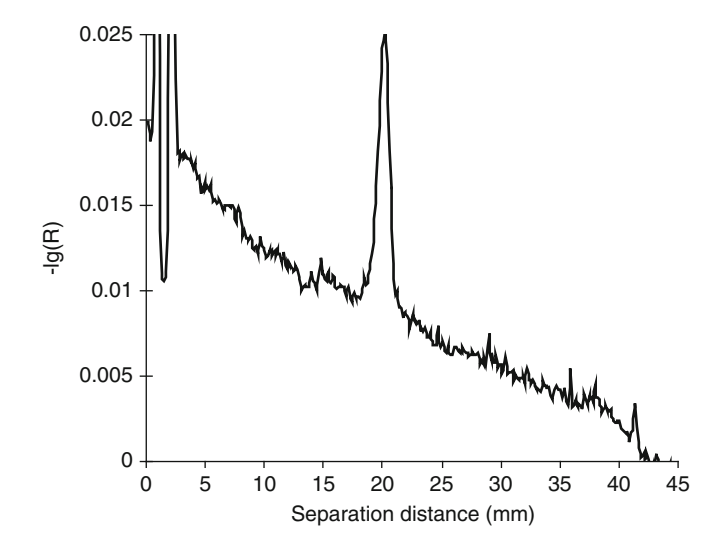


Fig. 7.12 Separation of 50 ng patulin on silica gel using the mobile phase dichloromethane–acetone (9+1, V/V). The plate was heated at 130° C for 20 min in the presence of a small amount of ammonium bicarbonate and evaluated by absorption at 280-320 nm. The sloping baseline is a result of inadequate drying of the layer before heating in the presence of the reagent

zones. The dried plate is heated at 160°C in the presence of the reagent. The coloured zones show a yellow or red fluorescence when illuminated at 366 nm. The reagent is suitable for silica gel layers.

7.3.3 Formic Acid Reagent

The fluorescence of quinine and quinoline is enhanced if a silica gel plate is contacted with formic acid vapours at room temperature for several minutes [2].

7.3.4 Hydrogen Chloride Reagent

The vapour of concentrated hydrochloric acid (36% HCl dissolved in water) reacts with anticonvulsants, digitalis glycosides, sugars, diazepam, testosterone, alkaloids, anabolic active compounds, penicillin acid, and many other compounds forming coloured compounds many of which are fluorescent. During the reaction, the analytes undergohydrolysis. The dried plate is placed in a TLC chamber at 110°C for 30 min in the presence of a few drops of concentrated hydrochloric acid. The reaction temperature can be used to distinguish different compounds. Sugars, such as glucose, fructose, fucose, and galactose; amino sugars; and N-acetylglucosamine, gangliosides, and N-acetylneuraminic acid can be separated on silica gel with chloroform-methanol-water (60+35+8, V/V). After dipping or spraying with 18% aqueous hydrochloric acid and heating these compounds form fluorescent zones. N-Acetylneuraminic acid and gangliosides react when the plate is covered by a glass plate and heated to 100°C for 10 min followed by 2 min with the cover plate removed. Sugars and amino sugars react (covered) only when heated to 150-170°C for 10 min [77]. Adapting the temperature can enhance selectivity among fluorescent compounds. Dipping the plate in liquid paraffin-dichloromethane (3+7, V/V) enhances fluorescence at 366 nm.

7.3.5 Trichloroacetic Acid Reagent

Trichloroacetic acid stains steroids, alkaloids, digitalis glycosides, vitamin D3, and benzodiazepin-2-one derivatives forming light blue fluorescent zones when illuminated at 365 nm. The dried plate is heated to 120°C for 10 min. Dipping in liquid paraffin–dichloromethane (3+7, V/V) enhances the fluorescence when illuminated with UV light at 366 nm. The reagent can be used with silica gel and cellulose layers.

7.3.6 Nitric Acid Reagent

Nitric acid in the vapour phase at $160-180^{\circ}\text{C}$ reacts with many aromatic compounds, testosterone, sugars, and phospholipids forming coloured and often fluorescent zones. The dried plate is exposed for 15 min. Dipping in liquid paraffin–dichloromethane (3+7, V/V) enhances the fluorescence when illuminated at 366 nm. All layer types can be used.

7.4 Thermal Treatment of TLC Plates

The thermal reaction of carbonyl compounds with 3-aminopropylsiloxane-bonded silica gel layers at appropriate temperatures is well known [78–85]. In a simple heating step all compounds containing aldehyde or ketone groups produce a brilliant fluorescence on a non-fluorescent background. The substances probably undergo a Maillard reaction, losing water and forming a Schiff base similar to the reaction with ammonia vapours [79]. Mostly an oven temperature of 150°C is not exceeded. Besides the reaction of sugars [78, 79] with HPTLC-NH₂ plates, reactions are described with catecholamines, creatine, creatinin and uric acid [80], twice catecholamines [81], steroid hormones [82], the artificial sweetener sucralose[®] (which needs 190°C for the reaction) [83], sterigmatocystin [84] and glucosamine [85].

Many compounds are transformed into fluorescent compounds simply by heating while in contact with the layer. This effect was first described for aluminium oxide layers, but these reactions usually work on silica gel as well. Testosterone, as an example, can be separated on aluminium oxide layers with the mobile phase toluene–propan-1-ol (10+1, V/V). Heating at 180°C for 20 min transforms the analyte into a fluorescent zone. The fluorescence intensity can be enhanced by a factor of 25 by dipping in a mixture of triton-X-100 and chloroform (1+4, V/V) [1]. The detection limit for testosterone is 2 ng per zone. In general, all analytes with an aromatic ring undergo this kind of reaction [86, 87].

7.5 Activity Analysis Using Chemical Reagents

Classical analysis is only possible if the analyte is available as a pure standard. In classical analysis the sample is compared with a reference standard to indicate whether the sample contains the analyte or not. The information measure is called a "bit" (the smallest information unit). A bit (binary digit) is defined as "yes" or "no", the simplest information an experiment can provide. If the sample contains the analyte, this is described as "yes" and we call it a 1-bit result, and a 0-bit result

means "no" analyte in the sample. A 1-bit analysis result is commonly called qualitative analysis.

In quantitative analysis, the analyte content is described as a figure with a resolution of >1 bit. This figure refers to the quality of the analysis. It can also be described as "resolution", the ability to distinguish different contents. For example, no more than eight different colours can be distinguished by using universal indicator papers for pH analysis. Such pH analysis provides a resolution of three bits ($2^3 = 8$) because only eight different colours can be distinguished.

Activity analysis is broader than this simple illustration with the purpose of identifying a class of analytes defined by a common activity and not simply a single compound by its similarity to a reference standard. This is the basis of screening tests for substances not available as a reference standard and for new compounds showing a particular biological activity.

7.5.1 Folin-Ciocalteu Reagent

The Folin–Ciocalteu reagent was initially intended for the analysis of proteins taking advantage of its reactivity with tyrosine. The assay was extended to the analysis of total phenols in wine and is nowadays used to measure a sample's reducing capacity, mainly for phenolic antioxidants. The reagent is made by first boiling 10 g of sodium tungstate (Na₂WO₄·2 H₂O) and 2.5 g of sodium molybdate (Na₂MoO₄·2 H₂O) in 10 mL concentrated HCl (36%), 5 mL H₃PO₄ (85%), and 70 mL water for 10 h. After boiling, 15 g of lithium sulphate (Li₂SO₄·4 H₂O) is added to the mixture to give an intense yellow solution. This solution is then refluxed for 15 min and made up to 100 mL with water. Contamination by reducing compounds leads to a green colour, which can be restored to yellow by adding a drop of bromine. The exact chemical composition of the reagent is unknown.

The plate is first dipped for 2 s into a 2% (W/V) aqueous sodium carbonate solution and then in a solution of Folin–Ciocalteu reagent diluted 1:10 with water. Reducing compounds such as phenols or vitamin C produce blue zones on a light yellow background [2, 3, 88].

7.5.2 Checking for Free Radical Scavenger Activity Using DPPH Reagent

Identifying radical scavenger properties provides valuable indications when testing pharmaceutically active substances in plant and fungal organisms. The radical-containing reagent DPPH [2,2-di-(4-*tert*-octylphenol)-1-picrylhydrazyl] is usually used to detect substances with anti-oxidant properties. DPPH is a stable radical with a purple colour. The compound turns yellow when reduced by a radical scavenger.

The dried plate is immersed in a solution of 25 mg DPPH in 50 mL acetone or methanol. Alternatively, the layer is sprayed with this solution. Any free radical scavenger activity will turn the blue radical into yellow at least 30 s after dipping [89, 90].

Structure of 2,2-di-(4-*tert*-octylphenol)-1-picrylhydrazyl (DPPH-reagent)

7.5.3 Nucleophilic Reaction Ability

Compounds reacting as a nucleophile are always suspected to cause cancer. The substance 4-(4-nitrobenzyl) pyridine (NBP) has a free electron pair at the pyridine-nitrogen which can combine with alkylating substances, such as halogenated alkylamines, diazoalkanes, aziridine, epoxides, activated olefines, cumarin, antrachinon, and pyrethroides, to produce bluish to red-violet zones on a colourless background that darkens when treated with alkali [1, 91]. NBP reagent is prepared by dissolving 1.2 g NBP in 40 mL acetone. The layer is dipped for 2 s in the reagent and then heated to 120–150°C for 15–30 min, allowed to cool, and exposed to ammonia or triethylamine vapour (Fig. 7.9).

The reagent can be used with silica gel, cellulose, cyano, and reversed-phase layers. The reagent solution is stable for several days if stored in a refrigerator [1].

Reaction 7.9 Forming a red-violet compound by a nucleophilic reaction

References 197

References

 Jork H, Funk W, Fischer W, Wimmer H (1990, 1994) Thin Layer Chromatography, Volume 1a, Physical and chemical detection methods, Volume 1b, Reagents and detection methods. VCH Verlagsgesellschaft mbH, Weinheim

- 2. Dyeing reagents for thin layer and paper chromatography. Merck-Company. http://www.cob.uha.fr/site%20cot/toolbox.php_files/TLC%20bible.pdf
- 3. Krebs KG, Heusser D, Wimmer H (1969) In: Stahl E (ed) Thin-layer chromatography, a laboratory handbook. Springer, Berlin, pp 854–909
- Touchstone JC, Dobbins MF (1978) Practise of thin layer chromatography. Wiley, New York, pp 135–187
- 5. Touchstone JC (1992) Practice of thin layer chromatography. Wiley, New York, pp 129-183
- 6. Kraus Lj, Koch A, Hoffstetter-Kuhn S (1995) Dünnschichtchromatographie. Springer, Berlin
- Cimpan G (2001) In: Nyiredy Sz (ed) Planar chromatography, a restrospective view for the third millennium. Springer, Budapest, pp 410–445
- 8. Randerat K (1965) Dünnschicht-Chromatographie. Chemie, Weinheim
- Wagner H, Bladt S (1996) Plant drug analysis. A thin layer chromatography atlas, 2nd edn. Springer, Berlin
- Reimann K (1972) Schnellnachweis von Schwermetallionen mittels Dünnschicht-chromatographie der Dithizonate aus Wasser, Abwasser und Schlamm. Wasser-und Abwasser-Forschung 1:3–7
- 11. Baranowska I, Poreba R, Baranowski J, Aleksandrowicz R (1992) Separation and identification of metals in the human placenta by TLC. J Planar Chromatogr 5:469–471
- 12. Bruno P, Caselli M, Fracassi F, Traini A (1984) HPTLC separation and densitometric determination of some metallic dithizonates at subnanogram levels: applications to real samples. Anal Lett 17:397–412
- 13. Baranowska I, Baranowski J, Norska-Borówka I, Pieszko C (1996) Separation and identification of metals in human bones, placenta and milk and in air by absorption and ion-exchange thin-layer chromatography. J Chromatogr A 725:199–202
- 14. B. Spangenberg Unpublished results
- König K-H, Kessler I, Schuster M, Steinbrech B (1985) Zur Chromatographie von Metallen.
 XV. Dünnschicht-Chromatographie von Rh, Pd, Ir und Tt mit 1-Hydroxy-2-pyridinthion.
 Fresenius Z Anal Chem 322:33–35
- Steinbrecher B, König K-H (1983) Zur Chromatographie von Metallchelaten. XII.
 Dünnschicht-Chromatographie (DC) und Hochdruck-Flüssigkeits-Chromatographie (HPLC)
 der Metallchelate des 1-Hydroxy-2-pyridinthin (HPT). Fresenius Z Anal Chem 316:685–688
- 17. König K-H, Kessler I, Schuster M, Steinbrech B (1984) Zur Chromatographie von Metall-chelaten. XV. Dünnschichtchromatographie von Rh, Pd, Ir und Pt mit 1-Hydroxy-2-pyridinthin. Fresenius Z Anal Chem 319:66–69
- Brozovic-Pohl K, Altorfer A, Perlia X (1992) A new (limit) test for heavy metals. Fresenius Z Anal Chem 343:348–351
- Siembida R, Rozylo TK, Jamrozek-Manko A (1998) Aspects of the exact quantitative determination of formaldehyde in tooth tissue by TLC. J Planar Chromatogr 11:417–420
- Funk W (1994) Derivatisierungsreaktionen im Bereich der quantitativen Dünnschicht-Chromatographie. Fresenius Z Anal Chem 318:206–219
- Moosbach E, Rosenboom J, Hartkamp H (1999) Thin-layer detector tubes a new system for the determination of trace gases in air by gas/solid reactions followed by remission photometric determination. Gefahrstoffe – Reinhalt Luft 59:71–78
- 22. Kim SS, Gallaher DD, Csallany AS (1999) Lipophilic aldehydes and related carbonyl compounds in rat and human urine. Lipids 34:489–496
- Büldt A, Karst U (1999) N-Methyl-4-hydrazino-7-nitrobenzofurazan as a new reagent for air monitoring of aldehydes and ketones. Anal Chem 71:1893–1898
- 24. B. Spangenberg Unpublished results

- 25. Gübitz G, Wintersteiger R, Frei RW (1984) Fluorigenic labelling of carbonyl compounds with 7-hydrazino-4-nitrobenzo-2-oxa-1,3-diazole (NBD-H). J Liq Chromatogr 7:839–854
- Jork H, Funk W, Fischer W, Wimmer H (1988) In situ pre-chromatographic derivatization.
 J Planar Chromatogr 1:280–292
- Miller JM, Kirchner JG (1953) Chromatostrips for identifying constituents of essential oils.
 Anal Chem 25:1107–1109
- Kofoed J, Korczak-Fabierkiewicz C, Lucas GHW (1966) A study of the conversion of phenothiazine derivates to the corresponding sulfoxides on thin-layer plates. J Chromatogr 23:410–416
- Wilk M, Hoppe U, Taupp W, Rochlitz J (1967) Reaktions-Chromatographie, ein Identifizierungsverfahren für Aromaten bei der Papier- und Dünnschichtchromatographie. J Chromatogr 27:311–316
- 30. Wilk M, Bez W, Rochlitz J (1966) Neue Reaktionen der carcinogenen Kohlenwasserstoffe 3,4-Benzpyren, 9,10-Dimethyl-1,2-Benzanthracen und 20-Methylcholanthren. Tetrahedron 22:2599–2608
- 31. Baggiolini M, Dewald B (1967) Kontrollierte Hydrolyse auf Kieselgel-Platten mit chromatographischer Trennung der Spaltprodukte. J Chromatogr 30:256–259
- 32. Elgamal MHA, Fayez MBE (1967) A new application of thin-layer chromatography. Chemical reactions induced on the adsorbent. Fresenius Z Anal Chem 226:408–417
- 33. Purdy SJ, Truter EV (1963) Constitution of the surface lipid from the leaves of Brassica oleracea. Isolation and quantitative fractionation. Proc Royal Soc (London), Ser B 158:536–543
- Young-Duck Ha, Bergner K-G (1981) Dünnschichtchromatographische Untersuchung von Phenylharnstoff- und N-Phenylcarbamat-Rückständen. Dtsch Lebensm Rundschau 77:102–106
- 35. Krüger D, Wichtl M (1985) Digitalisglykoside. Identifizierung und Strukturaufklärung mittels Reaktions-Dünnschichtchromatographie. Dtsch Apoth Ztg 125:55–57
- Schütz C, Schütz H (1973) Unterscheidung ungesättigter Barbiturate mittels Reaktionschromatographie. Dtsch Apoth Zrg 113:1559–1562
- 37. Polesuk J, Ma TS (1971) Organic synthesis on microgram scale. VIII. Chlorination of acetanilide and related compounds by means of molecular chlorine. Mikrochim Acta 662–666
- Gänshirt H (1963) Nachweisverfahren für dünnschichtchromatographisch getrennte Wirkstoffe von Antineuralgie- und Schlaftabletten. Arch Pharmaz 296:73–79
- Cargill DI (1962) The separation of cholesterol from related stanols and stanones by thin-layer chromatography. Analyst 87:865–869
- Schütz C, Schütz H (1973) Unterscheidung von 3,5-Dioxo-1,2-diphenyl-4-n-butyl-pyrazolidin (Phenylbutazon) und 3,5-Dioxo-1,2-diphenyl-4-prenyl-pyrazolidin (Prenazon) mit Hilfe der Reaktionschromatographie. Arzneim Forsch 23:428–431
- 41. Wintersteiger R (1982) Determination of morphine and morphine-6-nicotinate by an in situ reaction on chromatograhic plates with dansyl chloride. Analyst 107:459–461
- 42. Gertz Chr, Böschemeyer L (1980) Verfahren zur Bestimmung verschiedener Mykotoxine in Lebensmitteln. Z Lebensm Unters Forsch 171:335–340
- Goliński F, Grabarkiewics-Szczesna J (1984) Chemical confirmatory tests for ochratoxin A, citrin, penicillic acid, sterigmatocystin, and zearalenone performed directly on thin layer chromatographic plates. J Assoc Off Anal Chem 67:1108–1110
- 44. Frei RW, Lawrence JF (1973) Fluorigenic labelling in high-speed liquid chromatography. J Chromatogr 83:321–330
- Scholten AHMT, van Buren C, Lawrence JF, Brinkman UATh, Frei RW (1979) A residue technique for urea herbicides using catalytic hydrolysis on silica gel plates. J Liq Chromatogr 2:607–617
- 46. Wintersteiger R (1988) Fluoreszenz-Derivatisierung in DC und HPLC. GIT 32:5-11
- 47. Marcus BJ, Ma TS (1968) Organic synthesis on the microgram scale II. Mikrochim Acta 436–441

References 199

48. Spangenberg B (2006) Fluorescence spectroscopy in planar chromatography. International symposium for thin layer chromatography, Berlin, October 2006

- Müller D, Morlock G (2006) New validated method for determination of acrylamide on potato chips by planar chromatography. International symposium for thin layer chromatography, Berlin, October 2006
- 50. Gübitz G, Wintersteiger R (1980) Identification of drugs of abuse by high-performance thinlayer chromatography. J Anal Toxicol 4:141–143
- Junker-Buchheit A, Jork H (1988) Prächromatographische in situ-Derivatisierung von Fettsäuren im Picomol-Bereich. Teil I: HPTLC fluoreszierender Monodansylpiperzin- und cadaverin-Derivate. Fresenius Z Anal Chem 331:387–393
- 52. Lankmayr EP, Budna KW, Müller K (1979) Bestimmung von Thiolverbindungen durch selektive Fluorescenzderivatisierung und HPLC. Fresenius Z Anal Chem 295:371–374
- Lankmayer EP, Budna KW, Müller K, Nachtmann F, Rainer F (1981) Determination of D-penicillamine in serum by fluorescence derivatization and liquid column chromatography. J Chromatogr 222:249–255
- 54. Wintersteiger R, Gübitz G, Hartinger A (1980) Derivatisation of sympathomimetics with primary amino groups on thin-layer plates by spotting the sample spots with fluorescamine. Chromatographia 13:291–294
- Pataki G, Borko J, Curtis HCh, Tancredi F (1968) Some recent advances in thin-layer chromatography. New applications in aminoacid peptide and nucleic acid chemistry. Chromatographia 1:406–417
- Minyard JP, Tumlinson JH, Thompson AC, Hedin PA (1967) Gas-liquid thin-layer chromatographic derivatisation technique for the identification of alcohols. J Chromatogr 29:88–93
- Junker-Buchheit A, Jork H (1989) Monodansyl cadaverine as a fluorescent marker for carboxylic acids – in situ prechromatographic derivatization. J Planar Chromatogr 2:65–70
- 58. Wintersteiger R, Wenninger-Weinzierl G (1981) Neues, empfindliches Verfahren zur dünnschicht-chromatographischen Analyse von Substanzen mit alkoholischer Hydroxylgruppe durch Reaktion mit Naphthylisocyanat. Fresenius Z Anal Chem 309:201–208
- Stahl E (ed) (1969) Thin-layer chromatography, a laboratory handbook. Springer, Berlin, pp 854–909
- 60. Postaire E, Sarbach Ch, Delvordre P, Regnault C (1990) A new method of derivatisation in planar chromatography: overpressure derivatisation. J Planar Chromatogr 3:247–250
- Reich E, Schibli A (2006) High-performance thin-layer chromatography for the analysis of medicinal plants. Thieme, New York
- Spangenberg B, Lorenz K, Nasterlack St (2003) Fluorescence enhancement of pyrene measured by thin-layer chromatography with diode-array detection. J Planar Chromatogr 16:328-334
- 63. Jaryj E, Lorenz K, Spangenberg B (2008) A simple method for the quantification of urethane in spirits. J Liq Chromatogr Rel Technol 31:1–9
- 64. Wall PE (1997) Argentation HPTLC as an effective separation technique for cis/trans isomers of capsaicin. J Planar Chromatogr 10:4–9
- 65. Neu R (1954) Tetraphenyl-diboroxyd aus Natriumtetraphenylborat. Chem Ber 87:802-805
- 66. Göcer M, Hoferer K, Zipfel J, Spangenberg B (2009) A new method for the quantification of paraquat, diquat, difenzoquat, mepiquat and chloromequat in water by thin-layer chromatography. J Planar Chromatogr 22:59–63
- 67. Hiegel K, Spangenberg B (2009) A new method for the quantification of dequalinium-cations in pharmaceutical samples by absorption and fluorescence diode array thin-layer chromatography. J Chromatogr A 1216:5052–5056
- Machata G, Schütz H, Bäumler J, Daldrup T, Gibitz H-J (1989) Empfehlungen zur klinischtoxikologischen Analytik. Folge 5: Empfehlungen zur Dünnschichtchromatographie. VCH, Weinheim

- 69. Becker G, Eichler D, Nolting H-G, Thier H-P (1987) Dünnschichtchromatographie in der Rückstandsanalytik von Pflanzenschutzmitteln und deren Metaboliten. VCH, Weinheim
- 70. Broszat M, Brämer R, Spangenberg B (2008) A new method for quantification of melamine in milk by absorption diode-array chromatography. J Planar Chromatogr 21:469–470
- 71. Cimpan G (2001) In: Nyiredy Sz (ed) Planar chromatography. A retrospective view for the third millennium. Springer, Budapest, pp 410–445
- 72. Mohammad A (1997) Thin-layer chromatographic methods for the identification, estimation and separation of toxic metals in environmental samples. J Planar Chromatogr 10:48–54
- Mohammad A, Ajmal M, Anwar S, Iraqi E (1996) Twenty-two years report on the thin-layer chromatography of inorganic mixtures: observations and future prospects. J Planar Chromatogr 9:318–360
- Ahmad J (1996) Use of alumina stationary phase for thin layer chromatography of inorganic and organometallic compounds. J Planar Chromatogr 9:236–246
- 75. Spangenberg B Unpublished results
- Segura R, Gotto AM (1974) A new fluorimetric procedure for the detection and quantitation of organic compounds in thin-layer chromatography. J Chromatogr 99:643

 –657
- 77. Hayakawa T, Hirati M (2003) An assay of ganglioside using fluorescence image analysis on a thin-layer chromatography plate. Anal Chem 75:6728–6731
- 78. Klaus R, Fischer W, Hauck HE (1989) Use of a new adsorbent in the separation and detection of glucose and fructose by HPTLC. Chromatographia 28:364–366
- 79. Klaus R, Fischer W, Hauck HE (1990) Application of a thermal in situ reaction for fluorimetric detection of carbohydrates on NH₂ layers. Chromatographia 29:467–472
- Klaus R, Fischer W, Hauck HE (1991) Qualitative and quantitative analysis of uric acid, creatine and creatinine together with carbohydrates in biological material. Chromatographia 32:307–316
- Klaus R, Fischer W, Hauck HE (1993) Extension of the application of the thermal in-situ reaction on NH₂ layers to the detection of catecholamines in biological materials. Chromatographia 37:133–143
- 82. Klaus R, Fischer W, Hauck HE (1994) Analysis and chromatographic separation of some steroid hormones on NH_2 layers. Chromatographia 39:97–102
- 83. Stroka J, Arranz I, Mac Court J, Spangenberg B (2003) Simple and reliable working HPTLC quantification method for Sucralose[®]. J Liq Chromatogr Rel Technol 26:2729–2739
- 84. Stroka J, Dasko L, Spangenberg B, Anklam E (2004) Determination of the mycotoxin sterigmatocystin, by thin-layer chromatography and reagent-free derivatisation. J Liq Chromatogr Rel Technol 27:2101–2111
- 85. Bleichert M, Eckhardt H-S, Klein K-F, Spangenberg B (2008) A simple and reliable method for quantification of glucosamine in nutritional supplements. J Planar Chromatogr 21:55–59
- Caissie GE, Mallet VN (1976) The fluorimetric detection of pesticides on aluminium oxide layers. J Chromatogr 117:129–136
- 87. Baeyens WRG, Lin Ling B (1988) Thin layer chromatographic applications with fluorodensitometric detection. J Planar Chromatogr 1:198–213
- 88. Prior RL, Wu X, Schaich K (2005) Standardized methods for the determination of antioxidant capacity and phenolics in food and dietary supplements. J Agric Food Chem 53:4290–4302
- 89. Hostettmann K, Terreaux Ch, Marston A, Potterat O (1997) The role of planar chromatography in the rapid screening and isolation of bioactive compounds from medicinal plants. J Planar Chromatogr 10:251–257
- 90. Yrjönen T, Peiwu Li, Summanen J, Hopia A, Vuorela H (2003) Free radical-scavenging activity of phenolics by reversed-phase TLC. J Am Oil Chem Soc 80:9–14
- 91. Cee A (1978) New detection method for compounds with a labile halogen on thin-layer chromatograms. J Chromatogr 150:290–292

Chapter 8 Bioeffective-Linked Analysis in Modern HPTLC

The purpose of bioeffective-linked analysis is to bridge the gap between cause and effect, that is, primarily not to identify a given analyte, but to identify a class of compounds with a defined bioactivity. This is the basis of screening tests for substances with special properties (e.g. fungicides) and for screening tests on new compounds with a particular biological activity. This approach is of interest in the search for new compounds that show a particular biological activity and for investigating samples containing substances whose identity is unknown or unavailable as reference standards.

Hundreds of pesticides are in use currently worldwide. Routine testing on all these compounds is impossible if classical analysis is used because contaminants are often missed because the method does not check for them. Bioeffective analysis does not necessarily rely on standards. An activity analysis does not indicate that a sample contains a particular compound but conveys the information about whether the sample contains hazardous compounds or more specific molecules that can cause a defined biological (hazardous) reaction. Using bioeffective-linked analysis it is not necessary to test for all known pesticides. It is sufficient to test for a particular activity to verify contamination.

The effectiveness of a chromatographic analysis is determined by the selectivity of the chromatographic separation and the specificity of the detection method. In the case of high-performance thin-layer chromatography, the separated components can be detected and quantified directly on the chromatogram by physical and chemical methods. By coupling high-performance thin-layer chromatography with biological or biochemical inhibition tests it is possible to detect toxicological active substances in situ [1]. Furthermore the confirmation of toxic compounds by biological or biochemical tests increases the reliability of identification. Besides the detection and confirmation of bioeffective substances the use of bioeffective-linked analysis allows dose–effect relationships to be compiled.

8.1 Principle of the Method

Bioeffective-linked analysis is designed to integrate biological or biochemical tools for the detection of potentially adverse effects, physico-chemical fractionation procedures, and chemical—analytical methods for structure elucidation and toxicant quantification. This kind of analysis involves a coupling of two different methods. On the one hand, an analysis of contaminants using trace analytical methods is used for the determination of selected compounds and, on the other hand, the physical/chemical assessment is followed by a biological or biochemical toxicity test, thus, allowing a direct activity-dependent evaluation to be made after chemical/physical characterization.

8.1.1 Contaminant Analysis in the Environment and Food and the Principle of Bioactivity-Based Analysis

The investigation of samples, such as water, soil and air, and food for toxicologically relevant substances presents a number of problems. The use of biological toxicity tests or enzymatic inhibition tests in vivo or in vitro as screening procedures for the analysis of ground, drinking, surface, and wastewaters as well as food samples affords an initial indication of the presence of toxic contaminants. The results of this "bio-monitoring" generally yield a summation of the damaging effects of contaminants in a defined test system; however, it is not possible to identify individual substances.

In order to demonstrate the presence of one or more contaminants, which are responsible for the toxic effect in the test system, it is necessary to resort to instrumental analysis to detect and to quantify the smallest traces of these substances (e.g. in the nanogram to pico-gram range).

For its part, the use of instrumental analysis requires selective enrichment of the active substances from the matrix: usually, a chromatographic separation precedes identification with the aid of selected reference substances followed by their quantification. There are difficulties here in the selection of relevant reference substances. It is only possible to detect those substances that are actively sought by the analyst. The analysis of individual substances does not detect unknown substances or metabolites having adverse biological or toxicological effects in an environmental sample.

Bioeffective-linked analysis is based on the idea that the biological effect of the total sample or an extract on selected target systems (e.g. cell cultures, microorganisms, enzymes) is determined as a sum of effects. In case of conspicuous effects, a specific search is subsequently performed to identify the responsible substance(s) [2].

8.1.2 Aims and Fundamental Aspects of Bioeffective-Linked Analysis by Thin-Layer Chromatography

The aim of bioeffective-linked analysis must be to detect and identify bioeffective compounds such as pharmacologically active substances or contaminants from samples having biological activity at trace concentrations within the 100–200 ng/kg range. It is also possible to determine trends in bioactivity with respect to a sampling plan. The selected method should be as universal as possible, in order to detect contaminants with biological effects in the questionable sample. It is not the selectivity with respect to individual substances that is of importance, but rather the detection of all, or at least as many as possible of the contaminants, which are present in the sample. A further parameter, the enrichment factor, depends on the bioactivity of the active substance (e.g. their toxicity). It is possible to detect very small amounts of highly active substances by means of activity analysis, so that an enrichment procedure is not necessary. The problem at hand determines whether selective sample preparation is required to detect one active substance in the sample or whether a universal sample preparation is used to detect as many active substances as possible.

8.1.3 HPTLC as a Method for Bioeffective-Linked Analysis

Thin-layer chromatography (TLC) is one of the oldest methods used in the analysis of bioeffective compounds such as antibiotics or contaminants. As the analysis of plant protection agent residues immerged as important in the 1950s the only methods available to the analyst were spectrophotometry and paper chromatography. However, these were soon replaced by thin-layer chromatography, which made it possible to separate numerous plant protection agents and to detect and identify them with various colour reagents. Many publications during the last decade clearly reveal an emphasis on the analysis of pesticide residues with particular attention being paid to fungicides and insecticides [3-6]. The determination of plant protection agents in drinking water with the AMD method according to German DIN 38407, part 11 [7] describes a thin-layer chromatographic separation after enrichment of the contaminant by solid-phase extraction. This universal method involves the separation of the individual components by a stepwise multiple development on a silica gel layer, whereby the development commences with a polar mobile phase and finishes with a mobile phase or lower polarity. This allows the separation of substances of varying polarity, which is typical of normal contaminants and their metabolites. Identification and determination is carried out by in situ reflectance measurements at different wavelengths. The individual substances are subjected to preliminary identification on the basis of their position in the chromatogram and by comparison of the reflectance spectrum with a spectral

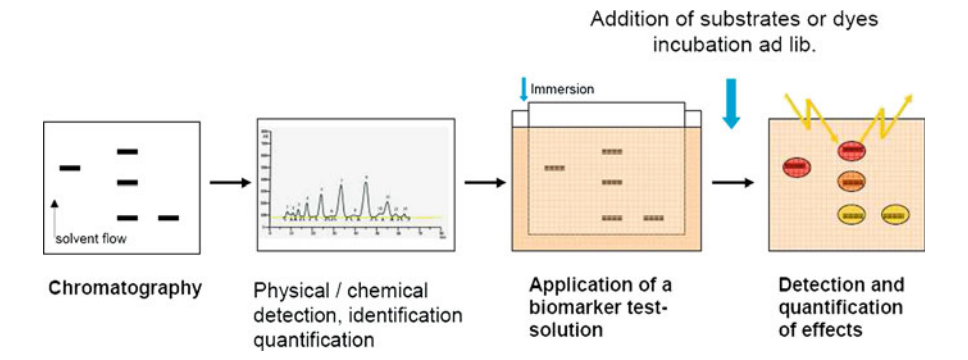


Fig. 8.1 Principle of bioeffective-linked analysis by AMD-HPTLC

library. In this case the detection limit is generally dependent on the absorption coefficients of the substance or of its derivative. Unknown contaminants are identified initially by comparing their retention factors with those of the reference substances or from their UV spectra. Chemical reactions carried out directly on the plate can be used to increase the reliability of identification. Although unknown contaminants can be identified using physical or microchemical techniques, it is also possible to determine these substances by a range of biological and biochemical test procedures. The second step consists of the detection of the active substance on the same chromatogram by coupling with a biological/biochemical toxicity test, involving damage to an appropriate organism that forms the test system, applied post chromatographically to the HPTLC plate (Fig. 8.1).

Final identification of compounds can be achieved through LC-MS or GC-MS analysis of TLC fractions exhibiting activity. Sample separation by planar chromatography offers several advantages over column chromatography for this purpose:

- (a) Separated components are preserved on the layer where they can be analysed using a combination of physical, chemical, and biological detection methods.
- (b) Separation of compounds of a wide polarity range (e.g. alkylphenols and alkylphenol ethoxylates) as well as a focusing effect can be achieved by using special development techniques, such as automated multiple development (AMD).
- (c) Up to 20 samples can be analysed simultaneously.
- (d) The HPTLC layer can be used as a growth surface for the bioassay test organism [8].

A key issue for the identification of bioeffective compounds is the establishment of suitable fractionation and isolation techniques. Test organisms, such as mould spores, yeast cells, bacteria, and cell organelles such as chloroplasts, in a suitable nutrient medium are applied to the layer. The biological signal, such as inhibition or stimulation of growth, inhibition or stimulation of luminescence, or inhibition of photosynthesis, is used to localize bioeffective substances on the chromatogram or to detect unknown bioeffective substances. In addition to the use of organisms or

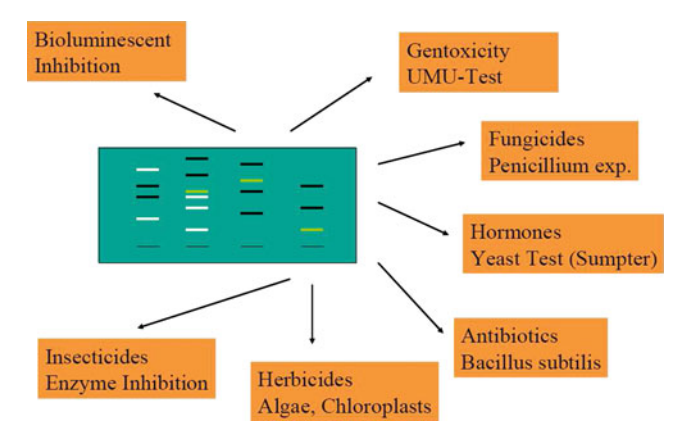


Fig. 8.2 Examples for in situ toxicological tests on HPTLC plates (From [1] with permission. © Akadémiai Kiadó.)

sub-organisms as test materials it is possible to use enzyme inhibition tests as a biochemical marker for toxicologically relevant substances (Fig. 8.2).

Documentation can be carried out by means of a flat bed scanner or a video camera and the inhibition can be reported quantitatively in defined toxicity units. The sensitivity depends on the toxicity of the substance with respect to each test system.

8.2 General Rules for the Analysis of Bioeffective Compounds

Biological and biochemical test procedures are used to detect bioeffective compounds, which are more or less separated by HPTLC. Specific enzyme inhibition tests on the thin-layer plate or test procedures involving organisms that use inhibition of bacterial growth, inhibition of bacterial luminescence, or inhibition of the growth of a yeast strain as the signal serve to detect the presence of biologically or toxicologically relevant compounds. The inhibition or stimulation of growth, inhibition or stimulation of luminescence, or inhibition of photosynthesis provides a selective signal to localize bioeffective substances on the chromatogram in order to detect unknown toxic substances in a sample.

Bioeffective-linked analysis in TLC couples two different methods. On the one hand the TLC plate is used as the stationary phase in a chromatographic system, pre-washed and activated at 100°C, optimized for the chromatographic development. On the other hand this stationary phase, contaminated with components of the mobile phase and bioeffective compounds, acts as the support for living organisms. Especially for biological assays the apparent pH of the sorbent has to be taken into account (Fig. 8.3).

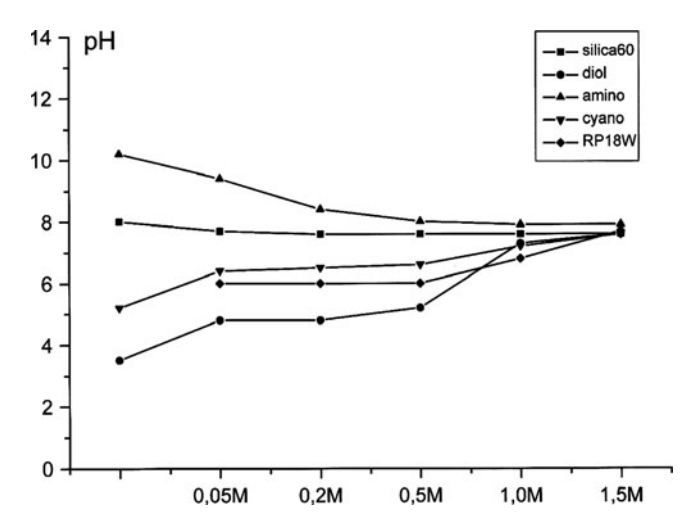


Fig. 8.3 Effect of ionic strength on the apparent pH of various sorbents impregnated with tris (hydroxymethyl)aminomethane–HCl buffer pH 7.6 [9]

Strong acids, such as those containing formic or aced acid, should be avoided. Toxic solvents like toluene should not be used. AMD separations commonly end by washing the layer with pentane or hexane. This has the advantage that interfering mobile phase constituents are washed out. A single plate development should always be succeeded by a development with pentane, a volatile solvent that will clean the plate. In general, the mobile phase has to be completely removed before application of the biological or biochemical assay organism.

8.3 Enzyme Tests

8.3.1 Urease-Inhibition Test for Heavy Metals

The detection of bioactive substances by enzyme-inhibition tests was known for more than 40 years. In 1972, Geike published an enzyme inhibition test for heavy metals.

The enzyme urease transforms urea into ammonium cations. Cadmium, zinc, copper, silver, mercury, and organic mercury compounds function as strong urease inhibitors. Surprisingly, lead does not inhibit this enzyme. For the enzyme solution, 30 mg of urease is dissolved in 10 mL of a 10^{-6} M pH 7 phosphate buffer. For the substrate solution, dissolve 500 mg urea in 12.5 mL of a 0.01% bromothymol blue solution and adjust to pH 7 with sodium carbonate. After development, the plate is dipped in 10 mL of enzyme solution and stored for 30 min at 80–90% humidity and 25°C. Subsequently, the plate is dipped for 2 s in the reagent solution. Zones

8.3 Enzyme Tests 207

containing heavy metals appear as yellow spots on a blue background [10]. Organic mercury compounds can be detected in the nanogram range [11].

8.3.2 Analysis Using Redox Enzymes

Oxidoreductases catalyse the transfer of electrons from an electron donor to an oxidant (which acts as electron acceptor). For sugars, such as galactose, N-acetyl-D-galactosamine, and 2-deoxy-D-galactose, galactose oxidase is a suitable enzyme. In this reaction O_2 is the oxidant forming H_2O_2 . Hydrogen peroxide can then be easily identified by reaction with colourless tetrazolium salts to form coloured compounds.

After separation, the dried plate is dipped into a solution of 125 units of galactose oxidase and 500 units of horseradish peroxidase suspended in 0.2 M pH 7.5 phosphate buffer. If the enzyme finds a substrate, it produces H_2O_2 , which is identified as a blue zone after reaction with a 0.5% solution of o-toluidine in ethanol [12] or with 2-(4-iodophenyl)-3-(4-nitrophenyl)-5-phenyl-2H-tetrazolium chloride (INT) forming a pink formazan dye.

 3β -Hydroxysteroids can be identified directly on the plate, using a solution of 10 units of 3β -hydroxysteroid oxidase, 100 units of peroxidase, 15 mg phenol, 2 mg 4-aminoantipyrine and 0.02 mL Triton X-100 in 20 mL 0.1 M pH 7.0 phosphate buffer. After separation, the dried plate is dipped in the reagent solution and incubated at 37° C for 30 min. Pink zones are formed on a colourless background [13]. Dehydrogenase activity is indicated by oxidation of a colourless tetrazolium salt to form a dark pink formazan compound, thereby differentiating between living and dead cells. This reaction is the basis for the test on living cultures (e.g. *Bacillus subtilis*).

 3α -Hydroxysteroids react with NAD⁺forming 3-ketosteroids and NADH. In Reaction 8.1 NAD⁺ is the oxidant forming NADH. The co-enzyme NADH reacts with TPH to form a pink formazan dye. The reaction is catalysed by a diaphorase

Reaction 8.1 Enzymatic reaction of TPH (2,3,5-triphenyltetrazolium chloride). The *white* compound is enzymatically reduced to *red* TPF (1,3,5-triphenylformazan) in living tissue

enzyme (dihydrolipoamide reductase from *Clostridium kluyveri*, type II-L). The reagent solution contains 6 mg INT or TPH, 1 unit of 3α -hydroxysteroid dehydrogenase, 50 units of diaphorase, and 5 μ mol β -NAD⁺ in 10 mL 0.2 M pH 8.5 K_2 HPO₄ buffer. After separation, the dried plate is immersed in the reagent solution and incubated at 37°C for 30 min and 80% relative humidity with zones containing NADH coloured pink [14].

8.3.3 The Detection of Cholinesterase Inhibitors

Mendoza published a summary of the application of enzyme-inhibition techniques in combination with thin-layer chromatography in 1973 [15–18]. He discussed the determination and identification of contaminants with cholinesterase inhibition properties in residue analysis of vegetable, soil, and water samples, together with the forensic toxicology of the results of the investigation of the metabolism of individual active substances. The report summarizes the detection limits for more than 100 phosphate esters [15-17] and carbamates [18]. In 1981, Ambrus et al. compared six TLC methods for the detection of 188 pesticides [19]. Besides the detection of pesticides, HPTLC-cholinesterase assays have been reported for the identification of inhibitors in plant extracts evaluated for the treatment of Alzheimer's disease [20-22]. The inhibition of cholinesterase has long been recognized as a biochemical method for the detection of the enzyme-inhibiting effects of organophosphate esters and carbamates. These materials are widely used as pesticides and have partially replaced persistent insecticides of the chlorinated hydrocarbon type. In contrast to organochlorine compounds, phosphate esters and carbamates are frequently characterized by a high toxicity, low stability towards hydrolysis, relatively high water solubility, and high mobility. The investigations were carried out using isolated enzymes and enzyme homogenates [9].

8.3.3.1 The Physiological Importance of Cholinesterase

Acetylcholine esterase exerts a key function in the control of cholinergic stimulus transmission. It is localized at the synaptic cleft of the peripheral and central nervous system. There it ensures rapid hydrolytic degradation of the acetylcholine that is produced during parasympathetic stimulation. Crystal structure analysis has made it possible to describe its function at the molecular level. Acetylcholine esterases are members of the family of serine hydrolases.

8.3.3.2 The Molecular Mechanism of Cholinesterase Inhibition

The inhibition of cholinesterase is the result of an irreversible phosphorylation or carbamylation of the serine hydroxyl groups in the active centre of the enzyme. The

8.3 Enzyme Tests 209

organophosphorus pesticides and carbamate insecticides inhibit the cholinesterase to very different degrees. Most irreversible inhibitors inhibit the enzymatic reaction completely, frequently by formation of a covalent bond if their concentration exceeds that of the reacting groups in the enzyme. The inhibition of serine hydrolases, such as cholinesterase from rabbit liver or B. subtilis and cutinase from F. $solani\ pisi$, has long been recognized as a biochemical method for the detection of the enzyme-inhibiting effects of organophosphate esters and carbamates. Irreversible inhibition is expressed mathematically by the following equations, where k_i is the constant for the formation of the enzyme-inhibitor conjugate:

$$E + I \xrightarrow{k_i} EI$$

$$k_i = \ln 2 \times t_{1/2}^{-1} c_I^{-1}$$

E enzyme

I inhibitor

 k_i inhibition constant [L/(mol min)] $t_{1/2}$ time for which half of c_I has reacted

 $c_{\rm I}$ concentration of inhibitor

The magnitude of the constant of inhibition k_i expresses the strength of the inhibiting effect of the inhibitor. Some pesticides and their metabolites exhibit differences in the ratios of their inhibition constants with respect to cholinesterase of up to 1:500.

Many organophosphorus derivatives, in particular thio- and dithiophosphate derivatives, inhibit cholinesterase to a very slight degree. However, their inhibiting effects can be increased by a factor of up to 1,000 if they are first oxidized to organophosphate analogues. Thio- and dithiophosphate esters are converted to their analogous, toxicologically active phosphonates using Br_2 as the oxidizing agent. Limits of detection (LOD) and quantification (LOQ) depend both on the insecticide and on the enzyme used (Table 8.1). The inhibitory effect of paraoxon, malaoxon, and carbofuran with different esterases was investigated by Akkad and Schwack [20] using rabbit liver esterase, B. subtilis esterase, and cutinase from F. solani pizi. LODs are for B. subtilis esterase and rabbit liver esterase, proving the high sensitivity of these esterases to organophosphorus and carbamate insecticides [20].

8.3.3.3 HPTLC-Cholinesterase Assay Procedures

Methods generally follow the steps sample application, (HP)TLC separation, dipping the plate into an enzyme solution, incubation (which means time for enzyme activity), spraying with or dipping into a substrate solution, stopping the enzyme reaction by heat or drying, and plate evaluation. The inhibitory effect is determined by the reduction of enzymatic substrate hydrolysis. Enzyme inhibition

 2.7×10^{4}

 1.6×10^{4}

 3.2×10^{3}

 1.6×10^{3}

 1.4×10^{5}

1.0 ×10

Cabaryl

Aldicarb

Oxamyl

Butoxycarboxim

Pentachlorophenol

Butocarboxim

carbamates, and pentachlorophenol. The inhibition constants are for cholinesterase from horse serum [23]		
Active substance (enzyme inhibitor)	Detection limit HPTLC-	Inhibition constant,
•	cholinesterase assay (ng)	k_i (L/mol/min)
Parathion (after oxidation)	0.045	_
Paraoxon-ethyl	0.013	4.9×10^{5}
Paraoxon-methyl	0.400	2.2×10^4
Mevinphos	0.200	1.4×10^{4}
Dichlorovos	0.200	5.2×10^4

0.200

0.400

0.100

0.800

0.800

20.00

Table 8.1 Detection limits using an HPTLC-cholinesterase assay for several organophosphates,

Reaction 8.2 Enzymatic reaction of cholinesterase on a TLC plate, (1) 1-naphthyl acetate, (2) αnaphthol, (3) fast blue salt B, and (4) diazonium dye [9]

is revealed by bands of different colours than the background, depending on the substrate. Acetylcholine esterase is able to hydrolyse various esters.

Cholinesterase Enzyme Solution

Dissolve 11 mg cholinesterase (50 U/mg) in 180 mL of 0.05 M pH 7.8 tris(hydroxymethyl)-aminomethane-HCl buffer, and add 100 mg of bovine serum albumin to 8.3 Enzyme Tests 211

dilute the enzyme and improve its stability on the layer [23]. Alternatively, an enzyme solution can be prepared from 5 g beef liver in 45 mL tris-buffer (pH 8.2, homogenized for 2 min). The supernatant obtained by centrifugation (4,000 U/min) can be stored in a refrigerator and diluted 1–4 with water if necessary [17, 18, 24]. Mix with tris (24.3 g/L) and 20 mL 0.1 M HCl as tris-buffer (25 mL 0.2 M) and top up with water to 100 mL.

Different Reagent Solutions

One of the first methods using cholinesterase inhibition is attributed to Ackermann [25]. After the separation the plate was dried and then dipped into a solution of the enzyme followed by a solution containing a mixture of 1-naphthyl acetate and a diazo-group reagent. The enzyme hydrolyses the 1-naphthyl acetate into acetic acid and 1-naphthol, which forms a dye in conjunction with the diazonium cation. Diazo dyes are not formed in inhibition areas because 1-naphthol is not available (Reaction 8.2).

The diazonium cation reagents (250 mg 1-napthyl acetate) in 100 mL absolute ethanol and 400 mg fast blue salt B [23] are dissolved in 160 mL water. Other diazonium cations like fast black salt K or 4-nitrobenzodiazonium tetrafluoroborate (400 mg in 100 mL acetone) [26] can be used. Dip the dried plate in the enzyme solution for 2 s and incubate at 37°C in a chamber at 90% relative humidity for 30 min. Then dip the plate for 2 s in a freshly made solution of the diazonium cation reagent. After about 3 min, colourless spots appear on a violet background, which can be evaluated at 533 nm [23]. The reagent solution can be used with silica gel, aluminium oxide, and cellulose layers. The enzyme solution can be stored at 4°C for about 3 weeks (Fig. 8.4).

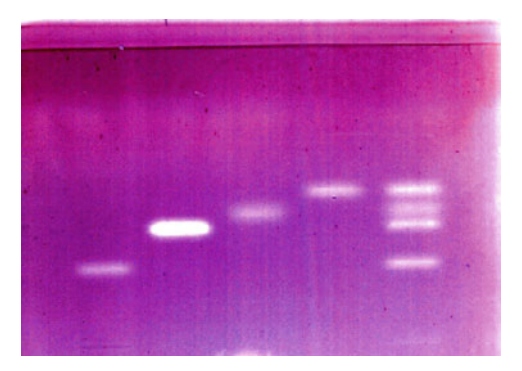
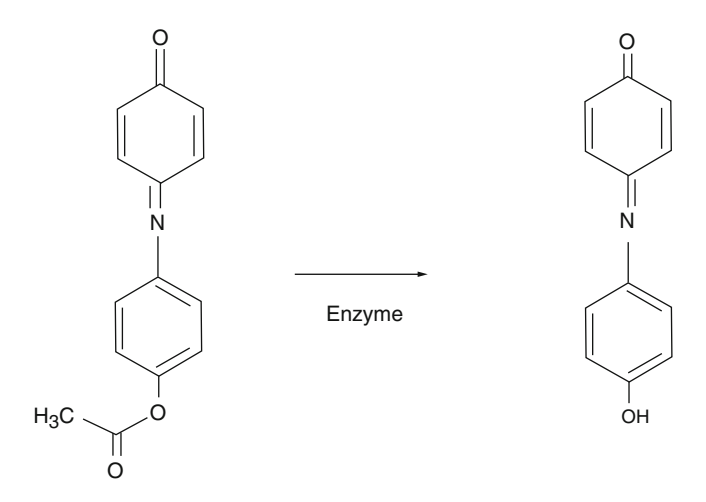


Fig. 8.4 HPTLC-cholinesterase assays with 1-naphthyl acetate as substrate coupled with fast blue salt B. From *left to right*: Paraoxon-methyl (0.4 ng/zone), paraoxon-ethyl (2 ng/zone), naled (0.4 ng/zone), and dichlorovos (2 ng/zone). Stationary phase HPTLC KG 60 F254 (10×10 cm), mobile phase, tetrahydrofuran–hexane, (7+25, V/V). The migration distance is 5 cm and the migration time is 15 min. For documentation a flatbed scanner was used [9]

Weins and Jork also used 1-naphthyl acetate as substrate in combination with fast blue salt B [23]. The detection limits are proportional to the inhibition constant of the particular substance and are in the lower pico-gram range (Table 8.1) [23]. As a fluorogenic reagent, maleimide CPM (7-diethylamino-3-(4'maleimidylphenyl)-4-methylcoumarin) was used by Hamada and Wintersteiger [27]; this reacts with thiocholine enzymatically released from acetylthiocholine to form a strong blue fluorescent background. In this way, the sites of enzyme inhibition by pesticides can be identified as dark spots. Different assays using chromogenic substrate systems have been reported [28–34]. Winterlin used colourless indophenyl acetate as an enzyme substrate transformed into blue indophenyl (see Reaction 8.3) [28]. He dissolved 10 mg of indophenyl acetate in 10 mL absolute ethanol and dipped the dry plate in the enzyme solution for 2 s followed by incubation in a chamber at 37°C and 90% relative humidity for 30 min. Then he dipped the plate for 2 s in the indophenyl acetate solution. White zones will appear on a light blue, non-fluorescent background. For thiophosphonate pesticides and carbamates, pre-treatment with bromide fumes before dipping in the enzyme solution strongly enhances the recognition level [17, 18].

The most widely used method, as mentioned above, is coupling enzymatic produced 1-naphthol with a diazonium cation to form a coloured substance, like the fast blue salt B [23]. An alternative is to enzymatically hydrolyse indoxyl acetate [24, 29], 5-bromo-4-chloroindoxyl acetate [30], *N*-methylindoxyl acetate [31], or bromoindoxyl acetate [32].

Reaction 8.4 shows the transformation of non-fluorescing indoxyl acetate into strongly fluorescing indoxyl. However, with oxygen, indoxyl is oxidized into non-fluorescent indigo blue. For the reagent, dissolve 10 mg indoxyl acetate in 6 mL of



Reaction 8.3 Enzymatic reaction of indophenyl acetate forming blue indophenyl

8.3 Enzyme Tests 213

Reaction 8.4 Enzymatic reaction of cholinesterase with indoxyl acetate forming indoxyl, which can react with oxygen forming indigo [29]

Reaction 8.5 Enzymatic reaction of resorufin acetate (non-fluorescing) forming resorufin (fluorescing) [29]

absolute ethanol [24, 29]. Another possibility is a 0.5% *N*-methylindoxyl acetate solution in acetone–water (2+3, V/V) [31].

An alternative reaction is followed by the hydrolysis of (non-fluorescent) resorufin acetate into fluorescent resorufin, whereby non-fluorescent zones appear on a fluorescent background (Reaction 8.5) (Fig. 8.5) [29].

As reagent, mix 2.85 mL tris-buffer (0.01 M, pH 7.4) with 0.15 mL 0.001 M resorufin acetate solution [29]. Dip the dry plate in the enzyme solution for 2 s and incubate at 37°C in a chamber at 90% relative humidity for 30 min. Then dip the plate in the reagent solution for 2 s. If using indoxyl acetate, white zones can be detected on a light blue, partially fluorescent background. If using resorufin acetate, non-fluorescing zones appear on a fluorescent background.

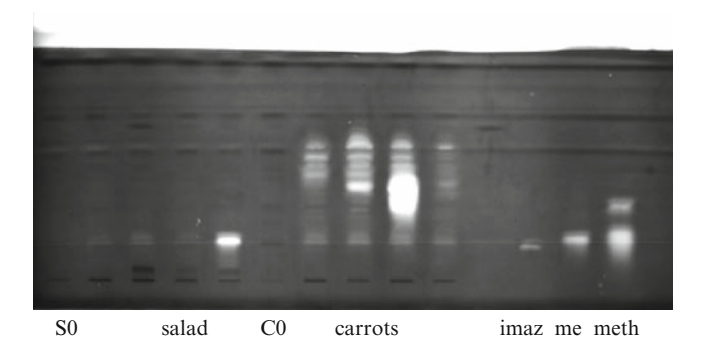


Fig. 8.5 Presence of esterase inhibitors in different plant food samples. *S0* control salad, *C0* control carrots, *Iiaz* imazalile 10 ng, *me* mercaptodimethur 30 ng, *meth* methiocarb 10 ng [9]

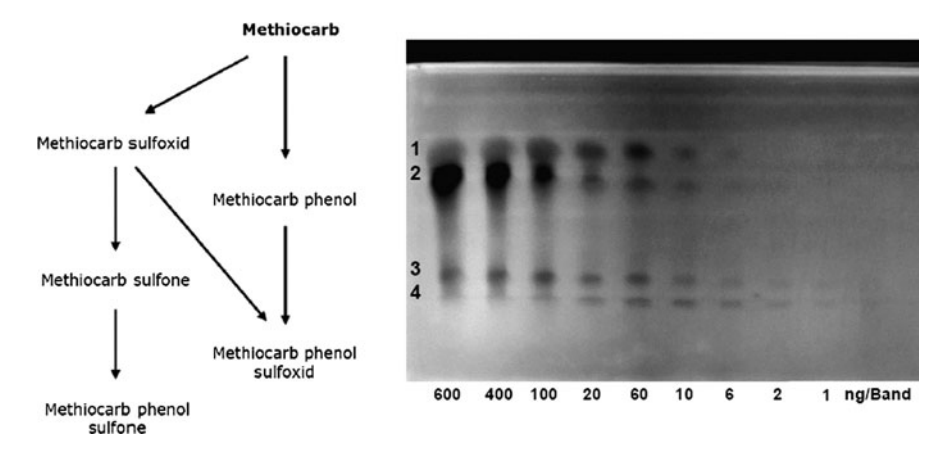


Fig. 8.6 Abiotic degradation of methiocarb and HPTLC-cholinesterase assay to detect its degradation products. Conditions for assay: stationary phase KG 60 F 254s (Merck); chromatography, automated multiple development AMD2 (Camag), documentation of the cholinesterase inhibition: SensiCam® (AVT Horn, Aalen, Germany); and identification, (1) methiocarb, (2) methiocarb sulphoxide, (3) methiocarb phenolsulphoxide, (4) methiocarb phenolsulphone [9]

Bioeffective compounds can be detected by TLC enzyme assay in the lower pico-gram range, which is often below the detection limit of instrumental methods. The method can be used to check the purity of chemical standards. Figure 8.6 shows a separation of methiocarb and its bioactive degradation product, which could be identified by an HPTLC-cholinesterase assay. Figure 8.6 underlines that the degradation product methiocarb sulphoxide (2) is much more effective in bioluminescence inhibition than methiocarb (1).

8.3 Enzyme Tests 215

8.3.3.4 Quantitative Analysis of HPTLC-cholinesterase Assays

The in situ quantification is performed either by absorbance measurement at 533 nm or by detecting the differences of colour intensities with a video-densitometric scanner.

A linear relationship between the signal of the enzyme inhibition and the concentration of its inhibitor is demonstrated using a solution of constant specific enzyme activity (units/mg protein) and constant incubation time (Fig. 8.7). For the optimized assay conditions, calibration can be performed over a wide range of concentrations. At the upper limit of the calibration curve, zone broadening results in large oval spots [20, 23].

The signal of the enzyme inhibition depends on the difference between the kinetics of the non-inhibited and inhibited enzyme when the substrate is converted to its specific product. Therefore the signal intensity is determined by the reaction time, which starts when the substrate of the enzyme has been added. Figure 8.8 shows the optimum of the signal intensity as a function of the reaction time. A peak maximum can be observed between 2 and 4 min.

For detection of a specific inhibitor by a selective enzyme the limits of detection (LOD) depend on:

- 1. The enzyme activity (units/mL solution) of the dipping solution (where time and conditions of storage can change the enzyme activity)
- 2. The specific enzyme activity (units/mg protein) of the dipping solution (where the content of biochemical inert protein, e.g. bovine serum albumin determines the amount of active enzyme protein on the layer)
- 3. The reaction time of the substrate catalysed by the enzyme (because the reaction time on the TLC plate affects the inhibition signal)

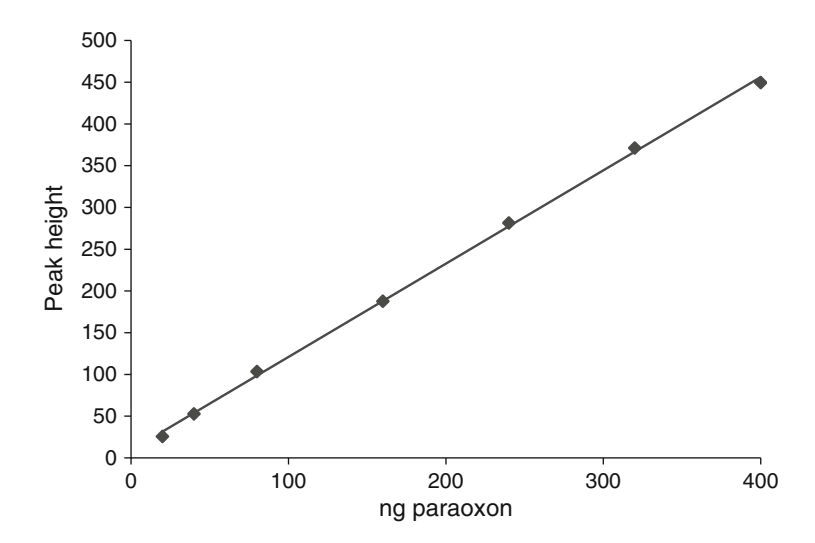


Fig. 8.7 Linear calibration for paraoxon in the range 20-400 pg per track. Peak heights are measured at 533 nm

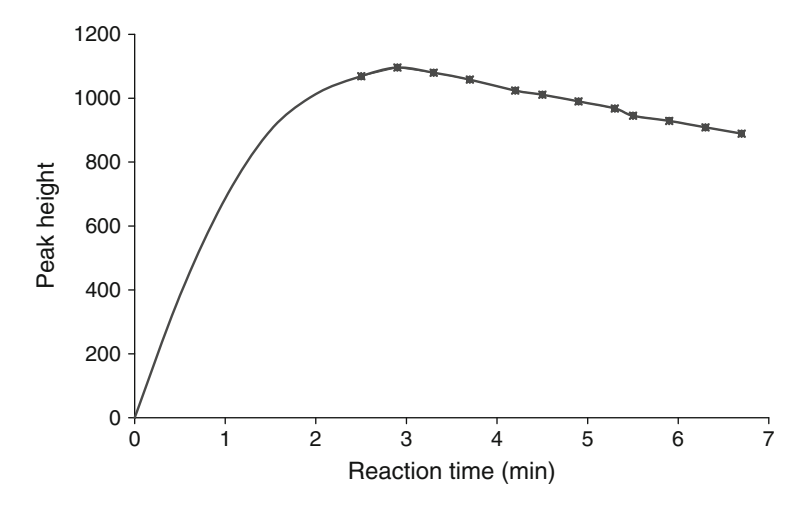


Fig. 8.8 Correlation of the inhibition signal of paraoxon with the reaction time, measured at 533 nm (TLC Scanner CD 60, Desaga Heidelberg, Germany)

8.4 Inhibition of Photosynthesis by Herbicides

Herbicides include many substances with different chemical structures that attack various parts of the plant organism to block its growth. The most important types by quantity are the triazines, such as atrazine, simazine, and terbuthylazine, which inhibit photosynthesis [35–38]. The basis of the chloroplast assay for the inhibition of photosynthesis is the inhibition of the Hill reaction. Isolated chloroplasts or chloroplast fragments from leaves are applied to the thin-layer plate after development to detect herbicidal active substances. The blue redox-indicator 2,6-dichlorophenolindophenol (DCPIP) is de-coloured by chloroplasts. DCPIP acts as an electron acceptor and loses its blue colour. The following method can determine about 40–45% of all commercially available herbicides [36].

8.4.1 Reagent Preparation

The chloroplasts are isolated from spinach leaves. Rinse 300 g fresh spinach leaves with distilled water and remove the leaf stems and veins. Place about 140 g of rinsed leaves and 20 g of ice in a container wrapped in aluminium foil in ice water, homogenize, and gradually add 30 mL of buffer solution (phosphate buffer pH 7.5, for which 700 mg KH₂PO₄ are dissolved in a litre of water). Filter this homogenized mixture through a fine gauze (e.g. bandage fabric) with slight hand pressure and then divide the filtrate between three falcon tubes (wrapped in aluminium foil). Centrifuge at 3,600 rpm at 14°C for 10 min. Dispose of the supernatant. The

chloroplast pellets are suspended in 30 mL phosphate buffer containing 3 g glycerine and then frozen in 5 mL portions. The chloroplast solutions must be stored in the dark. Dissolve 20 mg 2,6-dichlorophenolindophenol in 50 mL water. Mix 5 mL of the chloroplast solution with 45 mL water, and then mix this suspension with 2,6-dichlorophenolindophenol solution in the ratio 5:1.

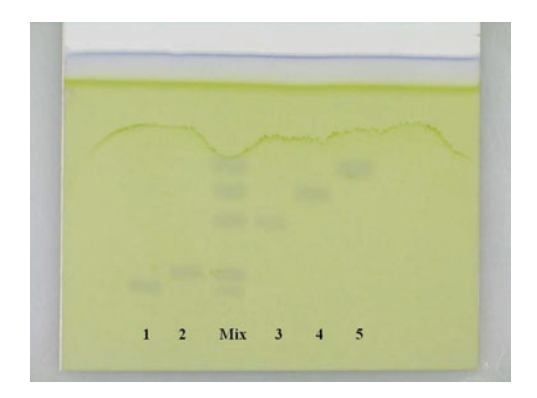
8.4.2 Hill Reaction

Dip the dry plate in the 5:1 mixture (see above) for 4 s [37]. Cover the TLC plate with another glass plate to keep the layer moist, and then expose the plate to intense white light (ca. 40 W) at a short distance for about 2–5 min. (Halogen floodlights are suitable for this purpose, placed at about 20 cm above the plate.) The light exposure should be stopped when the background stops fading. Hill reaction inhibitor substances show within 1–2 min blue-grey zones on a pale yellow-green background. To increase the contrast, the moist plate can be dipped into a solution of PEG-600 (10% PEG-600 in methanol) for 2 s. Afterwards, the plate should be scanned as soon as possible. PEG-600 enhances the red chlorophyll fluorescence in chlorophyll. The reagent can be used on silica gel and cellulose plates. Figure 8.9 shows the separation of five triazine herbicides. On track 1s and 2 as well as on tracks 4–6, standards are separated. The standard mixture is separated on track 3.

8.4.3 Detection Using Algae

Algaecide compounds, such as herbicides, copper-ions, or benzalkonium chloride, are detectable using the sweet water algae *Pseudokirchneriella subcapitata*. The algae are immersed in Jaworski medium for 2 weeks to grow [39]. The dry plate is

Fig. 8.9 Separation of triazine herbicides: (1) Atraton (2 ng per zone), (2) terbumeton (1 ng per zone), (Mix) mixture off all herbicides, (3) simazine (2 ng per zone), (4) atrazine (1 ng per zone), and (5) terbuthylazine (1 ng per zone) on silica gel with cyclohexane–methyl *tert*-butyl ether (1+1, V/V) as mobile phase



sprayed with a solution of 740 mg $CaCl_2 \cdot 2H_2O$, dissolved in 50 mL of water. The plate is then dipped in the algae suspension and incubated at 21°C in a water saturated humidity chamber for 1 day. The plate is then sprayed with a solution of 20 mg of triphenyltetrazolium chloride in 10 mL of water and incubated for another 1–2 days. Algaecide zones will appear yellow on a blue-violet background [39].

8.5 Detecting Bioeffective Compounds with Photobacteria

The non-pathogenic marine bacterium *Aliivibrio fischeri* (formerly *Vibrio fischeri*) and *Photobacterium phosphoreum* are especially suitable as a biological detector because their luminescence is directly connected with energy metabolism. Thus every disturbance of energy production in the cells will be indicated by a change in light emission [22, 40]. Because of the numerous ways of affecting energy production, the luminescent bacteria react to a wide range of substances. Currently known modes of action are:

- 1. Non-specific disturbance of the membrane structure (narcotic effect)
- 2. Effect on the proton gradient
- 3. Inhibition of electron transport because of the occupation of receptors [22, 27]

The comparatively quick and low-cost bioassay with the luminescent marine bacterium *Photobacterium phosphoreum*, strain NRRL-B-11177, has gained considerable popularity for the monitoring of industrial effluents and to assess the toxicity of different chemicals. Many toxic substances (nearly 1,350 individual organic compounds) show an inhibition of the bioluminescence of *P. phosphoreum* and *V. fischeri* in vitro [27].

After development, toxic substances on the layer are identified by dipping the plate for 1–2 s into a suspension of bacteria and determining the difference of photon emission using a cooled charged coupled device camera in a dark chamber. A linear correlation between the inhibition of bioluminescence of *P. phosphoreum* and the concentration of an inhibitor is obtained. A detection limit between 10 and 20 ng for pentachlorophenol and about 7.5 ng for dichlorophenol is obtained [23, 27].

8.5.1 Practical Use of Photobacteria

Dipping a TLC plate in a suspension of photobacteria is an elegant way of detecting toxic substances on the plate. Photobacteria emit light via luciferase enzymes using long-chained aldehydes as a substrate. Their bioluminescence depends directly on the metabolic status of the cell. If there is a certain concentration of these cells in the medium, this sets an auto-inducer free, $(N-(\beta-hydroxybutyryl)homoserin-lactone)$,

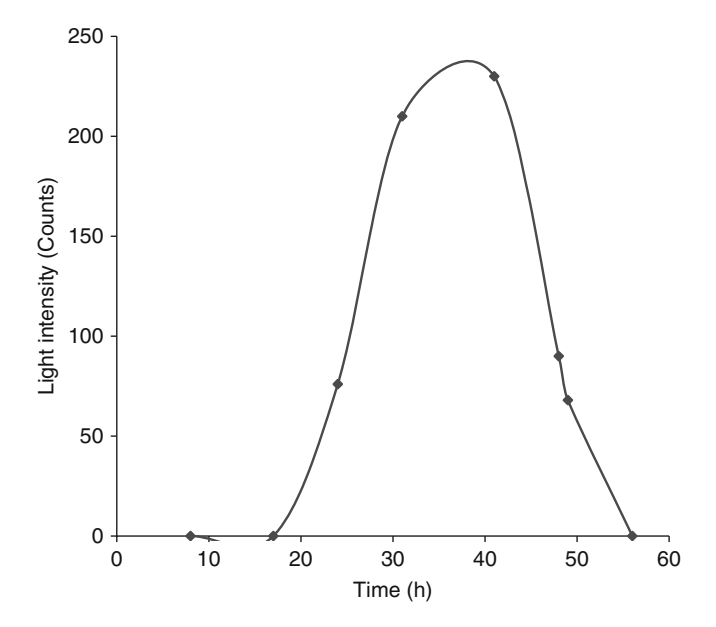


Fig. 8.10 Light emission from marine *bacterim V. fischeri* over a growth period (at 23°C). The emission maximum is attained after 38 h

which incites the bacteria to luminosity. This is the case when the (slightly shaken) bacteria have been kept incubated at room temperature for 24–40 h at ambient temperature. The luminous emission lasts for a maximum of about 20 h, shown in Fig. 8.10.

To start a bacteria culture all that is required is to pipette freeze-dried luminous bacteria into a reliable reactivating solution: a combination of the following salts, dissolved in 1 L of water and autoclave:

20 g NaCl 0.3 g KCl 2.035 g MgSO₄·7 H₂O

Then let the photobacteria grow in the following medium (calculated for 2 L and adjusted to pH 7.0 \pm 0.2):

60 g	NaCl
12.2 g	NaH ₂ PO ₄ ·H ₂ O
4.2 g	K_2HPO_4
0.4 g	MgSO ₄ ·7 H ₂ O
1.0 g	$(NH_4)_2HPO_4$
3.4 mL	glycerine (87%)
10 g	peptone from casein
1 g	yeast extract

The nutrient medium is heated at 121°C for 20 min and then stored in a refrigerator. The solution should have a pale yellow colour. For reactivation, thaw 5 mL of the bacteria (kept as cold as possible) in a reactivation solution. Leave the mixture to stand for 15 min and then pour into 220 mL of nutrient medium. Shake this mixture at room temperature for 25–30 h, after which it will be ready for use. Dip the TLC plate into the bacteria suspension for 3 s and then gently wipe off the dipping solution with a wiper. Place a clean glass plate on top of the layer and with a light-sensitive camera measure the luminescence for 2–20 min. Such photobacteria can only be used on silica gel, nylon, and cyanopropylsiloxane-bonded silica layers.

8.5.2 Reaction Time Optimization

Enzyme or bacteria inhibition is determined by the reaction time, which starts when the enzyme or the bacteria are added to the layer. Enzymes show an optimum signal inhibition after some minutes. The optimum reaction time for V. fischeri is in the range of hours. Figure 8.11 shows the separation of two diclophenac spots (containing 2 and 3 μ g dichlophenac) on cyanopropylsiloxand-bonded silica layers, measured at different times after V. fischeri incubation. The inhibition areas increase but the intensity of the background luminescence decreases because the

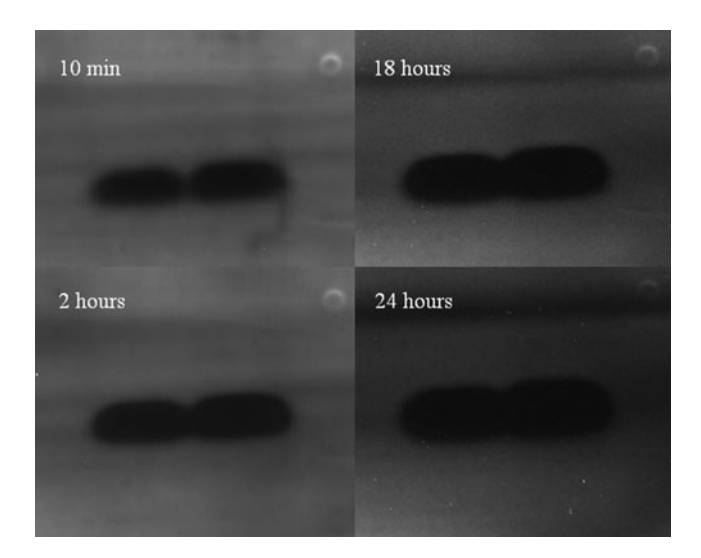


Fig. 8.11 Separation of 2 and 3 μ g diclophenac on cyanopropylsiloxane-bonded silica layers using dichloromethane—methanol—cyclohexane (95+5+30, V/V) as mobile phase and *V. fischeri* luminescence detection at different incubation times. The inhibition areas increase and the background luminescence intensity decreases depending on the time

bacteria cannot stay living at a TLC plate surface for more than some hours. The optimum signal, calculated as the maximum difference between signal and background, is observed after 1–2 h. This shows that in quantitative bioeffective-linked analysis the reaction time must be selected with care.

8.5.3 Applications of Photobacteria

Sample preparation plays an important role in bioeffective-linked analysis, which targets the detection of hazardous compounds in a sample rather than a huge number of chemical entities. For this purpose the sample has to be fractionated according to its polarity, molecular size, or acidity [40].

For evaluation of water in a rainwater overflow basin and in a creek near an expressway, sample pH was adjusted to 2 and 7. Enrichment was performed by solid-phase extraction (SPE); the enrichment factor was 500. Liquid-liquid extraction with methyl *tert*-butyl ether (MTBE) was used for the removal of matrix components. Samples (30 μ L) of the extracts were applied to the TLC plate. Analysis of the results indicated that inhibitions by extracts obtained by SPE were stronger than those from liquid-liquid extraction (Fig. 8.12) [41]. More inhibitory substances were present in the creek sample at both adjusted pH values than for rainwater from the storage reservoir.

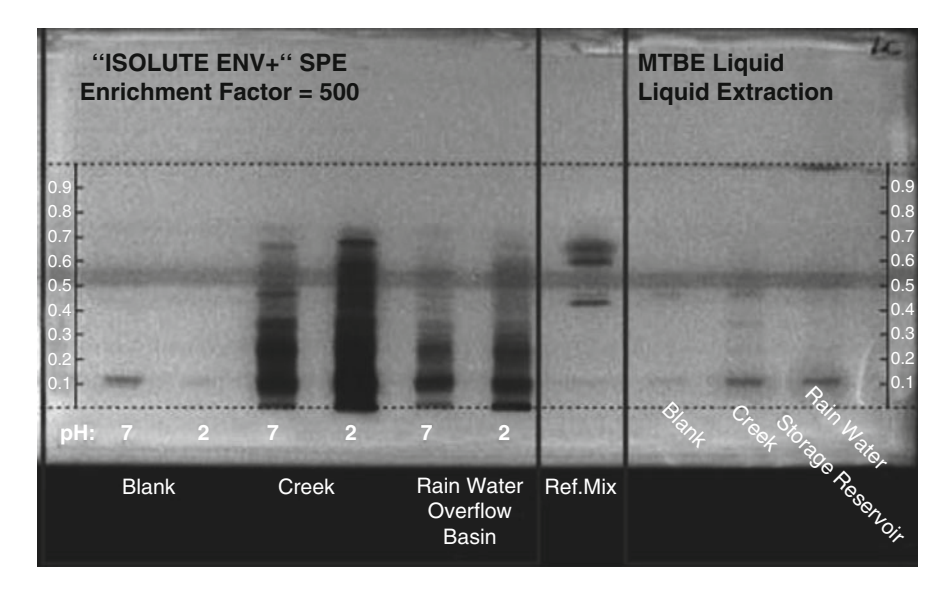


Fig. 8.12 Detection of inhibition of bioluminescence from expressway wastewater samples. Desmetryn, p-chlorophenyl methyl sulphone, and 3,4-dichloroaniline were used as reference compounds (From [41] with permission. © Akadémiai Kiadó.)

8.6 Detection of Fungicidal- and Antibiotical-Active Substances in Environmental Samples

There are about 300 permitted active substances in food and water samples, such that even the development of an analytical procedure for one group of substances involves a great deal of time and expense, while the possibility remains that a similar contaminant is released into the environment which is not detected by the measurement programme set-up. The presence of unknown harmful agents can only be detected by their biological effect. Bioactivity-based analysis using the combination AMD/HPTLC is of great importance because it is capable of identifying substances by fungal spores or yeast strain inhibition zones.

8.6.1 Determining Fungicides

The presence of fungicides that inhibit growth can be detected and quantified on a TLC plate using a suitable test organism. *Penicillium expansum*, ATCC 7861, in particular, has proved suitable for determining fungicides [42] besides other test organisms, such as Curvularia lunata, Aspergillus niger, Alternaria brassicicola, Cladosporium cucumerinum or Rhizopus sp. [19, 20, 43–48]. Candida albicans[49] and other bacterial groups are also suitable [50-53]. Normal household baking yeast can be used for this purpose as well [52]. For an overview of the various techniques, see [46]. The yeast strain *Rhodotorula rubra* is a useful test organism, which imparts a red colour to the layer when growing successfully. In the presence of a fungicidal active substance a white inhibition zone is produced, whose size depends on the amount of fungicide and on its specific activity [47]. Suitable for cultivation is a nutrient solution containing 7 g KH₂PO₄, 3 g Na₂HPO₄ · 7 H₂O, 4 g KNO₃, 1 g MgSO₄ · 7 H₂O, and 1 g NaCl in 1 L of sterilized water. Mix 10 mL of this solution with 60 mL of a sterilized 30% glucose solution in 0.1% Tween 20 solution. The suspension should contain 10^7-10^9 cells/mL. The dried plate is dipped into this suspension for 3 s and then incubated in a humid chamber at 25°C for 1-3 h [42]. The chamber should be draped with a piece of wet filter paper to keep the atmosphere moist. *Penicillin* spores will turn green and inhibition zones can be detected as white zones. This process can also be used for two-dimensional separations [48].

8.6.2 Screening of Pesticides in Food and Surface Water

The extraction of all plant protection agents was carried out according to the German Standard DFG S19. Plant materials, 100 g, were extracted by acetone and water (2+1, V/V). The water phase is separated from the organic fraction of the

homogenate by the addition of dichloromethane and 50-100 µL of the organic phase applied to two HPTLC plates and separated according to DIN 38 407 Part 11. One plate was dipped for 2 s into a *Penicillium* spore suspension and incubated at 21°C in a water saturated humidity chamber for 15 h [47]. The results from a screening experiment for fungicides in plant foods are shown in Fig. 8.13. The plate covered by *Penicillium* spores was documented by illumination with a light source of 254 nm. The inhibition spots are visible as bright zones due to excitation of the phosphorescence indicator in the stationary phase.

Detection of Compounds by Antibiotic Activity 8.6.3

It has been demonstrated that large numbers of antibiotic-resistant bacteria are present in the environment. They are released directly into the environment during the application of slurry and dung from intensive animal rearing, or they collect in water treatment plants arriving in the wastewaters from clinical and domestic sources [45]. The bacterium B. subtilis ATCC 6633 (hay bacteria) was shown to be useful for determining antibiotics. After AMD development B. subtilis was used as the indicator organism in the activity analysis that follows. The growth of the test organism on the thin-layer plate is inhibited by antibiotic active compounds and the zones of inhibition are detected by means of a bacterial vitality test, where the bacterial lawn on the thin-layer chromatogram is sprayed with an MTT tetrazolium salt [54]. The nutrient solution consists of 1,000 mL of meat broth (boiled minced meat) with 10 g of peptone, 3 g of NaCl, and 2 g of Na₂HPO₄ – all mixed together to a pH optimum of 5.5–8.5. The nutrient solution must be sterilized by autoclaving at 121°C for 20 min before use. The bacterial suspension is added under sterile

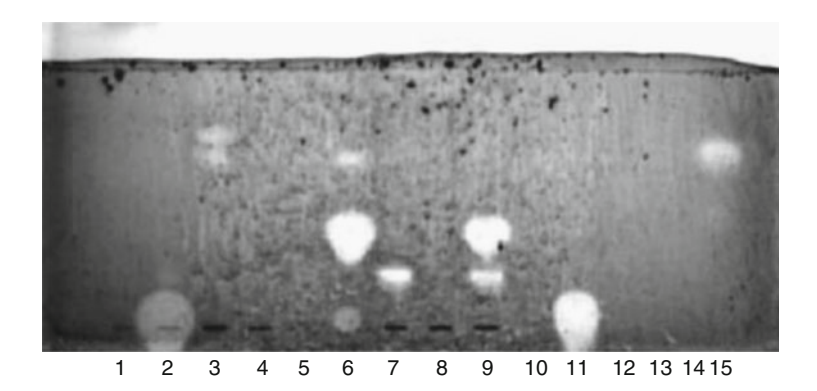


Fig. 8.13 Presence of fungicides in different plant food samples: (1) control strawberries, (2–5, 9) strawberries, (6) control raisins, (7, 8, 10) raisins, (11–15) fungicide standards (30 ng fenpropathrine, 10 ng imazalile, 30 ng mercaptodimethur, and 10 ng procymidome per zone) (From [1] with permission. (C) Akadémiai Kiadó.)

conditions to the nutrient. The dried TLC plate is dipped into the suspension of bacteria or yeast and the bacteria or yeast is allowed to grow directly on the plate surface at 23–35°C in a humid chamber for 19 h [52, 53]. Most important is that the plate should not contain solvent residues leftover from the mobile phase. In some cases it is necessary to develop the plate with pentane after the separation to wash out mobile phase residues. For the reagent solution, dissolve 20 mg of triphenylte-trazolium chloride in 10 mL of water. The incubated plate in dipped in the dye solution for 2 s. Yellow inhibition zones appear on a blue-violet background after 5–30 min.

The size of the inhibition zones is determined by the sample amount applied to the layer and by the specific activity of the substance. Figure 8.14 shows the separation of different amounts of chloroamphenicol, oxytetracycline, and lasalocide. After separation the plate was dipped in a *B. subtilis* suspension, incubating for 16 h, and stained with 3-(4,5-dimethylthiazol-2-yl)-2,5-diphenyltetrazolium bromide (MTT). The stained plate was scanned by a simple flatbed scanner. Inhibition zones show white areas on a blue-red background. Dehydrogenase activity (which indicates living bacteria) is detected by an oxidation of the light yellow MTT to a blue-red formazone dye.

Target bacterial cells in the logarithmic growth phase were found to be the most sensitive for reaction with appropriate reagents on TLC plates [54]. Detecting aflatoxin B1 by *Pseudomonas savastanoi* pv. *Phaseolicola* bacterial cell suspensions, the formaldehyde capturer L-arginine decreased, whereas the formaldehyde generator—mobilizer Cu(II) ions increased, the antibacterial toxic effect [54]. Direct bioautography performed with luminescence gene-tagged bacteria like luminescent *B. subtilis* enables an almost real time detection of antimicrobial compounds. The light emission of engineered luminescent bacteria has no complex control; it depends only on the metabolic state. In this way transgenic luminescent microorganisms tagged with different Lux gene constructs combine the advantages of luminescence detection with the ability of measuring antibacterial effects. Using this method the detection of chamomile (*Matricaria recutita*) components having

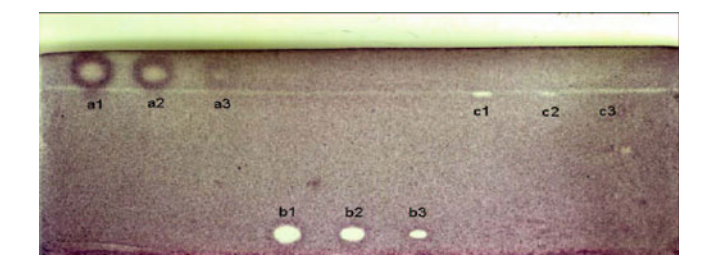


Fig. 8.14 Separation of different amounts of chloroamphenicol (a1–a3), oxytetracycline (b1–b3), and lasalocide (c1–c3, 25 ng, 15 ng, and 5 ng each). After separation the plate was dipped in a *B. subtilis* suspension, incubated for 16 h, and stained with 3-(4,5-dimethylthiazol-2-yl)-2,5-diphenyltetrazolium bromide (MTT) [9]

antibacterial effect against luminescent *B. subtilis* soil bacteria was more sensitive compared with the commonly used bioautographic visualization method of staining with a tetrazolium salt [55].

8.7 Yeast Estrogen Screen

A wide variety of compounds are known to possess estrogenic properties, and new endocrine disrupting compounds are still being discovered. Estrogen receptor agonists include natural and synthetic hormones, phytoestrogens, and chemicals such as metabolites of alkylphenol ethoxylates, bisphenol-A, parabens, benzophenones, phthalates, and various UV filters. Many of these compounds have been found in wastewater or sewage treatment plant effluents and are known to be released into the environment. Investigations on endocrine disrupters are mostly done using either exclusively analytical or biological methods only [8]. Only a few publications use TLC [56, 57]. Determination of estrogens in environmental samples is possible by recombinant yeast (Saccharomyces cerevisiae) that contains a human estrogen receptor DNA sequence [8, 58]. The yeast cells grow on the TLC layer and, in the absence of estrogen-like substances, produce the enzyme β-galactosidase. The plate is sprayed with a solution of 4-methylumbelliferyl- β -digalactopyranoside, which, in the presence of the enzyme β -galactosidase, releases the strongly fluorescent 4-methylumbelliferon [8]. Chlorophenol red β -D-galactopyranoside can also be used to measure β -galactosidase activity. In the presence of the enzyme β-galactosidase, the yellow compound turns into a red dye, which can be detected by absorption at 540 nm [58].

The yeast estrogen screen (YES) was introduced as a new bioautographic detection method for HPTLC analysis [58]. In 2004, Müller, Dausend, and Weins [8] selected the YES screen from the then existing in vitro bioassays for estrogenic compounds, because the yeast cells are more suitable for cultivation on HPTLC plates than other test organisms or organelles, such as the E-screen assays based on vitellogenin formation or receptor binding assays. Recombinant yeast cultures can be grown directly on HPTLC silica gel plates, where in the presence of estrogenic substances the enzyme β-galactosidase is produced. Chlorophenol red-β-D-galactopyranoside (CPRG) and 4-methylumbelliferyl β-D-galactopyranoside (MUG) are used as enzyme substrates (100 mg/100 mL of growth medium) [8]. Total test duration is 3 days. At day 1, a yeast culture was prepared. At day 2, silica gel plates were allowed to dry in air after development and before applying the yeast cell test culture. The dried plate was dipped in the test culture, which contains recombinant yeast and enzyme substrate, and was incubated at 32°C. At day 3, the dipped plate was sprayed with enzyme substrate solution (100 mg/100 mL) to enhance the staining contrast. CPRG conversion could be observed as a color change from yellow to red [8]. MUG conversion (after exposure to ammonia vapour) could be observed as fluorescence at 460 nm. The MUG sensitivity is improved by a factor of 20 in comparison to the substrate CPRG. As little as 2.75 pg of 17 β-estradiol

yielded a clearly detectable fluorescence signal on the HPTLC plate (Fig. 8.15). A quantitative correlation of 17 β -estradiol mass and the fluorescence signal was observed (see Fig 8.16).

The new HPTLC-YES procedure was applied to the analysis of estrone, estriol, nonylphenol, and octylphenol. While estrone and estriol could be detected by the HPTLC-YES assay, nonylphenol and octylphenol did not induce MUG conversion [8].

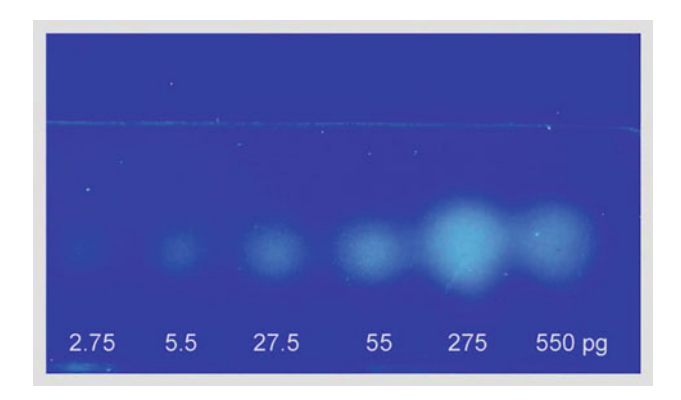


Fig. 8.15 Detection of hormones by HPTLC-yeast estrogen screen according to Routledge and Sumpter [8]. Detection limit for the HPTLC-YES test is 2.75 pg, using β -estradiol 4-methylum-belliferyl β -D-galactopyranoside (MUG) as substrate of induced β -galactosidase (From [1] with permission. © Akadémiai Kiadó.)

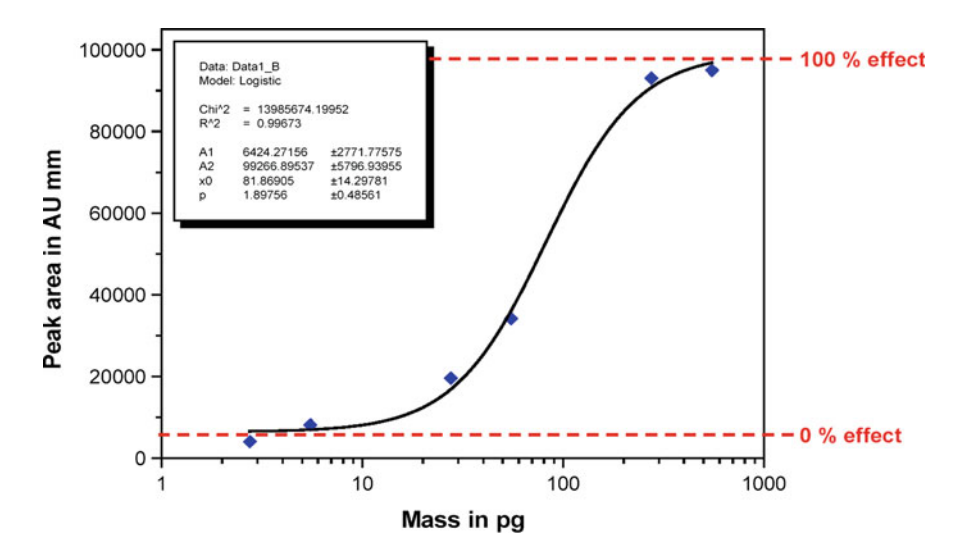


Fig. 8.16 HPTLC yeast estrogen screen (YES) assay. Illustrated is the quantitative correlation between the 17 β -estradiol mass and the fluorescence signal [8]

References 227

References

 Weins C (2008) Overview of bioactiveity-based analysis by HPTLC. Bridging the gap between cause and effect – HPTLC detection of bioactive compounds in the environment and in food. J Planar Chromatogr 21:405–410

- 2. Brack W (2003) Effect directed analysis: a promising tool for the identification of organic toxicants in complex mixtures. Anal Bioanal Chem 377:397–407
- Walker KC, Beroza M (1963) Thin-layer chromatography for insecticide analysis. J Assoc Off Agric Chem 46:250–261
- Mori H, Sato T, Nagase H, Sakai Y, Yamaguchi S, Iwata Y, Hashimoto R (1994) Rapid screening method for pesticides as the cause substance of toxicosis by TLC. Jpn J Toxicol Environ Health 40:101–110
- 5. Sherma J (2005) In: Cazes J (ed) Pesticide analysis by thin layer chromatography. Encyclopedia of Chromatography, 2nd edn. Dekker, New York, pp 1230–1238
- Sherma J (2005) Thin-layer chromatography of pesticides a review of applications for 2002–2004. Acta Chromatogr 15:5–30
- 7. Deutsches Institut für Normung (DIN) (ed) (1990) DIN 38407, part 11. Beuth, Berlin
- 8. Müller MB, Dausend C, Weins Ch, Frimmel FH (2004) A new bioautographic screening method for the detection of estrogenic compounds. Chromatographia 60:207–211
- 9. Weins C (2006) Dissertation Universität Basel (Prof. Dr. Michael Oehme)
- Geike F (1972) Verfahren zum dünnschicht-chromatographisch-enzymatischen Nachweis von Schwermetallen mit Urease. Fresenius Z Anal Chem 258:284–285
- 11. Geike F, Schuphan L (1972) Dünnschicht-chromatographischer Nachweis von Organoquecksilber-Verbindungen. J Chromatogr 72:153–163
- Pazur JH, Romanic BM (1979) Paper chromatography enzyme spray technique for the detection of sugar nucleotides with galactose and N-acetylgalactosamine residues. J Chromatogr 169:495–499
- 13. Yamaguchi Y (1979) Excretion pattern of 3ß-hydroxysteroids in patients with adrenal tumor, cushing's disease and 21-hydroxylase deficiency, and in pregnancy, using thin-layer chromatography and color development of 3ß-hydroxysteroids with 3ß-hydroxysteroid oxidase. J Chromatogr 163:253–258
- Yamaguchi Y (1980) Enzymic color development of urinary 3-hydroxysteroids on thin-layer chromatograms. Clin Chem 26:491–493
- 15. Mendoza CE (1972) Analysis of pesticides by thin-layer chromatographic-enzyme inhibition technique. Residue Rev 43:105–142
- Mendoza CE (1974) Analysis of pesticides by thin-layer chromatographic-enzyme inhibition technique, part II. Residue Rev 50:43–72
- Mendoza CE (1973) Thin-layer chromatography and enzyme inhibition techniques. J Chromatogr 78:29–40
- Mendoza CE, Shields JB (1973) Determination of some carbamates by enzyme inhibition techniques using thin-layer chromatography and colorimetry. J Agr Food Chem 21:178–184
- 19. Ambrus A, Hargitai A, Károly É, Fülöp G, Lantos A (1981) General method for determination of pesticide residues in samples of plant origin, soil, and water. II. Thin layer chromatographic determination. J Assoc Off Anal Chem 64:743–748
- Akkad R, Schwack W (2008) Multi-enzyme inhibition assay for detection of insecticidal organophosphates and carbamates by high-performance thin-layer chromatography.
 Basics of the method development.
 J Planar Chromatogr 21:411–415
- Marston A, Kissling J, Hostettmann K (2002) A rapid TLC bioautographic method for the detection of acetylcholinesterase and butyrylcholinesterase inhibition in plants. Phytochem Anal 13:51–54
- Rhee IK, van de Meent M, Ingkaninan K, Verpoorte R (2001) Screening for acetylcholinesterase inhibitors from amaryllidaceae using silica gel thin-layer chromatography in combination with bioactivity staining. J Chromatogr A 915:217–223

- Weins Ch, Jork H (1996) Toxicological evaluation of harmful substances by in situ enzymatic and biological detection in high-performance thin-layer chromatography. J Chromatogr A 750:403

 –407
- Schneider J (1986) Dünnschichtchromatographischer Nachweis von Methamidophos durch enzymatische Detektion. Die Nahrung 30:859–860
- Ackermann H (1968) Dünnschichtchromatographisch-enzymatischer Nachweis phosphororganischer Verbindungen. J Chromatogr 36:309–317
- Bhaskar SU, Nanda Kumar NV (1981) Thin layer chromatographic determination of methyl parathion as paraoxon by cholinesterase inhibition. J Assoc Off Anal Chem 64:1312–1314
- 27. Hamada M, Wintersteiger R (2003) Fluorescence screening of organophosphorus pesticides in water by an enzyme inhibition procedure on TLC plates. J Planar Chromatogr 16:4–9
- 28. Winterlin W, Walker G, Frank H (1968) Detection of cholinesterase-inhibiting pesticides following separation on thin-layer chromatograms. J Agr Food Chem 16:808–812
- Guilbault GG, Kramer DN (1965) Resorufin butyrate and indoxyl acetate as fluorogenic substrates for cholinesterase. Anal Chem 37:120–123
- Mendoza CE, Wales PJ, McLeod HA, McKinley WP (1968) Procedure for semi-quantitative confirmation of some organophosphorus pesticide residues in plant extracts. Analyst 93: 691–693
- 31. Štefanac Z, Štengel B, Vasilic Z (1976) Quantitative determination of organophosphorus pesticides by thin-layer densitometry. J Chromatogr 124:127–133
- 32. Wales PJ, McLeod HA, McKinley WP (1968) TLC-enzyme inhibition procedure to detect some carbamate standards and carbaryl in food extracts. J Assoc Off Anal Chem 51: 1239–1242
- 33. Vashkevich OV, Gankina ES (1990) Quantitative determination of organophosphorus pesticides by HPTLC with detection by enzyme inhibition. J Planar Chromatogr 3:354–356
- 34. Breuer H (1982) Sensitive and rapid detection of paraoxon by thin-layer chromatography and strips using enzyme inhibition and Ellman's method. J Chromatogr 243:183–187
- Kováč J, Kurucová M, Bátora V, Tekel J, Sterniková V (1983) Chronometric technique for the quantitative analysis of some photosynthesis-inhibiting herbicides. J Chromatogr 280:176–180
- Kováč J, Henselová M (1977) Detection of triazine herbicides in soil by a Hill-reaction inhibition technique after thin-layer chromatography. J Chromatogr 133:420–422
- Lawrence JF (1980) Simple, sensitive, and selective thin layer chromatographic technique for detecting some photosynthesis inhibiting herbicides. J Assoc Off Anal Chem 63:758–761
- 38. Sackmauerová M, Kovác J (1978) Thin layer chromatographic determination of triazine and urea herbicides in water by inhibition detection method. Fresenius Z Anal Chem 292:414–415
- Baumann U, Brunner C, Pletscher E, Tobler N (2003) Biologische Detektionsverfahren in der Dünnschichtchromatographie. Umweltwissenschaften und Schadstoff-Forsch 15:163–167
- 40. Eberz G, Rast H-G, Burger K, Kreiss W, Weisemann C (1996) Bioactive screening by chromatography-bioluminescence coupling. Chromatographia 43:5–9
- 41. Schulz W, Seitz W, Weins SC, Weber WH, Böhm M, Flottmann D (2008) Use of *Vibrio fischeri* for screening for bioactivity in water analysis. J Planar Chromatogr 21:427–430
- 42. Weins Ch, Collet P (2002) Bestimmung von Schadstoffen in Lebensmitteln Wirkungsbezogene Analytik, ein neues Konzept zur schnellen Erfassung von Pestiziden in einer Probe. Lebensmittelchemie 56:128–131
- 43. Adinarayana M, Singh US, Dwivedi TS (1988) A biochromatographic technique for the quantitative estimation of triphenyltin fungicides. J Chromatogr 435:210–218
- 44. Homans AL, Fuchs A (1970) Direct bioautography on thin-layer chromatograms as a method for detecting fungitoxic substances. J Chromatogr 51:327–329
- 45. Hamburger MO, Cordell GA (1987) A direct bioautographic TLC assay for compounds possessing antibacterial activity. J Nat Prod 50:19–22
- 46. Betina V (1973) Bioautography in paper and thin-layer chromatography and its scope in the antibiotic field. J Chromatogr 78:41–51

References 229

 Hostettmann K, Terreaux Ch, Marston A, Potterat O (1997) The role of planar chromatography in the rapid screening and isolation of bioactive compounds from medicinal plants. J Planar Chromatogr 10:251–257

- 48. Wehge DE, Nagle DC (2000) A new 2D TLC bioautography method for the discovery of novel antifungal agents to control plant pathogens. J Nat Prod 63:1050–1054
- Rahalison L, Hamburger M, Hostettmann K, Monod M, Frenk E (1991) A bioautographic agar overlay method for the detection of antifungal compounds from higher plants. Phytochem Analysis 2:199–203
- 50. Gafner J-L (1999) Identification and semiquantitative estimation of antibiotics added to complete feeds, premixes, and concentrates. J Assoc Off Anal Chem 82:1–8
- Vanderkop PA, McNeil JD (1989) Thin-layer chromatography/bioautography method for detection of monensin in poultry tissues. J Assoc Off Anal Chem 72:735

 –738
- 52. Eymann R, Fischer W, Hauck HE, Weins Ch (2001) Nachweis von Antibiotika in Futtermitteln durch wirkungsbezogene Analytik. Fleischwirtschaft 8:95–96
- Choma IM, Choma A, Komaniecka I, Pilorz K, Staszczuk K (2004) Semiquantitative estimation of enrofloxacin and ciprofloxacin by thin-layer chromatography direct bioautography. J Liq Chromatogr Rel Technol 27:2071–2085
- 54. Móricz ÁM, Adányi N, Horváth E, Ott PG, Tyihák E (2008) Applicability of the BioArena system to investigation of the mechanisms of biological effects. J Planar Chromatogr 21:417–422
- 55. Móricz ÁM, Tyihák E, Ott PG (2010) Usefulness of transgenic luminescent bacteria in direct bioautographic investigation of chamomile extracts. J Planar Chromatogr 23:180–183
- 56. Möller M, Landmark LH, Björseth A, Renberg L (1984) Characterisation of industrial aqueous discharges by the TLC/Ames' assay. Chemosphere 13:873–879
- 57. Houk VS, Claxton LD (1986) Screening complex hazardous wastes for mutagenic activity using a modified version of the TLC/Salmonella assay. Mut Res 169:81–92
- Routledge EJ, Sumpter JP (1996) Estrogenic activity of surfactants and some of their degradation products assessed using a recombinant yeast screen. Environ Toxicol Chem 15:241–248

Chapter 9 Planar Chromatography Detectors

From the beginning of the 1950s, paper chromatography was used to quantify samples. The paper was made transparent by liquids and transmitted light was measured according to the Lambert-Beer law. Silver-impregnated media were used as detectors, adapted from paper photography.

9.1 Transmittance Measurements in Thin-Layer Chromatography

In the mid-1960s, the techniques developed for the measurement of absorption in paper chromatography were transferred to thinly layered glass plates. Measurements were performed by transmittance using the Lambert-Beer law for quantification. Measuring the optical density led to the name "densitometric measurements". The optical density was plotted against the separation distance and this was called a densitogram. Densitograms could be viewed much quicker than scraping out separated zones and measuring them in a UV–visible spectrophotometric device, and in situ densitometric measurements were tenfold more sensitive [1].

In comparison to liquid measurements, in situ densitometry shows some peculiarities:

- The analyte is not uniformly distributed in the stationary phase and unlike for a liquid neither is the absorption density. The analyte signal is not only dependent on the analyte concentration but also dependent on its distribution within the zone [2].
- Due to the scattering effect, the length of the light path cannot be exactly determined, but it is obviously longer than the thickness of the layer, because light passes through the layer showing an enlarged spot size.
- A change in layer thickness has a distinct influence on the observed absorption, since light scattering and absorption both depend on the path length.

9.1.1 The Lambert-Reer Law

Transmittance measurements were described and quantified according to the Lambert-Beer law [2]. The probability of a photon being absorbed is considered to be proportional to the concentration of the absorbing molecules. This probability is expressed mathematically by the following equation:

$$\frac{\partial I}{I} = -kc\partial x.$$

In this equation I is the light intensity (at a particular wavelength), and ∂I is the change in light intensity by absorption in a thin layer of thickness ∂x containing a concentration c of absorbing molecules. The intensity of a light beam after passing through the distance d of the layer is

$$\int_{I_0}^{I_d} \frac{\partial I}{I} = -kc \int_0^d \partial x$$

$$\ln \frac{I_d}{I_0} = \ln(10) \lg \frac{I_d}{I_0} = -kcd.$$

It is convenient to use the logarithm to the base 10. With the introduction of the absorption (former: extinction) coefficient

$$\varepsilon = \frac{k}{\ln 10} = \frac{k}{2.303},$$

the final expression of the Lambert-Beer law is obtained:

$$A = -\lg \frac{I_d}{I_0} \equiv -\lg T = \varepsilon c d. \tag{9.1}$$

where

A absorbance

 I_d light intensity after passing through the layer a distance d

 I_0 incident light intensity

T relative transmitted light $(T \equiv I_d/I_0)$

ε molaric absorption coefficient

c concentration of the analyte in the spot

d layer thickness

The Lambert-Beer law describes the relationship between the incident light and the remaining light after absorption. The equation is valid only for absorptions in non-scattering media because the light lost during passage through the layer (the light intensity difference between I_0 and I_d) is attributed only to absorptions by the sample. Light lost as a result of scattering by the layer is not taken into account.

The expressions for light intensities (I and I_0) are physical parameters and contain a unit, which depends on the kind of measurement. The expression for the transmitted light intensity $T \equiv I_d/I_0$ (the light intensity which remains after passage through the layer) is introduced as a unit-less light intensity function.

TLC transmittance measurements have some noticeable disadvantages. The Lambert-Beer law is not applicable for TLC evaluations, because TLC plates scatter light. The most commonly used stationary phase (silica gel) as well as the glass support shows decreasing transmittance below 300 nm. Therefore the range below 300 nm is not available for TLC transmittance measurements. Nevertheless, in contrast to reflectance measurements, transmittance measurements afford higher light intensity and were recommended for a long time [1]. In 1967, Jork experimentally verified a correlation between transmittance intensity and layer thickness [3], which is reasonable in view of the Lambert-Beer law. The crucial point was his finding that reflectance measurements are independent of the layer thickness [3]. After this publication, measurements in the transmittance mode for TLC virtually ceased. Today transmittance measurements are used only for scanning polyacrylamide gels.

9.2 Reflectance Measurements in TLC and HPTLC

The term "volume reflectance" describes the process of light penetrating into a scattering sample and reemerging from the surface. Sometimes this is also called "diffuse reflectance". The term "regular reflection" describes light reflected in parallel from a plain surface, which is what happens when a mirror reflects light. Rough surfaces reflect light diffusely, i.e. light is reflected in all directions. This kind of light reflection is called "diffuse reflectance".

In 1964, Jork described a scanner, which was able to record a TLC separation in the reflectance mode using a light beam of nearly monochromatic light [1, 4]. Figure 9.1 shows the principle of transmission and reflectance measurements.

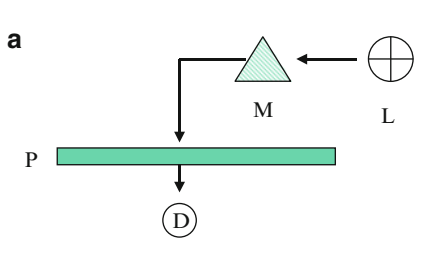


Fig. 9.1 The principles of **(a)**. TLC transmittance measurement in comparison to **(b)** a TLC reflectance measurement. *L* lamp, *M* monochromatic device, *P* TLC plate, and *D* detector

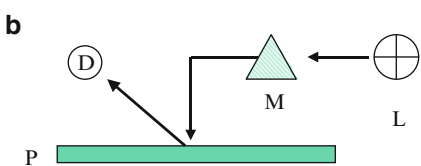




Fig. 9.2 Typical TLC scanner with optical path shown. The plate is illuminated by monochromatic light from above. The position of the detector, a photomultiplier, can be varied. Reflectance measurements are carried out by the detector (placed above) and transmittance measurements by the detector placed below the TLC plate (Photo published with permission from DESAGA, Heidelberg, Germany.)

The difference lies in the position of the detector. For reflectance measurements, the lamp and the detector are positioned above the TLC plate. This measurement principle has not changed in modern times. A monochromatic light beam of low intensity illuminates the plate surface from above (Fig. 9.2). The detector at an angle of 45° measures the scattered light that leaves the plate surface in all directions. The wavelength range generally lies in the range of 200 nm up to 700 or 800 nm. The wavelength dispersion device of the scanner illuminates the plate in the range ± 2.5 nm of the chosen wavelength. Measurements at several wavelengths require additional scanning of the track.

The incidental light spot is scattered in all directions within the layer, to an extent of more than 150 μm . Therefore the spatial resolution cannot be better than 300 μm . One disadvantage of the TLC scanner is the laborious method of recording UV–visible spectra. The light beam must be spatially fixed in the spot centre or sides, and the monochromatic device illuminates the spot with light of different wavelengths. The intensity of the reflected light is measured and plotted against the illumination wavelengths producing a conventional spectrum, which is a time-consuming process. In contrast, scanning a single track at a given wavelength can be completed within seconds.

9.2.1 The Kubelka-Munk Equation

In 1905, Schuster was the first person to investigate light scattering in fog [5]. He described two equations, which were later used by Kubelka and Munk to

describe painted walls [6]. According to the definition of the transmitted light intensity $T \equiv I_d/I_0$, Schuster defined a remission function which describes the remaining light I of the incident light intensity I_0 after scattering:

$$R_{\infty} = \frac{I}{I_0}$$
.

A detailed discussion based on the ideas of Schuster, Kubelka, and Munk is presented in Chap. 10 [7]. The important point is that Kubelka and Munk described an expression for multi-scattered light measured in the reflectance mode [6, 9]. To reduce the complexity of the mathematical expressions, Kubelka and Munk assumed that light inside the scattering medium is homogeneously scattered in all directions. The Kubelka–Munk expression adapted to TLC measurements is [9–11]

$$KM = \frac{(1 - R_{\infty})^2}{2R_{\infty}} = \frac{a}{s} = 2.3 \frac{\varepsilon}{s} c = 2.3 \frac{\varepsilon}{s} \frac{n}{dA},$$
 (9.2)

where

 R_{∞} absolute reflectance of an infinitely thick layer

a absorptivity (absorption coefficient)

ε molar absorption coefficient

s scattering coefficient

c TLC spot concentration

n analyte amount

A spot area

d layer thickness

The Kubelka-Munk function provides an approximate solution for TLC evaluations. The equation is valid for an infinitely thick TLC layer without regular reflection. All the light must be reflected from the top surface of the layer. No light losses may occur by transmittance (Kubelka and Munk assumed an infinitely thick layer of the scattering medium), and the layer itself may absorb no light. Furthermore, the analyte should be uniformly distributed within the analyte zone. It is obvious that TLC plates do not fulfil all these demands. The simple fact that the transmittance measurements are possible although the Kubelka-Munk theory assumes no light losses at the backside of a TLC layer shows that the Kubelka-Munk theory has only limited validity for TLC evaluations. The TLC layer thickness of 100 or 200 µm is far too thin to avoid transmitted light losses. Increasing the layer thickness does not increase the diffuse reflectance but will help to reduce light losses at the backside of the plate. A disadvantage of thick layers is that if d is extended with constant spot area yA, the detection limit (n)will decrease. Besides these disadvantages, (2.24) demonstrates that the chromatographic resolution decreases with increasing layer thickness. A possible way of increasing reflectance (and thus avoiding light losses) is to use aluminium sheets as a layer support, which can act as a mirror [12]. This increases the

intensity of the reflected light but cannot avoid loss of light due to absorption by the layer particles.

Despite the above considerations, reflectance measurements are the best way to evaluate TLC separations and especially for HPTLC plates, because reflectance increases with smaller particles [7, 8, 11, 12]. Both the absorptivity and the scattering coefficient increase with increasing layer thickness. Therefore the quotient of both should be independent of the layer thickness. Variations in the layer thickness should thus have no influence on reflectance measurements. This is exactly what Jork verified experimentally [3].

A uniformly distributed analyte zone is achieved by bandwise sample application and should be evaluated using slit scanning with a small spatial resolution [13]. In this way, segments of the sample on different tracks at the same separation distance exhibit the same uniform distribution. Regular reflection on TLC or HPTLC plates can be observed only at low incident light angles. Then the plate reflects light like a mirror. To avoid such regular reflections, incident light should illuminate the plate at a perpendicular angle to the layer.

A crucial point is the kind of sample application. The Kubelka–Munk expression describes a relationship between the transformed signal (KM) and the analyte amount n in the spot. In fact the observed signal depends on the concentration and the spot area. Different analyte amounts on different tracks should thus be applied in such a way as to obtain constant spot sizes after development. For quantification purposes it is essential that the developed spots have the same areas. This can be achieved by always applying the same sample volume or by applying the sample in bands of constant size [7, 13].

Due to the above-mentioned restrictions, Kubelka–Munk's equation is not often used for TLC evaluations. The reason is that according to the Kubelka–Munk theory, only absolute reflectance values are proportional to the analyte amount in the spot. Absolute reflectance implies reflection of all light if no absorption is present. The absolute reflectance of such a clean layer will be $R_{\infty}=1$ resulting in a KM value (according to (9.2)) of zero, indicating no absorption (a=0). If the layer shows no absolute reflectance, light losses cannot be counted as analyte absorption; it could also be due to light absorption of the layer itself.

There is no compound known that reflect all light without absorption. Thus, measurements of absolute reflectance cannot be expected from a TLC or an HPTLC plate. Fine MgO particles, freshly precipitated BaSO₄, or MgCO₃ may show nearly absolute reflectance and can be used to approximately determine the absorptivity of a stationary phase.

Nevertheless, some attempts in using the Kubelka–Munk theory for TLC evaluations have been published [1, 7, 11, 14–17]. Figure 9.3 shows a typical densitogram. Caffeine was separated using silica gel 60 as the stationary phase and 2-propanol–cyclohexane–aqueous ammonia (25%) (7+2+1, V/V) as the mobile phase. The track was scanned at 273 nm and transformed using the Kubelka–Munk equation. If their theory is valid, the integrated caffeine peak (the sum of all caffeine signals) should show a direct relationship to the caffeine mass.

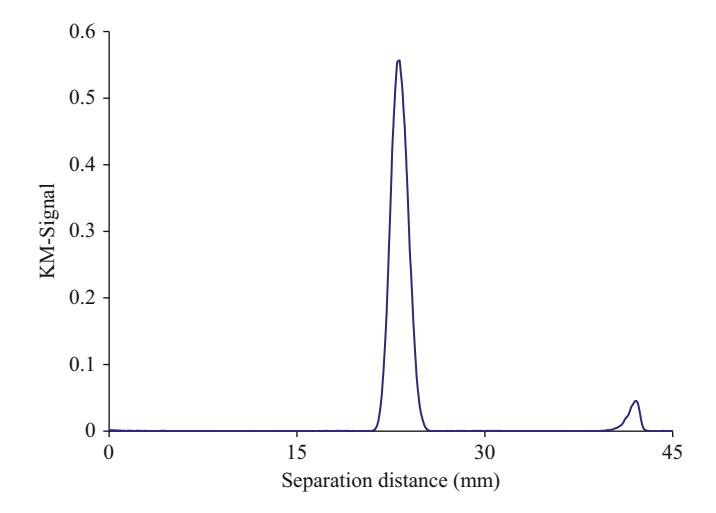


Fig. 9.3 Densitogram of caffeine with a solvent front migration distance of 42 mm. The caffeine peak can be seen at a separation distance of 20 mm, measured at 273 nm and transformed by using (9.2)

9.2.2 Reflectance Measurements with a Diode-Array Scanner

Figure 9.4 shows a 3D plot of the same caffeine separation from Fig. 9.3 measured with a diode-array scanner. The separation distance is plotted as the *x*-axis from left to right. The small solvent front signal at about 42 mm can be seen at the right-hand edge of the figure. The wavelength range was plotted as the *y*-axis and the Kubelka–Munk transformed data as the *z*-axis. A diode-array scan provides much more information than simply measuring a densitogram at a given wavelength, as provided by a single-wavelength scanner. In Fig. 9.4 the 3D plot of the caffeine signal is shown at different wavelengths instantly providing the spectral characteristics of the separated compound. These spectral data can be used for compound identification, for choosing the optimum quantification wavelength, and for checking peak purity.

A TLC or an HPTLC track is not usually represented as a 3D plot but as a contour plot such as the one shown in Fig. 9.4 at the bottom. A contour plot contains all the track spectra. The caffeine contour plot in Fig. 9.5 comprises 450 single spectra in the wavelength range from 195 to 345 nm over a separation distance of 45 mm. Because the spatial resolution is better than 100 μm , it is possible to measure ten spectra per millimetre using an array with 512 diodes. Consequently, the contour plot comprises 450 spectra and 512 densitograms. Software allows the desired densitograms for quantifications to be selected after scanning.

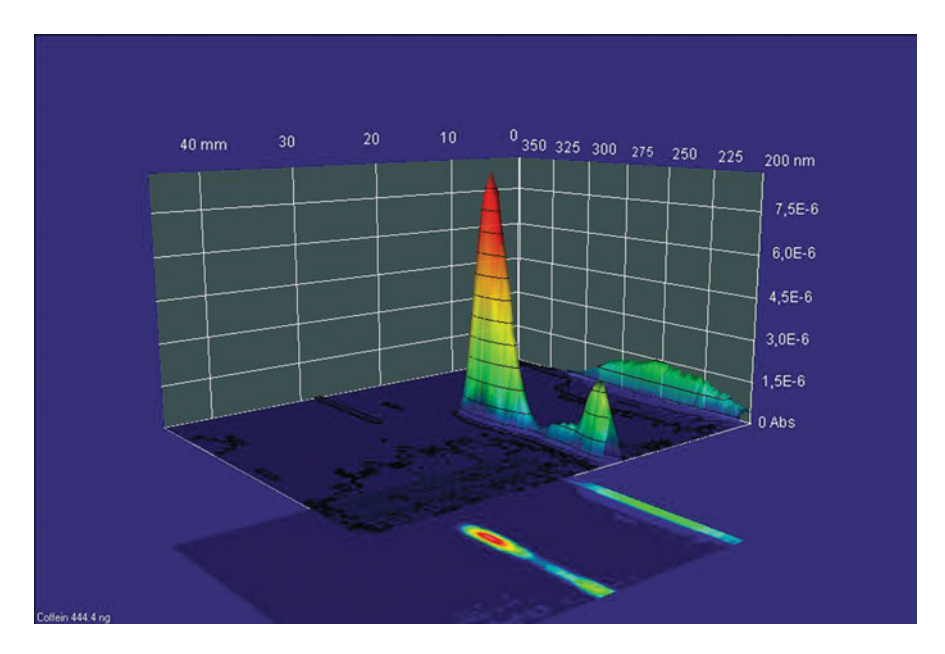


Fig. 9.4 A 3D plot of a caffeine separation recorded with a diode-array scanner. The *x*- and *y*-axes are the separation distance (from *left to right*, with the front seen at the right-hand side) and the wavelength range, respectively, and KM signal is taken on the *z*-axis

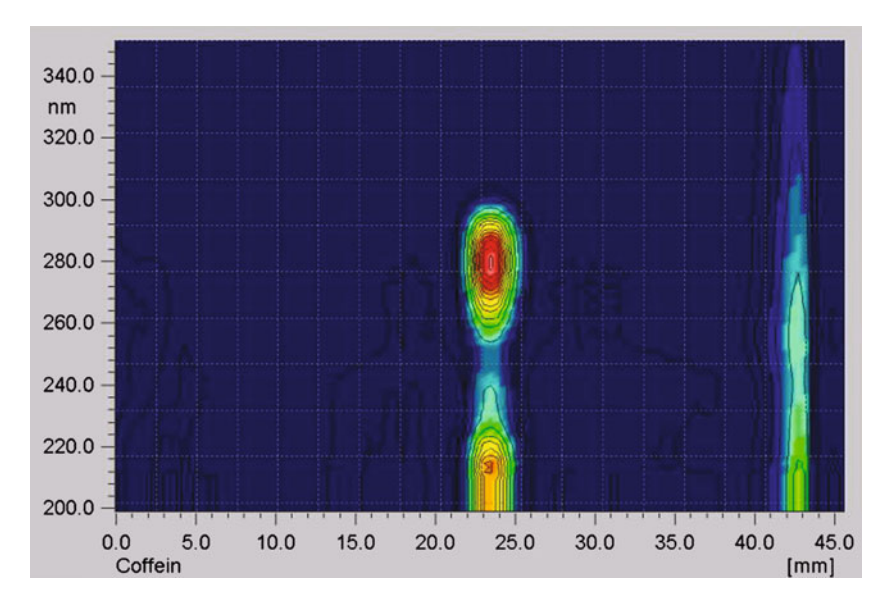


Fig. 9.5 The contour plot for a caffeine separation with the separation distance plotted as the x-axis and the wavelength range as the y-axis. A TIDAS TLC 2010 system (J&M Aalen, Germany) was used for scanning

9.2.3 Spatial Resolution on the Plate

The first evaluation of a TLC separation using the diode-array technique was published by Gauglitz and Bayerbach in 1989 [18]. The basic idea of using a diode-array for evaluating TLC separations was first included in a thesis written by Wuthe [19]. The first light-fibre scanner for TLC separations was built in 1966 [20]. Using UV transparent light-fibres in combination with a new interface enabled the development of a commercially available scanner whose fibres transport light to the plate and the reflected light back to the detector [21]. Placing the layer horizontally on a mechanical stage, which can be adjusted by two motors, allows the scanning of the layer. The linear slide system operates with constant velocity during reflection measurements. The whole device needs no lenses, filters, or slitwidth adjustments. The measuring principle is illustrated in Fig. 9.6. The light-fibre interface of the TIDAS TLC 2010 system consists of 50 identical optical fibres, each with 100 µm diameter. These fibres transport light of different wavelengths from a deuterium lamp to the TLC plate and back to the diode-array detector. The light source and detector are both placed 450 µm above the surface of the TLC plate for detection. The most commonly used scanners require an angle of 45° between the light-emitting device and the bulky detector. Due to the Lambert cosine law $[I=I_0\cos(\alpha)]$, the angle (α) is responsible for a reflected light intensity reduction (I)of nearly 30% but the light-fibre array overcomes this limitation [8]. For dense light intensities the light emitting and the detecting fibres should be arranged parallel to one another because this is the only arrangement where the Lambert cosine law predicts an optimum response.

Various optical fibre configurations can be constructed for scanning. The simplest way to arrange the interface of light-emitting and light-detecting fibres is to

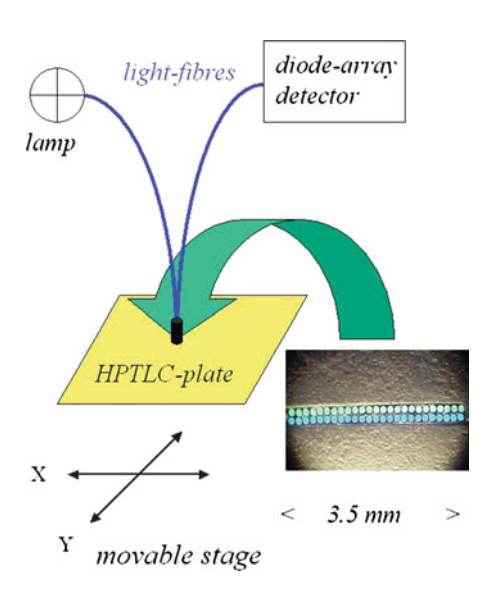


Fig. 9.6 The principle of light-fibre diode-array scanning [18, 21]

place them alternately in the array, thus forming a single row. The spatial resolution of this interface is nearly 140 µm at a distance of 450 µm above the layer [21]. A double-row interface has a set of 25 fibres arranged in a separate line to transport light to the plate. The detecting channel also forms a line, fixed close to the illuminating row. This double-row array is nearly 3 mm long and results in resolution on the plate of better than 100 µm [21]. Remember that according to the Kubelka–Munk theory the size of the scanning slit should be as small as possible in order to measure an almost constant concentration distribution in the substance zone. Each illuminating fibre forms a light spot on the TLC plate, which itself depends on the numerical aperture of the fibre used. The light spot is nearly 300 µm in size (Fig. 9.7). The detecting fibres register spots of identical size in the same way but in a position of 100 μm to the side [21]. A third version of the interface consists of three light-fibre rows with the centre fibre line forming the detecting row. Both rows on the sides are used to illuminate the plate with light from various sources. The usual configuration of the TIDAS TLC 2010 system has one row of fibres to emit light from a combined deuterium and tungsten lamp while the other row transports light from an LED and is only switched on for fluorescence measurements.

This fibre-array measurement input is a function of all the overlapping areas in the illuminating and detecting fibre spots. The result is a small scanning slit, smaller than $100~\mu m$, which is mainly dependent on the fibre array distance above the layer. Establishing the optimum distance between the fibre arrangement and the TLC plate is the only adjustment needed.

9.2.4 Spectral Distribution on HPTLC Plates

Single-wavelength scanners illuminate the layer with monochromatic light. The principle of the diode-array technique differs in this aspect. Here polychromatic light illuminates the layer and then, after interaction with layer and analyte, the light is split into different wavelengths. The advantage of this approach is discussed in



Fig. 9.7 Photograph of a double-row interface with a light-fibre diameter of 100 µm

the following chapters. The disadvantage is a high illumination light intensity, which may interact with the analyte. Nevertheless, light-sensitive compounds like benzo[a]pyrene are not degraded even after multiple scans and the strong light intensity does not seem to present a problem. The spectral distribution of the reflected light at intensity $J(\lambda)$ establishes the raw data used for further evaluation. This wavelength-dependent intensity is the difference between the spectral intensity distribution of the incident light $I_0(\lambda)$ minus the light intensity absorbed by the plate $I_{\rm abs}(\lambda)$, which is described by (9.3):

$$J(\lambda) = I_0(\lambda) - I_{abs}(\lambda), \tag{9.3}$$

where

 $J(\lambda)$ reflectance

 $I_0(\lambda)$ incident light intensity

 $I_{abs}(\lambda)$ light absorbed by the plate

Figure 9.8 shows the spectral distribution measured on a clean HPTLC plate. It can be seen that the deuterium lamp emits light ranging from 200 to 350 nm. Above 350 nm, nearly all reflected light comes from the tungsten lamp, which emits light up to 1,000 nm. To induce fluorescence, an LED (light-emitting device) which emits light at 364 nm, is used. LEDs produce sharp signals with ± 10 nm peak width

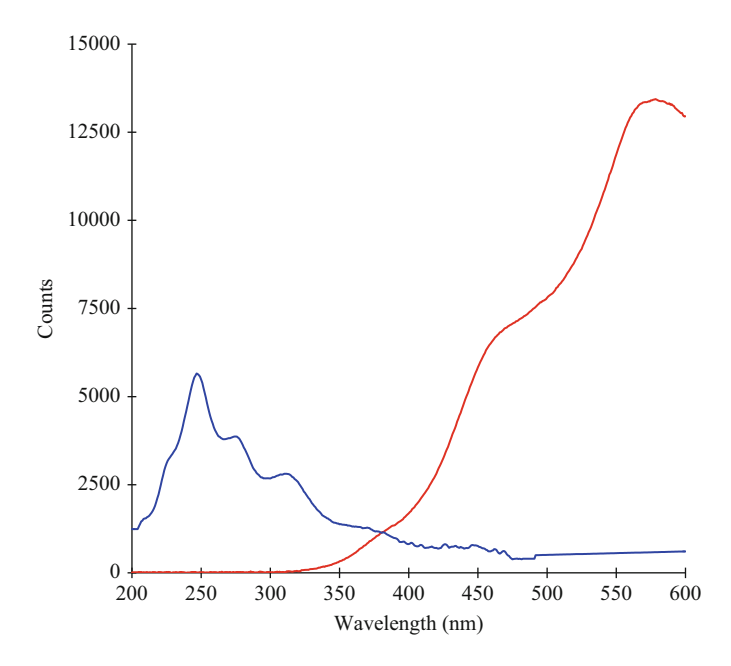


Fig. 9.8 Reflectance spectra from a silica gel layer using a deuterium lamp (blue) and a tungsten lamp (red)

[22, 23]. The main advantage of LED technology is the constant intensity of the emitted light, which makes these devices so valuable for fluorescence measurements.

The relative reflectance is calculated from the analyte reflectance divided by the reference reflectance. The reference spectrum is measured on a clean HPTLC plate:

$$R(\lambda) = \frac{J_{\text{sample}}(\lambda)}{J_{\text{reference}}(\lambda)} = \frac{J(\lambda)}{J_0(\lambda)},$$
(9.4)

where

 $R(\lambda)$ relative reflectance

 $J(\lambda)$ intensity distribution of the analyte zone

 $J_0(\lambda)$ intensity distribution of the clean layer

Thus lamp-independent spectra can be achieved because relative reflectance takes the layer absorption into account and absolute reflectance values are no longer necessary. The reference spectrum is commonly taken from a track position where there is no analyte present. An advantage of this approach is that it allows the spectrum to be read independent of the type of stationary phase.

9.2.5 Spectral Evaluation Algorithm

All TLC scanners register reflected light from the source with three possible reasons for light losses. The light emitted by the source can be partially absorbed by analyte and layer, and light is scattered by the particles. To make the situation more complicated, light can also be produced as fluorescence. Light losses by scattering and absorption by the layer can be compensated for by using the relative reflectance measured on each plate. The big question is "how can analyte absorption and fluorescence be detected while achieving linearity between the signal and sample amount?" Figure 9.9 shows the spectra from analytes reference zones from a benzo [a]pyrene spot. In the 200–400 nm range, a benz[a]pyrene spot absorbs more light than the clean layer. Between 400 and 470 nm, the spot emits more light than the clean layer, a phenomenon induced by fluorescence of the compound. Between 400 and 470 nm, the relative reflectance values are larger than 1. In summary, light absorption leads to relative reflectance values smaller than 1 and fluorescence to values larger than 1. For the case of no absorption and no fluorescence, the expression R = 1 is valid. With increasing analyte amounts we observe increasing light absorptions from decreasing relative reflectance values. A suitable expression is needed to obtain a linear response with increasing analyte amounts. Therefore it is necessary to transform the relative reflectance into absorptions and fluorescence data showing linearity between the measurements and analyte amounts.

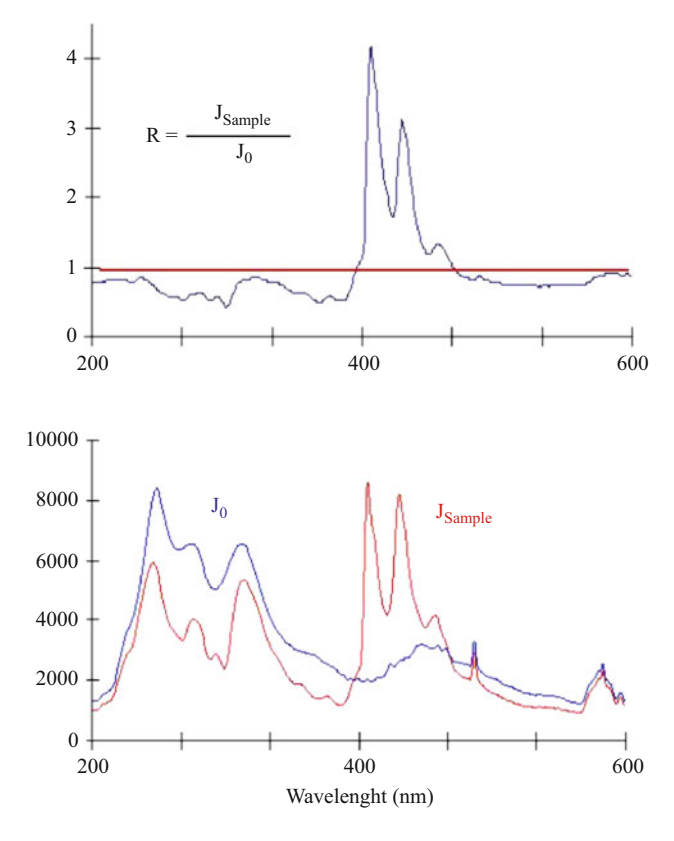


Fig. 9.9 Relative reflectance spectrum of a benzo[a]pyene spot (*above*) and the reflected light emissions (in counts) from a clean HPTLC plate (J_0) and the reflectance from a spot containing 125 ng benzo[a]pyrene (*below*)

There are various ways to turn a decreasing relative reflectance function into an expression showing increasing values with increasing analyte amount in a detection zone. Three different transformation algorithms have been proposed [24]:

$$DA(\lambda) = 1 - R(\lambda), \tag{9.5}$$

$$LB(\lambda) = \ln\left(\frac{1}{R(\lambda)}\right) = -\ln R(\lambda), \tag{9.6}$$

$$A(\lambda) = \frac{1}{R(\lambda)} - 1. \tag{9.7}$$

Expression (9.5) describes the relative light loss as a difference between the incident light and the absorbed light. Expression (9.6) is identical to the

transformation expression for the Lambert–Beer's law and is further denoted as the "logarithmic transformation" or "absorbance". Expression (9.7) is referred to as "reciprocal expression" or "reflectance" [2, 24]. The resulting spectral functions of both the absorption and the logarithm transformation show identical curvature, but their values differ. The relative reflectance increases with increasing fluorescence. Fluorescence normally increases with increasing analyte amount in the spot. If there is no analyte in the spot then fluorescence should be zero. A suitable transformation algorithm for fluorescence is therefore [7, 24]

$$F(\lambda) = R(\lambda) - 1. \tag{9.8}$$

Fluorescence measurements can also include scattered light and both sources of light will be observed at the layer surface. The incidental light is directed to the bottom part of the layer. In their theory, Kubelka and Munk assume that the light inside the layer is homogeneously scattered in all directions. This is called an isotropic scattering behaviour. The Kubelka–Munk theory therefore simply describes the mean of expressions (9.7) and (9.8), which is illustrated by (9.9) [8]:

$$KM(\lambda) = \frac{(1 - R(\lambda))^2}{2R(\lambda)} = \frac{1}{2} \left(\frac{1}{R(\lambda)} - 1 \right) + \frac{1}{2} (R(\lambda) - 1) = \frac{a}{s}, \tag{9.9}$$

where

 $R(\lambda)$ relative reflectance

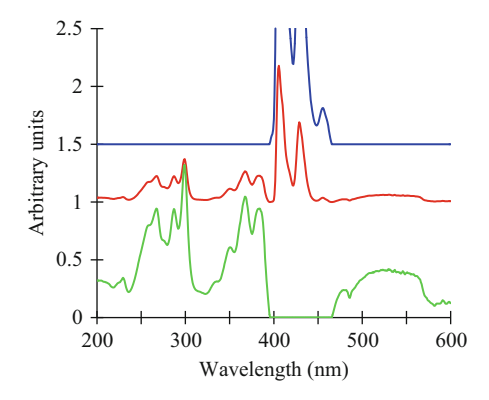
a total absorption coefficient

s scattering coefficient

As for (9.5)–(9.7), expression (9.9) transforms decreasing relative reflectance into increasing values and can therefore be used as a transformation algorithm.

In Fig. 9.10 the reflectance spectrum of a benz[a]pyrene-containing zone from Fig. 9.9 is plotted as the transformation spectra using the relationships given in

Fig. 9.10 The fluorescence spectrum $F(\lambda)$, the Kubelka–Munk spectrum $KM(\lambda)$ and the absorption spectrum $A(\lambda)$ from a zone containing 125 ng benz[a]pyrene (shown from *top to bottom*)



(9.7)–(9.9). The absorption spectrum is shown as lowest. The range from 200 to 400 nm and 470 to 600 nm shows a positive curve, which is correct because the benzo[a] pyrene spot absorbs light in this range. The fluorescence formula (at the top of Fig. 9.10) renders the relative reflectance as positive in the range from 400 to 470 nm, which is also correct because the benzo[a]pyrene spot shows fluorescence in this wavelength range. The Kubelka–Munk transformation algorithm (in the middle of Fig. 9.10) renders both fluorescence and absorption data as positive values representing the average of the fluorescence and absorption expressions as indicated by (9.9). A contour-plot transformation according to Kubelka–Munk instantly reveals light absorption and fluorescence for a TLC track.

9.2.6 Video-Densitometric Measurements

Modern TLC scanners can measure absorption and fluorescence by reflectance and transmittance. TLC scanners cover the whole wavelength range from 200 up to 1000 nm. The disadvantage of TLC scanners is their high purchase and maintenance costs. Most TLC applications are designed to work in the wavelength range from 400 to 800 nm, with the human eye as a detector. Scanning equipment such as CCD camera (charge coupling device camera) or flatbed scanner working in the visible range is inexpensive and can be used for plate evaluation [25, 26]. Since 1985 these have been increasingly used for this application [27, 28]. The term video densitometer was introduced for such scanning devices. The disadvantage of the video densitometer is that spectra are not available. This makes peak identification and peak-purity tests by spectral acquisition impossible. Otherwise, most substances show no light absorption or fluorescence in the visible range. To make TLC separations more specific, we recommend a staining step, which often makes spectral identification and peak-purity testing unnecessary.

What features should be taken into consideration when buying a CCD camera? Quantitative video-densitometric measurements require a camera, which can linearly digitize light intensity measurements. Double-fold light intensity must result in double signal values, which can be checked by changing the measurement time (doubling the measurement time must result in a doubling of the measured values). The digital resolution of commonly used cameras is 8 bit. A signal is rendered in $2^8 = 256$ different increments, which is not sufficient for quantification purposes. At least 12-bit capacity is necessary for general quantification purposes ($2^{12} = 4,096$ increments). CCD cameras with a resolution of 16 bits are much better. Such cameras render $2^{16} = 65,536$ greyscales, so check whether the evaluation software can manage 12 or 16 bits. Relatively inexpensive cameras with suitable software that meet these requirements are available for astronomical observations. These cameras produce TIFF pictures, because the TIF Format (tagged image file format) supports 16-bit data storage.

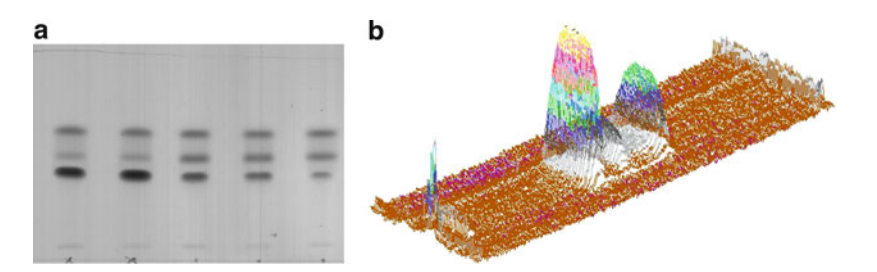


Fig. 9.11 Separation of cobalt–dithizone, dithizone, and zinc–dithizone with toluene on a silica gel plate recorded with a simple hand scanner: at *left* the separation of fife tracks (**a**) and at *right* the separation of a single track, visualized as a contour plot (**b**) (from [29])

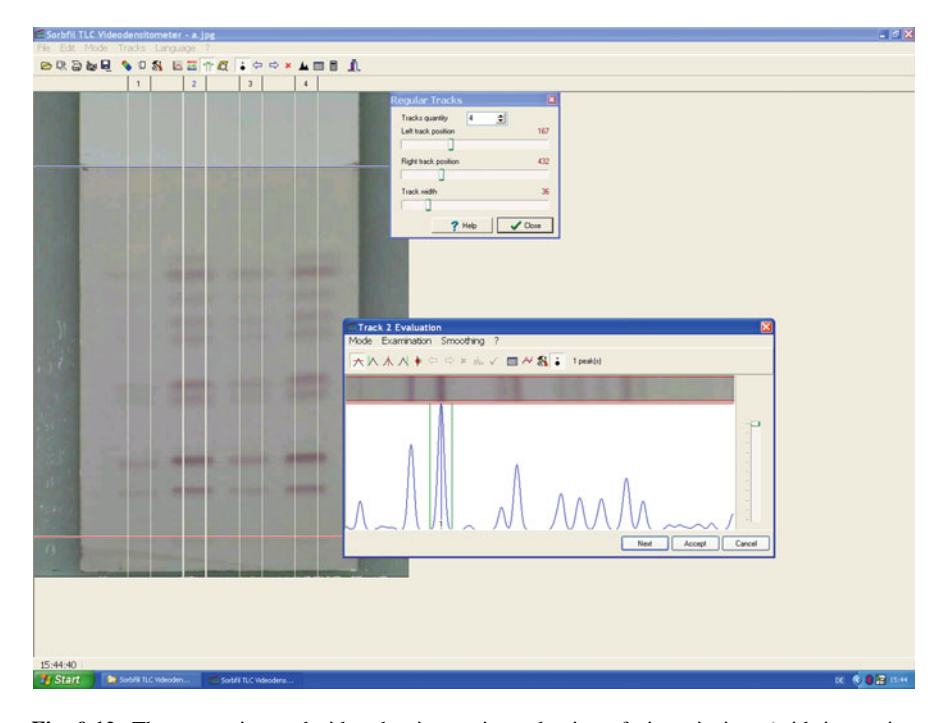


Fig. 9.12 The separation and video-densitometric evaluation of nine triazines (with increasing $R_{\rm f}$ values: prometon, desmetryn, simazine, ametryne, atrazine, terbutryne, atraton, prometryne, and metribuzine), separated on a silica gel layer with a mobile phase of methyl *tert*-butyl ether–cyclohexane (1+1, V/V). For visualization the plate was treated with chlorine and stained with the iodine/starch reagent. The densitogram of the second track is also shown. Quantification was performed with SORBFIL TLC Videodensitometer software (version 1.8)

Although inexpensive flatbed scanners and cameras are not linearly calibrated, it is nevertheless possible to quantify TLC separations. The output from an inexpensive hand scanner is plotted in Fig. 9.11. The metal complexes cobalt—dithizone and

zinc-dithizone are quantified, but the working range covers only a single order of magnitude due to the non-linear working range of the detector [29].

Commonly used flatbed scanners can also be used for evaluation of TLC separations. These scanners illuminate the plate with white light and can scan coloured zones. Figure 9.12 shows the results from an evaluation by video densitometry. Nine triazines were separated on a silica gel plate with the mobile phase methyl *tert*-butyl ether–cyclohexane (1+1, V/V). The plate was stained with iodine/starch reagent after treatment with chlorine. The densitograms can be used to quantify the triazines with a restricted calibration range less than one order of magnitude. The various measurements from a single track were combined in a single densitogram. The averaged data reduces noise. It is important for all tracks to be evaluated with the same number of measurements. All tracks must also be evaluated using the same position within the track and the same evaluation widths, as shown in Fig. 9.12. This inexpensive approach for evaluation of TLC separations is available to all laboratories requiring only widely available office equipment. It is also possible to use a simple UV lamp for plate illumination to record TLC separations in the fluorescence mode [28].

9.3 Infrared and Raman Detection in Thin-Layer Chromatography

9.3.1 Analysis of Thin-Layer Chromatograms by Diffuse Reflectance Infrared Fourier Transformation

By far the most important range for TLC measurements is from 200 to 800 nm. This range was extended to beyond 800 nm by the use of the so-called DRIFT technique [30]. DRIFT is the abbreviation for "Diffuse Reflectance Infrared Fourier Transformation" for measurements in the IR wavenumber range from 400 to 4,000 cm⁻¹ (2.5–25 μm). Intense silica gel absorption bands from 1,000 to 1,350 cm⁻¹ and above 3.550 cm⁻¹ restrict the available wavenumber range for in situ measurements by the usual scanning methods. For DRIFT measurements, a commercially available Fourier-transform IR spectrometer is connected via mirrors and lenses to the surface of the TLC plate [31]. The IR light beam is moved over the plate surface and interacts with the stationary phase. The wavenumber dependent intensity of the reflected light is calculated by the use of a Michelson interferometer. Glasssupported layers 200 µm thick formed from 10 µm particles with a narrow size distribution are suitable for this application but a 1:1 mixture of silica gel and magnesia tungstenate particles is regarded as best. The spectra measured by the DRIFT technique show more structured bands than those measured by UV-visible spectroscopy. The method is useful for substance identification [30]. Its disadvantages lie in its high costs and poor detection limits (50-fold higher than typical for UV-visible measurements). Kovar demonstrated an in situ linear calibration curve for caffeine over the range 0.5–2 μg obtained using reflectance measurements transformed according to the Kubelka–Munk equation [32]. Fourier-transformed infrared photoacoustic spectroscopy (FTIR-PAS) is an alternative to commonly used FTIR detectors, which offer similar detection limits, but the photoacoustic technique is not often used [33].

9.3.2 Analysis of Thin-Layer Chromatograms by Near-Infrared FT-Raman Spectroscopy

Raman spectroscopy is a technique for studying molecule vibrations named after Raman, who invented it in 1928. It relies on the non-elastic scattering of monochromatic light when it interacts with matter. A laser or an LED is commonly used as a source. The Raman effect occurs when light interacts with the bonded electron cloud of a molecule transferring energy to it so that the molecule enters an excited state. For a spontaneous Raman effect, the molecule is excited from its basic state to a virtual energy state and then relaxes into a vibrationally excited state. The light emitted during the relaxation period is called "Rayleigh scattering", with two series of lines around this central vibrational transition. They correspond to the complimentary rotational transitions. Anti-Stokes lines correspond to rotational relaxation whereas Stokes lines correspond to rotational excitation. Raman emission is not the result of an absorption process. The scattered light (in wavelength ν) changes its wavelengths depending on the status of the molecules, which scatters the light. The scattered light can increase its energy $(v + v_0)$ by transferring rotation energy from the molecule to the light (anti-Stokes emission). The scatted light can also lose energy $(v - v_0)$ by transferring its energy to the molecule where it is stored as rotational energy (Stokes emission). The electron cloud is deformed during Rayleigh scattering. Deformation is required for the molecule to exhibit the Raman effect. The amount of deformation (change in polarizability) will determine the Raman scattering intensity. Therefore easily polarized molecules result in strong Raman emissions. This is complementary to infrared absorption where polar group vibrations show strong absorption. Technically, Raman spectroscopy is carried out by illuminating a sample with an Nd-YAG laser beam of 1,064 nm to avoid fluorescence [34]. Light from the illuminated spot is collected with a lens and sent through a monochromator. Due to elastic Rayleigh scattering, wavelengths near the laser line are filtered out while the rest of the collected light is dispersed onto a detector. Raman spectra are nearly as highly structured as IR spectra [34, 35] and are suitable for compound identification. The detection limit is reported to be in the lower microgram range (>2 µg per spot) [34]. Raman measurements show a rather high background, which must be subtracted from the sample spectra [35].

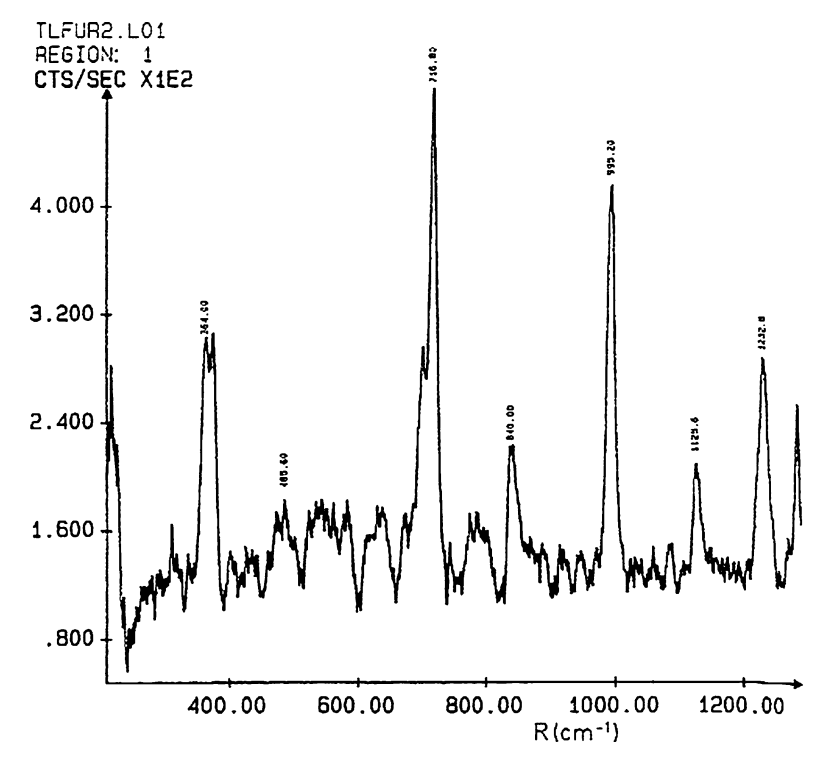


Fig. 9.13 SERS/HPTLC spectrum of dibenzofuran (50 pg) on an HPTLC silica gel 60 plate activated with a silver colloid (From [37] with permission © Akadémiai Kiadó.)

9.3.3 Analysis of Thin-Layer Chromatograms by Surface-Enhanced Raman Scattering Spectrometry

An alternative to the FT-Raman method is surface-enhanced Raman scattering spectrometry (SERS) [36, 37]. Spraying an HPTLC plate with a silver colloidal solution produces a remarkable increase in Raman intensity. Raman scattering from molecules adsorbed on metal surfaces are enhanced by a factor of 10^5 – 10^6 . After separation, the dried plate is immersed in a silver colloid solution prepared from one volume of 1 mM aqueous silver nitrate solution added dropwise to three volumes of a 2 mM sodium borohydride solution in water [37]. SERS spectra can be measured from 400 up to 1,600 cm⁻¹ using a Raman spectrometer. With a 632 nm laser, 50 pg of dibenzofuran can be detected on an HPTLC plate within 3 s. The spectrum is plotted in Fig. 9.13.

9.4 Mass Spectrometric Detection in TLC

Mass spectrometry (MS) has a significant advantage in speed, sensitivity, and specificity over other methods of spectrochemical analysis. The combination of mass spectrometry with TLC extends the scope of planar separations, because all TLC-MS systems provide mass densitograms with structural information for the analytes. The direct coupling of TLC and MS has been of interest for many years [38–40]. Several approaches that differ in the method used for ionization and technique to liberate the analyte from the surface of the layer have been pursued. If a liquid or gas jet is used for desorption and ionization, the methods DESI (desorption electrospray ionization), EASI (easy ambient sonic spray ionization mass spectrometry), and DeSSI (desorption sonic spray ionization) are used. DeSSI works in contrast to DESI with no voltage but needs a high gas velocity. If a laser is used for desorption and ionization, the methods are known as LDI (laser desorption ionization), MALDI-MS (matrix-assisted laser desorption/ionization mass spectrometry) and AP-MALDI-MS (atmospheric pressure matrix-assisted laser desorption/ionization mass spectrometry). If a collision with particles is used for desorption and ionization, the methods are called FAB (Fast Atom Bombardment) and SIMS (secondary ion mass spectrometry), as well as other possibilities. Methods employing thermal desorption with secondary ionization are known as DART (direct analysis in real time), APCI-MS (laser desorption/atmospheric pressure chemical ionization mass spectrometry), and APGD-MS (atmospheric pressure glow discharge mass spectrometry). Zones of interest can also be extracted by liquid using LMJ-SSP (liquid microjunction surface sampling probe) and SSSP (sealing surface sampling probe). LMJ-SSP systems directly extract an analyte from a surface by contacting the surface with a confined liquid stream. For SSSP, the inlet capillary of a stainless steel plunger is sealed to the surface of the layer and the sample transferred in solution to the ion source of the mass spectrometer. The zone of interest is eluted by a solvent that flows through the sealed TLC zone. In this section, we focus on those interfaces that are commercially available.

9.4.1 Direct Plate Extraction (SSSP)

The "ChromeXtractor" device [41-43] affords a universal interface for TLC layers compatible with any mass spectrometer designed for HPLC applications. This extractor is a 4×2 mm stamp, which is placed over the analyte zone. An HPLC pump is used to force mobile phase through the selected part of the layer extracting the analyte, which is transported to the ionization source of the mass spectrometer (see Fig. 9.14). This simple and robust technique has a spatial resolution of 2 mm. The detection limit is in the nanogram per extracted zone range, depending on the MS system used [41]. This extractor can also be used to obtain FTIR Raman spectra from sample zones on a TLC plate.

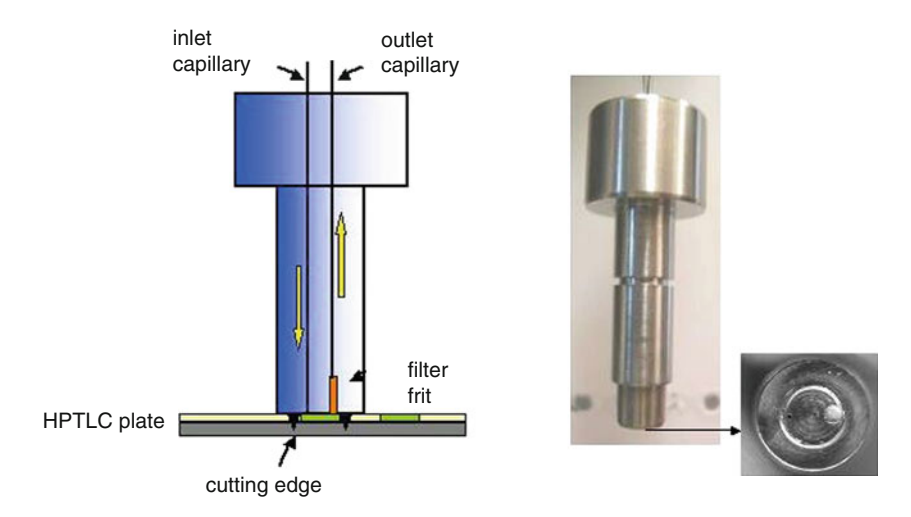


Fig. 9.14 The ChromeXtractor device (With permission from Morlock and Luftmann)

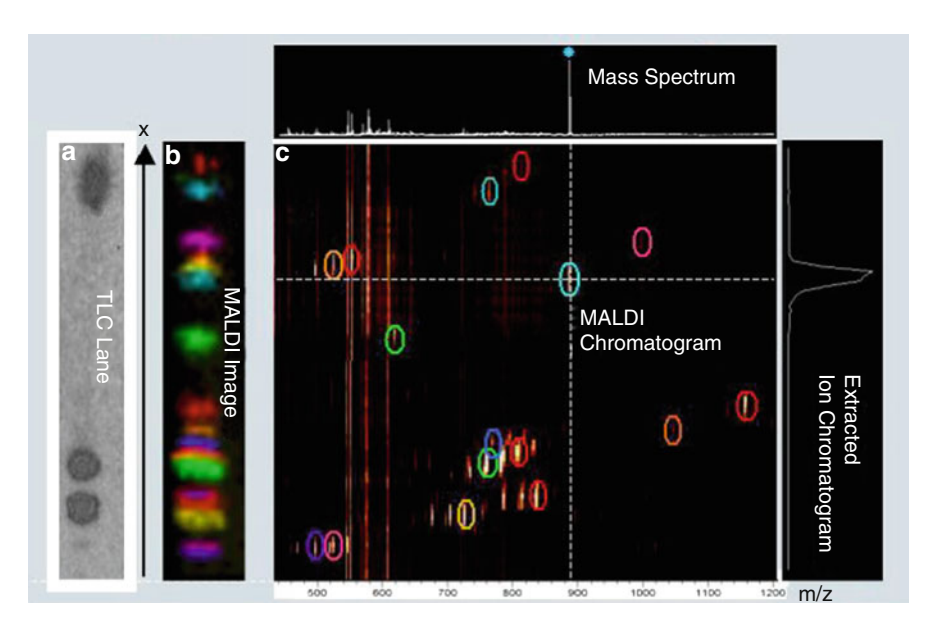


Fig. 9.15 TLC-Maldi chromatogram of phospholipids. (a) Classical primuline staining of the separated lipids on an HPTLC plate; (b) HPTLC-MALDI imaging analysis of an identical HPTLC plate with matrix coating; (c) TLC readout as provided by the HPTLC-MALDI software, permitting direct access to all molecular species (*m/z* values on the *x*-axis) and the chromatographic separation on the *y*-axis. The *coloured circles* correspond to the compounds visualized in the HPTLC-MALDI image (With permission from Bruker Daltonik GmbH, Bremen, Germany.)

9.4.2 MALDI Techniques (MALDI-MS)

For MALDI-MS, the plate must be prepared prior to analysis [44–46]. The plate is dipped in a coating solution (e.g. 2,5-dihydroxybenzoic acid), which will absorb the laser energy for ablation. The suitably impregnated plate is then placed under high vacuum. Figure 9.15 shows MALDI-TOF mass spectra of membrane lipids measured directly from an HPTLC plate. Erythrocyte membrane phospholipids were extracted from cells using chloroform—methanol—water (2+1+1, V/V) and then separated by TLC in a horizontal developing chamber using chloroform—ethanol—water—triethylamine (35+35+7+35, V/V) as mobile phase [45, 46]. A 100 mg/ml solution of dihydroxybenzoic acid in acetonitrile/water (1+1, V/V) was used for manual matrix application. The mass spectrometric information was subsequently read out automatically. The spatial resolution is better than 200 µm [45].

9.4.3 Atmospheric Pressure Mass Spectrometry

The general aim of recent research as stated by van Berkel is to liberate the mass analysis from the constraints of getting the surface to be sampled into a vacuum system [39]. The number and type of ambient or atmospheric pressure (AP) techniques suitable for HPTLC sampling is rapidly expanding. Several techniques are now available for desorption from the layer and ionization [40], such as DART [47, 48], EASI-MS [49], APCI-MS [50], and DESI [51–54]. All these methods are able to measure the parent ion mass and characteristic fragments produced during the measurement process at atmospheric pressure. This is important information to identify - in combination with UV-visible spectra - individual TLC zones. Nevertheless, quantification is possible only by using an internal standard, since the desorption processes are not sufficiently reproducible for quantification purposes. A new commercial form of APCI-MS based on thermal desorption (TD) was introduced recently under the name DART [47] and was shown to be suitable for evaluating HPTLC separations [48]. The DART system employs an excited helium gas stream, forming protonated water clusters from the surrounding air. These clusters transfer their energy to the analyte, forming molecular cations. This device has a spatial resolution of better than 3 mm on an HPTLC plate and a detection limit that lies in the lower nanogram range [48]. EASI-MS offers a simple ionization interface. The desorption and ionization from the HPTLC surface is performed by the charged droplets produced by sonic spraying a 1:1 acidic (0.01% formic acid) water/methanol solution. The spatial resolution on plate is 330 μm [49]. DESI employs high voltages and a methanol and/or formic acid spiked nitrogen gas for nebulization [52, 53]. In Fig. 9.16 a DESI evaluation of a 2D separation by TLC is shown. The DESI emitter is described in detail in [53]. A 7–13-cm-long stainless steel tube (0.84 mm i.d, 1.27 mm o.d.) to reach out over the TLC plate surface was press fit into a standard heated atmospheric pressure sampling capillary maintained

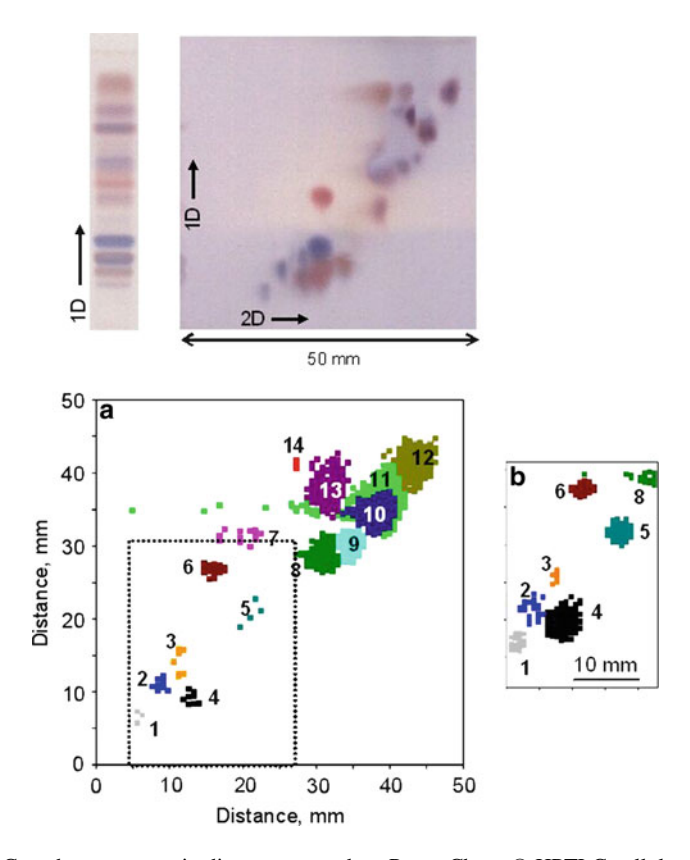


Fig. 9.16 Cytochrome c tryptic digest separated on ProteoChrom® HPTLC cellulose layer and stained with ProteoChrom® Color Peptide Stain. The image on the *left* is a 1D separation and the images on the *right* 2D separation. The 2D maps showing the peptide distribution acquired using an LCQ Deca Ion Trap Mass Spectrometer (Thermo Scientific, San Jose, CA, USA) are shown in (a) and (b) (*below*). *Inset*: peptide distribution acquired using an LTQ FT Ultra Hybrid (Thermo Scientific). *Dotted lines* indicate the approximate region scanned in (b) (From [52] with permission © Wiley-VCH)

at 200° C. A high voltage of 4 kV was applied to the stainless steel body [52]. The tip of the DESI spray emitter was mounted 2–3 mm above the surface of the layer at an angle of \sim 55° to the surface [52]. Figure 9.16 shows a 2D HPTLC/DESI-MS image of a separation of a tryptic protein digest [52]. The total amount of \sim 20 µg protein was applied 10 mm from each edge of the left corner of an HPTLC cellulose plate. The development was carried out in a normal chamber using 2-butanol-pyridine–acetic acid–water (45+30+9+36, V/V) as mobile phase for the first dimension and butanol–pyridine–aqueous ammonia–water (39+34+10+26, V/V) for the second dimension. The migration distance was 50 mm in each direction. To determine the masses, the plate was dried and an LCQ Deca Ion Trap and an LTQ FT Ultra Hybrid mass spectrometers were used [52]. Raster scanning of the tryptic digest was performed with a pixel size of 700 µm. For the digest, an area measuring

45 mm \times 47 mm was imaged (Fig. 9.16a) resulting in a total analysis time of \sim 8.5 h [52]. DESI-MS can be used with a spatial resolution on the layer of better than 100 µm [52]. Raster scanning of a 10×10-mm surface area at 100 µm/s was published in 2006 [53]. To visualize the spots, the plate was sprayed with Proteo-Chrom Color Reagent (Merck, Darmstadt, Germany). After drying at room temperature for 5 min, the plate was sprayed with ninhydrin solution and heated to 120°C for 1–2 min. The zones of the tryptic digest appear as coloured spots. (Coloured peptide staining can also be achieved using Folin's reagent or ninhydrin–collidine reagent 100 mg ninhydrin dissolved in 70 mL methanol mixed with 2.9 mL 2,4,6-trimethylpyridine and 21 mL acetic acid), which is heated to 90°C after spraying.)

All the atmospheric pressure methods are in some way complementary to MALDI-MS, since MALDI is primarily suited for the detection of large molecules (>500 Da), such as peptides, proteins, and phospholipids. DESI, EASI, APCI, and DART are suitable for the detection of smaller molecules (<500 Da).

9.5 Thin-Layer Radiochromatography (TL-RC)

Radioactive isotopes have been used for decades to elucidate biochemical pathways, and thin-layer chromatography plays an important role in this approach. Radionuclides are used as tracers in pharmaceutical and biological researches. Appropriate compounds are labelled with ³H, ¹⁴C, ³⁵S, ³²P, ¹⁸F, ⁹⁹Tc, or ¹²⁵I, usually, and then separated by TLC. The β - or γ -radiation from these compounds is then measured with a special scanner, using techniques such as gas counting, β-positron-Geiger-Müller counter, γ-scintillation counter, or storage phosphor screen imaging scanner. The instrumentation for these methods is described in [55]. The classical TL-RC detection methods are liquid scintillation and autoradiography. In liquid scintillation the zone of interest is scraped out and mixed with a scintillation cocktail to convert the kinetic energy of the nuclear particles into light. The light intensity is proportional to the radioactivity of the zone. The photons are measured by the use of a photomultiplier. In autoradiography the TLC plate is placed in direct contact with a photographic (X-ray) film, which shows the plate image after development [55]. Quantification is made by densitometric measurements of the film. Slit scanners, digital cameras, or flatbed scanners can be used for this purpose. Modern equipment offers radioactive scanning without a film.

9.5.1 Direct Radioactivity Measurements on TLC Plates

For direct digital gas counting of all β - and γ -emitting isotopes, a counting gas is ionized by interaction with the radioactive TLC zone. This produces a pulse of

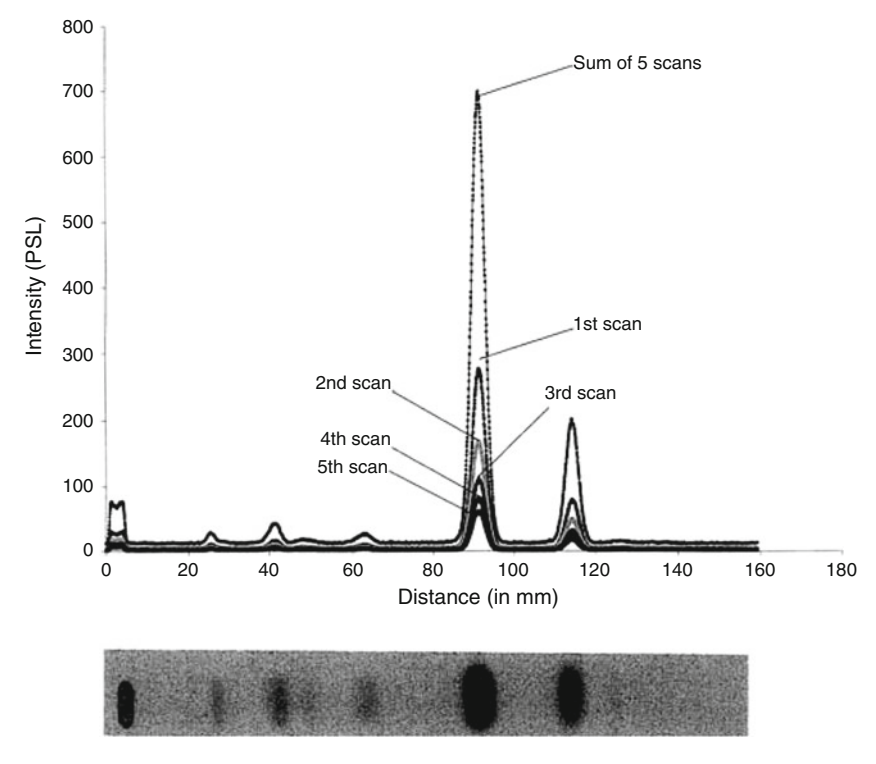


Fig. 9.17 Chromatogram obtained from the serum of a rat dosed with a ¹⁴C-labelled substance, and the corresponding intensity profiles of subsequent readings. The adsorbent was silica gel 60 F254 and the mobile phase chloroform–*n*-hexane–ethanol 25% (W/V) aqueous ammonia (75+15+9+1, V/V). Radioluminographic detection was performed with an exposure time of 65 h (From [56] with permission © Akadémiai Kiadó)

electrons that is proportional to the amount of radioactive compound in the separated zone. ³H-labelled compounds can be measured only by the use of an open window gas flow-through counter. The open-window configuration can lead to difficulties for routine operations. For example, the high voltage counting wire can attract dust. Closed-window gas counting avoids this. Isotopes with medium-energy emission such as ¹⁴C can be detected because the emitted radiation is able to pass through a very thin Mylar foil, which closes the ionization chamber. For high energy β-emissions, the simplest detection method is to use a Geiger-Müller counter. During a scan of a TLC track the radioactive material may decay due to its short half-life. To avoid loss of radioactivity by decay, the Geiger-Müller scanner moves relatively quickly over the track many times. All instruments show high sensitivity, linearity over 4–5 decades of activity, and a spatial resolution on the layer of 0.5–3 mm [56]. A TLC track can be measured within 1–10 min, depending on the isotope.

9.5.2 Phosphor Imaging

Storage phosphor screen imaging is an advantageous method for detecting radioactivity of compounds separated by TLC. After the separation of the radionuclide-labelled compound, the TLC plate is exposed to a phosphor imaging plate. The phosphor imaging plate provides a flexible and reusable image sensor in which the crystals of a photostimulatable phosphor are coated as a film. The exposure time can be quite long, even overnight. The imaging plate accumulates and stores the radioactive energy as a latent image [56]. After this exposure, a laser beam in a dedicated instrument scans the phosphor imaging plate. The resulting photostimulated luminescence of the exposed zones on the phosphor imaging plate

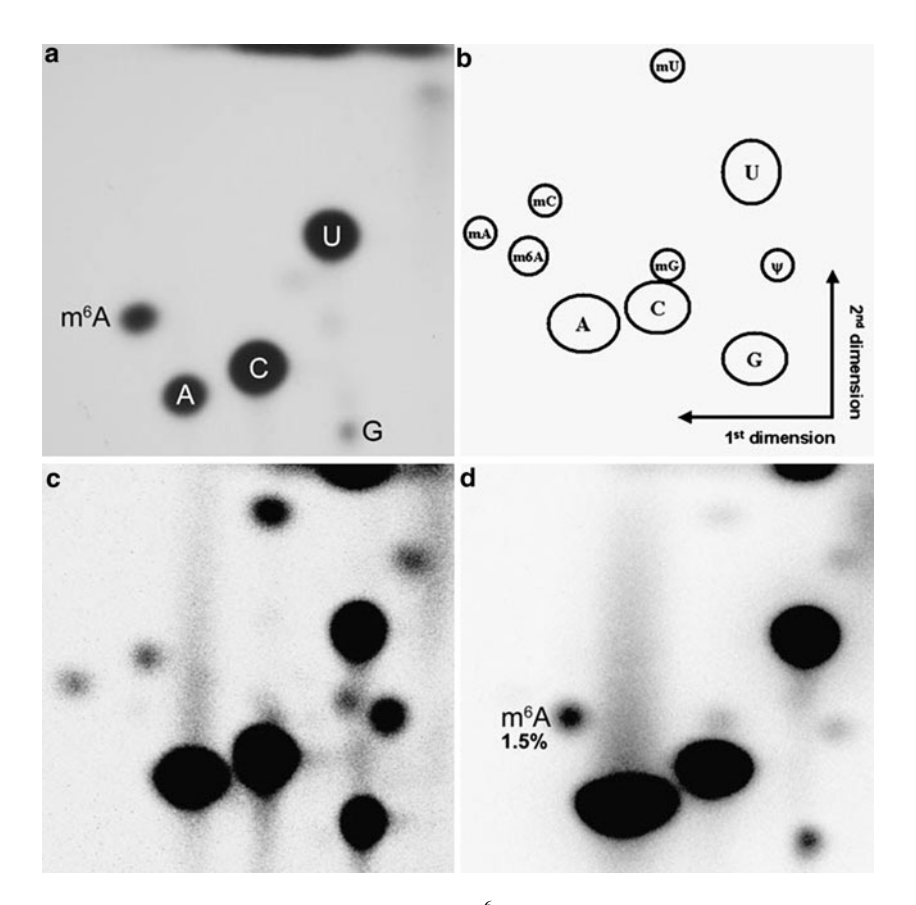


Fig. 9.18 Two-dimensional TLC detection of m^6A in *Arabidopsis* poly(A) RNA. (a) Two-dimensional TLC analysis of in vitro transcribed RNA containing m^6A and normal adenosine. (b) The relative positions of nucleotide spots (A adenosine, C cytosine, G guanosine, U uracil, and (mA, mC, mU, mG, m^6A) methylated nucleotides. (c) Two-dimensional TLC analysis of total RNA extracted from 2-week-old *Arabidopsis* seedlings. (d) Two-dimensional TLC analysis of poly(A) RNA from 2-week-old *Arabidopsis* seedlings. The m^6A :A ratio is 1.5%

References 257

(photostimulated luminescence, PSL) is measured by a photomultiplier and plotted as a densitogram. For TLC separations, the linearity, sensitivity, and resolution are excellent [56].

The high sensitivity of the phosphor imaging analyser can be further increased by multiple reading of the image plates, which increases the signal intensity. Summing of the chromatograms obtained in successive readings results in an increased signal-to-noise ratio. This allows either the exposure period to be shortened or higher sensitivity to be achieved [56]. Figure 9.17 shows a chromatogram obtained from the serum of a rat dosed with a ¹⁴C-labelled substance. For measurement purposes, the TLC plates were wrapped with protective foil to prevent contamination. The imaging plates were placed in direct contact with the layers. A bio-imaging analyser (Fuji Photo Film, Japan) was used to scan the latent image, using BAS Reader software, from Raytest Isotopenmessgeräte GmbH (Staubenhardt, Germany). Plate reading (50 µm pixel size, 8 bits/pixel) was performed immediately after release of the imaging plate from the cassette (in subdued light to avoid signal loss) [56].

Phosphor image detection results in better spatial resolution than for digital autoradiography and is able to scan 2D separations, as shown for N^6 -methyladenosine (m⁶A) in Fig. 9.18 [57]. N^6 -Methyladenosine is a ubiquitous modification identified in the mRNA of numerous eukaryotes, where it is present within both coding and non-coding regions. For separation by TLC, mRNA from tissue was extracted and then labelled using 10 units of T4 polynucleotide kinase in the presence of 1 mL of [γ -³²P]ATP (6,000 Ci/mmol). Sample amounts, 2 μ L, were applied to 20 \times 20 cm cellulose TLC plates and developed in a solvent system of isobutyric acid–0.5 M aqueous ammonia (5+3, V/V) in the first dimension and 2-propanol–hydrochloric acid–water (70+15+15, V/V) in the second dimension. The identification of labelled nucleotide zones was carried out using synthetic methylated and non-methylated RNAs. Quantification was carried out using a storage phosphor screen (K-Screen; Kodak) and Bio-Rad Molecular Imager FX [57].

References

- 1. Touchstone JC, Sherma J (1979) Densitometry in thin layer chromatography, practice and applications. Wiley, New York
- Klaus R (1964) Einige kritische Betrachtungen zur photometrischen Auswertung von Dünnschichtplatten. J Chromatogr 16:311–326
- Jork H (1967) Die direkte quantitative d\u00fcnnschicht-chromatographische Analyse. Fresenius Z Anal Chem 234:310–326
- Jork H (1966) Direkte spektralphotometrische Auswertung von Dünnschicht-Chromatogrammen im UV-Bereich. Fresenius Z Anal Chem 221:17–33
- 5. Schuster A (1905) Radiation through a foggy atmosphere. Astrophys J 21:1–22
- Kubelka P, Munk F (1931) Ein Beitrag zur Optik der Farbanstriche. Z Tech Physik 11a:593–601
- Spangenberg B (2006) Does the Kubelka-Munk theory describe TLC evaluations correctly?
 J Planar Chromatogr 19:332–341
- 8. Kortüm G (1969) Reflextionsspektroskopie. Springer, Heidelberg

- 9. Kubelka P (1948) New contributions to the optics of intensely light-scattering materials. Part I. J Opt Soc Am 38:448–457, 1067
- Kortüm G, Vogel J (1958) Die Theorie der diffusen Reflexion von Licht an pulverförmigen Stoffen. Z Physik Chem 18:110–122
- Ebel S, Kussmaul H (1974) Auswertung von Dünnschicht-Chromatogrammen über die Kubelka-Munk-Funktion. Chromatographia 7:197–199
- 12. Eckert Th, Knie U (1981) Zum Einfluss reflektierender Trägermaterialien bei der quantitativen in situ Hochleistungs-Dünnschichtchromatographie. Untersuchungen am Beispiel einer Kieselgel 60-Beschichtung, J Chromatogr 213:453–462
- Klaus R (1969) Quantitative in situ Auswertung bandförmig aufgetragener Substanzen in der Dünnschichtchromatographie. J Chromatogr 40:235–243
- 14. Goldmann J, Goodall RR (1968) Quantitative analysis on thin layer chromatograms: a theory for light absorption methods with an experimental verification. J Chromatogr 32:24–42
- 15. Huf FA (1987) In: Treiber LR (ed) Quantitative thin-layer chromatography and its industrial applications. Dekker, New York, pp 17–66
- Tausch W (1972) Quantitative Auswertung von Dünnschicht-Chromatogrammen durch direkte Photometrie. Messtechnik 2:38–44
- Poole CF, Poole SK (1989) Progress in densitometry for quantification in planar chromatography. J Chromatogr 492:539–584
- 18. Bayerbach S, Gauglitz G (1989) Spectral detection in thin-layer chromatography by linear photodiode array spectrometry. Fresenius Z Anal Chem 335:370–374
- 19. Wuthe W (1986) Rechnergesteuerte Auswertung in der Dünnschichtchromatographie mit Photodiodenarray-Scanner. Thesis Würzburg
- Hamman BL, Martin MM (1966) A versatile spectrophotometric scanner for large TLC Plates. Anal Biochem 15:305–312
- Spangenberg B, Klein K-F (2000) Fibre optical scanning with high resolution in thin-layer chromatography. J Chromatogr A 898:265–269
- 22. Stroka J, Arranz I, MacCourt J, Spangenberg B (2003) A simple and reliable HPTLC method for the quantification of the intense sweetner Sucralose[®]. J Liq Chromatogr Rel Technol 26:2729–2739
- Bleichert M, Eckhardt H-S, Klein K-F, Spangenberg B (2008) A simple and reliable method for quantification of glucosamine in nutritional supplements. J Planar Chromatogr 21:55–59
- Spangenberg B, Klein K-F (2001) New evaluation algorithm in diode-array thin-layer chromatography. J Planar Chromatogr 14:260–265
- Ford-Holevinski TS, Agranoff BW, Radin NS (1983) An inexpensive, microcomputer-based, video densitometer for quantitating thin-layer chromatographic spots. Anal Biochem 132: 132–136
- 26. ProŠek M, Medja A, Katic M, Kaiser RE (1984) Quantitative evaluation of TLC. Part 7: scanning with micro D-cam. CAL 4:249–251
- Mustoe S, McCrossen S (2001) TLC image capture and analysis by use of a prototype device for visualizing fluorescence. J Planar Chromatogr 14:252–255
- Stroka J, Peschel T, Tittelbach G, Weidner G, van Otterdijk R, Anklam E (2001) Modification
 of an office scanner for the determination of aflatoxins after TLC separation. J Planar
 Chromatogr 14:109–112
- Spangenberg B, Stehle St, Ströbele Ch (1995) Quantitative DC mit einem Handscanner: Co²⁺-Bestimmung. GIT 39:461–464
- 30. Rager IOC, Kovar K-A (2001) In: Nyiredy Sz (ed) Planar chromatography. A retrospective view for the third millennium. Springer, Budapest, pp 247–260
- 31. Glauninger G, Kovar K-A, Hoffmann V (1990) Possibilities and limits of an on-line coupling of thin-layer chromatography and FTIR-spectroscopy. J Anal Chem 338:710–716
- 32. Kovar K-A, Hoffman V (1991) Möglichkeiten und Grenzen der direkten DC-FTIR-Kopplung. GIT 35:1197–1201

References 259

33. White RL (1985) Analysis of thin-layer chromatographic adsorbates by Fourier transform infrared photoacoustic spectroscopy. Anal Chem 57:1819–1822

- 34. Petty C, Cahoon N (1993) The analysis of thin layer chromatography plates by near-infrared FT-Raman. Spectrochim Acta 49:645–655
- 35. Sollinger St, Sawatzki J (1999) TLC-Raman für Routine-Anwendungen. GIT 43:14-18
- 36. Séquaris J-ML, Koglin E (1987) Direct analysis of high-performance thin-layer chromatography spots of nucleic purine derivatives by surface-enhanced Raman scattering spectrometry. Anal Chem 59:525–527
- Koglin E (1989) Combining HPTLC and micro-surface-enhanced Raman spectroscopy (Micro-SERS). J Planar Chromatogr 2:194–197
- 38. Busch KL (2001) In: Nyiredy Sz (ed) Planar chromatography. A retrospective view for the third millennium. Springer, Budapest, pp 261–277
- van Berkel GJ, Pasilis SP, Ovchinnikova O (2008) Established and emerging atmospheric pressure surface sampling/ionization techniques for mass spectrometry. J Mass Spectrom 43:1161–1180
- Cocan S (2009) Hyphenated techniques in thin-layer chromatography. Adv Chromatogr 47:353–453
- 41. Luftmann H (2004) A simple device for the extraction of TLC spots: direct coupling with an electrospray mass spectrometer. Anal Bioanal Chem 378:964–968
- 42. Alpmann A, Morlock G (2006) Improved online coupling of planar chromatography with electrospray mass spectrometry: extraction of zones from glass plates. Anal Bioanal Chem 386:1543–1551
- 43. Luftmann H, Aranda M, Morlock GE (2007) Automated interface for hyphenation of planar chromatography with mass spectrometry. Rapid Commun Mass Spectrom 21:3772–3776
- 44. Dreisewerd K, Kolbl S, Peter-Katalinic J, Berkenlcamp S, Pohlentz G (2006) Analysis of native milk oligosaccharides directly from thin-layer chromatography plates by matrixassisted laser desorption/ionization orthogonal time-of-flight mass spectrometry with glycerol matrix. J Am Soc Mass Spectrom 17:139–150
- 45. Fuchs B, Schiller J, Süß R, Zscharnack M, Bader A, Müller P, Schürenberg M, Becker M, Suckau D (2008) Analysis of stem cell lipids by offline HPTLC-MALDI-TOF MS. Anal Bioanal Chem 392:849–860
- 46. Fuchs B, Schiller J, Süß R, Nimptsch A, Schürenberg M, Suckau D (2009) Capabilities and disadvantages of combined matrix-assisted laser-desorption/ionisation time-of-flight mass spectrometry (MALDI-TOF MS) and high-performance thin-layer chromatography (HPTLC) analysis of egg yolk lipids. J Planar Chromatogr 22:35–42
- 47. Cody RB, Laramee JA, Dupont DH (2005) Versatile new ion source for analysis of materials in open air under ambient conditions. Anal Chem 77:2297–2302
- 48. Morlock G, Ueda Y (2007) New coupling of planar chromatography with direct analysis in real time mass spectrometry. J Chromatogr A 1143:243–251
- Haddad R, Milagre HMS, Catharino RR, Eberlin MN (2008) Easy ambient sonic-spray ionisation mass spectrometry combined with thin-layer chromatography. Anal Chem 80: 2744–2750
- Peng S, Edler M, Ahlmann N, Hoffmann T, Franzke J (2005) A new interface to couple thinlayer chromatography with laser desorption/atmospheric pressure chemical ionization mass spectrometry for plate scanning. Rapid Commun Mass Spectrom 19:2789–2793
- Ford MJ, Kertesz V, Van Berkel GJ (2005) Thin-layer chromatography/electrospray ionization triple-quadrupole linear ion trap mass spectrometry system: analysis of rhodamine dyes separated on reversed-phase C₈ plates. J Mass Spectrom 40:866–875
- Pasilis SP, Kertesz V, Van Berkel GJ, Schulz M, Schorcht S (2008) HPTLC/DESI-MS imaging of tryptic protein digests separated in two dimensions. J Mass Spectrom 43: 1627–1635

- van Berkel GJ, Kertesz V (2006) Automated sampling and imaging of analytes separated on thin-layer chromatography plates using desorption electrospray ionization mass spectrometry. Anal Chem 78:4938–4944
- 54. van Berkel GJ, Ford MJ, Deibel MA (2005) Thin-layer chromatography and mass spectrometry coupled using desorption electrospray ionization. Anal Chem 77:1207–1215
- 55. Sherma J, Larkin JD, Larkin FH (2009) A field guide to instrumentation. J AOAC Int 92:29A-35A
- 56. Hazai I (2004) Use of multiple readings to increase the sensitivity of phosphor image detection in TLC. J Planar Chromatogr 17:449–453
- 57. Zhong S, Li H, Bodi Z, Button J, Vespa L, Herzog M, Fray RG (2008) MTA is an arabidopsis messenger RNA adenosine methylase and interacts with a homolog of a sex-specific splicing factor. Plant Cell 20:1278–1288

Chapter 10 Diffuse Reflectance from TLC Layers

In planar chromatography light is used for detecting separated sample zones. To achieve this the stationary phase is commonly illuminated from the top by light of known intensity. Light of reduced intensity reflected from the top surface of the layer is used for quantification. The difference in intensity between the illumination and reflected light is a measure of the sample amount within the stationary phase. Increasing sample amounts will induce a decrease in the intensity of the reflected light. Therefore a transformation algorithm is needed, which turns the decreasing light intensities into increasing signal values and ideally shows linearity between the signals and sample amounts [1–3].

10.1 The Lambert Cosine Law

The first attempt to theoretically understand diffuse reflectance at macroscopic surfaces was made by Bouguer in 1760. Bouguer assumed that diffuse reflections occur through regular reflections from tiny crystals, which are distributed statistically over all angles. From direction α , the plate surface F still has the apparent size $dF = F\cos(\alpha)$. The light intensity I, therefore, describes the fraction dI, which is still the cosine portion of the incident light intensity I_0 (Fig. 10.1). According to the Lambert cosine law, the share of the diffuse reflected light dJ is

$$dJ(\alpha) = I_0 dF \cos(\alpha), \tag{10.1}$$

where

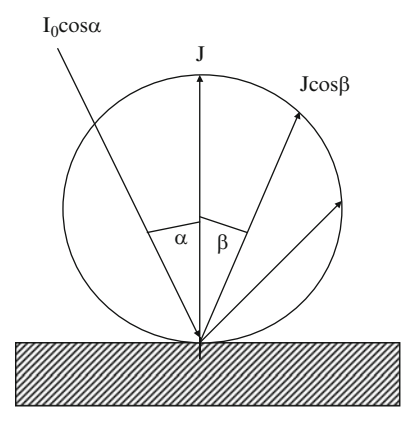
 I_0 incident light intensity

dF share of plate area

α angle of the incident light

dJ fraction of diffuse reflected light

Fig. 10.1 A Lambert emitter [3]



The Lambert cosine law does not determine exactly the angle distribution of the diffuse reflection from TLC plates. The plate acts more as a Seliger emitter due to direct reflections [3]. TLC plates glitter if the daylight is directly reflected at a small angle.

The incident light is scattered by the layer particles in all directions. Assuming this scattered light is isotropic (showing the same intensity in all directions), the fraction of light intensity dJ at the plate surface dF can be calculated according to the Lambert cosine law:

$$d\Im = \int dF \, dx = dx \int_0^{\pi/2} \frac{dJ}{I_0 \cos(\alpha) d\alpha} d\alpha.$$

The angle dependent distribution of the isotropic light is

$$\frac{\mathrm{d}J}{\mathrm{d}\alpha}2I_0\sin(\alpha)\cos(\alpha)$$

and further

$$d\Im = dx \int_0^{\pi/2} 2\sin(\alpha)d\alpha = 2 dx.$$
 (10.2)

For the fraction of the incident light travelling through the layer and passing the layer thickness share dx, the scatted light distance is 2dx. In other words, scattered light travels twice the absorption distance [3]. That makes the incredible detection power of HPTLC plates understandable, although absorption distances are so small. That is the reason why plate evaluation using light without destroying the stationary phase is so interesting.

The plate is illuminated by incoming light (the incident light) and is evaluated by the detection of the reflected light. The most convenient way to detect separated compounds on the plate is simply to use your eyes. Unfortunately this works only in the spectral range from 400 to 800 nm. In situ densitometry offers a way of measuring the optical density of the separated zones directly on the plate in the spectral range from 190 to 1,000 nm, and a scanner is recommended. The angular distribution of the reflected light whether as a Lambert emitter or Seliger emitter shows that illumination perpendicular to the plate surface results in maximum reflectance [1]. To achieve optimum diffuse reflection and minimal reflection of direct light, measurements should be done perpendicular to the plate. This is possible only by the use of light fibres with small diameters, which transport light to the plate top and back to the detector. Only light fibre interfaces have fibres for incident light and fibres for the reflected light in parallel. The rather small linear operating range is a general weakness of scanners. Indeed, most publications report a range of linearity, which does not exceed one order of magnitude. But this is not a general weakness of all planar methods. It arises from the use of incorrect transformation algorithms to establish a linear relationship between the sample amount in a zone and the observed signal. Even in the simple case of light, absorption in a non-scattering media results in a non-linear relationship between the observed signal and sample concentration.

10.2 Theory of Diffuse Reflectance

In the case of a scattering material like TLC plates, part of the scattered light is emitted as diffuse reflectance J when viewed perpendicular to the plate surface. Figure 10.2 shows an overview [3–7]. In general the vector I represents the light

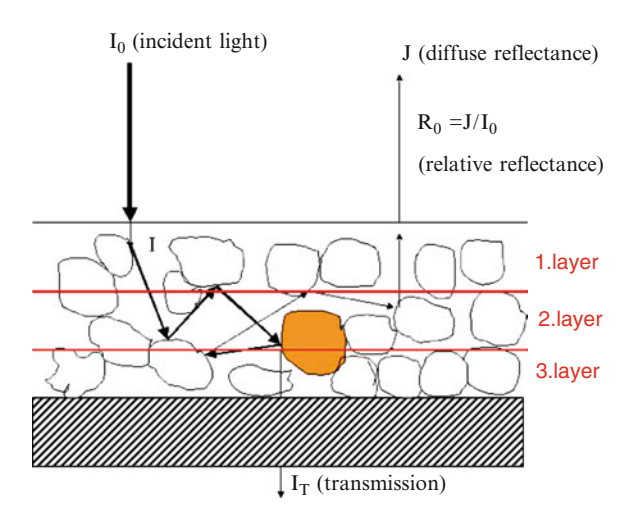


Fig. 10.2 Three virtual layers illustrating the interactions of an absorbing and scattering thin layer with incident light

flux in the direction of the incident light and the vector J describes the light intensity in the anti-parallel direction. To a first approximation, the incident light beam with intensity I_0 is scattered by particles inside the layer in all directions, and some radiation may be absorbed by either the sample or the layer itself. The diffuse reflected light J provides the desired information of how much light is absorbed by the sample.

If J is the scattered light in the direction of the layer surface and $I_{\rm abs}$ is the abbreviation for the light absorbed by the layer and sample, the incident light intensity I_0 is split into scattered and absorbed light. The abbreviation a stands for the absorption coefficient and s stands for the scattering coefficient:

$$I_0 = J + I_{\text{abs}} = sI_0 + aI_0 = I_0(s+a).$$
 (10.3)

Here.

 I_0 incident light intensity

J diffuse reflectance at the plate surface $(J=sI_0)$

s scattering coefficient

a absorption coefficient

 $I_{\rm abs}$ light absorption

In (10.3), the absorbed share of the incident light I_0 is aI_0 and the fraction of scattered light is sI_0 . Both coefficients (a and s) are assumed to be constant (e.g. show a constant distribution) over the whole layer. If all incident light is either absorbed or scattered and there is no other light loss, the sum of both shares must be the original incident light intensity. There is a simple connection between the scattering coefficient and the absorption coefficient [8, 9]:

$$s = (1 - a). (10.4)$$

It is well known that both the coefficients a and s are often proportional to each other, so that only the quotient a/s is constant [3, 7]. This is the main result of the socalled Kubelka-Munk theory, which is often used to describe reflectance on TLC plates [5]. To understand why a decreasing particle size causes a decrease of light absorption [3], consider the compound CuSO₄·5 H₂O, for example. This compound is blue in crystal form and turns nearly white when heavily ground. The reason is simple. Scatter increases with decreasing particle size and results in smaller path lengths within the layer for the incident light, which in turn reduces its absorption properties. The more the scattering the less light that can be absorbed and thus the brighter is the reflected light [3]. The Kubelka-Munk theory is commonly used to describe scattering and absorption in TLC layers and the Kubelka-Munk formula describes how to transform optical density measurements. But it is also said that this theory simplifies the real situation and is therefore not applicable to TLC. Perhaps it is the complex writing in the form of two differential equations, which makes it difficult to understand the Kubelka-Munk theory and its limitations. It probably will help to understand the complex processes of scatter and absorption by using a model that describes the TLC plate as an assembly of different layers [10]. Modern

HPTLC plates have a layer thickness of $100\text{--}200~\mu m$. If we assume an absorbent particle diameter of approximately 5 μm and a layer thickness of $100\text{--}200~\mu m$, this plate will have at least 20--40 virtual layers. Light absorption and scattering probably occurs in the upper part of these virtual layers. In Fig. 10.2 three virtual layers are drawn according to the particle size.

What happens with light within the different layers? In addition to sample absorption there is also absorption by the layer to be considered. The absorption coefficient a comprises both kinds of absorptions. The absorption coefficient determines the fraction of incident light aI_0 , which is absorbed. The non-absorbed radiation will be scattered inside the layer and only scattered light is emitted from the layer surface at the first virtual layer as I_1 :

$$J_1 = I_0 - I_{\text{abs}} = I_0 - aI_0 = I_0(1 - a). \tag{10.5}$$

If it is assumed that scattering between virtual layers is isotropic (that means we have constant light intensity in all directions) the same scattered light intensity J_1 that leaves the layer from the layer surface illuminates the top of the second virtual layer by leaving the first virtual layer at the bottom. From this light the fraction aJ_1 is absorbed and the fraction $J_1(I-a)$ is scattered. Therefore, the remaining light J_{sec} of the second layer is

$$J_{\text{sec}} = J_1(1-a) = I_0(1-a)^2. \tag{10.6}$$

Half of this light is scattered as J_2 towards the first virtual layer and illuminates the first virtual layer from the bottom. The other half illuminates as I_2 , the third virtual layer from above. In detail, the light intensity within the first layer comes from half of the non-absorbed share of the incident light $[I_0(1-a)/2]$ and half of the non-absorbed light from layer 2, which is the share $[J_2(1-a)/2]$. The sum of both intensities is emitted to the top as J_1 and illuminates layer 2 as $I_2(J_2 = I_2)$:

$$J_1 = \frac{1}{2}(1-a)I_0 + \frac{1}{2}(1-a)J_2 = \frac{(1-a)}{2}I_0 + \frac{(1-a)^3}{2^3}I_0.$$

The assumption that isotropic scattering takes place within TLC layers is not necessarily true. In the case of particles with a diameter larger than the wavelength of the scattered light, scattering becomes asymmetrical. The larger the quotient of the particle diameter and light wavelength, the smaller the scattering towards the layer surface compared with the scattered light in the incident light direction [1]. If we assume that every layer will illuminate the next layer above and below it with different light intensities, we need to introduce a backscattering factor k. The factor k describes the fraction of the remaining light in a virtual layer, which is scattered in the direction of the layer surface. Logically the fraction (1-k) describes the remaining light in a virtual layer, which is scattered in the direction of the plate bottom, which is also the direction of the incident light. In Fig. 10.3 the interactions of the incident light (I_0) with at least five layers is shown schematically. To make the situation clear, the abbreviations q = k(1-a) for the fraction of non-absorbed

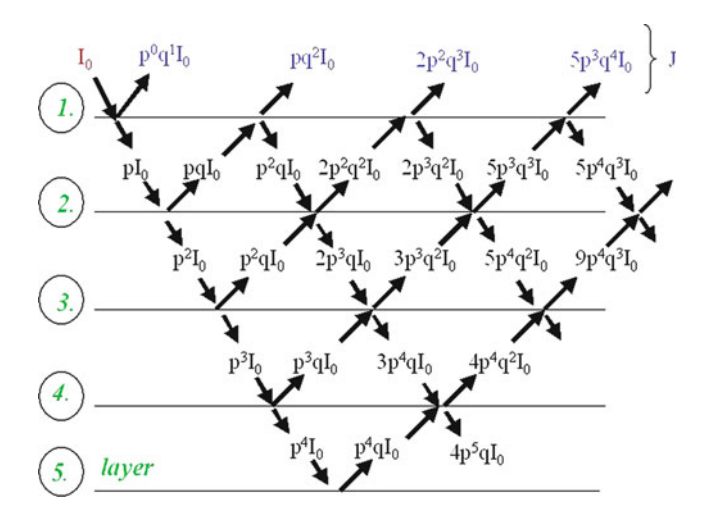


Fig. 10.3 The interactions of the incident light (I_0) with at least five virtual layers. The fraction q of I_0 is reflected to the top and the fraction p is scattered in the incident light direction. The expression for reflectance from the top five virtual layers is $J = qI_0 + pq^2I_0 + 2p^2q^3I_0 + 5p^3q^4I_0 + 14p^4q^5I_0 + \cdots +$. With p = q the expression for reflectance from the first five virtual layers is $J = qI_0 + q^3I_0 + 2q^5I_0 + 5q^7I_0 + 14q^9I_0 + \cdots$

light in the direction of the layer surface and p = (1-k)(1-a) for the fraction of light in the direction of the incident light are used.

For the light intensity of the first layer J_1 the layer model is expressed as

$$\frac{J_1}{I_0} = 2^0 q + \frac{1}{1 \times 2} 2^1 p q^2 + \frac{1 \times 3}{1 \times 2 \times 3} 2^2 p^2 q^3 + \frac{1 \times 3 \times 5}{1 \times 2 \times 3 \times 4} 2^3 p^3 q^4
+ \frac{1 \times 3 \times 5 \times 7}{1 \times 2 \times 3 \times 4 \times 5} 2^4 p^4 q^5 + \frac{1 \times 3 \times 5 \times 7 \times 9}{1 \times 2 \times 3 \times 4 \times 5 \times 6} 2^5 p^5 q^6 + \cdots$$

The relative reflectance value R_0 , defined as the quotient of J_1 and I_0 , converges to an expression containing a and k only:

$$R_0 = \frac{J_1}{I_0} = q + pq^2 + 2p^2q^3 + 5p^3q^4 + 14p^4q^5 + 42p^5q^6 + 132p^6q^7 + 429p^7q^8 + \dots = \frac{1}{2(1-a)(1-k)} \left(1 - \sqrt{1 - 4k(1-a)^2(1-k)}\right).$$

$$(10.7)$$

If this equation is resolved to an expression as a function of the absorption coefficient, a modified Kubelka–Munk equation results [10]:

$$KM(R_0, k \ge 0, k \le 1) = k\left(\frac{1}{R_0} - 1\right) + (1 - k)(R_0 - 1) = \frac{a}{(1 - a)}.$$
 (10.8)

Here,

 R_0 relative reflectance $(R_0 = J/I_0)$

k backscattering factor $(k \ge 0 \text{ and } k \le 1)$

a absorption coefficient

Equation (10.8) contains two parts: the fraction of incident light absorbed and the back-scattering correction. The first term in (10.8) describes the light absorption, whereas the second term shows a negative connection with the absorption coefficient (R_0 -1=-a), as shown by (10.5). Diffuse multiple scattering within a TLC layer results in an isotropic distribution of scattered light in any case and even directed incident light becomes isotropic after scattering in at least two layers [4]. Most scanners do not use diffuse illumination but most of the incident light is scattered in the first layer in any case. It cannot be excluded, however, that some light is asymmetrically scattered. Equation (10.8) can be used to establish whether the system scatters light isotropically or not [10].

10.2.1 Special Case a: The Reversal Reflectance Formula

The value of k can be larger than 0 and smaller than 1. For the extreme case of k = 1, we must assume that no scattered light illuminates the top of the second virtual layer. All light is absorbed in the first virtual layer as I_0a or is scattered from the top of the first virtual layer as $J_1 = I_0(1-a)$. With $R_0 = (1-a)$, we observe

$$RR(\lambda) = \left(\frac{1}{R_0} - 1\right) = \frac{a}{(1-a)}.$$
 (10.9)

This expression describes a TLC plate in which all the light is scattered at least within the first virtual layer to the plate surface. No light reaches the second virtual layer. This expression, therefore, transforms all light absorptions into positive values [9–11]. In Fig. 10.4 the contour plot of benzo[a]pyrene is shown. A contour plot comprises the observed absorbance data for a single track at different wavelengths. The relative reflectance is therefore a wavelength-dependent function. On the track, the benzo[a]pyrene spot is observed as a peak along the *x*-axis and as a spectrum along the *y*-axis with positive reversal reflectance values in the range from 200 to 400 nm.

The separation was performed on an HPTLC plate containing a fluorescent dye. The fluorescence-quenching signal can be seen between 500 and 550 nm.

10.2.2 Special Case b: The Fluorescence Formula

For the second extreme case of (10.8) in which k = 0, the transformation formula for fluorescence is obtained [10–12]:

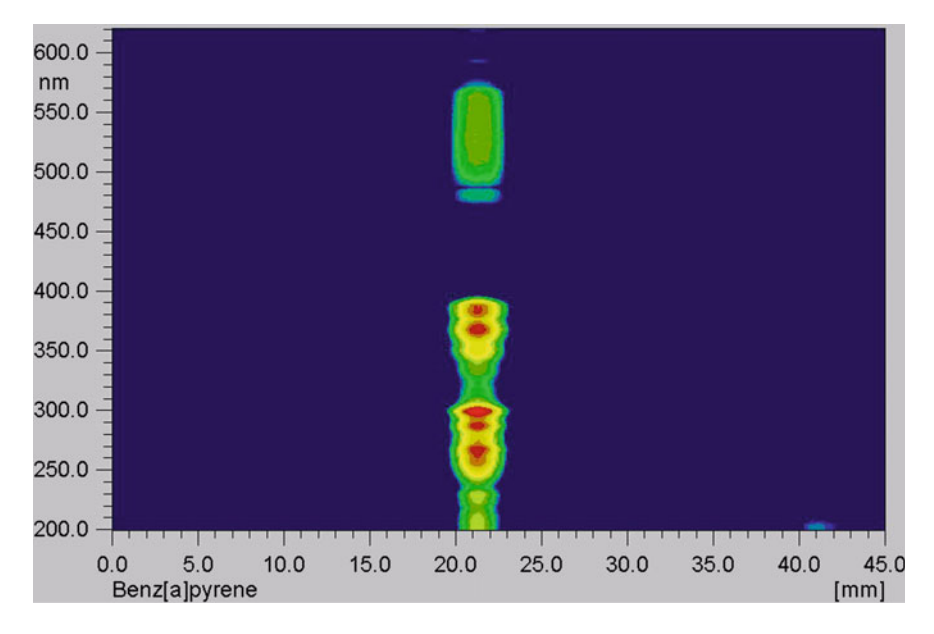


Fig. 10.4 Contour plot of a separation of benzo[a]pyrene calculated according to (10.9). The benzo[a]pyrene was separated on RP-18 silica gel layer containing a fluorescent dye with methanol–acetone (8+3, V/V)

$$FL(\lambda) = (R_0 - 1).$$
 (10.10)

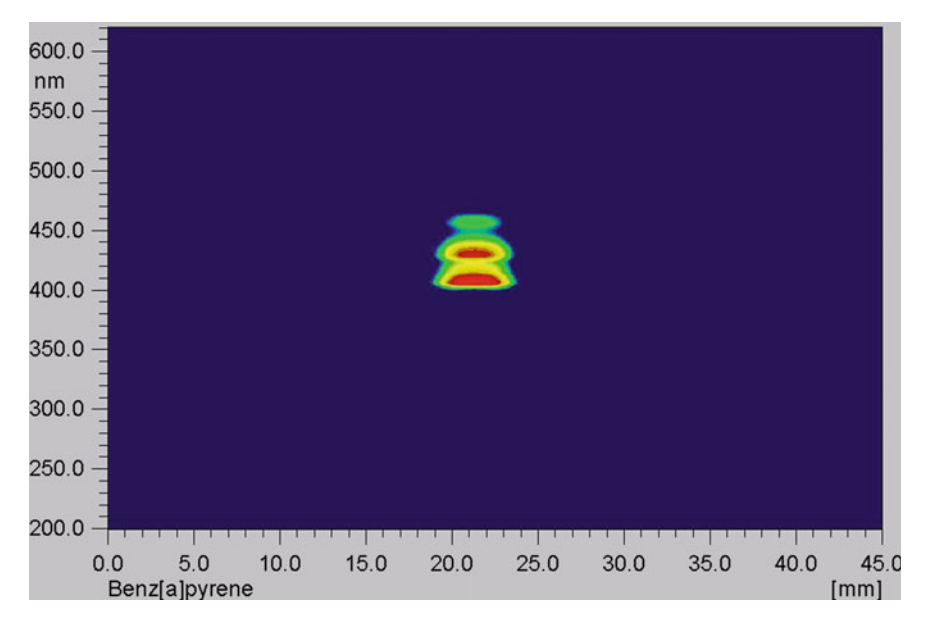
A contour plot evaluated by the use of the fluorescence formula instantly reveals compounds within the track scanned that fluoresce (Fig. 10.5).

10.2.3 Special Case c: The Kubelka-Munk Expression

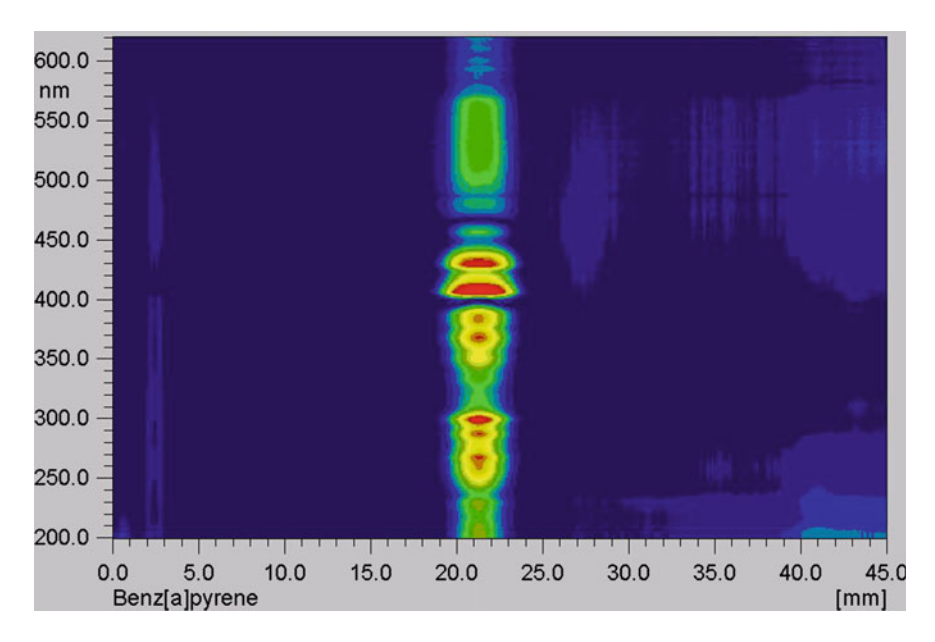
The Kubelka–Munk theory was first published in the year 1931 and is based on the assumption that half of the scattered flux is directed forward and half backward [1, 3, 4]. Both fluxes show the same intensity. According to Kubelka and Munk [3], scattering in every layer will illuminate the next layer above and below it with half of its non-absorbed light intensity:

$$KM(\lambda) = \frac{1}{2} \left(\frac{1}{R_0} - 1 \right) + \frac{1}{2} (R_0 - 1) = \frac{(1 - R_0)^2}{2R_0} = \frac{a}{(1 - a)} = \frac{a}{s}.$$
 (10.11)

In Fig. 10.6, a benzo[a]pyrene spot is evaluated according to Kubelka–Munk equation (10.11).



 $\textbf{Fig. 10.5} \ \ \text{Contour plot of a benzo[a]} pyrene \ separation \ calculated \ according \ to \ the \ fluorescence formula$



 $\textbf{Fig. 10.6} \ \ \text{Contour plot of a benzo[a]} pyrene \ separation \ calculated \ according \ to \ Kubelka-Munk \ equation \ (10.11)$

The Kubelka–Munk equation comprises both the absorption and the fluorescence signals [10, 11]. This expression is therefore recommended for a quick overview of a separation.

10.3 Mass-Dependent Reflection

Equation (10.8) demonstrates a linear relationship between the sample amount and the total absorption coefficient. It is assumed that the total absorption coefficient a is constant within the layer, which means a constant sample concentration in the whole layer. In TLC, the layer absorption is constant but the sample absorption is not. The sample distribution within a spot has a distribution of unknown shape. Layer models profoundly demonstrate that this (unknown) sample distribution is very important for the intensity of the reflection signal. If it is simply assumed that the whole sample is located in the first virtual layer and absorbs half of the incident light while half of the non-absorbed light is scattered to the plate surface and half to the second layer, the diffuse reflection is $R_1 = 0.2$, if we do not take the fraction of the scattered light in the direction of the other layers into account. In a second example, the same amount of sample is totally located in the second layer. From the first layer, half of the incident light is scattered in the direction of the plate surface and half illuminates the second layer. In the second layer, half of the illumination from the first layer is absorbed and the rest is scattered. If we do not take this scattered light into account the diffuse reflection will be $R_2 = 0.5$. This represents a tremendous difference between these two values, although we have the same sample amount, but now it is simply located in the neighbouring layers. These calculations show the importance of the sample distribution within the layer because the deeper a sample is located within the layer the weaker its absorption signal is. Quantitative TLC does not need a constant sample concentration within the layer, which cannot be verified experimentally. Essential for quantitative TLC is a constant sample distribution for each sample zone. This makes the evaporation of the mobile phase from the layer before scanning so important because uneven drying of the layer results in different sample distributions for the same compound in different tracks [10].

The stationary phase in TLC will absorb light as does the sample. Besides this loss of incident light by absorption, light is also lost by transmission $I_{\rm T}$ from the backside and edges of the layer. We can gather all losses of light in the absence of sample into the expression $I_{\rm abs,u}$. $I_{\rm abs,s}$ describes the light absorbed by the sample. The scattered light in the direction of the layer surface J is

$$J = I_0 - I_{abs} = I_0 - (I_{abs,u} + I_{abs,s}).$$
 (10.12)

With this expression, we assume that these two different types of absorption occur simultaneously. A sample, therefore, "sees" the light intensity I_0 of the

illumination lamp minus the light absorbed by the layer $I_{abs,u}$. The sample absorption coefficient is now defined as

$$a_{\rm s} \equiv \frac{I_{\rm abs,s}}{I_0 - I_{\rm abs,u}}.\tag{10.13}$$

The same is true for the absorption of light by the layer, which is illuminated by I_0 minus the light which is absorbed by the sample. The plate absorption coefficient is therefore defined as

$$a_{\rm u} \equiv \frac{I_{\rm abs,u}}{I_0 - I_{\rm abs,s}}.\tag{10.14}$$

The replacement of $I_{abs,u}$ from (10.14) in (10.13) and vice versa gives

$$\frac{I_{\text{abs,s}}}{I_0} = \frac{a_{\text{s}} - a_{\text{s}} a_{\text{u}}}{1 - a_{\text{s}} a_{\text{u}}} \text{ and } \frac{I_{\text{abs,u}}}{I_0} = \frac{a_{\text{u}} - a_{\text{s}} a_{\text{u}}}{1 - a_{\text{s}} a_{\text{u}}}.$$

The absorption coefficient of the layer and sample is then the sum of both the factors [8, 9].

$$a = \frac{I_{\text{abs,s}}}{I_0} + \frac{I_{\text{abs,u}}}{I_0} = \frac{a_s + a_u - 2a_s a_u}{1 - a_s a_u}.$$
 (10.15)

This absorption factor describes all absorptions within the layer. To prove whether the quotient of a and the scattering factor (1-a) is linear with respect to the sample mass m, (10.15) is substituted into (10.8).

$$\frac{a}{1-a} = \frac{a_{\rm s}(1-2a_{\rm u}) + a_{\rm u}}{(1-a_{\rm s})(1-a_{\rm u})}.$$

The light intensity which is absorbed by the sample mass m depends on the mass absorption coefficient $a_{\rm m}$ and must be written as

$$I_{\text{abs.s}} \equiv ma_{\text{m}}I_0$$
.

The rest of the light either leaves the layer or is absorbed by the stationary phase

$$I_{\text{abs u}} = (1 - m)a_{\text{m}}I_{0}.$$

It follows then that the sample absorption coefficient a_s becomes

$$a_{\rm s} = \frac{ma_{\rm m}}{1 - a_{\rm m}(1 - m)}.$$

Replacement of a_s leads to the following expression:

$$\frac{a}{(1-a)} = \frac{ma_{\rm m}(1-2a_{\rm u}) + a_{\rm u}[1-a_{\rm m}(1-m)]}{[1-a_{\rm m}(1-m) - ma_{\rm m}](1-a_{\rm u})}$$

and further

$$\frac{a}{(1-a)} = m \frac{a_{\rm m}}{(1-a_{\rm m})} + \frac{a_{\rm u}}{(1-a_{\rm u})}.$$
 (10.16)

There is a linear connection between the mass m of a compound and its corresponding signal. The intercept in (10.16) contains the constant a_u only and therefore describes the layer absorption [8, 9]. Equations (10.8), (10.9), and (10.11) demonstrate linearity between the transformed intensity data and the quotient a/(1-a) and direct linearity between the transformed data and the sample mass. With transformed intensity data according to (10.8), the fraction of the light absorbed by the sample can be separated from the light absorbed by the layer. The diffuse reflected light intensity J_0 can be determined at a position of the layer surface free of absorbing compounds. If this signal is used in (10.17) instead of the lamp intensity I_0 to calculate the relative reflection R, we assume that the TLC plate does not show any loss of light instead of sample absorption. The corrected relative reflection R can be written as

$$R = \frac{J}{I_0 - I_{\text{abs u}}} = \frac{J}{J_0}.$$
 (10.17)

As a result, the plate absorption intensity $I_{\rm abs,u}$ becomes zero, but in fact the light intensity of the lamp I_0 is only replaced by J_0 . Mathematically the original light flux of the lamp I_0 is reduced by all loss of light at the plate surface to J_0 , and hence we assume $I_{\rm abs,u}$ to be zero, which in turn means that $a_{\rm u}$ is zero as well. With (10.8), (10.16), and (10.17), we obtain the fundamental expressions (10.18) for quantitative HPTLC:

$$k\left(\frac{1}{R}-1\right) + (1-k)(R-1) = m\frac{a_{\rm m}}{(1-a_{\rm m})},$$

$$k\left(\frac{1}{R}-R\right) + (R-1) = m\frac{a_{\rm m}}{(1-a_{\rm m})}.$$
(10.18)

R relative reflectance

K backscattering factor $(k \ge 0 \text{ and } k \le 1)$

 $a_{\rm m}$ mass absorption coefficient

m sample mass

This equation affords a linear relationship between the sample mass and the transformed signal with no intercept [9, 10].

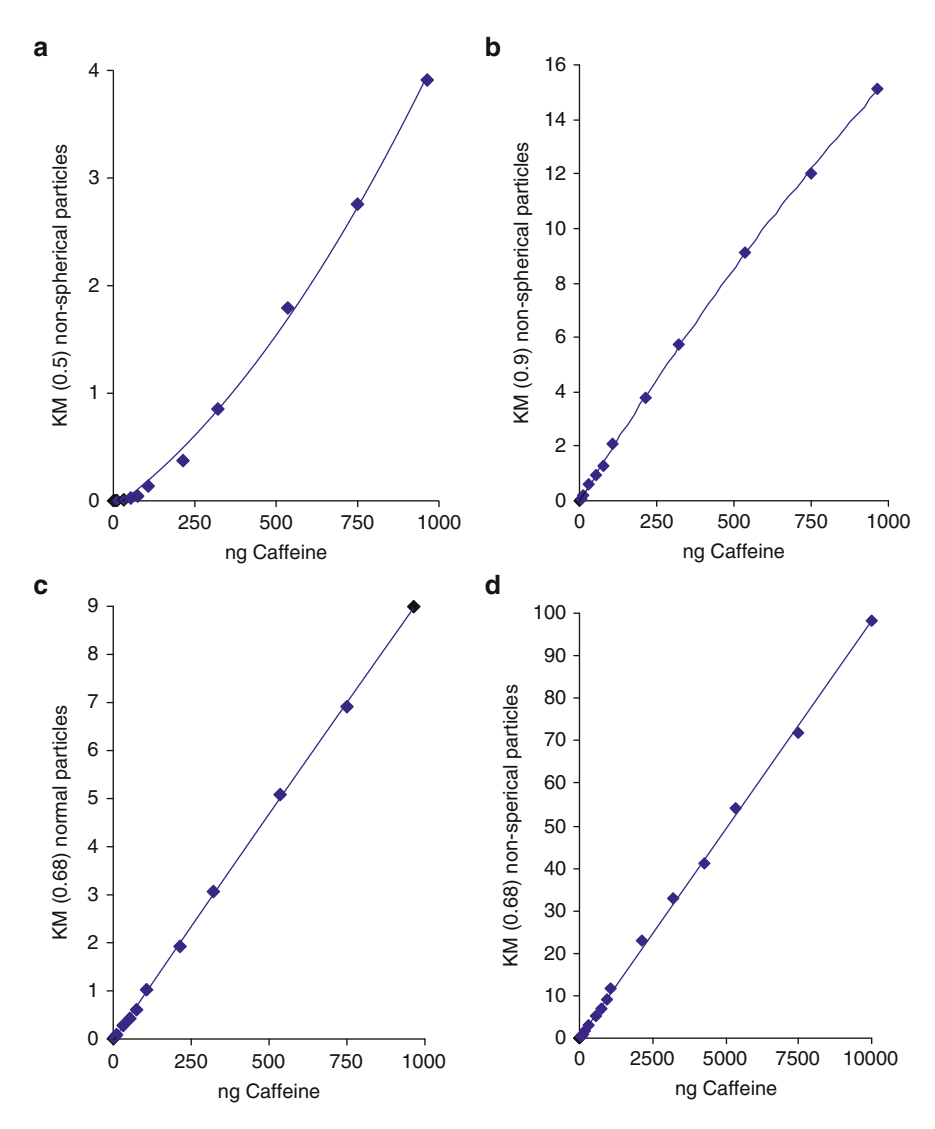


Fig. 10.7 Calibration curve for caffeine after separation with a mobile phase of 2-propanol-cyclohexane–25% (W/V) aqueous ammonia (7+2+1, V/V) on silica gel 60. (a) Raw data evaluation according to Kubelka–Munk equation (10.18) with k = 0.5; (b) Raw data evaluated according to (10.18) with k = 0.9; (c, d) Raw data evaluated according to (10.18) with k = 0.68

To confirm the theoretical considerations, different amounts of caffeine were separated on silica gel layers without fluorescent indicator and the responses were measured with a diode-array detector [10]. The calibration curves for caffeine over the range 1–1,000 ng and 1–10,000 ng are shown in Fig. 10.7. In Fig. 10.7a, the raw data are evaluated using the original Kubelka–Munk equation (10.11) illustrating the absence of linearity for the full working range. There are some deviations from

linearity in Fig. 10.7b evaluated with (10.18) and a backscattering factor k = 0.9. The response relationship is slightly curved [13]. The *curve* in the response relationship is fully compensated (linear) over the whole working range from 1–10,000 ng caffeine when using (10.18) with a backscattering factor of k = 0.68 (Fig. 10.7c, d).

10.4 Simplifying the Expression

Equation (10.18) shows linearity over a large concentration range without an intercept, as shown in Fig. 10.7. The backscattering factors of nearly all HPTLC plates are in the range from k = 0.6 to k = 1.0. For many applications, it is sufficient to use (10.18) with a factor of k = 1. Using a backscattering factor of k > 0.5, approximation (10.19) is absolutely sufficient for planar chromatographic evaluations:

$$\frac{k(1-R)^{1/k}}{R} \approx m \frac{a_{\rm m}}{(1-a_{\rm m})}.$$
 (10.19)

The values for this expression do not differ too much from (10.18). As an approximation for k values, the formula $3(1 - R)^{1.3}/4R$ holds for $k \approx 0.75$. Similar expressions can be found in [14, 15].

References

- Jork H (1966) Direkte spektralphotometrische Auswertung von Dünnschicht-Chromatogrammen im UV-Bereich. Fresenius Z Anal Chem 221:17–33
- Ebel S, Hocke J (1976) Computer controlled evaluation in thin-layer chromatography. J Chromatogr 126:449–456
- 3. Kortüm G (1969) Reflextionsspektroskopie. Springer, Berlin
- 4. Schuster A (1905) Radiation through a foggy atmosphere. Astrophys J 21:1-22
- Kubelka P, Munk F (1931) Ein Beitrag zur Optik der Farbanstriche. Z Tech Physik 11a:593–601
- Ebel S, Post P (1981) Theory of reflectance measurements in quantitative evaluation in TLC and HPTLC. 1. Multilayer model of reflectance and transmittance. J High Resolut Chromatogr 4:337–342
- 7. Kubelka P (1948) New contributions to the optics of intensely light-scattering materials. Part I. J Opt Soc Am 38:448–457, 1067
- 8. Post P (1979) Massenverteilung und densitometrische Detektion in der DC. Thesis, Marburg
- Spangenberg B, Post P, Ebel S (2002) Fibre optical scanning in TLC by use of a diode-array detector – linearization models for absorption and fluorescence evaluations. J Planar Chromatogr 15:88–93
- Spangenberg B (2006) Does the Kubelka-Munk theory describe TLC evaluations correctly?
 J Planar Chromatogr 19:332–341
- Spangenberg B, Klein K-F (2001) New evaluation algorithm in diode-array thin-layer chromatography. J Planar Chromatogr 14:260–265

References 275

12. Spangenberg B, Weyandt-Spangenberg M (2004) Quantitative thin-layer chromatography using absorption and fluorescence spectroscopy. J Planar Chromatogr 17:164–168

- 13. Treiber LR (1974) Standardization of the direct spectrophotometric quantitative analysis of chromatograms. IV. A comparative study on the most common mathematical treatments of thin-layer densitometric problems. J Chromatogr 100:123–135
- Loyalka SK, Riggs CA (1995) Inverse problem in diffuse reflectance spectroscopy: accuracy of the Kubelka-Munk equation. Appl Spectrosc 49:1107–1110
- Dahm DJ, Dahm KD (2007) Interpreting diffuse reflectance and transmittance. NIR, Chichester

Chapter 11 Fluorescence in TLC Layers

The measurement of fluorescence in planar chromatography is a sensitive method for the determination of fluorescing substances [1–9]. Fluorescence emission provides more selectivity and increased sensitivity compared to UV–visible absorption. Molecular fluorescence can be described as the immediate emission of energy from a molecule after irradiation. During absorption (this process is called radiative excitation), a molecule is excited from a lower to a higher electronic state by absorption of a photon. During de-excitation, a molecule emits a photon and changes from a higher to a lower electronic state. A transition between states of the same multiplicity is known as fluorescence and a transition between states of different multiplicities is called phosphorescence.

11.1 Theory of Fluorescence and Phosphorescence

Fluorescence or phosphorescence occurs at longer wavelengths compared with excitation. Some compounds do not show fluorescence. In this case, the absorbed energy is dissipated by the medium or emitted as phosphorescence, which has a longer lifetime for the excited state. Fluorescence is usually observed in the case of $n \to \pi^*$ or $\pi \to \pi^*$ transition states. The $n \to \pi^*$ transition state of an electron from a non-binding ground state to a first excited π -state has a longer lifetime than a pure $\pi \to \pi^*$ transition. Due to their longer lifetime, excited electrons from $n \to \pi^*$ transitions are more likely to experience energy dissipation than excited electrons from $\pi \to \pi^*$ transitions. Polycyclic aromatic compounds, such as pyrene and benzo[a]pyrene, or compounds without non-binding electrons are more likely to exhibit fluorescence than compounds with non-binding electrons, such as ethers or carbonyls. Biphenyl and stilbene, for example, show fluorescence because they have a large number of π -electrons. The lowest transition state for diphenyl ketone is a n $\rightarrow \pi^*$ transition. This substance does not fluoresce. The lifetime of the excited state is of the order of 10^{-9} – 10^{-7} s. If the lifetime of the excited electron exceeds 10^{-3} s the process is called phosphorescence. Fluorescence occurs from a single state because the absorbed light is – after internal stabilization by dissipation – directly emitted from this excited state. The internal dissipation (internal conversion) to a lower energy level explains why fluorescence is emitted at longer wavelengths than the absorbed light. Phosphorescence is emitted from a triplet state. The excited electron undergoes intersystem crossing to a triplet state, which is blocked from light emission. This is the reason for the large phosphorescence lifetime.

Fluorescence spectra often show a mirror-like structure compared with absorption spectra. This is shown in Fig. 11.1 for benzo[a]pyrene, absorption spectrum (left) and fluorescence spectrum (right). The π -electron system of benzo[a]pyrene is excited to different vibration states. After internal conversion, all electrons are energetically located in the lowest excited state and emit light by "falling" down to the different vibration levels of the ground state. This is schematically shown in Fig. 11.1. The energy of the fluorescence emission is generally lower than that of absorption. This is caused by the loss of energy during the internal conversion process. This energy difference between the absorption and fluorescence spectra is known as "Stokes shift" named after Stokes, who first described this in 1858.

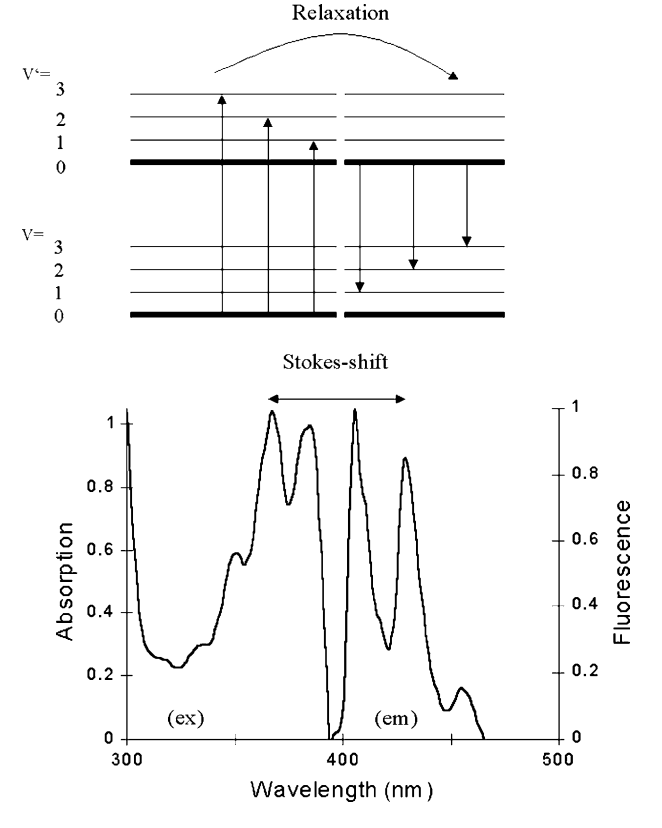


Fig. 11.1 A Jablonski energy level diagram for benzo[a]pyrene (*above*). The absorption spectrum (*left*) and the fluorescence emission (*right*) for benzo[a]pyrene on a TLC plate is shown below

The mirror-like structure of fluorescence absorption and emission spectra can easily be explained by assuming that during the absorption process the different vibration levels increase in energy in the opposite direction to the fluorescence process [9].

Fluorescence is observable only if the absorbed energy is not fully dissipated during internal conversion. Compounds in contact with the stationary phase usually lose some energy by transfer to the layer diminishing their fluorescence intensity. Compounds that fluoresce weakly in solution may show no fluorescence at all when adsorbed onto silica gel or may show fluorescence at much longer wavelengths than observed in solution. In TLC, an excited molecule rapidly dissipates its vibrational energy as heat to the surrounding medium, that is to say, the activated molecules distribute their excess photons to neighbouring molecules or to the TLC layer. If a thermal de-activation pathway reduces fluorescence, the term "quenching" is commonly used. Studies of fluorescence quenching in solution as a function of solvent viscosity identify two quenching processes: a viscosity-independent process, referred to as static quenching, and a diffusion-controlled process, referred to as dynamic quenching [10].

In TLC, static quenching is attributed to contact between molecules in the layer and with the layer itself. Dynamic quenching results from the formation of complexes in an excited state by diffusion-controlled encounters of excited and ground state molecules [10]. The probability of a collision between excited and unexcited molecules in a TLC layer increases at higher sample concentrations. The interaction of an excited molecule with an unexcited molecule can lead to transfer of its excitation energy to either molecules of the same species or to the layer. An energy transfer between molecules of the same species is referred to as excitation migration. Aromatic hydrocarbons, for example, do not associate in the ground state but may form molecular complexes in concentrated solutions [10]. The spectrum of a concentrated pyrene sample (1.7 μ g/spot) is shown in Fig. 11.2 before (blue bold line) and after dipping in an aqueous solution of sodium pentanesulphonate (thin red line). First of all, a remarkable difference can be seen between the absorbance spectrum for pyrene on the dipped and the undipped layer.

The pyrene spot on the undipped layer shows broad and unstructured absorption bands slightly shifted towards lower wavelengths in comparison to the pyrene absorption spectrum on the dipped layer. The absorption spectrum shows a sharp structured shape between 200 and 360 nm. The pyrene fluorescence spectra are different as well. On the native silica gel layer the pyrene spot shows a weak and unstructured fluorescence around 480 nm caused by pyrene–pyrene interactions. After dipping, the pyrene spectrum shows an additional well-structured peak between 360 and 440 nm. This peak is identical to the fluorescence spectrum for monomeric pyrene in solution [10]. Taking the range from 360 to 600 nm into account, dipping the layer in the sodium pentanesulphonate solution is responsible for a tenfold fluorescence enhancement. For 420–600 nm the fluorescence enhancement is about sixfold. Pyrene in dilute solution exhibits a rich structured violet fluorescence emission band around 380 nm, which is characteristic for an excited monomer [11]. The concentration quenching of this fluorescence is accompanied by the appearance of a broad structure-less green

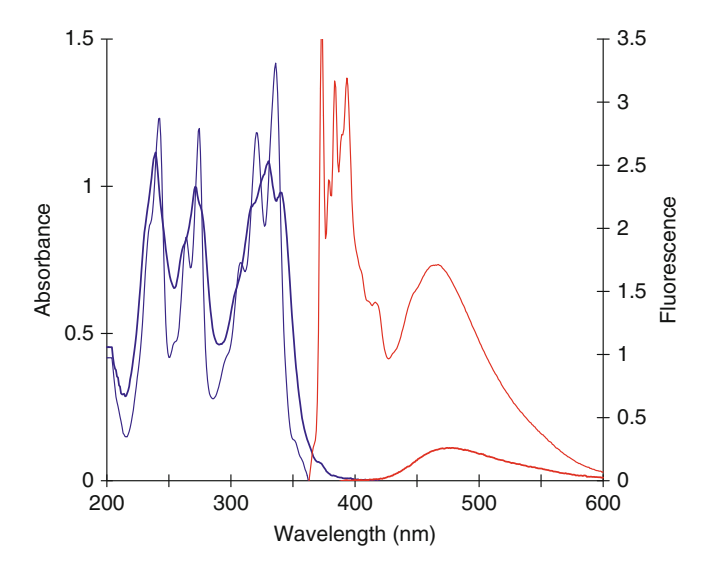


Fig. 11.2 Absorption and fluorescence spectra of $1.7 \mu g$ pyrene, measured on a silica gel layer. The sample not dipped in the sodium pentanesulphonate solution shows broad and unstructured absorption bands whereas the dipped sample shows sharp structures and a large fluorescence

fluorescence around 480 nm. The structure-less emission band is due to the fluorescence of excited pyrene dimers, formed by collisional interaction of excited and unexcited pyrene molecules. The fluorescence of excited pyrene dimers is not caused by the absorption of pyrene ground state dimers, because no concentration-dependent change in the absorption spectra (e.g. peak broadening) is observed. This indicates that the excited pyrene dimers, responsible for the 480 nm fluorescence, are dissociated in the ground state [11]. The term excimer was introduced to distinguish between excited dimers, which are dissociated in the ground state, and normal dimers in an excited state [11]. Figure 11.3 shows the fluorescence spectra for different amounts of pyrene applied to a silica gel plate. At higher pyrene concentrations, an increase in the excimer emission and a decrease in the monomer emission can be observed.

The sharp structure of the monomer emission bands broadens with increasing pyrene concentration. The calibration plot of the fluorescence taken below 400 nm shows a negative slope due to the dramatic concentration quenching. Thus, this concentration range is unsuitable for quantitative evaluations.

11.2 Fluorescence Enhancement

To improve the fluorescence intensity, thermal de-activations should be effectively suppressed. Numerous papers recommend spraying or dipping plates in a liquid to enhance and stabilize fluorescence signals [8, 12–19]. The term

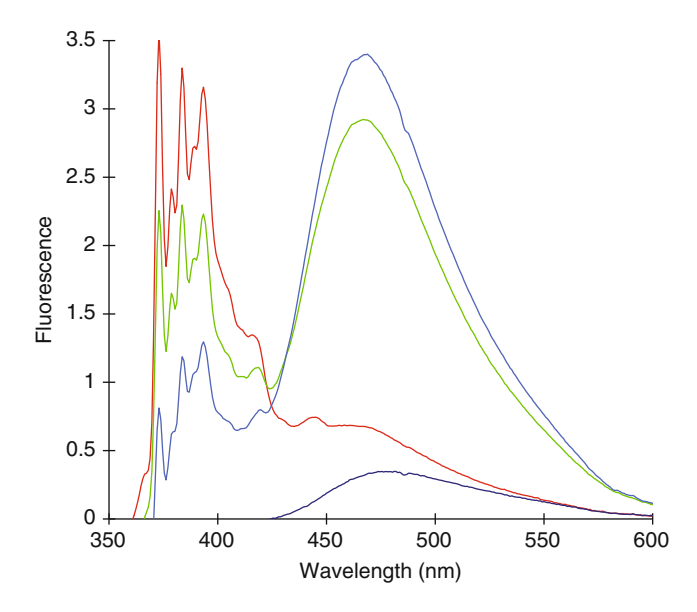


Fig. 11.3 Fluorescence spectra for different pyrene concentrations (from *top to bottom* 11.7 μ g, 5.1 μ g, 3.4 μ g, and 1.7 μ g after dipping the plate in a solution of sodium pentanesulphonate and the 11.7 μ g and 1.7 μ g without dipping) on a silica gel TLC plate

"enhancement" of fluorescence is the change in the observed signal after spraying or dipping the layer in a solution of a viscous liquid in a volatile organic solvent. This phenomenon is frequently observed for compounds adsorbed on silica gel and less so for the same compounds adsorbed on chemically bonded layers [17]. Otherwise, dipping in solutions containing fluorescing substances is often used to visualize lipophilic substances after TLC separation [12]. Figure 11.4. shows the fluorescence spectra for pyrene on an RP-18 layer (red) and after dipping in a solution of sodium pentanesulphonate (blue). The excimer signals around 480 nm are decreased significantly after dipping, indicating a reduction in the excited dimer formation. The monomer fluorescence signal increases slightly. Impregnating the layer with sodium pentanesulphonate prevents pyrene from forming the excited dimers and is also responsible for the increase in monomeric fluorescence [11].

Impregnating the layer with a solvent or an enhancing reagent enhances fluorescence by blocking pyrene-layer contact. Fluorescent signals for pyrene monomers can be seen because radiation-less pathways are no longer available. This is the main enhancement effect, restricted to low concentrations of pyrene on silica gel. Dipping the layer in an enhancing reagent mainly causes the enhancement effect on RP-18 plates by the blocking of pyrene-to-pyrene interactions. This minimizes eximer fluorescence and increases monomer fluorescence. Thus, the enhancement effect is a shielding effect of the dipping solution, which reduces molecular interactions with the stationary phase or other molecules located in the stationary

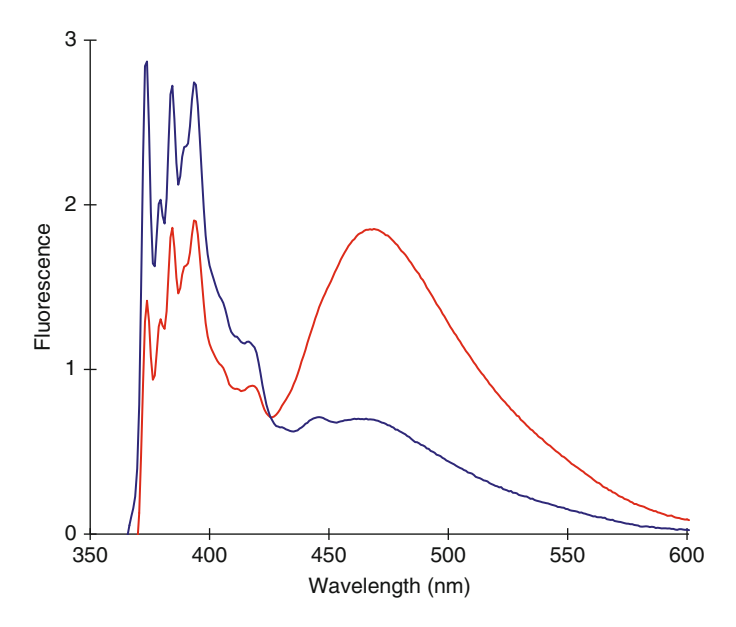


Fig. 11.4 Fluorescence spectra for pyrene on an RP-18 layer (*red*) and after dipping in a solution of sodium pentanesulphonate (*blue*)

phase. An excellent overview of dipping or spraying for fluorescence enhancement was given by Jork [12]. The theoretical background of this important method of making TLC more sensitive has often been controversially discussed [8, 13, 14, 18, 19]. Impregnating the layer with an enhancing reagent is an intended contamination of the analyte, which may appear strange, since impurities normally quench fluorescence.

11.3 Quantification in TLC by Fluorescence

Sample molecules in a light scattering medium exhibit fluorescence $J_{\rm F}$ if the absorbed light is transformed into fluorescence emission. The extent of this transformation is described by the quantum yield factor $q_{\rm F}$. The light intensity absorbed by the sample can be calculated from the light intensity reflected from the clean plate surface (J_0) minus the light intensity (J) reflected from the sample:

$$J_{\rm F} = q_{\rm F}(J_0 - J) = q_{\rm F}J_0(1 - R), \tag{11.1}$$

where

 $J_{\rm F}$ emitted fluorescence intensity

 $q_{\rm F}$ fluorescence quantum yield factor

 J_0 light intensity reflected from a clean plate surface

J light intensity reflected from the sample

R relative reflectance $(R = J/J_0)$

11.3.1 Low Sample Concentration Fluorescence in Light Scattering Media

In the case of trace analysis (which means we have k-values near $k \sim 1$), we observe linearity according to the extended Kubelka–Munk equation (10.18) for the reflectance formula (1/R)-1. The quotient $R=J/J_0$ is a relative measure of the scattered light from a sample zone compared with the scattered light for the excitation source. By multiplying (11.1) by 1/R and taking (10.4) and (10.18) into account, we get

$$\frac{J_{\rm F}}{J_0 R} = q_{\rm F} \frac{(1-R)}{R} = q_{\rm F} m \frac{a_{\rm m}}{s}.$$
 (11.2)

If R is substituted by R = s/(a + s) (derived from expression (1 - R)/R = a/s) and if we take into account (s + a) = 1, (11.3) results from (11.2):

$$J_{\rm F} = mJ_0q_{\rm F}\frac{a_{\rm m}}{s}\frac{s}{(a+s)} = mJ_0q_{\rm F}a_{\rm m}.$$
 (11.3)

The reflected light intensity J of the sample is the sum of light scattering $J_{0\rm F}$ and fluorescence at the fluorescence wavelength ($J_{\rm F}=J-J_{0\rm F}$). Equation (11.3) can be rewritten as

$$\frac{J - J_{0F}}{J_{0F}} = R_{F} - 1 = \frac{J_{0}}{J_{0F}} m q_{F} a_{m}. \tag{11.4}$$

Here.

J scattered light intensity of the sample (at the wavelength of the fluorescence)

 $J_{0\rm E}$ intensity of the reference at the wavelength of the fluorescence

 J_0 intensity of the reference at the wavelength of absorption

m sample mass

 $q_{\rm F}$ fluorescence quantum yield factor

 $a_{\rm m}$ mass absorption coefficient

In trace analysis the fluorescence intensity is directly proportional to the sample amount in the layer. Here, we can see a crucial advantage of fluorescence measurements compared with absorption: the fluorescence signal increases with increasing source intensity [20, 21].

11.3.2 High Sample Concentration Fluorescence in Light Scattering Media

To measure the fluorescence of a sample at high concentration, the extended Kubelka–Munk equation (10.18) with $k \sim 0.5$ describes a linear dependency between fluorescence intensity and sample mass:

$$KM = \frac{(1-R)^2}{2R} = \frac{a}{s} = m\frac{a_{\rm m}}{s}.$$
 (11.5)

The sample absorbs light and the fluorescence emission J_F is described by the quantum yield factor q_F according to $J_F = q_F J_0 (1 - R)$ (11.1). If this equation is squared and the denominator extended by 2R, and if the Kubelka–Munk equation (11.5) is taken into account, (11.6) results [21]:

$$\frac{J_{\rm F}^2}{J_0^2 2R} = q_{\rm F}^2 \frac{(1-R)^2}{2R} = q_{\rm F}^2 m \frac{a_{\rm m}}{s}.$$
 (11.6)

Substituting for R (derived from (10.4) and (11.5)) as

$$R = \frac{1}{s} - \frac{1}{s}\sqrt{1 - s^2} = \frac{1}{\frac{1}{s} + \frac{1}{s}\sqrt{1 - s^2}} = \frac{s}{1 + \sqrt{1 - s^2}}$$

gives

$$J_{\rm F}^2 = mJ_0^2 q_{\rm F}^2 \frac{2a_{\rm m}}{1 + \sqrt{1 - s^2}}.$$

If we take into account that for large sample amounts (with strong light absorption) the scattering coefficient is $s \ll 1$, (11.7) results:

$$J_{\rm F}^2 = mJ_0^2 q_{\rm F}^2 a_{\rm m},\tag{11.7}$$

where

 $J_{\rm F}$ emitted fluorescence intensity

m sample mass

 $q_{\rm F}$ fluorescence quantum yield factor

 J_0 light intensity reflected from a clean plate surface

 $a_{\rm m}$ mass absorption coefficient

For large sample masses, the squared fluorescence intensity is directly proportional to the sample amount in the layer. High sample concentrations in a zone are only suitable for quantitative evaluations if eximers are not formed. Flurpitin does not form eximers and its calibration plot is linear up to 5 µg per zone (Fig. 11.5) [21].

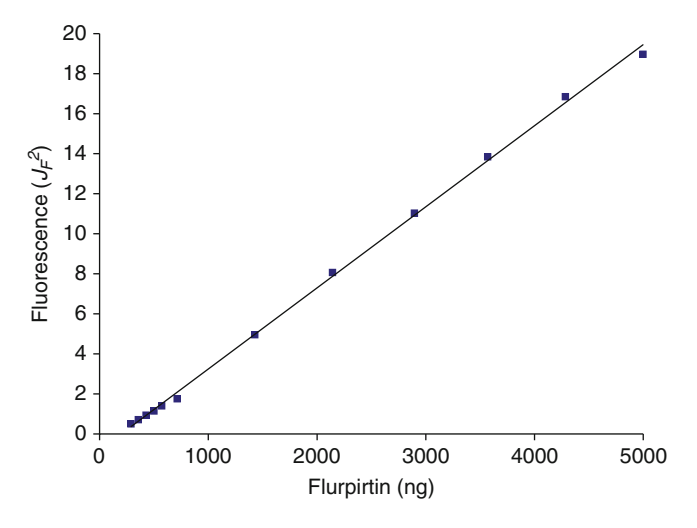


Fig. 11.5 Calibration curve for flurpitin (a centrally acting non-opioic analgesic compound) evaluated using (11.7). The fluorescence detection limit for flurpitin is 200 ng [21]

11.4 Contour Plots for Fluorescence Evaluation

The visualization of fluorescence emission using (11.4) or (11.5) gives a quick overview of all fluorescent compounds separated on a single HPTLC track. For all reflectance values R the expression (R-1) shows positive values only for fluorescence:

$$R - 1 = \frac{J_0}{J_{0F}} q_F a_{\rm m} m. \tag{11.8}$$

Figure 11.6 shows a separation of four aflatoxins B_1 , B_2 , G_1 , and G_2 as a contour plot. Both G_1 and G_2 aflatoxins fluoresce above 470 nm. This is observed as a green fluorescence (hence the abbreviation G). The B-aflatoxins show blue fluorescence only below 470 nm (hence the abbreviation B). The G-aflatoxins' fluorescence spectra can be measured easily at concentrations less than 100 pg per zone. Scanning densitometry also facilitates the determination of peak purity of separated zones and aids compound identification using fluorescence spectral libraries.

11.5 TLC Plates Containing a Fluorescent Dye

For the detection of UV absorbing substances, which show no native fluorescence, layers containing a fluorescence indicator can be used. Commonly, inorganic dyes are homogeneously incorporated in the layer for this purpose. Manganese-activated

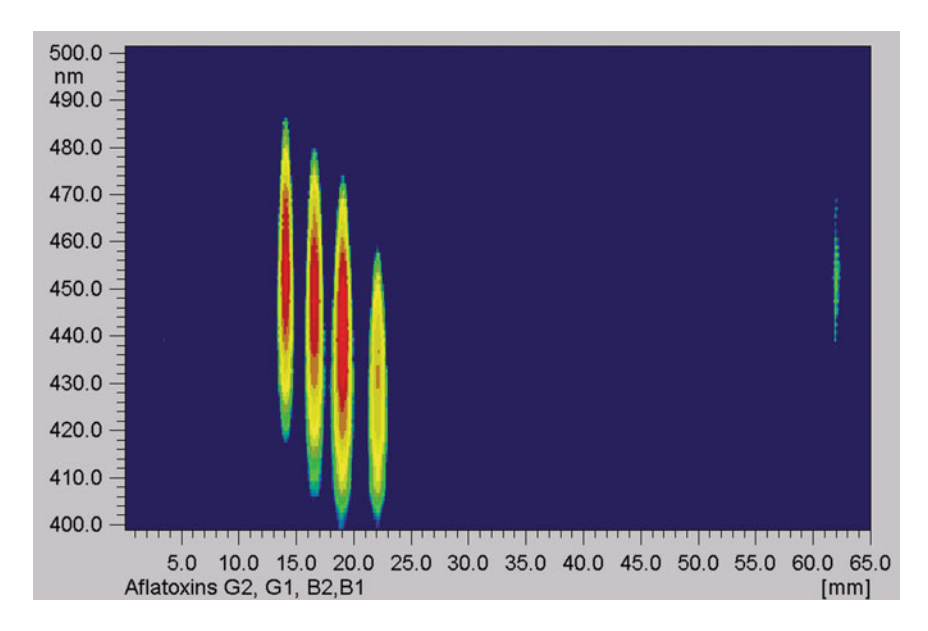


Fig. 11.6 Fluorescence contour plot for an aflatoxin separation on silica gel (0.1 mm layer thickness) with the mobile phase methyl *tert*-butyl ether (MTBE)–water–methanol–cyclohexane (240 + 2.5 + 10 + 5, V/V). The zones correspond to 210 pg aflatoxin B_1 and G_1 and 70 pg aflatoxin B_2 and G_2 [22]

zinc silicate is used for green fluorescence and magnesium tungstate for blue fluorescence. These dyes absorb light at 254 nm exhibiting a green or blue fluorescence in the range \sim 480 to \sim 570 nm. Sample molecules in the layer cover the fluorescent dye and inhibit absorption of light by the dye. In comparison to an uncovered area, sample zones exhibit lower light intensity in the visible region because the covered fluorescent dye cannot transform absorbed light into fluorescence emission. Dark zones on a coloured fluorescent background indicate the position of light absorbing compounds. The term "fluorescence quenching" is often used for this decrease of fluorescence intensity.

Figure 11.7. shows the spectra of doxepin and zopiclone (two pharmaceutical substances). Both spectra have been measured from an HPTLC plate containing a fluorescent dye. Doxepin shows a strong absorption at 254 nm and in its remission spectrum an additional large signal at 520 nm is caused by the fluorescent dye in the layer. This signal represents the light loss of the sample spot at 520 nm in comparison to a sample-free zone. Zopiclone in contrast shows nearly no absorption at 254 nm.

Therefore, the fluorescence inhibition signal at 520 nm is very weak. This is an indication that only compounds with a strong absorption at 254 nm will exhibit fluorescence inhibition.

Figure 11.8. shows the contour plot of a doxepin and zopiclone separation on an HPTLC plate containing a fluorescent dye. The fluorescence quenching signals can

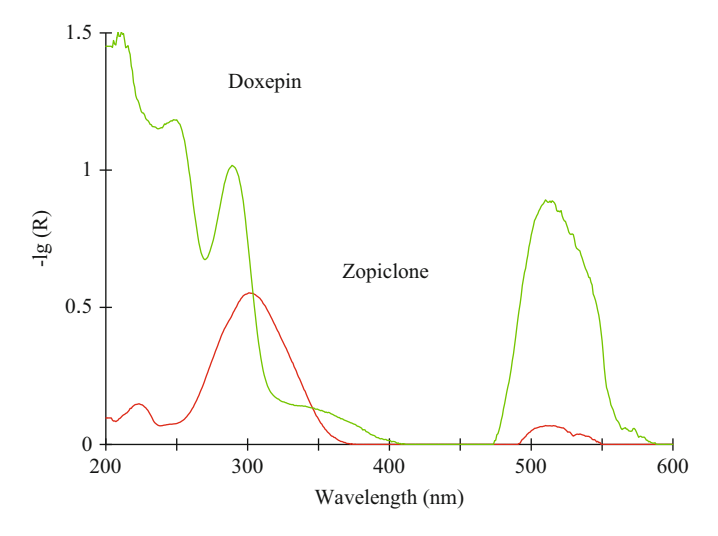


Fig. 11.7 Absorption spectra of doxepin (green) and zopiclone (red). The fluorescence quenching signals can be seen around 550 nm

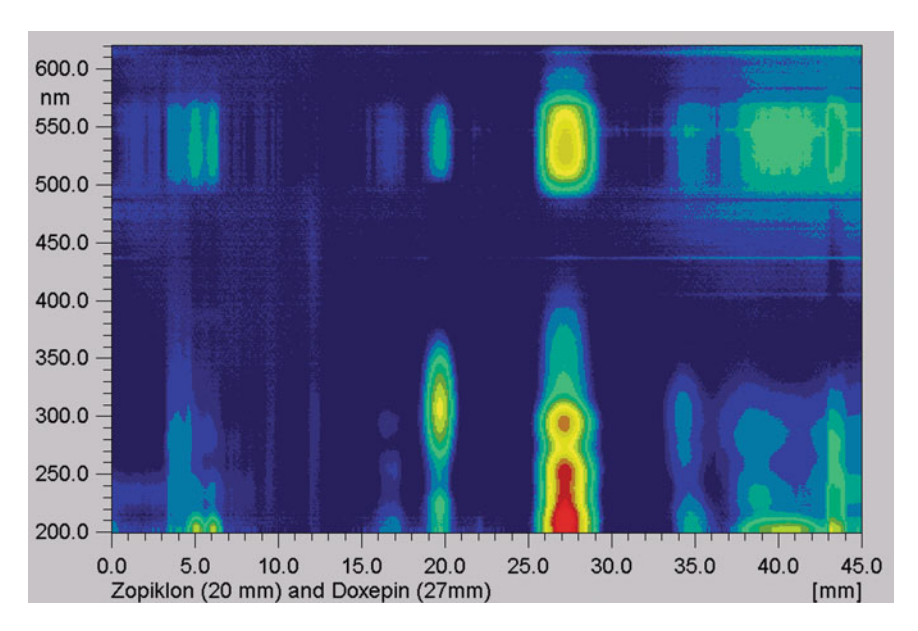


Fig. 11.8 Contour plot of a doxepin and zopiclone separation on an HPTLC plate containing a fluorescent dye. The fluorescence quenching signals can be seen around 550 nm

be seen between 500 and 570 nm. The strong fluorescence quenching signal of doxepin at 27 mm can be clearly seen. Fluorescence quenching signals can be used for calibration purposes. However, the sensitivity of this detection method is lower than for reflection measurements.

References

- 1. Sherma J, Fried B (eds) (1996) Handbook of thin-layer chromatography. Dekker, New York
- 2. Nyiredy Sz (ed) (2001) Planar chromatography, a retrospective view for the third millennium. Springer, Budapest
- Oelkrug D, Kortüm G (1968) Zur Berechnung der Lumineszenzabsorption bei pulverförmigen Substanzen. Z Physik Chemie 56:181–188
- Pollak V (1972) The quantitative assessment of fluorescence on thin media chromatograms.
 A theoretical study. J Chromatogr 72:231–239
- Goldmann J (1973) Quantitative analysis on thin-layer chromatograms. Theory of absorption and fluorescent densitometry. J Chromatogr 78: 7–19
- Pollak V (1977) Fluorescence photometry of thin-layer chromatograms and electropherograms. J Chromatogr 133:49–57
- Prosek M, Medja A, Kucan E, Katic M, Bano M (1980) Quantitative evaluation of thin-layer chromatograms. The calculation of fluorescence using multiplayer models. J High Resolut Chromatogr 3:183–188
- 8. Poole CF, Poole SK, Dean TA, Chirco NM (1989) Sample requirements for quantitation in thin layer chromatography. J Planar Chromatogr 2:180–189
- 9. Hurtubise RJ (1981) Solid surface luminescence analysis. Decker, New York
- 10. Birks JB (1970) Photophysics of aromatic molecules. Wiley, London
- Spangenberg B, Lorenz K, Nasterlack St (2003) Fluorescence enhancement of pyrene measured by thin-layer chromatography with diode-array detection. J Planar Chromatogr 16:328–334
- 12. Jork H, Funk W, Fischer W, Wimmer H (1990, 1994) Thin Layer Chromatography, Volume 1a, Physical and chemical detection methods, Volume 1b, Reagents and detection methods. VCH Verlagsgesellschaft mbH, Weinheim
- 13. Uchiyama S, Uchiyama M (1978) Fluorescence enhancement in thin-layer chromatography by spraying viscous organic solvents. J Chromatogr 153:135–142
- 14. Uchiyama S, Uchiyama M (1980) Thin-layer chromatography-fluorometry of ethoxyquin using triton X-100. J Liq Chromatogr 3:681-691
- 15. Linares RM, Ayala JH, Alfonso AM, Gonzales V (1998) Effect of non-ionic surfactants as mobile phase additives on the fluorescence intensity of dansyl derivatives of biogenic amines in high-performance thin-layer chromatography. Analyst 123:725–729
- Kartnig Th, Göbel I (1996) Effect of fluorescence intensifiers on the fluorodensitometric determination of flavones and flavonols after detection with diphenylboric acid 2-aminoethyl ester. J Chromatogr A 740:99–107
- Baeyens WRG, Lin Ling B (1988) Thin layer chromatographic applications with fluorodensitometric detection. J Planar Chromatogr 1:198–213
- Diaz AN (1991) Fibre-optic remote sensor for in situ fluorimetric quantification in thin-layer chromatography. Anal Chim Acta 255:297–303
- Shaun SJ, Ho H, Butler T, Poole CF (1983) Fluorescence enhancement of polycyclic aromatic hydrocarbons separated on silica gel high-performance thin-layer chromatography plates. J Chromatogr 281:330–339
- Spangenberg B, Klein K-F (2001) New evaluation algorithm in diode-array thin-layer chromatography. J Planar Chromatogr 14:260–265
- 21. Spangenberg B, Weyandt-Spangenberg M (2004) Quantitative thin-layer chromatography using absorption and fluorescence spectroscopy. J Planar Chromatogr 17:164–168
- 22. Broszat M, Welle C, Wojnowski M, Ernst H, Spangenberg B (2010) A versatile method for quantification of aflatoxins and ochratoxin A in dried figs. J Planar Chromatogr 23:193–197

Chapter 12 Chemometrics in HPTLC

Chemometrics is the application of mathematical or statistical methods to chemical data. The aim is to extract the maximum information about the analyte using mathematical methods. Chemometric methods aid the selection of optimal separation conditions; calibration of analytical instruments; as well as suggesting advanced methods for analyzing chemical data. In this chapter, chemometric methods are used to facilitate compound identification, to confirm the purity of separated zones, and to deconvolute inadequately separated compounds.

12.1 Calculation of R_F Values

The oldest chemometric procedure in TLC is the accurate determination of $R_{\rm F}$ values. Originally, $R_{\rm F}$ values were measured using a ruler held over the layer, but today, a scanner in combination with a computer is used. Nevertheless, results can vary, whatever method of measurement is used, but mistakes can be avoided by following some simple rules.

Normal phase retention varies strongly with the water content of the stationary phase. Humidity, therefore, has a decisive influence on the separation conditions. This results in seasonally dependent $R_{\rm F}$ values despite using the same type of TLC plates. To obtain constant $R_{\rm F}$ values, it is absolutely essential to use layers with a constant water content. Before use, silica gel plates should be dried at 120°C and then stored at a constant humidity. A humidity of 38% is a good general choice for storing TLC plates. Special development chambers for pre-conditioning plates are available, which allow selection and maintenance of a constant humidity. In addition, the water content of silica gel layers should be controlled during the sample application process. This can be achieved by a system, which applies the sample quickly and accurately and, if necessary, under a stream of dry nitrogen. The estimation of $R_{\rm F}$ values is best done by scraping out the stationary phase where the solvent flow should end. That enables all pores to be filled after a stop of

the solvent flow. If a plate is simply removed from the chamber, the calculated $R_{\rm F}$ values differ from those of a plate with a scraped-out stop line. When the solvent front reaches a virtual stop line, not all pores near the front are completely filled with mobile phase. If the plate is removed from the chamber, the flow instantly stops because of the missing feed. If the front reaches the scraped-out line, the flow will not stop before all pores are filled. During this pore-filling process, zones will move and will thus alter their $R_{\rm F}$ values. The layer thickness also influences $R_{\rm F}$ values. If the layer thickness differs from plate to plate, different amounts of mobile phase are required to fill the layer pores. The different flow rates result in different $R_{\rm F}$ values.

In forensic sciences, a series of standard substances with known $R_{\rm F}$ values are run in a separate track on the same plate as samples and used to standardize the measurement of $R_{\rm F}$ values to facilitate identification by searching $R_{\rm F}$ libraries [1]. Standardized $R_{\rm F}$ values are mostly given as percents of the front. For this, the "normal" $R_{\rm F}$ values are multiplied by 100 and indicated as an $R_{\rm F}$ (%) value. A standard mixture is used to correct the measured $R_{\rm F}$ values to the established values for the standards. The $R_{\rm F}$ values for the standards should cover the whole range of $R_{\rm F}$ (%) values from 10 up to 90. To correct $R_{\rm F}$ values, the reference $R_{\rm F}$ values are plotted against the measured $R_{\rm F}$ values. If the reference and measured values are identical, a regression line with a slope of 1 and no intercept will result. If the reference and the measured values differ, a curved line with a characteristic shape like Fig. 12.1 is obtained. This plot can be used to correct the measured $R_{\rm F}$ values according to the scale for the standards. The corrected $R_{\rm F}$ values or $R_{\rm F}$ (%) values are calculated from different regions of the graph. For example, the measured $R_{\rm F}$ (%) value is $R_{\rm F}(m)=60$, the corrected value is $R_{\rm F}(k)=55$ using the regression function.

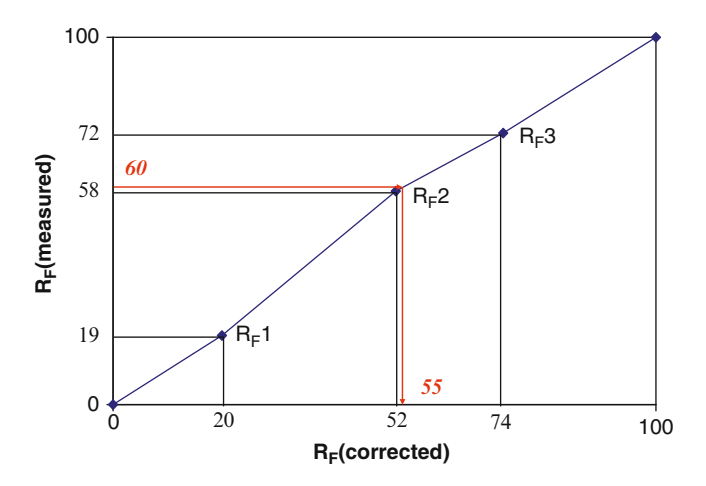


Fig. 12.1 Method for correcting $R_{\rm F}$ values

For numerical calculations, the line which connects pairs of R_F values (e.g. R_F 2 and R_F 3) is used to transform the measured R_F value R_F (m) into the corrected value R_F (c). The following regression function is used.

$$R_{\rm F}(c) - R_{\rm F}(c)_0 = a [R_{\rm F}(m) - R_{\rm F}(m)_0].$$
 (12.1)

In (12.1), the abbreviation "c" indicates corrected and "m" the measured $R_{\rm F}$ values and a stands for the slope of the regression function. The indication "0" describes the lower value of the pair of corrected $R_{\rm F}(c)$ values bracketing the measured $R_{\rm F}(m)$ value. The measured value $R_{\rm F}(m)=60$ lies between $R_{\rm F}2$ and $R_{\rm F}3$. The value $R_{\rm F}(c)_0$ is, therefore, $R_{\rm F}2_{\rm c}$. The slope can be calculated as $a=(R_{\rm F}3_{\rm c}-R_{\rm F}2_{\rm c})/(R_{\rm F}3_{\rm m}-R_{\rm F}2_{\rm m})$. The corrected $R_{\rm F}$ value is 55.

$$\begin{split} R_{\rm F}({\rm c}) &= \frac{(R_{\rm F}3_{\rm c} - R_{\rm F}2_{\rm c})}{(R_{\rm F}3_{\rm m} - R_{\rm F}2_{\rm m})} [R_{\rm F}({\rm m}) - R_{\rm F}2_{\rm m}] + R_{\rm F}2_{\rm c} \\ &= \frac{74 - 52}{72 - 58} (60 - 58) + 52 = 55. \end{split}$$

The use of corrected $R_{\rm F}$ values is a versatile tool for data interchange and for compound identification [1]. In practice, these corrected $R_{\rm F}$ values are reliable in the presence of numerous interferences.

12.2 Compound Identification Using UV-Visible and Fluorescence Spectra

The advantage of modern scanner technology is that spectra are available directly from the TLC plate. Commonly used single wavelength scanners can place a light spot in the centre of a zone of interest, which is then illuminated by light of different wavelengths. The spectrum is calculated from the reflected light. Diode-array technology provides spectral information directly as a contour plot from the measured data. Both methods make it possible to identify a compound via its spectrum. It is even more important to check zone purity to ensure that a complete separation was achieved. Checking zone purity is a general requirement for quantification. Spectral data can also be used to minimize the total analytical error.

Using diode-array technology, a contour plot is the preferred approach to obtain an overview of a separation in an individual track. This requires the selection of a suitable spectral reference $[I(\lambda)_0]$ to calculate all spectra from the scanned track. Typically, a clean section of the TLC plate is used [2, 3], usually an area between the plate edge and the sample application zone. It is important that no substance-containing zones are selected. In the past, dual scanners were recommended to correct for background contributions. This was achieved by simultaneously scanning the sample track and the clean plate area between sample tracks.

This background scan is then subtracted from the sample track [4, 5]. Sometimes, it is convenient to choose a reference zone close to the zone of interest. This is a simple way to subtract the background track signal [2].

In planar chromatography, measured absorption spectra are almost identical with spectra measured in solution according to the Lambert–Beer law [6].

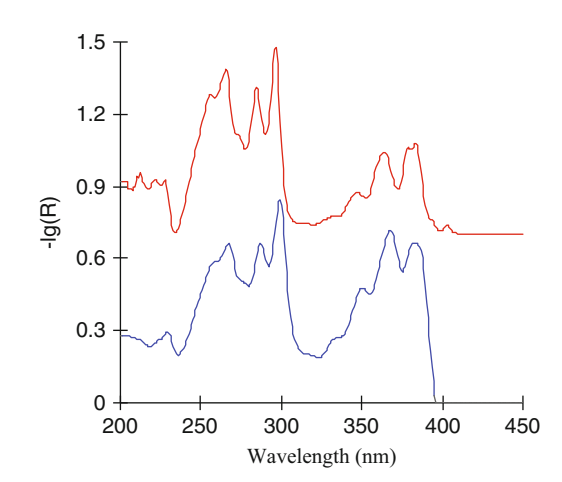
A convenient way to transform reflectance data into mass-dependent signals is to use (12.2).

$$LB(J,\lambda) = -\ln R(\lambda) = -\ln \frac{J(\lambda)}{J_0(\lambda)}.$$
 (12.2)

The logarithm transformation shows identical curvature with the absorption function (12.3), but their values differ. This logarithmic expression sets all wavelength-dependent intensities smaller than I_0 to positive values. The result is similar to the spectrum for benzo[a]pyrene measured in solution. In Fig. 12.2, the benzo[a]pyrene spectrum (500 ng) of a spot on a TLC plate is compared with the benzo[a]pyrene spectrum of a sample dissolved in methanol. Both spectra are almost identical. Small differences can be seen when peak heights are compared. In addition, the plate spectrum is slightly shifted to longer wavelengths. Spectra measured using the logarithmic expression, therefore, are suitable for compound identification [6].

This is true also for fluorescence spectra. Figure 12.3 shows the pyrene fluorescence spectrum measured on a silica gel HPTLC plate. For illumination purposes, a deuterium lamp was used. The spectrum was measured using a diode-array detector. The pyrene fluorescence spectrum in solution is shown on the right-hand side of Fig. 12.3 [7]. Both spectra are nearly identical, which also make fluorescence spectra suitable for substance identification [8].

Fig. 12.2 The spectrum for 500-ng benzo[a]pyrene measured on a HPTLC plate shown below, after transformation according to (12.2) and the benzo[a]pyrene absorption spectrum measured in methanol (above)



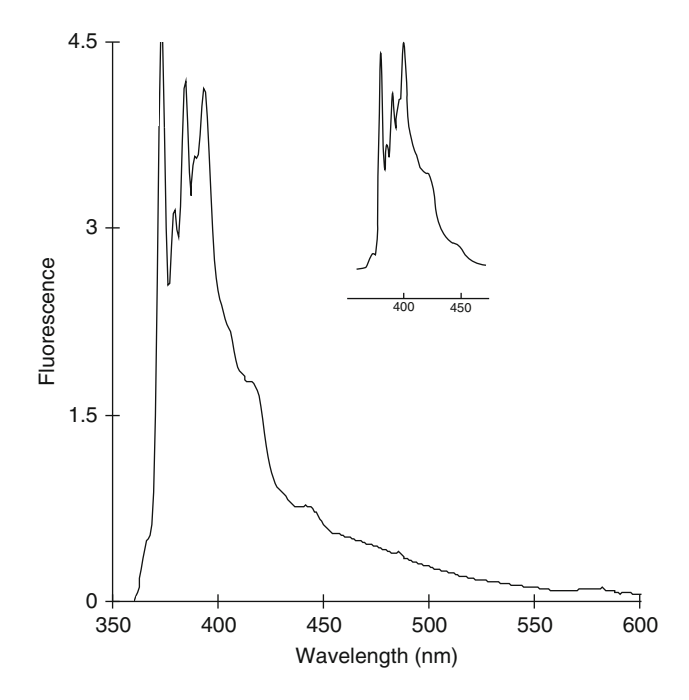


Fig. 12.3 Pyrene fluorescence spectrum measured from an HPTLC plate (*left*) and in solution (*right*) (From [7] with permission: Royal Society of Chemistry)

Matching spectra in the UV-visible range makes it possible to identify compounds quickly and reliably. An algorithm for spectral comparison is essential.

12.3 Correlation Spectroscopy

Diode-array scanners offer a fast survey of a TLC separation and facilitate the application of various chemometric techniques. For compound identification, a cross-correlation function is the best way to compare UV–visible sample spectra with appropriate library spectra. The cross-correlation function can also be used for zone purity testing.

12.3.1 Theory of Correlation Spectroscopy

For spectra identification, the cross-correlation function of two spectra is obtained by gradual multiplication of the target spectrum (the sample spectrum) and the reference spectrum. The reflected light intensity from an HPTLC plate at different wavelengths $J(\lambda)$ is measured for the chosen range. The relative reflectance $R(\lambda)$ is calculated according to (12.2). For this purpose, the measured spectra $J(\lambda)$ are divided by the reference spectrum $J_0(\lambda)$ measured from a clean region on the HPTLC plate.

Generally, a logarithmic transformation (12.2) or the reverse transformation (12.3) provides the best results [6].

$$A(\lambda) = \frac{1}{R(\lambda)} - 1. \tag{12.3}$$

If the target compound is fluorescent, or the zone of interest has a high concentration, the corresponding spectrum can be calculated by use of the extended Kubelka–Munk theory.

The simultaneously measured values at different wavelengths are bundled in the data field \(\mathbb{S} \), which contains the desired transformed measurement data at different wavelengths.

$$\mathfrak{F} = \begin{pmatrix} \lambda_1, A_1 \\ \lambda_2, A_2 \\ \vdots & \vdots \\ \lambda_n, A_n \end{pmatrix}.$$

The auto-correlation vector is calculated by multiplying each wavelength-dependent value with itself. For n values, the vector \Im results [9].

$$\Im \Im = \begin{pmatrix} A_1 & * & A_1 \\ A_2 & * & A_2 \\ \vdots & * & \vdots \\ A_n & * & A_n \end{pmatrix}.$$

The auto-correlation vector of the reference spectrum $\Re\Re$ is obtained in a similar way. For evaluation of the cross-correlation functions, the sample values A_J are multiplied wavelength-wise by the values A_R of the reference spectrum. The resulting data vector is $\Im\Re$.

$$\mathfrak{R} = \begin{pmatrix} A_{J1} & * & A_{R1} \\ A_{J2} & * & A_{R2} \\ \vdots & * & \vdots \\ A_{Jn} & * & A_{Rn} \end{pmatrix}.$$

All data vectors have to be summed over the desired wavelength range to calculate the rate of percentage identity \aleph .

$$\aleph = \frac{\sum_{1}^{n} \Im \Re}{\sum_{1}^{n} \Re \Re} \sqrt{\frac{\sum_{1}^{n} \Re \Re}{\sum_{1}^{n} \Im \Im}} \times 100(\%). \tag{12.4}$$

The value of \aleph represents the percentage fit of the sample spectrum compared with the reference spectrum. A spectral fit of 100% means complete agreement between the sample and the reference spectra. A fit of above 90%, or a difference of 5% to the next sample fit to a reference spectrum, is usually regarded as sufficient for a definite identification [9–11]. Confirmatory visualization of sample and reference spectra increases the certainty of identification, but a computer-produced hit list of candidates on the basis of a library search accelerates sample identification.

The quality of directly measured UV–visible spectra allows identification of compounds even in difficult matrices. For example, it is even possible to identify diphenhydramine in urine, although diphenhydramine has a weak UV spectrum with little fine structure. Figure 12.4 compares unsmoothed sample and reference spectra of diphenhydramine. The fit is 95%, which provides adequate certainty in the identification of the compound. This is a powerful tool for sample identification when used in combination with $R_{\rm F}$ values.

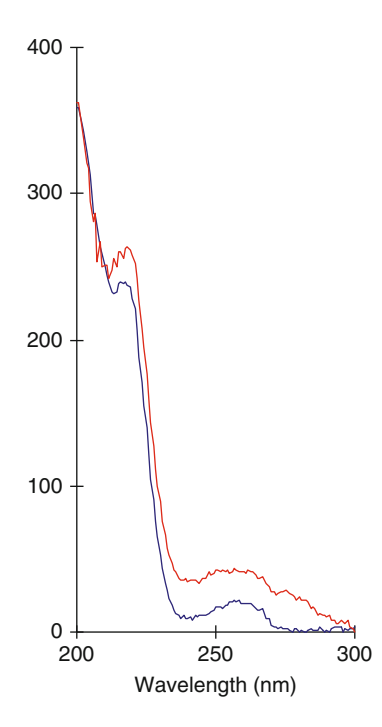


Fig. 12.4 Reference (*blue*) and sample spectrum (*red*) of diphenhydramine in a urine sample

12.3.2 Combination of R_F and UV-Visible Spectral Library Search

For critical compound identification, the UV–visible spectrum match must be supported by additional information for the compound. The combination of the spectral fit with standardized R_F values according to (12.5) provides the best results [10, 11].

$$\aleph_{R_{\rm F}} = \aleph \times [1 - \Delta R_{\rm F}]. \tag{12.5}$$

In this expression, the spectral fit value is corrected with the positive difference between the sample and the reference $R_{\rm F}$ values, indicated as $\Delta R_{\rm F}$. If there is no difference in $R_{\rm F}$ values, the combined fit equals the spectral fit. If there is a (positive!) difference for the $R_{\rm F}$ values, the spectral fit is multiplied by a figure smaller than 1. It must be emphasized that constant separation conditions are essential to use $R_{\rm F}$ values for this kind of compound identification.

The combination of the spectral fit with the three different separations on the same TLC plate makes it possible to identify e.g. 28 benzodiazepines with very similar UV spectra [10]. This set of four values (the spectral fit factor and three $R_{\rm F}$ values) is compared with the reference data set. The extended expression (12.6) is used for the calculation of the combined fit.

$$\aleph_{R_{\rm F}} = \aleph \times [1 - \Delta R_{\rm F}] \times [1 - \Delta R_{\rm FB}] \times [1 - \Delta R_{\rm FC}]. \tag{12.6}$$

As an example, to separate benzodiazepines in a first run, the solvent system dichloromethane—methanol (95 + 5, V/V) was used [10]. This system shows $R_{\rm F}$ values on silica gel that are less than 0.5. After 10 min, the track can be scanned to obtain mobile phase-independent spectra. After scanning, the plate is developed again with the mobile phase ethyl acetate—cyclohexane—25% (w/v) aqueous ammonia (500 + 400 + 1, V/V). This system saturates active sites on the silica gel layer changing the properties of both the layer and the mobile phase. After scanning, the plate is developed a third time using the system cyclohexane—acetone—methyl *tert*-butyl ether (3 + 2 + 1, V/V). The use of four compound-specific data allows the reliable identification of an individual benzodiazepine in a relatively short time. On a single 10×10 -cm HPTLC plate, at least six samples and two reference tracks can be applied, developed, and scanned within 1 h [10].

12.3.3 Zone Purity Check

The aim of a TLC separation is, in general, the identification and quantification of the analytes. The first step is to identify the analyte-containing zone. The second step is to verify that the zone contains pure analyte. The commonly used TLC scanners allow spectra to be measured at a defined layer location. For zone purity

confirmation, it is usually sufficient to measure spectra at the peak maximum and at the peak inflection points. Overlaying the three spectra in a single diagram instantly reveals whether the spectra vary, thus indicating zone contamination. The diodearray technique is better suited in confirming zone purity because all zone spectra are available after scanning. A peak measured by a diode-array scanner comprises usually 10-30 individual spectra. Of course, they contain more information than the three spectra per peak typically measured by a scanning densitometer. Figure 12.5 illustrates the separation of a urine sample. Eight different substances can be identified. For example, the compound codeine at a separation distance of 13.6 mm can be identified either via its typical UV spectrum or via its characteristic $R_{\rm F}$ value. The symmetrical shape of the codeine peak is an indication that the codeine zone is completely separated from the matrix. More than ten spectra are measured from this codeine zone. The average of 7-9 spectra near the peak maximum represents the spectral properties of the peak quite well, effectively reducing spectral noise. Such an averaged spectrum of a chosen substance can be used for a library search. It is also possible to compare a reference spectrum with all the measured spectra of a single track.

This combines sample recognition with a zone purity check. A fit-function results when a codeine reference spectrum is compared according to (12.4) with all the measured spectra of the HPTLC track. The resulting fit function and the track densitogram measured at 273 nm are plotted in Fig. 12.6. The fit function comprises all codeine-fit factors for the measured spectra.

A symmetrical peak shape with a fit of nearly 98% can be observed at a migration distance of about 13.6 mm. The rectangular fit function indicates a pure peak and the good fit identifies the peak as codeine. Beside peak identification,

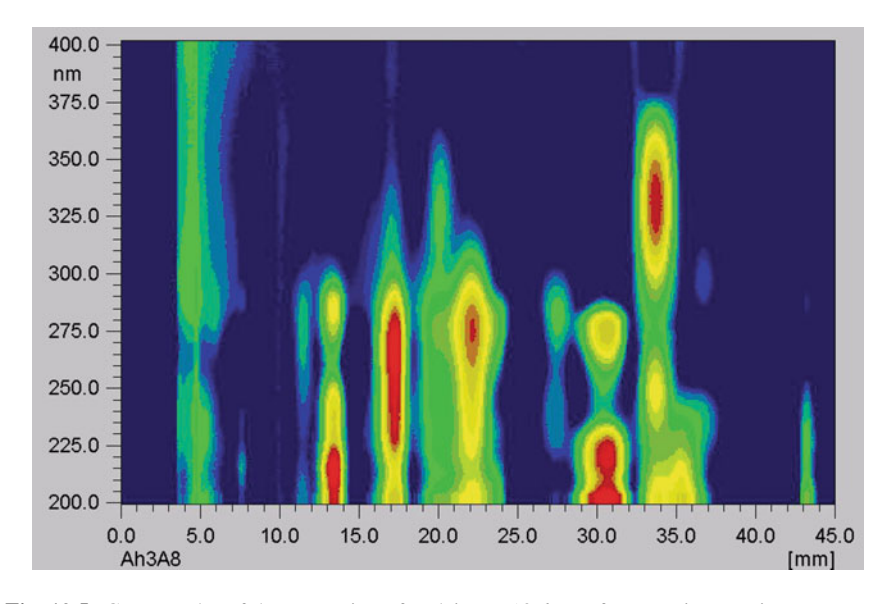


Fig. 12.5 Contour plot of the separation of codeine at 13.6 mm from a urine matrix

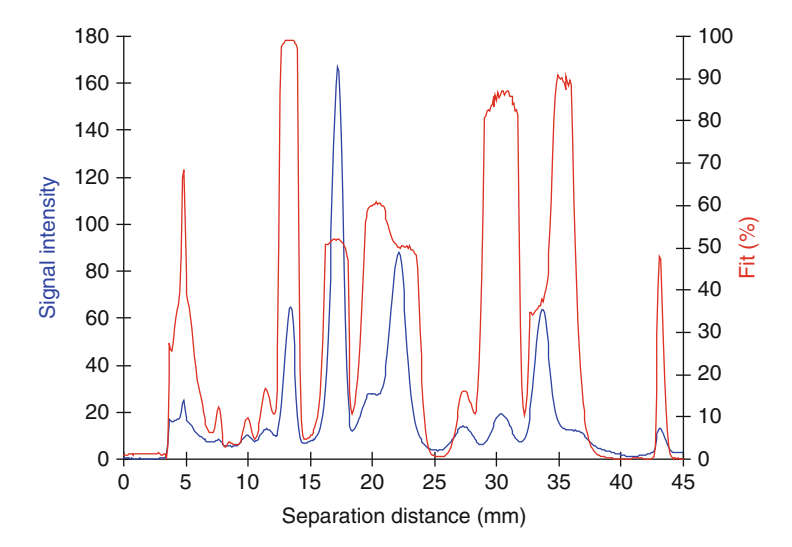


Fig. 12.6 Densitogram of a urine sample measured at 273 nm (blue) in combination with the codeine fit-function (red) according to (12.4)

a diode-array scanner in combination with (12.4) makes zone purity evaluations readily available. It is not necessary to choose individual wavelength combinations for zone purity investigations. Peak identification and purity can be carried out automatically and parameter free. For example, HPTLC tracks are compared with a library of relevant compounds. If a fit signal exceeds 90%, the track is marked and the fit function saved. All saved fit functions contain information about whether a zone is pure or contaminated. Subsequent quantification is valid only after a successful zone purity check.

Figure 12.7 shows a contaminated zone at a 23-mm separation distance. The densitogram allows us to speculate that the very broad peak at 23-mm consists of more than one substance. A caffeine reference spectrum is compared with all the spectra recorded for the track, which results in the fit function plotted above the densitogram. The decisive fact is that this fit function is not rectangular (shows an asymmetrical peak shape) confirming that the zone is contaminated. The fit function has a high peak on the right-hand side of the caffeine zone indicating that caffeine is incompletely resolved from matrix components. Even in this contaminated peak, the unresolved caffeine can be identified with a fit of nearly 98%!

12.4 Selection of the Measurement Wavelength

In situ scanning densitometry provides a simple means of quantification by measuring the optical density of the separated zones directly on the layer. To quantify the analyte peak in the densitogram, all peak data are summed up to give a single

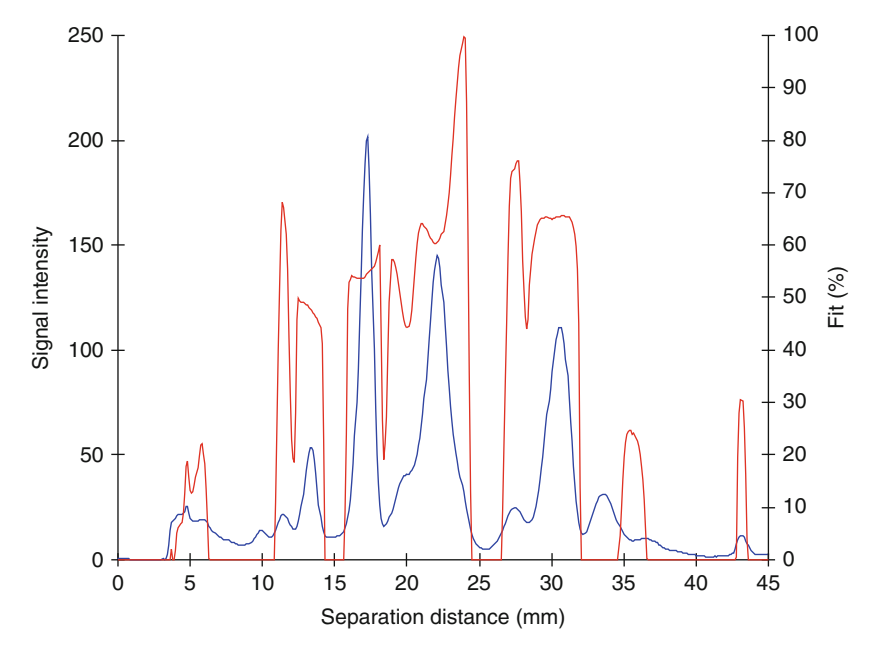


Fig. 12.7 Densitogram of a urine sample measured at 280 nm (blue) in combination with the caffeine fit-function (red) according to (12.4)

value. Single wavelength scanners need to know at which wavelength the track should be measured. Diode-array scanning does not. The track is scanned and the contour plot reveals the best wavelengths for quantification. If more than a single wavelength measurement is necessary, a single wavelength scanner must scan the whole track again. This is unnecessary using diode-array scanners. All densitograms at different wavelengths are thus measured and stored in the contour plot, ready for evaluation. Commonly, the wavelength showing the highest signal is used for evaluation. A better decision is sometimes to select a wavelength where side peaks indicate minimum interference.

Figures 12.8 and 12.9 illustrate the separation of 16 polycyclic aromatic hydrocarbons. The low zone capacity of HPTLC makes it impossible to separate all 16 PAHs in single run [6]. Due to the richly structured PAH spectra, diodearray detection enables quantification of all 16 PAHs on one track. Although the separation is incomplete, every one of the 16 compounds can be quantified using suitable wavelengths. Figures 12.8 and 12.9 present contour plots of the separation of the 16 PAHs on an RP-18 layer [6]. Evaluation took place using the Kubelka–Munk function over the wavelength range from 200 to 400 nm. The starting point is at 1.2 mm and the front can be seen at 45.8 mm. Nearly all PAHs show strong fluorescence in the wavelengths range from 400 to 440 nm. The most sensitive method of quantification is a group detection scheme employing the

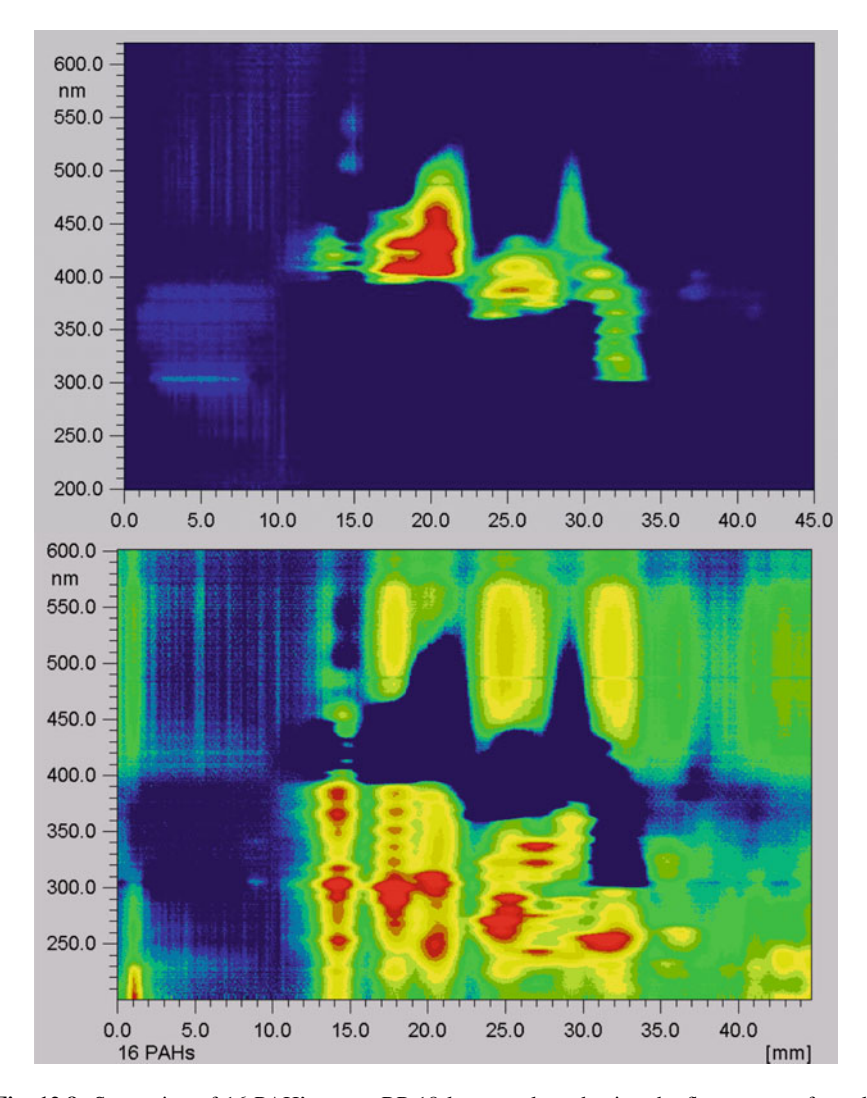


Fig. 12.8 Separation of 16 PAH's on an RP-18 layer evaluated using the fluorescence formula (*above*) and the absorption expression (*below*). The Kubelka–Munk function would merge the two figures into one. Methanol–acetone (8+3, V/V) was used as the mobile phase [6]

wavelength range indicated above. For the case of inadequate separation, the measurement wavelengths are fixed, because the wavelength with the highest resolution must be used for quantification. In principle, fully separated zones can be measured at any chosen wavelength, although the measurement error will not be constant.

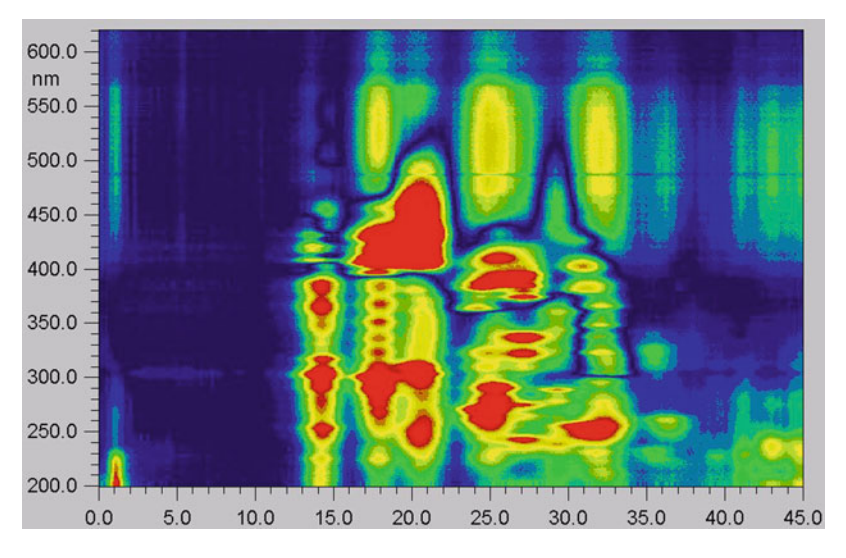


Fig. 12.9 Separation of 16 PAH's on an RP-18 layer evaluated using the Kubelka–Munk function [6]

12.5 Statistical Photometric Error (Detector Variance)

Scanners consist of different parts contributing statistically defined noise to the measurement. The most important are the light source, the detector, the signal amplifier, and the A/D converter. Two different spectra containing noise, the sample spectrum, and the spectrum of a reference must be combined into a single expression for quantification. A set of reflectance values $R(\lambda)$ at different wavelengths is calculated from the light reflected from the layer surface $J(\lambda)$ corrected by a reference value obtained at a blank area of the layer. Any noise in these two data sets will make the final result uncertain.

$$R(\lambda) = \frac{J}{J_0}. (12.7)$$

The variation of the relative mass $\partial m/m$ with reflectance, assuming a constant instrumental detection error, can be derived from the different transformation expressions. Expression (12.7) is calculated from two error-dependent values J and J_0 , which project their uncertainty into the reflectance R. In other words, both measurements contribute to the total error in R.

12.5.1 Reciprocal Model

Using the reciprocal formula for quantification, we assume a linear relationship between the mass in the zone of interest and the reversed reflectance data.

$$m = \text{const.} \times \left(\frac{1}{R} - 1\right).$$

The variation of the mass in the zone is dependent on the reflectance and leads to

$$\frac{\partial m}{\partial R} = \frac{\partial}{\partial R} \left[\text{const.} \times \left(\frac{1}{R} - 1 \right) \right] = -\frac{\text{const.}}{R^2}.$$

The relative error in mass for the reciprocal formula is

$$\frac{\partial m}{m} = -\frac{\text{const.}}{R^2} \frac{1}{\text{const.}} \left(\frac{R}{1 - R}\right) \partial R.$$

The final result is

$$\frac{\partial m}{m} = -\frac{1}{(1-R)} \frac{\partial R}{R}.$$
 (12.8)

The important point is whether the variation of the reflectance ∂R is independent of the reflectance R itself [12–16]. If we take thermal noise into account, we can propose the relationship $\partial R \cong \sqrt{R}$. The variation of R changes the relative mass variation $\partial m/m$ according to (12.8). The resulting function is shown in Fig. 12.10. This figure presents the uncertainty of the mass variation (the error for the mass determination), which depends on the value of R. The minimum error for this transformation is at R=0.5. The practical conclusion from this calculation is that a minimum detection error can be observed only near values of R=0.5. From Fig. 12.10, we can conclude that the measurement uncertainty strongly increases above the values R=0.9 and below R=0.1.

12.5.2 Absorbance Model

The relative mass error for the logarithmic expression, used as transformation algorithm,

$$m = -\text{const.} \times \ln R = \text{const.} \times \ln \left(\frac{1}{R}\right)$$

is

$$\frac{\partial m}{\partial R} = \frac{\partial}{\partial R} \left[-\text{const.} \times \ln R \right] = -\text{const.} \times \frac{1}{R},$$

$$\frac{\partial m}{m} = \frac{-\text{const.}}{-\text{const.} \times \ln R} \frac{1}{R} \partial R = \frac{1}{\ln R} \frac{\partial R}{R}.$$
(12.9)

The minimum error for this transformation is at R = 0.4343.

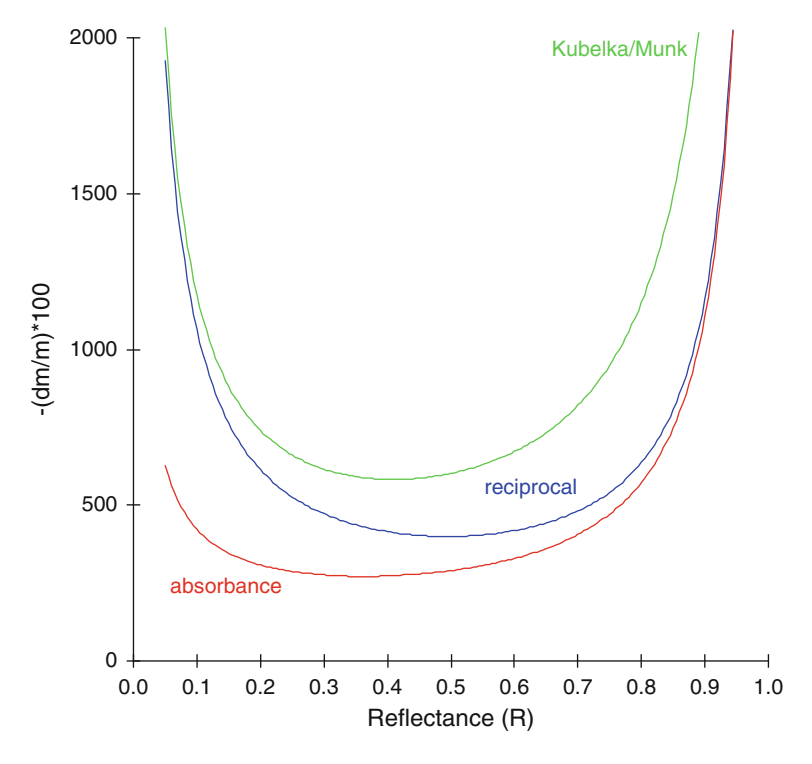


Fig. 12.10 Error values as a function of reflectance for the three transformation models discussed in the text. (From *top* to *bottom*: Kubelka–Munk, reciprocal model, and absorbance model)

12.5.3 Kubelka-Munk Model

The Kubelka–Munk function is more complicated than the two transformation methods used above. The relationship between the sample concentration in the stationary phase and the observed reflectance is:

$$m = \text{const.} \times \frac{(1-R)^2}{2R} = \text{const.} \times \left(\frac{1}{2R} - 1 + \frac{R}{2}\right)$$

The variation of the concentration leads to

$$\frac{\partial m}{\partial R} = \frac{\partial}{\partial R} \operatorname{const.} \times \left[\frac{1}{2R} - 1 + \frac{R}{2} \right] = \operatorname{const.} \times \left[-\frac{1}{2R^2} + \frac{1}{2} \right] = \operatorname{const.} \times \frac{R^2 - 1}{2R^2}.$$

The relative mass error for the Kubelka-Munk function is

$$\frac{\partial m}{m} = \frac{(R^2 - 1)}{(1 - R)^2} \frac{\partial R}{R}.$$
 (12.10)

This expression is identical to the following [17].

$$\frac{\partial m}{m} = \frac{(R+1)}{(R-1)} \frac{\partial R}{R}.$$

The minimum error for this transformation is at R = 0.4139.

Figure 12.10 combines the error function of all the three transformation algorithms discussed above. Kubelka–Munk transformed data should be used in the range R > 0.1 and R < 0.8 [12].

A reflectance of R = 0.5 means that half of the incident light is absorbed and half reflected back to the detector. This scenario exhibits the lowest error and should be used for quantification. The reflectance R = 0.1 describes a situation in which only 10% of the incident light is reflected. This is the case for zones with high sample concentrations. The reciprocal and Kubelka-Munk transformations both exhibit the same error curve. The logarithmic transformation (absorbance) is the best. For high concentrations in a zone, it is recommended to use the Kubelka-Munk transformation, because only this algorithm shows a linear relationship between high mass concentrations and the transformed reflectance. A reflectance of R = 0.9means that 90% of the incident light is reflected from the layer, conditions typical for trace analysis. For measurements of low mass concentrations in a zone, the Kubelka-Munk algorithm is error prone and unsuitable for general use. For the three models, errors arise at reflectance values larger than 0.9 and an error minimum is observed for reflectance values between 0.1 and 0.9. Figure 12.10 clearly shows that the Kubelka-Munk equation should be used with care at reflectance values larger than 0.8!

12.5.4 Fluorescence model

The fluorescence formula is a special case for error propagation of the detector noise in the final measurement value. We have the expression

$$m = \text{const.} \times [R-1].$$

The expression for the relative concentration error of the fluorescence formula can be calculated as:

$$\frac{\partial m}{m} = \frac{\partial R}{(R-1)}. (12.11)$$

The function shows large values near $R \approx 1$, decreasing with increasing R values. The uncertainty of the fluorescence measurements is greatest at large reflectance values. In other words, the stronger the fluorescence the smaller the measurement error!

12.5.5 Minimizing the Statistical Photometric Error

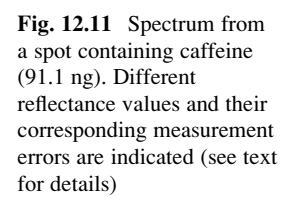
Looking at the general picture for absorbance measurements, the experimental error will be minimized for reflectance values near R=0.5. The measurement wavelength, therefore, should be selected to obtain a reflectance value close to R=0.5. In practice, scanning TLC layers mostly results in low light intensities with R<0.5, especially for high sample concentrations.

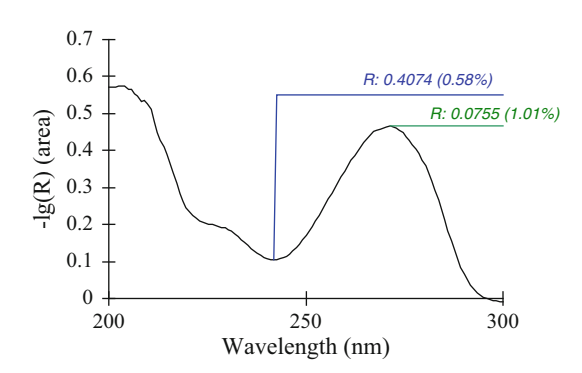
To reduce the total error, the selection of the measurement wavelengths should be done carefully, according to the desired reflectance values and not according to a spectral absorption maximum! For example, Fig. 12.11 shows the spectrum of 91.1-ng caffeine. The determination of nine caffeine applications at the absorption maximum (273.6 nm) shows a larger error (1.01%) than the same measurements at the absorption minimum of 241.1 nm (0.58%). The error is determined by the best reflectance and not by the peak maximum. In this example, the reflectance value of R=0.4074 is a better choice for measurements than R=0.0755 at the absorption maximum!

Figure 12.12 shows two densitograms of the same sample, separated over 12 and 30 mm. The caffeine concentration in the zone is very low. Different tracks with the same applied amount and migration distance show a significantly larger error (2.23%) at the unfavourable reflection value of R = 0.928. A shorter separation provides better results (1.17% error) due to the better reflectance value (R = 0.895). This example of the better caffeine separation does not result in a lower quantification error.

12.6 Diode Bundling and Data Smoothing

An important advantage of diode-array scanning is the possibility of bundling different diode signals into a single densitogram. This is an effective means of reducing noise [18] and enhancing signal-to-noise ratios without smoothing. Using





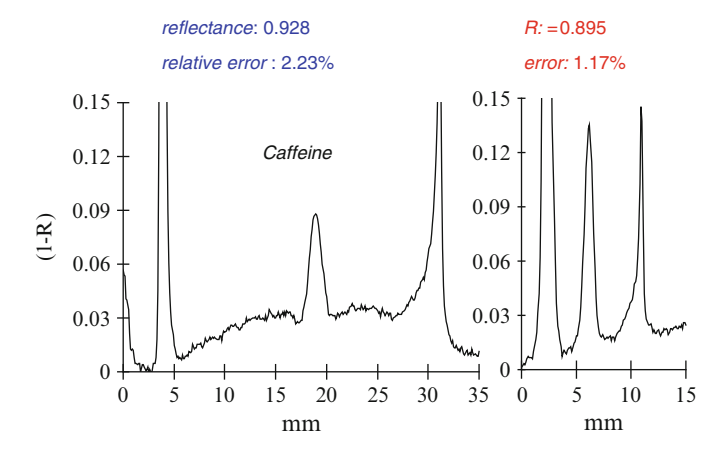


Fig. 12.12 Two caffeine separations with a solvent front migration distance of 35 mm and 15 mm on silica gel with 2-propanol-cyclohexane-25 % (w/v) aqueous ammonia (7+2+1, V/V) as mobile phase. The *left-hand plot* contains the greater total error

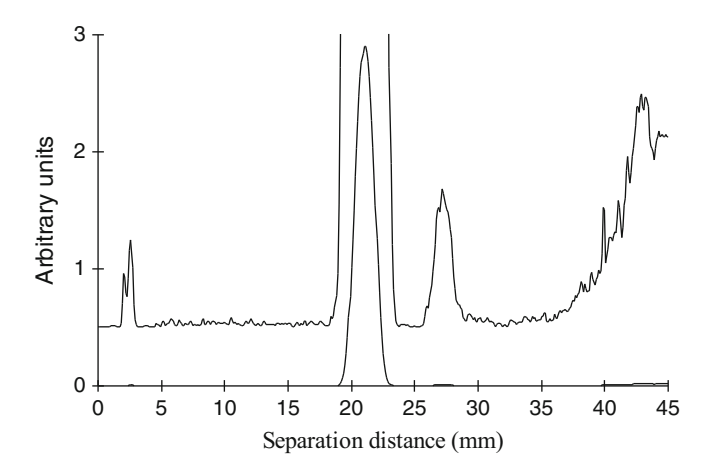


Fig. 12.13 Densitogram of 250-ng benzo[a]pyrene (below) and 100-fold enhanced densitogram (above)

a modern diode-array scanner, a single diode measures a spectral range of about 1 nm. UV-visible spectra typically show broad absorption peaks larger than 30 nm. By combining the signals from 25 single diodes, the wavelength range is extended by a factor of 25 compared to a single diode. The benefit lies in noise reduction by a factor of $\sqrt{25} = 5$, which directly improves the signal-to-noise ratio. Ratio values of 5,000:1 and more are achievable. In Fig. 12.13, the densitogram for 250-ng benzo[a]pyrene measured in the wavelengths range from 403 to 436 nm is shown as an averaged signal of 42 single diodes. In the amplified densitogram, the starting

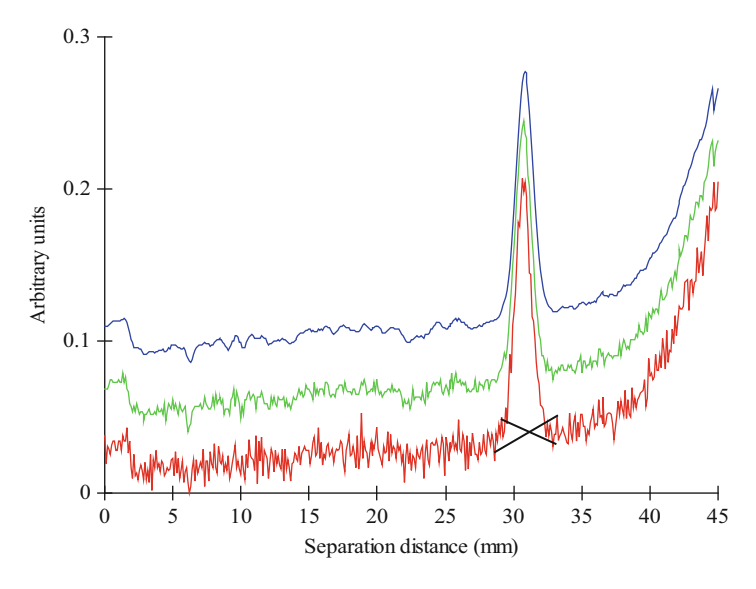


Fig. 12.14 Densitogram for 125-ng diphenhydramine measured at 200 nm by a single diode (*bottom*), averaged signals from seven diodes in the range 200–204 nm (*middle*), and smoothed densitogram (average of five data points, *top*). The *bottom* of the densitogram is manually cross-linked for integration

point at 2 mm and the solvent front position at 43 mm can be clearly seen, as well as the side signal at 27 mm. The side peak area represents 0.3% of the benzo[a]pyrene peak area.

Figure 12.14 illustrates a densitogram for 125 ng of diphenhydramine measured at 200 nm by use of a single diode (bottom) and the averaged signals of seven diodes in the range 200–204 nm (middle). The noise reduction can be clearly seen. Noise can be further reduced using a five-point moving average for smoothing [18, 19]. The disadvantage of smoothing is peak broadening, which will reduce chromatographic resolution. Smoothing makes it more convenient to integrate peaks but should be used with care.

12.7 Signal Integration: Area or Height Evaluation?

Peaks must be integrated after transformation of the measured data. An integration sums all responses within chosen peak limits. The integral of the Gauss-function from $-\infty$ to $+\infty$ is 1. The sum of all measured responses represents the sample amount for the zone.

$$f(x) = n \int_{-\infty}^{+\infty} \frac{1}{\sigma\sqrt{2\pi}} e^{-\frac{(x-z_S)^2}{2\sigma^2}} dx = n.$$

Peak integration is a mini—max calculation method [20]. The aim is to collect as much peak area as possible, using the minimum number of data points. Commonly, integration software automatically selects peak limits. Some software allows manual selection of peak limits as well. Manual setting of peak limits is of course arbitrary but the user (and not the program) must take responsibility for the final result. It is often difficult to integrate noisy signals. Noise affects both the baseline and the signal. For noisy baselines, the best results are usually observed for manual cross-integration. The first baseline is constructed from the noise maximum before the peak and ends at the noise minimum after the peak. A second baseline is constructed the other way round. The final result is the average of both the estimated peak areas. An example is given in Fig. 12.14 for the bottom trace. Peak height can be measured from the point where both baselines cross.

A question often discussed is whether peak area or peak height should be used for quantification. For a Gaussian function, there is a simple dependence between peak height H, sample amount n, and peak width σ .

$$H = n \frac{1}{\sigma \sqrt{2\pi}}. (12.12)$$

As stated in Chap. 2, the peak width σ depends on the $R_{\rm F}$ value. If $R_{\rm F}$ values differ from track to track, even though the same sample amounts are applied, different peak heights will result. Trace evaluations using peak height will often result in lower uncertainties compared with peak area evaluations. The reason is that in trace analysis peak sides often show unfavourable reflectance values of R>0.9. Reflectance values of R<0.9 are often observed only for the peak maximum. Therefore, height evaluation is recommended by the detection error theory. It should be noted that the measurement of a single peak height can result in incorrect values, for example, in the case of a spike in the peak. Averaging peak height values near the maximum will provide better results. It is nearly impossible to estimate peak limits when peaks are not fully resolved. In this case, all peaks should be evaluated using their heights.

12.8 Deconvolution of Overlapping Peaks

Figure 12.15 illustrates the incomplete separation of uracil and thymine. The peak at 53 mm is not a single-component peak. This results in a typical peak in the densitogram with a "shoulder". Perhaps more obvious are the results shown for the contour plot with its non-symmetric shape. Even though a compound is not sufficiently separated from other substances, quantification is possible. It only needs a substantial difference in the UV–visible spectra of the two unresolved compounds at a minimum of two different wavelengths. It is not even necessary to know the identity of the interfering substance.

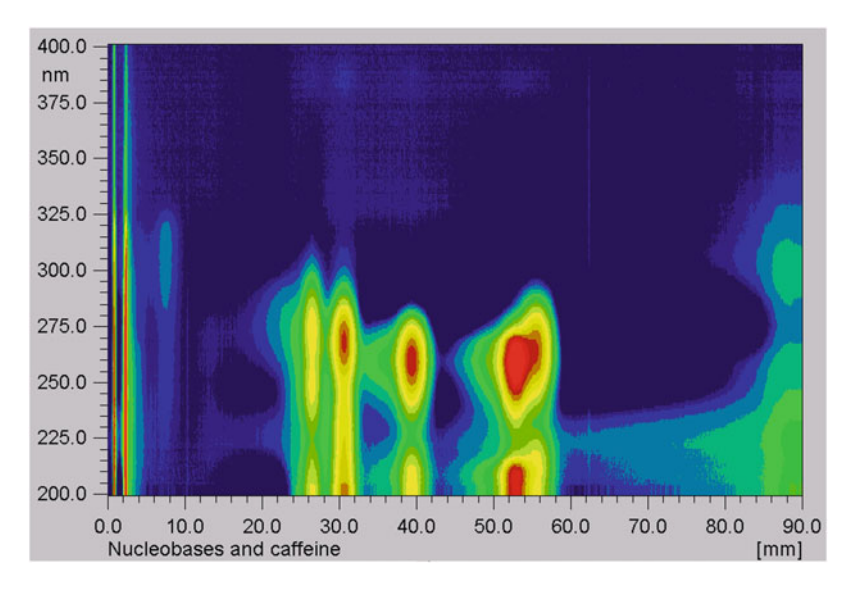


Fig. 12.15 Separation of nucleobases and caffeine. Guanine, cytosine, and caffeine are adequately separated while uracil and thymine at 53 mm are not fully resolved [21]

For calculation, it is assumed that the unresolved peak consists of two compounds A and B. Assuming linearity between the transformed measurements and sample amounts, the peak spectrum is the sum of the two single substance spectra. The responses at suitable wavelengths are assumed to be proportional to the masses m_A and m_B of the two compounds.

$$KM(\lambda)_{mixture} = \varepsilon'_A(\lambda)m_A + \varepsilon'_B(\lambda)m_B.$$

This model can be verified using the extended Kubelka–Munk theory for transformation purposes. In this theory, linearity between signal and sample amount is guaranteed. Using a diode-array scanner, an area of constant mass m_A or m_B is simultaneously measured at different wavelengths, exhibiting different spectral properties. In the case of two chosen wavelengths with significantly different spectral properties, two measurements $KM(\lambda_1)$ and $KM(\lambda_2)$ are obtained.

$$KM(\lambda_1)_{\text{mixture}} = \varepsilon_A'(\lambda_1)m_A + \varepsilon_B'(\lambda_1)m_B,$$

$$KM(\lambda_2)_{\text{mixture}} = \varepsilon_A'(\lambda_2)m_A + \varepsilon_B'(\lambda_2)m_B.$$

This results in two equations with two unknown masses m_A or m_B . A solution requires the measurement of responses at two different wavelengths λ_1 and λ_2 . To suppress noise, the averaged signal is calculated, for example, of seven diodes around the two chosen wavelengths. The properties of each compound are measured from the spectra of the single compounds. It is also possible to assume

peak purity on the left-hand and right-hand sides of a combined peak. Spectral properties ε can thus be extracted from the contour plot of the track, indicating measurement values as y-values and masses as a and b. The spectral properties at different wavelengths are indicated as x-values. The following system of equations will result.

$$y_1 = ax_{11} + bx_{12},$$

 $y_2 = ax_{21} + bx_{22}.$

This can be transformed into the matrix

$$\begin{vmatrix} x_{11}x_{12} \\ x_{21}x_{22} \end{vmatrix} \begin{vmatrix} a \\ b \end{vmatrix} = \begin{vmatrix} y_1 \\ y_2 \end{vmatrix}.$$

The determinant det(X) of this matrix is calculated as

$$\det(X) = x_{11}x_{22} - x_{12}x_{21}$$
.

The coefficients can be extracted according to Cramer's rule

$$a = \frac{1}{\det(X)} x_{22} y_1 - x_{12} y_2, \tag{12.13}$$

$$b = \frac{1}{\det(X)} x_{11} y_2 - x_{21} y_1. \tag{12.14}$$

Thus, using a simple calculation will result in two densitograms in which both substances are resolved (Fig. 12.16). The densitograms in 2.7, 2.8, 6.9, 6.10, 6.12 and 6.19 were evaluated using this algorithm.

12.9 New Visualization Methods for Plots

When using single wavelength scanners, separations are generally visualized as densitograms. Diode-array scanning provides much more information. Figure 12.17, for example, shows the separation of a rosmarini folium extract separated on silica gel with toluene—ethyl acetate—formic acid (5+4+1, V/V) as mobile phase and stained with the tetraphenyl borate/HCl reagent. The middle of the plot contains an inset identifying compounds that fluoresce when excited at 366 nm. The left side shows the absorption contour plot for the range 200–600 nm. The right side shows the fluorescence contour plot for the range 400–800 nm. Blue zones emit fluorescence below 600 nm. Red zones emit fluorescence between 650 and 700 nm.

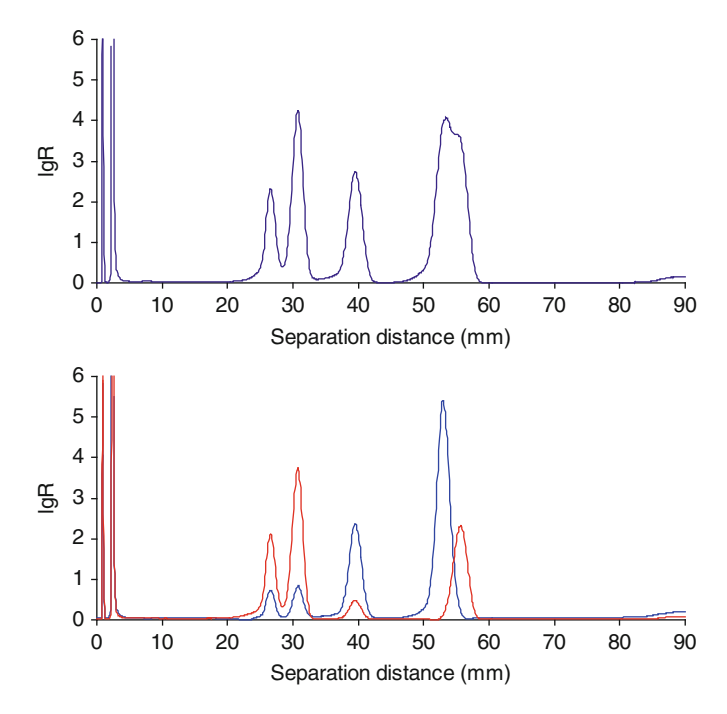


Fig. 12.16 Comparison of the original densitogram showing an unresolved peak and two densitograms calculated at different wavelengths, showing separated peaks for uracil and thymine [21]

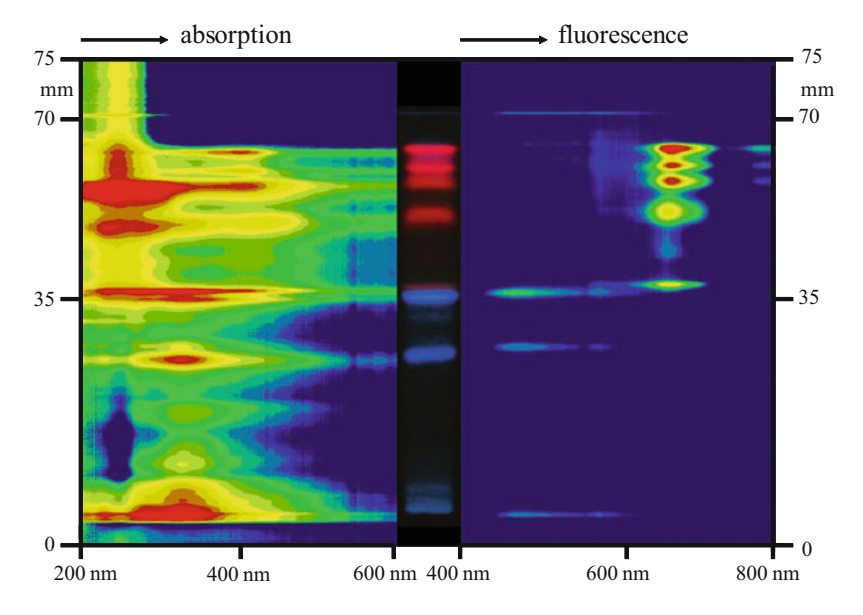


Fig. 12.17 Separation of a rosmarini folium extract on silica gel with toluene–ethyl acetate–formic acid (5+4+1, V/V) as mobile phase and stained with tetraphenyl borate/HCl reagent. A photograph of the track is located between the two contour plots. The absorption contour plot is on the *left side* and the fluorescence contour plot on the *right side*

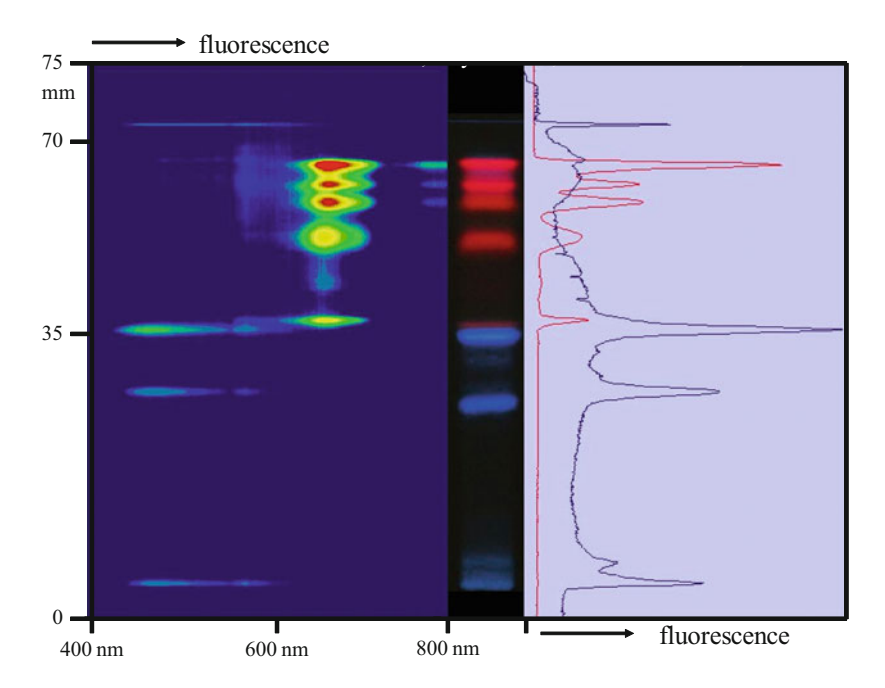


Fig. 12.18 Separation of a rosmarini folium extract stained with the tetraphenyl borate/HCl reagent. A photograph of the track is located between the two contour plots. The fluorescence contour plot is shown on the *left side* and the densitograms at 460 and 680 nm on the *right side*

The absorption plot shows a number of unresolved and light-absorbing zones. In contrast, all fluorescence zones are baseline separated.

Figure 12.18 illustrates the fluorescence contour plot and densitogram at 460 and 680 nm. Peak heights from the densitograms provide semi-quantitative information for the different compounds in the extract. A combination of different contour plots can enhance the separation information simply by visualizing different attributes of the recorded data.

The use of different detection conditions can be used to describe a sample according to different decision criteria. In Fig.12.19, 50 mL of sewage plant water was evaporated at room temperature and reconstituted with 20 μ L of methanol. The whole sample was applied to a 10 \times 10-cm cyanopropylsiloxane-bonded silica layer and developed for 7 cm in the first direction using dichloromethane—methanol—n-pentane (95 + 5 + 10, V/V) and after drying in the second direction using methyl tert-butyl ether—methanol—dichloromethane—cyclohexane—25% (V/V) aqueous ammonia (96 + 4 + 4 + 2 + 2, V/V). For video-densitometric evaluation, the plate was measured under UV light at 255 and 366 nm. The plate was then dipped for 2 s in a $Vibrio\ Fischeri$ suspension and evaluated for 2 min using a ST-1603ME CCD camera.

It should be noted that the selectivity of the two mobile phases is different because the migration order of paracetamol and dichlophenac is reversed in each

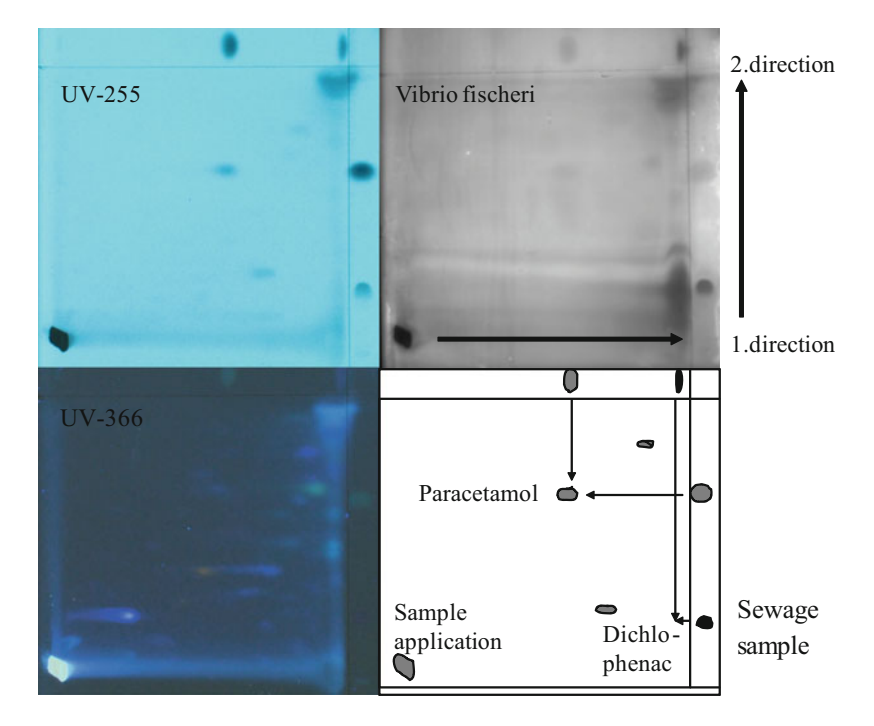


Fig. 12.19 The same 2D-separation of a sewage plant sample evaluated at 255 nm, 366 nm, and after dipping in a suspension of *Vibrio fischeri* luminescence bacteria. Paracetamol can be clearly identified in the 255-nm densitogram

development. The separation recorded at 366 nm reveals that the sample contains more than 15 contaminants with fluorescence. Paracetamol is clearly identified in the separation recorded at 255 nm as well as in the *Vibrio fischeri* evaluation. The *Vibrio fischeri* evaluation indicates a number of inhibition zones in the region of dichlophenac, but this compound could not be confidently identified [22].

References

- Machata G, Schütz H, Bäumler J, Daldrup T, Gibitz H-J (1989) Empfehlungen zur klinischtoxikologischen Analytik. Folge 5: Empfehlungen zur Dünnschichtchromatographie. VCH, Weinheim
- Spangenberg B, Post P, Ebel S (2002) Fibre optical scanning in TLC by use of a diodearray detector – linearization models for absorption and fluorescence evaluations. J Planar Chromatogr 15:88–93
- Spangenberg B, Ahrens B, Klein K-F (2002) Spektren zur Substanzidentifikation in der Dioden-Array Dünnschichtchromatographie. GIT Sep 22:22–24
- 4. Szepesi G (1990) Quantitation in TLC. In: Grinberg N (ed) Modern thin layer chromatography. Dekker, New York

- Touchstone JC, Levin SS, Murawec T (1971) Quantitative aspects of spectrodensitometry of thin layer chromatograms. Anal Chem 43:858–863
- Spangenberg B, Klein K-F (2001) New evaluation algorithm in diode-array thin-layer chromatography. J Planar Chromatogr 14:260–265
- Lloyd JLF (1975) Nitrogen heterocycle and polynuclear hydrocarbon fluorescence and adsorption effects in the presence of silica gel. Applications in high-pressure liquid and microcolumn chromatography. Analyst 100:529–539
- 8. Spangenberg B, Lorenz K, Nasterlack S (2003) Fluorescence enhancement of pyrene measured by thin-layer chromatography with diode-array detection. J Planar Chromatogr 16:331–337
- Ahrens B, Spangenberg B, Klein K-F (2001) TLC-analysis in forensic sciences using a diodearray detector. Chromatographia 53:S438–S441
- Spangenberg B, Seigel A, Kempf J, Weinmann W (2005) Forensic drug analysis by means of diode-array HPTLC using Rf and UV library search. J Planar Chromatogr 18:336–343
- 11. Ahrens B, Blankenhorn D, Spangenberg B (2002) Advanced fibre optical scanning in thinlayer chromatography for drug identification. J Chromatogr B 772:11–18
- 12. Spangenberg B, Klein K-F, Mannhardt J (2002) Proposals for error-reduction in planar chromatography, J Planar Chromatogr 15:204–209
- 13. Kortüm G (1962) Kalorimetrie, Photometrie und Spektrometrie. Springer, Berlin
- Wybourne G (1960) Optimum optical density for "shot" noise limited spectrophotometers.
 J Opt Soc Am 50:84–85
- 15. Pardue HL, Hewitt TE, Milano J (1974) Photometric errors in equilibrium and kinetic analyses based on absorption spectroscopy. Clin Chem 20:1028–1042
- Youmans HL, Brown H (1976) Selection of optimum ranges for photometric analysis. Anal Chem 48:1152–1155
- 17. Kealey D (1972) Quantitative reflectometry I. Principles and scope. Talanta 19:1563-1571
- Stroka J, Spangenberg B, Anklam E (2002) New approaches in TLC densitometry. J Liq Chromatogr Rel Technol 25:1497–1513
- 19. Savitzky A, Golay MJE (1964) Smoothing and differentiation of data by simplified least squares procedures. Anal Chem 36:1627–1639
- 20. Spangenberg B (1998) A new proposal for a parameter-free integration software. Fresenius J Anal Chem 360:148–151
- 21. Spangenberg B, Brämer R, Seigel A, Klein K-F (2001) Dünnschichtchromatographie mittels dioden-array detektion. GIT Sep 21:37–39
- 22. Spangenberg B Unpublished results

Chapter 13 Statistics for Quantitative TLC

In general, the aim of analytical measurements is the quantification of the analyte. The conversion of the observed signal into absolute sample amounts is usually achieved through calibration. For this purpose, response measurements are always indicated as the dependent variable (y-data), whereas the independent variable (x-data) is some function of the analyte amount. It should be noted that in this text a small letter represents a single observation or a single result. In reality, the analytical result is not calculated as a single figure but always calculated as a range.

13.1 The Mean Value

The mass m or the concentration c of the analyte and the random fluctuations of the measurement system affect observations. The random fluctuations are called noise. Noise comprises all effects caused by the measurement environment. We, therefore, observe that a duplicate or triplicate measurement does not result in two or three absolutely identical values. Single observations differ according to their noise. The question is which observation should be taken into consideration when calculating the analytical result? We may not be familiar with the measurement system so we can justify skipping the first observation, and perhaps we can also justify skipping our last observation, because we are tired of making measurements. We can also use an outlier test, which might identify the need to discard certain measured values according to a particular theorem. The crucial point behind all these considerations is that we should only delete an observation which we do not trust. But we should keep in mind, that we know nothing about the sample content, because the analytical result is unknown. If we know the result, we have no need to make a measurement! If the analytical result is unknown, we cannot argue that a single value differs significantly from other observations. In fact, by using outlier tests, we imply that multiple observations better describe reality than a single observation. But this might not be true. We should perform multiple measurements (a series of tests) to estimate the noise in our observations. We, therefore, tend to

trust in multiple observations with an assessment of the noise more than a single observation with unknown noise. Carl Friedrich Gauss (1777–1855) proved that we should indeed put more trust in multiple observations.

Gauss looked for a representative value, which best reflects all observations (i.e. in a democratic manner). The question is which value fits best? In his theory of errors, Gauss made the assumption that the best fit (in the least squares sense) is the smallest value of the sum of squared residuals (S_{sr}) . Gauss first described this method around 1794. In general, using least squares can be interpreted as a method of fitting data [1]. For i single measurements y_i , we can write:

$$\sum_{i} (y_i - \overline{Y})^2 \equiv \text{Minimum}$$

with \overline{Y} taken as a measure of central tendency for the data set. The deviation of the sum of squared residuals $S_{\rm sr}$ between the measurements and the optimally adjusted value for the central tendency \overline{Y} should assume a minimum. From this minimum condition, we can deduce that:

$$\frac{\partial \sum_{i} (y_{i} - \overline{Y})^{2}}{\partial \overline{Y}} = 0 = 2 \sum_{i} (y_{i} - \overline{Y}) (-1)$$
$$0 = -2 \sum_{i} y_{i} + 2 \sum_{i} \overline{Y} = -2 \sum_{i} y_{i} + 2n\overline{Y}.$$

After solving for \overline{Y} we observe:

$$\overline{Y} = \frac{1}{n} \sum_{i} y_{i}. \tag{13.1}$$

The best fit for the central tendency \overline{Y} is the mean value (the average) of all measurements. Please note that mean values will always be written in capital letters.

13.2 Variance and Precision

Each observation is corrupted by noise. Establishing constant measurement conditions for the different sample amounts is impossible since the measurement conditions, and therefore the measurement values, fluctuate by chance (randomly) in positive and negative directions due to the contribution from the noise.

13.2.1 Definition of Variance

By assuming that we measure no mass or concentration-dependant signals, we can directly measure the fluctuation as noise σ .

$$v = 0 \pm \sigma$$
.

For *n* data measured and squared, the values will have a constant (positive) noise if we assume constant measurement conditions. Thus we can write:

$$\sum_{i=1}^{n} y_i^2 = n\sigma^2.$$

If we assume that all observations are independent of one another, we must assume that the products of various different measurements are always zero (e.g. $\sigma_1\sigma_2=0$, but $\sigma_1\sigma_1=\sigma^2$). In this case, we can write:

$$\left(\sum_{i=1}^{n} y_{i}\right)^{2} = \sum_{i=1}^{n} y_{i}^{2} = n\sigma^{2}.$$

The sum of squared residuals in this particular measurement system can be written as:

$$\sum_{i=1}^{n} (y_i - \overline{Y})^2 = \sum_{i=1}^{n} y_i^2 - 2 \sum_{i=1}^{n} y_i \overline{Y} + \left(\sum_{i=1}^{n} \overline{Y}\right)^2.$$

With $\overline{Y} = \frac{1}{n} \sum_{i=1}^{n} y_i$, we obtain:

$$\sum_{i=1}^{n} (y_i - \overline{Y})^2 = n\sigma^2 - 2\sum_{i=1}^{n} y_i \frac{1}{n} \sum_{i=1}^{n} y_i + \left(\sum_{i=1}^{n} \frac{1}{n} \sum_{i=1}^{n} y_i\right)^2$$

$$= n\sigma^2 - \frac{2}{n} \left(\sum_{i=1}^{n} y_i\right)^2 + n\frac{1}{n^2} \left(\sum_{i=1}^{n} y_i\right)^2$$

$$\sum_{i=1}^{n} (y_i - \overline{Y})^2 = n\sigma^2 - \frac{1}{n} \left(\sum_{i=1}^{n} y_i\right)^2 = n\sigma^2 - \sigma^2.$$

After resolving for noise, we get:

$$\sigma^2 = \frac{1}{n-1} \sum_{i=1}^{n} (y_i - \overline{Y})^2.$$
 (13.2)

For this special case, we can calculate the noise from the measured data and the mean value. If we observe a measured value larger than zero (e.g. +z), (13.2) can be used as well, because $\sum_{i=1}^{n} \left[(z+y_i) - (z+\overline{Y}) \right]^2 = \sum_{i=1}^{n} (y_i - \overline{Y})^2$.

13.2.2 Relative Variance

The squared noise of a single observation is called *sample variance*. The sample variance is the averaged noise for multiple measurements. We assume that all the single values of this multiple measurement have the same averaged variance. The related *error* is the square root of the variance. We call this the *standard deviation* σ . The total *relative variance* ($\sigma_{\rm rel}^2$) can be calculated from the square root of the total variance divided by the mean of the data.

$$\sigma_{rel}^2 = \frac{\sigma^2}{\overline{Y}}.\tag{13.3}$$

The square root of the variance is the standard deviation, which can be used as an indication of the *precision* or *uncertainty*. If the variance of a multiple measurement is low, the measurements have high precision. The aim of good analytical work is to measure precisely, which means keeping uncertainties small [2–8]. The question is "what causes uncertainty in (HP)TLC?" The total statistically defined error comprises the detection variance (σ_D^2) of the measurement system, the uncertainty in sample preparation (σ_P^2), the variance of applying the desired sample volume to the layer (σ_V^2), and the uncertainty of chromatography itself (σ_C^2) [5]. Two features of the measurement uncertainty are generally poorly distinguished in the literature: the evaluation variance (σ_E^2) and the calibration variance (σ_K^2) [6]. The evaluation variance represents all uncertainties produced by inappropriate use of raw data after plate scanning. The variance of the manual integration and the variance using peak areas instead of peak heights contribute to the evaluation variance. Calibration variance comprises all uncertainties arising from a chosen calibration function. All these uncertainties form the total variance (σ^2).

$$\sigma_{\rm rel}^2 = \sigma_{\rm rel,P}^2 + \sigma_{\rm rel,V}^2 + \sigma_{\rm rel,C}^2 + \sigma_{\rm rel,D}^2 + \sigma_{\rm rel,E}^2 + \sigma_{\rm rel,K}^2$$

 $\sigma_{\mathrm{rel}\ P}^2$ is the relative variance of sample pre-treatment, $\sigma_{\mathrm{rel}\ V}^2$ the relative variance of sample application, $\sigma_{\mathrm{rel}\ C}^2$ relative variance of the chromatographic separation, $\sigma_{\mathrm{rel}\ D}^2$ the relative variance of the detector, $\sigma_{\mathrm{rel}\ E}^2$ the relative variance of evaluation, and $\sigma_{\mathrm{rel}\ K}^2$ is the relative variance of calibration.

Practical experience shows that the sample application error and the sample preparation error are by far the largest contributors to the total error. The uncertainty in sample preparation ($\sigma_{\rm P}^2$) is caused by all sample pre-treatment steps and can be effectively reduced if the sample is applied directly on the layer without further cleanup steps. The variance of the sample application volume ($\sigma_{\rm V}^2$) is mainly caused by manual spotting and can be significantly reduced if a computer controlled sample application device is used. The uncertainty in chromatography ($\sigma_{\rm C}^2$) is caused by inappropriate development conditions. It is mainly a positioning error and is caused by incorrect placement of the layer in the development chamber [7]. The detection variance is composed of measurement errors from inadequate

instrument adjustments, varying plate thickness, positioning error within the light beam, and instrumental measurement errors. Modern HPTLC equipment enables the analyst to do fully automated sample application and the use of modern glass fibre interfaces for slit scanning avoids most positioning errors [8]. Modern diodearray TLC scanners do not need any adjustments, such as wavelengths selection, which can affect the measurement precision of single wavelength scanners [9, 10]. The only adjustment a light fibre diode-array scanner needs is the choice of the distance of the interface above the layer, but this only influences the spatial resolution on the layer [8]. The analysis of variances is a powerful validation tool, because it reveals the weak points of a TLC method. How to quantify the different types of errors is described elsewhere [1, 5]. Total errors between 1 and 2% have been reported for modern TLC [5]. In practice, total analytical errors of less than 5% are difficult to achieve.

13.2.3 Quantification of Relative Variance

How can we improve analytical precision? Variance sizes are often very different and cannot be influenced. Mostly it is sufficient to reduce the largest contribution to the total variance. The simple quantification of caffeine in coffee can be used to illustrate how analysis of variance can contribute to improvements in the analytical precision [6]. Quantification of caffeine in beverages using HPTLC avoids the sample preparation uncertainty (σ_p^2) , because the undiluted sample is applied directly to the layer. If we perform a 7-mm band-wise application, the chromatographic uncertainty (σ_C^2) is negligible because the scanner measures 7-mm broad bands with a slit width of 3.5 mm. We can exclude uncertainties from inappropriate development conditions due to a positioning error in the development chamber. The combination of applicator and scanner in one system minimizes track-positioning errors. The system finds the exact position of the sample on the track without further information. The evaluation variance $(\sigma_{\rm F}^2)$ affects the accuracy but not precision using suitable integration software. Beside the sample application variance $(\sigma_{\rm V}^2)$ only the detection variance $(\sigma_{\rm D}^2)$ contributes to the total error. It is quite simple to determine the detection variance. The caffeine peak on a single track is measured six times without changing the plate position perpendicular to the direction of scanning. For this measurement, a relative error of 0.49% was calculated ($\sigma_{\rm rel~D}^2=0.49^{\bar 2}$) using the logarithm equation for data transformation (Chap. 12) [6]. The evaluation variance ($\sigma_{\rm E}^2$) cannot be clearly quantified, because all measurements were evaluated with the same algorithm. In Chap. 12, we showed that the logarithmic model produced the lowest error of all evaluation models. An appropriate evaluation model should be selected to suitably validate the HPTLC analysis. It is important to use reflectance values around R = 0.5 [8]. To reduce the total error, the selection of the measurement wavelength should be done carefully, according to the desired reflectance values and not according to a spectral absorption maximum [8].

The relative sample application variance for the caffeine sample $(\sigma_{\rm rel~V}^2)$ can be calculated as the difference between the total error and the detection error. To calculate this, nine caffeine samples were applied to the layer, separated, and measured resulting in a total relative variance of 1.23% [8]. The relative sample application error for the caffeine determination is calculated as $\sqrt{1.23^2-0.49^2}=1.129$ % indicating the good performance of the application device. The relative detection error from nine different standard caffeine tracks evaluated with the absorption formula is 1.18% [8]. Let us take this as the calibration uncertainty. Thus, the total relative variance of the analysis can be calculated as:

$$\begin{split} \sigma_{\text{rel P}}^2 + \sigma_{\text{rel V}}^2 + \sigma_{\text{rel C}}^2 + \sigma_{\text{rel D}}^2 + \sigma_{\text{rel E}}^2 + \sigma_{\text{rel K}}^2 &= \sigma_{\text{rel E}}^2 \\ &= 0 + 1.129^2 + 0 + 0.49^2 + 0 + 1.18^2 = 1.705^2. \end{split}$$

The total error is 1.705%, which illustrates that uncertainties below 2% are achievable in thin-layer chromatography. The result is precise within an uncertainty of 2%. Thus, in a 3-figure result, the last figure is uncertain.

13.3 Trueness, Precision, and Accuracy

Until now we have spoken about error in the sense of precision or uncertainty. Error was indicated as the noise, which corrupts the observation. Why should repeated measurements of a single quantity give different values? Well, no measurement is ever absolutely exact, but beside noise, incorrect functioning of equipment or mistakes made by the experimenter is possible. We did not include these in our discussion! We see that two types of errors are possible. These are random errors, which are a statistical error, and systematic (systemic) errors. A systematic error is the result of a miss-calibrated or incorrectly functioning device, or a mistake in the procedure made by the analyst. We, therefore, distinguish between precision (the observed repeatability of a measurement due to random errors) and trueness (the lack of systematic errors). A result shows high accuracy (correctness) in the sense of both trueness and precision [1]. Experiments are performed to establish the best values for certain quantities. Statistics in the form of analysis of variance helps to reveal the underlying causes of poor precision. Even more important is to reveal a weakness in the trueness. The aim of any chemical analysis is to determine the true value of the sample to achieve accuracy. It could be that we measure extremely precisely, that is, we observe a very low variance. That does not mean that we have determined the true value for that sample. Perhaps, we made a mistake during sample preparation. If only a single sample is prepared, the sample preparation error is an error in the trueness. Therefore, it is necessary to process several subsamples to obtain a representative estimate of the true value of an analyte [2–8]. The error in trueness is the difference between the measured value and the true value for the sample. A single measurement value never reveals a random

error, and a single incorrectly functioning measurement can never reveal a lack in trueness. We need to use another item in the hope that it will work correctly to allow observation of the difference in comparison to the incorrectly working item. We will never reveal a lack in trueness if we use a single sample for multiple measurements and if we make a mistake during the pre-treatment procedure. To check accuracy we, therefore, have to carry out multiple error-dependent steps on the way to the final result. In particular, Kaiser notes that the chromatographic separation itself often produces the largest error [2–4]. In general it is like shooting a gun: the smaller the target, the more frequently you miss it. Measuring small concentrations will generally result in large variances, but this does not mean that the result is not true.

13.4 The Gauss Distribution

An error in precision is caused by the change in individual measurements. This kind of error is quantified by the variance or the relative variance. The distribution of random measurements often conforms to the shape of a Gaussian curve. A Gaussian curve, also called a *normal distribution* (the bell curve), is plotted in Fig. 13.1. Its range is from $-\infty$ to $+\infty$, although measurement values can never have negative values. Mathematically the Gauss distribution is written as

$$f(x) = \frac{A}{\sigma\sqrt{2\pi}} e^{-\frac{(x-\mu)^2}{2\sigma^2}}$$
 (13.4)

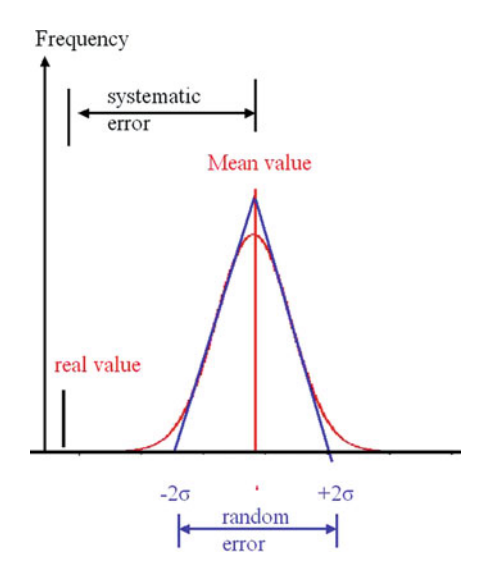


Fig. 13.1 Illustration of a random error and a systematic error according to the mean μ and the standard deviation σ of a Gauss distribution

with height:

$$H = \frac{A}{\sigma\sqrt{2\pi}} = 0.3989 \frac{A}{\sigma}.\tag{13.5}$$

A is the area of the function, H the height of the function, σ the standard deviation, and μ is the maximum value of the Gauss function.

13.4.1 Area of the Gauss Distribution

The area of the function is the integral of all single function values. The width of the function σ is the square root of the variance and is called the *standard deviation*. The height is a function of the inverse standard deviation and its area (13.4). The area in the range $\pm 1\sigma$ around the maximum covers 68% of the total function area. The range $\pm 2\sigma$ (exactly: $\pm 1.96\sigma$) covers 95%, and the range $\pm 3\sigma$ (exactly: $\pm 3.09\sigma$) covers 99.8% of the total area.

Measurement results are mostly distributed according to the Gauss function, which allows the calculation of the mean [according to (13.1)] and the variance [according to (13.2)]. If there is no systematic error, the Gauss distribution offers a measure of certainty. If we address the range around the mean as $\pm 2\sigma$, we can assume that the true value is located within this range with a certainty of 95%. In other words, the error probability is 100%-95%=5%. The area of the Gauss distribution is one. Therefore, if we choose a significance level of $\alpha=0.05$, we get a certainty of $(1-\alpha)=0.95$. A significance level of $\alpha=0.05$ is commonly used in chemical analysis. If a result is specified with a significance level of $\alpha=0.05$ as $\mu\pm2\sigma$, we assume that the true value is within this range, with a probability of 95%.

13.4.2 Quantiles of the Gauss Distribution

Analytical results are calculated as a range corresponding to a section on the x-axis. If the question arises whether a result is less than a given value, we have to decide whether the result is contained within this range or not. To decide this, we first have to choose a significance level α . In other words, we have to define the error we are prepared to accept for the test. In mathematical terms, we need to define the area of the normal distribution, which covers the area $(1-\alpha)$ of the *Gauss* function. For this purpose, the normal distribution must be integrated from $-\infty$ to a level which exactly provides the value $(1-\alpha)$.

$$F(z) = 1 - \alpha = \int_{-\infty}^{z_{\alpha}} \frac{A}{\sigma \sqrt{2\pi}} e^{-\frac{(z-\mu)^2}{2\sigma^2}} dz.$$

The upper integration level (z_{α}) is called a quantile. Quantiles are points placed at regular intervals in the normal distribution. They are the data values that mark the boundaries between consecutive subsets. If the quantile value is smaller than the test value, the analytical result is specified as smaller than the test value with a certainty of $(1-\alpha) \times 100\%$.

The area of the Gauss distribution

$$F(z) = \alpha = \int_{z_{-}}^{\infty} \frac{A}{\sigma \sqrt{2\pi}} e^{-\frac{(z-\mu)^2}{2\sigma^2}} dz$$

represents a measure of the error probability. The decisions "less than" or "more than" describe single-side decisions. The decisions "equal and less" (range \leq level) or "equal and more" (range \geq level) describe two-side test decisions (13.6). This is because of the "equal" in the decision. Asking for "equal" implies that a measured range is tested within an upper and lower limit. With the chosen significance level, we have two integration levels. The area of the normal distribution is the integrated function in the range from the lower level $-z_{\alpha/2}$ to the upper level $+z_{\alpha/2}$.

$$F(z) = 1 - \alpha = \int_{-z_{\pi/2}}^{+z_{\pi/2}} \frac{A}{\sigma\sqrt{2\pi}} e^{-\frac{(z-\mu)^2}{2\sigma^2}} dz.$$

For a decision (range \geq level) or (range \leq level) with a significance level of $\alpha = 0.05$, the test value is $(1-\alpha/2)$. We, therefore, have to use a normal distribution table for $\alpha = 0.025$ (Fig. 13.2).

The quantiles z_{α} of the normal distribution are commonly tabulated with respect to significance level α , for single-side certainties $p=1-\alpha$ or for double-sided certainties $p=1-2\alpha$. The quantiles z_{α} or $z_{\alpha/2}$ for single- or double-sided questions can be easily approximated using the Hasting expression.

$$z_p = q - \frac{a_0 - q(a_1 + a_2 q)}{1 + q(b_1 + q(b_2 + qb_3))}$$
(13.6)

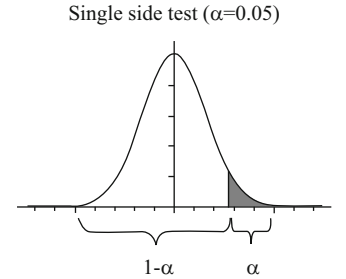
with

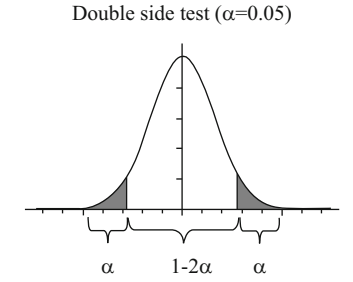
$$q = \sqrt{-2\ln(1-p)}$$

 $a_0 = 2.515517$, $a_1 = 0.802853$, $a_2 = 0.010328$, $b_1 = 1.432788$, $b_2 = 0.189269$, and $b_3 = 0.001308$.

This approximation is valid for certainties in the range $0.5 . Quantiles for the certainties <math>0 can be calculated from mirrored negative values <math>(z_p = -z_{I-p})$. These quantiles are also necessary to calculate the critical limit for the trend test according to von Neumann.

Fig. 13.2 Gauss distributions for a single-side test (for $\alpha=0.05$) and a double (duplicate) side test for $\alpha=0.01$



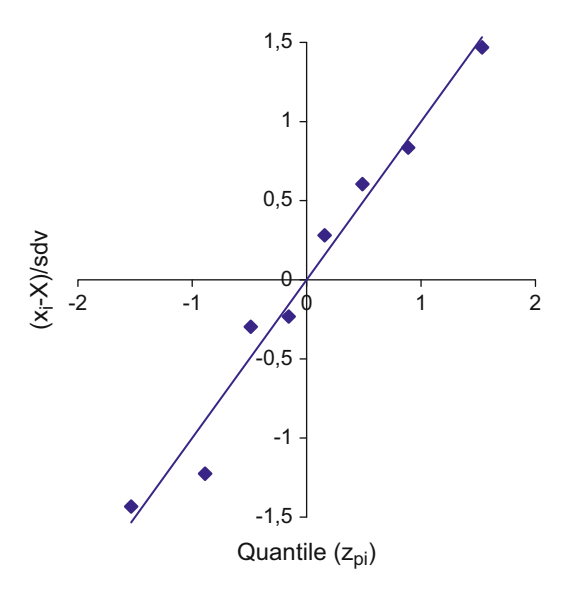


13.4.3 Test for a Normal Distribution

The first question at the beginning of an analytical evaluation is whether the data are distributed according to a normal distribution or not. Several tests, such as the Kolmogoroff-Smirnov-Lilliefors test, are available to answer this question. The quantile-quantile plot (O-O plot) in which the measured data are compared directly with the data of the normal distribution is easy to perform. For example, let us take eight measurements from a chloromequat determination. Chloromequat, 500 ng, was applied several times to a HPTLC plate, separated, stained, and measured by fluorescence, resulting in the peak areas: 2.974, 2.773, 2.728, 2.988, 3.099, 3.169, 3.219, 3.356. The mean of these data according to (13.1) is $(\overline{Y} =$ 3.0383) and the standard deviation is sdv = 0.21636. The mean value is subtracted from the measured data, and each value is divided by the standard deviation, and these values are then rank ordered. The mean value of this standardized set of data is zero. For the eight measurements, the appropriate quantiles from the normal distribution are calculated according to (13.6). For this, the whole range is divided into eight equally distant certainties $(p_1 = 0.0625, p_2 = 0.1875, p_3 = 0.3125,...,$ $p_8 = 0.9375$). The calculated quantiles (z_{pi} -values) are then plotted against the ranked measurements. For a normal distribution of the data, a straight line without an intercept is expected.

Figure 13.3 clearly indicates that a single value deviates further from the best fit line than the other values. This test is often misused as an *outlier test* to eliminate inconvenient data.

Fig. 13.3 A Q-Q plot for eight measurements of chloromequat. The measured data are normally distributed because all data form a straight line passing through the origin



13.5 Student's Distribution (t Distribution)

The standard distribution is valid for an infinite number of independent measurements. As a general rule, the standard distribution can be reliably used if more than 30 measurements are available for each sample. This is rarely the case for chromatographic measurements, since it is generally too time consuming to acquire this level of data. In this case it is not the standard distribution but the student distribution, which is valid. Gosset first published the derivation of the t distribution in 1908 under the pseudonym Student, while he was working at a brewery in Dublin. The t test and its associated theory became well known through the work of Fisher, who called the distribution "Student's distribution", often simply called t distribution. The student distribution is a little bit flatter and broader than the normal distribution. This can be corrected by a constant factor called the student factor $t_{\alpha,n}$. This factor is dependent on the significance level α and the number of data points n, which defines the number of degree of degree of degree and degree is significance level $\alpha = 0.05$, the following equation is obtained:

$$2^{2}\sigma^{2} = t_{(\alpha=0.05)}^{2} \operatorname{var}(y)_{n<30}. \tag{13.7}$$

The abbreviation var(y) stands for the sample variance, calculated according to (13.2) for any number of data points less than 30. The variance according to (13.2) can be redefined as follows:

Table 13.1	The t factors
for the signi	ficance levels
of $\alpha = 0.05$, 0.01, and 0.002

α			
\overline{f}	0.05	0.01	0.002
1	12.706	63.657	318.309
2	4.303	9.925	22.327
3	3.182	5.841	10.214
4	2.776	4.604	7.173
5	2.571	4.032	5.893
6	2.447	3.707	5.208
7	2.365	3.499	4.785
8	2.306	3.355	4.501
9	2.262	3.250	4.297
10	2.228	3.169	4.144
11	2.201	3.106	4.025
12	2.179	3.055	3.930
:	:	:	:
60	2.000	2.660	3.232
:	:		:
∞	1.960	2.576	3.090

$$var(y)_{n<30} = \frac{1}{n-1} \sum_{i=1}^{n} (y_i - \overline{Y})^2.$$
 (13.8)

The standard deviation sdv(y) is calculated from the square root of the variance as:

$$sdv(y)_{n<30} = \sqrt{\frac{1}{n-1} \sum_{i=1}^{n} (y_i - \overline{Y})^2}.$$
 (13.9)

The number of degrees of freedom is calculated from the number of data points minus the number of statistical values calculated from the data, e.g., if the mean is calculated for n measurements then the number of degrees of freedom is f = n - 1. The number of degrees of freedom is used to determine the student t factor (Table 13.1).

13.6 Error Propagation

The laws of error propagation describe the approach used to combine several sources of random error into a single value. This is necessary because we commonly have to measure more than a single quantity to obtain a final result. The laws of error propagation define the way in which data uncertainties propagate through the calculation, thus resulting in a final uncertainty. Let us discuss the question in which way the error in two independent values will be propagated

into the sum of both values. Let us take the mean value of two single measurements as an example.

$$m_{\text{end}} = (m_1 + m_2)/2.$$

The term variance was introduced as a measure of error. If we assume that both data $(m_1 \text{ and } m_2)$ have the same variance, what will be the variance in the final result? Thus, we can write the following, taking the measurement uncertainty $\pm \sigma_1$ and $\pm \sigma_2$ for both data sets into account:

$$2m_{\rm end} \pm 2\sigma_{\rm end} = m_1 \pm \sigma_1 + m_2 \pm \sigma_2$$
.

For the uncertainty of the final result, we obtain:

$$\pm 2\sigma_{\rm end} = \pm \sigma_1 + \pm \sigma_2$$
.

Squaring the equation eliminates negative values.

$$4\sigma_{\rm end}^2 = \sigma_1^2 + \sigma_2^2 + 2\sigma_1\sigma_2$$

The product of two different variances $(\sigma_1\sigma_2)$ is called a *co-variance*. Commonly, data are measured sequentially. If we do it properly, these measurements are independent of one another. Thus, we make a measurement error while actually carrying out the measurement. We never make a mistake in the measurement of the second value while measuring the first. While measuring σ_1^2 the variance of $\sigma_2^2=0$! In general, a covariance of two independent measurements is always zero. We can write:

$$4\sigma_{\rm end}^2 = \sigma_1^2 + \sigma_2^2$$

With these partial derivatives

$$\left(\frac{\partial m_{\rm end}}{\partial m_1}\right) = 1; \left(\frac{\partial m_{\rm end}}{\partial m_2}\right) = 1,$$

we obtain:

$$4\sigma_{\rm end}^2 = \left(\frac{\partial m_{\rm end}}{\partial m_1}\right)^2 \sigma_1^2 + \left(\frac{\partial m_{\rm end}}{\partial m_2}\right)^2 \sigma_2^2.$$

Gauss was the first to formulate the law of error propagation. It says: for the estimation of the uncertainty of an analytical result, all sources of uncertainty must

be taken into account. Assuming equality of the variances, the expression must be partially derived and squared with respect to all the expressions for the uncertainty. The result is multiplied by the variance of the uncertain value. Usually, only the measurements (y-values) are regarded as uncertain, although the x-values (the concentration of the standards) are uncertain as well. In general, it is assumed that the x-values are error free.

According to Gauss' law of error propagation, the variance of the mean value is calculated as:

$$\sigma_{\overline{Y}}^2 = \sum_{i=1}^n \left[\left(\frac{\overline{\partial Y}}{\partial y_i} \right)^2 \sigma_i^2 \right] = \left(\frac{1^2}{n^2} \sigma_1^2 + \dots + \frac{1^2}{n^2} \sigma_n^2 \right) = n \frac{1}{n^2} \sigma^2, \tag{13.10}$$

$$\sigma_{\overline{Y}}^2 = \frac{1}{n} \sigma^2.$$

For measurements with fewer than 30 data points (typical of chromatography), we can write:

$$\operatorname{var}(\overline{Y}) = \frac{1}{n} \operatorname{var}(y). \tag{13.11}$$

The standard deviation of the mean value is smaller than the standard deviation of a single value by a factor of \sqrt{n} .

$$\operatorname{sdv}(\overline{Y}) = \frac{1}{\sqrt{n}}\operatorname{sdv}(y). \tag{13.12}$$

In other words, we can reduce noise by a factor of \sqrt{n} by using multiple measurements. That is the reason why averaging spectra and densitograms reduce noise so effectively.

13.7 Calibration Methods

For quantification of the analyte, we need a function to transform the observations (the measured data) into analytical results. The function used to define the relationship between the measurement data and the sample amount is called the calibration function. Establishing the calibration function is usually a component of the analytical method. Thus, a series of samples containing a known amount of analyte (standard samples) are measured to estimate their resulting responses. In other words, a calibration starts with *x*-values in order to estimate *y*-values. The calibration function shows the functional dependence:

$$y = f(x)$$
.

13.7 Calibration Methods 329

After solving for x, the *calibration function* then becomes the *analytical function*. The analytical result is a function of the observation.

$$\{x_{\mathbf{a}}\} = f^{-1}(y).$$

Inserting the observation y into the analytical function, we obtain the analytical result x.

13.7.1 The Linear Calibration Function

The functional interdependence between analyte content (x-value) and measurement signal (y-value) is commonly described as:

$$y(x) = b + ax$$
.

The regression coefficient a is called the slope and is a measure of sensitivity [1]. The intercept on the y-axis is named b and can be calculated according to Gauss as the best fit between the measurements (y_i -values) and the optimally adjusted regression function y(x). The squared residuals $S_{\rm sr}$ should result in a minimum:

$$S_{\rm sr} = \sum_{i=1}^{n} (y_i - y(x))^2 = \text{Minimum}.$$

The deviation of S_{sr} with respect to the intercept is:

$$\begin{aligned} \frac{\partial S_{\text{sr}}}{\partial b} &= \frac{\partial}{\partial b} \sum_{i=1}^{n_{\text{C}}} (y_i - b - ax_i)^2 = 0, \\ \frac{\partial S_{\text{sr}}}{\partial b} &= \sum_{i=1}^{n_{\text{C}}} 2(y_i - b - ax_i)(-1) \\ &= -2 \sum_{i=1}^{n_{\text{C}}} y_i + 2n_{\text{C}}b + 2a \sum_{i=1}^{n_{\text{C}}} x_i = 0. \end{aligned}$$

Dividing this equation by 2 and rearranging gives for the intercept:

$$b = \frac{1}{n_{\rm C}} \sum_{i=1}^{n_{\rm C}} y_i - a \frac{1}{n_{\rm C}} \sum_{i=1}^{n_{\rm C}} x_i = \overline{Y_{\rm C}} - a \overline{X_{\rm C}}.$$

There are problems with the term "intercept". The intercept value describes the measurement data at a mass or a concentration of zero. The calibration function

covers the range from the lowest up to the highest calibration values. Outside this range, the function is mathematically defined but not verified by experiment. The intercept is often misunderstood as a blank value, although it is not part of the calibration range [9]. We stated that measurement data are nearly always distributed according to a normal distribution. A blank value can only be described mathematically as a normal distribution if the measurements are located around zero. This is only the case if we assume negative masses or concentrations. The logical consequence must be to avoid the regression coefficient "intercept" in each calibration function.

We can achieve this by shifting the origin of the system y(x) = b + ax from 0/0 to $\overline{Y_C}/\overline{X_C}$. Thus, a new calibration function results, avoiding the term "intercept" [5, 7, 9, 10].

$$Y(x) - \overline{Y_{C}} = a(x - \overline{X_{C}}). \tag{13.13}$$

The procedure is illustrated in Fig. 13.4.

13.7.2 Estimating $\overline{X_C}$

To find the best fit for the x-values, set the squared residuals $S_{\rm sr}$ calculated from the x-values and the optimally adjusted mean value of the standards $\overline{X}_{\rm C}$ for $n_{\rm C}$ data points to a minimum.

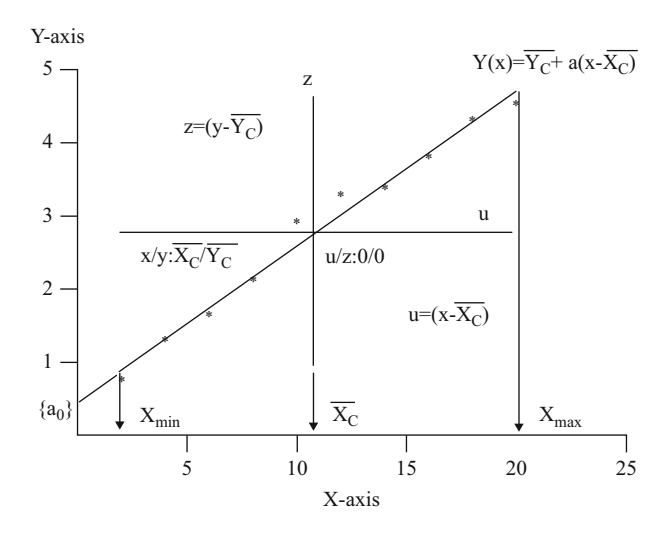


Fig. 13.4 Illustration of the shift of the calibration expression from y(x) = ax + b to $Y(x) = \overline{Y_C} + a(x - \overline{X_C})$

13.7 Calibration Methods 331

$$S_{\rm sr} = \sum_{i=1}^{n} (x_i - \overline{X_{\rm C}})^2 = \text{Minimum}.$$

With respect to the mean value of the standards, the deviation of $S_{\rm sr}$ is:

$$\frac{\partial S_{\text{sr}}}{\partial \overline{X}_{\text{C}}} = \frac{\partial}{\partial \overline{X}_{\text{C}}} \sum_{i=1}^{n_{\text{C}}} \left(x_i^2 - 2x_i \overline{X}_{\text{C}} + \overline{X}_{\text{C}}^2 \right)$$
$$= -2 \sum_{i=1}^{n_{\text{C}}} x_i + 2n_{\text{C}} \overline{X}_{\text{C}} = 0.$$

The mean value of the standard is defined as:

$$\overline{X_{\rm C}} = \frac{1}{n_{\rm C}} \sum_{i=1}^{n_{\rm C}} x_i. \tag{13.14}$$

This is of course the same function derived for the mean value of a test series. In TLC, the independent variable x is the amount of substance applied to the layer. This variable is assumed to be free of error. Obviously, this is not the case because we may have an error in preparing the solution, in applying the sample, and in measuring the response. But if we assume x to be free of error, we transfer all x-errors into y-values. This procedure makes calculations simpler without forgetting that x-values are corrupted by errors in reality. The variance var(y) for n_C measurements is dependent on the number of degrees of freedom. The number of degrees of freedom is f = n - 2, because we need to estimate the two regression coefficients a and \overline{Y}_C from a calibration series of n_C data. The sum of the squared residuals S_{sr} can be used to estimate regression variance in the same way as shown in (13.2).

$$var(y) = \frac{S_{sr}}{f} = \frac{1}{n_{C} - 2} \sum_{i=1}^{n_{C}} (y_{i} - \overline{Y_{C}} - a(x_{i} - \overline{X_{C}}))^{2}.$$
 (13.15)

We just have to take into account that we want to fit the data to the regression equation (13.13) and not into a single value as shown in (13.2).

13.7.3 Estimating a and \overline{Y}_{C}

To find the best fit according to Gauss, the squared residuals $S_{\rm sr}$ between the measurements and the optimally adjusted regression function y(x) for $n_{\rm C}$ data points should assume a minimum

$$S_{\rm sr} = \sum_{i=1}^{n} (y_i - Y(x))^2 = \text{Minimum}.$$

The regression coefficient a is calculated from the partial derivative of the squared residuals according to a.

$$\begin{split} \frac{\partial S_{\rm sr}}{\partial a} &= \frac{\partial}{\partial a} \sum_{i=1}^{n_{\rm C}} \left(y_i - \overline{Y_{\rm C}} - a(x_i - \overline{X_{\rm C}}) \right)^2 = 0, \\ \frac{\partial S_{\rm sr}}{\partial a} &= \sum_{i=1}^{n_{\rm C}} 2 \left(y_i - \overline{Y_{\rm C}} - a(x_i - \overline{X_{\rm C}}) \right) \left(-(x_i - \overline{X_{\rm C}}) \right) \\ &= \sum_{i=1}^{n_{\rm C}} -2 \left(y_i - \overline{Y_{\rm C}} \right) \left(x_i - \overline{X_{\rm C}} \right) + 2a \sum_{i=1}^{n_{\rm C}} \left(x_i - \overline{X_{\rm C}} \right)^2 = 0. \end{split}$$

We can carry out the same procedure for $\overline{Y_C}$.

$$\begin{split} \frac{\partial S_{\text{sr}}}{\partial \overline{Y_{\text{C}}}} &= \frac{\partial}{\partial \overline{Y_{\text{C}}}} \sum_{i=1}^{n_{\text{C}}} \left(y_i - \overline{Y_{\text{C}}} - a(x_i - \overline{X_{\text{C}}}) \right)^2 = 0\\ \frac{\partial S_{\text{sr}}}{\partial \overline{Y_{\text{C}}}} &= \sum_{i=1}^{n_{\text{C}}} 2 \left(y_i - \overline{Y_{\text{C}}} - a(x_i - \overline{X_{\text{C}}}) \right) (-1)\\ &= -2 \sum_{i=1}^{n_{\text{C}}} y_i + 2 \left(n_{\text{C}} \overline{Y_{\text{C}}} \right) + 2a \sum_{i=1}^{n_{\text{C}}} \left(x_i - \overline{X_{\text{C}}} \right) = 0. \end{split}$$

It should be noted that according to (13.14) the equation $\sum_{i=1}^{n_C} (x_i - \overline{X_C}) = 0$ is valid. Both equations for the determination of a and $\overline{Y_C}$ divided by 2 can be written as:

$$n_{C}\overline{Y_{C}} + a \sum_{i=1}^{n_{C}} (x_{i} - \overline{X_{C}}) = \sum_{i=1}^{n_{C}} y_{i}$$

$$0\overline{Y_{C}} + a \sum_{i=1}^{n_{C}} (x_{i} - \overline{X_{C}})^{2} = \sum_{i=1}^{n_{C}} (y_{i} - \overline{Y_{C}}) (x_{i} - \overline{X_{C}}).$$

It is possible to use a matrix to estimate a and $\overline{Y_C}$:

$$\begin{vmatrix} n_{C} + 0 \\ 0 + \sum_{i=1}^{n_{C}} (x_{i} - \overline{X_{C}})^{2} \end{vmatrix} \begin{vmatrix} \overline{Y_{C}} \\ a \end{vmatrix} = \begin{vmatrix} \sum_{i=1}^{n_{C}} y_{i} \\ \sum_{i=1}^{n_{C}} (y_{i} - \overline{Y_{C}})(x_{i} - \overline{X_{C}}) \end{vmatrix}$$

13.7 Calibration Methods 333

We can use some abbreviations to shorten the matrix.

$$\begin{vmatrix} n_{\mathbf{C}} & 0 \\ 0 & S_{xx} \end{vmatrix} \begin{vmatrix} \overline{Y_{\mathbf{C}}} \\ a \end{vmatrix} = \begin{vmatrix} \sum y_i \\ S_{xy} \end{vmatrix}.$$

As shown in Chap. 12, we can solve the matrix using Cramer's rule to extract the expression for \overline{Y}_C , which of course is the mean value of the calibration data. With the determinant of the matrix $\det(X) = x_{11}x_{22} - x_{12}x_{21}$, we can calculate the regression coefficient:

$$\overline{Y_{\rm C}} = \frac{1}{n_{\rm C} S_{xx}} S_{xx} \sum y_i = \frac{1}{n_{\rm C}} \sum_{i=1}^{n_{\rm C}} y_i.$$
 (13.16)

The expression for the slope a (the measure of sensitivity) can be calculated in the same way.

$$a = \frac{1}{n_{\rm C}S_{xx}} n_{\rm C}S_{xy} = \frac{S_{xy}}{S_{xx}}.$$
 (13.17)

13.7.4 Estimating the variances of a and $\overline{Y_{\rm C}}$

For the calculation of a und $\overline{Y_C}$, we do not necessarily need to use a matrix expression. For the calculation of the *confidence interval* (the scatter of measured values around the regression line), it is helpful to use the inverse matrix. The inverse matrix S^{-1} multiplied by the variance of the calibration series according to (13.15) provides the variances of the regression coefficients.

$$\begin{vmatrix} \operatorname{var}(\overline{Y_{C}}) & \operatorname{cov}(\overline{Y_{C}}, a) \\ \operatorname{cov}(a, \overline{Y_{C}}) & \operatorname{var}(a) \end{vmatrix} = \frac{1}{n_{C}S_{xx}} \begin{vmatrix} S_{xx} & -0 \\ -0 & n_{C} \end{vmatrix} \operatorname{var}(y),$$

$$\operatorname{var}(\overline{Y_{C}}) = \frac{1}{n_{C}}\operatorname{var}(y), \tag{13.18}$$

$$var(a) = \frac{1}{S_{xx}} var(y). \tag{13.19}$$

From the matrix expression, it can be seen that there is no covariance cov() between the two regression coefficients. We find two zeros in the matrix at the covariance positions. When using the regression function y(x) = ax + b, we will observe the expressions $-\Sigma x_i$ for the covariance. The regression coefficients are not independent of one another in this regression function.

13.8 The *F*-Test

We should now discuss a very important restriction for calibration functions. It is assumed that the variance for a series of measurements is constant over its whole range, but this is not always the case. We, therefore, have to check this assumption. Thus, the variance must be measured in different sections of the calibration range. The term for this is checking *homoskedasticity*. It is sufficient to measure the variance at the extreme positions in the calibration range, because that is where we expect the largest differences. Measure at least six standards at the lowest and the highest calibration level and calculate the variance according to (13.2).

Statistically, we must answer the question whether the two variances are equal. Fisher's F-test is best suited for this. If equation $var(y_A) = var(y_B)$ is valid, the quotient value of T_F will be 1.

$$T_{\rm F} = \frac{\operatorname{var}(y_A)}{\operatorname{var}(y_B)}. (13.20)$$

It should be noted that the larger figure must be assigned to the nominator to fulfil the condition $T_{\rm F} > 1$.

The test value $T_{\rm F}$ has to be compared with the F-distribution values at a chosen significance level and for the correct number of degrees of freedom (Table 13.2). A significance level of $\alpha=0.05$ is commonly chosen. For example, for six measurements at the outer extremes of the calibration range, we find with $f_{\rm N}=f_{\rm D}=5$ the value 5.05. Variances should not be combined if the value of the test ($T_{\rm F}$) is greater than this figure. In this case, the calibration range must be reduced.

13.9 The Linear Regression Variance

For the estimation of the total linear regression variance, all sources of uncertainty must be taken into account. Thus, the linear regression function Y(x) must be partially derived and squared with respect to all the uncertainties of (13.13). There are no co-variances, which make calculations easier.

freedom	The F-dist	ribution for	the signii	icance level	or $\alpha = 0.03$	for different	degrees of
$f_{\rm N}/f_{\rm D}$	2	3	4	5	6	7	8

$f_{\rm N}/f_{\rm D}$	2	3	4	5	6	7	8
2	19.00	19.16	19.25	19.30	19.33	19.35	19.37
3	9.55	9.28	9.12	9.01	8.94	8.89	8.85
4	6.94	6.59	6.39	6.26	6.16	6.09	6.04
5	5.79	5.41	5.19	5.05	4.95	4.88	4.82
6	5.14	4.76	4.53	4.39	4.28	4.21	4.15
7	4.74	4.35	4.12	3.97	3.87	3.79	3.73
8	4.46	4.07	3.84	3.69	3.58	3.50	3.44

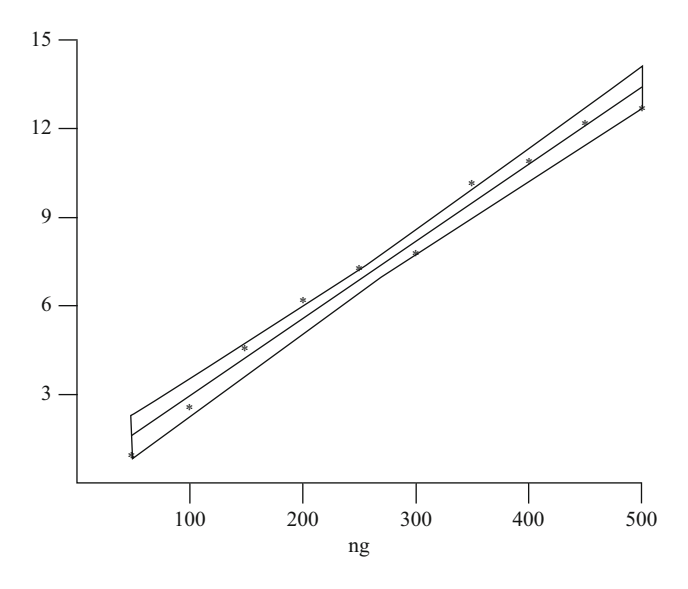


Fig. 13.5 The confidence interval for a linear calibration function

$$\operatorname{var}Y(x) = \left(\frac{\partial y(x)}{\partial \overline{Y_{C}}}\right)^{2} \operatorname{var}(\overline{Y_{C}}) + \left(\frac{\partial y(x)}{\partial a}\right)^{2} \operatorname{var}(a)$$
$$= \frac{\operatorname{var}(y)}{n_{C}} + (x - \overline{X_{C}})^{2} \frac{\operatorname{var}(y)}{S_{xx}}.$$

The confidence interval of the calibration function is even more interesting. For calibration data $n_{\rm C} < 30$, we have to take the Student t factor into account. With (13.13), we obtain the confidence interval for linear regression as:

$$\operatorname{cnf}\{Y(x)\} = Y(x) \pm t_{C} \sqrt{\frac{\operatorname{var}(y)}{n_{C}} + \frac{\left(Y(x) - \overline{Y_{C}}\right)^{2}}{a^{2} S_{xx}} \operatorname{var}(y)}.$$
 (13.21)

The confidence interval describes the uncertainty of data in the *y*-direction and the uncertainty of the slope. The confidence interval is, therefore, a function of *x*. The lowest uncertainty is observed at position \overline{X}_C , which is the mean of the values for the standards as shown in Fig. 13.5. The central region of the calibration curve is exactly where the analyte should be measured [5, 7, 9, 10]!

13.10 The Analytical Function of Linear Regression

First, the calibration function must be established after which the amount of analyte in individual samples can be determined. A series of n_a measurements are made for each sample. The results are combined to give a mean value of the analyte $\overline{Y_a}$, which is given as:

$$\overline{Y_{\mathbf{a}}} = \frac{1}{n_{\mathbf{a}}} \sum_{i=1}^{n_{\mathbf{a}}} y_i.$$

The mean value of the analyte is then inserted as x-values into the regression function and the equation rearranged to give the analyte amount $\{X_a\}$. Graphically, we project a mirror image of the y-data onto the x-axis by using the calibration function. The analytical function for linear regression is given by (13.13) as:

$$\{X_a\}_{LR} = \frac{\overline{Y_a} - \overline{Y_C}}{a} + \overline{X_C}.$$
 (13.22)

All sources of uncertainty must be taken into account to estimate the total variance of the final result. There are uncertainties in all the y-values and in the slope, and these can be derived from the measurements using (13.17).

$$\begin{aligned} \operatorname{var}\{X_{\mathbf{a}}\}_{\mathsf{LR}} &= \left(\frac{\partial \{X_{\mathbf{a}}\}_{\mathsf{LR}}}{\partial \overline{Y_{\mathbf{C}}}}\right)^{2} \operatorname{var}(\overline{Y_{\mathbf{C}}}) + \left(\frac{\partial \{X_{\mathbf{a}}\}_{\mathsf{LR}}}{\partial a}\right)^{2} \operatorname{var}(a) \\ &+ \left(\frac{\partial \{X_{\mathbf{a}}\}_{\mathsf{LR}}}{\partial \overline{Y_{\mathbf{a}}}(x)}\right)^{2} \operatorname{var}(\overline{Y_{\mathbf{a}}}). \end{aligned}$$

There is no covariance between calibration and analyte data, because both sets of measurements are made independently. A single plate should be used for these measurements, and all tracks are evaluated independent of one another. If the scanner interface is not correctly located, side-by-side tracks may be scanned simultaneously. This would be a typical example for a covariance, because one sample influences its neighbours; in other words, both sample tracks are measured together and not independently. Assuming no co-variance, the total variance of the analytical function becomes:

$$\operatorname{var}\{X_{\mathbf{a}}\}_{\mathsf{LR}} = \frac{\operatorname{var}(\overline{Y_{\mathsf{C}}})}{\left(-a\right)^{2}} + \left(\frac{\overline{Y_{\mathsf{a}}} - \overline{Y_{\mathsf{C}}}}{-a^{2}}\right)^{2} \operatorname{var}(a) + \frac{\operatorname{var}(\overline{Y_{\mathsf{a}}})}{a^{2}}.$$

The analyte variance is calculated according to $var(\overline{Y_C})$ described in (13.18).

$$\operatorname{var}(\overline{Y_{\mathbf{a}}}) = \frac{1}{n_{\mathbf{a}}} \operatorname{var}(y).$$

The values of the calibration variance and the variance of the analyte should be identical, which can be checked by Fisher's F-test. Both can be combined as var(y). The calibration range must be reduced if the different variances are not equal. If the identity of the different variance (within their uncertainties) is confirmed, the

averaged value of both variances can be used for further calculations. A better choice is to use the larger variance for further calculations, because this avoids describing the final result too optimistically.

The expressions for $var(\overline{Y_C})$ and var(a) [(13.18) and (13.19)] have to be included.

$$\operatorname{var}\{X_{\mathbf{a}}\}_{\mathsf{LR}} = \frac{\operatorname{var}(y)}{a^2} \left[\frac{1}{n_{\mathbf{a}}} + \frac{1}{n_{\mathsf{C}}} + \frac{\left(\overline{Y_{\mathbf{a}}} - \overline{Y_{\mathsf{C}}}\right)^2}{a^2 S_{xx}} \right].$$

If the different Student t factors of the regression equation (13.13) are included, the range for the confidence interval becomes:

$$\operatorname{cnf}\{X_{\mathbf{a}}\} = X_{\mathbf{a}} \pm \sqrt{\frac{\operatorname{var}(y)}{a^{2}} \left[\frac{t_{n_{\mathbf{a}}-1}^{2}}{n_{\mathbf{a}}} + \frac{t_{n_{\mathbf{C}}-2}^{2}}{n_{\mathbf{C}}} + \frac{t_{n_{\mathbf{C}}-2}^{2} \left(\{X_{\mathbf{a}}\}_{\mathbf{LR}} - \overline{X_{\mathbf{C}}} \right)^{2}}{S_{xx}} \right]}.$$
 (13.23)

Figure 13.6 shows the analyte variance transformation with regard to the confidence interval. It starts with two equal variances $(var(y_1) \text{ and } var(y_2))$ at different values. The total uncertainty contains both the analyte variance and the variance of the calibration function. The uncertainty of the final result is least at the middle of the calibration range and so the equation $cnf\{x_1\} < cnf\{x_2\}$ is valid. To achieve the lowest uncertainty in the final result, measurements should always be carried out in the centre of the calibration range.

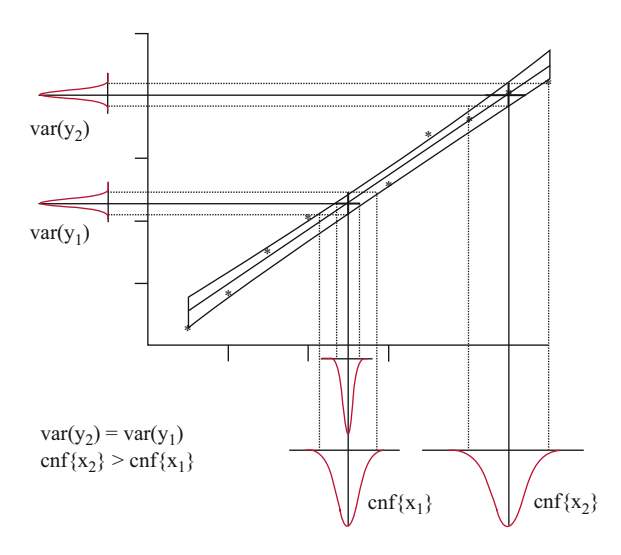


Fig. 13.6 Illustration of the confidence interval and the uncertainty propagation for two samples with the same variance. The transformation to x-values in the centre of the calibration range results in a lower uncertainty

The important influence of the slope can be seen in Fig. 13.6. The slope is called the measure of sensitivity: the larger the slope, the lower the uncertainty of the analytical result [5, 7, 9, 10]. A large slope is preferable, thus determining the method of choice for quantification.

Calibration is laborious because multiple measurements are needed to obtain a final result with an acceptable uncertainty. A linear calibration requires a minimum of at least six measurements for the standards. Thus, all error-dependent steps (weighting, sample pre-treatment procedure, sample application, separation, and scanning) must be done independently. To save time pre-treatment procedures may be applied to a single sample, which is then applied to the layer in different amounts for calibration. This does not establish the true variance for the whole method but only the variance that accompanies the steps after sample application. This approach may reduce random errors due to the smaller number of pre-treatment steps at the expense of an increase in the risk of a systematic error! At least six independently weighed standards should be used for a linear calibration. If the standard solutions are stable, these standards can be used for further calibrations for as long as the solutions are stable. This approach requires some check on the stability of the standards. A simpler solution is to randomly discard one of the six standard solutions before performing calibration [11]. The discarded standard is replaced by a freshly prepared standard. Thus, the calibration solutions are routinely replaced over time avoiding the need for stability checks. The above protocol represents a reduction of work by nearly a factor of two [11].

13.11 Quantitative Analysis Using External Standards

To evaluate a quantification method for a new problem, first test the linear regression method. This results in values for a slope, intercept, and a range over which the calibration is linear, all properties that can be evaluated by statistical parameters for suitability. In the case of a small linearity range, the use of a second-order (non-linear) calibration function is recommended. The external standard method can be used if the intercept is zero within its confidence interval. In this case, the calibration function y = ax is valid for its linear range. The simplification that result from using the external standard method is the reason behind attempts to linearize calibration measurements.

Using a single-level calibration (the external standard method), the sample and the external standard are commonly measured as a series of paired values [5]. As already mentioned, a single series comprises its mean value, which can be used to represent the series:

$$\overline{Y_{\mathbf{a}}} = \frac{1}{n} \sum_{i=1}^{n} y_{\mathbf{a}i}.$$

If $\overline{X_a}$ is the mean value of the analyte (which is to be determined) and $\overline{X_S}$ is the mean value of the standard, the mean of the measurements are abbreviated as $\overline{Y_S}$ and $\overline{Y_a}$. The quotient of both calibration functions can be written as:

$$\frac{a\overline{X_{a}}}{a\overline{X_{S}}} = \frac{\overline{Y_{a}}}{\overline{Y_{S}}}.$$

The measures of sensitivity are identical because we determine the same analyte in the sample and the standard. The slope can be eliminated and after rearranging the general expression for the external standard method is obtained:

$$\overline{X_a} = \overline{X_S} \frac{\overline{Y_a}}{\overline{Y_S}} \tag{13.24}$$

The total variance is available from the law of error propagation. The variance of the final result is assuming only *y*-values as uncertain:

$$\begin{split} var(\overline{X_a}) &= \left(\frac{\delta \overline{X_a}}{\delta \overline{Y_a}}\right)^2 var(\overline{Y_a}) + \left(\frac{\delta \overline{X_a}}{\delta \overline{Y_S}}\right)^2 var(\overline{Y_S}) \\ &= \left(\frac{\overline{X_S}}{\overline{Y_S}}\right)^2 var(\overline{Y_a}) + \left(-\frac{\overline{X_SY_a}}{(\overline{Y_S})^2}\right)^2 var(\overline{Y_S}). \end{split}$$

The variances of the mean values for n data points can be calculated according to (13.10) or (13.18) as:

$$\operatorname{var}(\overline{Y_a}) = \frac{\operatorname{var}(y)}{n}$$
.

The range of confidence for n analyte measurements and m standard measurements, taking the different Student t factors into account, is:

$$\operatorname{cnf}(\overline{X_y}, t) = \overline{X_a} \pm \frac{\overline{X_s Y_a}}{\overline{Y_s}} \sqrt{\operatorname{var}(y) \left(\frac{t_{n-1}^2}{n \overline{Y_a}} + \frac{t_{m-1}^2}{m \overline{Y_s}}\right)}.$$
 (13.25)

Assuming m = n, the range of the confidence interval increases by the factor $\sqrt{2}$ in comparison with a series of single measurements [5].

13.12 Second-Order Calibration Function

Calibration functions in planar chromatography are not necessarily linear. In the case of non-linearity, a second-order regression analysis can be used to fit the data [1]. A second-order calibration function is also called a two-dimensional linear

regression [5]. Higher dimension regression analysis is not suitable for TLC evaluations. The greater number of regression coefficients that need to be determined the more data that must be measured. Non-linear calibration data, which are not transformed using the extended Kubelka–Munk equation, can be adequately fit by a second-order calibration function. Once again to avoid the problematic intercept, (13.26) is recommended as a second-order regression function [5, 10].

$$\hat{y}(x) = \overline{Y_C} + a_1(x - \overline{X_C}) + a_2(x^2 - \overline{X_C}^2). \tag{13.26}$$

The notation of (13.26) explains the expression "two-dimensional linear regression". The function is linear with respect to a_1 and second order with respect to a_2 . The *measure of sensitivity* (MS) is given in (13.27) and is the first derivative of the regression function.

$$MS(x) = a_1 + 2a_2x. (13.27)$$

In contrast to the linear regression function, here the measure of sensitivity depends on the mass or the concentration. The mean values for $n_{\rm C}$ data points can be calculated as previously mentioned. The squared mean value is calculated as:

$$\overline{X_{\rm C}}^2 = \frac{1}{n_{\rm C}} \sum_{i=1}^{n_{\rm C}} x_i^2.$$

The two regression coefficients a_1 and a_2 can be calculated to find the best fit between the measurements and the optimally adjusted regression function via the minimum of the squared residuals. For second-order calibration, the following quantities assist in the calculations:

$$\begin{split} S_{xx} &= \sum_{i=1}^{n_{\text{C}}} \left(x_i - \overline{X_{\text{C}}} \right)^2, \\ S_{x^2} &= \sum_{i=1}^{n_{\text{C}}} \left(x_i^2 - \overline{X_{\text{C}}}^2 \right), \\ S_{xx^2} &= \sum_{i=1}^{n_{\text{C}}} \left(x_i - \overline{X_{\text{C}}} \right) \left(x_i^2 - \overline{X_{\text{C}}}^2 \right), \\ S_{x^2x^2} &= \sum_{i=1}^{n_{\text{C}}} \left(x_i^2 - \overline{X_{\text{C}}}^2 \right)^2, \\ S_{xy} &= \sum_{i=1}^{n_{\text{C}}} \left(x_i - \overline{X_{\text{C}}} \right) \left(y_i - \overline{Y_{\text{C}}} \right), \\ S_{x^2y} &= \sum_{i=1}^{n_{\text{C}}} \left(x_i^2 - \overline{X_{\text{C}}}^2 \right) \left(y_i - \overline{Y_{\text{C}}} \right). \end{split}$$

The regression coefficients a_1 and a_2 can be calculated by taking the partial derivatives of the squared residuals $S_{\rm sr}$ with respect to the coefficients. The following equations result:

$$\frac{\partial S_{\text{sr}}}{\partial a_1} = 0 = \left(-S_{xy} + a_1 S_{xx} + a_2 S_{xx^2} \right),$$

$$\frac{\partial S_{\text{sr}}}{\partial a_2} = 0 = \left(-S_{x^2y} + a_1 S_{xx^2} + a_2 S_{x^2x^2} \right).$$

The two equations can be resolved using matrix notation.

$$\begin{vmatrix} S_{xx} & S_{xx^2} \\ S_{xx^2} & S_{x^2x^2} \end{vmatrix} \begin{vmatrix} a_1 \\ a_2 \end{vmatrix} = \begin{vmatrix} S_{xy} \\ S_{x^2y} \end{vmatrix}.$$

The regression coefficients a_1 and a_2 can be calculated according to Cramer's rule.

$$a_1 = \frac{S_{x^2x^2}S_{xy} - S_{xx^2}S_{x^2y}}{S_{xx}S_{x^2x^2} - (S_{xx^2})^2},$$

$$a_2 = \frac{S_{xx}S_{x^2y} - S_{xx^2}S_{xy}}{S_{xx}S_{x^2x^2} - (S_{xx^2})^2}.$$

The inverse matrix S^{-1} ,

$$S^{-1} = \frac{1}{\det(S)} \begin{vmatrix} S_{x^2x^2} & -S_{xx^2} \\ -S_{xx^2} & S_{xx} \end{vmatrix},$$

multiplied by the variances of a series of measurements will result in the variance/co-variance matrix. The variances of the regression parameter are directly available via this matrix.

$$\begin{vmatrix} \operatorname{var}(a_1) & \operatorname{cov}(a_1, a_2) \\ \operatorname{cov}(a_2, a_1) & \operatorname{var}(a_2) \end{vmatrix} = \frac{1}{\det(S)} \begin{vmatrix} S_{x^2 x^2} & -S_{xx^2} \\ -S_{xx^2} & S_{xx} \end{vmatrix} \operatorname{var}(y).$$

The determinant det(S) is:

$$\det(S) = S_{rr}S_{r^2r^2} - (S_{rr^2})^2.$$

The variance/co-variance matrix clearly shows that co-variances exist and must be taken into account for calculating the final variance. The abbreviation

var(y) describes the variance of the test series. Three values $(a_1, a_2 \text{ and } \overline{Y_C})$ must be calculated from these calibration data. The residual variance of the test series is calculated from the differences between the measured and the fitted data, divided by n_C-3 .

$$var(y) = \frac{1}{n_{C} - 3} \sum_{i=1}^{n_{C}} \left(\hat{y}_{i} - \overline{Y_{C}} - a_{1}(x_{i} - \overline{X_{C}}) - a_{2}(x_{i}^{2} - \overline{X_{C}}^{2}) \right)^{2}.$$

The second-order calibration function has three error-dependent regression coefficients, \overline{Y}_C , a_1 , and a_2 . According to the law of error propagation, the total calibration variance var(y(x)) is:

$$\operatorname{var} \hat{y}(x) = \left(\frac{\partial \hat{y}(x)}{\partial \overline{Y_{C}}}\right)^{2} \operatorname{var}(\overline{Y_{C}}) + \left(\frac{\partial \hat{y}(x)}{\partial a_{1}}\right)^{2} \operatorname{var}(a_{1}) + \left(\frac{\partial \hat{y}(x)}{\partial a_{2}}\right)^{2} \operatorname{var}(a_{2}) + 2\left(\frac{\partial \hat{y}(x)}{\partial a_{1}}\right) \left(\frac{\partial \hat{y}(x)}{\partial a_{2}}\right) \operatorname{cov}(a_{1}, a_{2}).$$

The variances $var(a_1)$ and $var(a_2)$ can be calculated from the variance/co-variance matrix. The variance $var(\overline{Y_C})$ of the mean is calculated according to the linear regression expression.

$$\operatorname{var}\{\hat{y}(x)\} = \frac{\operatorname{var}(y)}{n_{C}} + (x - \overline{X_{C}})^{2} \frac{S_{x^{2}x^{2}}}{\det(S)} \operatorname{var}(y)
+ (x^{2} - X_{C}^{2})^{2} \frac{S_{xx}}{\det(S)} \operatorname{var}(y)
+ 2(x - \overline{X_{C}}) \left(x^{2} - \overline{X_{C}}^{2}\right) \frac{-S_{xx^{2}}}{\det(S)} \operatorname{var}(y)$$
(13.28)

The Student t factor depends on the number of degrees of freedom, which is given as $f = n_{\rm C} - 3$. The confidence interval of the second-order calibration function is:

$$\operatorname{cnf}\{\hat{y}(x)\} = \hat{y}(x) \pm t_{\text{C}} \operatorname{sdv}\{\hat{y}(x)\}.$$
 (13.29)

This confidence interval as well as the confidence interval of the linear regression is defined only in the y-direction. It describes the uncertainty of the calibration function calculated from the y-data. It differs from the linear regression function because we have two minima, which are located at \overline{X}_C and \overline{X}_C^2 as shown in Fig. 13.7.

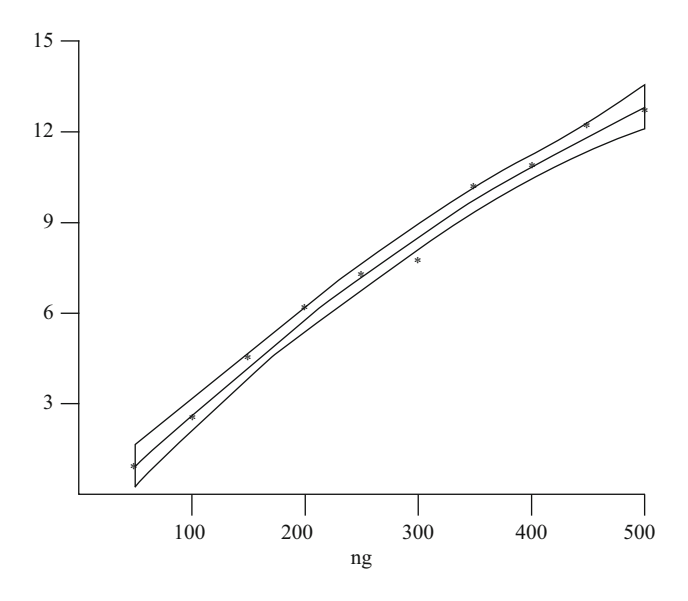


Fig. 13.7 The confidence interval of the second-order regression function with its two minima

13.13 Analytical Function of the Second-Order Calibration

The second-order calibration function (13.26) rearranged with respect to x_a results in the rather complicated expression (13.30). The data for the analyte is compressed to the mean value \overline{Y}_a . Two results are possible, but obviously the negative result is analytical non-sense.

$$\{x_{\rm a}\}_{\rm soc} = \sqrt{\frac{\overline{Y_{\rm a}} - \overline{Y_{\rm C}} + a_1 \overline{X_{\rm C}}}{a_2} + \overline{X_{\rm C}}^2 + \left(\frac{a_1}{2a_2}\right)^2} - \frac{a_1}{2a_2}.$$
 (13.30)

The final variance of the analytical function is calculated according to the law of error propagation, taking the four error-dependent values a_1 , a_2 , $\overline{Y_C}$, and $\overline{Y_a}$ into consideration.

$$\begin{aligned} \operatorname{var}\{x_{\mathrm{a}}\}_{\mathrm{soc}} &= \left(\frac{\partial\{x_{\mathrm{a}}\}_{\mathrm{soc}}}{\partial \overline{Y_{\mathrm{C}}}}\right)^{2} \operatorname{var}(\overline{Y_{\mathrm{C}}}) + \left(\frac{\partial\{x_{\mathrm{a}}\}_{\mathrm{soc}}}{\partial a_{1}}\right)^{2} \operatorname{var}(a_{1}) \\ &+ \left(\frac{\partial\{x_{\mathrm{a}}\}_{\mathrm{soc}}}{\partial a_{2}}\right)^{2} \operatorname{var}(a_{2}) + \left(\frac{\partial\{x_{\mathrm{a}}\}_{\mathrm{soc}}}{\partial \overline{Y_{\mathrm{a}}}(x)}\right)^{2} \operatorname{var}(\overline{Y_{\mathrm{a}}}) \\ &2 \left(\frac{\partial\{x_{\mathrm{a}}\}_{\mathrm{soc}}}{\partial a_{1}}\right) \left(\frac{\partial\{x_{\mathrm{a}}\}_{\mathrm{soc}}}{\partial a_{2}}\right) \operatorname{cov}(a_{1}, a_{2}). \end{aligned}$$

It should be remembered that according to $n_{\rm C}$ and $n_{\rm a}$ two different Student t factors must be taken into account. With the contraction

$$A = \sqrt{\frac{\overline{Y_{a}} - \overline{Y_{C}} + a_{1}\overline{X_{C}}}{a_{2}} + \overline{X_{C}}^{2} + \left(\frac{a_{1}}{2a_{2}}\right)^{2}}$$

and the derivatives

$$\begin{split} &\frac{\partial \left\{x_{\mathrm{a}}\right\}_{\mathrm{soc}}}{\partial \overline{Y}_{\mathrm{C}}} = -\frac{1}{2a_{2}A},\\ &\frac{\partial \left\{x_{\mathrm{a}}\right\}_{\mathrm{soc}}}{\partial a_{1}} = \frac{1}{2a_{2}A} \left(\overline{X}_{\mathrm{C}} + \frac{a_{1}}{2a_{2}}\right) - \frac{1}{2a_{2}},\\ &\frac{\partial \left\{x_{\mathrm{a}}\right\}_{\mathrm{soc}}}{\partial a_{2}} = -\frac{1}{2a_{2}^{2}A} \left(-(\overline{Y}_{\mathrm{a}} + \overline{Y}_{\mathrm{C}}) - a_{1}\overline{X}_{\mathrm{C}} - \frac{a_{1}^{2}}{2a_{2}}\right) + \frac{a_{1}}{2a_{2}^{2}},\\ &\frac{\partial \left\{x_{\mathrm{a}}\right\}_{\mathrm{soc}}}{\partial \overline{Y}_{\mathrm{a}}} = \frac{1}{2a_{2}A} \end{split}$$

and the different variances

$$\operatorname{var}(\overline{Y_{C}}) = \frac{1}{n_{C}} \operatorname{var}(y),$$

$$\operatorname{var}(a_{1}) = \frac{S_{x^{2}x^{2}}}{S_{xx}S_{x^{2}x^{2}} - (S_{xx^{2}})^{2}} \operatorname{var}(y),$$

$$\operatorname{var}(a_{2}) = \frac{S_{xx}}{S_{xx}S_{x^{2}x^{2}} - (S_{xx^{2}})^{2}} \operatorname{var}(y),$$

$$\operatorname{cov}(a_{1}, a_{2}) = \frac{-S_{xx^{2}}}{S_{xx}S_{x^{2}x^{2}} - (S_{xx^{2}})^{2}} \operatorname{var}(y),$$

$$\operatorname{var}(Y_{a}) = \frac{1}{n_{2}} \operatorname{var}(y),$$

we obtain the final confidence interval for the second-order analytical function (13.31).

$$\operatorname{cnf}\{x_{\mathrm{a}}\}_{\mathrm{soc}} = x_{\mathrm{a}} \pm t \sqrt{\operatorname{var}\{x_{\mathrm{a}}\}_{\mathrm{soc}}}.$$
 (13.31)

As a general rule, a minimum of three data points should be measured for each regression coefficient [10]. For linear regression, a calibration set of six data points and for the second-order calibration, at least nine data points are required. Calculate the different confidence intervals and then select the method with the lowest confidence interval to calculate the final result. The lowest final uncertainty should determine the method!

13.14 Risk of Systematic Error

It is assumed that a chromatographic analysis is *selective*. A method is selective when it is able to determine all the relevant substances. A problem can arise for acids and bases because their identity depends on the pH value. It is possible that the neutral and ionized form co-exist in the sample. In this case, both forms must be determined. A method is selective if it is certain that the simultaneous presence of other substances in the matrix does not lead to incorrect results [1]. The common assumption is that all the analytes are measured without matrix interference. The methods we have presented (external standard, linear regression, and second-order calibration) merely allow calculating the confidence intervals of the final result, but these methods give no information about potential systematic errors! Nevertheless, it cannot be excluded that a systematic error is present, perhaps caused by matrix interference. Systematic errors can be divided into two groups: constant and proportional systematic errors.

13.14.1 Constant Systematic Error

A constant systematic error comprises all influential factors independent of the mass or the concentration of the analyte. Two different measurement methods are recommended to reveal a constant systematic error. If both methods result in the same value, no constant error is present. In planar chromatography, absorption and fluorescence measurements can be used to reveal a constant error as well as specific staining in conjunction with the measurement of the unstained zone. Often the main source of potential error is the sample pre-treatment procedure and not the separation or measurement. Often the analyte is lost during pre-treatment. In principle, using an internal standard or addition of standard to the sample can reveal this error.

13.14.2 Proportional Systematic Error

A proportional systematic error depends on the analyte concentration. Adding different amounts of standard to the sample can reveal this error. The added amounts are plotted against the measured data. The resulting regression function will have a slope of one if there is no proportional systematic error. A slope with a value less than one indicates a proportional systematic error. A constant systematic error results in a regression function with an intercept other than zero.

13.15 Use of Internal Standards

If a systematic error is indicated, the use of an internal standard can compensate for this error as long as the calibration plot is linear and has no intercept. The internal standard should be a compound with similar properties to the analyte. If a mass detector is available, an isotopically labelled copy of the analyte is considered a good choice as an internal standard. The internal standard is mixed with the sample, and all the analytical works are carried out simultaneously for the analyte and the internal standard. The amount of analyte is x_a and its observed signal is y_a . The expression $y_a = ax_a$ describes a linear relationship without an intercept. The amount of internal standard in the reference is x_{s1} and the amount of analyte x_r . The appropriate measurement data should be $y_{s,r}$ and y_r . The quotient of both calibration expressions can be combined as:

$$\frac{x_{\rm r}}{x_{\rm s1}} = \frac{a_{\rm r}y_{\rm r}}{a_{\rm s}y_{\rm s,r}} = K \frac{y_{\rm r}}{y_{\rm s,r}}.$$

The different calibration slopes are combined in the constant value K giving:

$$K = \frac{x_{\rm r} y_{\rm s,r}}{x_{\rm s1} y_{\rm r}}.$$

The amount of analyte in the sample x_a and its observed response y_a as well as the internal standard in the sample x_{s2} and its observed response $y_{s,a}$ have the same dependence on K, as described above.

$$\frac{x_{\rm a}}{x_{\rm s2}} = K \frac{y_{\rm a}}{y_{\rm s,a}}.$$

The constant *K* and the amount of analyte in the sample can be determined from all the four measurements. Multiple measurements are usually performed, using the mean values for calculation.

$$\overline{X_a} = K \frac{\overline{X_{s2}Y_a}}{\overline{Y_{s,a}}} = \frac{\overline{X_rY_{s,r}}}{\overline{X_{s1}Y_r}} \frac{\overline{X_{s2}Y_a}}{\overline{Y_{s,a}}}.$$
(13.32)

The total variance of the final result is calculated according to the law of error propagation. All sources of uncertainty must be taken into account. Taking the squared partial derivatives with respect to all y-values gives:

$$\begin{split} var(\overline{X_a}) &= \left(\frac{\delta \overline{X_a}}{\delta \overline{Y_a}}\right)^2 var(\overline{Y_a}) + \left(\frac{\delta \overline{X_a}}{\delta \overline{Y_{s,a}}}\right)^2 var(\overline{Y_{s,a}}) \\ &+ \left(\frac{\delta \overline{X_a}}{\delta \overline{Y_r}}\right)^2 var(\overline{Y_r}) + \left(\frac{\delta \overline{X_a}}{\delta \overline{Y_{s,r}}}\right)^2 var(\overline{Y_{s,r}}). \end{split}$$

The variances of the mean values are the variance of a series of data var(y) divided by the number of data points n.

$$\operatorname{var}(\overline{Y}) = \frac{1}{n} \operatorname{var}(y).$$

Assuming constant variance for each data series, we can shorten the expression to:

$$\operatorname{var}(\overline{X_{a}}) = \left(\frac{\overline{X_{r}Y_{s,r}}}{\overline{X_{s1}Y_{r}}} \frac{\overline{X_{s2}Y_{a}}}{\overline{Y_{s,a}}}\right)^{2} \left[\frac{2 \operatorname{var}(y)}{n\overline{Y_{a}}} + \frac{2 \operatorname{var}(y)}{m\overline{Y_{s}}}\right].$$

The confidence interval cnf() for n sample and m standard measurements is:

$$\operatorname{cnf}(X_{y},t) = \overline{X_{a}} \pm 2\left(\frac{\overline{X_{r}Y_{s,r}}}{\overline{X_{s1}Y_{r}}}\frac{\overline{X_{s2}Y_{a}}}{\overline{Y_{s,a}}}\right)\sqrt{\operatorname{var}(y)\left(\frac{t_{n-1}^{2}}{n\overline{Y_{a}}} + \frac{t_{m-1}^{2}}{m\overline{Y_{s}}}\right)}.$$
(13.33)

The internal standard method needs four measurements (in contrast to external standard calculations which needs only two) and shows reduced precision by a factor of $\sqrt{2}$ compared with the external standard method. The internal standard method compensates for sample losses during analysis and avoids systematic errors. The method can also be used to compensate for improper sample application. Most modern sample applicators can apply a constant sample amount to the layer with high accuracy. If such equipment is unavailable, manual application with glass pipettes is the only practical alternative. Internal standard measurements compensate for variances in the applied sample amount and help reduce the analytical standard deviation.

13.16 Standard Addition Method

In many cases, the analyte is adequately separated from the matrix. Then it does not matter that the calibration standards have a different matrix to the sample. Standards are commonly prepared using pure solvents, and as a consequence, the measured values for calibration standards and actual samples do not possess the same matrix and the statistical structure. This can result in measurements of lower precision [1]. In this case, calibration standards must be dissolved in the sample matrix to avoid a systematic error. Using the standard addition method, the sample is divided into a series of equal volume aliquots to which is added a varied amount of standard except for one aliquot. The response for the sample and samples containing added analyte are now measured in a common matrix. Therefore, a calibration (a change in concentration) is performed in a nearly unchanged sample matrix. This reduces the possibility of a systematic error caused by the

presence of the sample matrix. A proportional systematic dependence on the matrix (a proportional systematic error) is found if the slope of the standard addition calibration function differs significantly from the slope of the linear regression model. The standard addition method can be used to reveal systematic errors but also allows quantification of the analyte in an uncharacterized matrix. The method is more laborious than the external standard method but is capable of greater accuracy.

The standard addition method is based on a linear relationship between the analyte concentration and the measured values. If the analyte with mass x_0 (or the concentration x_0 , applied on the layer) exhibits a response y_0 , the direct proportionality of analyte concentration and the measured values is the slope A_a . From this we obtain the relation:

$$y_0 = A_a x_0. (13.34)$$

In the case of k-fold sample measurements, we can use the mean value:

$$\overline{Y_0} = \frac{1}{k} \sum_{i=1}^k y_{0_i}.$$

After the addition of various known concentrations, slope A_a can be calculated from the response y plotted against the added mass x. If we imagine that mass x_a is added to the sample, providing the response y_a , then the mass (or the concentration) in the separated zone x_a is only responsible for the measurement increase $(y_a - y_0)$. Thus, for the sample concentration x_a , we obtain [12]:

$$y_{a} - y_{0} = A_{a}x_{a}$$
.

The combination of both equations results in:

$$A_a x_0 - y_0 = 0 = A_a x_a - y_a + y_0.$$

The appropriate mean values are

$$\overline{X_{a}} = \frac{1}{n} \sum_{i=1}^{n} x_{ai} \text{ and } \overline{Y_{a}} = \frac{1}{n} \sum_{i=1}^{n} y_{ai}.$$

After resolving for x_0 , we get:

$$x_0 = \frac{1}{A_a} \left(2\overline{Y_0} - \overline{Y_a} \right) + \overline{X_a}. \tag{13.35}$$

The sample should be measured k-fold and the standard added and measured m-fold. Slope A_a is available according to (13.17) as:

$$A_{\mathbf{a}} = \frac{\sum_{i=1}^{m} \left(y_{\mathbf{a}i} - \overline{Y}_{\mathbf{a}}\right) \left(x_{\mathbf{a}i} - \overline{X}_{\mathbf{a}}\right)}{\sum_{i=1}^{m} \left(x_{\mathbf{a}i} - \overline{X}_{\mathbf{a}}\right)^{2}} = \frac{S_{xy}}{S_{xx}}.$$

To estimate the uncertainty of the analytical result, all sources of uncertainty must be taken into account. The variance of x_0 must be calculated according to Gauss' law. Assuming constant variances, the expression for x_0 must be derived from the partial differential with respect to all the uncertainties in expression (13.35). Usually, only measurements (y-values) are seen as uncertain, although the x-values, the volumes of the standards, are also uncertain. However, these errors are projected into the general uncertainty of the measurements. The standard addition method shows no co-variance terms (no cross-terms), because all measurements are accomplished independently of each other. The variance of x_0 is calculated according to the Gaussian law of error propagation as:

$$\operatorname{var}(x_0) = \left(\frac{\partial x_0}{\partial A_a}\right)^2 \operatorname{var}(A_a) + \left(\frac{\partial x_0}{\partial \overline{Y_a}}\right)^2 \operatorname{var}(\overline{Y_a}) + \left(\frac{\partial x_0}{\partial \overline{Y_0}}\right)^2 \operatorname{var}(\overline{Y_0}).$$

The variance of the slope is

$$\operatorname{var}(A_{\mathbf{a}}) = \frac{1}{S_{yy}} \operatorname{var}(y).$$

The variances of the mean values $\overline{Y_a}$ and $\overline{Y_0}$ are

$$\operatorname{var}(\overline{Y_{\mathbf{a}}}) = \frac{1}{m} \operatorname{var}(y)$$

and

$$\operatorname{var}(\overline{Y_0}) = \frac{1}{k} \operatorname{var}(y).$$

For the fraction of the variance x_0 , we can calculate the following deviations

$$\left(\frac{\partial x_0}{\partial A_a}\right)^2 \text{var}(A_a) = \left(-\frac{2Y_0 - Y_a}{A_a^2}\right)^2 \frac{1}{S_{xx}} \text{var}(y),$$

$$\left(\frac{\partial x_0}{\partial Y_a}\right)^2 \text{var}(Y_a) = \left(\frac{-1}{A_a}\right)^2 \frac{1}{m} \text{var}(y),$$

$$\left(\frac{\partial x_0}{\partial Y_0}\right)^2 \text{var}(Y_0) = \left(\frac{2}{A_a}\right)^2 \frac{1}{k} \text{var}(y).$$

The total variance of the standard addition using k-fold sample measurements and m-fold standard additions is:

$$var(x_0) = \frac{1}{A_a^2} \left[\frac{4}{k} var(Y_0) + var(Y_a) \left(\frac{1}{m} + \frac{(x_0 - \overline{X}_a)^2}{\sum_i (x_{a_i} - \overline{X}_a)^2} \right) \right].$$
 (13.36)

The confidence interval (cnf) of the sample amount x_0 is given by [12]

$$\operatorname{cnf}(x_0) = x_0 \pm \frac{1}{A_a} \sqrt{\frac{4t_{k-1}^2 \operatorname{var}(Y_0) + \operatorname{var}(Y_a)t_{m-2}^2 \left(\frac{1}{m} + \frac{\left(x_0 - \overline{X}_a\right)^2}{\sum_i \left(x_{a_i} - \overline{X}_a\right)^2}\right)}$$
 (13.37)

The conclusion from theory is obvious. To minimize the uncertainty in the measurement, increase the added standard amount by twofold for each addition. For the standard addition method, the following equation $\left(x_0 - \overline{X}_a\right)^2 = 0$ is valid, which minimizes the statistically defined error and leads to the simplified confidence interval:

$$\operatorname{cnf}(X_0)_{X_a=2X_0} = x_0 \pm \frac{1}{A_a} \sqrt{\frac{4t_{k-1}^2}{k} \operatorname{var}(Y_0) + \frac{t_{m-2}^2}{m} \operatorname{var}(Y_a)}.$$
 (13.38)

Four samples (k=4) and five standard additions (m=5) can be separated on a single 10×10 -cm HPTLC plate, allowing facile application of the standard addition method for HPTLC.

13.17 Mean *t* Test.

The mean t test evaluates the difference between two means obtained from two independent series of measurements. Based on the equation $\Delta x = \text{tvar}(y)$ Gosset (1908) used this to compare two mean values x_1 and x_2 with the variances var₁ and var₂. The question is whether both means are identical within their confidence intervals.

$$TV = \left| \frac{x_1 - x_2}{\text{sd} v_d} \right| \sqrt{\frac{n_1 n_2}{n_1 + n_2}},$$
 (13.39)

TV is the test value, sdv_d the combined standard variation, x_1,x_2 the mean values of two test series, n_1,n_2 the number of data points, var_d the combined variances of the series, and $var_{1,2}$ the test series variances.

References 351

The combined variances var_d must be calculated in the following way:

$$sdv_d = \sqrt{\frac{(n_1 - 1)var_1 + (n_2 - 1)var_2}{n_1 + n_2 - 2}}.$$

The calculated test value is compared with the appropriate Student t factor. A random difference is given for $TV \le t(f,p=95\%)$, a probable difference is observed for $TV \le t(f,p=99\%)$ and a significant difference is given for TV > t(f,p=99%) [1]. This test can be used to compare the results from two different methods. The test can be used to decide whether the result from a series of fluorescence or absorption measurements of the same sample indicate the same analyte concentration with the assigned probability level. The test is also suitable for deciding whether the mean of a group of n data is identical to a given mean. This is important for deciding whether data meet given limits.

A single-side test is used to decide whether a mean x statistically exceeds a maximum value or lies below a minimum value.

$$TV = \left| \frac{x - x_{\text{debit}}}{\text{sdv}_{\text{a}}} \right| \sqrt{n},$$

TV is the test value for a single-sided t test, x the mean value of a test series, x_{debit} the reference value, sdv_a the standard deviation of the test series, n the number of data points.

The calculated test value is compared with the appropriate Student t factor with f = n-1 number of degrees of freedom. In the case of TV $\leq t(f,p=95\%)$, the measured value does not exceed the given value.

References

- 1. Funk W, Dammann V, Vonderheid C, Oehlmann G (2007) Quality assurance in analytical chemistry, 2nd edn. Wiley-VCH, Weinheim
- Kaiser RE (2005) Methods of detecting and reducing systematic errors in quantitative planar chromatography. Part 1. Fundamentals of systematic quantitative errors. J Planar Chromatogr 18:51–56
- Kaiser RE (2005) Methods of detecting and/or reducing systematic errors in quantitative planar chromatography. Part 2. Systematic errors caused by separation systems. J Planar Chromatogr 18:118–126
- Kaiser RE (2005) Methods of detecting and/or reducing systematic errors in quantitative planar chromatography. Part 3. Evaluation and calibration errors. J Planar Chromatogr 18:256–263
- 5. Ebel S (1996) Quantitative analysis in TLC and HPTLC. J Planar Chromatogr 9:4-15
- Golc-Wondra A, Prošek M, Vovk I (2001) Quantifying uncertainty in quantitative TLC. J Planar Chromatogr 14:100–108

- Cimpoiu C, Hodisan S (2002) Quantitative thin layer chromatography analysis by photodensitometry. Rev Anal Chem 21:55–75
- Spangenberg B, Klein KF, Mannhardt J (2002) Proposals for error-reduction in planar chromatography. J Planar Chromatogr 15:204–209
- Ebel S (1983) Über den Vertrauensbereich kalibrierender Analyseverfahren. Teil 1: Lineare Kalibration. CAL 55–61
- 10. Ebel S (1983) Über den Vertrauensbereich kalibrierender Analyseverfahren. Teil 2: Nichtlineare Kalibrierfunktionen bei Approximation durch Polynome. CAL 172–177
- Ebel S, Lorz M, Weyandt-Spangenberg M (1989) Optimierte Kalibrierung, Fresenius Z Anal Chem 335:960–965
- 12. Spangenberg B unpublished results

Chapter 14 Planning an Analysis and Validation in TLC

This short overview section is dedicated to the planning stage of an analysis by TLC to ensure that the methods used are fit for their intended purpose. This process of evaluation is called validation. It consists of checking the quality of the whole analytical process and making improvements wherever necessary. Validation also encompasses documentation to demonstrate that expectations of quality have been met for the analysis.

14.1 Terms Used in Validation

Validation of analytical methods is discussed in different guidelines [1, 2]. These general guidelines can also serve as the basis of a method validation for thin-layer chromatography. Moreover, there are numerous publications that deal with the validation of various other measurement methods [3–5]. Most of these guidelines only provide broad definitions of the principles to be employed to validate a method. This serves to ensure that the same things are being discussed, but missing are details of the structure in which the principles should be applied to individual methods. According to Taylor, a better overview of the analytical process is disclosed in four hierarchical areas identified as technique, method, procedure, and correct protocol [4].

Technique means the applied scientific principle useful for providing the desired information [4]. If the technique "planar chromatography" is chosen, it generally means TLC or HPTLC plates used in combination with a solvent as mobile phase and a wavelength-dependent, optical measuring plate scanner. Method means a particular adaptation of the chosen technique for a selected measurement [4]. The ICH guideline gives the definition for the term procedure: "The analytical procedure refers to the way of performing the analysis. It should describe in detail the steps necessary to perform each analytical test. This may include but is not limited to: the sample, the reference standard and the reagents preparations, use of the apparatus, generation of the calibration curve, use of the formulae for the

calculation, etc. [1]". For HPTLC, it also includes considerations such as the choice of the separation system (reversed phase or normal phase), selection of the optimum wavelength for the measurement, selection of the developing chamber, and mobile phase composition. Procedure means written directions necessary to use a method [4]. The procedure describes the test method to be used as completely as possible so that the experiment can be repeated. Every detail of an operation should be described in the standard operating procedure (SOP) for each segment of the method, including the correct procedure for all operations such as from weighing the standard to calculating the final values.

The term *protocol* is the most specific name for a method. The protocol is a set of definitive directions that must be followed, without exception, if the analytical results are to be accepted for a given purpose. Typically, they are prescribed by an official body for use in a given situation [4]. For example, in the case of legislation limits, which could mean the refusal of a production lot or the public release of foodstuffs, the protocol must faithfully comply with the regulatory guidelines.

Validation is the process of confirming the reliability of a method to provide useful analytical data [4]. During validation all the above four steps are investigated to identify critical steps as a potential source of variance or bias. Thus, validating a method is the pre-condition for obtaining valid analytical data. Validating an analysis merely establishes whether a particular procedure meets the required standard for that analysis with regard to the documented performance of the method. A validation does not confirm whether this method also fulfils customer demands.

At the point that an HPTLC method has been chosen, further discussion about "technique" is rendered superfluous. Several publications discuss the validation of HPTLC methods [3, 6–15].

Method validation cannot be separated from the method development process, since the validation of the method development must indicate whether the method had achieved its intended purpose, which is the determination of correct analyte values. Publications on the subject of the validation of analytical methods mention certain concepts that stand for particular concrete values such as precision, accuracy (trueness), repeatability, specificity, detection limit, quantification limits, sensitivity, linearity, and range. An analytical method must normally be evaluated against each of these parameters.

14.2 Method Validation

14.2.1 Testing Specificity

The concept of specificity refers to an analytical method, which can quantify a particular analyte without disturbance. "Specificity is the ability to unequivocally assess the analyte in the presence of components, which may be expected to be

present. Typically these might include impurities, degradants, matrix, etc. Lack of specificity of an individual analytical procedure may be compensated by other supporting analytical procedure(s). This definition includes the following implications. Identification: to ensure the identity of an analyte. Purity tests: to ensure that all the analytical procedures accurately present the analyte impurities, i.e. accompanying substances test, heavy metals, residual solvents, etc. Assay (analyte content): to provide an accurate statement of the analyte content in a sample [1]". "For critical separations, specificity can be demonstrated by the resolution of the two components which elute closest to each other [1]".

This concept is often used to describe a satisfactory separation of a substance from all the other accompanying substances. The substance or substances to be identified in a sample are the analytes, which are surrounded by the accompanying substances (the so-called matrix). The term specific generally refers to a method that produces a response for a single analyte. Alternatively, the expression selectivity is often used for a separation. The term selectivity refers to a method that provides responses for a number of chemical compounds, which may or may not be distinguished from each other. If the analyte response is distinguished from all the other responses, the method is said to be selective. The concept of selectivity refers to a method where no component other than the analytes contributes to the result. In a specific measurement, the analyte can be determined in a mixture or in the presence of matrix without interferences from any other components. Specificity is the desired state of selectivity. Specificity is either 100% selectivity or a high degree of selectivity [3]. To avoid confusion, the term specificity should not be used in the sense of selectivity. A method is either specific or it is not. Few, if any methods, are really specific [16]. Since there are few methods that provide a response for a single analyte only, the term selectivity is usually more appropriate than specificity for a typical chromatographic method.

An HPTLC method is specific (better to say selective) when it distinguishes sufficiently an analyte from all the other substances in a sample, and the analyte has an R_f value within the range 0.1–0.9. "Sufficiently separates" is generally defined as a minimum resolution of R=1.25. However, other values can be applied as a separation criterion. In order to make sure that a separated zone (a peak) does not contain other substances, peak purity should be checked by comparing the spectra of the peak at different locations (peak inflection points and peak maximum) with a reference spectrum. Both peak identification and peak purity determination can be easily carried out with a diode array optical scanner. A symmetrical peak shape in the contour plot is often sufficient for establishing peak purity. The use of deuterium and tungsten lamps for measuring spectra should be done with the $\lg(R)$ formula or the (1/R)-1 expression. Identification of substances from their fluorescence spectra (and the use of the extended Kubelka–Munk expression) should only be used when the excitation source emits light of a constant intensity.

If all by-products, impurities, or degradation products are known and available, specificity is established by demonstrating that all these substances are sufficiently separated from the analyte [9]. Generally speaking, you should always try to achieve the specificity required for a method primarily via variations in the

separation conditions. Only if a HPTLC separation does not perform satisfactorily, staining reactions should be used. However, if the separation is insufficient, in some cases it is sufficient to optimize the measurement wavelength to successfully achieve a specific determination. HPTLC's strength lies in its use of normal phase separations on silica gel, which should (nearly) always be the first choice for the stationary phase, because it also provides great flexibility in the choice of the mobile phase. If a separation is to be detected by fluorescence, a reversed-phase layer is recommended, because the fluorescence intensity is usually higher on chemically bonded layers than inorganic oxide layers. It is also advantageous to carry out partition-based separations on a cellulose phase. Two-dimensional separations often employ cyanopropylsiloxane-bonded silica layers. In Chap. 7, numerous more or less specific staining reactions are described. Few staining reactions are specific, but many exhibit selectivity. Nevertheless in some cases a selective staining reaction, similar to the reaction of the amino phase with carbonyl compounds, in conjunction with a separation, can render the method specific.

For planar chromatographic methods, 10×10 -cm or 20×10 -cm HPTLC plates are preferred because of their narrow particle size distribution, which provides sharper peaks in scanning densitometry in comparison to 20×20 -cm TLC plates. The mobile phase should be chosen so that critical pairs lie around an R_f value of 0.33, corresponding to optimum separation performance. Peak broadening during development can be minimized by using a fast-running solvent. A solvent with high viscosity should only be used in exceptional cases!

The sample application method influences the quality of the separation. For quantitative analysis, the sample should be sprayed on because that is the only way that the plate surface will not be damaged by the sample applicator. The narrower the application zone, that is the less sample applied, the better the likely separation. For polar stationary phases, such as silica gel, the sample should be applied to the layer in a volatile solvent of low polarity, which is a good solvent for the sample. The opposite is true for non-polar phases, such as reversed-phase layers, where the solvent should be volatile and as polar as possible. It should be noted though that some samples with high water content do not wet certain RP-18 layers. In that case, wettable RP-18 layers may be a better choice. The optimum application area is about 10 mm from the lower edge of the plate or about 5 mm above the solvent immersion line on the HPTLC plate. The sample should be applied in lines so that a maximum sample amount with optimum peak resolution can be achieved. Inserting a drying step is often recommended between application and separation so that the application solvent residues (very often water!) do not interfere in the separation.

HPTLC methods are generally expected to sufficiently separate the analyte from all known sample contaminants. A suspected contaminant in pure form is often added to the sample to test the separation performance. If identity of likely contaminant is unknown, the analyte can be stressed along with the matrix. Samples can be stressed by treatment with an acid or base, by treatment with an oxidant, by humidity, by treatment with a reducing agent, or by exposing the sample to UV light and/or high temperatures. The degradation products formed in these reactions are likely sample contaminants. After separating the stressed sample, the peak purity of

the analyte is evaluated by spectroscopic methods and/or by two-dimensional development with a different solvent.

14.2.2 Quantifying Analytes

For pharmaceutical products, not only the analyte but also its known contaminants must often be quantified. To simultaneously quantify both analyte and contaminants in one run, HPLC methods are often used for economic reasons. Although HPTLC does not achieve the same separation performance as HPLC, it can attain sufficient selectivity to be competitive, and this together with its capability of parallel development allows a large number of samples to be analysed relatively quickly and at low cost.

14.2.2.1 General Quantification Remarks

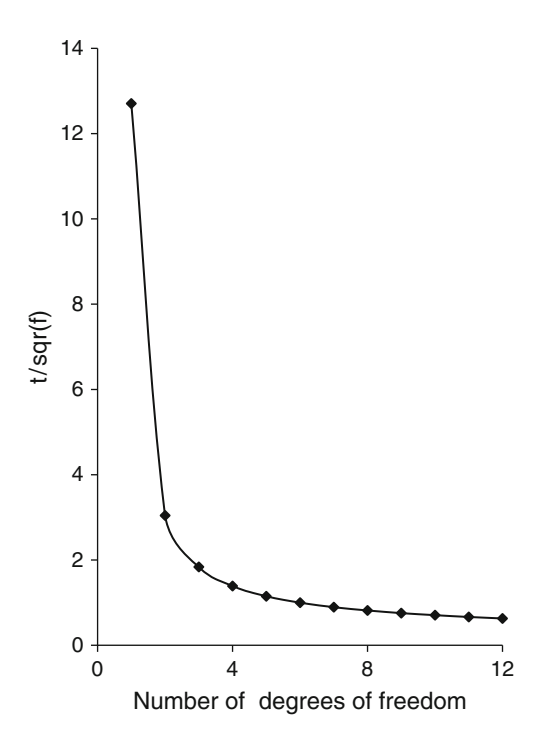
The number of measurements decisively influences the quality of the analytical result. How often a sample should be measured depends on the required confidence interval. The confidence interval for a mean value is calculated from the variance of the mean value var(y), the Student t factor, and the number of measurements n as follows:

$$Y \pm cnf(Y) = \sqrt{\frac{t_{n-1}^2}{n} var(y)} = \frac{t_{n-1}}{\sqrt{n}} var(y).$$
 (14.1)

The expression t/\sqrt{n} in (14.1) is included in all the expressions for the confidence interval. For calibration, the number of degrees of freedom f and not the number of measurements n must be used in the square root expression. If the number of degrees of freedom is plotted against this square root expression, the resulting error function is shown in Fig. 14.1. It can be seen that a minimum value of f=5 should be used, because the error function achieves a minimum value that changes little with higher values of f. Therefore, a mean determination requires six measurements, a linear calibration requires at least seven measurements, and a second-order polynomial calibration requires at least eight measurements.

The analyte should definitely be sprayed on the layer as bands for automated quantitative evaluation of HPTLC plates. This is the only way for a slit-scanning densitometer to measure light absorption under optimal conditions. The application bands should be placed at an approximate distance of 5 mm from the side of an HPTLC plate. For light fibre slit-scanning measurements, the application width should be between 5 and 7 mm, depending on the width of the measuring interface. In any case, the application band must be broader than the measuring interface and scanning should be done in the middle of the band.

Fig. 14.1 Expression t/\sqrt{n} plotted against the number of degrees of freedom, calculated for p = 0.95%



To scan a track, the scan speed should be chosen so that the substance peak will include at least 25 independent data points. The remission values should lie within the range R=0.1–0.9 to minimize the measurement uncertainty. Needless to say that the R_f values of the sample components must lie within the range $0.05 < R_f > 0.9$.

14.2.3 General Aspects of Calibration

Two types of calibration can be distinguished as physical and chemical calibration [5]. *Physical calibration* refers to the measuring capability of an instrument. For example, before using an HPTLC scanner, the dark current is measured and this value is then subtracted from all the following measurements. Also, the adjustment of the *x/y*-scanner table relative to a reference location is generally automatically carried out when the device is switched on. *Chemical calibration* reveals the functional relationship between a given amount (the calibration standards) and the sample amount. Calibration standards must be prepared and measured independently, which means each standard solution must be weighed, dissolved, and measured separately. A single weighing followed by sequential dilution is not permitted, since this procedure could result in a systematic error due to an incorrect

weighing. At least six and preferably ten calibration standards should be used for calibration. Calibration standards should be applied in random order and not in ascending or descending order. The working range should be established so that the expected sample response is located around the centre of the working range. The chemical calibration provides the mathematical relationship between the measured data and the sample content. With this information, the measured values can be transformed into sample concentration values. If different calibration sets are available (e.g. absorption and fluorescence data or results from unstained and stained plates), the calibration set with the largest slope (the largest measure of sensitivity) should be used (see Fig. 13.6).

14.2.4 Linearity and Working Range

The ICH-guideline gives the definition for the terms "linearity" and "range" as follows. "The linearity of an analytical procedure is its ability (within a given range) to obtain test results which are directly proportional to the concentration (amount) of analyte in the sample. The range of an analytical procedure is the interval between the upper and lower concentration (amounts) of analyte in the sample (including these concentrations) for which it has been demonstrated that the analytical procedure has a suitable level of precision, accuracy and linearity [1]".

14.2.4.1 Linearity in HPTLC

ICH guidelines [1, 2] only discuss the linearity of a calibration function as "directly proportional". This reflects the widespread use of UV-visible spectrophotometers (including HPLC spectrophotometric detectors) in analytical measurements that are based on the Lambert-Beer law, which provides a linear response against concentration up to high absorbance values. It should be emphasized that except for fluorescence measurements, calibration functions of optical detectors are generally non-linear. Measurement data from UV-visible spectrophotometers must be logarithmically transformed to achieve a linear calibration functions. The lowest total error function in HPTLC calibration is achievable with the same logarithmic transformation. However, its linear working range is short. The extended Kubelka-Munk transformation generally provides the smallest error over large working ranges, using the linear regression method of data analysis. For a linear calibration range of over 2-3 orders of magnitude, an extended Kubelka-Munk transformation with backscattering factors k = 3/4 to k = 1 is generally sufficient. In any case, a Kubelka-Munk transformation (with k = 1/2) is the only suitable method for evaluating higher concentrations because other models soon run into the saturation range and thus show no more sensitivity. For a more complete discussion see Chaps. 9, 10 and 11.

Nevertheless, the ICH guidelines take non-linear calibrations into account. We can read: "Some analytical procedures, such as immunoassays, do not demonstrate linearity after any transformation. In this case, the analytical response should be described by an appropriate function of the concentration (amount) of an analyte in a sample. For the establishment of linearity, a minimum of 5 concentrations is recommended. Other approaches should be justified [1]". ICH guidelines describe in detail how linearity should be evaluated: "Linearity should be evaluated by visual inspection of a plot of signals as a function of analyte concentration or content. If there is a linear relationship, test results should be evaluated by appropriate statistical methods, for example, by calculation of a regression line by the method of least squares. In some cases, to obtain linearity between assays and sample concentrations, the test data may need to be subjected to a mathematical transformation prior to the regression analysis [1]".

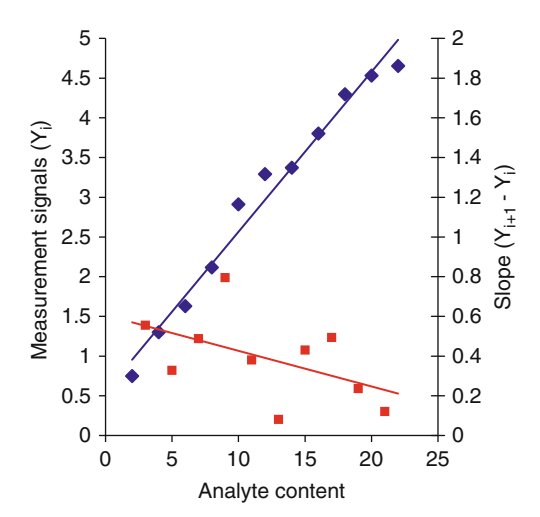
14.2.4.2 Working Range in HPTLC

If a very large working range is required, then a polynomial transformation is preferred. A second-order calibration function is usually quite sufficient. It is not necessary to use higher-order polynomial functions or the sometimes recommended Michaelis-Menten regression formula. However, you must take into account that non-linear calibration functions need more calibration data than a linear function, due to the greater number of regression parameters. A disadvantage of a non-linear calibration model is that calculations according to the external standard, internal standard, and the standard addition methods are not possible. For calibration, at least eight roughly equidistant concentrations are recommended [7]. The smallest and the largest concentrations should each be applied twice (ten data points in total). Moreover, the variance of the calibration data must be constant over the whole calibration range (homoskedasticity). To confirm this, determine the variances of six applications at the minimum and the maximum value of the calibration range. Both must be identical, which can be evaluated using Fisher's variance test. If unequal variances are found at the ends of the working range, the range must be reduced to a value where variance equality reigns.

14.2.5 Choosing a Calibration Function

The calibration function should be chosen so as to minimize the residual values for the fit of the model to the data. During method development, a decision has to be made to adopt either a linear or a polynomial calibration model. For this, the measurement data must be tested (calibration and measured analyte data) via various calibration functions and different linearization models (e.g. extended Kubelka–Munk equation). The model selected is the model providing the smallest error while explaining the data as completely as possible. This would also make all linearity tests superfluous. Correlation coefficients are often adopted as a way of

Fig. 14.2 Measurement responses evaluated by linear regression (*blue*) and trend analysis with slope values between neighbouring data (*red*)



sanctioning a linear calibration model. In most cases, these show values of around one, thus often defining all types of calibrations as linear [10]. To demonstrate that a calibration function is linear, a better test is to plot the individual slopes between neighbouring measurements against the analyte amount or concentration as shown in Fig. 14.2. The linear regression model provides an innocent-looking regression function (blue line in Fig. 14.2). The correlation coefficient is calculated as 0.99152, thus indicating high-grade linearity. The differences between sequentially measured segments are shown in red in Fig. 14.2. These rising values indicate a clear negative trend. This demonstrates that the data would have been better evaluated using a polynomial function.

Instead of a graphic tool, a trend can also be evaluated by comparing the scattering of the measured values around the mean value (var(y)) and the variation of the differences between sequentially measured data. This method is known as von Neumann's trend test. We have already introduced the variance as the squared deviation of the measured values from the mean value (14.2).

$$var(y) = \frac{1}{n_{\rm C} - 1} \sum_{i=1}^{n_{\rm C}} (y_i - \overline{Y_{\rm C}})^2.$$
 (14.2)

If in the expression for the mean variance var(y) the mean $\overline{Y_C}$ is replaced by the previous measured value, one obtains the mean square successive difference (for $n_C - 1$ differences). The test value T_N is defined as the ratio of the mean square successive difference to the variance (14.3).

$$T_N = \frac{\Delta^2}{\text{var}(y)} = \frac{\sum_{i=1}^{n_{C-1}} (y_{i+1} - y_i)^2}{\sum_{i=1}^{n_C} (y_i - \overline{Y_C})^2}.$$
 (14.3)

If trend-free measurements follow a normal distribution, then Δ^2 will be twice as big as var(y).

As soon as a trend is obvious, the mean sequential differences will be reduced and thus it follows: $\Delta^2 < \text{var}(y)$. The approximation V_N (for n > 5) can be used as a quantile for Neumann's trend test, which is calculated according to (14.4) from the quantile of the normal distribution (z_α) .

$$V_N = 2 - 2z_\alpha \sqrt{\frac{n-2}{(n-1)(n+1)}}. (14.4)$$

The test value T_N is now compared with the V_N quantile for a chosen significance level. If the data exhibit a trend, then $T_N < V_N$ results from the calculation.

14.2.6 External Standard Calculation

Routine analysis is often carried out using the *External Standard Method* to avoid calibration. The method of external standards employs multiple measurements of the sample and direct determination of the analyte by the rule of proportion. This procedure is only applicable when a linear relationship exists between the measured data and the analyte concentration, and this relationship has a zero intercept. If only one of these conditions is fulfilled, external standard calibration results in systematically incorrect values. Therefore, before using this method, the linearity of the calibration function and its working range must be established. To evaluate HPTLC separations over a wide concentration range with the external standard method, application of the extended Kubelka–Munk theory is more or less obligatory.

14.2.7 Optimized Calibration Methods

When the external standard method is determined to be unsuitable, we recommend standards near below and above the analyte concentration using the linear regression model for calculation. In HPTLC there is nearly always a linear dependence between the measured value and the range of 80–120 % of the analyte concentration. Therefore, almost all of the transformation methods presented in Chaps. 9 and 10 can be used. Whether the calibration function has an intercept or not is not important for measurements with two standards near the analyte concentration using the linear regression model. The number of calibration measurements can be considerably reduced using the *Optimized Calibration Method* [17]. Only a single calibration set is needed for several determinations. For each new analysis, some calibration data are eliminated at random and then measured again. Such a

calibration takes place continually, together with quantification, thus considerably reducing the time and effort for measurements as well as facilitating the recognition of systematic errors [17].

14.2.8 Precision

The ICH guidelines define precision as: "The precision of an analytical procedure expresses the closeness of agreement (or degree of scatter) between a series of measurements obtained from multiple sampling of the same homogeneous sample under prescribed conditions. Precision may be considered at three levels: repeatability, intermediate precision, and reproducibility. Precision should be investigated using homogeneous, authentic samples. However, if it is not possible to obtain a homogeneous sample, it may be investigated using artificially prepared samples or a sample solution. The precision of an analytical procedure is usually expressed as the variance, standard deviation, or coefficient of variation for various measurements [1]". A precision test describes the random error of repeated measurements for the complete analytical procedure, consisting of sample preparation, measurement, and calculation. A value should always be given as relative precision corresponding to the analyte amount or concentration.

ICH guidelines define the precision of a method at three different levels: *repeatability* (for a repeated analysis), *intermediate precision* (for analysis repetitions over a period of time), and *reproducibility* (for repetitions in different laboratories). "Repeatability expresses the precision under the same operating conditions over a short interval of time. Repeatability is also termed intra-assay precision. Intermediate precision expresses within-laboratories variations: different days, different analysts, different equipment, etc. Reproducibility expresses the precision between laboratories (collaborative studies, usually applied to standardization of methodology) [1]".

Measurement repeatability is expressed as the percent relative standard deviation for repeated measurements using a homogeneous sample. The guidelines suggest at least six sample determinations within a short time, carried out by the same person. Repeatability is defined as the precision under the same operating conditions over a short period of time. Repeatability can also be termed intra-assay precision [1]. Intermediate precision is determined by measuring the same sample on various days by different analysts using different equipment, with the relative standard deviation calculated at the end. Intermediate precision expresses variations within a laboratory, on different days, with different analysts, with different equipment, etc. For repeatability over time, a method must be tested with several different sets of equipment and persons involved in the analysis [1]. Reproducibility expresses precision maintained between laboratories (collaborative studies, usually applied to methodology standardization). The reproducibility of measured results obtained in various laboratories with identical samples at different times. Reproducibility is important for methods that are to be transferred to other laboratories [1].

In general, the ICH guidelines state: "The standard deviation, relative standard deviation (coefficient of variation) and confidence interval should be reported for each type of precision investigated [1]".

How can the method precision be improved for an HPTLC method? For quantification, remission values must lie within a range of R=0.1–0.9. This can be achieved by adjusting the sample application amount so that the signal values fall into the required range. Moreover, a reference spectrum should be chosen to facilitate the calculation of the remission values near the peak to be quantified. The highest precision is obtained for evaluations with the absorbance formula [-lg(R)]. Experience has also shown that using software for peak integration mostly yields smaller standard deviations than "manual integration".

14.2.9 Accuracy

The ICH guidelines state: "The accuracy of an analytical procedure expresses the closeness of agreement between the value which is accepted either as a conventional true value or an accepted reference value and the value found. This is sometimes termed trueness [1]". Accuracy describes the difference (also known as bias) between the measured values and the true value for the sample. Therefore, the better term to use here is "trueness". For example, evaluation of a certified reference sample can be used to establish accuracy. The method is obviously accurate if it provides a value close to the certified value for the reference sample. The method can also be tested with a second independent measurement process. For HPTLC, quantifications by two nearly independent analytical processes, for example, by determining absorption and fluorescence of a sample zone or by determining a pure and a stained sample zone, afford an indication of accuracy. The matrix often has a decisive influence on the accuracy of the analytical result. Therefore, pretreatments should be performed under the same conditions for standards and samples. Mostly it is too complicated to prepare an artificial matrix for the standard, which will contain all interfering substances. In this case, either the Internal Standard method or the Standard Addition Method is recommended. The internal standard method requires the sample to be mixed with a substance having properties similar to the analyte and performing all pre-treatment steps with this modified sample. If a mass selective detector is available, the internal standard can be the isotope-labelled analyte. The internal standard method can compensate for analyte losses during sample preparation. For the standard addition method, various amounts of standard are mixed with the sample. In contrast to the internal standards method, the standard itself is measured in the presence of the matrix, and this method is preferred over the internal and external standard methods for obtaining accurate values. The recovery rate for a reference material is usually expressed as the percent value for the measured results (c_m) compared with their certified

value ($c_{\text{certified}}$). For n measurements, the percent recognition rate w is calculated according to the following formula:

$$w = \frac{100\%}{n} \sum_{i=1}^{n} \frac{c_{\rm m}(i)}{c_{\rm certified}(i)}.$$
 (14.5)

This method is valid for a standard, which is measured externally, without matrix. We recommend mixing the sample with various defined amounts of analyte. Then the analyte amounts are determined and given as a percentage recovery rate, calculated according to the content of the added mixture. The best way to test the accuracy of a method is to compare the slopes (and intercepts) of the calibration functions with and without the sample.

In Fig. 14.3, various amounts of an anionic tenside (perfluorooctanesulfonic acid) extracted by ethyl acetate from water (values in blue) and from a chrome-containing galvanic bath (values in red) were separated by HPTLC, and the resulting fluorescence signals were plotted against the added standard amounts. Both slopes are identical, which can be tested by a mean *t*-test. Identical slopes (measure of sensitivity) show that the matrix exerted no influence on determining the analyte.

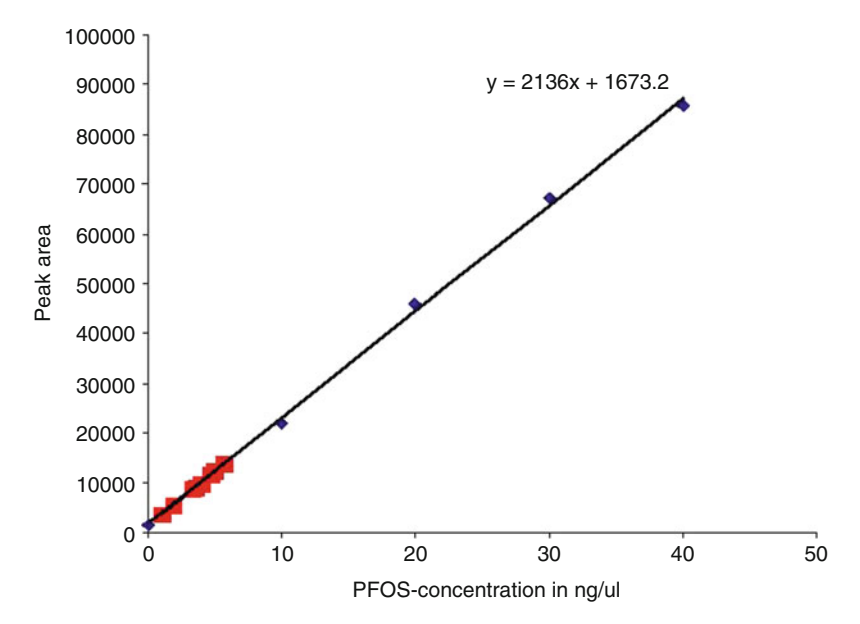


Fig. 14.3 Amount of a pinacryptol yellow/tenside ion pair extracted from water (*blue*) and from a galvanic sample (red). The anionic tenside sample (pH < 5) 10 mL and 1 mL of the cationic dye pinacryptol-yellow solution (100 mg in 100 mL methanol) was extracted with 2-mL ethyl acetate. The extract was separated on silica gel 60 with n-propanol-methanol-2.5 M NaCl/NH $_3$ (25%) (3 +1 + 1 + 1, v/v) and measured by fluorescence at 480 nm

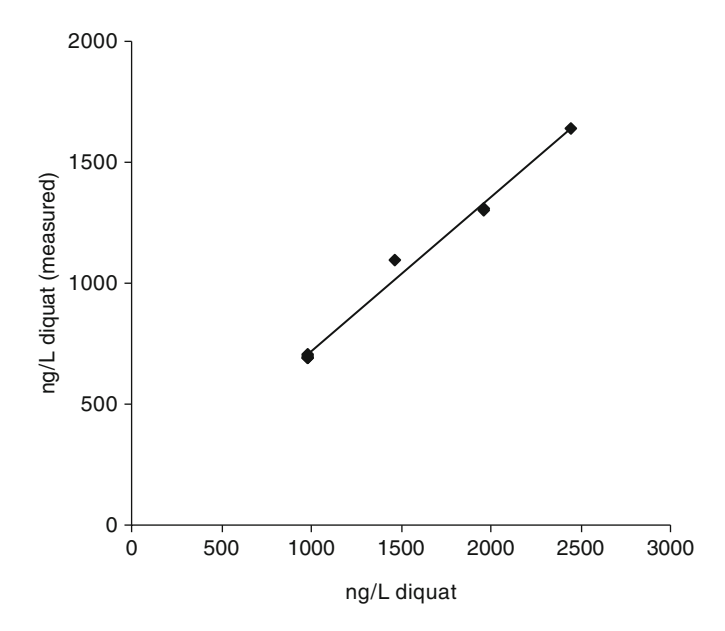


Fig. 14.4 Diquat recovery function in water: the slope is $a=0.638\pm0.023$ ng/L and the intercept 79.7 \pm 88 ng/L diquat [18]

This method is suitable, therefore, for quantifying very low amounts of anionic tenside in the presence of a complicated matrix.

To reveal *proportional systematic errors*, the recovery rate can be graphically evaluated by plotting the theoretical values (the added standard amounts) against the amounts determined for the sample. The ideal recovery function will have a slope = 1 and an intercept = 0. If the intercept is other than 0, then a *constant systematic error* has occurred. This systematic error is independent of the analyte and identical to the intercept value [5]. If the slope differs from 1, there must be an analyte-dependent systematic error [5]. This error can be determined as a percent difference from the ideal slope.

In Fig. 14.4, various amounts of the pesticide diquat were extracted from a litre of water using ion exchange columns [18]. The added amounts are shown on the X-axis and the measured values on the Y-axis. The slope in the recovery function is $a=0.638\pm0.04$. This means that only about $63.8\pm4\%$ of the added diquat amounts were observed. This indicates an analyte-dependent systematic error. The intercept 79.7 ± 88 establishes the absence of a constant systematic error for the determination of the analyte. If all the recovery values lie within the range of 95% of the calculated confidence intervals for slope and intercept, the accuracy of the method is stated as proven.

Most systematic errors arise from the pre-treatment procedure. In any case, systematic errors must be taken into consideration in the final results! A method can still be acceptable, even if it has a systematic error. The important point is that

the error has been recognized and is taken into account and that the same systematic error is observed for each sample.

14.2.10 Confidence Interval

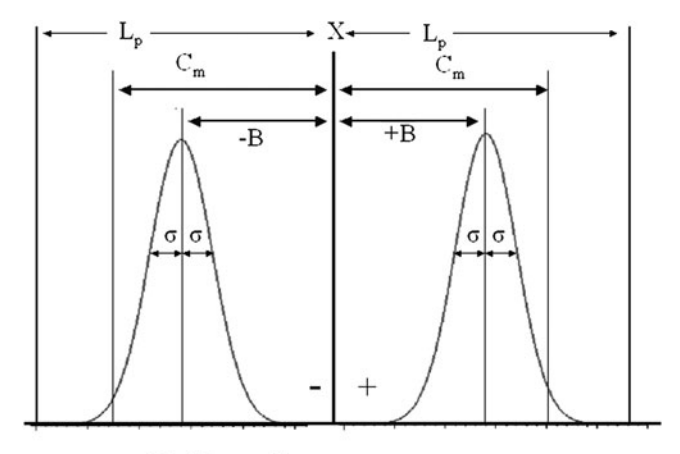
The confidence limits (C_m) for the mean of n replicate measurements is calculated from the mean variance var(x) (the random error) and the bias B (the systematic error). The confidence interval is generally defined for an error probability of 5% which is considered in the student factor (t_{n-1}) for f = n-1 degrees of freedom.

$$C_{\rm m} = \pm \left[B + \frac{t_{n-1} \operatorname{var}(x)}{\sqrt{n}} \right]. \tag{14.6}$$

Obviously, regarding the prescribed tolerance limits (L_p) , the confidence limits (C_m) of a measurement must be less than $L_p[5]$ (Fig. 14.5).

14.2.11 Limit of Detection and Limit of Quantification

Many suggestions have been made for calculating a limit of detection (LOD) and a limit of quantification (LOQ) [14]. The ICH guidelines state: "The detection limit of an individual analytical procedure is the lowest amount of analyte in a sample which can be detected but not necessarily quantified as an exact value [1]".



X : Mean value

σ : Standard deviation (random error)

B: Bias (systematic error)

Fig. 14.5 Calculation of the confidence intervals $C_{\rm m}$, consisting of a random error and a systematic error, compared with the mean X and tolerance limits L_p (according to [5])

14.2.11.1 Limit of Detection

Generally speaking, the observed response measured in triplicate must be three times larger than the standard deviation of a blank. In other words, a peak is recognized as a peak if the signal-to-noise ratio exceeds the value 3 (LOD \geq 3:1 S/N). This proof-limit was first suggested by Kaiser whose "detection limit" is known as the student factor for the probability p=0.9973 with an endless number of degrees of freedom [19]. This factor is $t_{(p=0.9987,\infty)}=3.00$. On this subject, *Kaiser* wrote: "to definitely recognize a substance, the difference between the analytical measured size x and the mean blank value of this measurement must be larger than a determined multiple standard deviation of three blank values [19]". The signal-to-noise value (S/N value) is the reciprocal value of the relative variance. According to Kaiser this should be more than 3 to definitely distinguish the value x from the accompanying noise var(x).

$$\frac{S}{N} = \frac{x}{\operatorname{var}(x)} = \frac{1}{\operatorname{rel var}(x)} \ge 3. \tag{14.7}$$

The ICH guidelines state: "Determination of the signal-to-noise ratio is performed by comparing measured signals from samples with known low concentrations of analyte with those of blank samples and establishing the minimum concentration at which the analyte can be reliably detected. A signal-to-noise ratio between 3 or 2:1 is generally considered acceptable for estimating the detection limit [1]".

Based on the standard deviation of the response and the slope, the detection limit is expressed according to the ICH guideline as [1]:

$$LOD = \frac{3.3 \text{ var}(x)}{A}.$$
 (14.8)

The slope A may be estimated from the calibration curve of the analyte. The residual standard deviation of a regression line may be used as the standard deviation [1]. This is described in (13.15).

14.2.11.2 Limit of Quantification (Quantitation Limit)

The definition of the limit of quantification in the ICH guidelines is: "The quantitation limit of an individual analytical procedure is the lowest amount of analyte in a sample which can be quantitatively determined with suitable precision and accuracy. The quantitation limit is a parameter of quantitative assays for low levels of compounds in sample matrices, and is used particularly for the determination of impurities and/or degradation products [1]". "The quantitation limit is generally determined by the analysis of samples with known concentrations of analyte and by establishing the minimum level at which the analyte can be quantified with acceptable accuracy and precision [1]".

Based on the above definition, the limit of quantification is often set as a S/N ratio of LOQ \geq 10:1. This value is prescribed in the European Pharmacopoeia and is now part of the ICH guidelines.

The ICH guidelines recommend calculation of the limit of quantification based on the signal-to-noise approach.

"This approach can only be applied to analytical procedures that exhibit baseline noise. Determination of the signal-to-noise ratio is performed by comparing measured signals from samples with known low concentrations of analyte with those of blank samples and by establishing the minimum concentration at which the analyte can be reliably quantified. A typical signal-to-noise ratio is 10:1 [1]".

$$LOQ = \frac{10 \text{ var}(x)}{A}.$$
 (14.9)

The slope A and estimate of var(x) can be obtained from the calibration curve for the analyte. A specific calibration curve should be studied using samples, containing an analyte in the range of the LOQ. The residual standard deviation of a regression line (13.15) may be used as the standard deviation [1].

The EURACHEM approach defines a quantification limit, which involves evaluating five different concentrations of a sample whose content lies close to the quantification limit and plotting the relative standard deviations against the measured concentrations [2].

The corresponding limit of quantification can be read from this graph, starting from a just about acceptable relative standard deviation (e.g. 10% or 20%). An example is plotted in Fig. 14.6. These relative standard deviations are often given as 10% for contamination in pure substances and 15% in mixtures or manufactured end products [1, 2].

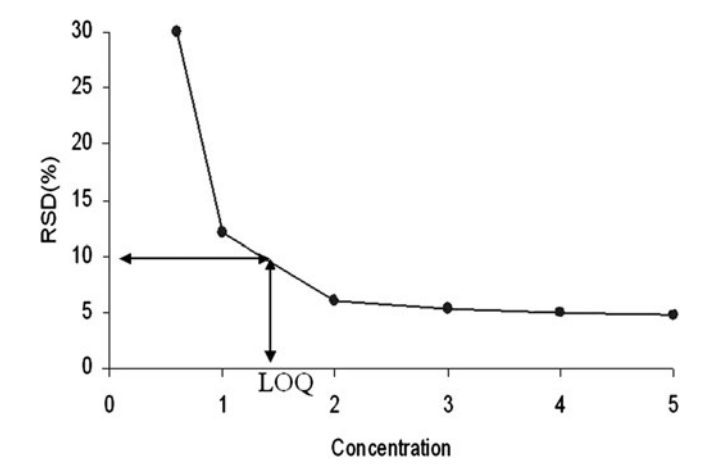


Fig. 14.6 Calculation of the limit of quantification (LOQ) by the EURACHEM approach

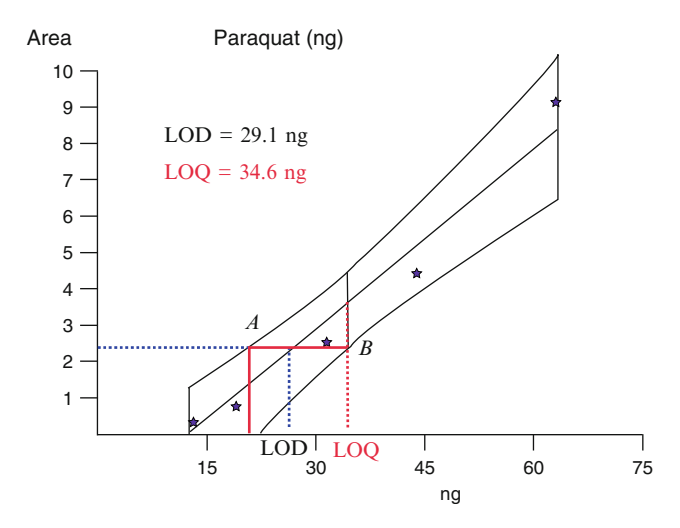


Fig. 14.7 Calculation of a limit of detection (LOD) and limit of quantification (LOQ) according to W. Funk [14]

Calculating the detection and quantification limits from the confidence range of a calibration function is described in [14]. In this approach, there is no need to assign a relative standard deviation as required by the EURACHEM approach. The calibration function is simply plotted with the corresponding confidence interval.

The detection limit is defined as the crossing point of the lower confidence band with the x-axis, where the y-value of the lower confidence range equals zero. In Fig. 14.7, this corresponds to 22 ng. To extract the detection limit from Fig. 14.7, the value of the upper confidence band at this crossing point (A) is marked and has coordinates of x = 22 ng and y = 2.5 (area units). From A, a straight line to the right (parallel to the x-axis) is drawn meeting the crossing point of the lower confidence band (B). The crossing point of this straight line with the calibration function at the x-axis defines the LOD, which lies at 29.1 ng. The crossing point of these straight lines with the lower confidence band (B) indicates at the x-axis the LOQ corresponding to 34.6 ng. The obvious advantage of this method is that no previous information is needed because LOD and LOQ can be constructed directly from the calibration function and its confidence interval.

14.2.12 Robustness

Concerning robustness the ICH guidelines state: "The robustness of an analytical procedure is a measure of its capacity to remain unaffected by small, but deliberate variations in method parameters and provides an indication of its reliability during normal usage [1]".

The evaluation of robustness should be considered during the development phase and depends on the type of procedure under study. It should show the reliability of an analysis with respect to deliberate variations in method parameters. If measurements are susceptible to variations in analytical conditions, the analytical conditions should be suitably controlled or a precautionary statement should be included in the procedure. One consequence of the evaluation of robustness should be that a series of system suitability parameters (e.g., resolution test) is established to ensure that the validity of the analytical procedure is maintained whenever used.

Examples of typical variations are:

- Stability of analytical solutions
- Extraction time
- Influence of variations of pH in a mobile phase
- Influence of variations in mobile phase composition
- Temperature [1]

For example, in all HPTLC methods, small changes in solvent composition should be investigated to check the behaviour of slightly incorrect prepared mixed solvents. This is particularly necessary in adsorption chromatography, where separation behaviour is influenced by small changes in the solvent's water content. Changes in humidity are often responsible for alterations in the separation behaviour because water deactivates the sorbent's active centres. Such influences on separation behaviour must be carefully investigated. If necessary, plates should be stored at a constant relative humidity and this must be included in the "procedure".

Do not underestimate the influence of layer irregularities on reproducibility of the separation and densitometer measurements. Sample application should be carried out across the direction used to apply the layer to its support, since this is the only way to counteract the effect of plate irregularities. Two sides of standard 10×10 -cm HPTLC plates are cut at right angles to the layer coating direction. If possible, sample application should be made at the sharply cut edge. It is also advisable to apply the sample and standards alternately to compensate for any unevenness in the plate surface. Under some circumstances, this could result in lower precision but always improves accuracy! Samples should be applied at least 0.5 cm from the plate edge.

Pre-conditioning the plate is not usually necessary. Reliable separations can be obtained using unconditioned, air-dried layers. In any case, a plate should never be pre-activated by heating to temperatures over 120° C, even if this is prescribed in the instructions! If R_F values vary widely due to variations in relative humidity, it is best to work in rooms with a stable humidity level. In addition, plates should be stored in stable climatically controlled conditions or an air-conditioned developing chamber should be used. Alternately, using RP phases can help to minimize this problem without reverting to the need for specialized equipment.

Developing chambers. Only horizontal chambers with unsaturated vapour phases or vertical chambers without chamber saturation should be used. These chambers allow use without significant delay, provide the most reliable results, and

require the least amount of solvent. Chamber saturation is required to avoid the formation of ß-fronts in horizontal chambers. In this case, small double-trough chambers are available in which the plates can also be pre-conditioned. This type of chamber provides the most stable results for many separations with different solvent mixtures. If vertical chambers are used, then exact conditions for preconditioning the chamber (use of filter paper, saturation time, temperature, conditioning time) must be described in the "procedure" and adhered too.

The separation distance in HPTLC should be about 3–8 cm. Separation distances between 4 and 5 cm are convenient and allow the plate to be simultaneously developed from both sides towards the centre using a horizontal developing chamber.

A small variation in any of the conditions discussed above should have little or no effect on the separation performance for a robust method. Otherwise, the tolerances for those factors which significantly influence the method should be documented in the procedure. To avoid unstable separating conditions, often a change in the stationary phase is the best solution.

The term "robustness" is often confused with the term "ruggedness". Robustness describes internal factors of the method and applies to research and development (R&D) laboratories, which usually develop analytical methods. When these analytical methods are transferred to production control laboratories, ruggedness of a method must be determined. The USP (US Pharmacopoeia) defines ruggedness as "degree of reproducibility of test results obtained by the analysis of the same sample under a variety of normal test conditions such as different laboratories, different analysts, different instruments, different assay temperatures, etc". These conditions are external conditions not affecting the internal conditions of the method development procedure. Therefore, tests on ruggedness are not the subject of this book.

14.3 Control Charts as Quality Indicators in Routine Analysis

Thin layer chromatography is a parallel method that can simultaneously measure many samples. The sample and the standard should be alternately applied onto a plate. Sometimes there is space remaining on an HPTLC plate after all samples have been applied. Some of this space can be occupied by a standard mixture for quality-control purposes. With such control samples, the resolution or other parameters of each separation can be documented and expressed as a function of time or separation conditions. The simplest way to detect trends in the method is to construct a control chart using the data collected for the standard mixture. In addition, a reference plate containing standards should be periodically developed in the same direction as the sample plate and at the same time as the sample plate. The measurements (resolution, R_F values, content, detection limit, separation distance, etc.) from such reference plates provide an excellent overview of the method's long-term stability. This can provide data for documenting the robustness of the method over a long time.

References 373

References

 ICH Guideline Q2(R1) (2005) Validation of analytical procedures: text and methodology. International conference on harmonization, 6 Nov 1996, incorp, Geneva. http://www.ich.org/ LOB/media/MEDIA417.pdf

- Guide EURACHEM (1998) Fitness for analytical methods English edition. LGC, Teddington, UK
- Ferenczi-Fodor K, Végh Z, Nagy-Turák AN, Renger B, Zeller M (2001) J AOAC Int 84:1265–1276
- 4. Taylor JK (1983) Validation of analytical methods. Anal Chem 55:600A-608A
- 5. Taylor JK (1981) Quality assurance of chemical measurements. Anal Chem 53:1588A-1596A
- Ferenczi-Fodor K, Végh Z, Nagy-Turák A, Renger B, Zeller M (2001) Validation of planar chromatographic procedures. In: Nyiredy SZ (ed) Planar chromatography: a restrospective view of the third millennium. Springer, Budapest, pp 336–352
- Szepesi G (1993) Some aspects of the validation of planar chromatographic methods used in pharmaceutical analysis. I. General principles and practical approaches. J Planar Chromatogr 6:187–197
- Ferenczi-Fodor K, Végh Z, Pap-Sziklay Z (1993) Validation of the quantitative planar chromatographic analysis of drug substances. 1: definitions and practice in TLC. J Planar Chromatogr 6:198–203
- 9. Renger B, Jehle H, Fischer M, Funk W (1995) Validation of analytical procedures in pharmaceutical analytical chemistry: HPTLC assay of theophylline in an effervescent tablet. J Planar Chromatogr 8:269–278
- Ferenczi-Fodor K, Nagy-Turák A, Végh Z (1995) Validation and monitoring of quantitative thin layer chromatographic purity tests for bulk drug substances. J Planar Chromatogr 8:349–356
- Nagy-Turák A, Végh Z, Ferenczi-Fodor K (1995) Validation of the quantitative planar chromatographic analysis of drug substances. III. Robustness testing in OPLC. J Planar Chromatogr 8:188–193
- 12. Sun SW, Fabre H, Maillols H (1994) Test procedure validation for the TLC assay of a degradation product in a pharmaceutical formulation. J Liq Chromatogr 17:2495–2509
- Sun SW, Fabre H (1994) Practical approach for validating the TLC assay of an active ingredient in a pharmaceutical formulation. J Liq Chromatogr 17:433–445
- 14. Funk W, Dammann V, Donnevert G (2007) Quality assurance in analytical chemistry, 2nd edn. Wiley-VCH, Weinheim
- Shewiyo DH, Kaale E, Risha PG, Dejaegher B, Smeyers-Verbeke J, Vander Heyden Y (2009) Development and validation of a normal-phase high-performance thin layer chromatographic method for the analysis of sulfamethoxazole in co-trimoxazole tablets. J Chromatogr A 1216:7102–7107
- Vessmann J (2001) Selectivity in analytical chemistry (IUPAC recommendations 2001).
 Pure Appl Chem 73:1381–1386
- Ebel S, Lorz M, Weyandt-Spangenberg M (1989) Optimierte Kalibrierung, Fresenius. Z Anal Chem 335:960–965
- 18. Spangenberg B unpublished results
- Kaiser H, Specker H (1956) Bewertung and Vergleich von Analysis Verfahren, Fresenius.
 Z Anal Chem 149:46–66

Index

A	Aldicarb, 65
Abbott, D.C., 111	Algae, 217
Absorbance, 243	Algaecide, 217
Absorption, 232	Alizarin reagent, 190
Absorption coefficient, 264	Alkaline reagents, 182
Absorptivity, 235	Alkaloids, 165, 173, 179, 180, 187, 189, 193
Accuracy, 320, 364	Alkylating substances, 196
Acetaldehyde, 160	Alkylphenol ethoxylates, 225
Acetanilides, 161	Allium species, 190
Acethylcholine, 182	Allobarbital, 122
Acetic anhydride, 163	Alternaria brassicicola, 222
Acetic esters, 163	Aluminium chloride reagent, 189
Acetone, 106, 158	Aluminium oxide, 62
Acetonitrile, 106	Alzheimer's disease, 208
Acetophenone, 164	Ambrus, A., 208
Acetylcholine, 208	AMD. See Automated multiple
Acetylcholine esterases, 208	development (AMD)
Acid constant, 100	Ametryne, 246
Acidic aluminium oxide, 62	Amines, 165, 166, 178–180, 184
Ackermann, H., 211	Amino acids, 165, 166, 168, 179–181, 185, 192
Acridine, 171	4-Aminoantipyrine, 177, 207
Acridine orange, 171	Amino-bonded silica gel plates, 194
Acrylamide, 175, 185	4-Amino-2,3-dimethyl-1-phenyle-
Activated olefines, 196	3-pyrazoline-5-one, 177
Activity analysis, 195	4-Aminohippuric acid reagent, 177
Activity of the stationary phase, 54	o-Aminophenol reagent, 177
Activity parameter (for Al ₂ O ₃), 85	Amino plate, 8
Adenine, 65	Aminopropyl phase, 21, 66
Adsorption, 16	Amino sugars, 193
Adsorption chromatography, 18, 53, 81	Ammonium bicarbonate reagent, 192
Adsorption energy, 56, 84	Ammonium molybdate (NH ₄) ₆ [Mo ₆ O ₂₁], 187
Adsorption isotherm, 19	Ammonium vanadate (NH ₄ ⁺) ₃ VO ₄ , 172
Aflatoxin B ₁ , 224, 286	Amphetamines, 173
Aflatoxin B_2 , 286	Anabolic active compounds, 193
Aflatoxins, 163	Analytical function, 329, 336
Akkad, R., 209	Analytical range, 315
Alcohols, 162, 166	Andreev, L.V., 59
Aldehyde reagents, 158, 173, 176, 177	Aniline-aldose reagent, 176

Aniline derivatives, 184	Bacteria, 204
Aniline-phthalic acid reagent, 175	Bacterial groups, 222
Anilines, 176, 181	Barbiturates, 162, 178
8-Anilino-naphthalen-1-sulfonic acid	Barrett, C.B., 9
reagent, 168, 171	Barton's reagent, 172
Anion exchangers, 70	Basic Al ₂ O ₃ , 62
Anisaldehyde reagent, 170, 174	Bayerbach, S., 9, 239
4-Anisidine reagent, 177	Beate-Smith, E.C., 28
ANS-reagent, 171	Belenkij, B., 47
Anthraquinones glycosides, 182	Bell curve, 321
Anthrone reagent, 176	Benzalkonium chloride, 217
Antibiotic-resistant bacteria, 223	Benzene, 82
Antibiotics, 174, 181, 203, 223	Benzenesulfonic acid, 107
Anticonvulsants, 193	Benzidine, 168
•	
Antimony-III-chloride reagent, 188 Anti-parallel gradient, 140	Benzo[a]pyrene, 242, 267, 292, 306 4-Benzochinon derivatives, 164
Anti-Stokes lines, 248	
Antrachinon, 196	Benzodiazepines, 162, 185 Renzodiazepine 2 one derivatives 103
	Benzodiazepin-2-one derivatives, 193
APCI-MS. See Laser desorption/atmospheric	Benzoic acid, 166
pressure chemical ionisation mass	Benzophenones, 225
spectrometry (APCI-MS)	3,4-Benzpyrenyl, 160
Application bandwidth, 110	Benzyl alcohol, 26, 27, 127, 128, 131, 141
Application position, 112	Berberine, 66, 171
Archer John Porter Martin, 6	Best fit, 330
Area of the Gauss distribution, 322	Besthorn reagent, 177
Ariabel red, 14	Beyerinck, M.W., 7
Aromatic amines, 162, 172, 175, 184, 185	Bias, 364
Aromatic hydrocarbons, 173, 178	Binary digit, 194
Aromatic hydroxyl ketones, 189	Bioeffective compounds, 203
Ascorbic acid, 171	Bioeffective-linked analysis, 201
Aspartic acid, 70	Biological/biochemical toxicity test, 204
Aspergillus niger, 222	Bio-monitoring, 202
Asymmetrical peak shape, 298	Bis-3,4-benzpyrenyl, 160
Atmospheric pressure glow discharge mass	Bisphenol-A, 225
spectrometry (APGD-MS), 250	Bits, 194, 245
Atmospheric pressure matrix-assisted laser	Bladt, S., 170
desorption/ionisation mass	Blocking the analyte-layer contact, 170
spectrometry (AP-MALDI-MS), 250	Boric acid, 64, 101
Atraton, 217, 246	Bornträger reaction, 182
Atrazine, 216, 217, 246	Borohydride, 161
Atropine, 187	Boron-containing reagents, 180
Automated multiple development (AMD), 143	Bouguer, P., 261
Average, 316	Bovine serum albumin, 72, 211
Average particle size, 60	Bratton-Marshall reagent, 184, 185
Average pore diameter, 61	Brenner, M., 123
Axial diffusion, 44	Bromination, 162
Azeotropic solvent mixtures, 96	Bromine, 161, 162, 188
Azinphos-methyl, 65	5-Bromo-4-chloroindoxyl acetate, 212
Aziridine, 196	Bromocresol green, 171
	Bromoindoxyl acetate, 212
B	4-Bromophenacyl bromide, 163
Bacillus subtilis, 207, 209, 223, 224	Bromothymol blue, 206
Backscattering factor, 267	Buffer systems, 100

Bundling different diode signals, 305 Chloromeguat, 101, 146, 182, 188 Burger, K., 143 7-Chloro-4-nitrobenzo-2-oxa-1,3-diazolreagent (NBD-chloride), 180 C Chlorophenol red β-D-galactopyranoside, 225 Cadmium, 206 p-Chlorophenyl methyl sulfone, 221 Caffeine, 65, 161, 183, 237, 298 Chlorophyll, 67 Calibration function, 328, 360 Chlorophyll fluorescence, 217 Chloroplasts, 204, 216 Camphor derivatives, 72 Cancer, 196 Chlorotoluron, 145 Cancer-causing substances, 82 Cholestanol, 162 Candida albicans, 222 Cholesterine, 183, 189 Cannabinols, 184 Cholesterol, 161, 171 Cholinergic stimulus transmission, 208 Capillary flow, 16 Capillary saturation, 120 Cholinesterase assays, 208 Carbamate esters, 175 Christian F. Schönbei, 2 Carbamates, 165, 185, 208, 212 Chromatogram, 4 Carbofuran, 209 Chromatography, 4 Carbon tetrachloride, 82 Chromato-plates, 7 Chromato strips, 7 Carbonyl group, 163 Carboxylic acids, 162, 172 ChromeXtraktor, 250 Carotene, 67 Ciba F-II, 14 Carr-Price reagent, 188 Cinnamaldehyde reagent, 175 Carvone, 164 Circular separations, 133-134 Catechin, 189 Citrinin, 189 Cladosporium cucumerinum, 222 Catecholamines, 194 Cation exchangers, 69 Clostridium kluyveri, 208 CCD camera, 245, 312 Cobalt-dithizone, 246 Cell organelles, 204 Codeine, 161, 173, 182, 297 Cellulose, 68 Collaborative studies, 363 Cellulose layer, 21 Confidence interval, 333, 335 Central tendency, 316 Confidence interval for the second-order Centrifugal, 135 analytical function, 344 Centrifugal development, 133 Confidence interval of the second-order Centripetal, 135 regression, 343 Cephalosporines, 64 Confidence limits, 367 Chamber saturation, 120, 123 Consden, R., 6, 148 Charge-transfer complexes, 66 Constant systematic error, 345, 366 Charring reagents, 172 Contact-spotting process, 114 Chemical calibration, 358 Contaminants, 203 Chemically bonded silica gel layers, 66 Contour plot, 238, 287, 291, 310 Chemical reagents, 156 Control charts, 372 Chemometrics, 289 Copper reagent, 173, 206 Chiral phases, 72 Correctness, 320 Chiral reagents, 101 Correlation spectroscopy, 293 Chloramine T NaOH reagent, 183 Corticoids, 188 Chloramine-T reagent, 183 Co-variances, 327, 341 Chloramine T trichloroacetic acid reagent, 183 Cramer, F., 8 Chlorination, 161, 183 Cramer's rule, 310, 333, 341 Chlorine, 161, 188 Creatine, 194 Chlorine atmosphere, 185 Creating gradients, 141 7-Chlor-4-nitrobenzo-2-oxa-1,3-diazole, 165 Creatinin, 194 Chloroamphenicol, 224 Cross-capillary analysis, 5

Chloroform, 121

Cross-correlation function, 293

G 4 101	D' ' 160
Crown ethers, 101	Diazo-cation, 162
Cumarin glycosides, 182	Diazonium compound, 184
Cumarins, 184, 196	Diazotisation reactions, 184
Curvularia lunata, 222	Diazotisations, 162, 184
Cutinase, 209	Dibenzofuran, 249
Cyanazine, 145	2,6,-Dibromochinone-4-chlorimide, 179
Cyano HPTLC plate, 8	Dichlophenac, 312
Cyanopropyl layer, 21	2,7-Dichlorfluoresceine, 171
Cyanopropyl plate, 312	3,4-Dichloroaniline, 221
Cyanuric acid, 161, 187	Dichlorophenol, 218
β-Cyclodextrin, 72	2,6-Dichlorophenolindophenol (DCPIP),
Cyclodextrins, 101	171, 216
Cytochrome c, 253	Dichlorovos, 211
Cytosine, 65	7-Diethylamino-3-(4'-maleimidylphenyl)-
•	4-methylcoumarin, 212
D	Diethyldithiocarbamate, 157
Dallas, M.S.J., 9	Diethyl ether, 82, 121
Dansyl aziridine, 165	Difenzoquat, 101, 146, 182, 188
Dansyl azirine, 164	Diffuse multiple scattering, 267
Dansyl chloride, 164	Diffuse reflectance, 233, 261, 263
Dansyl hydrazine, 164	Diffuse reflectance infrared
Dansyl semicadaverine, 166	Fourier transformation, 247
Dansyl semipiperizide, 166	Diffusion coefficient, 40, 41, 47
DART. See Direct analysis in real time (DART)	Digitalis glycosides, 183, 193
	DIH-reagent, 164
Dausend, C., 225	Dihydrolipoamide reductase, 208
2D-chromatography, 148	9,10-Dihydro-9-oxoanthracene, 176
Deconvolution of overlapping peaks, 308	1,3-Dihydroxy 5-methylbenzene, 175
Degree of freedom, 325	Dimedone, 158, 176
Degree of scatter, 363	Dimedone-phosphoric acid reagent, 176
Dehydrogenase activity, 207, 224	4-Dimethylaminobenzaldehyde, 174
Densitometer, 9	Dimethyl sulfoxide, 68
2-Deoxy-D-galactose, 207	3-(4,5-dimethylthiazol-2-yl)-2,5-
Desethylatrazine, 145	diphenyltetrazolium bromide
DESI. See Desorption electrospray	(MTT), 224
ionisation (DESI)	Dimroth, K., 93
Desmetryn, 221, 246	2,4-Dinitrobenzene ethers, 165
Desorption, 16	3,5-Dinitrobenzoylchloride, 166
Desorption electrospray ionisation (DESI),	2,4-Dinitrofluorobenzene, 165
249–250, 252	2,4-Dinitrophenylhydrazine, 158, 163
Desorption sonic spray ionisation (DeSSI), 250	2,4-Dinitrophenyl hydrazine reagent, 177
Detection variance, 318	Dinitrophenylhydrazone, 182
Detector variance, 301	Diode-array detector (DAD-detector), 9
Determinant, 310	Diode-array light scanner, 10
Deuterium lamp, 241	Diode-array scanner, 237
Developing chamber, 371	Diode-array scanning, 305
Development distance, 17	Diode bundling, 305
Development techniques, 119	Diol HPTLC plate, 8
de Zeeuw, R.A., 119	Dioxane, 82, 90, 106
2,3-Diaminonaphthalene, 158, 191	1,3-Dioxoindane, 176
Diaphorase enzyme, 207	Diphenhydramine, 295, 307
Diazepam, 193	2-Diphenylacetyl-1,3-indandion-
Diazoalkanes, 196	1-hydrazone, 164
•	

Diphenylboric acid anhydride, 180 Diphenylboric acid-β-ethylamino ester, 180 2,2-Diphenyl-1-oxa-3-oxonia-2-borata- naphthaline (DOOB) reagent, 181	Environmental screening, 145 Enzyme-inhibition techniques, 205, 208 Enzyme inhibition test for heavy metals, 206 Epoxides, 196
Dipping systems, 169	EP-reagent, 174
Diquat, 101, 146, 182, 188	Error propagation, 326
Direct analysis in real time (DART), 250, 252	Error values, 303
Direct radioactivity measurements, 254	Erythromycin, 72
Direct yellow 7, 171	Essential oils, 174
Dissociation equation, 99	Esterification, 162
Distribution coefficients, 18, 20, 28	17β-Estradiol, 225
Distribution equilibrium, 18	Estriol, 226
Disulfides, 190	Estrogenic properties, 225
2,2-Di-(4-tert-octylphenol)-1-	Estrogens in environmental samples, 225
picrylhydrazyl, 195	Estrone, 226
Dithiophosphate derivatives, 209	Ethanol, 90, 106
Dithizone, 157, 246	Ethyl carbamate, 175
Diurone, 165	Ethylenediamine, 68
DNFB-reagent, 165	Ethylene glycol, 68
Dosage quality, 109	EURACHEM approach, 369
Double-row interface, 240	Excimer, 280
Double trough chamber, 123	Excited dimers, 281
Doxepin, 287	Excited state, 277
Doxylamine, 156	Extended Kubelka–Munk theory, 294
3-D plot, 237	External standard method, 338, 362
DPPH-reagent, 195	Extinction, 232
Dragendorff reagent, 170, 187	Extiliction, 232
DRIFT, 247	F
	_
Drying the plate, 153	Fast atom bombardment (FAB), 250
Durasil®, 63	Fast black salt K, 211
Dynamic quenching, 279	Fast blue salt B reagent, 184, 210
T.	Fatty acids, 171, 192
E	Fenpropathrine, 223
EASI-MS. See Easy ambient sonic spray	Feundlich, H., 19
ionisation mass spectrometry (EASI-MS)	Fisher, R.A., 325
Easy ambient sonic spray ionisation mass	Fisher's F-test, 334
spectrometry (EASI-MS), 250	Fisher's variance test, 360
Ebel, S., 9	Flatbed scanner, 211, 224
Eddy-diffusion, 40	Flavonoids, 180, 188, 189, 192
EDTA, 64	Flavonoids and glycosides, 189
Effective plate number, 39, 137	Flavonols, 184
Ehrlich's reagent, 174	Fluorescamine, 165
Einstein's diffusion law, 41	Fluoresceine isothiocyanate, 167
Ekkerts' reagent, 174	Fluorescence, 9, 242, 277
Electron acceptor, 207	Fluorescence enhancement, 280
Eluotropic series, 85	Fluorescence enhancer, 170
Emission spectra, 279	Fluorescence formula, 244, 267, 304
Enamine ketones, 172	Fluorescence indicator, 285
	Fluorescence quantum yield, 282
Enantiomeric additives, 72	1 .
Enantiomers, 72	Fluorescence quenching, 286
Endocrine disrupters, 225	Fluorescent indicators, 73
Enhanced fluorescence, 66	Fluorescent resorufin, 213
Environmental analysis, 170	Fluorescing compounds, 171

380 Index

Fluorisi1 [®] , 62	Gordon, A.H., 6
Flurpitin, 285	Gosset, W.S., 325
Folin-Ciocalteu reagent, 195	Gotto, A.M., 192
Folin's reagent, 179, 253	Gradient chromatography, 134
Forced flow, 147–148	Gradient separation, 143
Forensic science, 170	Grafted TLC, 149–151
Forensic toxicology, 208	Greyscale, 245
Formaldehyde, 158, 173	Grinberg, N., 62
Formic acid reagent, 193	Group-specific pre-chromatographic
Fourier transformed infrared photoacoustic	reactions, 159
spectroscopy (FTIR-PAS), 247	Grüss, J., 5
Free radical scavenger activity, 195	Guanine, 65
Frei, R.W., 159, 163	Guiochon, G., 40
Friedlieb Ferdinand Runge, 2	Gypsum (CaSO ₄), 62
β-Front, 128	31
Frontal analysis, 3	Н
Front gradient, 81, 126	Hall, N.F., 7
Fronting, 19	Halogenated alkylamines, 196
Fructose, 193	Halpaap, H., 8
F-test, 334	Hamada, M., 212
Fucose, 193	Hamman, B.L., 9
Fungal spores, 222	Hasting expression, 323
Fungicides, 222, 223	Hay bacteria, 223
Funk, W., 158, 163, 370	H-chamber, 125
Furfural, 173, 175	HCl reagent, 193
Furfural reagent, 175	Heavy metals, 64, 157
Fusarium solani pisi, 209	Hefendehl, F.W., 9
r usartum sotum pist, 209	Height equivalent to a theoretical plate, 43
G	Heptobarbital, 122
D-Galactaric acid, 72	Herbicides, 216, 217
Galactose, 193, 207	Heterocyclic compounds, 184
Galactose oxidase, 207	HETP. See Height equivalent to a
β-Galactosidase, 225	theoretical plate
Gallic acid, 188	Hexachloroplatinic acid, 190
Gangliosides, 193	Hexazinone, 65
Gauglitz, G., 10, 239	<i>n</i> -Hexenesulfonate, 170
Gauss distribution, 321	Hexobarbital, 122
Gauss function, 32	High performance thin-layer chromatography
Gaussian curve, 321	
Gaussian function, 308	(HPTLC), 8, 46, 58 HILIC, 145
Geike, F., 206	•
	Hill-reaction, 216
Geiss, F., 45, 57, 87, 120, 125, 131, 140	Hill-reaction inhibitor, 217 Histidine, 70
Gibbs' reagent, 178	
Giddings, J.C., 44	Homoskedasticity, 334, 360
Gingko extract, 117	Honegger, C.C., 129
Glucosamine, 194	Horizontal chamber, 15, 125, 371
Glucose, 173, 176, 193	Hormones, 225
Glucose-reagent, 175	Horseradish peroxidase, 207
Glutamic acid, 70	HPTLC. See High performance thin-layer
Glycerine, 217	chromatography (HPTLC)
Glycol, 172	hR _f -value, 23
Glycosides, 174, 188	Human estrogen receptor DNA sequence, 225
Goppelsröder, F., 2, 22	Humidity, 132

Hydrazines, 181	Isothiosulfates, 172
4-Hydrazino-7-nitrobenzofurazane	Izmailov, N.A., 7
(NBD-hydrazine), 159, 166	
Hydrazones, 158, 177	J
Hydrogen peroxide (H ₂ O ₂), 172, 207	Jaworski medium, 217
Hydrolytic reactions, 161	Jensen's reagent, 183
Hydrophilic interaction chromatography, 145	Jork, A., 9
17-Hydroxicorticosteoids, 160	Jork, H., 212, 233, 282
•	Jost, W., 8
8-Hydroxychinoline, 190	Jost, W., 6
3-Hydroxy-4-methoxybenzaldehyde	V.
(vanillin), 173	K
8-Hydroxyquinoline reagent, 191	Kaiser, H., 368
3β-Hydroxysteroid oxidase, 207	Kaiser, R.E., 8, 47, 59, 109, 147, 321
3α-Hydroxysteroids, 207	Karrer, Paul, 1
3β-Hydroxysteroids, 207	Keller, G.J., 7
	Ketones, 158, 172, 176
I	Ketoses, 177
ICH-guideline, 353, 359, 360, 363, 364, 367,	3-Ketosteroides, 207
368, 370	Keto-sugars, 176
Imazalile, 214, 223	Kieselguhr, 67
Incident light, 262	Kirchner, J.G., 7, 9, 160, 163
Incomplete drying, 116	Klose, A., 125
Indanedione reagent, 176	Knox constants, 40, 46
Indole alkaloids, 162	Kolmogoroff–Smirnov–Lilliefors test, 324
Indoles, 178	Kovar, KA., 247
Indophenol, 14	Kraus, L., 125
Indophenyl acetate, 212	Kubelka–Munk equation, 234, 284
	Kubelka–Munk expression, 268
Indoxyl, 212	<u> </u>
Indoxyl acetate, 212	Kubelka–Munk function, 299, 303
Inhibition constant, 209	Kubelka–Munk theory, 264
Inhibition of electron transport, 218	Kubelka–Munk transformation, 359
Inhibition of photosynthesis, 216	Kubelka, P., 234
Integration, 307	Kuhn, Richard, 6
Intercepts, 329, 365	
Intermediate precision, 363	L
Internal standard method, 364	Labyrinth factor, 41
Intra-assay precision, 363	Lambert-Beer law, 231
Iodination, 162	Lambert cosine law, 262
Iodine-starch reagent, 186	Lasalocide, 224
Iodine vapour, 155, 162	Laser, 248
2-(4-iodophenyl)-3-(4-nitrophenyl)-5-phenyl-	Laser desorption/atmospheric pressure
2H-tetrazolium chloride (INT), 207	chemical ionisation mass spectrometry
Iodoplatinate reagent, 189	(APCI-MS), 250
Ionenaustauscherharze, 71	Laser desorption ionisation (LDI), 250
Ion-exchange chromatography, 53	Layer quality, 38
Ion pair interactions, 101	LED. See Light emitting device (LED)
Ion trap, 253	LiChrospher [®] , 63
Iron-(III)-chloride reagent, 189	Liesegang, R.E., 5
Isocratic separation, 13	Light emitting device (LED), 241, 248
Isocyanates, 166	Light fibre, 9
	Light-fibre diode array scanning, 239
Isoleucine, 70	
Isonicotinic acid hydrazide, 163, 177	Like dissolves like, 82, 94
Isoquinoline, 162	Limit of detection (LOD), 367

Limit of quantification (LOQ), 367	Measure of sensitivity, 329, 333, 340
Linear chambers, 123	Mediator, 127
Linearity, 359	Meinhardt, J.E., 7
Linear regression function, 334	Melamine, 161, 185, 187
Linurone, 165	Mendoza, C.E., 208
Lipid acids, 166	Menthone, 164
Lipophilic analytes, 171	Mepiquat, 101, 146, 182, 188
Lipophilic compounds, 155	Mercaptanes, 165, 190
Liquid-liquid extraction, 221	Mercaptodimethur, 214, 223
Liquid microjunction surface sampling probe	Merck (Darmstadt, Germany), 8, 61
(LMJ-SSP), 250	Mercury, 206
Liquid paraffin, 194	Mesitylene, 26, 27, 127, 128, 131, 141
Lithium sulfate (Li ₂ SO ₄ ·4H ₂ O), 195	Metal-cations, 190
Local plate height, 42	Methiocarb, 214
Logarithmic expression, 302	Methiocarb phenolsulfone, 214
Logarithmic transformation, 243	Methiocarb phenolsulfoxide, 214
Long-chained aldehydes, 218	Methiocarb sulfoxide, 214
Longitudinal spot spreading, 41	Methobromuron, 145
Luciferase enzymes, 218	Method development, 354
Luftmann, H., 251	4-Methoxybenzaldehyde (anisaldehyde), 174
Luminescence, 204, 218	3-Methyl-2-benzothiazolin-3-one hydrazone
Luminescent bacteria, 218	HCl (MBTH), 177
Luteine, 67	Methyl carbamate, 175
	Methyl ethyl ketone, 90
M	Methyl-NBD-hydrazine, 159
Macherey-Nagel (Düren, Germany), 63	Methyl-phenobarbital, 122
Macrolide antibiotics, 72	4-Methylumbelliferon, 225
Magnesium silicate, 62	4-Methylumbelliferyl-β-
Magnesium tungstate, 73	digalactopyranoside, 225
Maillard reaction, 194	Metoclopramide, 156
Making your own plates, 73	Metoxuron, 65, 165
Malaoxon, 209	Metribuzine, 246
MALDI-MS. See Matrix-assisted laser	Michaelis-Menten regression, 360
desorption/ionisation mass	Michelson interferometer, 247
spectrometry (MALDI-MS)	Miller, J.M., 7, 160
Mandelins reagent, 172	Minimum error, 304
Manganese reagent, 173	Mobile phase, 81, 356
Marquis'-reagent, 173	Mobile phase composition, 26
Martin, A.J.P., 20	Modified Kubelka-Munk equation, 266
Martin, M.M., 9	Modifier, 54
Martin relationship, 29	Molar absorption coefficient, 235
Martin-Synge equation, 24, 29	Molecule diffusion coefficient, 41
Mass-dependent reflection, 270	Molybdatophosphoric acid (H ₃ Mo ₁₂ O ₄₀ P), 173
Mass spectrometry (MS), 249	Monuron, 65, 145
Matricaria recutita, 224	Morlock, G., 10, 251
Matrix, 106	Morphine, 164, 173
Matrix-assisted laser desorption/ionisation	Morphine derivatives, 164
mass spectrometry (MALDI-MS), 250	Mould spores, 204
Matrix interference, 345	MTBE. See tert-butyl methyl ether (MTBE)
Mean, 321	MTT tetrazolium salt, 223
Mean t-test, 350	Müller, M.B., 225
Mean value, 316	Multi-K dual phase, 149
Measurement wavelengths, 300	Multiple development, 142

36 : 136 1 1 6 107	37 - 1 12 1 - 1
Munier and Macheboeuf, 187	N-methylindoxyl acetate, 212
Munk, F., 234	<i>N</i> -(1-naphthyl)ethylendiamine
Mycotoxins, 163, 174, 189	dihydrochloride, 185
	N,N'-dicyclohexylcarbodiimide, 166, 167
N	N,N-dimethylaminobenzene, 14
N-acetyl-D-galactosamine, 207	N,N-dimethyl-1,4-phenylenediammonium
<i>N</i> -acetylglucosamine, 193	dichloride (DPDD-reagent), 185
N-acetylneuraminic acid, 193	N,N,N',N'-tetramethyl-1,4-
NAD ⁺ , 207	phenylenediammonium dichloride
NADH, 207	(TPDD), 186
Naled, 211	Noise, 316
Nano-DurasilR®, 63	Nonylphenol, 226
1,3-Naphthalenediol, 175	Normal distribution, 321
α-Naphthol, 162	Normal phase systems, 53
1-Naphthol reagent, 171, 175, 211	Nucleophilic reaction, 196
1,2-Naphthoquinone-4-sulfonate, 179	Nucleophilic reaction ability, 196
1-Naphthyl acetate, 211	Nucleotides, 185
Naphthylamines, 162	Number of equilibria, 32
± •	•
Naphthylisocyanate, 167	Number of measurements, 357
Narceine, 187	Number of theoretical plates, 34
Narcotic effect, 218	Nutrient, 224
NBD-chloride reagent, 165, 180	Nyiredy, Sz., 92, 97, 147
NBD-hydrazine, 159	Nylon 66, 107
N-(β-hydroxybutyryl)homoserin-lactone), 218	
NBP-reagent, 196	0
N-chambers, 123–124	Ochratoxin A, 163, 189
Nd-YAG laser, 248	<i>n</i> -Octane, 90
Neoxanthine, 67	<i>n</i> -Octanesulfonate, 170
Nernst distribution, 21	Octylphenol, 226
Neu, R., 180	Oestriol, 164
Neu-reagent, 180	Oestrogens, 183
Neutral Al ₂ O ₃ , 62	Omori, T., 114
Nicotine, 187	OPLC. See Optimum performance laminar
Niederwieser, A., 123, 129	chromatography
Nile red, 171	Optical fibres, 239
Ninhydrin, 167, 253	Optimized calibration method, 362
Nitrations, 162	Optimum performance laminar
Nitric acid reagent, 194	chromatography (OPLC), 46, 147–148
Nitrite ions, 184	Orcinole reagent, 175
<i>m</i> -Nitroaniline, 71	Organic acids, 176
o-Nitroaniline, 71	Organic mercury compounds, 206
<i>p</i> -Nitroaniline, 71	Organic polymers, 62
Nitroaromatic compounds, 185	Organisms, 204
4-Nitrobenzodiazonium tetrafluoroborate,	Organochlorine compounds, 208
184, 211	Organophosphate esters, 208
4-(4-Nitrobenzyl) pyridine (NBP), 196	Outlier test, 315, 324
Nitrogen-containing compounds, 187	Over-pressure layer chromatography, 147–148
Nitromethane, 90	Overspotting, 161
Nitrophenyl esters, 182	Oxidant, 207
o-Nitrophenylisocyanat, 166	Oxidation reactions, 183
N^6 -methyladenosine, 257	Oxidations, 160
N-methyl-4-hydrazino-7-nitrobenzofurazane	Oxidoreductases, 207
(Methyl-NBD-hydrazine), 159, 166	Oxytetracycline, 224

P Phosphate esters, 208 PAHs. 299 Phosphate ions, 187 Palladium dichloride reagent, 190 Phospholipids, 64, 171, 188, 189, 194, 251 Papaverine, 182 Phosphorescence, 277 Paper chromatography, 20 Phosphor imaging, 255 Paperstrips, 4 Photobacterium fischeri, 218 Parabens, 225 Photobacterium phosphoreum, 218 Paracetamol, 312 Photomultiplier, 256 Paraffin, 193 Photo-stimulated luminescence (PSL), 256 Paraoxon, 209, 215 Photosynthesis, 204 Paraoxon-ethyl, 211 Phthalates, 225 Paraoxon-methyl, 211 Physical calibration, 358 Paraguat, 101, 146, 182, 188 Phytoestrogens, 225 Particle size, 16 Phytonalysis, 170 Particle size distribution, 46, 57, 60 Picric acid, 168 Partisil® K6, 63 Pilocarpine, 182 Partition chromatography, 20, 53, 81, 87 Pinacryptol yellow, 171, 365 Partition coefficient, 25 Piperidine derivatives, 179 Patulin, 163, 164, 192 Planar chromatography detectors, 231 Paulys' reagent, 184 Plate numbers, 34, 36, 42 Peak area, 308 Plate overloading, 116 Peak height, 308 Polarity scale, 91, 102 Peak integration, 308 Polyamide-6, 70 Peak width, 35 Polyamide-11, 70 PEG-600, 217 Polyamide phases, 70 Pendimethaline, 145 Polycyclic aromatic hydrocarbons, 162, 299 Penicillin acid, 193 Polyethylene glycol, 188 Penicillin-derivatives, 190 Polyethylene glycol 600 (PEG 600), 170 Penicillin spores, 222 Polyethylene glycol 4000 (PEG 4000), Penicillum expansum, 222 170, 180 Pentachlorophenol, 210, 218 Poole, C.F., 112 Pentanesulphonate, 279 Pore volume, 61 Peptides, 165, 179, 180 Post-chromatographic reactions, 168 Peptone, 223 Potassium hexacyanoferrate (III), 172, 177 Permeability, 16 Pre-chromatographic reactions, 157 Permeability constants, 16 Precision, 318, 320, 363 Perry, J.A., 143 Precision of an analytical procedure, 363 Pesticides, 201, 208 Pre-conditioning the plate, 371 Pharmaceutical analysis, 170 Pre-loading, 120, 122 Pharmacologically active substances, 203 Primary amines, 181 Phenobarbital, 122 Primary aromatic amines, 184 Phenolic antioxidants, 195 Primulae flos extract, 182 Phenolic aromatic sulfides, 179 Primuline staining, 251 Phenolic steroids, 162, 172 PRISMA model, 98 Phenols, 165, 172, 174, 177, 178, 180, 184 Probable difference, 351 Phenothiazine, 160, 187, 189, 190 Procedure, 353 Phenoxyethanol, 189 Procymidome, 223 Phenylbutazone, 162 Prometon, 246 Phenylenediamine, 168 Prometryn, 65, 246 o-Phenylenediamine reagent, 176, 177 2-Propanol, 106 Phenylhydrazine, 163, 164, 177 Propazine, 145 Phenylisocyanates, 166 Proportional systematic errors, 345, 366 pH-indicator substances, 171 Prosek, M., 9

Prostaglandins, 174	Reed, Lester, 3
Proteins, 195	Reflectance, 9, 235, 241, 243
Proton acceptor character, 92	Reflectance measurements, 233
Proton donator character, 92	Reflectance spectrum, 203
Proton gradient, 218	Reflexion, 9
Pseudomonas savastanoi pv. Phaseolicola, 224	Regression coefficient, 332
Purines, 183, 192	Regular reflection, 233
Purity of chemical standards, 214	Reichard's dye, 93
Pyrene, 279	Reichardt, C., 93
Pyrene fluorescence, 293	Reitsema, R.H., 7
Pyrethroides, 196	Relative detection error, 320
Pyridat, 65	Relative humidity, 132
Pyridine, 162, 163	Relative reflectance, 242, 267
Pyridoxal, 174	Relative variance, 320
4-(2-Pyridylazo)resorcinol (PAR), 157	Repartition coefficient, 19
Pyrimidines, 192	Repeatability, 363
Pyrrole, 162	Reproducibility, 363
- y,	Resolution, 37, 195
Q	Resorufin acetate, 213
Quantile, 323	Retardation factor (R_f) , 22
Quantile–quantile plot (Q–Q plot), 324	Retention factors, 25, 31, 204
Quantitation limit, 368	Reversal reflectance formula, 267
Quaternary ammonium compounds, 182, 189	Reversed phase, 8
QuEChERS approach, 105	Reversed reflectance, 301
Quick, easy, cheap, effective, rugged and	R_f factor, 22
safe, 106	R _F values, 289
Quinine, 193	R _F (%) values, 290
Quinoid derivatives, 162	
Quinoline, 162, 193	Rhizopus sp., 222
Quinonne, 102, 193	Rhodamine B, 171 Rhodamine 6G, 171
R	
	Rhodotorula rubra, 222
Rabbit liver, 209	R_m -values, 29
Radical scavenger properties, 195	Robustness, 370, 372
Radioactive isotopes, 254	Rohrschneider, L., 89
Rainwater overflow basin, 221	Rosmarini folium, 310
Raman spectroscopy, 248	Rotation planar chromatography, 147
Randerath, Kurt, 7	Routledge, E. J., 226
Random difference, 351	RP. See Reversed phase
Random errors, 320, 321	RP-2, 66
Range, 359	RP-8, 66
Raoult's law, 120	RP-18, 66
Rayleigh scattering, 248	Rubeanic acid reagent, 190, 191
Reactions via the gas phase, 191	Ruggedness, 372
Reaction time of the substrate, 215	
Reagent sprayer, 169	S
Real number of theoretical plates, 34	Saccharomyces cerevisiae, 225
Real plate height, 50	Salicylic aldehyde, 181
Reciprocal expression, 243	Salkowsky, 189
Recovery function, 366	Sample application, 105, 371
Recovery rate, 364	Sample contamination, 356
Reducing agents, 171	Sample preparation, 105
Reducing capacity, 195	Sample variance, 318
Reductions, 161	Sapogenins, 188, 192

386 Index

Saunders, D.L., 136 Scan speed, 358 Scatter, 244

Scattering coefficient, 235, 244, 264

Scatter of measured values, 333

S-chamber, 124 Schiff base, 173, 194 Schiff, H., 173 Schlitt, H., 125 Schreiber, M.S., 7 Schuster, A., 234 Schwack, W., 209 Screening tests, 195, 201

Sealing surface sampling probe (SSSP), 250

Secondary ion mass spectrometry (SIMS), 250

Second-order calibration function, 339

Segura, R., 192 Selective, 345 Selectivity, 355 Selectivity factor, 92 Selectivity term, 39 Selenium, 158

Selenium determination, 191 Selenomethionine, 191 Seliger emitter, 262 Sennosides, 182 SensiCam®, 214

Separation number, 47, 108 Sequence spraying, 168 Serine hydrolases, 208, 209

Sherma, J., 10 SH-groups, 180

Signal-to-noise ratio, 306, 368 Significant difference, 351 Silica gel, 63, 356

Silica gel 60, 63 Silica gel 50,000, 68

Silver, 206 Silver colloid, 248 Silver nitrate, 189

Silver nitrate reagent, 188 Simazine, 216, 217, 246 Single-level calibration, 338

Siouffi, A., 40

Size-exclusion chromatography, 53

Slopes, 333, 365 Small chamber, 124 S/N ratio, 369

Snyder, L.R., 55, 84, 136 Snyder's adsorption model, 55 Snyder's equation, 38 Snyder's polarity index, 93

Sodium molybdate (Na₂MoO₄·2H₂O), 195

Sodium nitrite, 162

Sodium nitroprusside (Na₂[Fe(CN)₅NO]), 168 Sodium tungstate (Na₂WO₄·2H₂O), 195 Solid-phase extraction (SPE), 106, 221

Solvent, 81 Solvent additives, 99 Solvent monolayer, 55 Solvent permeation, 83 Solvent strength, 85, 92 Solvent viscosity, 83

SOP. See Standard operating procedure (SOP)

Sorbent particle size distribution, 61 SORBFIL TLC videodensitometer, 246

Sorbinic acid, 166 Sorptive saturation, 120 Specific enzyme activity, 215

Specificity, 354

Specific surface area, 60

Spectra, 9

Spectral comparison, 293 Spectral distribution, 241 Spectral fit, 295

Spinach leaves, 216 Spong pad, 170 Squared residuals, 331 SRS-technique, 151–152 Stahl, E., 7, 58, 124

Staining reaction, 156

Standard addition method, 347, 364 Standard deviation, 33, 318, 321, 322, 324 Standard deviation of a single value, 328 Standard deviation of the mean value, 328 Standard operating procedure (SOP), 354

Starch solution, 155 Stationary phase, 53 Statistical error, 320

Statistical photometric error, 301

Statistics, 315

Sterigmatocystin, 163, 189 Sterins, 183, 188, 192 Steroid hormones, 194 Steroid ketones, 164

Steroids, 172, 174, 182, 183, 188, 192, 193 Stir bar sorptive extraction (SBSE), 108

St. John's word, 181 Stokes, G.G., 278 Stokes lines, 248 Student distribution, 325 Student factor, 325 Substance amount, 21 Sucralose®, 194

Sucraloser, 129 Sudan blue II, 14

Sudan IV, 14	Thionyl chloride, 161
Sugar analysis, 64	Thiophosphonate pesticides, 212
Sugars, 172, 174, 175, 192–194, 207	Thiophosphoric acid pesticides, 182
Sulfonamides, 161, 165	Thiophosphoric ester, 190
Sulfones, 179	Thiosulfate, 172
Sulfoxides, 179, 189	Thiourea derivatives, 172
Sulphonamides, 180, 184	Thomas, J., 111
Sulphur containing compounds, 190	Thymine, 65, 308
Sum of squared residuals (S _{sr}), 316	Thymol, 173
Sumpter, J.P., 226	TIDAS TLC 2010 system, 239
Surface-Enhanced Raman Scattering	Tillmans' reagent, 171
Spectrometry (SERS), 248	Tin-(IV) chloride reagent, 192
Surface tension, 16	TLC-gradient, 140
Surfactants, 170	TLC-scanner, 9
Symmetrical peak shape, 297	o-Toluidine, 186
Synge, R.L.M., 6, 20	Total phenols, 195
Systematic error, 320, 321	Toxic effect, 202
	Toxicity, 203
T	Toxicity test, 202
Tagged image file format (TIF-format), 245	Tramadole, 156
Tailing, 19	Transferring retention data, 28
Tanning agents, 184	Transformed intensity data, 272
Tannins, 189	Transition states, 277
Taylor, J.K., 353	Transmittance, 9, 245
t-distribution, 325	TRANSPOT [™] 1010, 114
Technique, 353	Trend test, 323
Teflon® tape, 114	Triazine herbicides, 161
Temperature on thin layer separations, 29	Triazines, 185, 216
Tenside ion pair, 365	1,3,5-Triazine-2,4,6-triamine, 187
Terbumeton, 217	Trichloroacetic acid reagent, 183, 193
Terbuthylazine, 216, 217	Triethanolamine, 170
Terbutryne, 246	Trifluoroacetic acid, 160
Terpenes, 188, 192 <i>tert</i> -butyl methyl ether (MTBE), 82	Trifluoroacetic anhydride, 163 Trifluralin, 65
Tertiary alcohols, 162	Triglycerides, 64, 189
Testosterone, 183, 193, 194	2,4,6-Trihydroxy-1,3,5 triazine, 187
Tetracyclines, 64	1,3,5-Triphenylformazan, 207
Tetrahydrofuran, 82, 106	Triphenyltetrazolium chloride, 218
Tetraphenyl borate reagent, 101, 146, 182, 311	2,3,5-Triphenyltetrazolium chloride, 207
Tetrazole blue, 171	7.8 tris(hydroxymethyl)-aminomethane-
Tetrazolium salts, 207	HCl buffer, 210
Thebaine, 173	Triton-X-100, 170, 194, 207
Theobromine, 183	Trough chamber, 123
Theophylline, 183	Trueness, 320, 364
Theory of fluorescence, 277	True R_f -value, 24
Thermal reaction of carbonyl compounds, 194	Tswett, M.S., 1, 3
Thiabendazole, 172	Tungsten lamp, 241
Thin-layer radiochromatography	Turnbull's blue, 172
(TL-RC), 254	Tween 20, 222
Thiobarbiturates, 162	Two-dimensional linear regression,
Thio ether, 189	339–340
Thioflavine, 171	Tyihák, E., 147
Thiols, 189	Tyrosine, 70, 195

388 Index

U	Video densitometric evaluation, 246
Umbelliferone, 171	Vinclozoline, 145
Uncertainty, 318, 320	Violaxanthine, 67
Uncertainty propagation, 337	Virtual layers, 263
Universal reagents, 172	Viscosity, 16
Unresolved peak, 309	Vitamin A, 188
Uracil, 65, 308	Vitamin D3, 193
Urea, 161, 177	Vitamins, 172
Urea-HCl reagent, 177	von Neumann's trend test, 361
Urea herbicides, 165	
Urea-pesticides, 185	\mathbf{W}
Urease, 206	Wagner, H., 170
Urethane, 185	Weins, Ch., 212, 225
Urethane derivates, 64	Westall, R.G., 28
Uric acid, 65, 194	Wetting angle, 16
UTLC, 60	Whatmann company, 149
UTLC plate, 75	White-standard, 75
UV–visible spectrum, 296	Willstädter, Richard, 6
o v visiole spectrum, 250	Winterlin, W., 212
V	Wintersteiger, R., 163, 212
Validation, 353, 354	Winterstein, Alfred, 6
Validation of analytical methods, 354	Working range, 359
Valine, 70	Wursters red reagent, 185
Vanadate (V)-sulphuric acid reagent, 172	Wusters blue reagent, 185
van Berkel, G., 252	Wusters reagents, 185
van Deemter equation, 43	Wuthe, W., 239
Van Dijck, H., 133	W utile, W., 239
Vanillin reagent, 170, 173	Y
van Urk's reagent, 174	=
	Yeast, 222
Vapour phase, 119, 130	Yeast cells, 204
Vapour phase fluorescence (VPF), 192	Yeast estrogen screen, 225
Variance, 33, 318	7
Variance equality, 360	Z
Variance of calibration, 318	Zearalenone, 189
Variance of evaluation, 318	Zinc, 206
Variance of sample application, 318	Zinc-dithizone, 246
Variance of sample pre-treatment, 318	Zinc silicate, 73
Variance of the chromatographic	Zlatkis, A., 59
separation, 318	Zone broadening, 40
Variance of the detector, 318	Zone compression factor, 137
Vario-KS-chamber, 123, 125, 131	Zone purity, 291
Vertical chamber, 372	Zone purity confirmation, 296–297
Vibrio fischeri, 218, 312	Zopiclone, 156, 287
Video densitometer, 245	Zulkowsky, 186